Recovery: Oxygen Transport Membrane-Based OxyCombustion for CO_2 Capture from Power Plants

Final Technical Report

For Reporting Period Starting April 1, 2007 and Ending September 30th 2015

DOE AWARD NO. DE-FC26-07NT43088

Principal Investigator: Sean Kelly
Praxair Program Manager: Joan Geary
Business Officer: Shrikar Chakravarti

Principal author: Jamie Wilson

Contributing authors: Max Christie, John Peck, Juan Li, Jonathan Lane, Javier Gonzalez, Yunxiang Lu, Mahesh Biradar, Chuck Robinson, Jiefeng Lin, Pawel Plonczak, Zigui Lu, Sadashiv Swami, Ines Stuckert

Praxair, Inc.
175 East Park Drive
Tonawanda, NY 14150
Contact: Sean Kelly
Tel: (716) 879-2635
Fax: (716) 879-7931
email: Sean_Kelly@praxair.com

Report Issue Date: December 22, 2015

DISCLAIMER:

ABSTRACT:

This Final report documents and summarizes all of the work performed for the DOE award DE-FC26-07NT43088 during the period from April 2007 - June 2012. This report outlines accomplishments for the following tasks: Task 1 – Process and Systems Engineering, Task 2 – OTM Performance Improvement, Task 3 – OTM Manufacturing Development, Task 4 - Laboratory Scale Testing and Task 5 – Project Management.

Executive Summary

The purpose of the OTM based oxycombustion program is to assess the feasibility of integrating Oxygen Transport Membranes (OTM) into a coal fired power plant for cost effective CO_2 capture and sequestration. This program was undertaken in two phases and included the following tasks:

Task 1: Process and Systems Engineering [Phase I and II]

Task 2: OTM Performance Improvement [Phase I]

Task 3: OTM Manufacturing Development [Phase I and II]

Task 4: Laboratory Scale Testing [Phase I and II]

Task 5: Project Management [Phase I and II]

For Task 1, the Advanced Power Cycle for OTM integration in a coal fired plant was developed and cost estimates for several design variants were completed and reported upon in a Phase I topical report. The most cost effective process case reported upon in Phase I included incorporation of warm gas cleanup for sulfur removal as well as an ultra-supercritical steam cycle. Over a range of coal prices, the cost model for this case predicted a <35% cost of electricity increase, meeting the DOE program goal.

The Advanced Power Cycle includes two modes of OTM operation. The first OTM mode is an OTM POx unit which heats high pressure syngas from a gasifier by oxidizing a portion of the syngas with oxygen transferred across the membrane. This syngas is expanded to produce power. The second mode is an OTM Boiler unit which heats supplied boiler feedwater

to produce steam by oxidizing low pressure syngas with oxygen transferred across the membrane. This steam partakes of a Rankine cycle that produces additional power. A more detailed approach to predicting the cost of the OTM POx and OTM Boiler units was undertaken as part of the Phase II work. A subcontract with Shaw Energy and Chemical enabled a basic design and cost estimate to be conducted for pilot-scale versions of the OTM boiler and OTM POx units. The process economics of the Advanced Power Cycle were updated reflecting changes in the configuration of the OTM POx and expander configuration that were chosen to reduce design risk. The cost models updated in Phase II indicated that that the Advanced Power Cycle is still an attractive option for CCS, especially with higher coal costs, but not able to meet the 35% COE increase threshold at lower coal prices.

Within Task 2, fundamental tests were performed which indicated that the porous support and the fuel oxidation layer were the main contributors to performance losses. A new porous support material ("ENrG" advanced substrate technology) with enhanced mass transport characteristics was developed by ENrG Inc. in a NYSERDA program under agreement number 10080, and jointly implemented and evaluated in the OTM technology by ENrG Inc. and Praxair. This new material was shown to exceed performance targets. However, The ENrG "advanced" substrate technology implemented in tubular form was less robust then the "standard" support technology. A new fuel oxidation activation layer with enhanced catalytic capability was also developed that met performance targets, which has since been fully transitioned to manufacturing. Task 2 was completed within the Phase I period of this program.

As part of Task 3, three manufacturing methods and procedures for production of laboratory-scale porous supports (cold isostatic pressing (CIP), extrusion, and ENrG advanced substrate technology) were developed and evaluated. Cost models were developed for each

manufacturing method, and by the end of Phase I extrusion was selected as the preferred low cost porous support manufacturing method, due to improved mechanical robustness of the OTM tube, and lower manufacturing cost. By the end of Phase II, the extruded tubular support structures manufactured in Praxair's ceramic membrane pilot manufacturing facility in Indianapolis, IN, had been scaled from laboratory scale to pilot scale. In addition, construction of an apparatus for automated deposition of the active layers at Praxair, allowed for improved OTM tube reproducibility. In April of 2011, a search for a high-volume ceramics manufacturing partner concluded with the formation of a partnership between Praxair and Saint-Gobain for Phase III of this program, which focuses on pilot-scale manufacturing and demonstration activities.

For Task 4, a single tube reactor was constructed at Praxair's facility in Tonawanda for testing OTM tubes of increased length (1/3 pilot size), with simulated fuels including sulfur containing species (H_2S and COS) and under high pressure (up to 200 psi) on the fuel side. OTM tubes exhibited stable operation in simulated coal-derived fuel gas including sulfur impurities, and OTM tubes exhibited significantly higher performance when tested in elevated fuel-side pressures.

A multi-tube reactor was constructed at the University of Utah and combined with a Hot-Oxygen-Burner (HOB) coal gasifier produced by Praxair for testing OTM tubes in coal-derived syngas. Stable operation (~ 80 hours) of OTM tubes in the coal syngas fuel environment was demonstrated. Ash accumulated on the surface of the OTM tube, but did not appear to cause a decrease in OTM performance. After testing, the OTM tubes were delivered to the University of Connecticut for post-test analysis. OTM tube analysis revealed: no reactions between the OTM components and the coal ash, no evidence of solid or liquid

(slagging) compound formation, and no observed plugging of the porous support with the ash particles.

Laboratory-scale tests conducted within Task 4 demonstrated that transport rates for oxygen flux through OTMs prepared with the standard material set met the target performance levels in the OTM POx environment, but did not meet the target in the OTM boiler environment. OTM tubes prepared with the advanced material set developed in Task 2 were shown to exceed the performance target in the OTM boiler environment. OTM tubes prepared with the advanced material set exhibited significantly higher oxygen flux than OTM tubes prepared with the standard materials set at low pressure and over a wide range of fuel utilization conditions. However, OTM tubes prepared with the advanced porous support failed when tested at elevated pressures, which was attributed to insufficient strength/robustness of the advanced support. Therefore, of the advanced materials developed, only the active layers: the fuel oxidation layer, dual-phase gas separation, and air activation were transitioned to Phase II and III of the program. Development of a robust, high performance and low manufacturing cost porous support is a major focus area for the current Phase III effort.

For Task 4, a heat transport computational model of the OTM system was also developed. Comparison of the model predictions to thermocouple measurements established the importance of radiation as a heat transport mechanism within the OTM system.

Table of Contents

DISCLAIMER: **2**
ABSTRACT: … **2**
EXECUTIVE SUMMARY **3**
LIST OF FIGURES: **8**
LIST OF TABLES **12**
LIST OF APPENDICES: **14**
1. INTRODUCTION **15**
2. PROGRAM TASKS **15**
2.1. TASK 1: PROCESS AND SYSTEMS ENGINEERING 15
2.1.1. SUBTASK 1.1 PROCESS AND SYSTEMS EVALUATION 16
2.1.2. SUBTASKS 1.2 AND 1.3 PILOT PLANT – CONCEPTUAL AND ENGINEERING DESIGN 65
2.2. TASK 2: OTM PERFORMANCE IMPROVEMENT. 102
2.2.1. SUBTASK 2.1 OTM PERFORMANCE IMPROVEMENT PLAN 105
2.2.2. SUBTASK 2.2 POROUS SUPPORT STRUCTURE 108
2.2.3. SUBTASK 2.3 GAS SEPARATION LAYER 117
2.2.4. SUBTASK 2.4 ACTIVATION LAYERS 121
2.3. TASK 3: OTM MANUFACTURING DEVELOPMENT 129
2.3.1. SUBTASK 3.1 AND 3.3 MANUFACTURING PROCESS DEVELOPMENT I &II 130
2.3.2. SUBTASK 3.2 COMMERCIAL SCALE ASSESSMENT 136
2.3.3. SUBTASK 3.4 MANUFACTURING SCALE-UP 137
2.4. TASK 4: LABORATORY SCALE TESTING 140
2.4.1. SUBTASK 4.1 SHORT TUBE TESTING 142
2.4.2. SUBTASK 4.2 AND 4.4 TUBE SECTION TESTING SHORT TUBE PRESSURE TESTING 146
2.4.3. SUBTASK 4.3 AND 4.5 COAL TESTING I & II 153
2.4.4. SUBTASK 4.6 TUBE-SECTION HEAT TRANSFER TESTING 167
2.5 TASK 5: PROJECT MANAGEMENT 176
REFERENCES **179**

List of Figures:

Figure 1 Advanced Power Cycle using WGCU technology for sulfur removal 19
Figure 2: Slip-stream configuration for POx units 28
Figure 3: Temperature duty diagram for a traditional pulverized coal power plant 29
Figure 4: Temperature duty diagram for a boiler feedwater preheat system in a traditional PC Power Plant 30
Figure 5: OTM boiler detail 31
Figure 6: Representative temperature enthalpy diagram for the Advanced Power Cycle 32
Figure 7: Advanced Power Cycle with WGCU and Sulfur containment 46
Figure 8: Escalation of cost from original 2008 study 61
Figure 9: PFD of OTM boiler process unit 66
Figure 10: Oxygen Flux Profile 67
Figure 11: 3-dimensional Schematic of Final Boiler Module (Concept 2) 73
Figure 12: Geometry of boiler module section used for CFD modeling 75
Figure 13: Close-up of boiler CFD geometry showing OTM tubes running cross-flow to the steam tubes (fluid domain shown) 75
Figure 14: CFD model boundary conditions 77
Figure 15: Fuel Gas Temperature Profiles of full module and close up 79
Figure 16: Temperature Profiles in between OTM and Steam Tubes 79
Figure 17: Velocity Profiles at OTM tube cross section 81
Figure 18: Velocity Profiles in between OTM and Steam Tubes 81
Figure 19: Velocity Profile showing recirculation region at the top of the module 82
Figure 20: Predicted OTM temperatures as a function of steam temperature 83
Figure 21: Isometric view of boiler assembly. (Approximately 110'x45'x45') 87
Figure 22: Side Elevation View of OTM Boiler 88
Figure 23: End Elevation View of OTM Boiler 89
Figure 24: Sectional View of OTM Boiler Module within Assembly 89
Figure 25: Low Pressure POx Process 93
Figure 26: 3d Model of Pilot Scale OTM POx System 98
Figure 27: Alternate View of OTM POx System 98
Figure 28: Image of OTM Tube and Illustration of Multilayer, Multifunctional Architecture 103

Figure 29: Relative membrane performance for OTM tubes, combining improvements in porous support and fuel oxidation (Tube 1: Standard support, Tube 2: Improved support, Tube 3: Improved fuel oxidation, Tube 4: Improved support & Improved fuel oxidation). 105
Figure 30: Contributions of OTM components to performance limitations within the standard material set (a) Boiler conditions, (b) POX conditions. Purple = Porous Support, Red = Fuel Oxidation Activation Layer, Green = Gas Separation Layer, Blue = Oxygen Incorporation Activation Layer 106
Figure 31: Contributions of OTM components to performance limitations within the advanced material set (a) Boiler conditions, (b) POX conditions. Purple = Porous Support, Red = Fuel Oxidation Activation Layer, Green = Gas Separation Layer, Blue = Oxygen Incorporation Activation Layer 108
Figure 32: Normalized porosity over tortuosity ratio for three types of porous supports prepared with variations of the "standard" support technology, and two porous supports prepared with variations of the "advanced" support technology 110
Figure 33: Normalized oxygen flux achieved for OTM discs prepared with "standard" and "advanced" supports in CO/CO2 fuel and H2/CO2 fuel compositions at a temperature of 1000°C. 112
Figure 34: Strength of the Praxair "Standard" Support and the ENrG "Advanced" Support 112
Figure 35: Normalized Porosity/Tortuosity of OTM porous support tubes. 114
Figure 36: Normalized Porosity/Tortuosity of OTM porous support tubes prepared in the original and upgraded manufacturing facilities. 114
Figure 37: Peak compressive force supported by O-ring sections cut from OTM tubes. Measurements were normalized by the same value of force, to show relative magnitude. The axial length of the O-ring sections was 1" for A and F, 0.5" for B and E, and 0.25" for C and D. 116
Figure 38: Normalized oxygen flux for OTM disks with gas separation layers that possessed the standard thickness (GS1) and 50% of the standard thickness (GS2), over a span of operating temperatures in gas composition 1 (a CO/CO2 mixture) 120
Figure 39: Normalized oxygen flux for OTM disks with gas separation layers that possessed the standard thickness (GS1) and 50% of the standard thickness (GS2), over a span of operating temperatures in fuel composition 2 (a H2/CO2 mixture). 120
Figure 40: Normalized area specific polarization resistance of candidate fuel oxidation layer materials tested at 1000°C in two gas compositions as a function of development time. Gas composition 1 was a CO/CO2 mixture, and gas composition 2 was a H2/CO2 mixture, and gas composition 2 was a H_2/CO_2 mixture 123

Figure 41: Fraction of target ASR of standard and advanced fuel oxidation layers in a CO/CO2 mixture, over a span of operating temperatures. 123
Figure 42: Normalized oxygen flux achieved for OTM disks tested at 1000°C in two gas compositions. Gas composition 1 was a CO/CO2 mixture (90% CO / 10% CO2), and gas composition 2 was a H2/CO2 mixture (85 H2 / 15% CO2). 126
Figure 43: Normalized ASR of two cathodes materials during a 1000 hours life test in air at a temperature of 1000°C. 127
Figure 44: Normalized ASR of three cathode materials tested in air as a function of operating temperature. 128
Figure 45: 36" long, OTM Tubes with Standard Support Manufactured by Isopressing. 131
Figure 46: Image of a green OTM tube prepared with the advanced support concept 133
Figure 47: Room temperature OTM substrate burst strength as a function of porosity. Porous substrates were pressured by expanding a rubber bladder inside of the porous tube. 134
Figure 48: Pilot production furnace in Indianapolis illustrating H2/N2 gas manifold. 136
Figure 49: Levels for characterizing oxygen flux in an OTM-based oxygen delivery system. 139
Figure 50: Average oxygen flux versus fuel utilization map for OTM tubes tested in conditions appropriate for the Phase I and Phase II advanced boiler at ambient pressure, in a simulated synthesis fuel gas, and at approximately 900°C furnace temperature 142
Figure 51: Normalized oxygen flux of OTM tubes tested in CO/H2/CO2 fuel. Temperature was 900°C and fuel utilization was typically between 60 – 80%. 143
Figure 52: Average oxygen flux versus fuel utilization map for OTM tubes tested at ambient pressure, in a simulated synthesis fuel gas, at 900°C furnace temperature 144
Figure 53: Normalized oxygen flux of OTM tubes tested in a CO/H2/CO2 synthesis gas composition over a range of operating temperatures and at atmospheric pressure. 145
Figure 54: High pressure, single tube, OTM reactor at Praxair, Tonawanda, NY. 148
Figure 55: Normalized oxygen flux of an OTM tube prepared with the "standard" material set as a function of fuel (85%H2/15%CO2) pressure at 850°C and 900°C 149
Figure 56: Normalized oxygen flux of an OTM tube prepared with the "standard" material set with a membrane temperature of 1020°C and ambient fuel pressure versus H2S content of the simulated BGL syngas 150
Figure 57: Normalized oxygen flux of an OTM tube prepared with the "standard" material set at about 1000°C as a function of pressure with a simulated BGL syngas containing 10,000 ppm of H2S in comparison to the simulated BGL syngas without H2S. 151

Figure 58: Normalized oxygen flux as a function of fuel utilization for OTM tubes tested with syngas at ambient pressure and at 900°C furnace temperature. 152
Figure 59: OTM Coal Gas Reactor at the University of Utah 155
Figure 60: Praxair Hot Oxygen Burner for Coal Syngas Production 156
Figure 61: Comparison of OTM Performance in syngas compositions derived from Illinois/PRB and Utah/PRB coal blends 159
Figure 62: OTM performance as a function of operating time in syngas derived from a Utah/PRB coal blend. 160
Figure 63: OTM performance as a function of operating time in syngas derived from an Illinois/PRB coal blend. 161
Figure 64: Ash on surface of OTM tube 162
Figure 65: OTM performance in Illinois/PRB coal derived synthesis gas with various conditions of accumulated ash 162
Figure 66: XRD pattern obtained from the ash deposit. Chemistry and melting point are also shown. 163
Figure 67: (a) Ash deposited on the OTM. (b) Powdery deposit, (c) smooth deposit, and (d) localized ash deposit formed on the porous channel. 165
Figure 68: Micrograph of OTM polished cross section 165
Figure 69: Predicted temperature profiles of the OTM tubes as a function of axial position. (a) no radiative heat transport, (b) moderate OTM emissivity, (c) high OTM emissivity 173
Figure 70: Normalized average oxygen flux versus fuel conversion for three OTM tubes evaluated in the HPR. The initial inlet fuel flow and composition was the same for all three tubes. 175
Figure 71: Residence time versus fuel conversion, for 3 OTM tubes evaluated in the HPR. The initial inlet fuel flow and composition was the same for all three tubes. 176
Figure 72: Project Spend for Phases I and II 178

List Of Tables

Table 1: Steam Cycle Conditions 20
Table 2: Ambient and Cooling Water Conditions 20
Table 3: OTM-ASU Operating Conditions 20
Table 4: CO2 Product Specifications 21
Table 5: Coal Composition 21
Table 6: Power Cycle Operating Costs 24
Table 7: COE Comparison Basis 24
Table 8: Case List 45
Table 9: Case 1 Stream Summary 47
Table 10: Case 1 power, industrial gas and environmental performance summary 48
Table 11: Case 1 Capital Cost 49
Table 12: Case 1 COE Estimate 50
Table 13: Case 2 Stream Summary 51
Table 14: Case 2 power, industrial gas and environmental performance summary 52
Table 15: Case 2 Capital Cost Estimate 53
Table 16: Case 2 COE Estimate 54
Table 17: Case 3 Stream Summary 55
Table 18: Case 3 power industrial gas and environmental performance summary 56
Table 19: Case 3 Capital Cost Estimate 57
Table 20: Case 3 COE Estimate 58
Table 21: Calculated COE for 3 OTM cases at various coal prices compared to the Air-PC reference case (no capture) 59
Table 22: Percent increase in COE over the reference case for various coal prices. 60
Table 23: COE for all cases assuming the steam cycle cost from Praxair's 2008 estimate 62
Table 24: Percent increase in COE assuming steam cycle cost from 2008 Praxair estimate 62
Table 25: Cost of CO2 avoided and removed for the 3 OTM cases at various coal prices 63
Table 26: Boiler Design Basis 68
Table 27: Typical Syngas Feed to OTM Boiler 68
Table 28: Table of flow conditions for CFD boiler model 76
Table 29: Pilot Boiler Cost Estimate Summary 91
Table 30: Pilot Boiler Cost Detail 92
Table 31: POx Process Design Basis 94

Table 32: Assumed Syngas Feed to POx Units 94
Table 33: OTM Pilot POx unit Cost Summary 100
Table 34: OTM Pilot POx unit Equipment Cost Breakdown 101
Table 35: OTM tubes used in strength testing, including porous support type, tube ID and average wall thickness. 115
Table 36: Gas Separation Layer Ambipolar Conductivity as a function of temperature 118
Table 37: Gas Separation Layer Ambipolar Conductivity as a function of gas composition at 1000°C. 118
Table 38: Ultimate and proximate analysis of coals (wt%) 157
Table 39: Trace species analysis of synthesis gas, ppm 157
Table 40: Fuel compositional analysis (dry vol%) 158
Table 41: Typical surface and gas temperatures on OTM tubes tested in CO/CO2 and synthesis gas (CO/H2/CO2) mixtures in the low pressure reactor 169
Table 42: Typical surface temperatures of OTM tubes tested in CO/CO2 and syngas (H2/CO/CO2/N2/CH4/H2O) fuel gas environment at ambient pressure with furnace at 900°C 170
Table 43: Measured emissivity values of OTM materials 171

List of Appendices:

Appendix A: Phase 1 Techno-economic evaluation of the Advanced Power Cycle Concept … A1

Appendix B: Shaw Energy and Chemical Final Report …… B1

Appendix C: University of Utah Final Report …….. C1

Appendix D: International Conference on Greenhouse Gas Control Technologies 2010 Paper… D1

Appendix E: Clearwater Papers 2007 – 2010 ……..… E1

Appendix F: Clean Coal Today Publication (2008) …… F1

Appendix G: Florida Turbine Technologies 2012 Report …….. G1

Appendix H: Patents …….. H1

1. Introduction

The objective of this project is to evaluate feasibility and demonstrate proof-of-concept of a novel oxy-combustion process based on oxygen transport membranes (OTM) for capturing carbon dioxide from coal-fired power plants. The proposed technology has the potential to capture greater than 90 percent of the carbon dioxide from a coal power plant while keeping the associated increase in cost of electricity (COE) to 7 to 20 percent less than integrated gasification combined cycle (IGCC) plants that can be built today and to less than a 35 percent increase in COE for pulverized coal power plants. Such high performance is possible because oxygen transport membranes can deliver oxygen for oxy-combustion with only 20 to 30 percent of the energy consumed by a cryogenic process. Praxair aims to develop a process for integrating OTMs into a power generation process such that coal-fired power plants with carbon dioxide capture have high efficiency and low COE while maintaining high environmental performance. A successful outcome of the project shall be an OTM-based oxy-combustion process evaluation that meets DOE goals for carbon dioxide capture and sequestration and laboratory-scale demonstration of OTM technology that meets commercial targets for oxygen flux, strength, and cost.

2. Program Tasks

2.1. Task 1: Process and Systems Engineering

The purpose of this task was to develop a process design and perform a techno-economic cost estimate of a coal-fired 550 MWe power plant with CCS utilizing OTM to enable oxy-combustion. The process developed during this task is identified as the Advanced Power Cycle (APC) concept. For a first-pass, the cost estimate was performed as a lumped estimate assuming an allocated cost per square foot of membrane area and applying that to all

units involving OTM including vessels, refractory, and process ducting/piping. Using this method, the potential benefits of the Advanced Power Cycle were quantified. As part of a Phase II effort, detailed designs and cost estimates were performed for pilot-scale OTM units (boiler and POx) to improve both technical and economic understanding of these reactors. The pilot-scale units were used as a basis to project scale-up costs to a commercial-scale power plant. A detailed understanding of the OTM units allowed for a much more accurate and higher confidence cost estimate of a commercial-scale OTM-based Advanced Power Cycle. Section 2.1.1 describes the design and cost estimate of the commercial scale power cycle. Section 2.1.2 describes the detailed design of pilot scale OTM boiler and POx units that were scaled up for the commercial scale design.

2.1.1. Subtask 1.1 Process and Systems Evaluation

There are three leading technology families which can be used in the power generating industry for carbon capture and sequestration (CCS) from power plants (in the relatively near term): pre-combustion (integrated gasification combined cycle, IGCC), oxy-combustion, and post-combustion capture (PCC). Praxair's Advanced Power Cycle concept represents a more efficient, although longer term, solution to CO_2 capture that relies on OTM (oxygen transport membranes) for oxy-combustion of a fuel. In conventional oxy-combustion, fuel is oxidized with a mixture of oxygen and recycled flue gases to mimic the boiler temperatures and heat transfer profile of an air-fired scenario. Oxygen is supplied from a cryogenic air separation unit (cryo-ASU); which is currently the lowest cost technology for large scale oxygen supply. The goal of OTM technology in an oxy-combustion application is to make a step-change reduction

in the parasitic power required for oxygen supply and thus achieve a step-change in efficiency improvement for a power plant.

The Advanced Power Cycle concept uses a coal gasifier to produce pressurized syngas which is then heated by oxy-combustion of syngas occurring on the OTM membranes. The hot syngas is expanded to produce a portion of the plant gross electric power. The resulting near-atmospheric pressure syngas is oxidized on the surface of the OTM membranes in the OTM boiler. As the syngas is combusted in the OTM boiler, heat is transferred to produce steam and the remaining power is produced using a steam turbine. The flue gas is roughly equivalent to conventional oxy-combustion flue gas (but with a slightly higher CO_2 concentration) and may be processed in the same manner for CO_2 purification and pressurization. Figure 1 shows a process flow diagram for the OTM Advanced Power Cycle.

Compared to other power generation processes enabling CCS (pre-combustion, post combustion, and oxy-combustion), the OTM cycle has an energy efficiency advantage because the power generation cycle contains several stages of high temperature expansion of syngas (Brayton cycle feature) in addition to a more conventional steam cycle (Rankine cycle feature). While this is similar to an IGCC cycle, the OTM-based cycle operates at an advantage to IGCC cycles with respect to the steam (Rankine) cycle because a higher pressure and temperature steam cycle can be used. In the Advanced Power Cycle fuel is oxy-combusted at atmospheric pressure and at around 1000°C in the boiler section.

In comparison to conventional oxy-combustion, much of the electrical parasitic load associated with a large cryo-ASU is avoided due to the low power consumption required of the OTM membrane system. Additionally, no flue gas recirculation is needed because the rate of fuel combustion and temperature is regulated by control of the OTM membranes. When using OTM membranes, the parasitic cost of oxygen production is essentially equal to the blower power needed to convey low-pressure air through the OTM membrane assemblies. This is, of course, substantially less than the compressor power used in a cryogenic air separation plant. However, cryogenic oxygen is still used in the Advanced Power Cycle. Gaseous oxygen is used in the coal gasifier, where the environment for OTM membranes would not be appropriate, as well as in a finishing combustor section of the boiler where low heating value fuel gases are inefficiently consumed by OTM membranes alone. With the use of OTM membranes, only 30% of the cryogenic oxygen required of a traditional oxy-combustion boiler is used representing an energy savings for oxygen production of ~70%. The flue gas is similar in composition to that from a conventional oxy-combustion power plant so in comparison to post-combustion capture technologies, there is no large thermal parasitic load associated with stripping CO_2 from an amine or other solution/absorbent.

The process mass and heat balance have been modeled with Aspen Plus™ and Thermoflow's Steam Pro™ product. Shaw Energy and Chemical employed in-house steam design know-how, quoted equipment costs, and Thermoflow's Peace™ software for cost estimation of the steam turbine system and calculation of convective heat transfer surface requirements, etc. A BGL gasifier was chosen for the APC due to its low specific oxygen consumption. BGL gasifier cost data was supplied by Allied Syngas and DOE reports while

cryo-ASU, OTM and CPU (CO_2 Processing Unit) capital cost was estimated by Praxair. In the first-pass cost estimate as part of the Phase I activity, a low incremental COE impact was obtained from the APC with a Warm-Gas Clean-Up desulfurizer, and an ultra-supercritical steam cycle for power generation. This case was chosen because it was the most economical configuration from the Phase I work with a commercially available steam cycle.

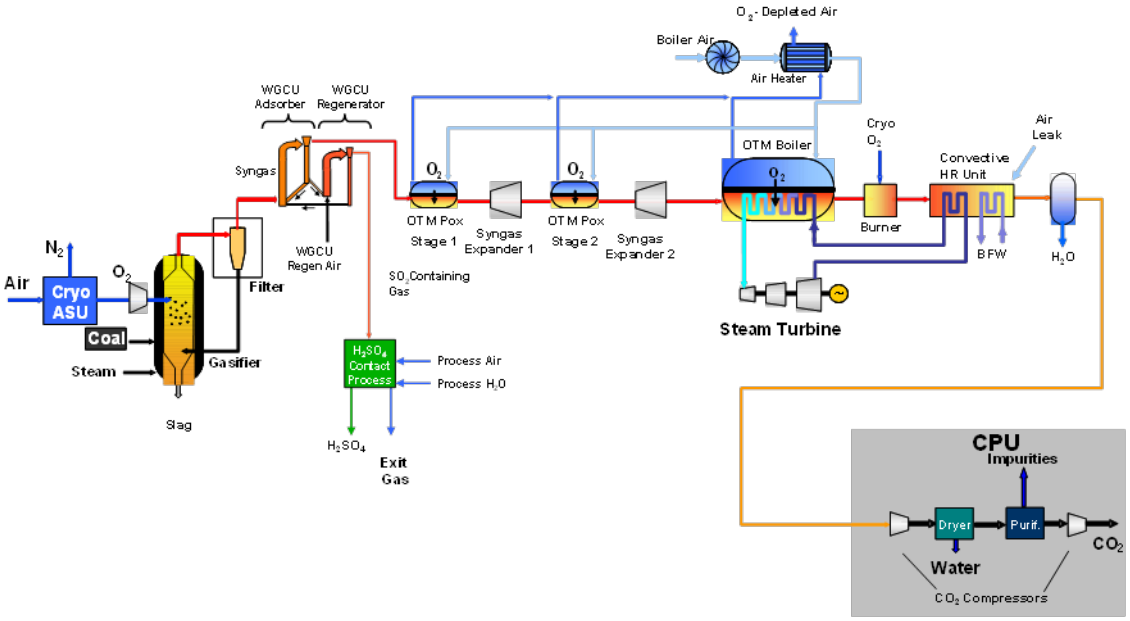

Figure 1 Advanced Power Cycle using WGCU technology for sulfur removal

Design Basis and Assumptions

A baseline OTM case has been analyzed with updated information obtained from the basic engineering design of the pilot-scale 7.5MWth OTM Boiler and 5 tpd O_2 capacity POx unit (see Section 2.1.2). Since the first expander in the cycle is currently not a commercially available unit, two alternate cases were considered that ease some of the requirements on the expander. The main case is a forward-looking estimate assuming the first expander could be developed. The steam cycle was modeled as an ultra-supercritical cycle. The sulfur recovery

process considered was a Warm Gas Clean Up (WGCU) option, using RTI's WGCU process, where sulfur species (H_2S and CO_S) are captured following the gasifier.

The steam cycle conditions are shown in Table 1. The ambient conditions and cooling water assumptions are shown in Table 2. Table 3 shows the assumed characteristics of the OTM-ASU and Table 4 shows the specifications for the CO_2 product.

Table 1: Steam Cycle Conditions

Steam Cycle Conditions	
Cycle	**Conditions**
Ultra- Supercritical (USC)	4050psi 1080/1100/1100F
Condenser Pressure	0.93psia 99.3F

Table 2: Ambient and Cooling Water Conditions

Ambient Conditions	
temperature	59F
ambient pressure	14.7psia
relative humidity	60%
cooling water supply temperature	66.5F
cooling water return temperature	94.5F

Table 3: OTM-ASU Operating Conditions

OTM-ASU Operating Conditions	
operating temperature	1832 F (1000^{o}C)
O_2 recovery	70%
pressure drop in air circuit (pressure rise across air fan)	5 psi
approach temperature in regenerative heater	95 F

Table 4: CO2 Product Specifications

CO2 Product Specifications	
CO_2 Purity	>95%
CO_2 Pressure	2000 psia

Coal Composition:

The coal composition for this study was taken to be the same as that used by the DOE in the report on "Pulverized Coal Oxycombustion Power Plants," (DOE/NETL-2007/1291).

Table 5: Coal Composition

Coal Characteristics: Illinois #6 Coal

Proximate Analysis	As Received (%)	Dry (%)
Moisture	11.12	
Volatile Matter	34.99	39.37
Ash	9.70	10.91
Fixed Carbon	44.19	49.72

Ultimate Analysis	As Received (%)	Dry (%)
Carbon	63.75	71.73
Hydrogen	4.50	5.06
Nitrogen	1.25	1.41
Sulfur	2.51	2.82
Chlorine	0.29	0.33
Ash	9.70	10.91
Moisture	11.12	
Oxygen	6.88	7.74

HHV (btu/lb)	11666	13126
LHV (btu/lb)	11252	12660

Capital Cost Estimation and COE Calculation Method:

The plant cost estimate basis for the OTM power cycle plant was taken to be from 2008 because much of the original baseline analysis was performed in 2008, and this was also the basis for the 2008 versions of Thermoflow's SteamPro™ and Peace™ software. Comparison

cases from the DOE's report on "Pulverized Coal Oxycombustion Power Plants," (DOE/NETL-2007/1291) were updated from their 2007 costing basis to match the 2008 costing basis.

The DOE's reported plant cost values were updated from 2007-dollars to 2008-dollars by scaling the plant capital values ($/kW) found in the DOE/NETL-2007/1291 reference report using data from the SteamPro™ and Peace™ software. The Air Pulverized Coal based power plant, (DOE Case 1 with no CO_2 capture), was first analyzed using the 2007 version of SteamPro™. Both the plant performance and the capital cost values agree well between the DOE reported values and the SteamPro™/Peace™ simulated values. After verifying good agreement, the same DOE reference plant (DOE's Case 1) was then simulated using the 2008 version of SteamPro™/Peace™ software and the capital plant cost in Q3/2008 dollars was taken as the basis for comparison going forward. Between 2007 and 2008 SteamPro/Peace predicted roughly a 22% escalation in capital cost. This 22% capital cost escalation was also applied to DOE's Case 3 (Air-Pulverized Coal with Post Combustion Capture) for comparison against the OTM cases.

From the estimated plant capital costs a 20 year levelized COE was estimated where COE was estimated using total plant capital (TPC), operating costs (OC), plant utilized capacity factor (CF), capital cost factors (CCF) and levelization factors as defined below:

$$COE = \frac{CCF\ \ TPC}{CF\ \ kWh} + \sum \frac{OC\ \ LF}{CF\ \ kWh}$$

$$CCF = \frac{17.5\%}{yr}\ (High\ Risk)\ or\ \frac{16.4\%}{yr}\ (Low\ Risk)$$

$$LF \sim 116\%\ (General)\ or\ 120\%\ (Coal)$$

$$kWh : annual\ kWh\ power\ generated\ at\ 100\%\ capacity\ factor$$

$$CF : Capacity\ Factor$$

$$OC : Operating\ Cost$$

A levelization factor of 120% is used for fuel costs, and 116% is used for all other operating expenses. These are similar to the factors used by the DOE in DOE/NETL-2007/1291. A 'low risk' capital cost factor of 16.4%/yr is used for the standard air blown pulverized coal power plant while a 'high risk' CCF of 17.5%/yr is used for high risk processes such as OTM cases and the post-combustion capture reference case. The methodology and factors used are consistent to that used by the DOE in DOE/NETL-2007/1291.

Variable and fixed labor costs were assumed to be 30 and 40 $/(kW-yr), respectively. Variable labor expense scales with capacity factor while fixed labor costs do not. A capacity factor of 90% was used for all cases because an assumption is made that the cost comparison is for an n^{th}-of-a-kind plant with proven reliability.

Consumable and labor operating costs are shown below in comparison to DOE assumptions. Operating costs include gypsum disposal, ash disposal, limestone cost, water expense, and makeup & water reagent costs.

Table 6: Power Cycle Operating Costs

		Praxair OTM	OxyCombustion Cases DOE Report (DOE/NETL-2007/1291)
Variable Labor Cost	$/(kw.yr)	30	17.88
Fixed Labor Cost	$/(kw.yr)	40	16.43
Gypsum Disposal	$/ton	10	-
Ash Disposal	$/ton	16	15.45
Limestone Cost	$/ton	20	20.6
Water Cost	$/kgal	1	1.03
Makeup & Water Treatment cost	$/yr	$1.5MM	~$2.0MM
CCF	%/yr	17.5	17.5
Coal Levelization Factor	%	120.00	120.22
General O&M Levelization Factor	%	116.00	116.51

Table 7: COE Comparison Basis

Power Cycle		Praxair Air-PC (2008 SteamPro)		Praxair Air-PC (2007 SteamPro)	DOE Air-PC DOE/NETL-2007/1291	
CO2 sequestration		NO	YES	NO	NO	YES
Net Efficiency (HHV)		39.7	27.2	39.6	39.5	27.2
Cost Basis (Year)		3/2008	3/2008	2007	1/2007	1/2007
Plant Cost ($/kW)		$1,908	$3,488	$1,560	$1,563	$2,857
	Coal Price ($/MMbtu)					
COE ($/MWh)	1.8	$70.5	$115.2	$63.6	$63.0	$110
	3.0	$82.9	$133.2	$76.0		
	4.0	$93.2	$148.3	$86.3		

This COE comparison was performed for $1.8/MMBTU coal as this is the coal price used in the referenced DOE report. Much of the analysis for this report was done in 2008 when the market price for coal was elevated. As a result COE was calculated for a range of coal prices from $1.8/MMBtu to $4/MMBtu. Going forward, the basis for comparison against DOE goals is shown in the left column of Table 7, which is the Praxair/SteamPro™ simulated Air-Pulverized Coal power plant case (with no carbon capture). The expected coal price was

generally taken to be $3/MMBtu for nominal comparison with OTM cases, again because this was the expected coal price in 2008.

Cost of CO2 removed and avoided

Cost of CO_2 removed/avoided is calculated using a similar method as compared to the DOE in DOE/NETL-2007/1291. The reference case used to calculate the costs of CO_2 removed and avoided is the Praxair calculated analog of Case 1 from DOE/NETL-2007/1291. An additional cost of $4/short-ton CO_2 is also included in the COE calculation of the sequestration case which is for CO_2 transport, storage and monitoring. The DOE oxy-combustion analysis presented in DOE/NETL-2007/1291 also assumes a penalty for CO_2 transport, storage and monitoring.

$$\text{Removal Cost} = \frac{COE_{with\ CCS} - COE_{w/o\ CCS}}{CO_2 Total_{with\ CCS} - Emissions_{with\ CCS}}$$

$$\text{Avoided Cost} = \frac{COE_{with\ CCS} - COE_{w/o\ CCS}}{Emissions_{w/o\ CCS} - Emissions_{with\ CCS}}$$

Process Description

BGL gasifier and candle filters

The overall OTM boiler process starts with an oxygen-blown BGL (British Gas-Lurgi) gasifier where O_2, coal, steam and limestone are used in the gasifier to produce syngas. The product syngas is filtered hot for removal of any entrained particulates. This process has been modeled using the BGL gasifier for coal to syngas conversion because this gasifier type is highly efficient and requires less specific oxygen and steam compared to other gasification

technologies. In typical BGL gasification applications, the syngas is quenched for tar, oil, and particulate removal before the gas is used for its ultimate purpose (synthetic fuels production etc.). In this project, hot syngas is advantageous (because any quenched syngas would otherwise have to be reheated) so it is assumed that candle filters and cyclone separators will facilitate the removal of any solid material from the raw syngas stream. It is also assumed that this filtered syngas can directly proceed on to the OTM POx unit operations where any small residual tars, oils,, etc. contained in the syngas stream will not pose a problem for the following syngas turbines or OTM membranes.

It is assumed that the gasifier coal feed lock system can be operated using the purified CO_2 product instead of air. A slipstream of purified CO_2 is extracted from the CPU pure product compression train and recycled back to the gasifier for use in the gasifier coal delivery system.

In addition to steam, coal, cryo-ASU derived O_2, and coal delivery gas, the gasifier is also operated with some other feeds as indicated in EPRI BGL gasification reports. This includes limestone (as a fluxing agent) and a small flow of natural gas and air used in the gasifier's tuyere system. These minor feeds were also included in the mass and energy balance simulation of the Advanced Power Cycle system as well as in the economic analysis which includes limestone and natural gas expense.

Gasifier performance data was provided by Allied Syngas and through EPRI reports on the BGL gasification process. The system in this application includes 5 gasifiers with a single

spare. The nominal capacity of each gasifier is 1100 tpd of coal which is consistent with the Schwartz-Pumpe BGL gasifier capacity.

Syngas Turbines

Immediately following the gasifier and filter arrangement the syngas flows to a pressurized OTM POx unit where OTM membranes combust only enough syngas to raise the temperature to 900°C. The syngas is then expanded to an intermediate pressure and flows through another OTM POx heating stage, which again combusts only enough syngas to heat the stream to 930°C. The pressurized syngas then flows through the second syngas turbine and is expanded to near atmospheric pressure. Two expansion/POx stages, rather than one, are used to improve the efficiency of the overall Advanced Power Cycle. In this arrangement the OTM POx unit operation is essentially a substitute for the combustor in a similar-in-principle gas turbine system. One modification made during Phase II was to utilize a syngas slip-stream approach for the OTM fuel in the two POx stages. In the slip-stream approach, low pressure syngas from the outlet of the second expander is rerouted as feed for the OTM membranes in the POx units where it is used as the fuel for combustion on the OTM membranes. Heat from the oxy-combustion of the fuel is coupled to the high pressure syngas in a radiant section where heat released from the OTM surface is absorbed by metal tubes containing the high pressure syngas. This allows the ceramic membranes to be operated at low pressure while still heating a high pressure syngas stream ahead of the expanders. This approach allows for lower capital expenditures in the POx units as well overcoming issues with OTM and seal material integrity at high pressure and temperature. See Figure 2 for a diagram of the slip stream approach.

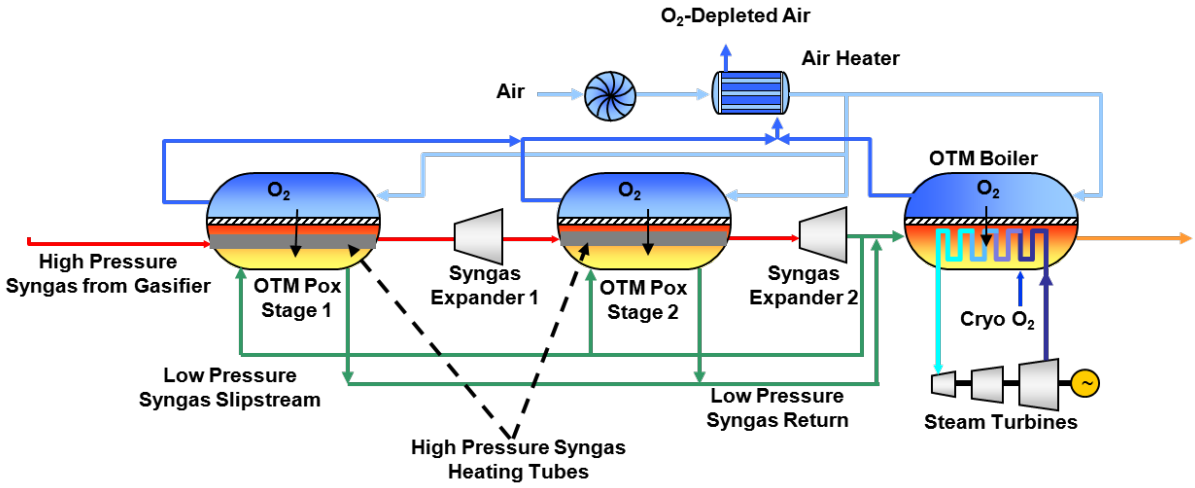

Figure 2: Slip-stream configuration for POx units

Currently the syngas expansion turbine is not a commercially available device because there is no existing market for this equipment. However, Florida Turbine Technologies (FTT) was contracted to do a feasibility study on the syngas expanders. FTT specializes in retrofitting existing industrial gas turbines (IGT) by removing the compressor section and utilizing only the expander portion of the IGT. Based on the study, FTT states: "In conclusion, OTM Syngas driven turbines are aerodynamically and structurally consistent with existing IGT technologies and therefore feasible."

In the Advanced Power Cycle concept, the expansion power of each turbine unit is similar to that of a GE Frame 5 Gas Turbine. Expansion performance end efficiency was estimated from the FTT study to be 85% for the first POx stage and 92% for the second POx stage.

Boiler (Excluding OTM), Feedwater Heaters (FWH) &Latent Heat Recovery

The non-standard OTM boiler arrangement differs significantly from the waterwall (or Benson type once-through boiler) radiative and convective sections in a standard pulverized coal or CFB power plant. A conventional Pulverized Coal boiler has a relatively standard arrangement of both convective and radiative heat transfer surface area. Figure 3 depicts a boiler temperature enthalpy diagram for a typical air-blown pulverized coal power plant. In this diagram the upper line (red) represents the flue gas stream cooling from right to left. As the flue gas cools this energy is used to heat water/steam (blue lines) in various radiative and convective heat exchangers including (from right to left) the 'waterwall', radiative superheater, convective superheater (CS2), convective reheater (CR2), convective superheater (CS1), convective reheater (CR1), economizer (ECO1) and lastly the air preheater. The waterwall and radiative superheater are in the same firebox section of the boiler.

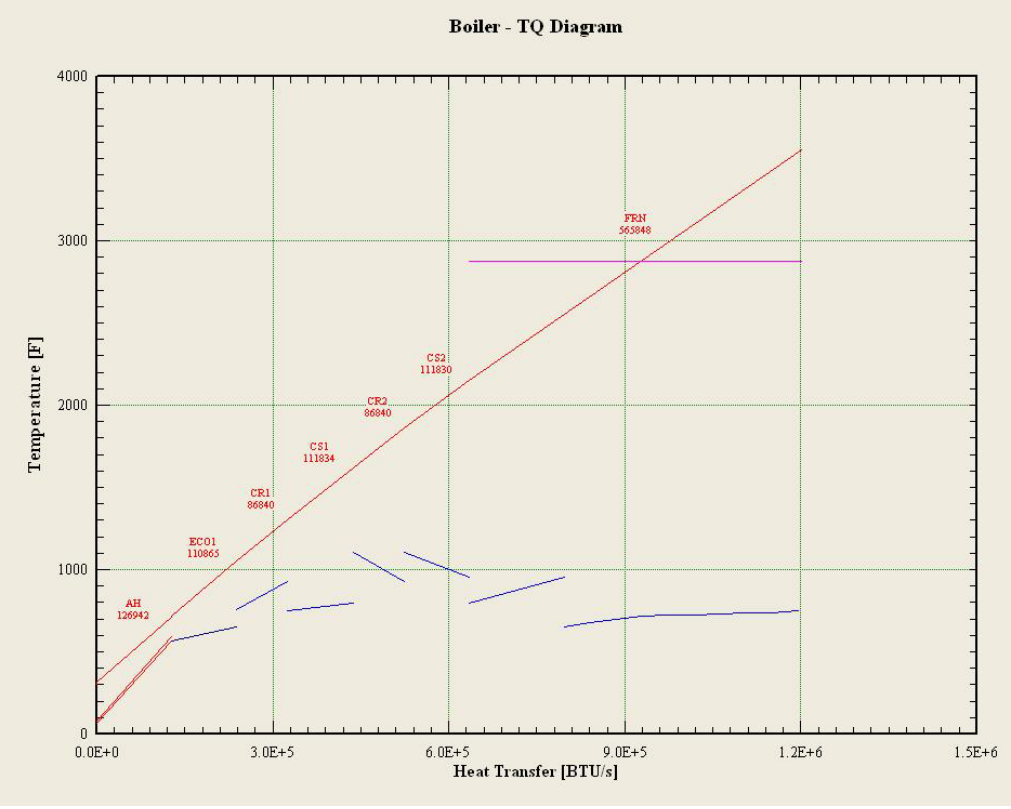

Figure 3: Temperature duty diagram for a traditional pulverized coal power plant

In this modern arrangement of boiler heat transfer surface area, the boiler feedwater is separately heated by steam extraction from various stages of the steam turbine. Figure 4 shows a temperature enthalpy diagram for the boiler feedwater train from a typical pulverized coal power cycle (air based combustion). The diagram shows boiler feedwater being heated (from right to left in blue) in 9 stages against extracted steam (magenta lines). Once heated to roughly 600°F the preheated boiler feedwater flows to the boiler's economizer and on to other convective and radiative heat transfer sections.

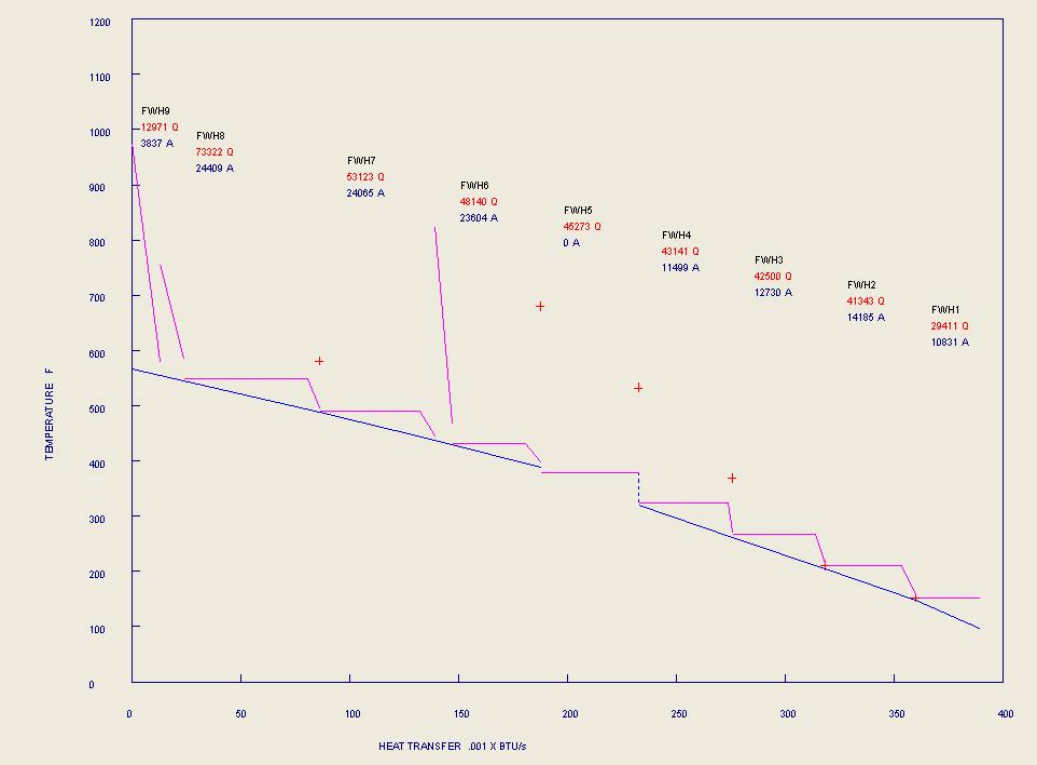

Figure 4: Temperature duty diagram for a boiler feedwater preheat system in a traditional PC Power Plant

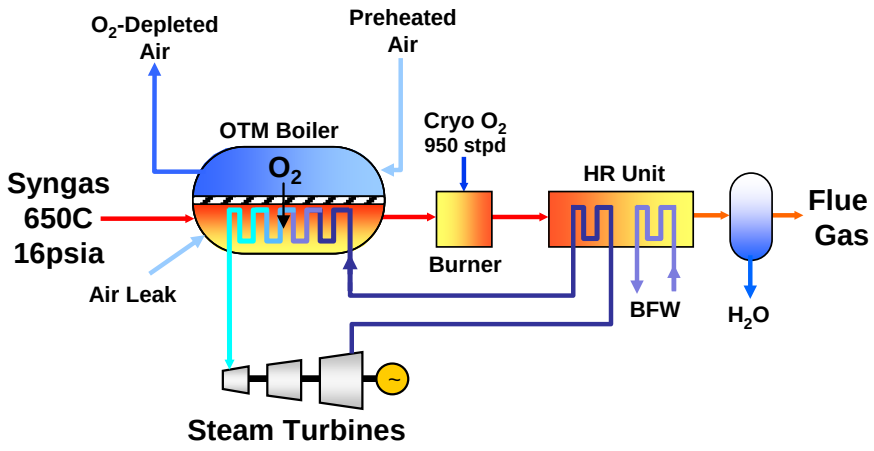

Figure 5: OTM boiler detail

Compared to the standard arrangement boiler and feedwater heat transfer surface, shown above in Figure 3 and Figure 4, the utility scale OTM system will have a different arrangement of heat transfer surface area because the OTM boiler system has a non-standard temperature profile. The operating temperature of the OTM boiler itself will be around 1000°C (1832°F). Following the OTM boiler, a gas phase O_2 combustor is used to combust the remaining syngas using cryogenically supplied oxygen. Here the temperature will increase above 1000°C. Following the gas phase combustor the flue gas is cooled by convective heat transfer and energy is transferred to high pressure water/steam as well as to low pressure boiler feedwater preheaters. See Figure 5 for a schematic of the OTM boiler including the supplemental combustor and heat recovery unit. The absence of a traditional air preheater in this OTM system means that additional energy is available to supplement the preheating of boiler feed water. Figure 6 shows a representative temperature enthalpy diagram for the OTM boiler system.

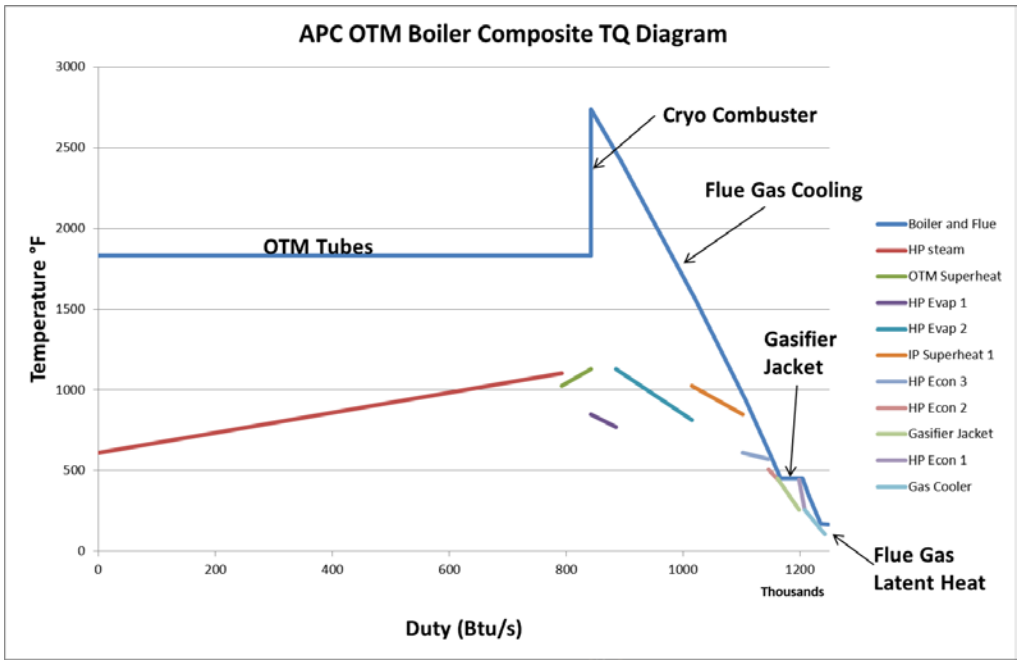

Figure 6: Representative temperature enthalpy diagram for the Advanced Power Cycle

The boiler Syngas/Flue gas stream is indicated by the top blue line and flows from left to right. The syngas first enters the OTM boiler and is heated to 1832°F/1000°C (preheat not shown on figure) via syngas combustion on the OTM surface. Once the syngas reaches 1832°F (1000°C) it continues to be combusted in the OTM boiler while energy is removed via heat transfer to steam. In the OTM boiler section, energy is transferred to steam heaters, superheater, and reheaters. In this entire section the radiant temperature is maintained at around 1832°F because this is the nominal operating temperature of the OTM tubes.

Following the last section of OTM tubes some syngas still remains in the gas stream (5-20%) because at low fuel heating value, the oxygen transport across the membrane starts to diminish, and hence it is uneconomical to attempt to combust all the syngas with OTM

membrane area alone. Cryogenically supplied oxygen is used here to combust the remaining syngas, and the flue gas temperature after the burner is increased due to this combustion (to roughly 2500°F). The flue gas is cooled first by radiative heat transfer and then via convective heat transfer against high pressure water in a section analogous to a standard economizer. Enough excess cryogenically supplied oxygen is used in the supplemental combustor to give a 1.2 mol% oxygen excess (wet basis) in the flue gas leaving the heat recovery section that follows the supplemental combustor.

Once the flue gas has cooled to sub-economizer temperatures the flue gas continues to cool against low pressure boiler feedwater (BFW). Due to the high moisture level in the flue gas some flue gas latent heat is transferable to the boiler feedwater stream. Some amount of moderate/low level energy is also available from the gasifier system because BGL gasifiers are operated with a water jacket. This gasifier energy is also used for BFW preheat. The remaining latent heat is transferred to the cooling water system and rejected to the environment.

In all cases the sensible flue gas energy, the recoverable flue gas latent heat, and the gasifier steam jacket energy is enough to completely heat the boiler feedwater from the condenser outlet temperature to the temperature needed to enter the BFW deareator (about 300°F).

Steam Turbine, Condensers, Cooling Tower, Pumps, Tanks

Steam turbine and condenser performance is estimated using the Thermoflex SteamPro™ software. The software estimates the performance of individual steam turbine

stages (including the boiler feed pump turbine), the steam seal system and steam turbine leakage. The SteamPro™ simulation also incorporates steam extractions used to drive compression in the cryo-ASU and CPU.

The steam turbine condenser pressure is held at 0.93 psia (99.32°F) and the condensed boiler feed water returns to the boiler feedwater preheat train. The condenser energy is rejected to a mechanical draft cooling tower. SteamPro™ calculates the power required for the mechanical draft cooling tower as well as for the cooling water forwarding pump. The SteamPro™-simulated cooling water system also takes into account the cooling water needed for flue gas latent heat condensation as well as the cooling water required for the cryo-ASU and CPU islands. Other miscellaneous steam/water pumps, tanks, etc. are included in the SteamPro™ peace simulation such as the condenser forwarding pump, FWH condensate forwarding pump, etc.

WGCU

The base case for the Phase II study was the Warm Gas Clean Up process (WGCU) used for H_2S and COS control following the gasifier and before the syngas flows to the first OTM Pox unit.

WGCU is a continuous process developed by RTI for removal of H_2S and COS from gas streams using a solid regenerable sorbent. In the WGCU unit syngas is processed immediately following the gasifier and candle filters at a temperature of about 1000°F and a pressure of about 340 psia. The process involves contact of the syngas with a solid metal oxide sorbent. The H_2S and COS in the gas stream react with recirculating solid metal oxide sorbent, typically

ZnO, forming metal sulfide, typically ZnS. This reaction occurs in the absorber portion of the WGCU unit. The solid sorbent continually circulates in the absorber portion of the WGCU unit.

A portion of the solid sorbent is continually withdrawn from the absorber, regenerated and re-introduced back to the absorber. In the regenerator portion of the WGCU process the spent solid sorbent is regenerated with air at near atmospheric pressure, producing ZnO and a SOx containing gas stream. The regenerated sorbent is then returned to the absorber portion of the WGCU unit while the SOx containing gas stream is processed for SOx control. The concentrated SOx containing gas stream has a significantly smaller molar flow rate as compared to the raw syngas flow or the eventual flue gas flow and is therefore easier to process for control of sulfur emissions.

The SOx containing regenerator off-gas stream has a high concentration of SOx, >10mol%, and can be treated for removal of SOx in different ways: 1) SOx can be further processed (oxidized) using the contact sulfuric acid process for recovery of the SOx as concentrated, potentially saleable, sulfuric acid (this is the method assumed in this report), 2) alternatively SOx can be reduced to elemental sulfur using a slipstream of cleaned syngas in a modified Claus process.

The SOx concentration in the regenerator off-gas stream is in the concentration range typically applicable for use in the contact process for conversion to H_2SO_4. As mentioned the alternative disposition of the sulfur in this gas stream is for conversion to elemental sulfur,

however this method is disadvantaged and not used in this report because using this method requires a considerable slip stream of cleaned syngas (roughly 2% of the total syngas in the case of high sulfur Illinois coal) would be needed. The use of a syngas slip-stream will reduce the efficiency of the overall power cycle, by roughly 2%, and will also reduce the carbon capture efficiency of the process by roughly 2% due to the carbon loss in the slip-stream.

Cryogenic ASU

A cryogenic ASU is used to supply gaseous oxygen to the gasifier and the supplemental combustor. The oxygen purity delivered by the ASU is 95.5mol% oxygen. The cryogenic ASU design is assumed to be that of a currently commercially realizable low purity, low pressure ASU. The portion of the cryogenically supplied O_2 going to the gasifier is compressed to 517 psia in a 5 stage compression train with each stage having 80% polytropic efficiency and 98% mechanical efficiency. This cryogenically supplied oxygen accounts for roughly 33% of the total oxygen consumed by the process (with the other 67% supplied using OTM membranes). ASU power and utilities (regenerated steam, cooling water, and auxiliary electrical power) are estimated by Praxair. It should be emphasized that the ASU specific power assumption is for a commercially realizable ASU design in 2008. As research continues on large scale, low purity ASU concepts, significant specific power and capital reductions are being made. Going forward these advances will further reduce the Cryo-ASU parasitic power demand and capital requirement.

OTM ASU (w/ air preheat, air fans/motors)

The OTM-ASU consists of air fans, air preheaters as well as the OTM-POX and OTM boiler unit operations that contain the actual OTM tubes. The OTM tube consists of two principle components: a porous support combined with a dense gas separation layer. The porous support provides mechanical strength to the OTM system. The dense gas separation layer facilitates the reduction of molecular oxygen (O_2) to oxygen ions (O^{2-}) on the surface of the air side of the OTM, the oxidation of fuel species on the surface of the fuel-side of the OTM, and transport of oxygen ions through the bulk of the membrane while preventing molecules in the air and fuel from crossing the membrane.

Praxair's OTM membranes are placed directly inside the boiler or partial oxidation unit operations where oxygen is consumed on the fuel-side of the membrane, where syngas is being oxidized. Because the combustion reaction occurs on the surface of the membrane, an extremely low oxygen partial pressure is achieved. A driving force for oxygen ion transport from the air-side to the fuel-side of the OTM membrane is established because air has a much higher oxygen partial pressure.

As air flows along the surface of the OTM tubes the air becomes depleted of oxygen. It is assumed that 70% of the air-side oxygen is transferred across the membrane for combustion with the remaining oxygen leaving in the O_2-depleted air stream. Hot oxygen-depleted air leaving the OTM tubes is used to preheat the air entering the OTM tubes, via a regenerative air preheater.

OTM POX

The first of two OTM POx units are located immediately after the WGCU sulfur removal process for all three cases. In all cases the second OTM POx unit is located after the first syngas expander. The purpose of the OTM POx units are to combust enough of the syngas to raise the gas temperature to >900°C. The OTM POx units consist of OTM tubes where O_2 from the air feed is separated and transported to the permeate side of the tube. The O_2 reacts with the low pressure slip-stream fuel to produce heat. The heat is radiated to metallic tubes that contain the high pressure syngas that is fed to the expanders. This low pressure slip-stream approach allows for the OTM tubes to operate at low pressure on both sides of the membranes which decreases costs and minimizes risk associated with operating a ceramic material under high pressure gradients. Detailed designs for the POx units are given in section 2.1.2

OTM Boiler

Following the second expander, the still mostly un-oxidized syngas flows to the OTM boiler where OTM tubes are used for combustion of up to 95% of the original syngas. In the OTM boiler, steam tubes are also arranged for removal of energy needed to keep the gas and OTM surface temperature at around 1000°C. The degree of syngas combustion via OTM membranes is an important optimization variable. Depending on OTM flux and OTM "cost allocation," 70-95% of the total syngas is combusted on the OTM membranes with the majority of the syngas combustion occurring in the OTM boiler.

Syngas flowing through the OTM boiler is combusted at atmospheric pressure and steam is used to remove energy. A non-traditional boiler arrangement will be required in order to

accommodate both the OTM surface and the steam tube surface. The section of the boiler containing OTM tubes should be maintained at between 900°C and 1100°C for optimal OTM performance. The OTM operating temperature was modeled as 1000°C for the purpose of this report. Detailed designs for the boiler are given in section 2.1.2

OTM Air Preheater

In the Advanced Power Cycle concept no standard flue gas-to-air preheater exists because air preheat/cooling for the OTM air is handled separately in a regenerative heat exchanger. The regenerator could be any type of thermal regenerator that uses a high temperature capable medium to store and transfer heat. One example of currently available technology at this scale is a fixed bed regenerator. The fixed bed regenerative heater concept is similar to that of a cyclically operated blast furnace stove (iron ore refining) where solid ceramic media is used to store and transfer thermal energy between gas streams. This type of air preheater was chosen over other types of air preheaters because 1) 1000°C temperature is within the current ability of such a heater (some modern hot blast stoves run at temperatures in excess of 1250C), 2) blast furnace stoves can be constructed at the large scale that would be required in this application and 3) regenerative heat exchangers offer some of the highest thermal efficiencies of available heat transfer equipment. Future applications could also use other types of regenerators such as rotating regenerators that use a rotating ceramic matrix to transfer the heat from the hot air to cold air streams.

Because air can be supplied to all OTM membranes at the same pressure, all of the air preheat can be integrated to a single system of regenerators. In other words, it is assumed that

separate air preheaters will not be necessary for each OTM POx stage and for the OTM boiler. The OTM air preheat system includes the fans and motors needed to convey air through the air preheater and OTM modules. A 5 psi pressure rise through the OTM air fan is assumed with an isentropic fan efficiency of 75% and mechanical efficiency of 95%.

CPU

The purpose of the Carbon Dioxide Processing Unit (CPU) is for compression and purification of the flue gas to a CO_2 product appropriate for sequestration. The CPU takes the flue gas following the latent heat removal operation. Flue gas is compressed to roughly 375 psi where it is treated for removal of mercury, water and some acid gases before the flue gas enters an auto-refrigerative process for inert removal. The raw flue gas is compressed in a 5 stage compression train with an average stage polytropic efficiency of ~85% and a mechanical efficiency of 98.5%.

In the auto-refrigerative process CO_2 is purified to a >95% CO_2 product with >97% recovery of CO_2. The cryogenic process also produces a vent stream which is enriched in atmospheric gases (N_2, O_2, Ar). Following the cryogenic portion of the CPU, the purified CO_2 stream is further compressed to 2000 psi. The purified CO_2 is compressed in a multistage compressor train having an average stage efficiency of 77% polytropic and a 98.5% mechanical efficiency. CPU auxiliaries include electricity for compressor operation, electricity for chiller operation, steam for dryer bed regeneration, and cooling water utility for intercooler/aftercooler duty.

Major Equipment Capital Cost Estimation

BGL gasifier and candle filters

BGL gasifier costs were estimated by costing data provided by Allied Syngas. In early 2009 the estimated BGL gasifier costs were evaluated against gasifier costs in DOE reports for IGCC systems. The BGL gasifier costs were shown to be in-line with gasifier costs reported in DOE report DOE/NETL-2007/1281 the gasifier cost estimate is around $450/kw which is in-line with other large scale gasifier systems not including the gas cleanup system. For all cases the gasifier cost is equivalent because the assumption is that in each case 5 gasifiers will be used plus one spare. Candle filter cost was estimated as roughly $1MM equipment cost per 1000 tpd coal usage. DOE/NETL-2007/1281 did not specifically separate cyclone/candle filter cost for the ConocoPhillips gasifier. The particulate removal equipment was estimated as roughly 5% of the "Gasifier, Syngas Cooler & Auxiliaries" equipment cost, which corresponds to roughly $1MM/1000tpd coal.

Syngas Turbines

The Syngas turbine cost was estimated to be the same as an entire GE Frame 5 Gas Turbine, with gas turbine cost data taken from the 2008 version of Thermoflex's GTPro™ and Peace™ software packages. In addition, equipment cost was increased by 50% based on the research and recommendation given in the report by Clean Energy Systems – 'Advanced Turbine Development for Pressurized Oxy-Combustion Commercial Scale-up'. (25 October 2011). This cost estimate is supported by the work carried out by Clean Power Systems, Inc., Florida Turbine Technologies, Inc and Siemens Power Generation, Inc. in their study 'Adapting

Gas Turbines to Zero Emissions Oxy-Fuel Power Plants.' The cost basis for the Advanced Power Cycle power plant was assumed to be for an n^{th}-of-a-kind plant so the development costs associated with this type of equipment were not included.

Steam Cycle Equipment

The SteamPro™/Peace™ software estimates the performance and cost for each heat exchanger of a typical power plant. The SteamPro™/Peace™ software estimates the area of each heat exchanger using the heat exchanger duty, LMTD, and calculated average heat transfer coefficient. Additionally SteamPro™/Peace™ generates a heat exchanger cost and an approximate heat exchanger weight.

Costs for the boiler feedwater heaters are estimated using SteamPro™ and Peace™ software. Low temperature boiler feedwater preheat is achieved through heat transfer against cooling flue gas. The cost of the heat transfer surface is estimated as expanded economizer surface relative to the SteamPro™/Peace™ economizer estimated cost, subject to the duty and LMTD of the heat exchanged. The cost of the latent heat recovery heat exchanger was estimated to be roughly the same per unit of exchanger duty compared to the low temperature economizer heat exchanger.

The cost of the higher temperature boiler feedwater preheaters including the deaerator and high pressure boiler feedwater preheaters (following the boiler feed pump turbine) are estimated directly by SteamPro™ and Peace™ software.

Steam turbine cost is estimated using the SteamPro™ and Peace™ software. It is assumed that SteamPro™ and Peace™ make reasonable assumptions for relative steam turbine price in the Ultra-Supercritical case. The cost of the boiler feedwater pump and boiler feed pump turbine are also estimated using information from the SteamPro™ and Peace™ software. The cooling system costs are taken from SteamPro™ and Peace™. This includes costs for the steam turbine condenser, boiler feedpump condenser, cooling towers, cooling water forwarding pump, cooling water piping, etc.

WGCU

Costs for the WGCU unit were taken from the DOE's 2008 report on current and future gasification technologies (DOE/NETL-2008/1337) which included a cost estimate for the WGCU process. Costs for the Contact Process plant used to convert SOx to H_2SO_4, was taken from a sulfuric acid technology textbook. Although the byproduct H_2SO_4 could be potentially sold in the H_2SO_4 market, no benefit (or disposal cost) was assumed for getting rid of the sulfuric acid byproduct. The sale price for sulfuric acid depends on geographical factors, acid purity, acid flow rate, etc and a net acid price of $0/ton is a conservative assumption. Even with a $0 sale price for acid the WGCU cases show a slight advantage over the FGD cases in terms of COE because there is no FGD limestone expense or FGD waste stream disposal expense.

Cryogenic ASU

Cryogenic ASU capital costs are estimated internally by Praxair. The Cryo-ASU costs were based on recently completed feasibility studies for 500+MW oxy-coal plants.

OTM Boiler and POX Units (w/ air preheat, air fans/motors, fired heater, burners)

There is still uncertainty regarding the OTM manufacturing, sealing, manifolding and installation cost, hence a "cost allocation" is used. The OTM "cost allocation" accounts for the installed cost of the OTM membranes in the OTM-POx and OTM-boiler units, which includes:

- Manufacturing the membrane surface
- Installing the OTM surface inside the OTM-POx and OTM boiler units

The Advanced Power Cycle OTM "cost allocation" range is not given here as Praxair internal numbers were used. The manifolds, reactor shell and other internals were estimated by Shaw.

The OTM/ POx pressure modules (minus the OTM tubes) are estimated as a scale-up from the pilot scale design that was engineered and cost-estimated by Shaw. Similarly the burners, fired heater with ID Fans for combustion completion, and the air blower /compressors were estimated by scaling from the pilot plant design study. See section2.1.2 for details of this study.

The air regenerative heat exchanger cost was estimated by scaling a quote for a smaller scale rotating ceramic regenerator. The scaling only made sense to a certain size and so 40 smaller parallel units were considered for the study. As will be seen, this fits in well with the modular approach for constructing the OTM boiler and POx units.

CPU

CPU cost has been determined by Praxair and includes the raw CO_2 compressors/motors, dryer beds, mercury removal, coldbox purification cycle, and purified CO_2 compressors/motors. The CPU costs were based on recently completed feasibility studies for 500+ MW oxy-coal plants.

Results

OTM Boiler with varying configurations of POx units and expanders:

Cases 1,2 and 3 are cases where the configuration of the expanders and POx units are considered. Case 1 is the base case with 2 expanders and 2 POx units. Case 2 adds an additional expander upstream of the first POx unit and case 3 considers only 1 POx unit and 2 expanders. The three cases use the same steam conditions defined previously. Refer to Figure 7 for the process schematic applying to the base case with 2 expanders and 2 POx units. In each of these cases the OTM membranes are used to combust 90% of the syngas. The remaining portion of syngas is combusted using cryogenically supplied oxygen.

The OTM flux values used in this analysis is taken from actual laboratory-measured flux performance of Praxair's advanced material OTM tubes.

Table 8: Case List

Case No.	Gasifier Type	OTM POx Units	Expander Units	Steam Conditions	OTM Fuel Combustion	OTM Type	SRU	CO2 Purification	Suppl. Comb. Oxidant Source	Air Leak	Flue Gas Recycle
1	BGL	2	2	USC	90%	Tube	WGCU	Yes	CryoASU	3%	No
2	BGL	2	3	USC	90%	Tube	WGCU	Yes	CryoASU	3%	No
3	BGL	1	2	USC	90%	Tube	WGCU	Yes	CryoASU	3%	No

For each of the three cases (Case 1, Case 2, and Case 3) the following performance information is given in Table 9 to Table 20:

- Stream Summary Table (corresponding to stream numbering in Table 9)
- Performance Summary
- Capital Cost Summary
- Cost of Electricity breakdown for a coal price of $3/MMBtu

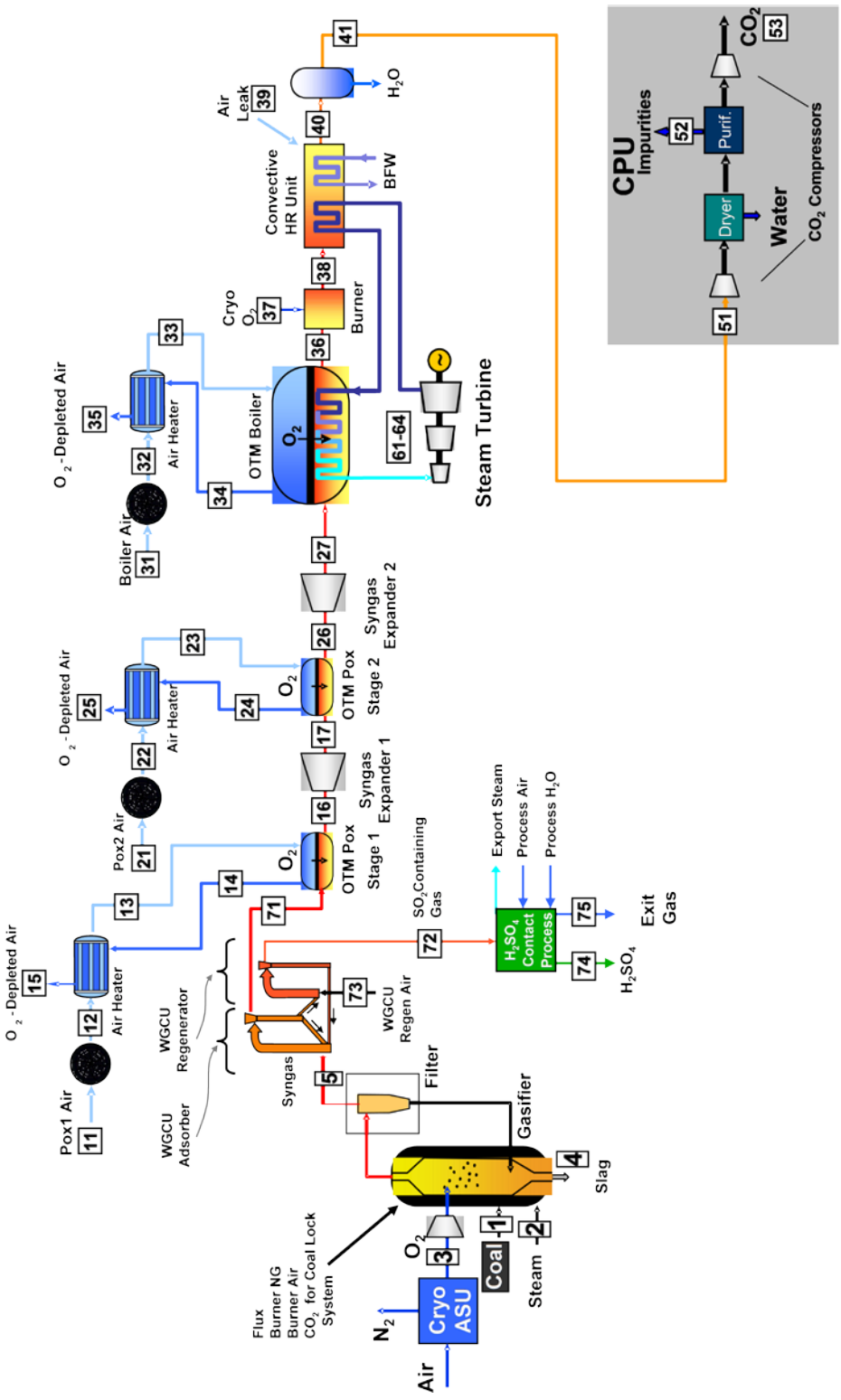

Figure 7: Advanced Power Cycle with WGCU and Sulfur containment

Table 9: Case 1 Stream Summary

	Stream	Coal	Gasifier Steam	Gasifier Cryo O2	Gasifier Slag	Gasifier Syngas	Pox 1 Air	Pox 1 Warm Air	Pox 1 Hot O2 Depleted	Pox 1 Cold O2 Depleted	Pox 1 Hot Syngas	Pox 2 Warm Syngas	Pox 2 Air	Pox 2 Warm Air
Stream #		1	2	3	4	5	11	13	14	15	16	17	21	22	23
Temperature	F	77	680	246	500	1000	59	1521	1832	150	1650	1266	59	119	1521
Pressure	psia	396.0	510.0	517.0	396.0	340.0	14.7	18.7	18.7	17.7	335.3	119.5	14.7	19.7	18.7
Flow	k lb/hr	427.5	124.1	215.3	47.6	778.6	181.1	181.1	146.4	146.4	766.5	766.5	125.6	125.6	125.6
Flow	lbmol/hr	-	6,889	6,696	-	38,849	6,275	6,275	5,190	5,190	38,515	38,515	4,354	4,354	4,354
Composition															
H2	mol%					30.0%					30.0%	30.0%			
CO	mol%					50.0%					51.0%	51.0%			
CH4	mol%					3.0%					3.0%	3.0%			
CO2	mol%					4.0%					4.0%	4.0%			
WATER	mol%		100.0%			9.0%	1.00%	1.00%	1.0%	1.0%	9.0%	9.0%	1.0%	1.0%	1.0%
OXYGEN	mol%			95.0%			21.00%	21.00%	4.0%	4.0%			21.0%	21.0%	21.0%
N2+AR	mol%			5.0%		2.0%	78.00%	78.00%	94.0%	94.0%	2.0%	2.0%	78.0%	78.0%	78.0%
H2S	mol%					1.0%									
SOx	mol%														
Solids	k lb/hr	427.5			47.6										

	Pox 2 Hot O2 Depleted	Pox 2 Cold O2 Depleted	Pox 2 Hot Syngas	Boiler Syngas	OTM Boiler Air	OTM Boiler Air	OTM Boiler Warm Air	OTM Boiler Hot O2 Depleted	OTM Boiler Cold O2 Depleted	Residual Syngas	Cryo O2 for Boiler	Hot Flue Gas	Air Leak	Warm Flue Gas	Cold Flue Gas	Lime-Stone	FGD Solids	Flue Gas to CPU	Syngas to 1st Expander
Stream #	24	25	26	27	31	32	33	34	35	36	37	38	39	40	41			51	71
Temperature	1832	150	1700	1317	59	119	1489	1832	150	1563	80	2738	77	365	120			120	1010
Pressure	18.7	17.7	106.3	38.9	14.7	19.7	18.7	18.7	17.7	17.2	17.0	17.0	15.0	15.0	14.0			14.0	340.0
Flow	101.6	101.6	766.5	766.5	2270.9	2270.9	2270.9	1791.1	1791.1	1305.0	115.8	1420.9	27.1	1448.0	1163.8			1163.8	766.5
Flow	3,602	3,602	38,515	38,515	78,227	78,227	78,227	63,234	63,234	42,640	3,595	43,687	936	44,624	28,849			28,849	38,515
Composition																			
H2			30.0%	30.0%						5.0%									30.0%
CO			51.0%	51.0%						8.0%									51.0%
CH4			3.0%	3.0%						1.0%									3.0%
CO2			4.0%	4.0%						48.0%		54.0%		53.0%	82.0%			82.0%	4.0%
WATER	1.0%	1.0%	9.0%	9.0%	1.0%	1.0%	1.0%	1.0%	1.0%	38.0%		43.0%		42.0%	11.0%			11.0%	9.0%
OXYGEN	4.0%	4.0%			23.0%	23.0%	23.0%	5.0%	5.0%		95.0%	1.0%	21.0%	1.0%	2.0%			2.0%	
N2+AR	94.0%	94.0%	2.0%	2.0%	76.0%	76.0%	76.0%	95.0%	95.0%	1.0%	5.0%	2.0%	79.0%	4.0%	5.0%			5.0%	2.0%
H2S																			
SOx																			
Solids																			

Table 10: Case 1 power, industrial gas and environmental performance summary

Power Production	
Steam Cycle (MW)	623.98
Expander 1	37.71
Expander 2	37.71
TOTAL GROSS POWER (MW)	**699.40**
Aux Load	
Cryo ASU	45.59
CO2 Compression/Purification	54.15
OTM ASU	11.49
Boiler Fuel Delivery	0.92
Flue Gas Desulfurization	0.00
Condenser Circulation Pump	3.74
Cooling Fan Tower	3.04
Condensate Pump	6.55
Additional Auxiliaries	5.17
Misc. Plant Auxiliaries	2.81
WGCU & DRSP	5.73
Gas Liquor Separation	2.69
Gas Liquor Treatment	0
TOTAL AUX LOAD (MW)	**141.88**
Net Power (MW)	**557.5**
Net Efficiency (%HHV)	**38.15%**
Coal Rate (tpd)	**5130**
Industrial Gases	
O2 Cryogenic ASU (tpd)	3974
O2 OTM ASU (tpd)	6462
CO2 Captured (tpd)	11806
CO2 Emissions (tpd)	687
CO2 Capture Efficiency (%)	97.1%
CO2 Purity (%)	95.8%

Table 11: Case 1 Capital Cost

Case 1: Captital Cost	Equipment Costs	Installation Costs	Bare Erected Cost	Eng'g Fee, EPC Profit	Contingency	Total	$/kw
Gasifier Costs			190,216,000	15,707,000	39,468,000	245,391,000	440.15
Candle Filter	5,034,000	3,524,000	8,558,000	856,000	1,712,000	11,126,000	19.96
Syngas Turbines	49,740,000	34,818,000	84,558,000	8,455,800	5,580,828	98,594,628	176.85
Steam Cycle-incl Cooling Towers	203,214,453	345,805,287	549,019,740	60,759,000	30,488,937	640,267,677	1,148.42
WGCU and Sulfur Recovery						159,355,000	285.83
Cryogenic ASU						116,774,000	209.45
OTM Boiler and POX units	309,050,433	216,335,303	525,385,736	51,325,119	51,325,119	628,035,974	1,126.48
CPU						170,031,000	304.98
					TOTAL	$ 2,069,575,279	3,712.11

* Does not include "Owners Costs," transportation costs, permit fees, owners CM expenses, owners contingency, escalation during construction, etc

Table 12: Case 1 COE Estimate

Case 1 COE Calculation				
Net Power Produced		**557.5**	**MW**	
Capacity Factor		90.0%		
Coal Cost		3	$/MMBtu	
Heat Rate (Including Sequestration)		8,945	Btu/kwh	
Capital Investment		**$x1000**		**$/kw**
Bare Erected Capital Cost	$	1,357,737		2,435
Engineering	$	137,103		246
Contingency	$	128,575		231
Total Plant Cost	**$**	**2,069,575**		**3,712**
Operating and Maintenance Cost		**$x1000**		**$/kw-yr**
Fixed O&M	$	22,301		40
Variable O&M	$	16,726		30
*Engineering & Contingency values shown do not include assumed values for Cryo ASU, CPU, WGCU				

COE Calculation		$x1000	factor	¢/kwh
O&M Cost				
Fixed O&M	$	22,301	1.16	0.589
Variable O&M	$	16,726	1.16	0.397
Consumable Operating Costs (less Coal)				
Limestone	$	869	1.16	0.023
Ash Disposal	$	3,022	1.16	0.080
Water	$	788	1.16	0.021
MU&WT Reagents	$	1,500	1.16	0.040
Natural Gas	$	1,514	1.2	0.041
Fuel Cost	$	117,958	1.2	3.220
Total Capital	$	2,069,575	0.175	8.240
Total 20 Yr Levelized COE (c/kwh)				**12.65**

Table 13: Case 2 Stream Summary

	Stream	Coal	Gasifier Steam	Gasifier Cryo O2	Gasifier Slag	Gasifier Syngas	Pox 1 Air	Pox 1 Air	Pox 1 Warm Air	Pox 1 Hot O2 Depleted	Pox 1 Cold O2 Depleted	Pox 1 Hot Syngas	Pox 2 Warm Syngas	Pox 2 Air	Pox 2 Air	Pox 2 Warm Air
Stream #		1	2	3	4	5	11	12	13	14	15	16	17	21	22	23
Temperature	F	77	680	246	500	1000							678	59	119	1521
Pressure	psia	396.0	510.0	517.0	396.0	340.0							99.0	14.7	19.7	18.7
Flow	k lb/hr	427.5	124.1	215.3	47.6	778.6							766.5	283.0	283.0	283.0
Flow	lbmol/hr	-	6,889	6,696		38,849							38,515	9,808	9,808	9,808
Composition																
H2	mol%					30.0%							30.0%			
CO	mol%					50.0%							51.0%			
CH4	mol%					3.0%							3.0%			
CO2	mol%					4.0%							4.0%			
WATER	mol%		100.0%			9.0%							9.0%	1.0%	1.0%	1.0%
OXYGEN	mol%			95.0%										21.0%	21.0%	21.0%
N2+AR	mol%			5.0%		2.0%							2.0%	78.0%	78.0%	78.0%
H2S	mol%					1.0%										
SOx	mol%															
Solids	k lb/hr	427.5			47.6											

	Stream	Pox 2 Hot O2 Depleted	Pox 2 Cold O2 Depleted	Pox 2 Hot Syngas	Boiler Syngas	OTM Boiler Air	OTM Boiler Air	OTM Boiler Warm Air	OTM Boiler Hot O2 Depleted	OTM Boiler Cold O2 Depleted	Residual Syngas	Cryo O2 for Boiler	Hot Flue Gas	Air Leak	Warm Flue Gas	Cold Flue Gas	Lime-Stone	FGD Solids	Flue Gas to CPU	Syngas to 1st Expander
Stream #		24	25	26	27	31	32	33	34	35	36	37	38	39	40	41			51	71
Temperature		1832	150	1700	1393	59	119	1489	1832	150	1564	80	2739	77	365	120			120	1014
Pressure		18.7	17.7	85.8	38.9	14.7	19.7	18.7	18.7	17.7	17.2	17.0	17.0	15.0	15.0	14.0			14.0	340.0
Flow		228.8	228.8	766.5	766.5	2292.4	2292.4	2292.4	1808.1	1808.1	1305.0	115.8	1420.9	27.1	1448.0	1163.8			1163.8	766.5
Flow		8,113	8,113	38,515	38,515	78,967	78,967	78,967	63,832	63,832	42,640	3,596	43,688	936	44,624	28,850			28,850	38,515
Composition																				
H2				30.0%	30.0%						5.0%									30.0%
CO				51.0%	51.0%						8.0%									51.0%
CH4				3.0%	3.0%						1.0%									3.0%
CO2				4.0%	4.0%						48.0%		54.0%		53.0%	82.0%			82.0%	4.0%
WATER		1.0%	1.0%	9.0%	9.0%	1.0%	1.0%	1.0%	1.0%	1.0%	38.0%		43.0%		42.0%	11.0%			11.0%	9.0%
OXYGEN		4.0%	4.0%			23.0%	23.0%	23.0%	5.0%	5.0%		95.0%	1.0%	21.0%	1.0%	2.0%			2.0%	
N2+AR		94.0%	94.0%	2.0%	2.0%	76.0%	76.0%	76.0%	95.0%	95.0%	1.0%	5.0%	2.0%	79.0%	4.0%	5.0%			5.0%	2.0%
H2S																				
SOx																				

Table 14: Case 2 power, industrial gas and environmental performance summary

Power Production	
Steam Cycle (MW)	631.51
Expander 1	21.73
Expander 2	21.77
Expander 3	21.77
TOTAL GROSS POWER (MW)	**696.78**
Aux Load	
Cryo ASU	45.59
CO2 Compression/Purification	54.15
OTM ASU	11.49
Boiler Fuel Delivery	0.92
Flue Gas Desulfurization	0.00
Condenser Circulation Pump	3.74
Cooling Fan Tower	3.04
Condensate Pump	6.55
Additional Auxiliaries	5.17
Misc. Plant Auxiliaries	2.81
WGCU & DRSP	5.73
Gas Liquor Separation	2.69
Gas Liquor Treatment	0
TOTAL AUX LOAD (MW)	**141.88**
Net Power (MW)	**554.9**
Net Efficiency (%HHV)	**37.97%**
Coal Rate (tpd)	**5130**
Industrial Gases	
O2 Cryogenic ASU (tpd)	3974
O2 OTM ASU (tpd)	6462
CO2 Captured (tpd)	11806
CO2 Emissions (tpd)	687
CO2 Capture Efficiency (%)	97.1%
CO2 Purity (%)	95.8%

Table 15: Case 2 Capital Cost Estimate

Case 2: Capital Cost	Equipment Costs	Installation Costs	Bare Erected Cost	Eng'g Fee, EPC Profit	Contingency	Total	$/kw
Gasifier Costs			190,216,000	15,707,000	39,468,000	245,391,000	442.23
Candle Filter	5,034,000	3,524,000	8,558,000	856,000	1,712,000	11,126,000	20.05
Syngas Turbines	53,719,200	37,603,440	91,322,640	9,132,264	5,935,972	106,390,876	191.73
Steam Cycle-incl Cooling Towers	202,198,380	344,076,261	546,274,641	60,455,205	30,045,105	636,774,951	1,147.55
WGCU and Sulfur Recovery						159,355,000	287.18
Cryogenic ASU						116,774,000	210.44
OTM Boiler and POX units	307,505,181	215,253,627	522,758,808	51,068,494	51,068,494	624,895,796	1,126.14
CPU						170,031,000	306.42
					TOTAL	$ 2,070,738,623	3,731.73

* Does not include "Owners Costs," transportation costs, permit fees, owners CM expenses, owners contingency, escalation during construction, etc

Table 16: Case 2 COE Estimate

Case 2 COE Calculation				
Net Power Produced		**554.9**	**MW**	
Capacity Factor		90.0%		
Coal Cost		3	$/MMBtu	
Heat Rate (Including Sequestration)		8,988	Btu/kwh	
Capital Investment		**$x1000**		**$/kw**
Bare Erected Capital Cost	$	1,359,130		2,449
Engineering	$	137,219		247
Contingency	$	128,230		231
Total Plant Cost	**$**	**2,070,739**		**3,732**
Operating and Maintenance Cost		**$x1000**		**$/kw-yr**
Fixed O&M	$	22,196		40
Variable O&M	$	16,647		30
*Engineering & Contingency values shown do not include assumed values for Cryo ASU, CPU, WGCU				

COE Calculation		$x1000	factor	¢/kwh
O&M Cost				
Fixed O&M	$	22,196	1.16	0.589
Variable O&M	$	16,647	1.16	0.397
Consumable Operating Costs (less Coal)				
Limestone	$	869	1.16	0.023
Ash Disposal	$	3,022	1.16	0.080
Water	$	788	1.16	0.021
MU&WT Reagents	$	1,500	1.16	0.040
Natural Gas	$	1,521	1.2	0.042
Fuel Cost	$	117,958	1.2	3.236
Total Capital	$	2,070,739	0.175	8.283
Total 20 Yr Levelized COE (c/kwh)				**12.71**

Table 17: Case 3 Stream Summary

	Stream	Coal	Gasifier Steam	Pox 2 Cold O2 Depleted	Pox 2 Hot Syngas	Boiler Syngas	OTM Boiler Air	Gasifier Slag	Gasifier Cryo O2	Gasifier Syngas	Add'l Expander Effluent	Pox 1 Air	Pox 1 Warm Air	Pox 1 Hot O2 Depleted	Pox 1 Cold O2 Depleted	Pox 1 Hot Syngas	Pox 2 Warm Syngas	Pox 2 Air	Pox 2 Air
Stream #		1	2		26	27	31	4	3	5		11	12	13	14	15	16	17	21	22
Temperature	F	77	680	150	1700	1481	59	500	246	1000	776	59	119	1521	1832	150	1650	1430	59	119
Pressure	psia	396.0	510.0	17.7	67.6	38.9	14.7	396.0	517.0	340.0	147.0	14.7	19.7	18.7	18.7	17.7	142.3	80.7	14.7	19.7
Flow	k lb/hr	427.5	124.1	62.7	766.5	766.5	2261.5	47.6	215.3	778.6	766.5	239.4	239.4	193.5	193.5	193.5	766.5	766.5	77.6	77.6
Flow	lbmol/hr	-	6,889	2,224	38,515	38,515	77,906		6,696	38,849	38,515	8,297	8,297	6,863	6,863	6,863	38,515	38,515	2,689	2,689
Composition																				
H2	mol%				30.0%	30.0%				30.0%	30.0%						30.0%	30.0%		
CO	mol%				51.0%	51.0%				50.0%	51.0%						51.0%	51.0%		
CH4	mol%				3.0%	3.0%				3.0%	3.0%						3.0%	3.0%		
CO2	mol%				4.0%	4.0%				4.0%	4.0%						4.0%	4.0%		
WATER	mol%		100.0%		9.0%	9.0%	1.0%			9.0%	9.0%	1.0%	1.0%	1.0%	1.0%	1.0%	9.0%	9.0%	1.0%	1.0%
OXYGEN	mol%						21.0%		95.0%			21.0%	21.0%	4.0%	4.0%	4.0%			21.0%	21.0%
N2+AR	mol%				2.0%	2.0%	78.0%		5.0%	2.0%	2.0%	78.0%	78.0%	94.0%	94.0%	94.0%	2.0%	2.0%	78.0%	78.0%
H2S	mol%					1.0%														
SOx	mol%																			
Solids	k lb/hr	427.5						47.6												

	Stream	Pox 2 Warm Air	Pox 2 Hot O2 Depleted	Pox 2 Cold O2 Depleted	Pox 2 Hot Syngas	Boiler Syngas	OTM Boiler Air	OTM Boiler Warm Air	OTM Boiler Hot O2 Depleted	OTM Boiler Cold O2 Depleted	Residual Syngas	Cryo O2 for Boiler	Hot Flue Gas	Air Leak	Warm Flue Gas	Cold Flue Gas	Lime-Stone	FGD Solids	Flue Gas to CPU
Stream #		23	24	25	26	27	31	33	34	35	36	37	38	39	40	41			51
Temperature		1521	1832	150	1700	1481	59	1489	1832	150	1563	80	2739	77	365			120	120
Pressure		18.7	18.7	17.7	67.6	38.9	14.7	18.7	18.7	17.7	17.2	17.0	17.0	15.0	15.0			14.0	14.0
Flow		77.6	62.7	62.7	766.5	766.5	2261.5	2261.5	1783.8	1783.8	1305.0	115.8	1420.9	27.1	1448.0			0.0	1163.8
Flow		2,689	2,224	2,224	38,515	38,515	77,906	77,906	62,974	62,974	42,640	3,596	43,688	936	44,624			0	28,850
Composition																			
H2					30.0%	30.0%					5.0%								
CO					51.0%	51.0%					8.0%								
CH4					3.0%	3.0%					1.0%								
CO2					4.0%	4.0%					48.0%		54.0%		53.0%	82.0%			82.0%
WATER		1.0%	1.0%	1.0%	9.0%	9.0%	1.0%	1.0%	1.0%	1.0%	38.0%		43.0%		42.0%	11.0%			11.0%
OXYGEN		21.0%	4.0%	4.0%			23.0%	23.0%	5.0%	5.0%		95.0%	1.0%	21.0%	1.0%	2.0%			2.0%
N2+AR		78.0%	94.0%	94.0%	2.0%	2.0%	76.0%	76.0%	95.0%	95.0%	1.0%	5.0%	2.0%	79.0%	4.0%	5.0%			5.0%
H2S																			
SOx																			

Table 18: Case 3 power industrial gas and environmental performance summary

Power Production	
Steam Cycle (MW)	634.60
Expander 1	30.37
Expander 2	30.37
TOTAL GROSS POWER (MW)	**695.34**
Aux Load	
Cryo ASU	45.59
CO2 Compression/Purification	54.15
OTM ASU	11.49
Boiler Fuel Delivery	0.92
Flue Gas Desulfurization	0.00
Condenser Circulation Pump	3.74
Cooling Fan Tower	3.04
Condensate Pump	6.55
Additional Auxiliaries	5.17
Misc. Plant Auxiliaries	2.81
WGCU & DRSP	5.73
Gas Liquor Separation	2.69
Gas Liquor Treatment	0
TOTAL AUX LOAD (MW)	**141.88**
Net Power (MW)	**553.5**
Net Efficiency (%HHV)	**37.88%**
Coal Rate (tpd)	**5130**
Industrial Gases	
O2 Cryogenic ASU (tpd)	3974
O2 OTM ASU (tpd)	6462
CO2 Captured (tpd)	11806
CO2 Emissions (tpd)	687
CO2 Capture Efficiency (%)	97.1%
CO2 Purity (%)	95.8%

Table 19: Case 3 Capital Cost Estimate

Case 3: Capital Cost	Equipment Costs	Installation Costs	Bare Erected Cost	Eng'g Fee, EPC Profit	Contingency	Total	$/kw
Gasifier Costs			190,216,000	15,707,000	39,468,000	245,391,000	443.38
Candle Filter	5,034,000	3,524,000	8,558,000	856,000	1,712,000	11,126,000	20.10
Syngas Turbines	44,766,000	31,336,000	76,102,000	7,610,200	4,946,600	88,658,800	160.19
Steam Cycle-incl Cooling Towers	201,791,952	343,384,644	545,176,596	60,455,000	30,275,514	635,907,110	1,148.97
WGCU and Sulfur Recovery						159,355,000	287.93
Cryogenic ASU						116,774,000	210.99
OTM Boiler and POX units	306,887,080	214,820,956	521,708,036	50,965,843	50,965,843	623,639,722	1,126.80
CPU						170,031,000	307.21
					TOTAL	**$ 2,050,882,632**	**3,705.57**

* Does not include "Owners Costs," transportation costs, permit fees, owners CM expenses, owners contingency, escalation during construction, etc

Table 20: Case 3 COE Estimate

Case 3 COE Calculation				
Net Power Produced		**553.5**	**MW**	
Capacity Factor		90.0%		
Coal Cost		3	$/MMBtu	
Heat Rate (Including Sequestration)		9,011	Btu/kwh	
Capital Investment		**$x1000**		**$/kw**
Bare Erected Capital Cost	$	1,341,761		2,424
Engineering	$	135,594		245
Contingency	$	127,368		230
Total Plant Cost	**$**	**2,050,883**		**3,706**
Operating and Maintenance Cost		**$x1000**		**$/kw-yr**
Fixed O&M	$	22,138		40
Variable O&M	$	16,604		30
*Engineering & Contingency values shown do not include assumed values for Cryo ASU, CPU, WGCU				

COE Calculation		$x1000	factor	¢/kwh
O&M Cost				
Fixed O&M	$	22,138	1.16	0.589
Variable O&M	$	16,604	1.16	0.397
Consumable Operating Costs (less Coal)				
Limestone	$	869	1.16	0.023
Ash Disposal	$	3,022	1.16	0.080
Water	$	788	1.16	0.021
MU&WT Reagents	$	1,500	1.16	0.040
Natural Gas	$	1,525	1.2	0.042
Fuel Cost	$	117,958	1.2	3.244
Total Capital	$	2,050,883	0.175	8.225
Total 20 Yr Levelized COE (c/kwh)				**12.66**

Cost Summary

The base case COE was calculated for a coal price of $3/MMBtu however the COE was calculated for other coal prices due to the volatility in coal prices in 2008. Table 21 below shows COE for coal prices of 1.8, 3.0 and 4.0/MMBTU for OTM cases 1 thru 3 as well as the

base case taken from Praxair's 2008 Phase I study. In all cases an installed OTM "cost allocation" was used for the ceramic material.

Table 21: Calculated COE for 3 OTM cases at various coal prices compared to the Air-PC reference case (no capture)

		Current OTM Cases			Previous OTM Study	Air-PC Case
Case		1 Main	2 3 Expanders	3 1 POx	4 Previous Study	Praxair/DOE No CCS SC
Net Efficiency		38.2	38	37.9	37.4	39.7
Cost Basis (year)		3/2008	3/2008	3/2008	3/2008	3/2008
Plant Cost ($/kW)		$3,712	$3,732	$3,706	$2,863	$1,908
	Coal Price ($/MMbtu)					
COE ($/MWh)	1.8	$113.6	$114.2	$113.6	$95.2	$70.5
	3	$126.5	$127.1	$126.6	$108.4	$82.9
	4	$137.2	$137.9	$137.4	$119.3	$93.2

For reference, also shown in Table 21 is the COE from the Praxair simulated version of the DOE's Supercritical Air-Pulverized Coal case which has been adjusted to match the 2008 capital basis for all the OTM cases. This reference case has been adjusted from Case 1 in the DOE oxy-combustion report DOE/NETL-2007/1291. This DOE-based reference case is the basis for calculating the % increase in COE for the OTM cases. The DOE goal for cost of electricity increase is <35% increase in COE for power cycles which enable CCS. Table 22 shows the calculated increase in COE over the reference case for the 3 OTM cases at the three different coal prices as well as the previous case from the 2008 study. The areas shaded in green denote that the case satisfies the DOE requirement for an increase in COE of less than 35%.

Table 22: Percent increase in COE over the reference case for various coal prices.

		Current OTM Cases			Previous OTM Study	Air-PC Case
Case		1 Main	2 3 Expanders	3 1 POx	4 Previous Study	Praxair/DOE No CCS SC
Net Efficiency		38.2	38	37.9	37.4	39.7
Cost Basis (year)		3/2008	3/2008	3/2008	3/2008	3/2008
Plant Cost ($/kW)		$3,712	$3,732	$3,706	$2,863	$1,908
	Coal Price ($/MMbtu)					
Increase in COE over Reference	1.8	61.1%	62.0%	61.1%	35.0%	
	3	52.6%	53.3%	52.7%	30.8%	
	4	47.2%	48.0%	47.4%	28.0%	

.

Several items contributed to the increase in cost from Praxair's previous study. Figure 8 gives a breakdown of this increase in cost. As can be seen most of the increase is due to steam/power generation cycle. This steam cycle is a standard cycle that would also be present in a non-OTM power plant. The increase in cost due to other factors such as the OTM boiler and POx units as well as the syngas expanders was only 4.5%. The steam cycle increased the cost by 12.3**%.**

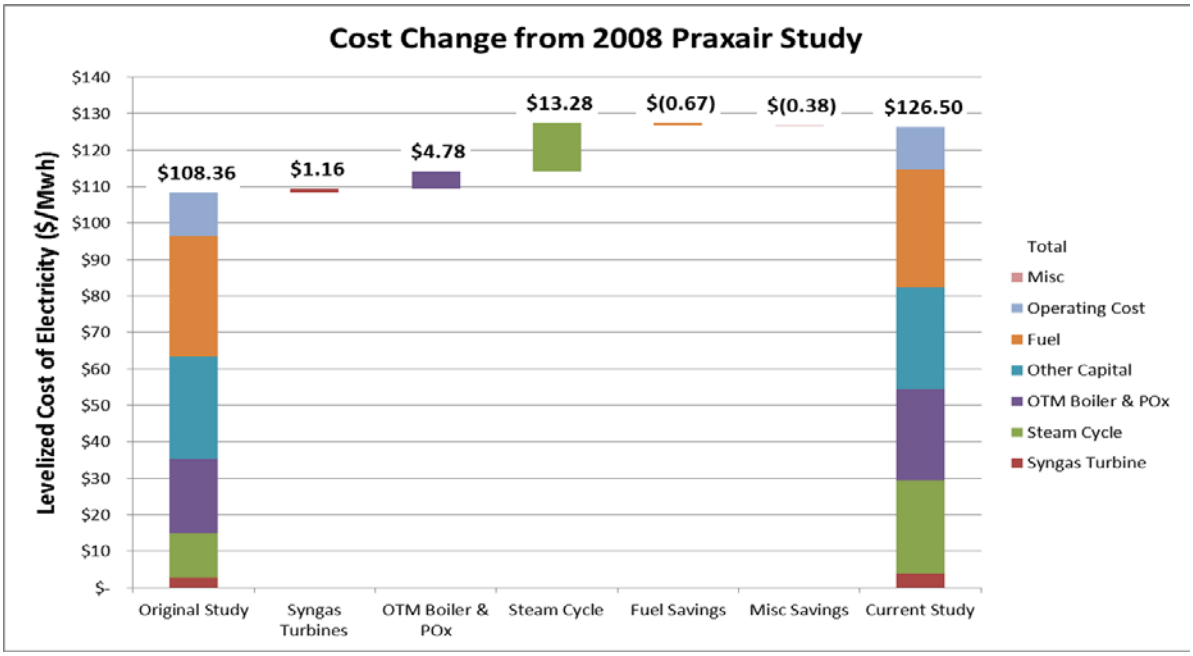

Figure 8: Escalation of cost from original 2008 study

There were no major configuration changes made to the steam cycle for this case. Therefore the difference in cost was due mainly to the group doing the estimating (Shaw vs. Praxair phase I study), and the total power allocated to the steam cycle. To make a fair comparison to the base case and Praxair's original 2008 study, Table 23 shows a cost comparison assuming the steam cycle did not increase in cost over the 2008 study. This makes the steam cycle cost more consistent with previous studies by Praxair and the NETL. This table shows that the increase in cost of electricity for a levelized steam cycle was much less dramatic. Table 24 shows the percent increase in COE for the levelized steam cycle. This shows that the updated cost estimate is still very close to the DOE goal of 35% increase in COE. The only case that is not very competitive is at the low coal price of $1.8/MMBtu.

Table 23: COE for all cases assuming the steam cycle cost from Praxair's 2008 estimate

		Current OTM Cases			Previous OTM Study	Air-PC Case
Case		1 Main	2 3 Expanders	3 1 POx	4 Previous Study	Praxair/DOE No CCS SC
Net Efficiency		38.2	38	37.9	37.4	39.7
Cost Basis (year)		3/2008	3/2008	3/2008	3/2008	3/2008
Plant Cost ($/kW)		$3,712	$3,732	$3,706	$2,863	$1,908
	Coal Price ($/MMbtu)					
COE ($/MWh)	1.8	$100.2	$100.7	$100.2	$95.2	$70.5
	3	$113.1	$113.7	$113.2	$108.4	$82.9
	4	$123.8	$124.5	$124.0	$119.3	$93.2

Table 24: Percent increase in COE assuming steam cycle cost from 2008 Praxair estimate

		Current OTM Cases			Previous OTM Study	Air-PC Case
Case		1 Main	2 3 Expanders	3 1 POx	4 Previous Study	Praxair/DOE No CCS SC
Net Efficiency		38.2	38	37.9	37.4	39.7
Cost Basis (year)		3/2008	3/2008	3/2008	3/2008	3/2008
Plant Cost ($/kW)		$3,712	$3,732	$3,706	$2,863	$1,908
	Coal Price ($/MMbtu)					
Increase in COE over Reference	1.8	42.1%	42.8%	42.1%	35.0%	
	3	36.4%	37.2%	36.6%	30.8%	
	4	32.8%	33.6%	33.0%	28.0%	

Cost of CO_2 avoided and cost of CO_2 removed is calculated as described in the Design Basis section. In all cases the cost of CO_2 avoided/removed reflects a $4/ton of CO_2 cost for transport, final sequestration, measurement, verification, etc. Costs of CO2 avoided/removed are shown below in Table 25. The relatively low cost of CO_2 avoided/removed for the Advanced Power Cycle of $30 to $40/ton CO_2 is due to the fact that the OTM based power cycle enables a high level of CO_2 capture with relatively low COE all while keeping a high net cycle HHV efficiency.

Table 25: Cost of CO2 avoided and removed for the 3 OTM cases at various coal prices

		Current OTM Cases			Previous OTM Study	Air-PC Case
Power Cycle Case		1 Main	2 3 Expanders	3 1 POx	4 Previous Study	Praxair/DOE No CCS SC
Net Efficiency		38.2	38	37.9	37.4	39.7
Plant Cost ($/kW)		$3,712	$3,732	$3,706	$2,863	$1,908
Coal Price ($/MMbtu)						
1.8	**Removal Cost ($/ton)**	$37	$38	$38	$31	
	Avoided Cost ($/ton)	$40	$41	$40	$34	
3	**Removal Cost ($/ton)**	$38	$39	$38	$32	
	Avoided Cost ($/ton)	$40	$41	$41	$35	
4	**Removal Cost ($/ton)**	$39	$39	$39	$33	
	Avoided Cost ($/ton)	$41	$42	$41	$36	

Conclusions and Recommendations

The Advanced Power Cycle calculated COE satisfies the DOE goal of less than 35% increase in COE in all cases when coal prices are $4/MMBtu. When coal is $3/MMBtu, is just above the 35% threshold at ~37%. In cases when coal prices are low ($1.8/MMBtu) the COE is not as competitive. Higher coal price decreases the % increase in COE due to the high efficiency of the Advanced Power Cycle.

The Advanced Power Cycle has a low cost of CO_2 removed and avoided due to three factors: 1) relatively low COE which in many cases meets the DOE's goal of <35% increase in COE, 2) high net cycle HHV efficiency, and 3) high CPU CO_2 capture efficiency. The net CO_2 capture efficiency of the CPU purification process is roughly 97% in all cases including the CO_2

losses for purifying the flue gas to >95% CO_2 product because the flue gas CO_2 concentration is relatively high from the start.

This high CO_2 recovery is achievable because of a few factors unique to the Advanced Power Cycle concept:

1) The OTM membranes effectively supply pure oxygen to the process with no other atmospheric gases as would be typical in an oxy-combustion power cycle where 'low purity' cryo-ASU oxygen is supplied to the boiler at between 95% and 97% purity.

2) The mechanism for oxygen transfer through the OTM membranes controls the rate of combustion in the boiler so flue gas recirculation is NOT necessary

3) A traditional air preheater is not used in this system. A typical regenerative air preheater is responsible for a large amount of air to flue gas leakage in a traditional power plant due to poor sealing in the heat exchanger. In the Advanced Power Cycle air preheat is achieved without any flue gas contact; this eliminates any possible air leakage to the flue gas side.

The results of this techno-economic evaluation show that the Advanced Power Cycle has the potential to meet the DOE goals for COE increase given the current level of OTM membrane performance and the current assumption for OTM cost allocation ($/ft^2). In addition, the confidence in the cost estimate has been greatly improved from Praxair's 2008 study due to the detailed design and cost estimate of the boiler and POx units. The detailed design is discussed in the following section of this report.

2.1.2. Subtasks 1.2 and 1.3 Pilot Plant – Conceptual and engineering design

Praxair engaged Shaw Energy & Chemicals to develop a Basic Engineering Design and cost estimate for a 7.5MWth Oxygen Transport Membrane (OTM) Boiler and 5tpd (of O_2 transported) OTM POx unit. The intent of this project was to identify a viable configuration for the boiler and POx unit that effectively utilized the OTMs in a tubular or planar format. The goal of the design effort was to inform and enable scale-up to a larger capacity with the intent for deployment in a 550MW coal-fired power facility. The estimated scale-up cost factors resulting from this study were used as inputs to the process economic evaluation detailed in the previous section of this report. Shaw was selected as a subcontractor to perform this task because of their extensive experience in high temperature furnaces, steam systems, power cycles, modelling of flow and heat transfer, project cost estimating, and a proven track record of deployment of new process technology.

Process Description

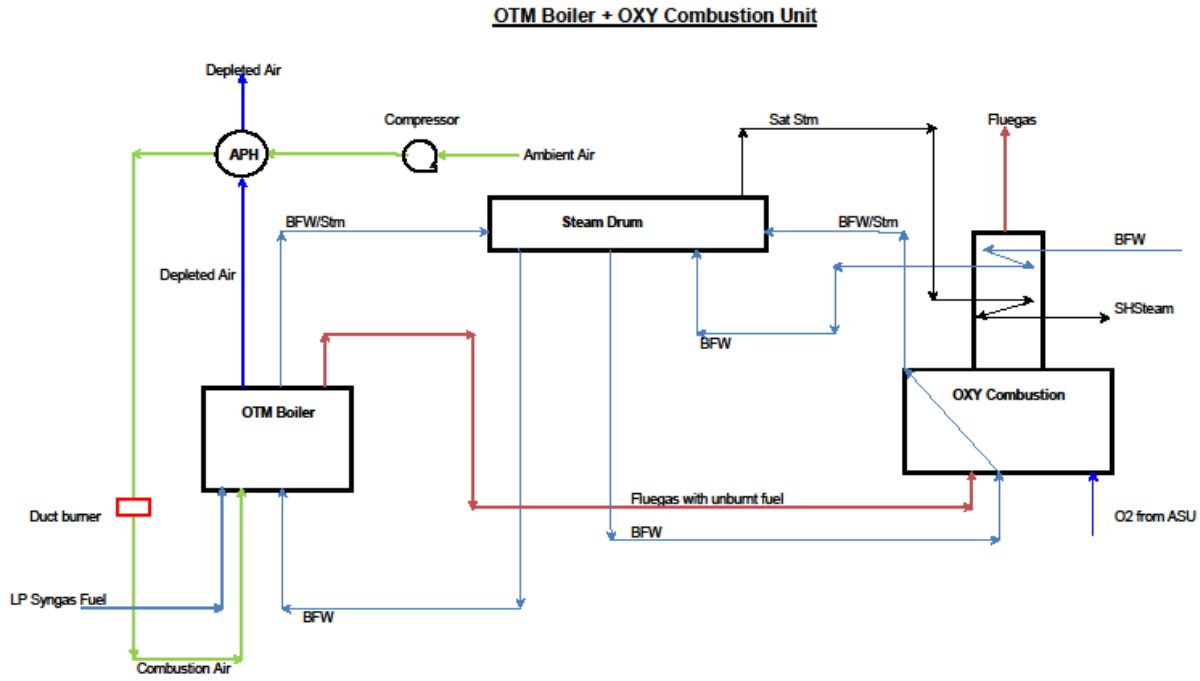

Figure 9: PFD of OTM boiler process unit

The OTM Boiler utilizes the heat release from the reaction of low pressure syngas fuel and oxygen (separated from air across the OTM) to partially vaporize boiler feed water (BFW). The BFW is fed to the OTM Boiler from a downcomer exiting the steam drum. The water/steam stream flows through a riser to the steam drum. The partially oxidized flue gas containing the remaining fuel is routed to the Oxy Combustion Fired Heater. Oxygen supplied from a cryogenic Air Separation Unit (ASU) (outside Shaw's scope) completes the combustion of the low pressure syngas in the radiant section of the Oxy Combustion Fired Heater. The heat released from the reaction of the low pressure syngas partially vaporizes the BFW that is fed from a downcomer pipe from the steam drum. The water/steam mixture flows thru a riser pipe to the steam drum. Additional heat is recovered in the overhead convection section to superheat steam and to preheat BFW. The BFW is preheated in the Economizer bank and is then fed to

the steam drum. The steam exiting the steam drum is fed to the convection section to be superheated in the Steam Superheat bank. The superheated steam is then routed to a Steam Turbine (outside Shaw's scope) for further energy recovery.

7.5 MW OTM Boiler Design and Cost Estimate

Design Basis and Assumptions

The design of the OTM boiler unit depends upon performance data for the OTM membranes under varying conditions. Praxair provided Shaw with actual experimental results on OTM membranes from which flux profiles and averages fluxes were used to guide various design calculations. The experimental data came from operation of OTM membranes with a coal derived syngas to best mimic the conditions in the Advanced Power Cycle (discussed in the previous section). Figure 10 shows a normalized flux profile obtained from OTM membranes.

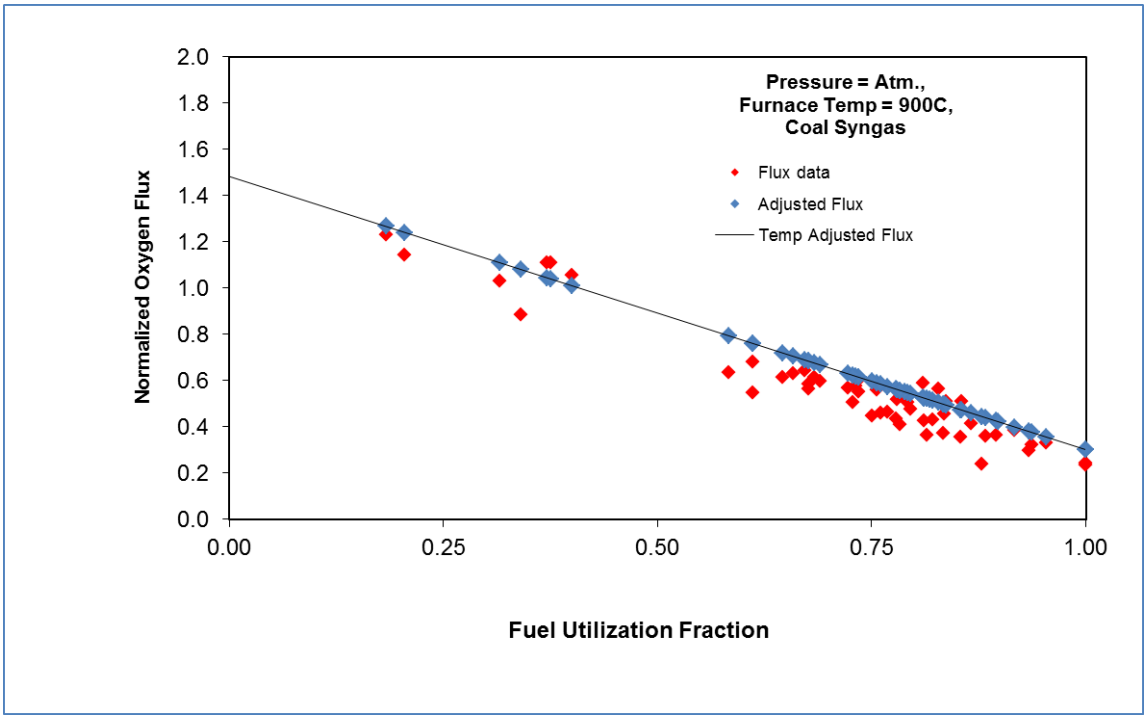

Figure 10: Oxygen Flux Profile

The Design Conditions for the OTM Boiler System are as follows:

Table 26: Boiler Design Basis

7.5 MW OTM Boiler Design Basis		
Air Inlet Temperature	°F	60
Air Pressure to OTM	psia	20
Relative Humidity	%	80
Atmospheric Pressure	psia	14.7
Air Preheat to OTM	°F	1400
BFW Inlet temperature	°F	250
Syngas Temperature to Boiler	°F	1250
Syngas Pressure to Boiler	psia	5
Cryo Oxygen Supply Temperature	°F	60
Cryo Oxygen Supply Pressure	psia	215
Steam Temperature	°F	700
Steam Pressure	psia	150
OTM Operating Temperature	°F	1832

The assumed syngas composition used for the study is show in Table 27.

Table 27: Typical Syngas Feed to OTM Boiler

Species	Base Case (mol%)	Range (mol%)
H_2	31.4	21.4 - 51.7
CO	44.6	24.4 – 44.6
CH_4	0.0	0.0 - 2.1
CO_2	10.1	5.6 – 10.1
H_2O	11.8	11.8 - 14.6
N_2	1.3	1.3 - 1.4
H_2S	0.7	0.0 – 0.7

Concept Development

An option selection meeting to determine the most favorable configuration of the Oxygen Transport Membranes developed by Praxair for the OTM Boiler was convened in Praxair's offices in Tonawanda, New York. Seven (7) Shaw proposed conceptual configurations for the boiler were reviewed and their merits considered. Selection criteria and priority weighting was determined by the joint Praxair/Shaw design team. The selection criteria included the following factors:

1. **Ease/ Ability of Manufacture/Design Simplicity/complexity/Cost**

   considering**:**

   - Ceramic
   - Balance of Reactor
   - Seals

2. **Technically Viable / Level of Risk**

   considering:

   - Ceramic
   - Balance of Reactor
   - Seals

3. **Safety**

   considering:

   - Leak Potential
   - Pressure Integrity

- Membrane Rupture Consequence

4. **Configuration Efficiency**

   considering:

   - Air Side Pressure Drop
   - Fuel side Pressure Drop

5. **Area Utilization for HT & Mass Transfer**
6. **Material Compatibility**
7. **Flexibility**

   considering:

   - Process optimization
   - Common features of Boiler vs POx units

8. **Serviceability**
9. **Scalability**

Priority weighting was highest for ceramic membrane and seal technical viability and risk. Safety and scalability were the next highest weighted criteria, respectively. A "Pugh's" analysis was conducted whereby design concepts were rated as better, worse, or the same as a baseline design with respect to each of the criteria. It was determined that "Boiler Concept 2", a tube array concept configured in cross flow with water in vertical tubes, air in horizontal OTM tubes, and syngas in the shell space surrounding the tubes, was the most favorable based on the analysis. The merits of this design included: vertical tubes (favorable orientation for steam

generation with elevated steam drum) and a low-risk, conventional OTM tube design where simple seals are used to seal the OTM tubes at low-pressure tube sheets.

Concepts

The concept development phase of the project was important to this project as it was the catalyst to a technical solution as well as defining the basis for the cost estimate. Due to the unique features of the OTM membrane, conventional boiler design was deemed not appropriate. Additionally, Praxair advised some key features and aspects of the OTM membrane that guided Shaw in the development of the concepts.

Key Concept Features:

- OTM membrane can be applied on the support structure (advanced ceramic material with porous construction) on either the air or gas side.
- The support structure will be ceramic based, so welding and other typical joining convention may be limited.
- The support structure can be either in tubular or planar form.
- OTM working temperature range required that there be continuous flow across the surface. The heat transfer cooling media needs to be uniform, to absorb and maintain the heat flux.

For each concept developed, a basic 3-dimensional rendering was produced to help with visualization and to aid in concept analysis and selection. The solid modeling used for these graphics also allowed the engineers at Shaw to extract the parts, make multiple view cuts, and to annotate descriptions on the renderings. Rejected concepts are shown in Appendix B.

Conception Selection

Boiler Concept 2 (see below) was deemed the best solution due to many factors:

- Best view factor between OTM tubes and steam tubes
- Ease of manufacturing for the module
- Scaling up was more feasible for a modular concept
- Safety can be addressed in the detailed design
- Design can be serviced/repaired

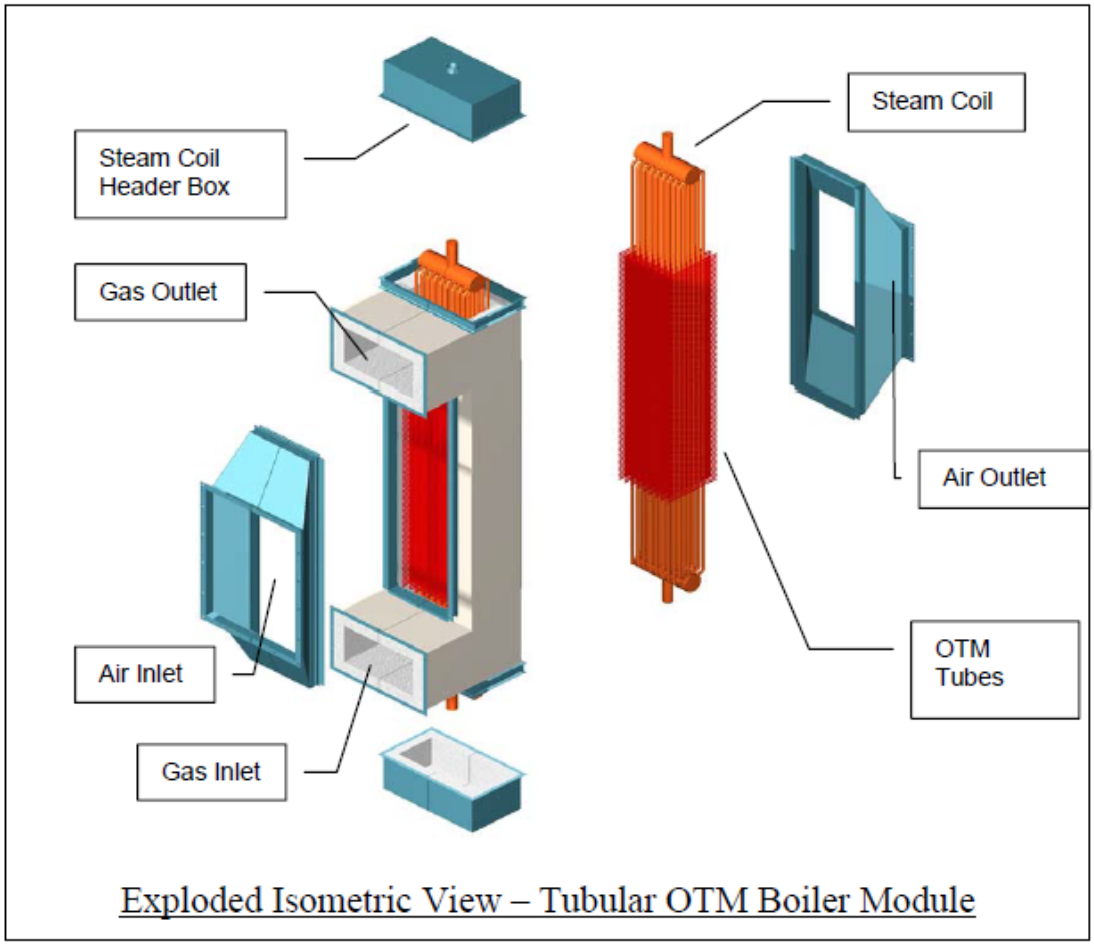

Figure 11: 3-dimensional Schematic of Final Boiler Module (Concept 2)

Figure 11 shows a 3-dimensional rendering of the final design for the boiler module. The orange tubes represent the steam tubes which sit vertically to accommodate an overhead steam drum. The OTM tubes run horizontally and are arranged between the rows of steam tubes. With this design, the fuel/syngas travels through refractory lined ducts on the exterior of the OTM tubes. The air flow travels within the OTM tubes. Multiple modules would be installed configured in parallel to meet the required steam flow for the application.

Computational Fluid Dynamics (CFD) Modeling

CFD modeling was performed in order to validate the selected boiler module design. In addition to validation, the modeling was used to aid in the specific geometrical design of the module. This ensures that the design will be able to facilitate the heat transfer (both radiative and convective) between the exothermic OTM tubes and the heat load (steam tubes). Improper geometry will result in lower steam production and/or low OTM temperatures and low flux/performance. A 3-dimensional CFD model of a vertical slice of the OTM boiler containing the OTM and adjacent steam tubes was created to study the effects of radiation and convection heat transfer inside the core of the Shaw-designed OTM Boiler module. A single column of 65 OTM tubes placed between two half rows of steam tubes as shown in Figure 12. The region between steam tubes was set as symmetry boundary for the computational domain.

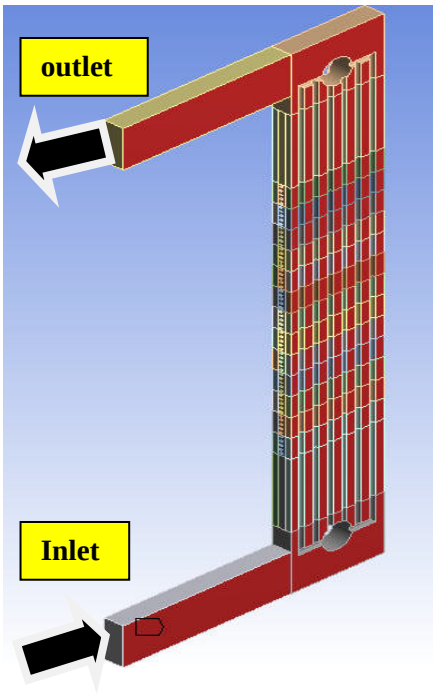

Figure 12: Geometry of boiler module section used for CFD modeling

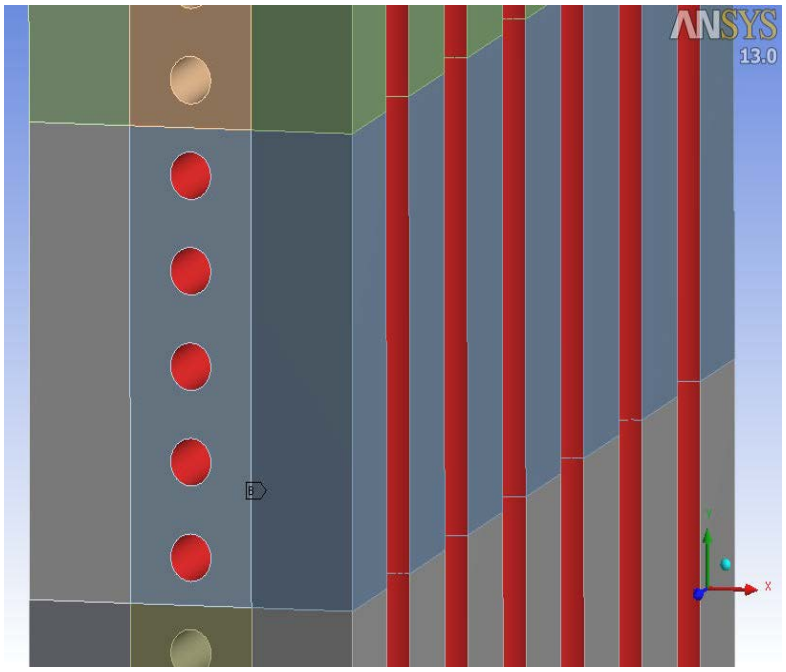

Figure 13: Close-up of boiler CFD geometry showing OTM tubes running cross-flow to the steam tubes (fluid domain shown)

Boundary Conditions

Flow conditions are documented in Table 28 . Flow rate was determined assuming even distribution to all OTM vertical arrays. A uniform velocity profile was assumed at the fuel feed duct inlet.

Table 28: Table of flow conditions for CFD boiler model.

		Inlet	Outlet	Average	MW
Pressure (psia)		20	20	20	
Mass flow (lb/hr)		8,123	12,290	10,206	
Temperature (°F)		400	1,168		
Molecular Weight		20.32	30.57	25.45	25.45
Species (mass %)	H_2	3.118	0.344		
	CO	61.543	6.781	38.64	19.4
	CO_2	21.897	67.732	44.81	44
	H_2S	1.175	0.129		
	N_2	1.794	1.185		
	H_2O	10.472	22.613	16.54	18
	SO_2	0.000	1.216		

The heat flux boundary conditions for the OTM tubes were set based on the flux performance curve supplied by Praxair, shown in Figure 10. Boundary conditions set in the model are described in Figure 14.

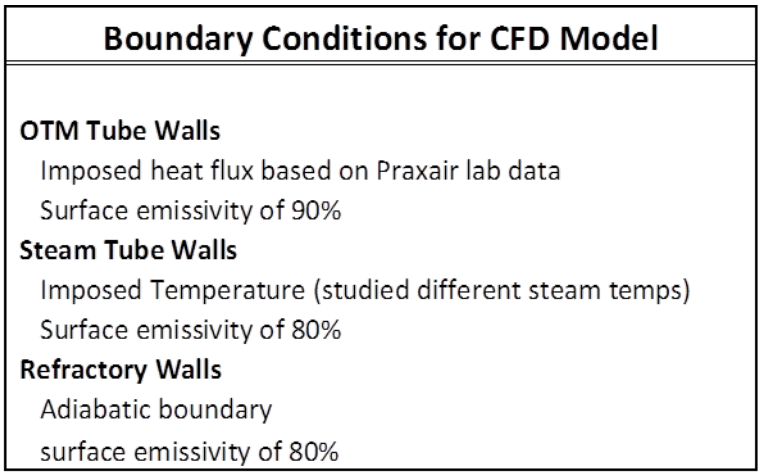

Figure 14: CFD model boundary conditions

Assumptions and Simplifications

Several simplifications were made to model the OTM boiler radiation and convection without embedded chemical reaction models. These included:

1. Imposed heat flux for OTM tube walls (based on the O_2 flux profile) based on a linear vertical variation with 13 points (the 65 OTM tubes were split into 13 bundles of 5 tubes each).
2. Only the main components of the gaseous mixture (i.e. CO_2, H_2O, and CO) were modeled. The syngas fuel was treated as a "gray" gas, having both absorption and emission properties with respect to radiation. Absorption coefficients were set to use the weighted-sum of the gray gas model based on CO_2 and H_2O partial pressure and vapor temperatures in the model domain.
3. The average syngas composition in each of the 13 defined zones along the vertical axis was estimated based upon the assumed oxygen flux profile, and

an average lumped value was applied to each of the 13 vertical elements. Average mass flow rate and properties for the gas mixture (inlet to outlet) were based on specific heat, thermal conductivity, viscosity, and molecular weight.

4. Only a fraction of the entire OTM boiler module geometry was modeled in order to reduce the computational cost: 1/10 slice by width and 1/9 slice by piping arrangement.
5. The OTM tubes are hollow and have no net mass flux in the modeling domain. The air flow and the heat and mass transfer between the air side and fuel side were not included in the model.
6. The enthalpy added to the system by oxygen flow is not considered.

Results

Figure 15 through Figure 18 depict the contours of temperature and velocity for the fuel gas throughout the computational domain. Figure 19 depict the flow recirculation regions that were predicted in the top and core of the module. Figure 20 shows predicted OTM tube temperature profile along the vertical axis as a function of steam temperature.

.

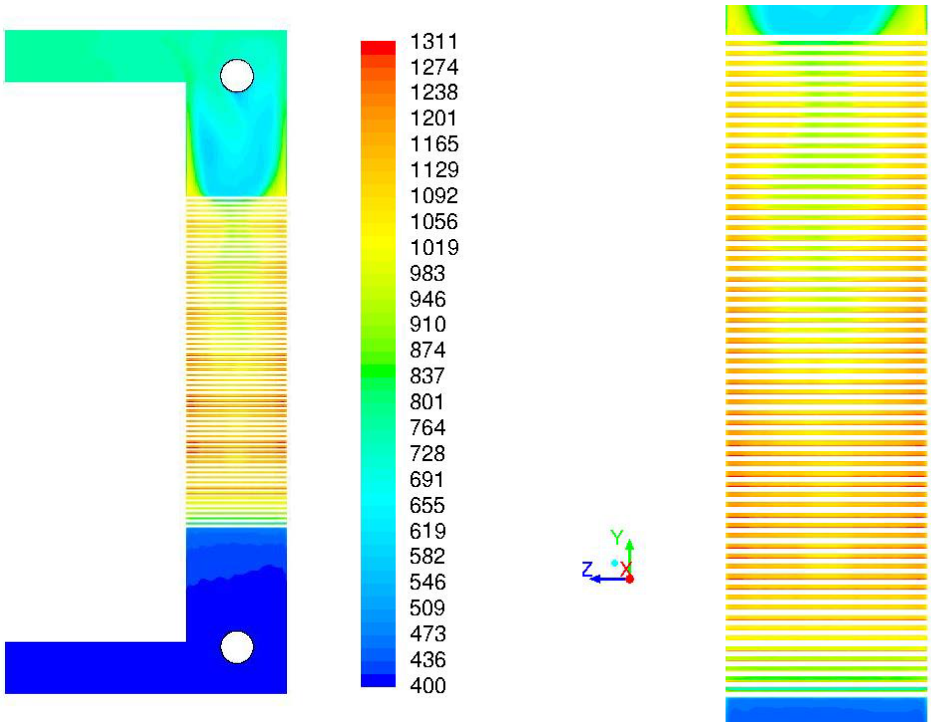

Figure 15: Fuel Gas Temperature Profiles of full module and close up

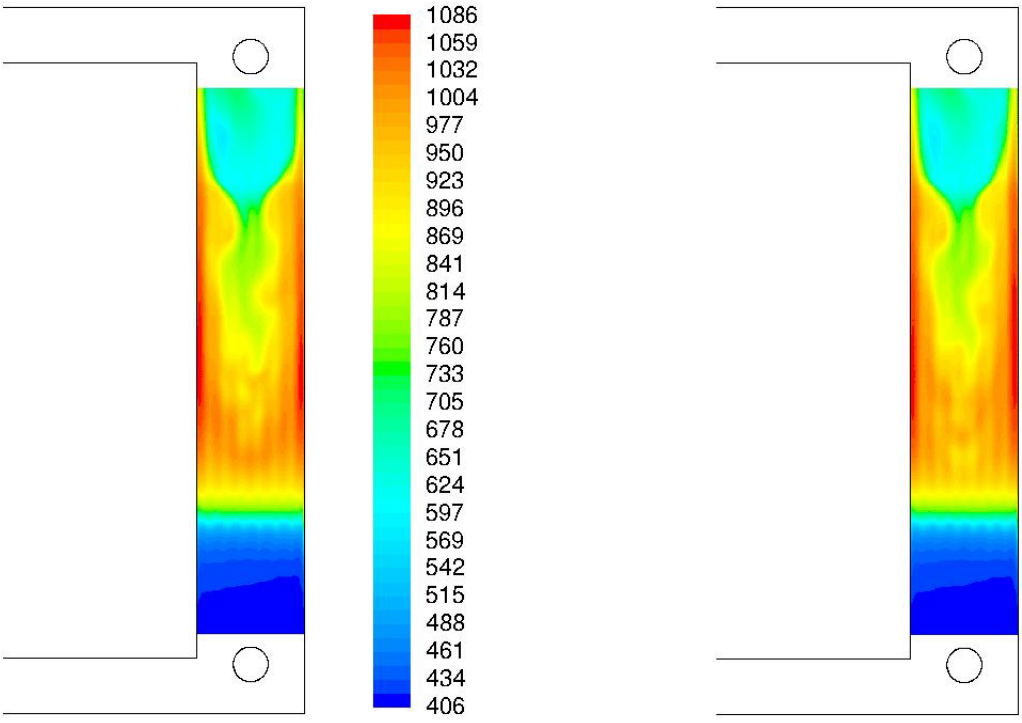

Figure 16: Temperature Profiles in between OTM and Steam Tubes

The temperature profiles in Figure 15 Figure 16 show a few issues with the initial design. In these figures, syngas fuel enters along the duct at the bottom of the boiler section and traverses vertically contacting OTM tube surface in cross-flow. Partially oxidized fuel is discharged from the boiler section along a duct at the top of the boiler. The results of the analysis indicate poor temperature distribution in the fuel gas with hot gas near the edges of the domain and the gas being very cool near the center of the duct. This was an unexpected result given that the heat release from the OTM surface would be expected to create the hottest gas down the center of the duct. The temperature mal-distribution is mainly due to the effect of the tubes containing steam which are relatively cold relative to the OTM surface and surrounding gas. The cold steam tube surfaces cool the syngas and cause sections where flow may reverse and recirculate in the duct. This can be seen more clearly by comparing the velocity profiles shown in Figure 17 and Figure 18. The negative velocity magnitudes in Figure 18 indicate syngas flow moving downward due to an increase in density at the lower temperature (reverse buoyancy).

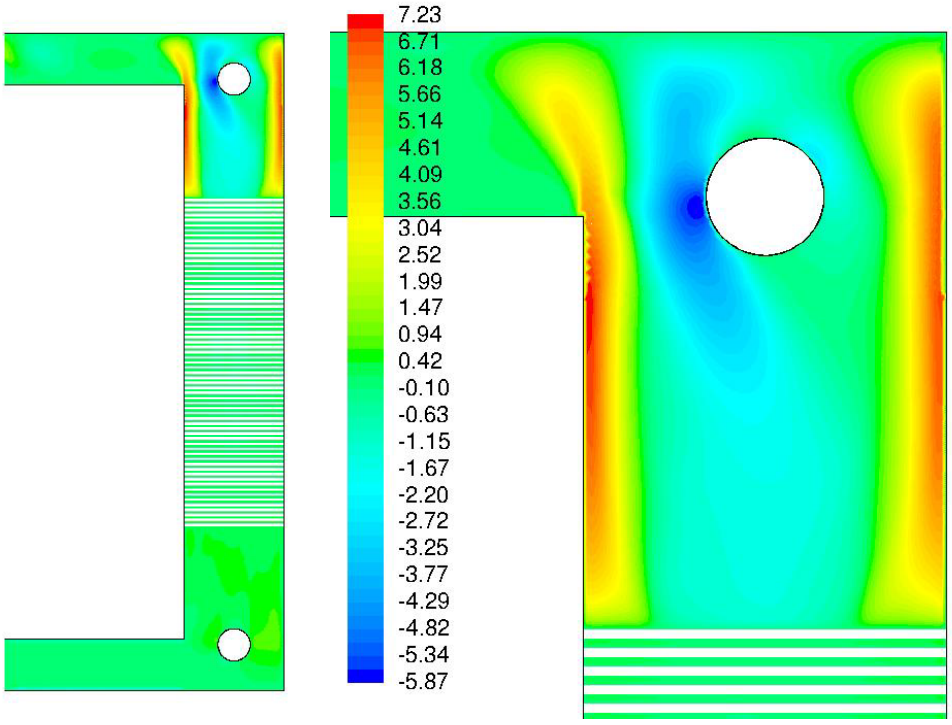

Figure 17: Velocity Profiles at OTM tube cross section

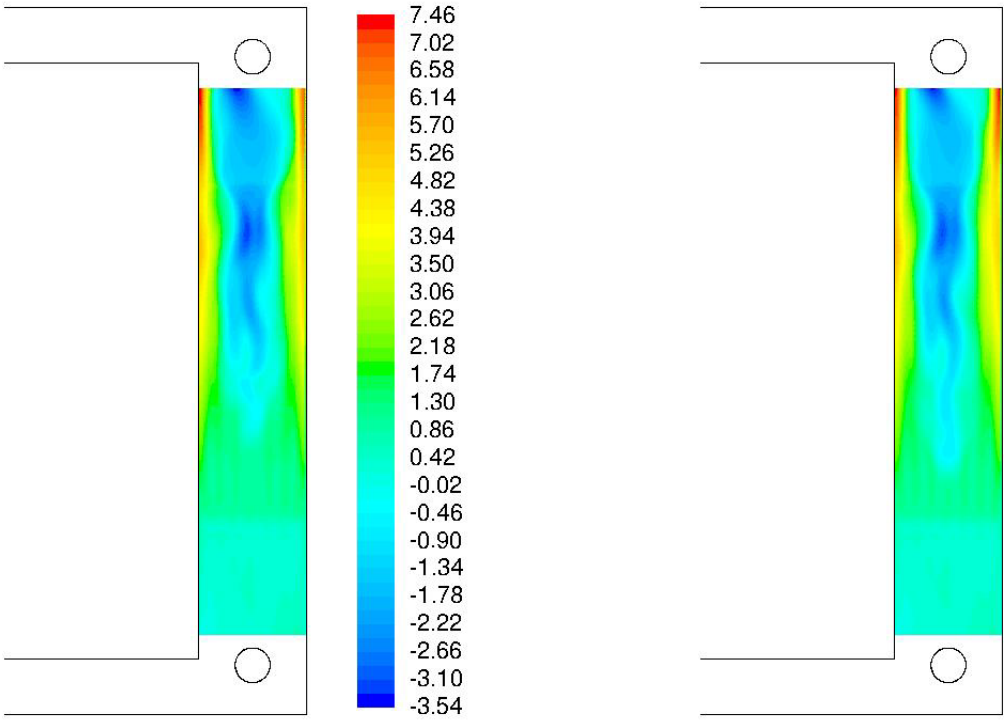

Figure 18: Velocity Profiles in between OTM and Steam Tubes

The model predictions suggested changes in the design such as the addition of screens and baffles to induce the velocity profile in the syngas duct to be more uniform. In principle, the flow direction of the syngas could be reversed so that cooled gas with higher density would be induced to flow in the direction of the bulk syngas flow. Additionally, the design was modified to have staggered OTM tubes rather than tubes in a straight vertical line. This should result in more fuel mixing and more uniform temperature and velocity profiles. Figure 19 shows a close-up vector plot of the recirculation region at the transition to the syngas exit duct. This region of the duct has much flow instability and the sharp edge at the right-angle turn of the duct further effects the distribution of the OTM section of the duct. A chamfered edge and potentially turning vanes have been proposed for this section of the duct.

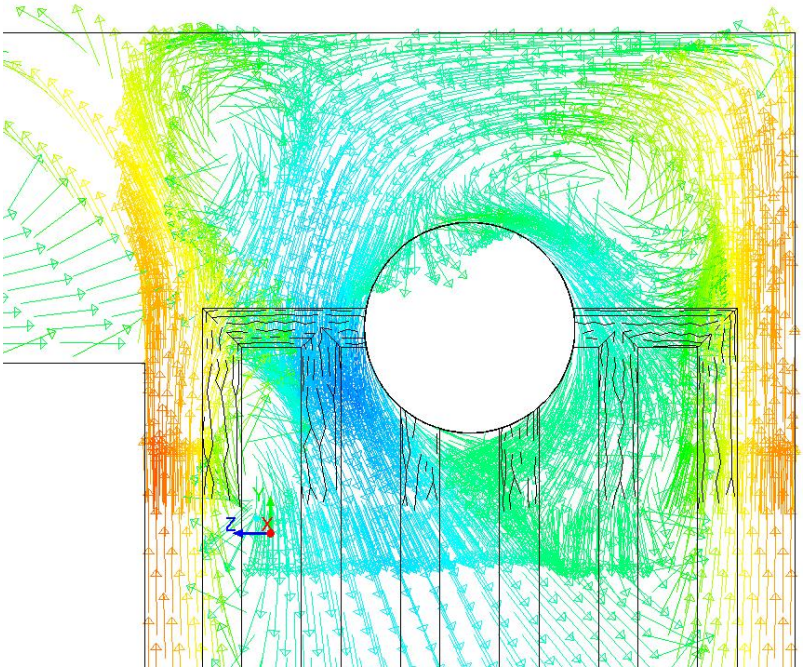

Figure 19: Velocity Profile showing recirculation region at the top of the module

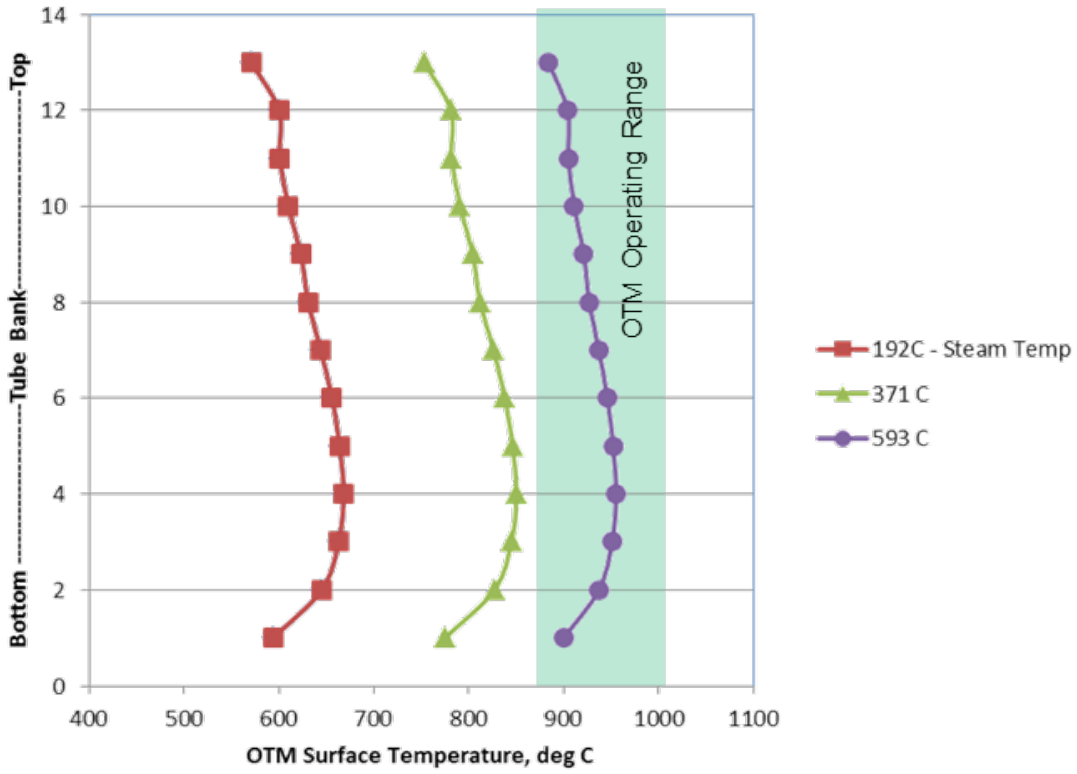

Figure 20: Predicted OTM temperatures as a function of steam temperature

Discussion of Results

The main purpose of the CFD calculations was to ensure that the module geometry and the OTM/steam tube layout were adequate to accommodate the required heat transfer. Since the steam tubes are at a constant temperature and the heat flux from the OTM tubes is specified, the model is solving for the OTM surface temperatures. Since the OTM tubes must be within a given temperature range (~875-1025°C) to operate effectively, the solution of the OTM surface temperatures is a good indicator of whether or not the geometry is adequate. If the temperature of the OTM tubes is calculated to be low, this implies that the steam tubes are creating too large of a heat sink which would render the OTM membranes in the reactor inoperable. If the temperatures on the OTM tubes are calculated to be too high, this implies that there is not

enough heat being removed by the steam and the OTM membranes would be at risk of exceeding a safe design temperature.

Due to these considerations, the module geometry was modeled at three steam temperatures. The pilot scale 7.5 MWth boiler was designed to produce low temperature steam (~450 °F) as compared to the full scale Advanced Power Cycle which produced high temperature supercritical steam (~1100°F). The low temperature steam assumed in the pilot unit simplified the steam design and removed complications of a supercritical steam cycle since the purpose of the pilot is to focus on demonstrating OTM and not a steam cycle. However, the design for the pilot unit was used as a reference for scale-up to the full Advance Power Cycle which would require high steam temperature. It is important to understand the effects that the steam temperature would have on the module geometry and tube layouts within the geometry.

The results in Figure 20 show that for the pilot scale unit with low steam temperature the predicted OTM tube temperatures are too low. They need to be above 875 °C for good flux performance. This implies that the designed module geometry is not sufficient for the low steam temperature. This is because there is not enough OTM area relative to steam tube area and that the low steam temperature provides too much of a radiative heat sink for the OTM tubes. To fix this problem, the OTM/steam area would need to be increased. An initial investigation was conducted whereby the number of steam tubes in each row was reduced. At low steam temperatures, there was low sensitivity of OTM temperatures to this change and adequate performance was not achieved with this method. However, if the steam temperature is higher (1100°F/539°C), Figure 20 shows that the OTM tubes are well within their operating range. This shows that the current module design will be adequate for the full-scale implementation of the Advanced Power Cycle which produces supercritical steam above 1100

°F. Since the purpose of the pilot design was to provide a scalable module for the full-scale system, the geometry was not modified further as part of this phase to accommodate lower steam temperatures. For a pilot system were low steam temperature is still desirable, modifications to the steam and OTM tube arrays may be made to adjust OTM temperatures into their required operating range.

Equipment Description

The OTM Boiler System is comprised of the following equipment:

(1) OTM Boiler Modules: There are eight (8) boiler modules. Each module consists of six hundred fifty (650) OTM tubes and fifty-four (54) 2.375" O.D. steam tubes. The OTM tubes are 1 meter long (effective) and the steam tubes are 3.25 meters long (effective). The eight (8) modules are designed to draw 50 tpd of O_2 across the OTM membranes by combusting a low pressure syngas and using the heat released to generate steam (from BFW at a 25/1 liquid/vapor ratio) to be fed into the steam drum. The absorbed steam duty is 7.66 MW.

(2) Oxy Combustion Fired Heater: The Oxy Combustion Fired Heater is a fired heater consisting of a radiant section (vertical cylindrical), a horizontal overhead convection section, three (3) floor burners and an Induced Draft (ID) fan. The remaining un-burnt fuel from the OTM Boiler is further combusted with oxygen (supplied from the ASU) in the radiant section via the floor burners. The radiant section has thirty-two (32) 4.5" O.D. steam generation tubes on 8" center-center spacing. The convection section is comprised of an Economizer and Steam Superheat banks. The Economizer bank has one (1) row of finned tubes (3.5"O.D) with 8 tubes across on six (6) inch spacing. The Steam Superheat bank has

two (2) rows of bare (shock) tubes (3.5" O.D.) and ten (10) finned rows of tubes (3.5"O.D) with 8 tubes across on six (6) inch spacing. The furnace draft will be provided by an ID fan. The draft is controlled by an inlet box damper (normally at a draft of 0.1 to 0.2 inches H_2O below the convection tube banks). The ID fan is sized at a flue gas flow rate 120% over the controlling case. The overall furnace efficiency is 88%.

(3) Steam Drum for OTM Boiler: The steam drum capacity is based on required steam production rates as well as liquid level process control within the drum. The change in steam drum liquid level is based on maximum steam make plus blowdown. The holdup time from normal liquid level to empty is 5 minutes. The steam drum blowdown is taken to be 1.0 percent of the BFW fed to the steam drum. The continuous and intermittent blowdown lines will be sized for 5.0 percent of the BFW rate to the steam drum. The steam drum is designed in accordance with ASME section VIII Division I.

(4) Duct Burner System for OTM Boiler: A duct burner combustion grid system is supplied to pre-heat the air for the OTM tubes in the boiler. During start-up the duct burners will supply enough heat to raise the air stream temperature from ambient to 1832°F (1000°C). Once initial reaction is achieved the burners are used to raise the air preheated temperature from 1180°F to 1400°F. The design fuel for the burners will be natural gas. The design duty is 13.2 MMBtu/hr (120% of Start-up).

(5) Air Preheater for OTM Boiler: An air preheater is supplied to heat the ambient air for reaction with the low pressure Syngas using superheated oxygen depleted air exiting from the OTM tubes. The design duty is 8.357 MMBtu/hr.

(6) Ambient Air Fan Compressor for OTM Boiler: A centrifugal air compressor is provided to supply ambient air at a maximum pressure of 20 psia. The compressor is sized for 120% flow rate for the controlling case.

3D Models of OTM Boiler Pilot Unit

Figure 21 through Figure 24 show 3-dimensional renderings of the entire OTM boiler pilot unit. These models were used in determining process and equipment layout. In addition, the models were used to aid in the cost estimate by determining quantities and sizes for piping, ducting, and supporting infrastructure.

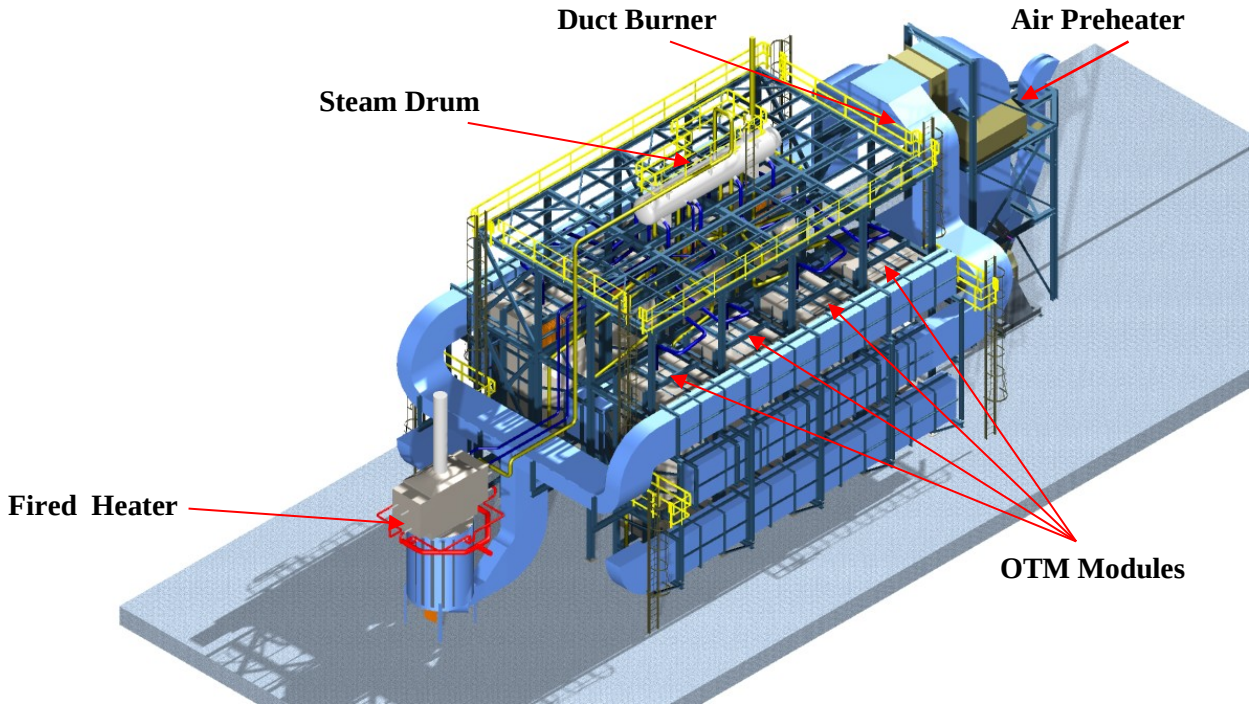

Figure 21: Isometric view of boiler assembly. (Approximately 110'x45'x45')

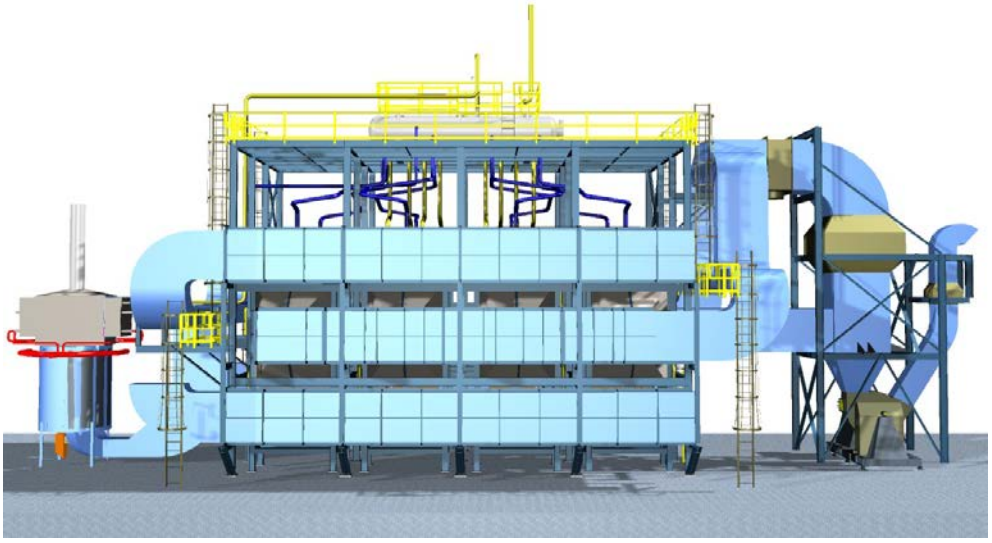

Figure 22: Side Elevation View of OTM Boiler

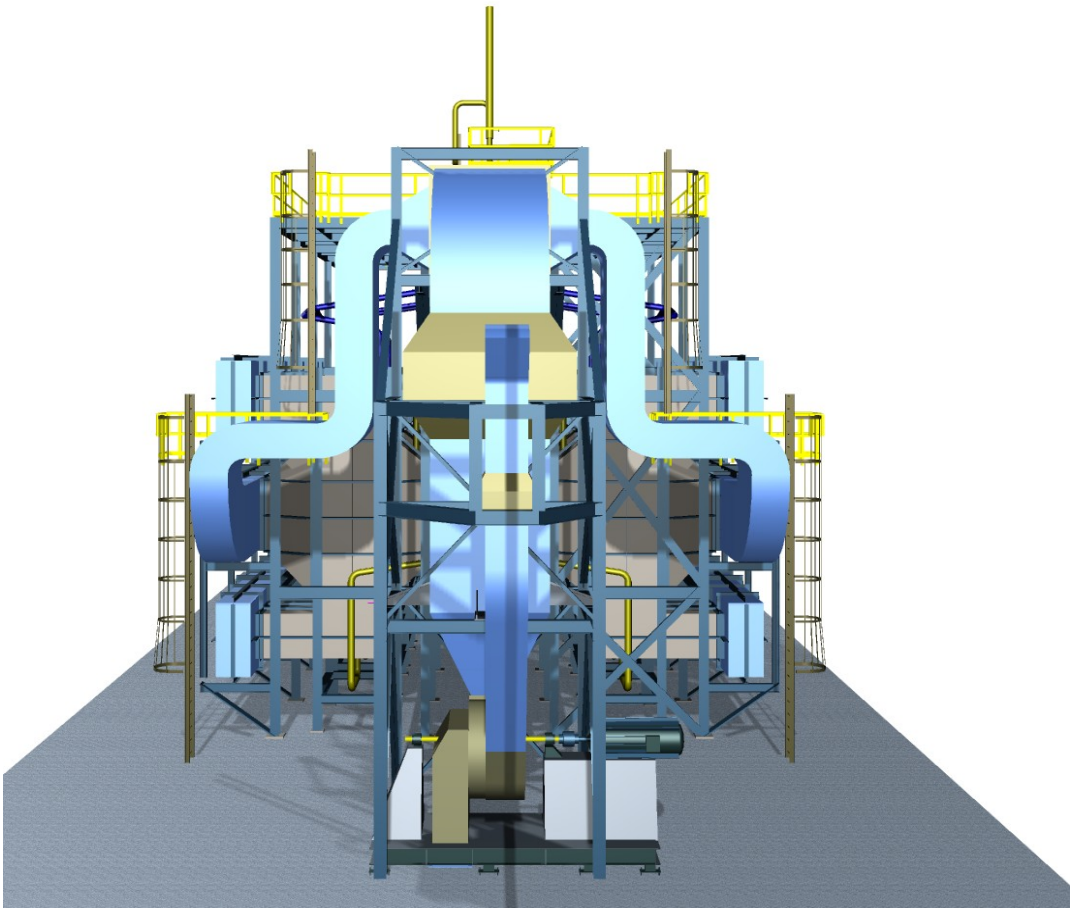

Figure 23: End Elevation View of OTM Boiler

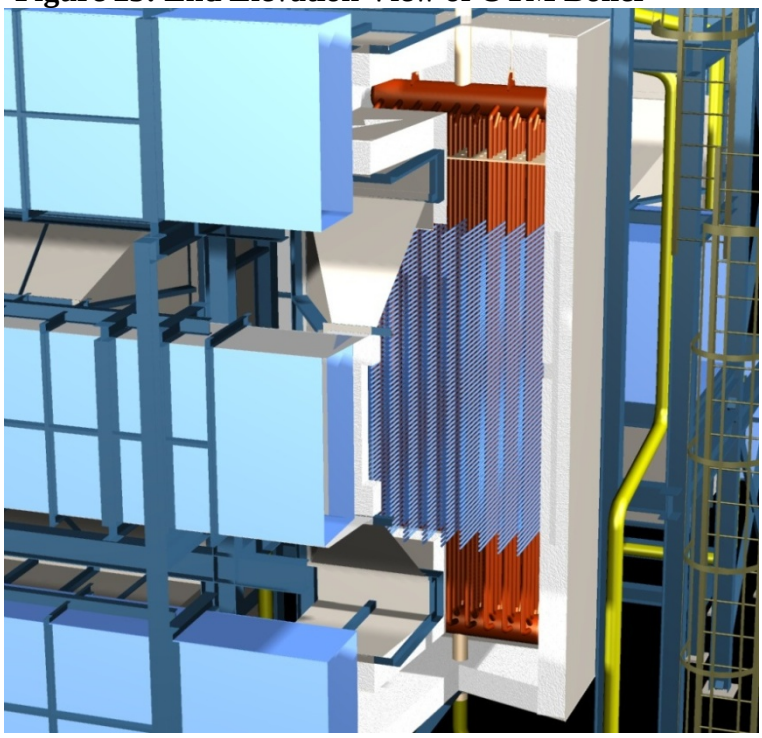

Figure 24: Sectional View of OTM Boiler Module within Assembly

Major Equipment Capital Cost Estimation

ESTIMATE BASIS: A total installed cost estimate was compiled for the OTM boiler based on the following:

Estimate Validity: Instantaneous (Escalation is EXCLUDED)

Currency: All costs were generated and expressed in equivalent US Dollars.

Engineering Documentation: Process data sheets for the major equipment/components of the boiler were generated and sent to vendors for quotation.

Drawings of the boiler module were generated for the concept selection study. The selected concept was developed further in detail and drawings were sent to fabrication specialists for pricing.

The 3-D model created to aid in the conceptual design of the OTM boiler module was also used to develop the made-to-order (MTO) documentation for the generation of the bulk material (such as piping and steel) for the cost estimate. The OTM boiler for this project consists of eight modules along with auxiliary equipment, a structural frame and interconnecting piping. The 3-D model is used to layout and prepare the take-off for the steelwork required for the modules and balance of structural steel and plate work. For the estimate the module steel is not included in the MTO as it is already included in the fabricated module cost. The balance of the steel, such as interconnecting ductwork, support frame, and platform, grating, handrail, and ladders are included in the MTO.

In addition to the steel, interconnecting piping is modeled from the modules to the steam drum and to/from the fired heater. All large bore piping is modeled and included in the MTO. Small bore piping is factored from the large bore piping.

The air ducts are refractory lined. The calculated volume of the refractory is provided for in-house estimating. The steel and piping MTO's are provided for in-house estimating.

Process control and instrumentation input to the cost estimate is provided.

Estimate Methodology: Equipment costs are vendor quotations for the OTM Boiler Module, Oxy-Combustion Module, Air Blower and ID Fan (92% of total), Client Estimate for the Air Preheater (3% of total), Engineering Estimate for the Boiler Duct Burner based on a previous vendor quotations (2% of total), and In-House-Estimates for the balance (3% of total).

The Bulk Material costs are developed using the engineering provided MTO and cost for instrumentation, MTO's for structural and piping, and the balance of bulk material quantities and costs using the FACES Shaw proprietary factored estimating system.

Freight is included at 8% of equipment costs and 4% of bulk materials except civil. Construction spares are included at 1.5% of equipment cost.

Home Office Services: These costs are developed using 1,500 workhours per equipment piece at $100 per workhour.

Construction: Direct workhours are developed using the FACES proprietary estimating system. Construction costs are developed using $95 per workhour as an all-in rate. Vendor servicemen required during construction are added at $0.50 per direct workhour.

Contingency: Contingency is not included.

Exclusions: Items not included in the cost estimate are the ceramic OTM tubes, commissioning, taxes, owner's cost, land cost, and permitting.

Cost Summary

The cost estimate for the 7.5MWth boiler is as detailed below (in thousand U.S. dollars):

Table 29: Pilot Boiler Cost Estimate Summary

	Equipment Cost M$	Bulk Material Cost M$	Construction Cost M$	Engineering Cost M$	Freight / Other M$	Total M$
7.5 MW Boiler	3,131	2,666	3,277	2,100	532	11,706

Other is: Vendor representatives, spare parts

The equipment cost breakdown can be detailed as follows (in thousand U.S. dollars)::

Table 30: Pilot Boiler Cost Detail

No.	Description	Quantity	Cost M$	Type	Estimating Methodology
APH-1	Air Preheater	1	85	Regenerative	Praxair
B-01	Duct Burner	1	75		Vendor Quote
C-1	Air Blower	1	117		Vendor Quote
D - 1	Steam Drum	1	90		Estimating Model
E-01	OTM Modules w/o membranes	8	2,280		Vendor Quote
F-01	ID Fan	1	34		Vendor Quote
H-1001	Fired Heater	1	450	Oxy-combustor	Vendor Quote

OTM POx Units

The purpose of the study was to design a 5 TPD (of O_2 fluxed) Partial Oxidation (POx) Unit, Syngas Expanders and all necessary interconnecting piping on a platform grid.

Alternative Power Cycle with Low Pressure Pox

The low pressure Pox process is shown below in Figure 25.

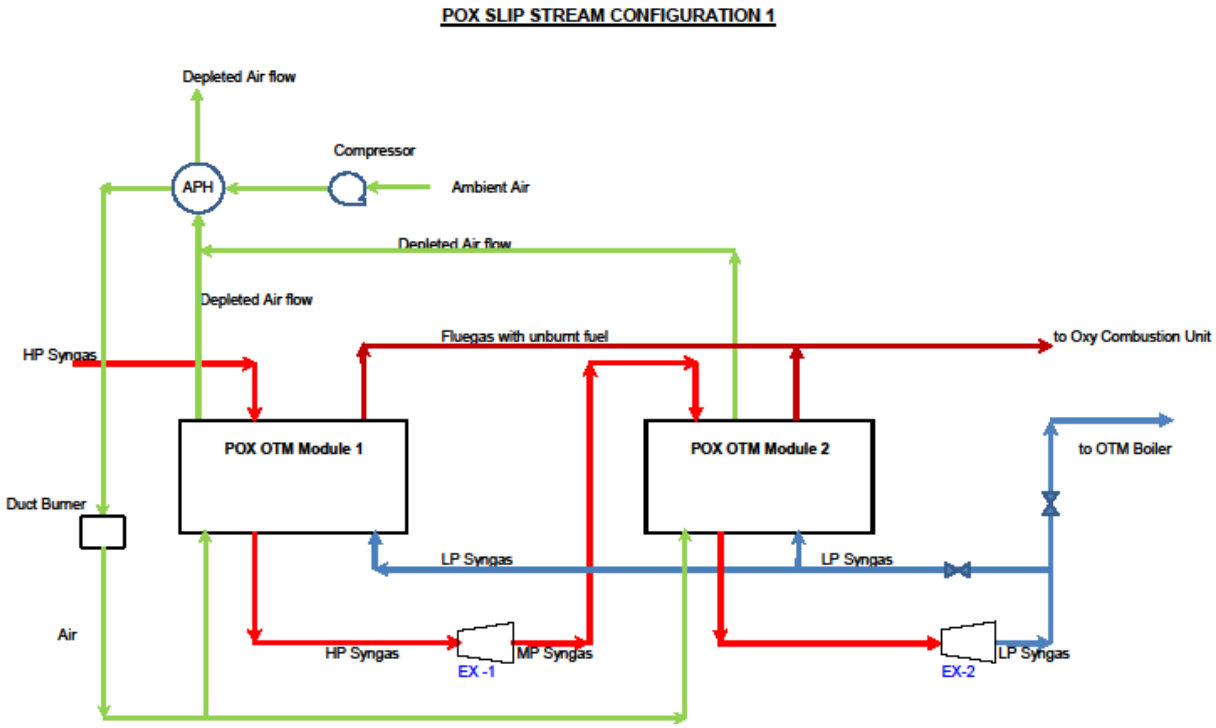

Figure 25: Low Pressure POx Process

The high pressure syngas is heated (in metallic tubes) by the reaction of low pressure syngas and the oxygen permeating across the membrane of the OTM tubes in two (2) stages of POx Units. After each stage the high pressure syngas is fed through an expander to recover energy. After the second stage the syngas is reduced in pressure to become low pressure syngas that is used as fuel for the Stage 1 & 2 POx Units and the OTM Boiler. The low pressure syngas

(after the 2nd stage POx Unit) is split into two (2) streams. The first stream is diverted back to the POx Units for heating the high pressure syngas and the second stream is fed to the OTM Boiler for heating the boiler feed water.

Design Basis and Assumptions

Design Conditions/Assumptions

Table 31: POx Process Design Basis

5 TPD POx Design Basis		
Air Inlet Temperature	F	60
Air Pressure to OTM	psia	20
Relative Humidity	%	80
Atmospheric Pressure	psia	14.7
Air Preheat to OTM	F	1400
High pressure Syngas Temperature	F	1000
High Pressure Syngas Pressure	psia	325
Target 2nd Stage Outlet Temperture	F	1742
OTM Operating Temperature	F	1832

Table 32: Assumed Syngas Feed to POx Units

	Base Case (mol%)	Range (mol%)
H_2	29.9	14.0 – 29.9
CO	50.3	12.0 – 50.3
CH_4	3.3	2.7 – 3.3
CO_2	4.3	4.3 - 14.0
H_2O	9.4	9.4 - 20.0
N_2	1.2	1.2 - 37.0
H_2S	0.8	0.0 – 0.8

Concept Development

Option Selection

The original scope of the project included two separate POx units, a low gas pressure (approximately 50 psig) and a high gas pressure design (approximately 325 psig). It was determined that the higher pressure would govern the design concept. Three separate concepts were developed for consideration and are shown in the appendix. However, after review and discussion on the constraints related to the OTM structure, it was deemed that the original design considerations for high pressure gas could not be accommodated. The areas of concern were:

1.) The porous ceramic structure would need to be of excessive thickness to support high pressure.
2.) The pressure differential between the gas side and air side was too high to realize a cost-effective design for the high-temperature seals and tubesheets separating the two flow streams.

Due to these issues, an alternate process scheme was developed. The resulting process flow is described above. In this scenario, the high pressure gas stream can be heated within available piping components and materials. In this manner, the POx unit can be designed with the same concept as that used for the low pressure OTM boiler. The difference being that the POx unit would have high pressure gas flow inside of the metallic tubes instead of water/steam as in the boiler. Conceptually, this allows for the OTM modules to have the same basic design arrangement as that of the boiler with the major difference being the ratio of OTM area to load tube area.

Equipment Description

The two (2) POx Units are comprised of the following equipment:

(1) Stage 1 and Stage 2 POx Units: Each POx Unit is identical in terms of quantity, diameter and length of tubes (both OTM and HP syngas). Each POx Unit is comprised of five hundred twenty (520) OTM tubes and twenty-eight (28) 2.375" O.D. high pressure (HP) syngas tubes. The OTM tubes are 1 meter long (effective) and the HP syngas tubes are 3.25 meters long (effective). Each module is designed to draw 5 TPD of O_2 across the OTM membranes by combusting a low pressure syngas and using the heat released to heat high pressure syngas. Energy from the superheated high pressure Syngas is recovered for power extraction and further processing in the advanced power cycle using two (2) Gas Expanders (one for each POx unit).

(2) Duct Burner System for POx Units: A duct burner combustion grid system will be supplied to pre-heat the air for initial reaction in the OTM tubes for the POx Units. The duct burners will supply enough heat to raise the air stream temperature from ambient to 1823°F (1000°C). Once the initial reaction is achieved the burners will be used to raise the air preheated temperature from 1276°F to 1400°F. The design duty is 2.65 MMBtu/hr (120% of Start-up). The design fuel for the burners will be natural gas.

(3) Air Preheater for POx Units: An air preheater will be supplied to heat the ambient air for reaction with the low pressure syngas using superheated oxygen depleted air exiting from the OTM tubes. The design duty is 1.511 MMBtu/hr.

(4) Ambient Air Fan Compressor for POx Units: A centrifugal air compressor will be provided to supply ambient air at a maximum pressure of 20 psia. The compressor will be sized for 120% flow rate for the controlling case.

(5) Expanders for POx Units: Each POx unit will be provided with a Gas Expander. Each Expander will provide 624 HP (0.47 MW). The Expander for POx Unit 1 reduces HP syngas pressure by 220 psi (to 101 psig) and the temperature by 357°F (to 1200°F). The Expander for POx Unit 2 reduces HP syngas pressure by 63 psi (to 19 psig) and the temperature by 350°F (to 1392°F).

3-D POx Models

Figure 26 and Figure 27 show 3D models of the entire OTM boiler pilot unit. These models were used in determining process and equipment layout. In addition, the models were used to aid in the cost estimate by determining quantities and sizes for piping, ducting, and supporting infrastructure.

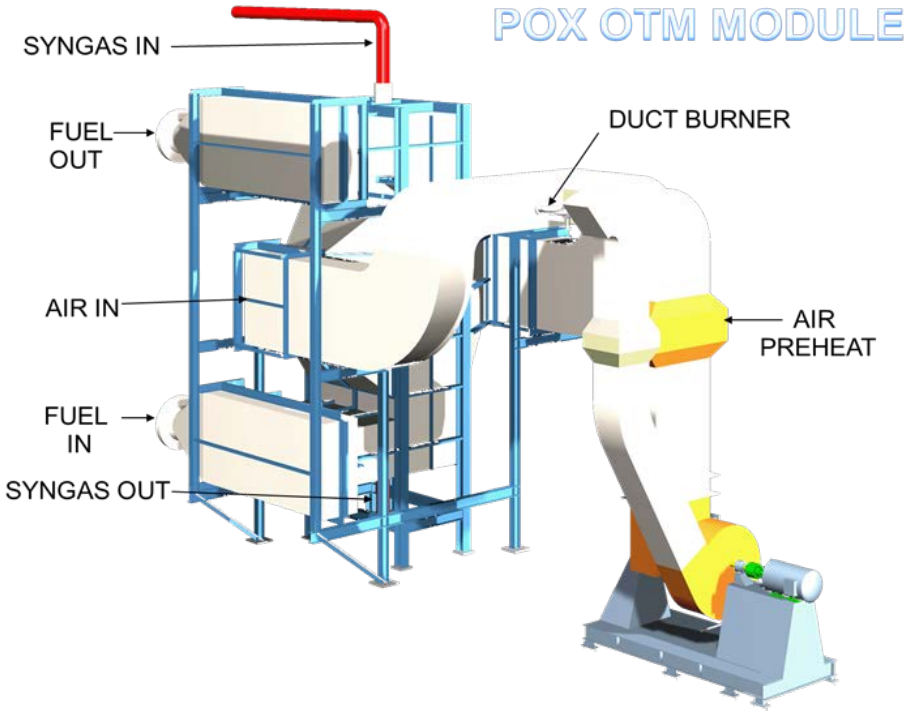

Figure 26: 3d Model of Pilot Scale OTM POx System

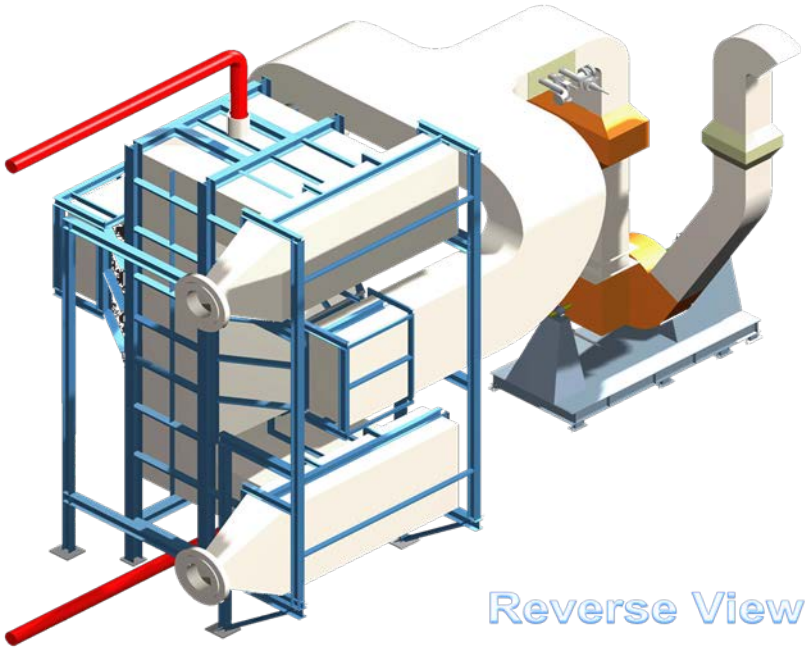

Figure 27: Alternate View of OTM POx System

Capital Cost Estimation

ESTIMATE BASIS: A total installed cost estimate was compiled for the POx unit based on the following:

Estimate Validity: Instantaneous (Escalation is EXCLUDED)

Currency: All costs were generated and expressed in equivalent US Dollars.

Engineering Documentation: Process data sheets for the major equipment/components of the boiler were generated and sent to vendors for quotation.

Drawings of the POx module were generated for the concept selection study. The selected concept was developed further in detail and drawings were sent to fabrication specialists for pricing.

A 3D model was created to aid in the conceptual design of the POx module. This model was also used to develop the MTO for the generation of the bulk material (such as piping and steel) for the cost estimate. Each POx unit consists of one module along with auxiliary equipment, a structural frame and interconnecting piping. The 3D model is used to lay out and prepare the takeoff for the steelwork required for the modules and balance of structural steel and plate work. For the estimate the module steel is not included in the MTO as it is already included in the fabricated module cost. The balance of the steel, such as interconnecting ductwork, support frame, and platform, grating, handrail, and ladders are included in the MTO.

The air ducts are refractory lined. The calculated volume of the refractory is provided for in house estimating.

Process control and instrumentation input to the cost estimate is provided.

Estimate Methodology: Equipment costs are from vendor quotations. The Bulk Material costs are developed using the engineering provided MTO and cost for instrumentation, MTO's for structural and piping, and the balance of bulk material quantities and costs using the FACES Shaw proprietary factored estimating system. Freight is included at 8% of equipment costs and 4% of bulk materials except civil. Construction spares are included at 1.5% of equipment cost.

Home Office Services: These costs are developed using 1,500 workhours per equipment piece at $100 per workhour.

Construction: Direct workhours are developed using the FACES proprietary estimating system. Construction costs are developed using $95 per workhour as an all-in rate. Vendor servicemen required during construction are added at $0.50 per direct workhour.

Contingency: Contingency is not included.

Exclusions: Items not included in the cost estimate are the ceramic OTM tubes, commissioning, taxes, and owner's cost

Cost Summary

The cost estimate for the 5 tpd O_2 POx pilot unit is as detailed below in Table 33 and Table 34 (in thousand U.S. dollars):

Table 33: OTM Pilot POx unit Cost Summary

	Equipment Cost M$	Bulk Material Cost M$	Construction Cost M$	Engineering Cost M$	Freight / Other Cost M$	Total M$
5tpd POx	720	811	1,074	750	142	3,497

Table 34: OTM Pilot POx unit Equipment Cost Breakdown

No.	Description	Quantity	Cost M$	Type	
APH-2	Air Preheater POx	1	38	Regenerative	Praxair
B-02	Duct Burner Pox	1	37		Vendor
C-2	Air Blower POx	1	75		Vendor
E-02	POx Module	1	285		Vendor

Conclusions:

The pilot boiler and POx unit design effort with Shaw Energy and Chemical resulted in several key findings. First, the selected design concept was among the simplest configurations considered. More complex arrangements did not offer increased value in the highly-weighted areas of safety, flexibility, and scalability, and generally added risk to a successful future execution. For the POx design effort, this proved to be decisive in that the conventional tube and shell design concepts were abandoned due to the challenges presented by high temperature and pressure seals and flow separators required. An innovation with the configuration of the POx units in the APC flowsheet allowed for low pressure operation of the OTM and a common design arrangement for both boiler and POx units. This common approach will generally lead to some economy and integration advantages at the powerplant level. While the changes to the POx units affected the economics of the APC somewhat, the overall result is an approach to the POx units that is more realistic and viable for the future. Secondly, with the addition of staggered tubes and baffling, the design approach to the boiler was determined to be qualified for generation of ultra-supercritical steam, but as steam temperature requirements are lowered enabling pilot-scale investigations, modifications will need to be made to the steam tube and OTM tube array. These challenges are manageable and will be addressed in context of the projects Phase III scope.

2.2. Task 2: OTM Performance Improvement.

In the 1998 – 2003 time frame, OTM architectures consisted of unsupported single phase perovskite materials and during that time, ceramic membrane failures were prevalent during heating, cooling, thermal cycling, and changes in fuel composition. These failures were

considered to be caused in part to mechanical strength deficiencies and to chemical and thermal expansion mechanisms associated with the single phase pervoskites that were utilized.

Under an NETL program (Advanced Oxyfuel Boilers and Process Heaters for Cost-Effective CO2 Capture and Sequestration – DE-FC26-01NT41447) that began in 2002, a number of design modifications were implemented that offered significant improvements in strength and reliability. A combination of dual-phase layers and the addition of a porous ZrO_2 support were implemented. By the end of NETL project in 2007, the OTM architecture consisted of a dense dual phase gas separation layer for oxygen ion transport, a porous dual-phase fuel oxidation layer (anode) located adjacent to the gas separation layer, a porous dual-phase oxygen incorporation layer (cathode) located adjacent to the gas separation layer and the air to promote rates of oxygen reduction, and a robust porous support located adjacent to the fuel oxidation layer (anode). This architecture is illustrated in Figure 28

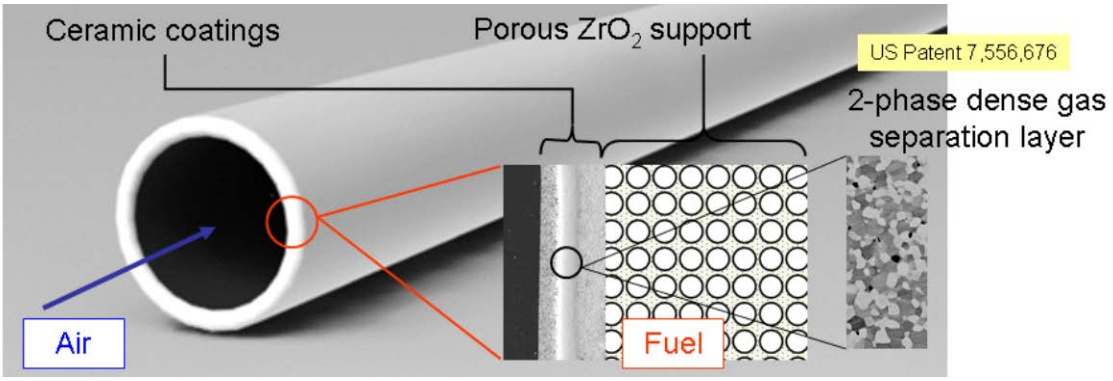

Figure 28: Image of OTM Tube and Illustration of Multilayer, Multifunctional Architecture

With this material set, the failure rate dropped to near zero in laboratory scale, single tube reactors. However, while the reliability of the system improved dramatically, the oxygen

flux performance suffered. Techno-economic analyses indicated that a performance improvement of at least 2X was required to achieve economic targets.

Task 2 of this program focused on achieving at least 2X performance improvement while maintaining material strength and material reliability. At the beginning of Phase I, standard OTM materials were available that were considered to have a good probability of meeting reliability targets but were limited in terms of oxygen flux performance. The fuel oxidation layer and the porous support were identified as rate limiting steps to OTM oxygen transport, and therefore the majority of effort was placed on improving those components. Efforts to reduce the mass transfer resistance of the porous support led to the identification and integration of the ENrG "advanced" substrate technology. Work on the ENrG "advanced" substrate technology was performed by ENrG Inc. in a NYSERDA program under agreement number 10080. Efforts to improve OTM fuel oxidation rates led to the development of an "advanced" fuel oxidation layer material. Figure 29 shows typical normalized performance levels measured on laboratory scale OTM tubes when implementing the "advanced" porous support and the "advanced" fuel oxidation layer, where performance levels are normalized to the performance measured on OTM tubes prepared with the standard materials set. Laboratory scale OTM tube tests demonstrated performance improvement of typically > 3X when implementing both of the advanced materials, as shown in bar 4 of Figure 29. When the improved performance values were fed back to the process and systems engineering task it was shown that the OTM process met the DOE requirements for economics of a power cycle with CO_2 capture and compression.

OTM tubes prepared with the "advanced" substrate were shown to be less robust than tubes prepared with the "standard" substrate technology and less able to meet mechanical

property requirements, especially when operating in the aggressive conditions of the partial oxidation unit, which includes high pressure differentials across the tube. However, under the less aggressive conditions of the advanced boiler unit, which operates at ambient pressure, the "advanced" substrate technology was considered to offer sufficient strength and reliability. Characterization of the oxygen flux of OTM tubes prepared with both generations of support was conducted and reported upon within task 4 of this program. In Phase II and Phase III, focus was placed on developing OTM tubes that could operate in aggressive conditions, and efforts shifted towards implementation of OTM tubes with a "standard" substrate and the "advanced" fuel oxidation layer, where typical performance levels when operating with this set of materials are shown in tube 3 of Figure 29.

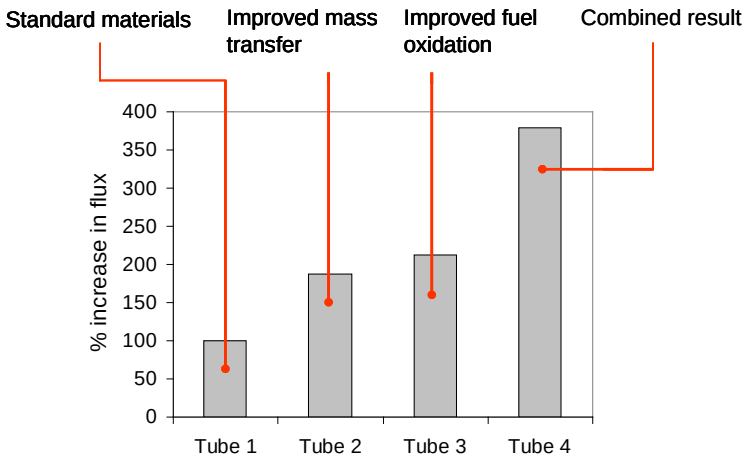

Figure 29: Relative membrane performance for OTM tubes, combining improvements in porous support and fuel oxidation (Tube 1: Standard support, Tube 2: Improved support, Tube 3: Improved fuel oxidation, Tube 4: Improved support & Improved fuel oxidation).

2.2.1. Subtask 2.1 OTM Performance Improvement Plan

A performance improvement plan was developed that involved independently measuring the contribution of each component (porous support, gas separation layer and activation layers) on overall performance. The independent tests used to evaluate each component were 1)

diffusivity measurements for the porous support, 2) blocking electrode measurements for the gas separation layer, and 3) electrochemical impedance measurements for the oxygen incorporation and fuel oxidation activation layers. These tests will be described in the subtask 2.2 – 2.4 sections of this report. An OTM model was developed that enables prediction of overall oxygen flux and fuel utilization – the main performance indicators – as a function of the component level capabilities as determined from independent tests. This model also computes the efficacy of each component and ranks the components in terms of their contribution to overall performance losses. The component properties of an OTM prepared with the standard materials as of the start of the program were input into the model and the model ranked the components in order of their contribution as a performance limitation.

Referring back to the Advanced Power Cycle described in Subtask 1.1, there are two regimes of interest 1) OTM Boiler conditions (low pressure, high fuel utilization > 70%) and 2) OTM POX conditions (high pressure, low fuel utilization < 30%). The components were ranked for each regime, and the results from those rankings are illustrated in Figure 30

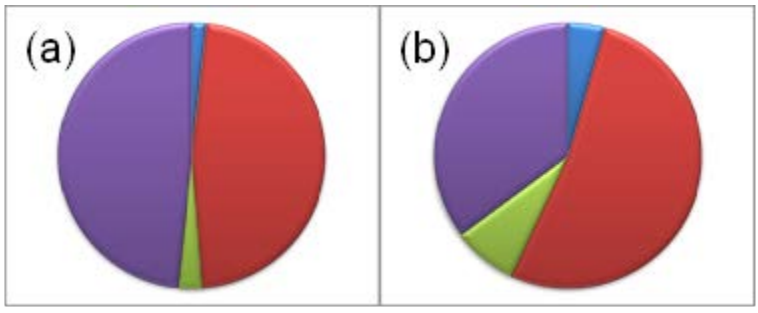

Figure 30: Contributions of OTM components to performance limitations within the standard material set (a) Boiler conditions, (b) POX conditions. Purple = Porous Support, Red = Fuel Oxidation Activation Layer, Green = Gas Separation Layer, Blue = Oxygen Incorporation Activation Layer

Figure 30 shows that under both sets of conditions the components in the OTM system were ranked in terms of their contribution to performance limitations as follows 1) Fuel Oxidation Layer, 2) Porous Support, 3) Oxygen Incorporation Activation Layer, and 4) Gas Separation Layer. The fuel oxidation layer and the porous support were predicted to have an almost equivalent large effect on overall performance, and the oxygen incorporation activation layer and gas separation layer were predicted to have an almost equivalent small effect on overall performance in the OTM boiler regime.

Advanced material sets for both the porous support and fuel oxidation layer were then developed and implemented, as discussed in the subtask 2.2 and subtask 2.4 section of this report. The performance properties of the advanced materials were measured independently and input into the OTM performance model where the contributions of each component to overall performance limitations were again predicted, as shown in Figure 31. Figure 31 indicates that the integration of the advanced porous support and advanced fuel oxidation activation layer will create a situation where the oxygen incorporation layer and gas separation layer will also impact the overall performance. The performance improvement plan was then expanded to include further investigations of the gas separation layer and the oxygen incorporation activation layer, as described in the Subtask 2.3 and Subtask 2.4 section of this report.

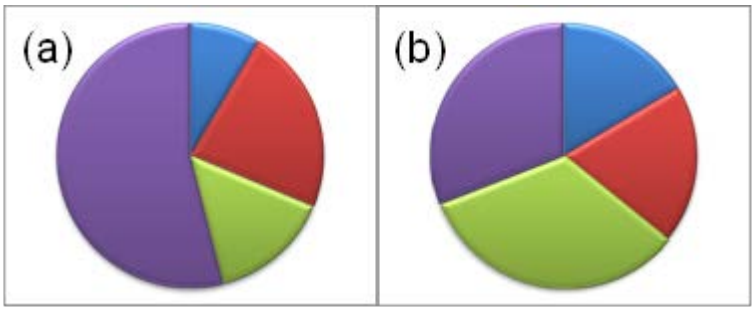

Figure 31: Contributions of OTM components to performance limitations within the advanced material set (a) Boiler conditions, (b) POX conditions. Purple = Porous Support, Red = Fuel Oxidation Activation Layer, Green = Gas Separation Layer, Blue = Oxygen Incorporation Activation Layer

2.2.2. Subtask 2.2 Porous Support Structure

The porous support, located between the fuel and the fuel activation layer, provides structural stability to the OTM, and therefore needs to be reliable. However, the porous support also inhibits performance by limiting the transport of gaseous fuel to the active membrane, and therefore needs to be optimized for mass transport capability. The standard porous support technology was considered to meet the reliability goals but fall short of mass transport targets. Therefore efforts were made to develop a support technology with improved mass transport properties that possessed comparable reliability and strength characteristics. Two development routes were pursued. The first route involved formation of porosity by fugitive pore formers that were burnt out during the sintering process. The second route involved implementing an "advanced" substrate technology, a technology that yielded structured pores. Development work on the "advanced" support in disc and tubular form was subcontracted to ENrG, Inc. Measurements performed to characterize the mass transport properties of the porous support

included diffusion coefficient measurements, permeability, SEM analysis, and mercury porosimetry. Measurements performed to characterize the reliability of the porous support included piston on ring strength tests on discs and compression tests on tubes.

In porous media, mass transport can take place by viscous flow, ordinary molecular diffusion or Knudson diffusion. Viscous flow is driven by pressure gradients, and since there is very little pressure gradient expected across the OTM porous support, viscous flow is neglected as a mechanism for gas transport. Ordinary molecular diffusion through a porous media and Knudson diffusion are considered to drive transport through the porous support, and these mechanisms are influenced by porosity, tortuosity and pore size. The porosity to tortuosity ratio, an architectural parameter, is considered the key characteristic driving mass transport, and was used as a metric for selecting porous support candidates throughout this program. A diffusion apparatus was used to measure the porosity to tortuosity ratio and the average pore size of porous support candidates. In the diffusion apparatus, at room temperature and atmospheric pressure (no pressure difference across the sample), a porous support disc or tube was placed in a gradient between air and nitrogen. Oxygen diffused from the airside to the nitrogen side. The oxygen flux was computed from the oxygen mass balance in the experiment and the effective diffusion coefficient of oxygen was calculated from the oxygen flux, porous support thickness and concentration gradient. The ratio of this effective diffusion coefficient and the molecular diffusion coefficient of oxygen in nitrogen yielded the porosity over tortuosity ratio of the porous support.

Several porous support candidates were considered and evaluated in disc form, prepared with the “standard” support technology and with the “advanced” support technology. Variations made to the porous support prepared with the “standard” support technology

included changes to the type and size of pore former, and changes to the volume fraction of pore former. Figure 32 shows the normalized porosity to tortuosity ratio of several candidate materials. The porous supports prepared with the ENrG "advanced" substrate technology had the highest porosity over tortuosity ratio, exceeding the target. A support prepared with the "standard" technology in disc form approached the target. Although the "Standard C" support approached the target, the porous support material "Standard B" and the porous support material "ENrG Advanced Support A", were selected for further evaluation, based on surface qualities that would enable coating and an initial evaluation of robustness.

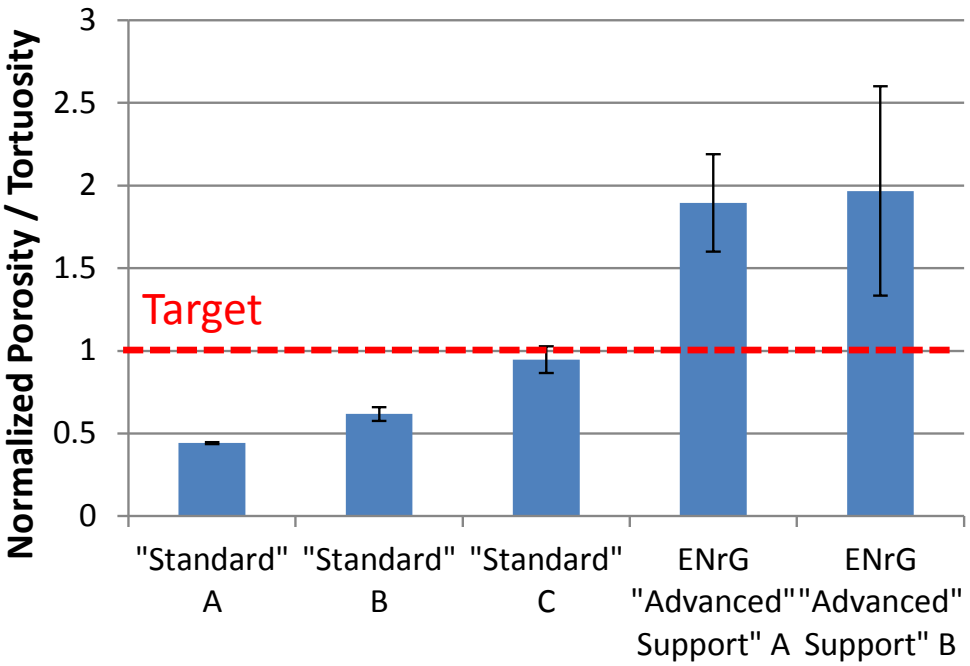

Figure 32: Normalized porosity over tortuosity ratio for three types of porous supports prepared with variations of the "standard" support technology, and two porous supports prepared with variations of the "advanced" support technology

Oxygen transport membranes were fabricated with supports prepared with the "standard" and "advanced" technologies in disc form, in order to measure performance values. Normalized oxygen flux values are reported in Figure 33 in CO/CO_2 and H_2/CO_2 fuel

compositions at a temperature of 1000°C. These performance levels were duplicated on several similar discs. The "advanced" porous supports (supports with structured pores) resulted in a ~2X improvement in oxygen flux in the CO/CO_2 gas environment and a ~ 20% improvement in oxygen flux in the H_2/CO_2 gas environment at an operating temperature of 1000°C when compared to OTM disks prepared with the standard support. As discussed in the subtask 2.4 section of this report, the highest performance levels were achieved in the disc reactor when combining the ENrG "advanced" support technology with the "advanced" fuel oxidation layer.

In disc form, the oxygen transport membranes are only able to oxidize about 10% of the fuel, and therefore the performance values are typically higher than those observed in tubular form, where fuel utilization levels of up to 90% can be reached. The oxygen flux targets set in task 1 are contingent on achieving a high fuel utilization level; therefore, even though Figure 33 shows performance levels in excess of the target, this performance level also needs to be demonstrated on OTM tubes which operate at higher fuel utilization levels. Oxygen flux values achieved on OTM tubes prepared with both the "Standard" and "Advanced" support are reported in the task 4 section of this report.

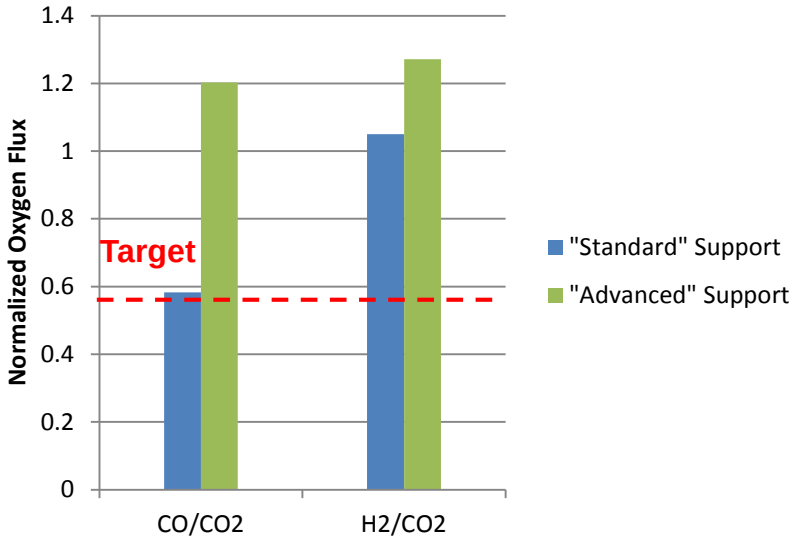

Figure 33: Normalized oxygen flux achieved for OTM discs prepared with "standard" and "advanced" supports in CO/CO2 fuel and H2/CO2 fuel compositions at a temperature of 1000°C.

A Piston on Ring Apparatus was assembled for strength measurements of porous supports discs. Figure 34 shows that the measured strengths of the ENrG "advanced" support and the Praxair "standard" support were comparable in disc form.

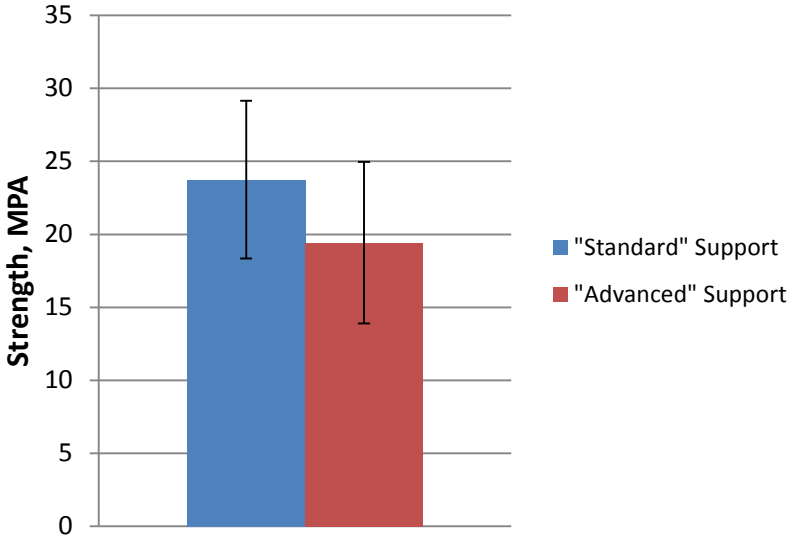

Figure 34: Strength of the Praxair "Standard" Support and the ENrG "Advanced" Support

.

A manufacturing protocol was developed in order to prepare tubes from the ENrG "Advanced" support material, as discussed in the task 3 section of this report. During manufacture of tubes with the "advanced" support, it was observed that a dense skin formed on the outside of the tube. The skin is typically removed by mechanical methods (e.g., grinding, sanding). Mass transport and strength properties were evaluated with the skin intact and with the skin removed. A cold isostatic pressing (CIP) process was put in place to manufacture OTM tubes prepared with the "standard" support. In both development routes, differences between manufacturing techniques used when fabricating discs and tubes yielded tube architectures that differed considerably from their disc counterparts. Mass transport measurements, strength measurements, and oxygen flux measurements were also performed on OTM tubes.

Figure 35 shows the normalized porosity to tortuosity ratio of OTM porous supports in tubular form. The porosity to tortuosity ratio is observed to be approximately 100% higher for tubes prepared with the "advanced" porous supports with the dense skin removed than that observed for the "standard" porous support. The porosity to tortuosity of porous support tubes prepared with the "standard" support technology were approximately 15% less than that of discs prepared with the same material. The porosity to tortuosity ratio of porous support tubes prepared with the "advanced" support technology were approximately 45% less than that of discs prepared with the same material. The OTM porous supports with the dense skin removed were prepared both in the original manufacturing facility and in an upgraded manufacturing

facility. The porosity to tortuosity ratio, as shown in Figure 36, was similar for OTM tubes prepared in both facilities.

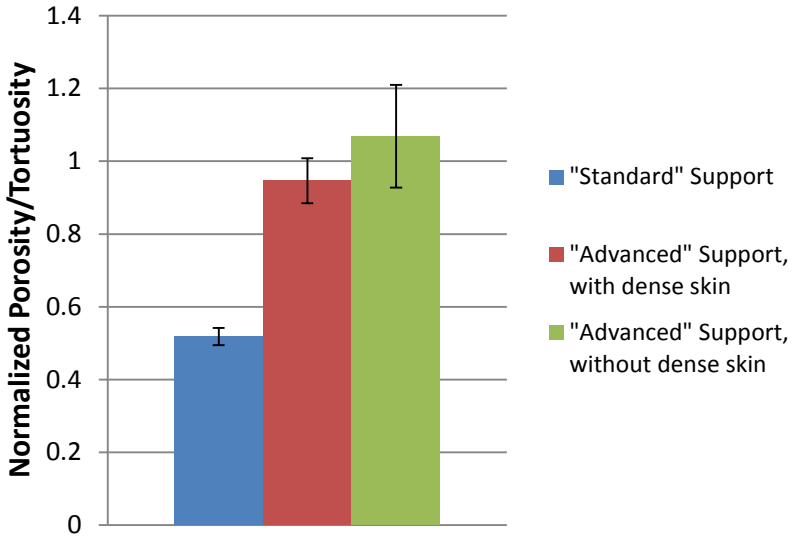

Figure 35: Normalized Porosity/Tortuosity of OTM porous support tubes.

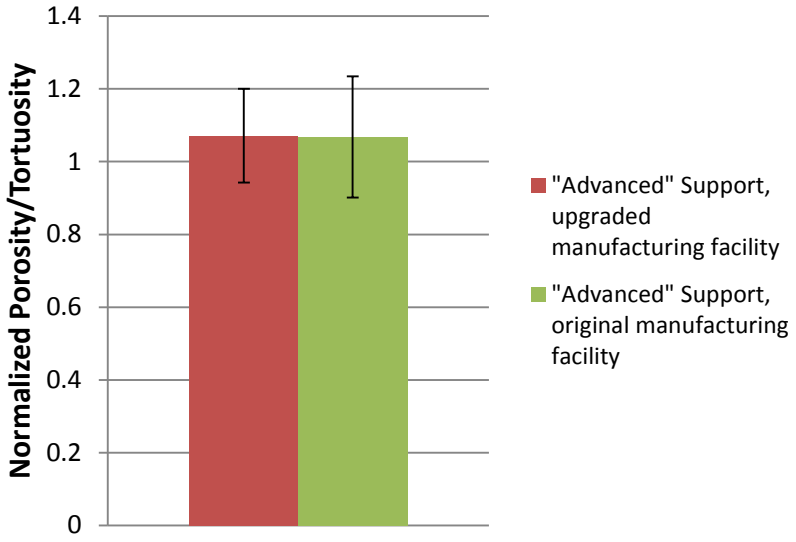

Figure 36: Normalized Porosity/Tortuosity of OTM porous support tubes prepared in the original and upgraded manufacturing facilities.

The strength of three OTM tubes, listed in Table 35, was evaluated by compression between two flat plates. Six sections were cut from three tubes, using a diamond cut-off saw, designated A through F.

Table 35: OTM tubes used in strength testing, including porous support type, tube ID and average wall thickness.

Porous support type	Tube ID	Average wall thickness, mm
"Standard"	6W091508C	1.9
"Advanced" – with skin	PXT 61-2	2.8
"Advanced" – skin removed	PXT 59-4	2.4

The peak compressive force sustainable by each O-ring section was measured and is presented in Figure 37, where the measurements were normalized by the same value of force, to show relative magnitude. For a given tube type, the compressive force increased with the axial length of the O-ring sections. The lack of symmetry in peak compressive force, for a given tube type, could result from variations in wall thickness and/or the presence of tube defects.

The OTM tubes prepared with the "advanced" support (PXT 59-4 and 61-2) exhibited a decrease in the sustainable peak compressive force, compared to the "standard" support (6W091508C). The decrease in strength was more dramatic for the "advanced" porous support which had the skin removed (PXT 59-4). It should be noted that the average wall thickness of "standard" porous support was approximately 2/3 the thickness of the "advanced" porous supports.

Sections A and B of the "advanced" support OTM tube with the skin removed (PXT 59-4) had visible cracks prior to compression testing. The lower than expected peak compressive force of the aforementioned sections is likely attributed to the presence of these cracks. It is unclear whether tube defects (i.e., cracks) were introduced during skin removal or O-ring cross sectioning.

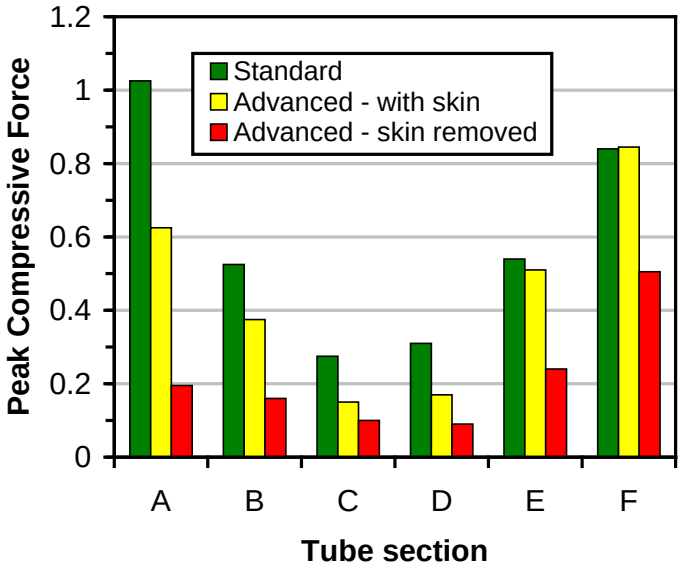

Figure 37: Peak compressive force supported by O-ring sections cut from OTM tubes. Measurements were normalized by the same value of force, to show relative magnitude. The axial length of the O-ring sections was 1" for A and F, 0.5" for B and E, and 0.25" for C and D.

Oxygen flux measurements on OTM tubes prepared with variations in the porous support are presented in the task 4 section of this report. In 2007, OTM tubes were typically prepared with the "standard" support A, in 2008, OTM tubes were typically prepared with the "standard" support B, and in 2009 OTM tubes were typically prepared with the ENrG "advanced" support with the dense skin removed. OTM tubes showed an improvement in overall oxygen flux when implementing the "advanced" porous support technology during ambient pressure tests (Boiler conditions). However, challenges arose when trying to seal and test OTM tubes prepared with the "advanced" support technology at elevated pressure (POx conditions).

Porous support optimization efforts continued into Phase III of this program where focus shifted from the "Advanced" support technology back to the "Standard" support technology which offered a more robust platform for pressurized operation. Improved methods of quantifying strength and reliability were implemented in Phase III, which include efforts to quantify creep mechanisms.

2.2.3. Subtask 2.3 Gas Separation Layer

The gas separation layer, located between the fuel oxidation layer and the oxygen incorporation layer, performs the function of transporting oxygen ions across the membrane from the air-side to the fuel side while preventing the passage of gaseous species. The gas separation layer therefore needs to be optimized for both fast oxygen ion transport and an architecture that lacks pinholes, cracks, or any other defects that could permit gas transport.
Leak targets were established at the start of the program and helium leak rate measurements were used to determine if OTM discs and OTM tubes met leak rate specifications prior to testing. Scanning Electron Microscopy (SEM) and bubble tests were also used to determine the location and nature of damage to the separation layer.

The oxygen ion transport performance of the separation layer is dependent on the separation layer ambipolar conductivity, the separation layer thickness, and the gradient of partial pressure of oxygen across the separation layer. The separation layer ambipolar conductivity can be controlled through material selection and the separation layer thickness can be controlled through manipulation of slurry viscosity or number of applications. The separation layer partial pressure of oxygen gradient is dependent on the operating conditions and the performance of the support and activation layers.

Work in this task focused first on an assessment of the separation layer ambipolar conductivity. A blocking electrode test was developed in order to assess the ambipolar conductivity of the gas separation layer over a range of oxygen partial pressures and temperatures. Table 36 and Table 37 show the ambipolar conductivity values measured over a range of temperatures and gas compositions. Activation energies between 70 kJ/mol and 130 kJ/mol were observed. The separation layer ambipolar conductivity and the separation layer thickness were then entered into the model described in subtask 2.1, and it was determined that the separation layer was not a rate limiting step.

Table 36: Gas Separation Layer Ambipolar Conductivity as a function of temperature

Air		**83% H_2 / 17% CO_2 (PO2 = 1E-16)**	
T (°C)	**σ_{amb}** (S/cm)	**T (°C)**	**σ_{amb}** (S/cm)
800	0.036	800	0.002
850	0.045	850	0.004
900	0.068	900	0.008
950	0.085	950	0.013
1000	0.132	1000	0.021

Table 37: Gas Separation Layer Ambipolar Conductivity as a function of gas composition at 1000°C.

Gas	**σ_{amb}** (S/cm)
83% H_2 / 17% CO_2 (PO2 = 1E-16)	0.021
32.7% H_2 / 67.3% CO_2 (PO2 = 2E-14)	0.026
4.6% H_2 / 95.4% CO_2 (PO2 = 3E-12)	0.031
83% CO / 17% CO_2 (PO2 = 3E-16)	0.023
32.7% CO / 67.3% CO_2 (PO2 = 3E-14)	0.028
4.6% CO / 95.4% CO_2 (PO2 = 3E-12)	0.034

A set of oxygen flux tests were performed on OTM discs with various separation layer thickness as a method to evaluate the impact of the separation layer thickness on performance. The performance of the separation layer is expected to be directly related to its thickness. An OTM disk was fabricated with the standard gas separation layer thickness and an OTM disk was fabricated with a gas separation layer that possessed 50% of the thickness of the standard separation layer. Figure 38 and Figure 39 show the results from oxygen flux measurements of disks with gas separation layers with the standard thickness and 50% of the standard thickness in tested in two fuel compositions over a range of temperatures. Fuel composition 1 (Figure 38) was 90% carbon monoxide mixed with 10% carbon dioxide. Fuel composition 2 (Figure 39) was 85% hydrogen mixed with 15% carbon dioxide. The measured oxygen flux for OTM disks tested in the hydrogen environment was in all cases higher the oxygen flux measured in the carbon monoxide environment. No dependence on separation layer thickness is observed, further suggesting that the gas separation layer is not a rate-limiting step.

However, after improvements were made to the mass transport capability of the porous support and the fuel oxidation rates of the fuel oxidation layer, the model described in subtask 2.1 was updated and showed that the contribution of the separation layer as a rate limiting step increased. Work was then performed to improve densification of the separation layer, through the use of sintering aids and processing conditions, in order to allow for production of OTM tubes with thinner separation layers. This work was continued into Phase III of this program, along with efforts to improve the experimental measurement of ambipolar conductivity.

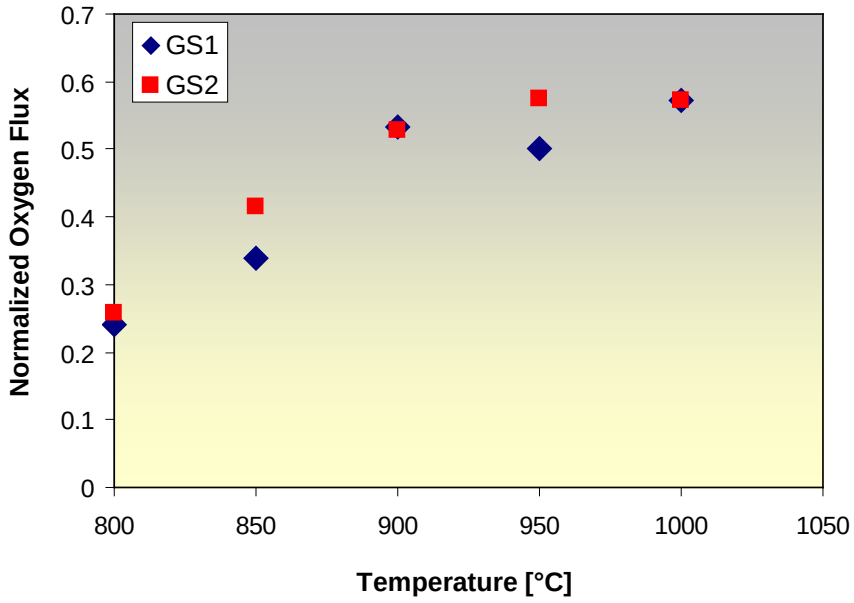

Figure 38: Normalized oxygen flux for OTM disks with gas separation layers that possessed the standard thickness (GS1) and 50% of the standard thickness (GS2), over a span of operating temperatures in gas composition 1 (a CO/CO2 mixture).

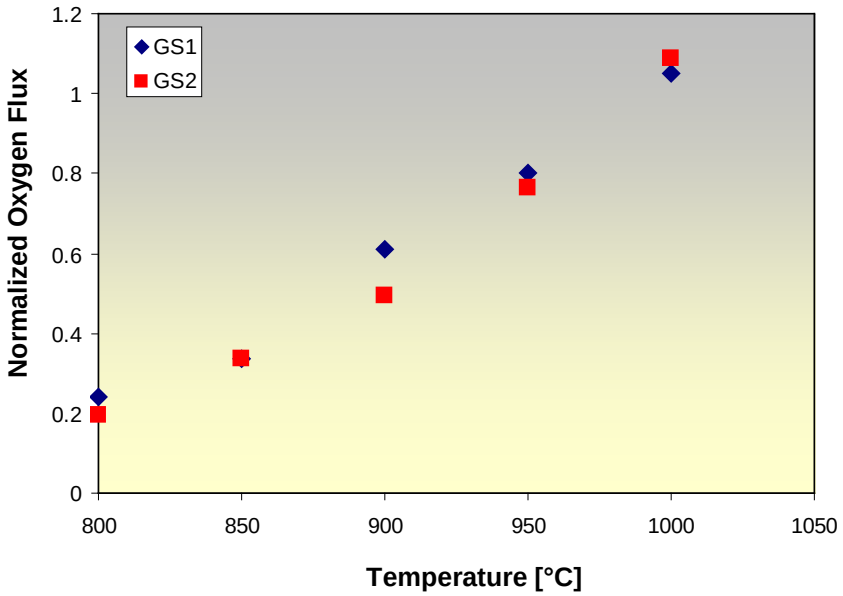

Figure 39: Normalized oxygen flux for OTM disks with gas separation layers that possessed the standard thickness (GS1) and 50% of the standard thickness (GS2), over a span of operating temperatures in fuel composition 2 (a H2/CO2 mixture).

2.2.4. Subtask 2.4 Activation Layers

There are two activation layers included in the layers of the Oxygen Transport Membrane. The first is a fuel oxidation layer (anode), which is located between the porous support and the gas separation layer. The function of the fuel oxidation layer is to incorporate oxygen ions from the gas separation layer interface, transport oxygen ions to active sites on the fuel/activation layer interfaces and to promote oxidation of fuel species on active sites. The fuel oxidation layer is porous and composed of an electronic conducting phase and an ionic conducting phase. The second activation layer is the oxygen incorporation layer (cathode), which is located between the air domain and the gas separation layer. The function of the oxygen incorporation layer is to promote the reduction of molecular oxygen to oxygen ions on actives sites on air/activation layer interfaces, to transport oxygen ions from surface sites to the interface between the activation layer and the gas separation layer and to transport oxygen ions into the gas separation layer. The oxygen incorporation layer is also porous and composed of an electronic conducting phase and an ionic conducting phase.

Fuel Oxidation Layer

The fuel oxidation layer (anode) was identified early in the program as a rate limiting step, as discussed in subtask 2.1. Candidate fuel oxidation materials underwent electrochemical impedance measurements as a method to isolate and characterize performance. Both symmetrical and half cells were constructed and loaded into a Probostat™ sample holder system where they were subject to high temperature and controlled atmospheres. The cells were electrically connected to a Solartron Analytical Potentiostat and Frequency Analyzer (FRA) through the Probostat™. The potentiostat and FRA were used to control the electrochemical

impedance tests, which resulted in impedance spectra that were broadly separated into ohmic resistance and polarization resistance contributions. Polarization resistance was used as a metric of selection. Candidate materials that exhibited low polarization resistance compared to the standard material were then integrated into OTM disks and OTM tubes and tested for oxygen flux.

Figure 40 shows normalized area specific polarization resistance of candidate fuel oxidation layer materials as a function of development time. Included in the fuel oxidation layer development work, were materials developed by Praxair and materials developed by NexTech Materials Ltd. Several materials were identified that offered an improvement over the material used at the beginning of the program, and a subsection of those materials were shown to meet the polarization resistance target. The majority of the materials that met or closely approached the target involved adding an additional catalytic component to the fuel oxidation layer[1]. Figure 41 shows an example of area specific polarization resistance values for one of the highest performing anodes with the added catalytic component ("Advanced Anode") and the highest performing anode material that did not include an additional catalytic component ("Standard Anode") as a function of operating temperature. A significant decrease in activation energy was observed on the "Advanced Anode", suggesting the addition of the catalytic component not only offers higher performance at the target operating temperature but also performance less sensitive to temperature over a wide range of operating temperatures. Lower activation energies were typical of anodes tested with a catalytic component.

[1] US Patent 8,323,463* "Catalyst Containing Oxygen Transport Membrane" G.M. Christie, J.R. Wilson, B. van Hassel, Issued December 04, 2012.

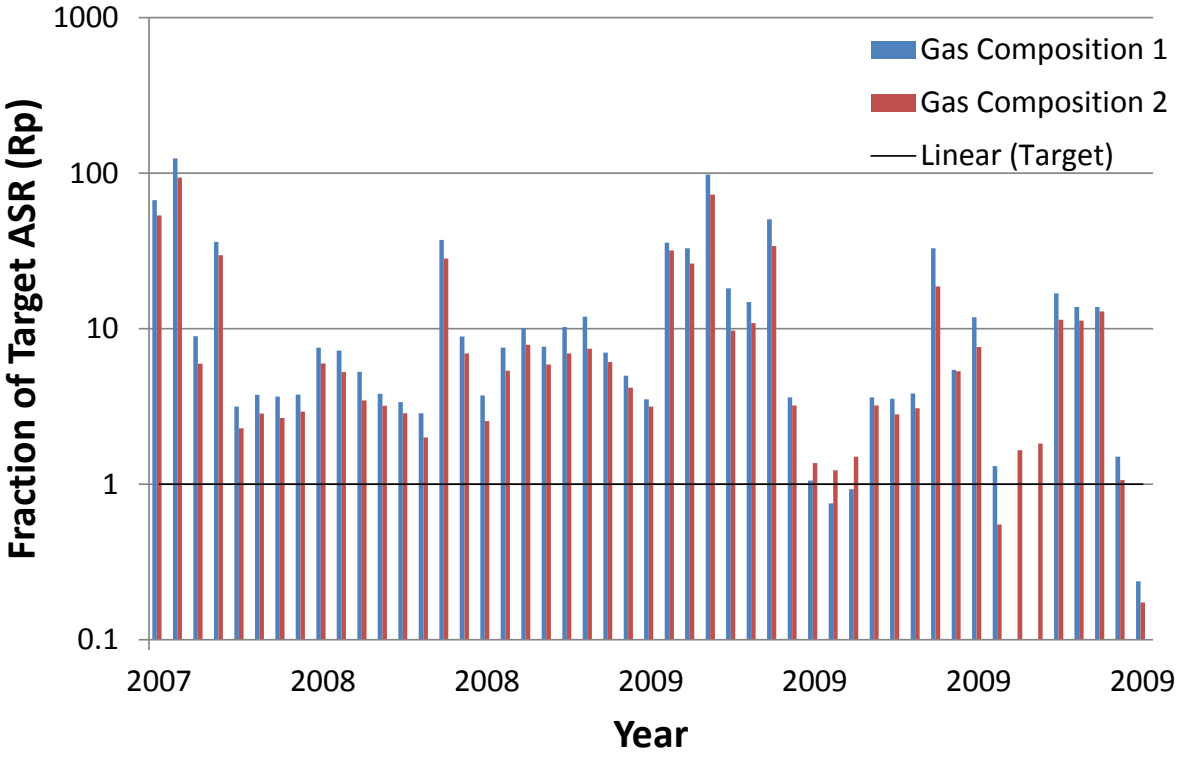

Figure 40: Normalized area specific polarization resistance of candidate fuel oxidation layer materials tested at 1000°C in two gas compositions as a function of development time. Gas composition 1 was a CO/CO2 mixture, and gas composition 2 was a H2/CO2 mixture, and gas composition 2 was a H_2/CO_2 mixture

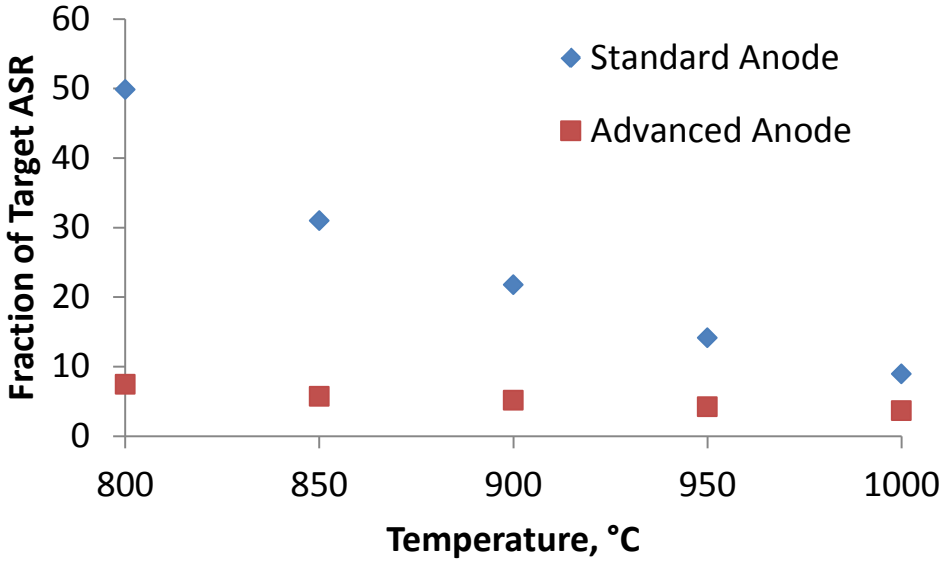

Figure 41: Fraction of target ASR of standard and advanced fuel oxidation layers in a CO/CO2 mixture, over a span of operating temperatures.

Several of the candidate fuel oxidation layer materials were integrated into OTM disks with and without catalytic components on both the standard and advanced porous supports. Figure 42 shows oxygen flux results from tests performed on a matrix of disks: (1) the standard cathode, the standard separation layer, the top anode candidate without an additional catalytic component ("Standard Anode") and the standard porous support, (2) the standard cathode material, the standard separation layer material, the top anode candidate with an additional catalytic component ("Advanced Anode"), and the standard porous support, (3) the standard cathode, the standard separation layer, the top anode candidate without an additional catalytic component ("Standard Anode") and the advanced porous support, and (4) the standard cathode material, the standard separation layer material, the top anode candidate with an additional catalytic component ("Advanced Anode"), and the advanced porous support. Fuel conversion is not measured when performing oxygen flux tests on disks, but is estimated to be about 10%.

The OTM disk with the "Advanced Anode" and standard support exhibited no change in performance compared to the OTM disk prepared with the "Standard Anode" and standard porous support when tested in the CO/CO_2 fuel, but did show a 15% performance improvement in the H_2/CO_2 fuel. SEM images showed that when the catalytic component is integrated into an OTM disc or tube with the standard support, the catalytic component does not achieve the target distribution on the surface of the anode. The OTM disk with the "Standard Anode" and advanced support exhibited a 110% performance improvement compared to the OTM disk prepared with the "Standard Anode" and standard porous support when tested in the CO/CO_2 fuel, and showed a 20% performance improvement in the H_2/CO_2 fuel. The OTM disk with "Advanced Anode" and advanced support exhibited a 140% performance improvement compared to the OTM disk prepared with the "Standard Anode" and standard porous support

when tested in the CO/CO_2 fuel, and showed a 70% performance improvement in the H_2/CO_2 fuel. The highest performance levels are achieved when coupling the “Advanced Anode” and the advanced porous support. SEM images showed an improved distribution of the catalytic component when implemented with the Advanced support. In summary, Praxair's "Advanced Anode" was the most promising fuel oxidation layer performance improvement method explored during Phase I.

The performance levels shown in Figure 42 for the OTM disk with both the advanced anode and the advanced porous support exceed the target oxygen flux in both fuel environments. However, since oxygen flux is expected to decrease with increasing fuel utilization, it is expected that the oxygen flux values measured on OTM tubes will be lower than measurements on OTM disks, because under the testing conditions available for discs fuel conversions of approximately 10% were achieved, whereas testing conditions available for OTM tubes enabled achieving higher fuel conversion levels in the range of the target fuel utilization (70-90%). Tests on OTM tubes are reported in the Task 4 section of this report.

After the conclusion of Phase I and Phase II of this program, the fuel oxidation layer (anode) continued to be a focus of materials development in Phase III. Emphasis in Phase III has been placed on characterizing and improving degradation behavior, in order to meet Phase III degradation targets.

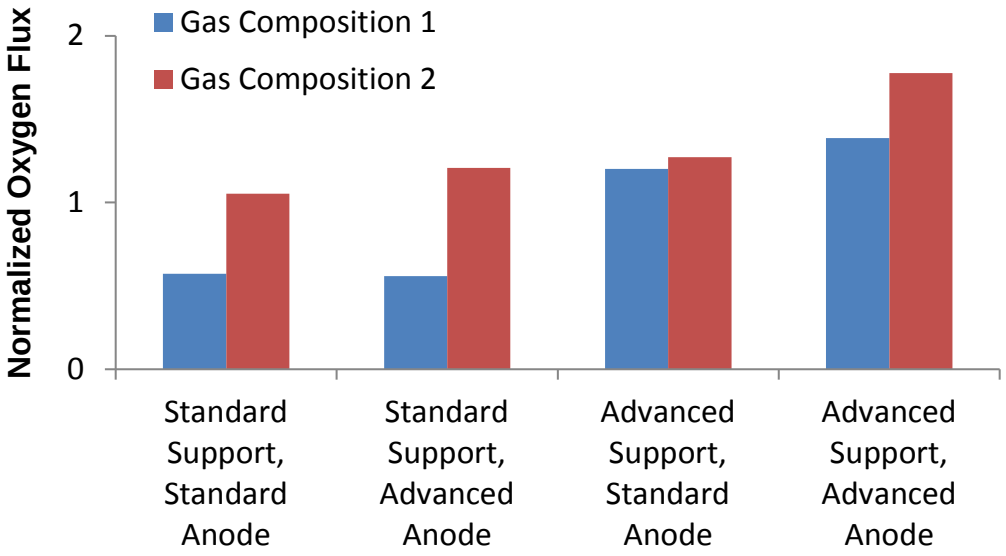

Figure 42: Normalized oxygen flux achieved for OTM disks tested at 1000°C in two gas compositions. Gas composition 1 was a CO/CO2 mixture (90% CO / 10% CO2), and gas composition 2 was a H2/CO2 mixture (85 H2 / 15% CO2).

Oxygen Incorporation Layer

The oxygen incorporation layer (cathode) was also characterized by electrochemical impedance spectroscopy, but was not found to be a rate limiting step. Three cathode materials (C1, C2 and C3) have been considered for use in the OTM system. Electrochemical measurements of the cathode compositions yielded low initial area specific resistances (ASR) in air at 1000°C, suggesting that each of the materials would be an acceptable candidate. However, long term (1000 hours) electrochemical tests (Figure 43) showed that the area specific resistance of C1 increased significantly with time while the area specific resistance of C2 increased minimally with time. The third material, C3, was not tested for the full 1000 hours, but had started to show degradation behavior similar to C1 at 200 hours. The composition C2 possessed area specific polarization resistance behavior that was better than the target value through the entire 1000 hour test and was therefore selected as the cathode composition.

Figure 44 shows the normalized area specific resistance of cathode materials C1, C2 and C3 tested in air as a function of operating temperature tested. Cathode material C2 had the highest activation energy, followed by C1 and C3. Although, a low activation energy material is preferable for operational stability, C2 continued to be the selected cathode material because of the low observed degradation behavior.

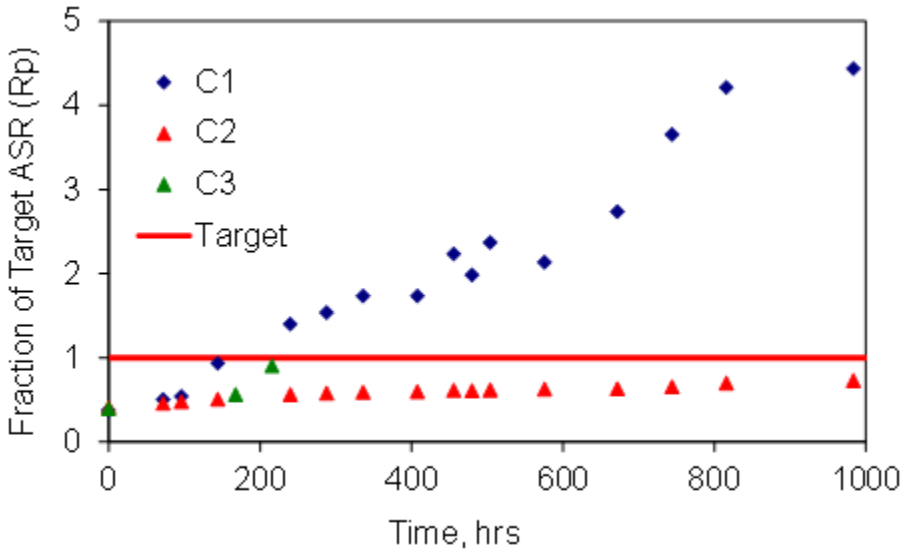

Figure 43: Normalized ASR of two cathodes materials during a 1000 hours life test in air at a temperature of 1000°C.

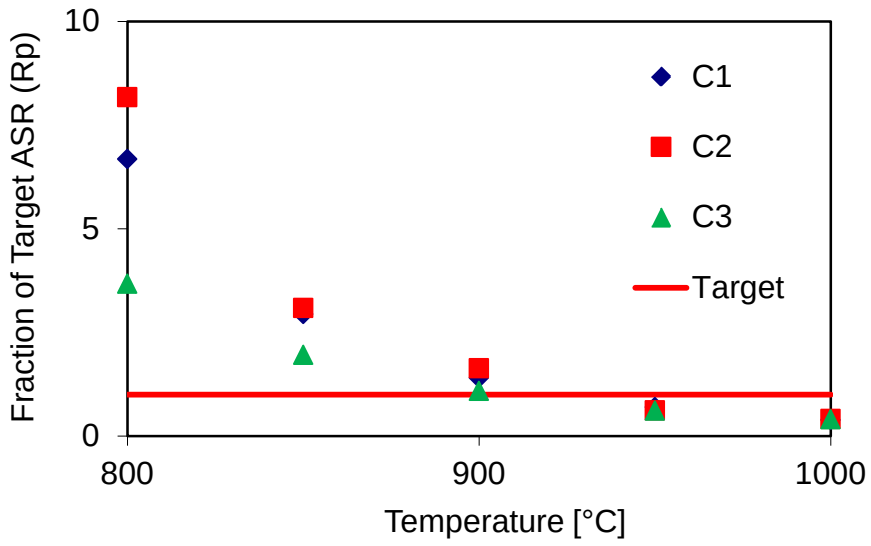

Figure 44: Normalized ASR of three cathode materials tested in air as a function of operating temperature.

After improvements were made to the mass transport capability of the porous support and the fuel oxidation rates of the fuel oxidation layer, the model described in subtask 2.1 was updated and showed that the contribution of the oxygen incorporation layer as a rate limiting step increased. Work was then performed to identify an oxygen incorporation layer with improved performance properties. This work was continued into Phase III of this program, and as with the fuel oxidation layer, emphasis in Phase III has been placed on characterizing and improving degradation behavior, in order to meet Phase III degradation targets.

2.3. Task 3: OTM Manufacturing Development

Task 3.0 efforts addressed development of cost effective and scalable manufacturing processes for production of Oxygen Transport Membranes and assembly of protocols for production steps. In Phase I, work focused on manufacturing of short laboratory scale OTM tubes (1/3 pilot scale), and in Phase II emphasis shifted to production of pilot size OTM tubes and cost estimation.

After development of new high performance materials within the performance improvement task (Task 2), the new materials were transferred to Task 3 for manufacturing. Three porous support technologies were identified and transitioned to manufacturing, two of the technologies involved production of porosity in the porous support through fugitive pore formers ("Standard" porous support technologies). The third technology, an "Advanced" porous support technology, was developed by ENrG, Inc. (Buffalo, NY) under subtask 2.2 of this program through a NYSERDA contract (agreement number 10080 and 10080-1). The "Advanced" porous support technology yielded a high permeability/high performance porous support. However, the "Advanced" porous support did not meet strength targets for pressurized operation (POx conditions). In the fourth quarter of 2010, it was decided that the first generation OTM module concepts would be assembled with OTM tubes with porous supports manufactured through one of the "Standard" porous support technologies.

The Task 3 manufacturing development work was initially carried out within Praxair's OTM pilot manufacturing facility in Indianapolis, IA. In early 2008 subtask 3.1, subtask 3.2 and subtask 3.3 were subcontracted to ENrG, Inc. At this time, the "Advanced" porous support technology developed in a joint subcontract by ENrG, Inc. was undergoing evaluation within performance improvement (task 2) and laboratory scale testing (task 4). ENrG was

subcontracted to produce and develop protocols for both OTM tubes prepared with "Standard" and "Advanced" porous supports. In early 2010, Praxair's pilot manufacturing facility for production of OTM tubes in Indianapolis, IN was brought back online to assist in production of pilot size OTM tubes prepared with the "Standard" porous support technologies. As Phase II and the manufacturing work subcontracted to ENrG concluded, a search was conducted for a partner for Phase III with substantial experience in high volume ceramics manufacturing. Early in Phase III, a technology partnership between Praxair and Saint-Gobain was initiated to support high volume production of ceramic membranes and modules, and to forecast manufacturing costs.

2.3.1. Subtask 3.1 and 3.3 Manufacturing Process Development I &II

Porous Support

The first step in production of an OTM tube is the formation of a porous support. The porous support forms the structural backbone of the OTM tube and must be able to maintain structural integrity in aggressive operating conditions. Specifically, high yield strength, low creep and high fracture toughness are targeted. The porous support must also enable high diffusion rates of fuel gases in order to support high oxygen flux. Manufacturing costs are also an important factor in evaluating porous support technologies. The competing drivers of high performance, high structural integrity and low manufacturing cost are porous support selection criteria. Three technologies were explored during this program for the formation of the porous support.

(i) Standard support - Isostatic Pressing (Praxair)

Laboratory-scale OTM tubes produced at the start of the program through isostatic pressing were approximately 6 inches long with outside diameters (OD) of one inch with one closed end and a cone like flange on the open end to facilitate sealing. Isostatic pressing has the advantage of facile formation of "shaped" tubes e.g. tubes could be manufactured in a single step. In the Praxair "standard support" that is formed by isostatic pressing, porosity is created by burning out fugitive pore formers i.e. carbon. This technology results in tubes that tend to have high strength, lower performance and relatively high cost for high volume production.

The tubes were scaled up in stages, with the final manufacturing process yielding 36 inch long, 1 inch OD tubes. Manufacturing protocols for porous support production were developed through each stage of scale up. Figure 45 shows a photograph of five 36" long OTM tubes formed by isostatic pressing.

Figure 45: 36" long, OTM Tubes with Standard Support Manufactured by Isopressing.
.

(ii) Standard Support – Extrusion (Praxair)

An extrusion process was also developed for production of "Standard" porous supports. Like isostatic pressing, the extrusion process involves creation of porosity through burn out of fugitive pore formers i.e. carbon. This technology results in tubes that tend to have high strength, lower performance and low cost for high volume production. The extruded tubular substrates have a higher green density than the isopressed and more pore former is required to be added to the mix in order to create the same level of porosity in the sintered substrate. Protocols were developed for both for the recipe of the extrusion mixture and for the extrusion process. By the end of Phase II, the extruded tubular support structures manufactured in Praxair's ceramic membrane pilot manufacturing facility in Indianapolis, IN, possessed an outside diameter of 3/8-inch and a length of 24 inches. The extrusion process was selected as the low-cost forming technique to be carried into Phase III. Effort in Phase III involved improvement of performance of OTM tubes prepared with extruded porous supports through optimization of the pore former type and concentration.

(iii) Advanced Support – Casting (ENrG)

ENrG Inc., through a contract with NYSERDA and with additional funding from Praxair, developed a high performance "Advanced" OTM substrate technology. ENrG originally demonstrated the technology in planar form, before translating it to tubular form. First generation OTM tubes prepared with the "Advanced" substrate were similar in geometry to the porous supports prepared by isostatic pressing, i.e. approximately 6 inches long with outside diameters (OD) of one inch with one closed end and with a cone like flange on the open end to facilitate sealing. Scale-up efforts yielded OTM tubes prepared with the "Advanced"

Supports of approximately 20 inches of length. Manufacturing protocols were developed for the first generation tube, and for subsequent generations during scale-up efforts. Figure 46 shows a photograph of a 6" long OTM tubes formed with the "Advanced" substrate technology.

Figure 46: Image of a green OTM tube prepared with the advanced support concept

The "Advanced" substrates enabled high performance levels, as shown in the Task 4 section of this report. However, strength values were significantly lower than that achieved for OTM tubes prepared with the "Standard" support technologies at comparable porosities, as shown in Figure 47. None of the tubes prepared with the "Advanced" substrate technology survived laboratory tests in the aggressive conditions expected in the partial oxidation unit. The partial oxidation unit requires testing under pressure differentials and in high fuel content gases. This technology resulted in tubes that tend to have low strength, high performance and relatively high cost for high volume production. The "Advanced" Support technology was not selected to be carried into Phase III.

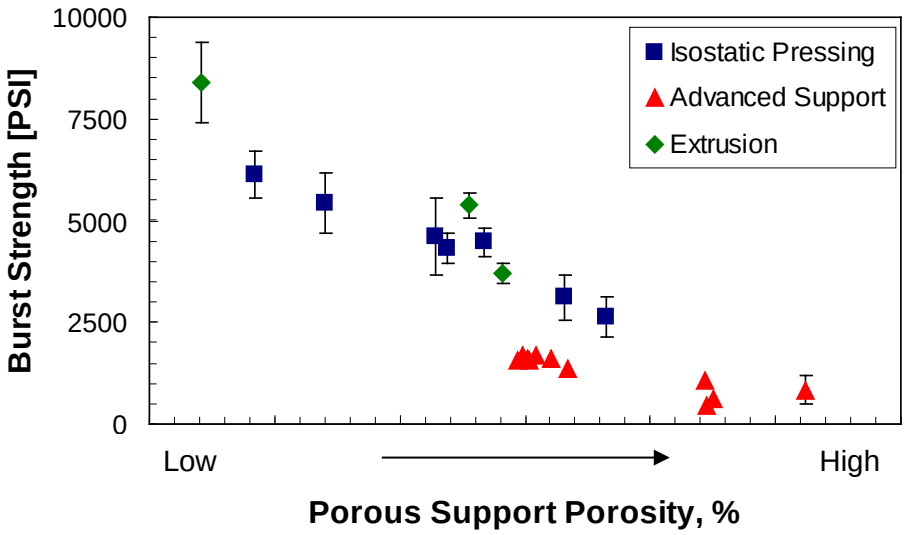

Figure 47: Room temperature OTM substrate burst strength as a function of porosity. Porous substrates were pressured by expanding a rubber bladder inside of the porous tube.

.

Porous Support Summary

Subtask 3.3 concluded with the decision that 1st generation OTM module concepts would be assembled from membranes in which porous support porosity is created by burning out fugitive pore formers. Although much higher support permeability and therefore higher OTM flux performance has been demonstrated on OTM tubes prepared with advanced methods of creating porosity in the porous support, there is concern over the strength and reliability of such structures for deployment in large scale power generation equipment. Both isostatic pressing and extrusion have been evaluated as techniques for manufacturing the conventional support structures which possess acceptable strength characteristics. Extrusion was selected as

it is considered to be the more cost effective, scalable technique for building tubular structures. In Phase III, emphasis will be placed on evaluation of creep behavior of porous supports, to assist in OTM tube lifetime predictions.

Activation and Gas Separation Layers

After production of the porous support, the support may be bisque fired at an intermediate temperature followed by the deposition of a fuel oxidation activation layer, a gas separation layer, and an oxygen incorporation activation layer. Activation layer and gas separation layer materials were down selected in Task 2 and transferred to Task 3. Several different slurry deposition techniques, with varying levels of automation, were developed both for coating the inside and coating the outside of OTM tubes. The slurry deposition techniques could be adapted to any of the porous support architectures. Control of layer thickness, coating reproducibility, ease of coating large tubes, and coating throughput were all considered when evaluating coating deposition techniques. A single technique was selected and transferred to manufacturing. After deposition of the fuel oxidation layer and gas separation layer, OTM tubes undergo sintering under controlled temperatures (1350^{o}C -1400^{o}C) and gas atmospheres (4%H_2 in N_2), in order to ensure density requirements for the gas separation layer are met. Figure 48 shows a pilot production furnace installed in the manufacturing facility in Indianapolis illustrating the manifold for the H_2/N_2 gas. Protocols were developed for slurry production for the activation and gas separation layers, layer deposition, and sintering steps.

Figure 48: Pilot production furnace in Indianapolis illustrating H2/N2 gas manifold.

OTM Module

In order to effectively deploy the membrane in demonstration OTM reactors during Phase III of this program, a cost effective, compact and reliable membrane bundle or repeat unit must be designed and demonstrated. Praxair has termed this repeat unit "OTM Module". The OTM module consists of a series of membranes that are provided with a fuel or air gas manifold. OTM operation temperature of 1000^{o}C leads to challenging sealing and manifolding issues that will need to be overcome during the technology demonstration phase. Although not contracted in Phase II as one of the DOE project tasks, using internal resources Praxair has generated several conceptual designs for OTM modules and seals, one variant of which is moving forward to prototype. During Phase III, OTM module development will be a large effort that will be executed jointly by Praxair and Praxair's ceramics manufacturing partner.

2.3.2. Subtask 3.2 Commercial Scale Assessment

A cost model was developed by Praxair to estimate the cost for manufacturing OTM tubes prepared with the "Standard" substrate technologies at Praxair's Indianapolis Pilot Manufacturing facility. ENrG, Inc. modified Praxair's cost model in order to estimate the cost of production of OTM tubes prepared with the "Advanced" substrate technology.

2.3.3. Subtask 3.4 Manufacturing Scale-Up

This subtask involves development of a commercialization plan for ceramic tube manufacture, which includes cost projections for large scale manufacture of OTM ceramic membranes. As efforts commenced to initiate cost projection work, it became clear that a high volume ceramic manufacturing partner would be required. In Phase II, Praxair sought and identified a technology partner who could lead efforts in large scale manufacture of OTM tubes, provide cost projections at commercial scale, and work jointly with Praxair in designing and building "OTM Modules". As Phase II concluded, Praxair reached an agreement with Saint-Gobain, and began setting up the multi-phase joint development program, which was formalized in Phase III. Work on the commercialization plan developed jointly by Praxair and Saint-Gobain continued into Phase III of this contract.

OTM Integration Levels for Commercial Scale Operation

Delivering the oxygen flow required at commercial scale necessitates the integration of large amounts of OTM surface area. It has been estimated that approximately 7000 tpd of OTM oxygen will be required by the advanced power cycle. In order to provide the required surface area, distinct OTM integration levels were identified, as illustrated in Figure 49. Integration

levels included in Figure 49 included element, module, reactor and system. In Figure 49, the flow of gas inside and outside the OTM elements is depicted by red and blue arrows, respectively. The directions depicted in Figure 49 are included merely as an example; in practice, the optimum direction (and magnitude) of gas flow, at each integration level, will be determined by analysis and testing.

OTM integration begins at the element level. The OTM element is the smallest discretely manufactured component within the system. It is analogous to a cell in a fuel cell stack. The size and shape of the individual elements are dictated by a number of factors, including cost, manufacturing limitations, and method of integration.

At the module level, OTM surface area is increased by connecting multiple elements. The flow of fuel and air across the opposite sides of the OTM may occur with the elements arranged in series, parallel or a combination of both. Manifolds are used to distribute gas flow to the elements within the module. OTMs operate at high temperature, and in some cases at high pressure.

Sealing the elements to the manifolds is a critical aspect of integration. During Phase I of this project Praxair used a seal technology based on a metal washer, ceramic rope and metal follower that was developed for use with single phase mixed conducting perovskite materials in OTM developments efforts that preceded this contract, for the purpose of forming a temporary seal appropriate for laboratory scale testing. In Phase II Praxair evaluated a series of glass ceramic and cement compositions for sealing the OTM tubes to ceramic manifolds, intended as a “permanent” seal for use in pilot tests. This seal and manifold arrangement cannot be reused but is required for both reliability and cost. In the event of a failure, a bundle of tubes arranged in a modular fashion with a ceramic manifold would be replaced as opposed to replacing

individual OTM tubes. Work evaluating sealing technologies and developing manifolds continued into Phase III of this program, as a joint project between Praxair and Saint-Gobain.

The fourth and fifth level of OTM integration (reactor and system) shown in Figure 49 are addressed within Task 7 of Phase III efforts.

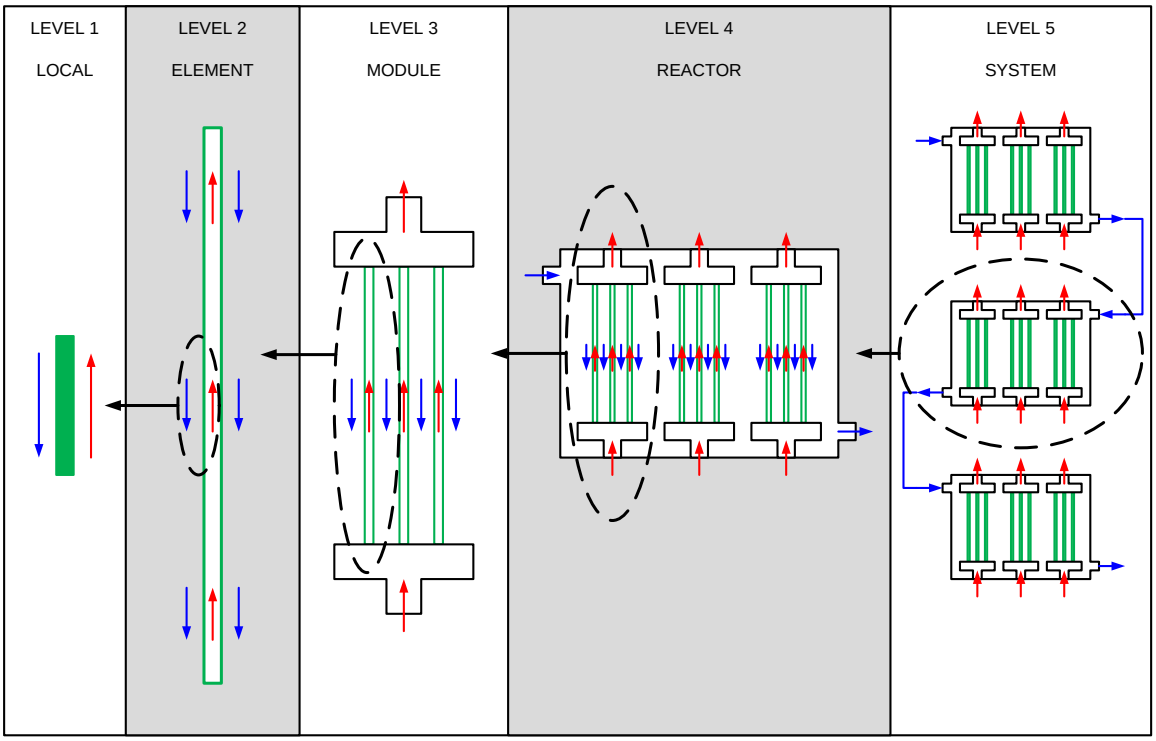

Figure 49: Levels for characterizing oxygen flux in an OTM-based oxygen delivery system.

.

2.4. Task 4: Laboratory Scale Testing

The objective of Task 4 was to generate OTM performance data under test conditions that mimic the environment foreseen in the process and systems engineering task (task 1). Two short-tube test rigs that were capable of testing OTM tube performance at ambient pressure in simulated fuels were used to test OTM tubes in an environment analogous to the advanced boiler defined in task 1, with results reported in subtask 4.1 of this report. A reactor was constructed at Praxair that enabled testing OTM tubes with simulated fuels including sulfur containing species (H_2S and COS), testing at high pressure (100-200 psi) and testing OTM tubes of increased length (1/3 pilot size) in environments analogous to both the advanced boiler and partial oxidation (POx) unit defined in task 1. The construction of the high-pressure reactor and performance results are reported upon in subtask 4.2 and 4.4 of this report. Properties necessary for reactor design, such as heat transport properties and residence time, were collected from both the ambient-pressure short-tube test rigs and the high-pressure reactor and are reported upon in subtask 4.6 section of this report. Subtask 4.1, 4.2, 4.4 and 4.6 work concluded at the end of 2010. However, tests performed on OTM tubes continued into Phase III of this program. Tests performed in Phase III were performed in operating conditions that mimic the environment foreseen in the process and systems engineering task (subtask 7.1 of the Phase III contract), where the operating conditions were different from the process conditions considered in task 1 of Phase I and Phase II of this program.

At the University of Utah (UofU), a bench-scale OTM coal reactor was designed and constructed. Both fluidized bed and fixed bed reactor configurations were evaluated, along with operation in direct and indirect firing modes. A fixed bed system in an indirect firing mode was

selected as the optimal configuration, where the coal was gasified in a hot oxygen burner (HOB) supplied by Praxair using externally-supplied oxygen, and the OTM tubes were exposed to the gasification products in a secondary stage to allow combustion of the synthesis gas. The construction of the coal reactor and results obtained from testing OTM tubes prepared with the "advanced" material set in the coal reactor are reported upon in subtask 4.3 and 4.5 of this report.

Oxygen Flux Map

An oxygen flux map shown in Figure 50 was assembled that includes data collected at conditions (fuel composition, pressure, temperature, etc.) appropriate to the process conditions expected for the advanced boiler considered in task 1. The data presented in Figure 50 was collected from multiple reactors across a wide range of fuel utilization conditions and was used to make decisions within the process and systems engineering task (task 1), the OTM performance improvement task (task 2) and the OTM manufacturing development task (task 3). In Phase III, new performance maps will be generated based on process conditions appropriate to Phase III.

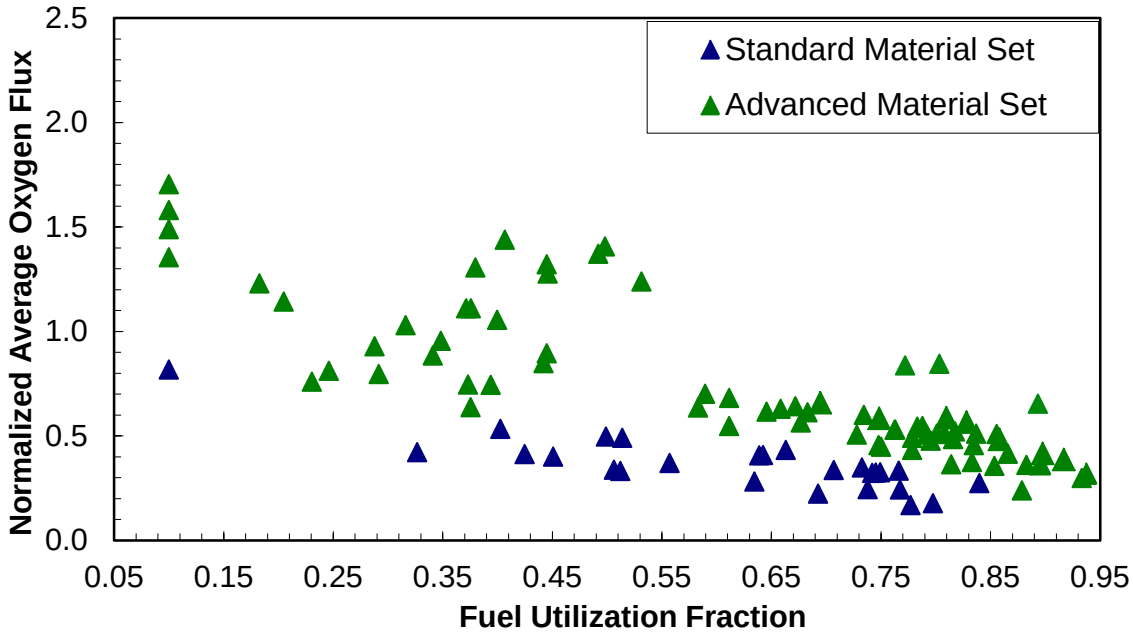

Figure 50: Average oxygen flux versus fuel utilization map for OTM tubes tested in conditions appropriate for the Phase I and Phase II advanced boiler at ambient pressure, in a simulated synthesis fuel gas, and at approximately 900°C furnace temperature

2.4.1. Subtask 4.1 Short Tube Testing

Two short-tube test rigs were used to evaluate and provide a feedback loop for OTM performance improvement (task 2) and OTM manufacturing development (task 3) at operating conditions similar to conditions expected for the advanced boiler considered in Phase I and II of this project. Oxygen flux as a percentage of the target, as initially defined in the process and systems engineering task (task 1), was measured and reported. Oxygen flux versus development time, oxygen flux as a function of fuel utilization, oxygen flux versus operating temperature, and results of thermal cycle tests are reported.

Seven OTM tubes were tested in 2007, nine OTM tubes were tested 2008, fifteen OTM tubes were tested in 2009 and nine tubes were tested in 2010 in the low-pressure test reactors. Figure 51 shows the normalized oxygen flux observed in OTM tubes from the beginning of the

Phase I and Phase II task 4.1 work in 2007 to the conclusion of the Phase I and Phase II task 4.1 work in 2010 tested in a $CO/H_2/CO_2$ fuel environment (a synthesis gas environment similar to that expected in the advanced boiler process) as a function of development time.

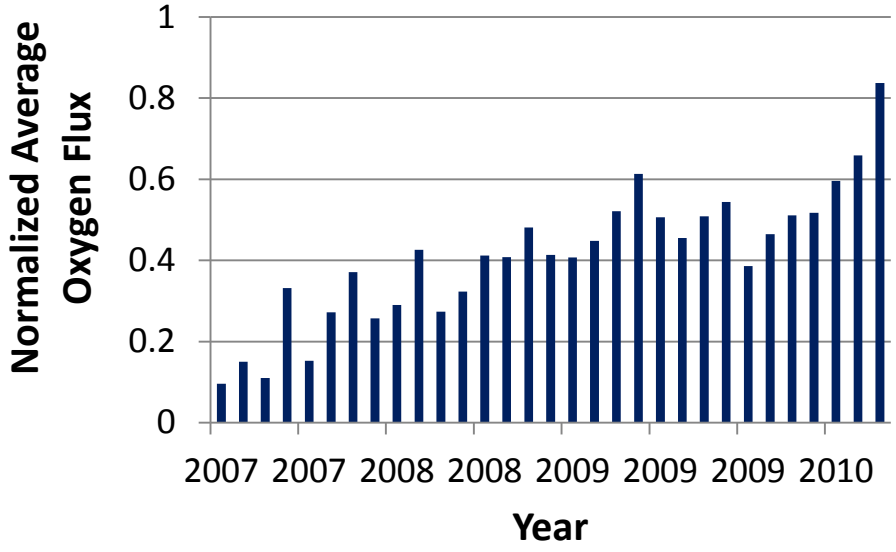

Figure 51: Normalized oxygen flux of OTM tubes tested in CO/H2/CO2 fuel. Temperature was 900°C and fuel utilization was typically between 60 – 80%.

Work performed in the performance improvement task (task 2) indicated that the porous support and the fuel oxidation layer (anode) were limiting performance. Work performed in task 2 also indicated potential improvements based on fundamental tests and analyses. Efforts were made throughout Phase I and II of the OTM program to improve the mass transport capability of the porous support, ending with implementation and optimization of the ENrG advanced support. Also, a higher performance fuel oxidation layer (anode) was identified in 2008, but was only efficiently implemented when prepared in conjunction with the ENrG advanced support. The majority of the performance improvement shown in Figure 51 was achieved with the implementation of the advanced ENrG support and advanced fuel oxidation (anode) layer in 2009 and optimization efforts also resulted in additional improvement in 2010.

Performance improvement was even more significant with the advanced material set when tested in the high-pressure reactor under lower fuel utilization levels, as described in the task 4.2 section of this report.

Typical testing conditions were as follows: ambient pressure (< 5 psig) air exposed to the inside of an OTM tube, and an ambient pressure (< 5 psig) simulated syngas (fuel) exposed to the outside of an OTM tube. Variables examined included furnace temperature, fuel flow and air flow. Varying the fuel flow rate allowed collection of performance data as a function of fuel utilization. This is important, considering the oxygen flux target determined in the task 1 work is contingent on achieving a specific fuel utilization level. Figure 52 shows oxygen flux vs. fuel utilization measured on OTM tubes throughout Phase I and Phase II in a regime of operating conditions analogous to those expected for the advanced boiler. Average oxygen flux decreased with increasing fuel utilization.

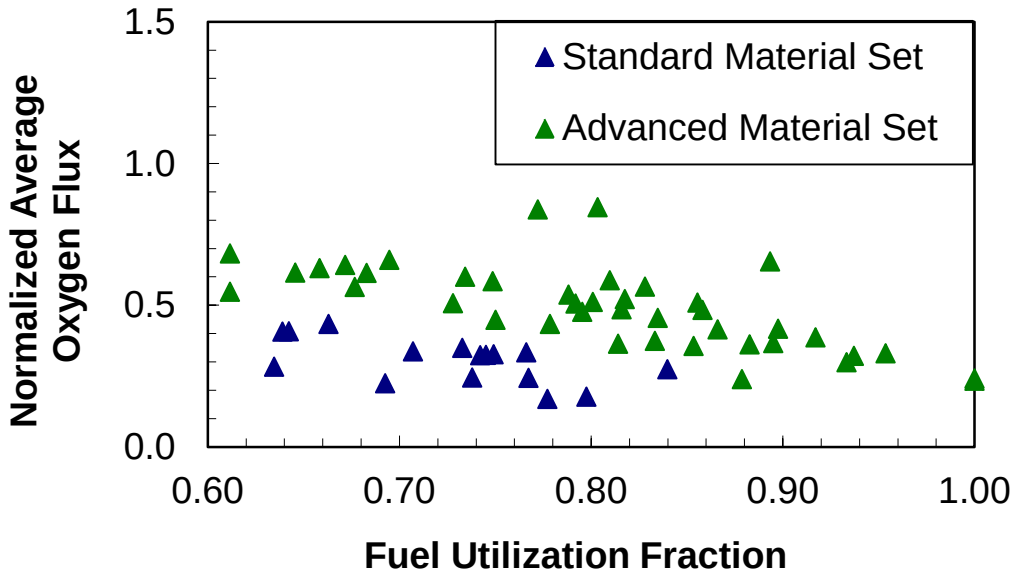

Figure 52: Average oxygen flux versus fuel utilization map for OTM tubes tested at ambient pressure, in a simulated synthesis fuel gas, at 900°C furnace temperature

Figure 53 shows typical oxygen flux performance values as a function of furnace set-point temperature. Data for both the standard material set and the advanced material set are presented. Performance was strongly influenced by the operating temperature. Experiments of this type were performed in order to better understand OTM performance capability, assist in identification of rate limiting steps, assist in selection of operating conditions, and assist in understanding of heat transport capability. Surface temperature of the activation layers, surface temperature of the porous support, and gas phase temperature at various locations were measured. These measurements were reported in the task 4.6 section of this report. Also reported in the task 4.6 section of this report are properties relevant to reactor design (e.g., packing density and residence time).

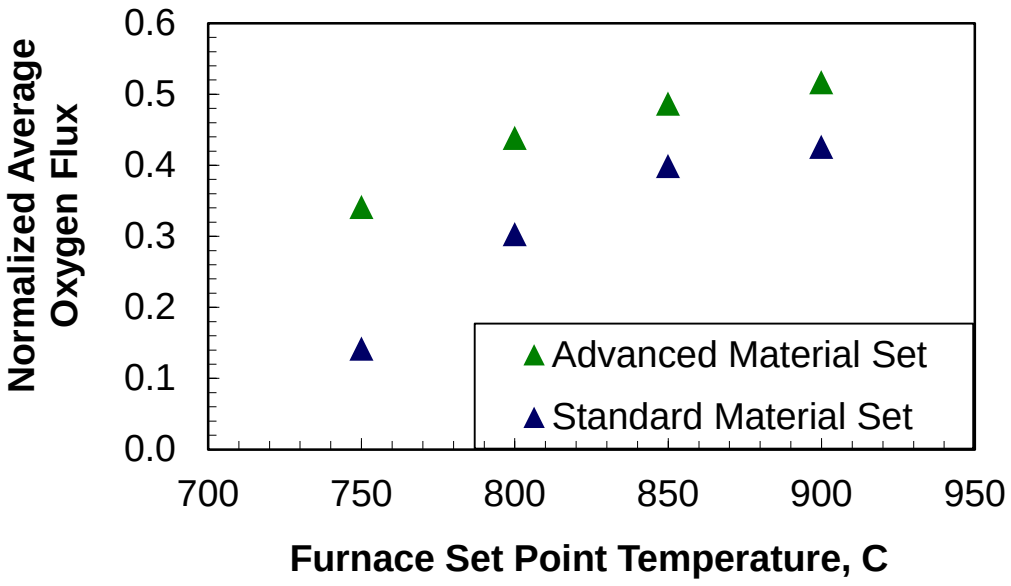

Figure 53: Normalized oxygen flux of OTM tubes tested in a CO/H2/CO2 synthesis gas composition over a range of operating temperatures and at atmospheric pressure.

In order to investigate the stability of the OTM performance, several of the OTM tubes prepared with the advanced material set underwent thermal cycle tests. The performance of the OTM tubes did not change appreciably after these tests.

Manufacturing development work performed in task 3 included making changes to the OTM manufacturing procedures. Included in this work were efforts towards increasing the length and diameter of the OTM tubes. OTM tubes of increased length and diameter were tested in the low-pressure reactors, and were found to have performance levels comparable to short laboratory scale tubes at comparable fuel utilization and temperature conditions.

In Phase III of this program a new process was developed, which required a different set of process conditions. Also, at the initiation of Phase III it was determined that the high performance ENrG advanced support did not offer sufficient structural characteristics to enable stability in high pressure conditions. A more robust porous support was implemented. Testing of OTM tubes in updated process conditions and with the more robust OTM porous supports in the short-tube low-pressure test rigs continued into Phase III of this program within task 6.5. The major focus of the testing within task 6.5 involves mapping out degradation behavior.

2.4.2. Subtask 4.2 and 4.4 Tube Section Testing Short Tube Pressure Testing

Summary

An OTM high pressure reactor (HPR) was designed and constructed at the Praxair Technology Center. The HPR was developed to test OTM tubes at harsh conditions, simulating operation in combustion or partial oxidation environments. HPR testing conditions included high temperature (800 – 1100 °C) and elevated pressure (up to 200 psig). In addition, sulfur-containing gas mixtures were used to simulate the syngas generated using a coal gasifier.

Special construction materials were utilized to ensure compatibility with the highly corrosive nature of sulfur species.

The performance of OTM tubes exposed to syngas mixtures was investigated using the HPR. Performance data included oxygen flux, fuel utilization ratio, and membrane stability. The key test results were:

1. OTM oxygen flux increased with fuel pressure.
2. OTM performance was stable even when exposed to syngas containing up to 10,000 ppm of H_2S.
3. OTM performance improved significantly with implementation of an "advanced" porous support and "advanced" anode layer.

HPR Construction

The HPR was designed to simulate the conditions of an OTM partial oxidation (POx) reactor, utilized as part of Praxair's OTM advanced power cycle (see US patents 7,856,829 and 8,196,387). In an OTM POx reactor, OTM tubes are exposed to a coal derived syngas, containing H_2S and COS, at high temperature and pressure. Simultaneously, the OTM tubes transport oxygen from a low pressure air stream, to a high pressure syngas stream.

A Process Hazard Analysis (PHA) and safety review were conducted to ensure the HPR design and controls adhered to Praxair's safety standards. Special materials were reviewed and selected for the reactor shell, considering sulfur impurities in syngas are highly corrosive.

As shown in Figure 54, the HPR consisted of a pressure vessel designed to support fuel pressure up to 200 psig, at OTM operating temperature. An electric clam-shell furnace was

utilized for preheat and reactor temperature control. A single OTM tube was loaded in the center of the pressure vessel with air flowing inside the OTM tube, and fuel flowing through the space between the OTM tube and pressure vessel wall. Fuel was a gas mixture of H_2, CO, CO_2, H_2O, CH_4, N_2, H_2S and COS. The mixtures were intended to simulate the syngas generated from a BGL coal gasifier.

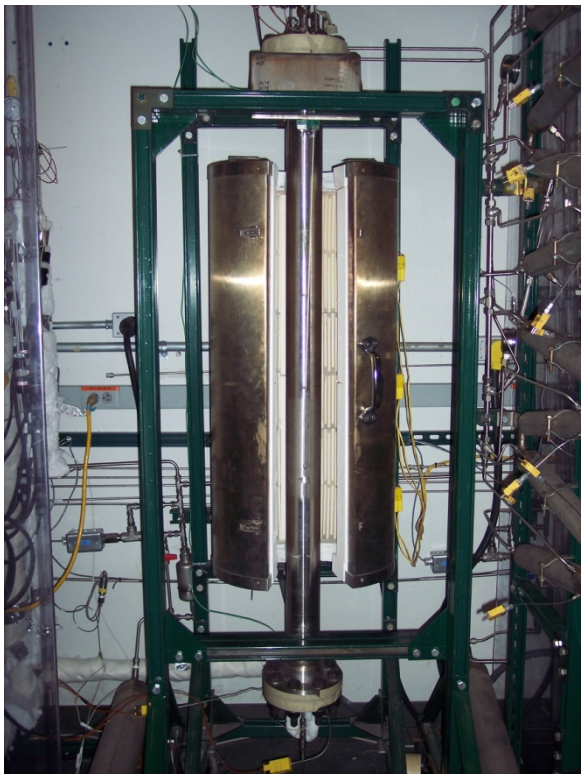

Figure 54: High pressure, single tube, OTM reactor at Praxair, Tonawanda, NY.

OTM Performance Testing

Tests using different fuel mixtures were conducted in the HPR at high temperature (~ 900°C) and elevated pressures (up to 200 psig). The following fuel mixtures were tested:

- 75%CO/25%CO_2
- 85%H_2/15%CO_2
- syngas without sulfur impurities (26%H_2/50%CO/4%CO_2/5%N_2/6%CH_4/9%H_2O)
- syngas with H_2S and COS of various concentration

In these tests, air was kept at constant flow rate and ambient pressure. Figure 55 demonstrates that OTM oxygen flux increased with an increase in fuel pressure. The change in oxygen flux with pressure appeared to level off at high pressures. In addition, the OTM oxygen flux increased with hydrogen concentration in the fuel mixture. For example, the oxygen flux with 85%H_2/15%CO_2 was higher than that of the syngas. The higher flux associated with hydrogen was attributed to the high diffusivity of hydrogen molecules, which can quickly diffuse through the porous support layer of the OTM tube to reach the membrane layer.

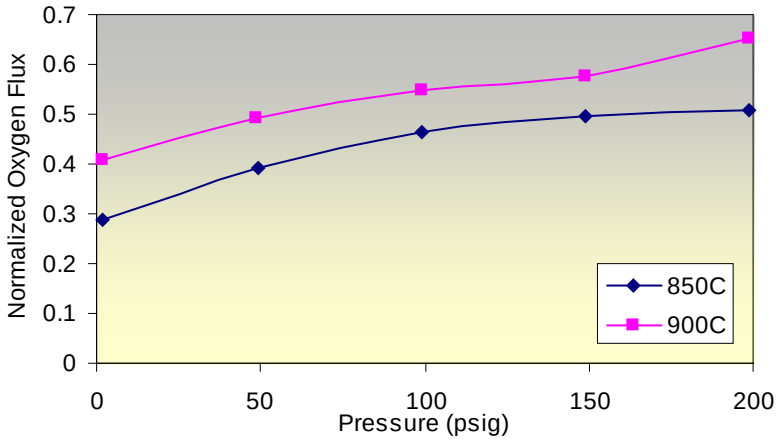

Figure 55: Normalized oxygen flux of an OTM tube prepared with the "standard" material set as a function of fuel (85%H2/15%CO2) pressure at 850°C and 900°C

To investigate the influence of sulfur impurities on OTM performance, OTM tubes were also tested using simulated syngas from a BGL coal gasifier that contained up to 10,000 ppm of H_2S. This was the maximum H_2S content available for testing. Figure 56 shows the normalized oxygen flux of an OTM tube versus H_2S concentration of the simulated BGL syngas at ambient

pressure. It demonstrated that the oxygen flux of the OTM tube was very stable even when exposed to a syngas with a high-sulfur content.

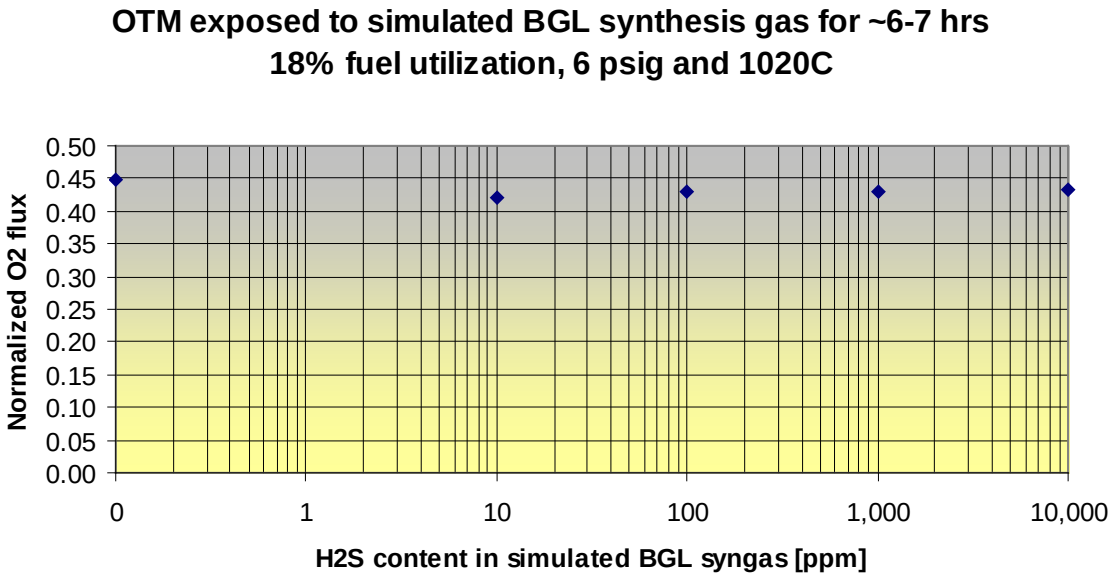

Figure 56: Normalized oxygen flux of an OTM tube prepared with the "standard" material set with a membrane temperature of 1020°C and ambient fuel pressure versus H2S content of the simulated BGL syngas

.

Oxygen flux measurements in the presence of H_2S were also performed at high pressure, as shown in Figure 57. The oxygen flux of the membrane increased with fuel pressure, and the membrane performance improved significantly through exposure to the H_2S containing syngas. SO_2 was observed in a low concentration in the reactor outlet, which indicates that H_2S behaves like a regular fuel for the oxygen transport membrane.

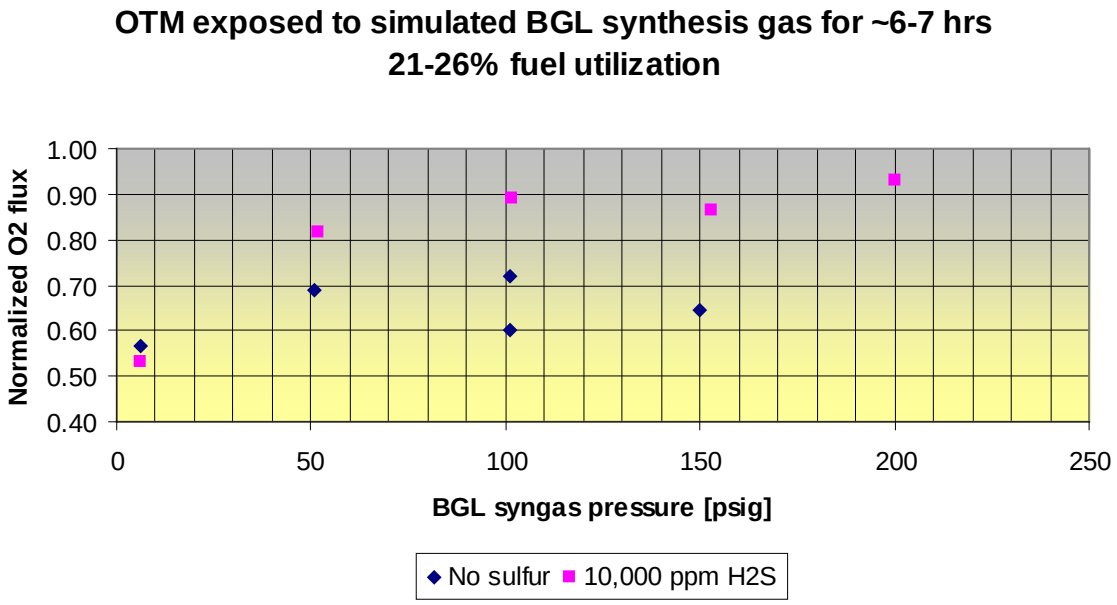

Figure 57: Normalized oxygen flux of an OTM tube prepared with the "standard" material set at about 1000°C as a function of pressure with a simulated BGL syngas containing 10,000 ppm of H2S in comparison to the simulated BGL syngas without H2S.

Syngas tests were also performed on OTM tubes prepared with the "advanced" support layer and "advanced" fuel oxidation layer (anode) at ambient pressures. As shown in Figure 58, the oxygen flux of OTM tubes with "advanced" materials improved significantly compared to those with standard materials. In HPR testing, fuel utilization was ranged from 30% to 60%. The improvement of OTM tube performance with the "advanced" material set was also observed in the low pressure reactor tests, in which fuel utilization was higher than 60%, as reported in subtask 4.1. Surface temperatures of the membrane and of the porous support were measured and are reported in the subtask 4.6 section of this report.

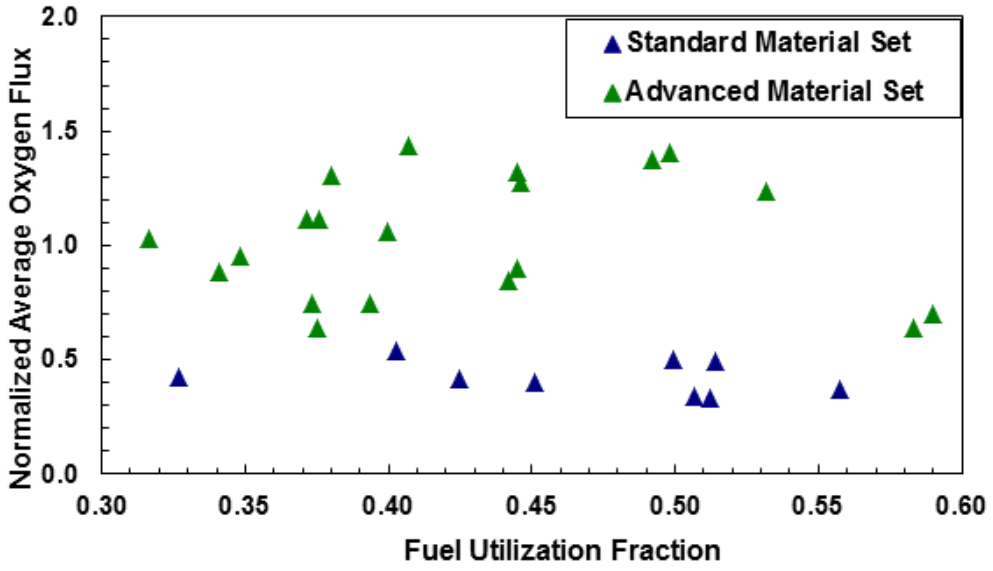

Figure 58: Normalized oxygen flux as a function of fuel utilization for OTM tubes tested with syngas at ambient pressure and at 900°C furnace temperature.

In addition, instantaneous oxygen flux tests were performed to simulate the situation when fuel flowing through a bank of OTM tubes in a partial oxidation reactor or OTM boiler. The instantaneous flux result was converted to average OTM flux based on active OTM area, which was used for OTM modeling as reported in subtask 4.6.

Because of the lower strength characteristics of OTM tubes prepared with advanced support, we were not able to test one at elevated pressure. However, the OTM tubes prepared with standard support are capable of testing under the high fuel pressure conditions expected in the partial oxidation reactor. OTM tubes of increased length were prepared with the standard support and the advanced anode, and were tested under elevated fuel pressures. Tests showed that both oxygen flux and fuel utilization increased with increasing fuel-side pressure, a trend also observed in earlier experiments on shorter length tubes. Developing long OTM tubes with robust support layer and increased performance is an important aspect of Phase III. The HPR

was modified to test new OTM tubes under different test conditions, and the test results are reported in task 6.5 of phase III.

2.4.3. Subtask 4.3 and 4.5 Coal Testing I & II

Summary

Utah Clean Coal Center (UC^3) at the University of Utah was subcontracted by Praxair to study the feasibility of operating Oxygen Transport Membrane (OTM) tubes in a coal environment. The University of Connecticut (UCONN) was subcontracted by Praxair to analyze the OTM tubes tested at the University of Utah. Testing OTM tubes in a coal environment established the ability of OTM tubes to operate in contact with tars, fines, fly-ash, HCl, H_2S, NH_3, and other impurities present in a coal derived fuel.

A multi-tube OTM reactor was constructed at the University of Utah. A number of tests in various coal derived synthesis gas environments were performed, including tests in coal gases derived from low sulfur and high sulfur coal blends. The key results from the tests are listed below:

1. OTM tube performance was stable for ~80 hours of operation for each coal blend
2. Ash accumulation on the surface of the OTM tube was observed, but did not appear to cause a decrease in OTM performance
3. OTM performance increased with increasing operating temperature
4. OTM performance increased with increasing partial pressure of O_2 on the air side
5. OTM performance was impacted by concentration of H_2 in the syngas fuel

No reactions between the OTM components and the coal ash were identified from the materials analysis work performed by UCONN, and there was no evidence of solid or liquid

(slagging) compound formation. The active layer exposed to the coal derived gas also remained stable and interactions with sulfur were not observed.

Coal Reactor Construction

The OTM reactor at the University of Utah was initially constructed to support both direct firing of coal (combustion) and indirect firing (gasification followed by syngas combustion) of coal, and was originally constructed as a fluidized bed reactor. Initial construction was completed in the fourth quarter of 2008, but experiments performed with the reactor in the direct-firing/fluidized bed configuration led to poor performance and OTM failures. It was thought that the low performance was due to the low concentration of active fuel species in the fluidized bed, and that the OTM tube failures were caused by direct contact of the OTM tubes with the coal particles and fluidized bed media. In the third quarter of 2009 the reactor was reconfigured as a fixed bed with indirect firing of coal. The first advantage of the fixed bed/indirect firing approach was that OTM tubes avoided direct contact with reacting coal particles and the fluidized bed media, as well as contact with the majority of the ash minerals in the coal. The second advantage was that a gas with a higher concentration of active fuel species interacted with the OTM tubes, since a fluidizing agent (e.g., CO_2) was no longer required.

The fixed bed OTM reactor consisted of three sections, as shown in Figure 59. The first section, the HOB section, housed the Praxair Hot Oxygen Burner (HOB) as shown in Figure 59 and Figure 60. The HOB was used to generate the coal derived synthesis gas using a hot oxygen jet to pyrolyze and gasify the coal. The second section, the OTM section, is where the OTM tubes were housed. During testing, a single OTM tube was typically positioned in the middle

port or top port of this section. Included on the right side are two sampling ports. These ports were used to sample synthesis gas before and after interaction with the OTM, when the OTM was positioned in the middle port. The third section, the afterburner section, was used to burn off the excess fuel generated by the HOB. The fuel is burned off by mixing O_2 with the syngas and then using a torch as an ignition source for the mixture.

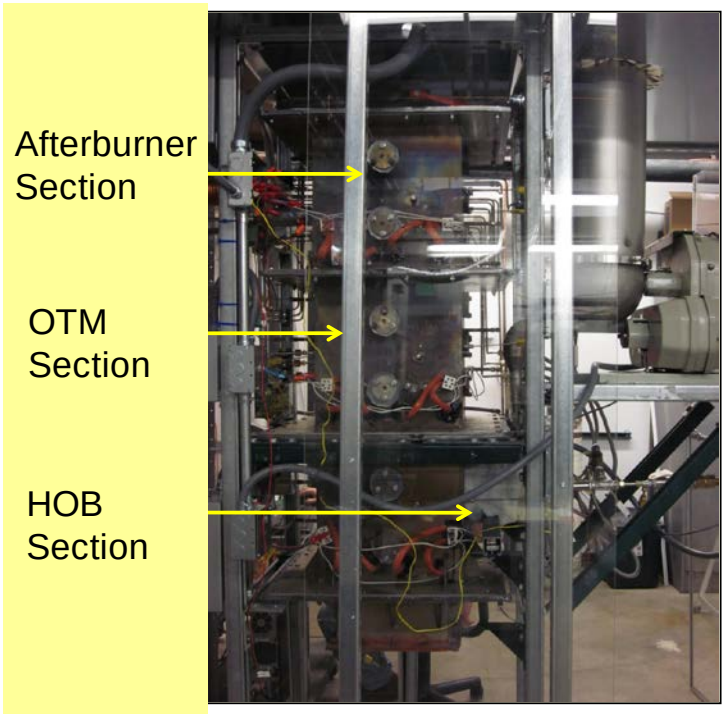

Figure 59: OTM Coal Gas Reactor at the University of Utah

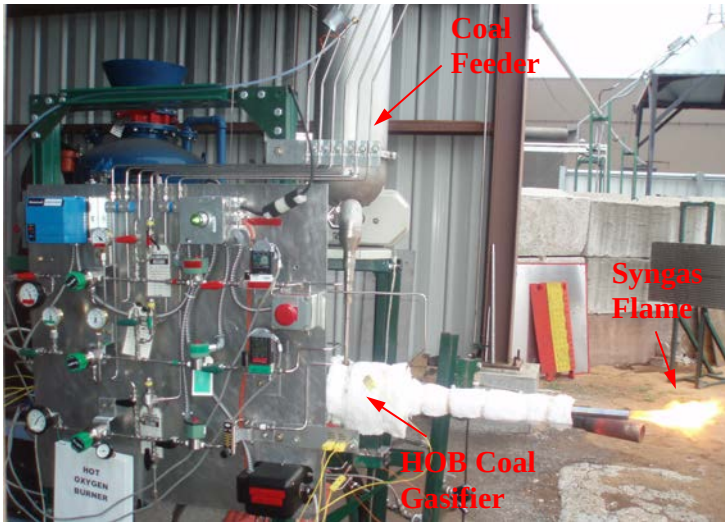

Figure 60: Praxair Hot Oxygen Burner for Coal Syngas Production

OTM Performance Testing

Two coal blends were used in performance tests. The coal blends were comprised of a low-sulfur bituminous Utah coal, a high-sulfur bituminous Illinois coal and a sub-bituminous low-sulfur North Antelope Powder River Basin (PRB) coal. The low-sulfur Utah coal was blended at 25 wt % to 75 wt % of the PRB coal. The high-sulfur Illinois coal was blended at 50 wt % to 50 wt % of the PRB. The ultimate and proximate analysis of each coal is given in Table 38.

Table 38: Ultimate and proximate analysis of coals (wt%)

Coal Type	LOD (105°C)	Ash (705°C)	C	H	N	S	O (by diff)	Volatile Matter	Fixed Carbon	HHV (BTU/lb)
Utah	3.18	8.83	70.6	5.41	1.42	0.53	13.21	38.6	49.39	12606
Illinois	9.65	7.99	64.67	5.59	1.12	3.98	16.65	36.78	45.58	11598
PRB	23.69	4.94	53.72	6.22	0.78	0.23	34.11	33.36	38.01	9078
Utah/PRB Blend (Calc.)	18.5625	5.9125	57.94	6.02	0.94	0.31	28.89	34.67	40.855	9960
Utah/PRB Blend (measured)	10.68	6.23	61.78	5.38	0.86	0.3	25.45	37.63	45.46	10544
Ill./ PRB Blend (calc.)	16.7	6.47	59.2	5.9	0.95	2.1	25.38	35.1	41.8	10338
Ill./PRB Blend (measured)	7.88	7.68	64.00	5.29	0.97	2.09	19.97	37.17	47.27	11134

The fuels produced from combustion of the coal blends in the HOB were sampled and analyzed by ALS Environmental in order to determine the concentrations of CH_4, C_2H_4, C_2H_6, H_2S, COS, CS_2, NH_3, HCN, and Cl. The fuel compositions are presented in Table 39. There was a large discrepancy in the concentrations of some of the species shown in Table 39. The most striking difference is between the H_2S concentrations provided for the first and second samples of syngas derived from the Illinois/PRB coal blend. An equilibrium calculation along with gas chromatography data collected with a Varian Micro GC suggested that the second set of data collected was not accurate, and that the H_2S concentration in the syngas derived from the Illinois/PRB coal blend was near 1600 ppm.

Table 39: Trace species analysis of synthesis gas, ppm

Coal Blend	CH_4	C_2H_4	C_2H_6	H_2S	COS	CS_2	NH_3	HCN	Cl
Illinois/PRB	3900	470	51	1700	260	6.6	<0.43	<0.047	<0.086
Illinois/PRB	5600	1400	88	0.052	340	29	2.3	<0.063	<0.11
Utah/PRB	7400	1300	66	<0.007	150	0.39	<0.57	<0.063	<0.11
Utah/PRB	15000	3000	120	<0.007	110	0.88	130	<0.063	<0.11

The gas chromatography results from the synthesis gas fuel analysis are shown in Table 40.

Table 40: Fuel compositional analysis (dry vol%)

	H_2	N_2	CO	CH_4	CO_2
Illinois/PRB	18.78 ± 0.4796	1.04 ± 0.1567	32	1.01 ± 0.093	43.67 ± 1.6901
Illinois/PRB	20 ± 1.6	0.93 ± 0.62	34.84 ± 3.41	0.86 ± 0.08	42.42 ± 5.54
Utah/PRB	32.24 ± 1.93	0.91 ± 0.03	50.72 ± 1.61	2.05 ± 0.04	14.08 ± 3.51
Utah/PRB	20.10 ± 2.22	0.89 ± 0.14	32.57 ± 3.23	1.71 ± 0.25	44.73 ± 4.61

Performance of the OTM tubes was evaluated in terms of the oxygen flux across the OTM membrane. Oxygen flux was calculated using a formula that considers how much O_2 is depleted from the air during operation. Normalized oxygen flux values for OTM tubes tested in synthesis gas environments derived from the two fuel blends are reported in Figure 61 as a function of temperature. Figure 61 shows that performance in the Utah/PRB blend was higher than performance in the Illinois/PRB blend over all of the temperatures probed. Figure 61 also shows that for the OTM tubes tested in syngas derived from both coal blends the performance increased linearly with temperature up to a temperature of approximately 920°C.

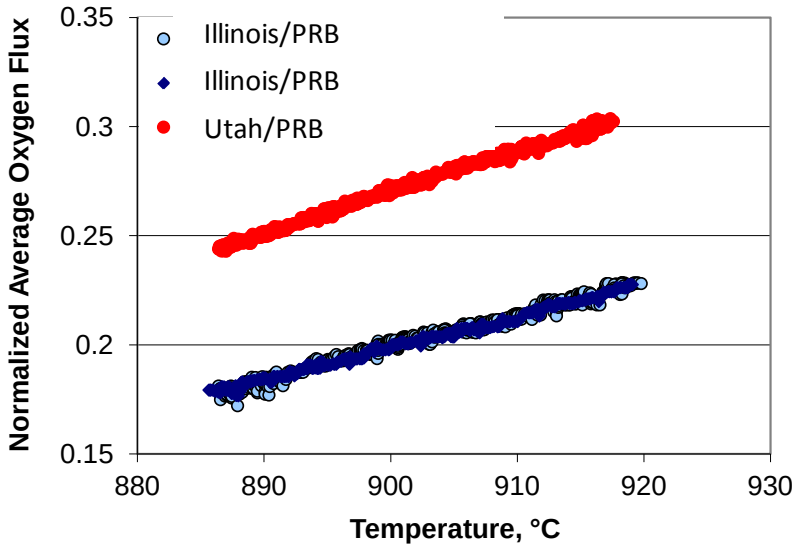

Figure 61: Comparison of OTM Performance in syngas compositions derived from Illinois/PRB and Utah/PRB coal blends

Oxygen flux is the primary performance metric used to evaluate the OTM tubes; however it is also important to be aware of the fuel conversion obtained during operation. During a test in the Illinois/PRB coal derived synthesis gas, gas chromatography measurements of the fuel composition prior to and after exposure to the OTM tube suggested that H_2 was consumed, CO was generated, CO_2 was consumed, CH_4 was consumed and C_2H_4 was consumed. One potential explanation for the CO result is that some entrained char was gasified between the two sampling ports to generate additional CO in the syngas. It is also possible that conditions for coking (i.e. CO_2 converted to CO) existed somewhere between the HOB and the gas chromatograph. This observation could also explain why the concentration of CO_2 decreased. It was determined that if the char combustion was affecting the sampled fuel compositions, that the samples could not be used to estimate the percent of syngas consumed by the OTM.

During test campaigns performed on OTM tubes in both coal derived synthesis gas environments no discernible performance degradation was observed. Performance consistency over time is illustrated in both Figure 62 and Figure 63 at various operating temperatures. The oxygen flux data obtained for the Illinois/PRB blend was generally more consistent that obtained for the Utah/PRB blend.

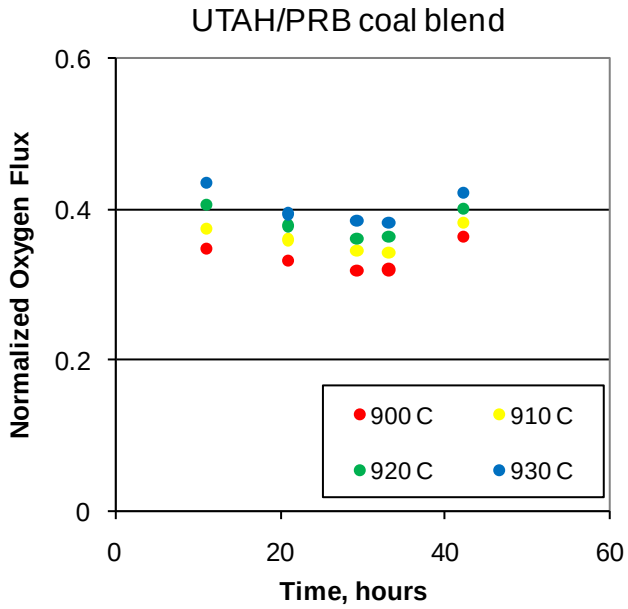

Figure 62: OTM performance as a function of operating time in syngas derived from a Utah/PRB coal blend.

.

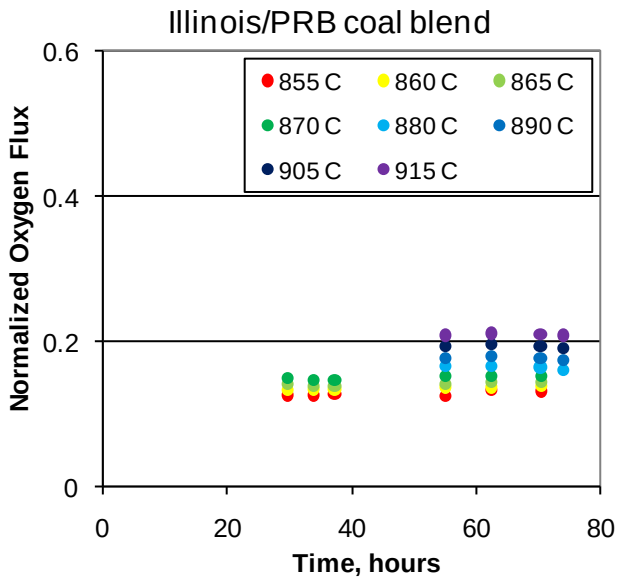

Figure 63: OTM performance as a function of operating time in syngas derived from an Illinois/PRB coal blend.

After performance testing of OTM tubes in coal derived syngas environments, buildup of loose and fixed ash on the outside of the OTM tube was observed, as shown in Figure 64. Though only ash is present on the pictured OTM, in actual operation there will be both ash and char in contact with the OTM tubes. The flow of char and ash into the OTM zone of the reactor was measured using an isokinetic probe at two points in the reactor, during one of the tests using the Utah/PRB coal derived synthesis gas. The sampled solids flow was between 2.15 and 2.56 g/s. Three sets of tests were performed to determine if the loose ash negatively affected the tube performance through the introduction of additional mass transport resistance. The loose ash was removed from the surface of the OTM tube through an air blower after the OTM had been cooled down. There is a possibility that some particles of ash fused to the ceramic support surface and remained after the loose ash was removed. The ash fused onto the surface of the tube will be referred to as fixed ash. It can be seen in Figure 65 that the O_2 flux measurements

with and without the loose ash are consistent over a range of operating temperatures. This result suggests that the collection of loose ash on the outside surface does not add a significant resistance to the transport of H_2 and CO to the OTM active layers. It is not currently known if the accumulation of fixed ash affects the performance of the OTM tube.

Figure 64: Ash on surface of OTM tube

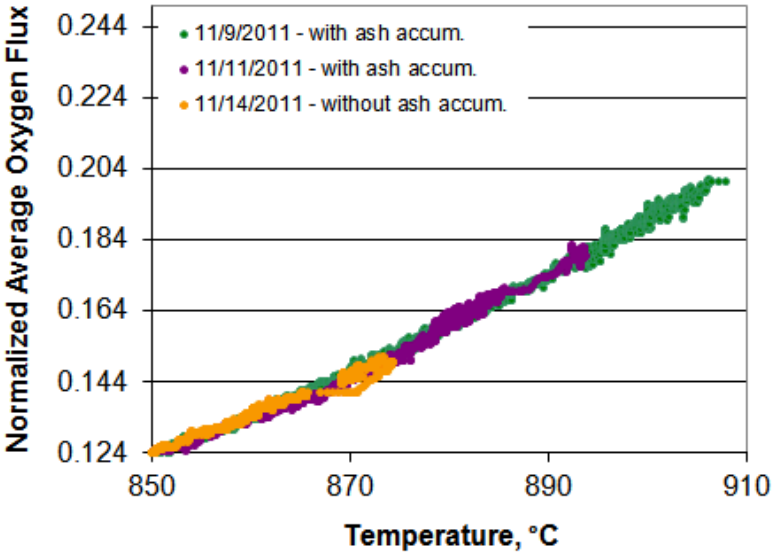

Figure 65: OTM performance in Illinois/PRB coal derived synthesis gas with various conditions of accumulated ash

Materials Analysis

In the fourth quarter of 2011, UCONN was subcontracted to analyze the material properties of the OTM tubes subjected to oxygen flux tests at the University of Utah. The oxygen flux tests involved synthesis gas environments generated from coal blends in an experimental coal gasifier. Surface, interface and bulk structure and chemistry were the subject

of the analysis. Interactions between the OTM and the surface ash deposit, electrochemically active cell components and the electrocatalyst were examined. Analytical tools and techniques such as FESEM, EDS, XRD, and DSC were used to characterize the OTM tubes. Materials stability was also analyzed using a standard thermochemical data base.

Samples of ash present on the surface of the OTM tube underwent XRD and SEM-EDS analysis. Complex silicates containing alkali, alkaline earth and transition metals were identified as possible compounds. X-ray diffraction results are shown in Figure 66. A literature search to understand the melting behavior of the silicates indicated the ash deposit on the OTM surface should not form liquid compounds under the experimental conditions. A complementary DSC analysis on the ash deposit indicated endotherms (indicative of melting) above 1000°C.

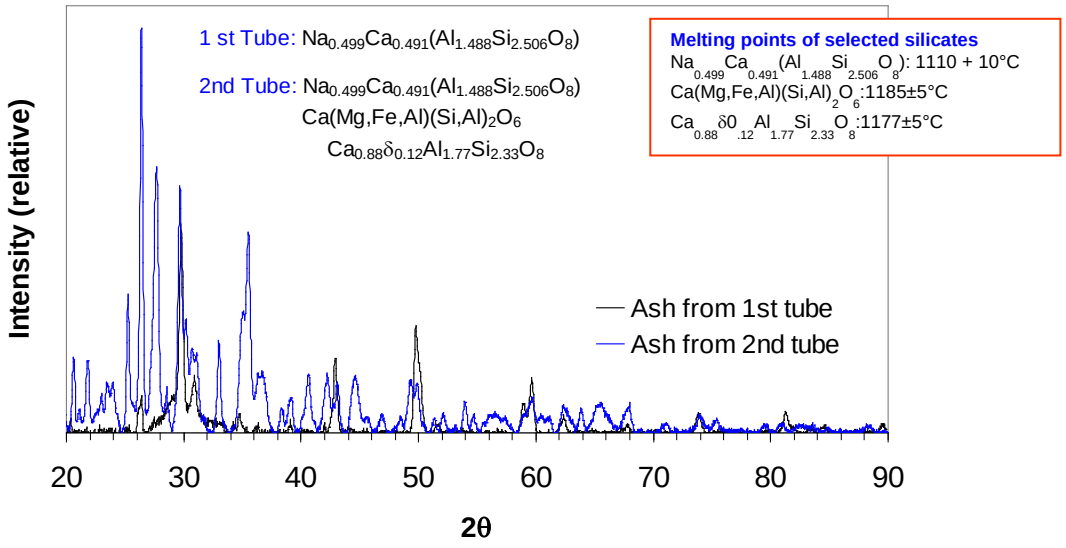

Figure 66: XRD pattern obtained from the ash deposit. Chemistry and melting point are also shown.

The porous support surface was analyzed by FESEM and EDS techniques to examine the possibility of interaction, molten compound formation and surface pore closure. Surface analysis and the morphology of the ash deposit is shown in Figure 67. The ash deposit

consisted of agglomerates showing both smooth and powdery regions. The ash particles deposited at the pore surfaces remained loose. There was no indication of surface compound or molten phase formation at the support tube surface. It was postulated that the molten phase present in the ash deposit formed in the gasifier at elevated temperature and was carried in the gas stream to the OTM surface.

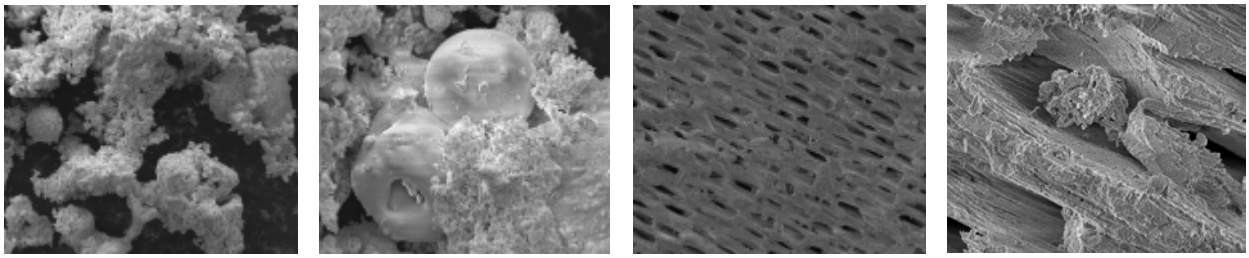

a b c d

Figure 67: (a) Ash deposited on the OTM. (b) Powdery deposit, (c) smooth deposit, and (d) localized ash deposit formed on the porous channel.

The microstructure of a polished cross section of one of the tested OTMs is shown in Figure 68. The microstructure clearly shows the activation layers, separation layer, and porous support. There are distinct and sharp boundaries between the layers indicating both the absence of interdiffusion between layers and the absence of interfacial compound formation. Such microstructural features can be attributed to (a) thermochemical stability of the compounds under the exposure conditions and (b) short reaction times.

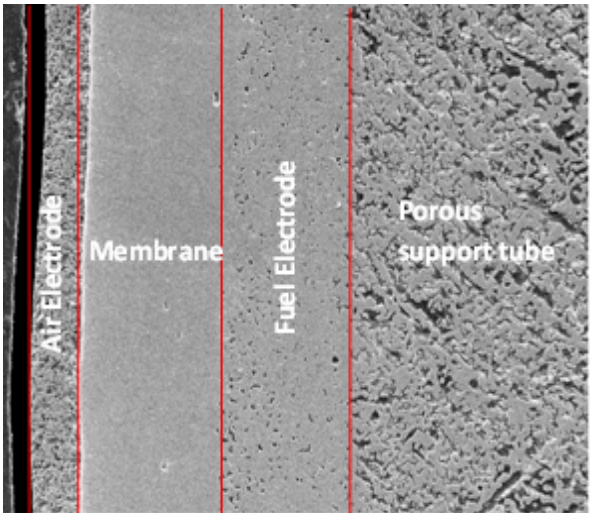

Figure 68: Micrograph of OTM polished cross section

Structural (secondary and backscattered mode analysis) and elemental analysis performed using FESEM and EDS. As expected, two distinct phases were identified in the membrane and the fuel oxidation layer. The electronic and ionic conductiving phases within the oxygen incorporation layer were not distinguishable, suggesting elemental interdiffusion. From EDS analysis, it was found that the electronic conducting phase of the fuel oxidation layer had a lower concentration of Fe than expected, suggesting elemental interdiffusion between phases.

Observations concerning the architecture of the OTM tubes from micrographs include:

- Porous oxygen incorporation layer (air electrode) showed evidence of localized sintering and densification attributed in part to local thermal conditions.
- Interfaces between oxygen incorporation layer (air electrode) and the dense membrane and between the fuel oxidation layer (fuel electrode) and the dense membrane showed minimal cationic interdiffusion. This is postulated to be due to shorter exposure time.
- Fuel oxidation layer (fuel electrode) showed dense layer formation and the development of a density gradient, consisting of a porous region near the separation layer and denser region near the porous support attributed in part to local thermal conditions.
- Presence of electrocatalyst was identified within the fuel oxidation layer.
- Presence of electrocatalyst was identified within the support.
- Fracture surface analysis showed that the catalytic material remained poorly adherent to the fuel oxidation layer and the porous support.
- Porous support tube did not show the presence of ash deposit

Conclusions

Highlights of the work performed at the University of Utah and the University of Connecticut included successful demonstration of OTM flux performance and thermal cycling in coal derived syngas, stability of OTM in a high sulfur atmosphere, and robustness of the material set to coal ash contamination. Material changes (densification) observed during this project were attributed to insufficient thermal stability, which is a major area of Phase III work.

2.4.4. Subtask 4.6 Tube-Section Heat Transfer Testing

Understanding the OTM heat transport capability is critical to designing OTM integrated steam generation equipment. Surface temperatures and emissivity values of the membranes were collected. A combined fluid flow, mass transport and heat transport model of a single tube was developed in COMSOL Multiphysics™. Temperature predictions from the model were compared to the measured temperatures, in order to assess the contributing heat transport mechanisms. In this subtask, work was also done to map out the performance of the larger pilot size OTM tubes and to collect information required for reactor design and scale up through performance of instantaneous oxygen flux and residence time measurements.

Heat Transport Properties

During experimental performance tests, temperatures on the surface of the OTM tube on both the coating side and the porous support side, along with temperatures in the gas adjacent to the OTM tube were recorded. Table 41 shows typical temperatures obtained on OTM tubes prepared with the ENrG advanced support and the advanced fuel oxidation layer material,

operated in the low pressure reactor. During these tests, two fuel mixtures were used; CO/CO_2 and syngas (a mixture containing $CO/H_2/CO_2$). The flow rate of either fuel mixture was 1 SLPM. Air flow rate was varied, depending on the fuel mixtures; it was 3 SLPM when operating in $CO/H_2/CO_2$ and 2 SLPM when operating in CO/CO_2. There were four thermocouples measuring the OTM outside surface temperature of the porous support, one thermocouple measuring the air temperature close to the OTM tip in line with the lance tube. The normalized position of 0.0 is representative of the OTM tip, and the normalized position 1.0 is representative of the OTM flange. For these experiments, the low pressure reactor was operated in a co-flow arrangement. For this case of co-flow operation, the tip of the OTM tube was exposed to both fresh fuel and air; the oxidized fuel and depleted air exited at the flange end of the OTM tube (i.e., end opposite from tip). The measured temperatures showed approximately 10°C difference between the air annulus and the coating surface at a normalized position of 0.0 when operating in a CO/CO_2 fuel, and an approximately 2°C difference between the air annulus and the coating surface at a normalized position of 0.0 when operating in a $CO/H_2/CO_2$ fuel. The small temperature differences reported between the air-side coating surface and the air annulus indicate that the heat generated in the coatings is able to be transported to the gas phase. Temperature differences of over 100°C were reported between the coating surface on the air-side and the porous support surface on the fuel-side. This indicates that the poor thermal conductivity of the "advanced" porous support is limiting heat from being transported.

Table 41: Typical surface and gas temperatures on OTM tubes tested in CO/CO2 and synthesis gas (CO/H2/CO2) mixtures in the low pressure reactor.

	Normalized Position	Temperature [C] CO/CO2	Temperature [C] Synthesis Gas
Air Annulus Temperature [C]	0	1120	1137
Surface Coating Temperature [C]	0	1109	1138
Porous Support Temperature [C]	0.25	981	1034
Porous Support Temperature [C]	0.5	1008	1015
Porous Support Temperature [C]	0.75	996	993
Porous Support Temperature [C]	1	983	976

Similar to tests conducted in the low pressure reactor, the temperatures of the OTM tube coating and porous support surface were measured during the oxygen flux tests in the high pressure reactor. Table 43 shows the typical temperature results from an OTM tube prepared with an advanced support and anode layers when tested with CO/CO_2 fuel and with sulfur-free syngas at ambient pressure and furnace at 900°C. In the tests, air flow rate was 6 SLPM, the CO/CO_2 mixture was 3.2 SLPM, and syngas was 3.6 SLPM. There were three thermocouples measuring the temperature of OTM porous support surface, and one thermocouple measuring the OTM coating temperature close to OTM tip. In the table, normalized position of 0.0 is representative of the OTM tip, and the normalized position 1.0 is representative of the OTM flange. As shown in Table 43, the surface temperature along the OTM tube was quite uniform (< 20°C) for both fuel tests. This was attributed to air and fuel operating in counter-flow configuration during this test. However, there was more than 100°C temperature difference between the coating surface on the air-side and the porous support surface on the fuel-side.

This indicates that the porous support was not efficient in transporting the heat generated in partial oxidation process on OTM membrane through the support layer.

Table 42: Typical surface temperatures of OTM tubes tested in CO/CO2 and syngas (H2/CO/CO2/N2/CH4/H2O) fuel gas environment at ambient pressure with furnace at 900°C

.

Thermocouple Location	Normalized Position	Temperature (°C)	
		CO/CO2	syngas
Surface Coating	0	1087	1134
Porous Support	0	986	1007
Porous Support	0.5	978	988
Porous Support	1	992	988

Three mechanisms are considered to be involved in OTM heat transport: convection, conduction and surface-to-surface radiation. The emissivity of the coatings and the porous support are important to assessing surface-to-surface radiation. Emissivity values of OTM materials and OTM reactor materials were evaluated and are presented in

Table 44. This data provides a preliminary input for modeling and reactor design calculations. This data was collected within a narrow range of wavelength (7 to 14 mm) and temperature (60°C to 250°C). Efforts to quantify OTM material emissivity continued into Phase III where OTM material emissivity values were measured at temperatures from 400K to 1300K and emissivity values in the range of 0.91 to 0.94 were reported.

Table 43: Measured emissivity values of OTM materials

	Emmissivity @ 60°C	Emmissivity @ 100°C	Emmissivity @ 250°C
Material 1	0.96	0.96	0.96
Material 2	0.89	0.9	0.9
Material 3	0.97	0.97	0.97
Material 4	0.91	0.91	0.91
Material 5	0.95	0.95	0.95
Material 6	0.88	0.88	0.88
Material 7	0.94	0.95	0.95
Material 8	0.93	0.94	0.94

Heat Transport Models

A 2D axisymmetric single tube OTM model was developed in COMSOL Multiphysics™, a modeling and simulation software package, to describe the fluid transport, mass transport, kinetics, and heat transport of the OTM tubes. Figure 69A - Figure 69C show examples of predicted temperature profiles of the OTM tube given three different sets of heat transport assumptions. The model used to generate the results in Figure 69A included heat transport via conduction and convection mechanisms, with no radiative heat transport. The model used to generate the results in Figure 69B included heat transport via conduction, convection and radiation mechanisms, and included a moderate emissivity value for the porous support material. The model used to generate the results in Figure 69C included heat transport via conduction, convection and radiation mechanisms, and included a high emissivity value for the porous support material.

These predictions can be compared to coating surface, porous support and air annulus temperatures measured in experiments reported in **Table 42**. Comparison indicates that radiation is a key heat transport mechanism, and that the emissivity values should be in the moderate to high range. Given these assumptions, OTM coating and air annulus temperatures

are expected to be very similar (within 50°C) and < 1200°C given a furnace set-point temperature of 900°C and moderate to high OTM emissivity values, as also indicated by experimental results in Table 41. The temperature of the OTM active layers is of interest because it drives the active layer performance and degradation mechanisms. If the coatings reach temperatures > 1200°C it is expected that they will be subject to enhanced degradation, and if the coatings achieve temperatures of < 900°C it is expected that they will be subject to poor performance.

In Phase III of this program, additional combined fluid transport, mass transport and heat transport simulations were performed. Specifically, a number of reactor design layouts were assessed in terms of their heat transport capability, with emphasis placed on the radiative properties of reactor layouts.

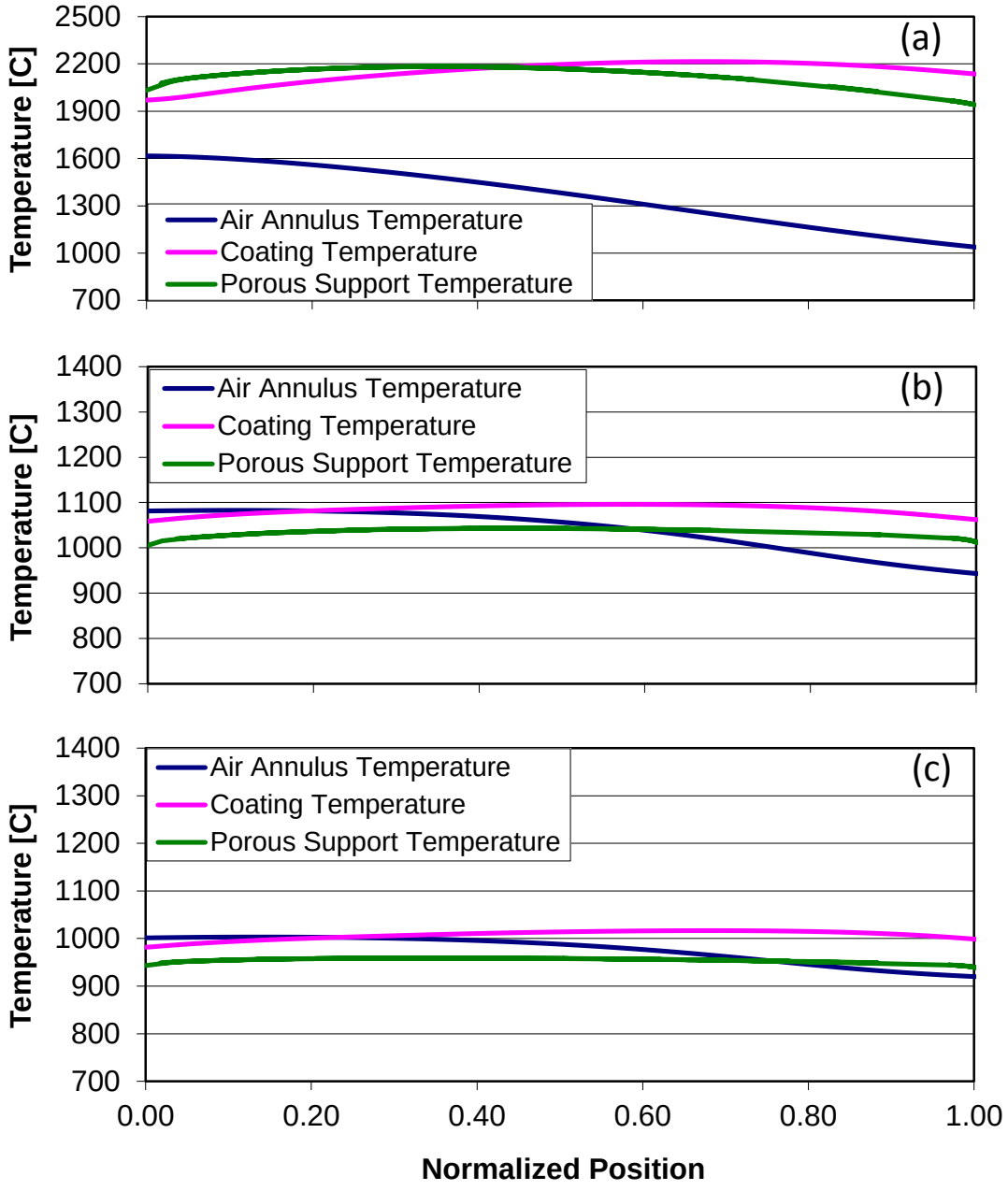

Figure 69: Predicted temperature profiles of the OTM tubes as a function of axial position. (a) no radiative heat transport, (b) moderate OTM emissivity, (c) high OTM emissivity

.

Performance Mapping

The method used to map the performance of OTM tubes in subtask 4.1 and 4.2 has been to evaluate the performance of different OTM materials by reporting average oxygen flux versus fuel utilization. A low fuel flow rate is typically used so that high fuel utilization could be probed on a short lab-scale tube in a single experiment. In order to simulate experimentation with longer OTM tubes or OTM tubes in a series configuration, a set of tests were developed to probe the instantaneous oxygen flux values over a range of fuel conversion in the high pressure reactor. The instantaneous (or local) oxygen flux was collected over narrow bands of fuel conversion, which was accomplished by increasing gas flow rates to permit small incremental changes to the fuel gas composition along the entire length of the tube. In order to collect this type of data, a series of experiments were conducted, where the outlet fuel composition of each experiment was used as the inlet composition for the subsequent experiment. The set of data collected was then converted into average oxygen flux. Figure 70 shows the oxygen flux vs. fuel conversion results of this type of analysis for three OTM tubes tested in the high pressure reactor, at ambient pressure. Tubes A and B were fabricated using the ENrG "advanced" support, and tube C was made from a standard support. Figure 70 demonstrates that the highest performing tube prepared with the ENrG advanced support (Tube A) exhibited a normalized average oxygen flux of > 0.6 at 80% fuel conversion, and the lowest performing tube prepared with the standard support showed an average oxygen flux of ~ 0.3 at 80% fuel conversion. These results are consistent with what was reported when testing performance with single experiments at low flow rates. In addition, these experiments provided the performance at lower fuel conversion values and can be used to better understand the performance trade-off of operating at lower fuel conversion.

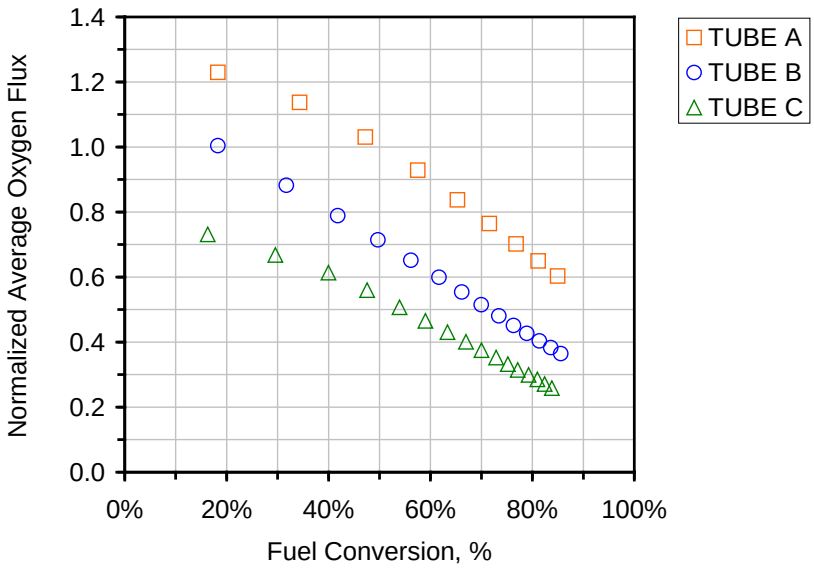

Figure 70: Normalized average oxygen flux versus fuel conversion for three OTM tubes evaluated in the HPR. The initial inlet fuel flow and composition was the same for all three tubes.

During OTM reactor design activities and capital cost estimation activities it is necessary to have a good estimate of required reactor volume. Residence time, as estimated from lab-scale data, can be used to better understand required reactor volume as a function of fuel conversion and this data can be used to study the cost trade-off associated with operating at different values of fuel conversion.

The residence time was measured in both the low pressure and high pressure reactor and over a number of different testing conditions. Figure 71 shows the residence time of the fuel gas required to yield a wide range of fuel conversion values for OTM tubes measured in the high pressure reactor. The dashed line indicates the expected trend in residence time versus fuel conversion. The corresponding flux data for these tubes was presented in Figure 70. As

expected, the tube with the highest flux (TUBE A) required the shortest residence times to accomplish a given fuel conversion.

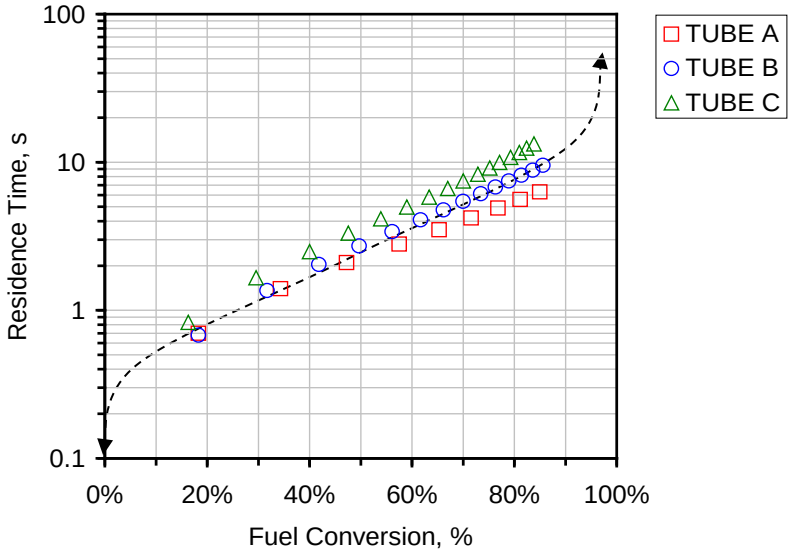

Figure 71: Residence time versus fuel conversion, for 3 OTM tubes evaluated in the HPR. The initial inlet fuel flow and composition was the same for all three tubes.

OTM operation can be divided into two main categories; (1) low fuel conversion and high oxygen flux (POx) or (2) high fuel conversion and low flux (combustion). Achieving higher conversion requires increased residence time. Efforts continued into Phase III to understand the trade-offs associated with operating at different regimes and in estimating required reactor volumes and reactor costs.

2.5 Task 5: Project Management

Project spending for Phase I and Phase II from year 2007 to 2012 is shown in Figure 72in terms of cumulative dollars spent per quarter. Actual spend value includes the labor rate

adjustment for the 6/30/12 ICE Submission. Figure 72also shows the total allotted contracted budget. The project was completed within budget in June of 2012.

During the first phase of this project, initiated April 1, 2007, resources were spent on down-selection and cost estimation of the Advanced Power Cycle for integration of OTM membranes in a coal fired power plant, development of a high performance OTM membrane technology, manufacturing of short laboratory scale OTM tubes (1/3 pilot scale) construction of reactors at Praxair and at the University of Utah for evaluation of OTM tubes in high pressure fuels with sulfur impurities and coal derived fuels, respectively and testing and characterization of OTM tubes in existing infrastructure. The first phase of this program was completed December 31, 2009.

During the second phase of this program, initiated January 1, 2010, resources were allocated towards cost estimates and engineering designs of the OTM Boiler and POx units, update of the Advanced Power System cost model, production of pilot size OTM tubes and manufacturing cost estimation, testing and characterization of OTM tubes including tests in both the high pressure reactor at Praxair and tests in the multi-tube reactor for testing in coal derived syngas environment at the University of Utah.

In October of 2010, the Phase III contract commenced. By this time, most of the Phase II work had been completed, with the exception of testing OTM tubes in the coal gas reactor at the University of Utah (Task 4), analysis of the OTM tubes at the University of Connecticut (Task 4), and the engineering design and cost estimate of the OTM POx and Boiler units prepared by Shaw Energy and Chemicals. The decrease in spending for Phase I and Phase II after October 2010 reflects a shift in the efforts towards Phase III activities.

During Phase II a search for a high-volume ceramics manufacturing partner was conducted for the selection of a partner for Phase III of this program, which focuses on pilot scale manufacturing and demonstration activities. In April of 2011, the search concluded with the formation of a partnership between Praxair and Saint-Gobain.

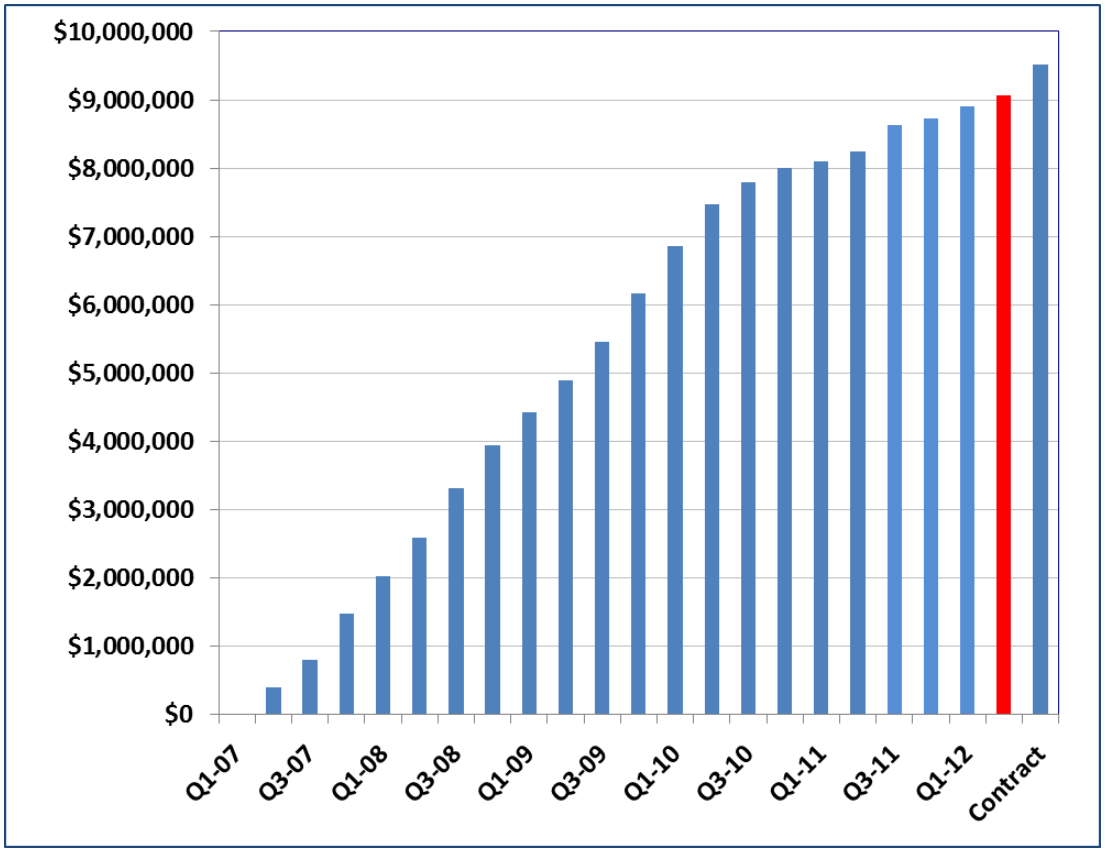

Figure 72: Project Spend for Phases I and II

During the course of this program, project results and status were reported at several conferences (Appendices D-F), and a white paper summarizing the Advanced Power Cycle titled, "The Advanced Power Cycle: A Cost Effective Solution for Carbon Capture and Sequestration from Coal Based Power Production" was submitted to the DOE in April of 2010

(Appendix A). Several inventions and discoveries led to patent applications during the course of this program (Appendix H).

References

[1] M. Christie, B. van Hassel, J. Li, and M. Shah, "OTM Based Oxycombustion for CO_2 Capture from Coal Power Plants", 32nd International Technical Conference on Coal Utilization & Fuel Systems, Clearwater, FL, 2007.

[2] J. Li, J. Wilson, N. Degenstein, M. Shah, B. van Hassel, and M. Christie, 33rd International Technical Conference on Coal Utilization & Fuel Systems,Clearwater, FL, 2008.

[3] J. Wilson, M. Christie, N. Degenstein, M. Shah, and J. Li, "OTM Based Oxy-fuel Combustion for CO_2 Capture", 34th International Technical Conference on Coal Utilization & Fuel Systems, Clearwater, FL, 2009.

[4] Christie, G.M., Degenstein, N., Li, J., Wilson, J. Peck, J., Corpus, J., Shah, M., Kelly, S.M., Rosen, L.,,"Oxygen Transport Membrane Based OxyCombustion for CO2 Capture from Coal Power Plants NT43088", 2010 CO2 Capture Technology Conference, Pittsburgh, PA, Sept 14th, 2010

[5] Rosen, L., Degenstein, N., M. Shah,, Wilson, J. , Kelly, S. Peck, John, Christie, M., International Conference on Greenhouse Gas Control Technologies GHGT10) 2010 Paper. 'Development of oxygen transport membranes for coal-based power generation (Energy Procedia Volume 4, 2011 pp. 750-755)

[6] Kelly, S.M., "Recovery Act: Oxy-combustion: Oxygen Transport Membrane Development" 2011 CO2 Capture Technology Conference, Pittsburgh, PA, August 24th, 2011

[7] Christie, G.M., "Recovery Act: Oxy-combustion: Oxygen Transport Membrane Development" 2012 CO2 Capture Technology Conference, Pittsburgh, PA, July 11th, 2012

Appendix A

OTM Based OxyCombustion for CO_2 Capture from Coal Power Plants

Phase 1 Techno-economic evaluation of the Advanced Power Cycle Concept

DOE AWARD NO. DE-FC26-07NT43088

OTM Based OxyCombustion for CO_2 Capture from Coal Power Plants

Phase 1 Techno-economic evaluation of the Advanced Power Cycle Concept

DOE AWARD NO. DE-FC26-07NT43088

Principal Author: Nick Degenstein
Contributing authors: Minish Shah, Jamie Wilson

Program Manager: Max Christie
Business Officer: Lee Rosen

Praxair, Inc.
175 East Park Drive
Tonawanda, NY 14150
Contact: G. Maxwell Christie
Tel: (716) 879-7738
Fax: (716) 879-7931
email: max_christie@praxair.com

Original Report Issue Date: February 26, 2010

Public Report Issue Date: May 29, 2012

Disclaimer

This report was prepared as an account of work sponsored by an agency of the United States Government. Neither the United States Government nor any agency thereof, nor any of their employees, makes any warranty, express or implied, or assumes any legal liability or responsibility for the accuracy, completeness, or usefulness of any information, apparatus, product, or process disclosed, or represents that its use would not infringe privately owned rights. Reference herein to any specific commercial product, process, or service by trade name, trademark, manufacturer, or otherwise does not necessarily constitute or imply its endorsement, recommendation, or favoring by the United States Government or any agency thereof. The views and opinions of authors expressed herein do not necessarily state or reflect those of the United States Government or any agency thereof.

Executive Summary

The Advanced Power Cycle is a concept for utility scale electricity generation which uses OTM (oxygen transfer membranes) for oxy-combustion. OTM technology represents a step change in oxygen separation efficiency in high temperature systems as compared to conventional cryogenic air separation technology. In the Advanced Power Cycle concept coal gasification is used to produce syngas which is combusted on OTM surface with the combustion energy transferred to steam for power production. Roughly 67% of the total oxygen used in the process is supplied using OTM technology.

A techno-economic evaluation of The Advanced Power Cycle was performed for 6 base cases for determination of cycle efficiency and cost of electricity (COE) in 2008 dollars. The six simulated base cases investigate the effect of 2 main parameters, steam cycle complexity and type of sulfur recovery unit.

The Advanced Power Cycle COE was determined for three coal prices for each of the base cases. Thirteen of the eighteen scenarios satisfy the DOE goal of less than 35% increase in COE. Higher coal price favors the Advanced Power Cycle COE due to the high efficiency enabled by OTM technology.

Further improvements to the COE can be made by adjusting the degree of fuel utilization in the OTM boiler. The optimal degree of fuel utilization depends on membrane flux performance, OTM "cost allocation" and parasitic cost of cryo-ASU supplied oxygen.

In comparison to other power cycles that enable carbon capture and sequestration (CCS), the Advanced Power Cycle has a uniquely low cost of CO_2 removed and avoided due to a relatively low COE, a high net cycle HHV efficiency, and high CO_2 capture efficiency.

The OTM-based Advanced Power Cycle is a promising technology for achieving DOE's goal of <35% impact on COE for power plants with CO_2 capture.

Table of Contents

DISCLAIMER **2**

EXECUTIVE SUMMARY **3**

TABLE OF CONTENTS **4**

LIST OF FIGURES **5**

LIST OF ACRONYMS **7**

1. INTRODUCTION **9**

2. DESIGN BASIS AND ASSUMPTIONS **12**

3. PROCESS DESCRIPTION **19**

4. MAJOR EQUIPMENT CAPITAL COST ESTIMATION **33**

5. RESULTS **38**

5.1. OTM CASES WITH FGD 38

5.2. OTM CASES WITH WGCU 53

5.3. COST SUMMARY 67

5.4. OPTIMUM 'EXTENT OF COMBUSTION' WITH OTM 70

6. CONCLUSIONS AND RECOMMENDATIONS **73**

List of Figures

Figure 1: Advanced Power Cycle with FGD for sulfur recovery 11
Figure 2: Advanced Power cycle using WGCU technology for sulfur removal 11
Figure 3: Advanced Power Cycle Case List 12
Figure 4: Steam Cycle Conditions 12
Figure 5: Ambient and Cooling Water Conditions 13
Figure 6: OTM-ASU Operating Assumptions 13
Figure 7: CO2 Product Specifications 13
Figure 8: Coal Composition 14
Figure 9: Power Cycle Operating Costs 16
Figure 10: COE comparison basis 17
Figure 11: Temperature Duty diagram for a traditional pulverized coal power plant. Diagram shows the traditional arrangement of heat transfer surface. 22
Figure 12: Temperature Duty diagram for a boiler feedwater preheat system of a traditional pulverized coal power plant. 23
Figure 13: OTM boiler detail 23
Figure 14: Representative Temperature Enthalpy Diagram for the Advanced Power Cycle 24
Figure 15: Advanced Power Cycle with FGD for Sulfur containment 39
Figure 16: Case 1 Stream Summary 40
Figure 17: Case 1 power, industrial gas and environmental performance summary 41
Figure 18: Case 1 capital cost estimate 42
Figure 19: Case 1 COE estimate. Contingency and Engineering costs reported here do not reflect contributions from the Cryogenic ASU or CPU equipment. 43
Figure 20: Case 2 Stream Summary 44
Figure 21: Case 2 power, industrial gas and environmental performance summary 45
Figure 22: Case 2 capital cost estimate 47
Figure 23: Case 2 COE estimate. Contingency and Engineering costs reported here do not reflect contributions from the Cryogenic ASU or CPU equipment. 48
Figure 24: Case 3 Stream Summary 49
Figure 25: Case 3 power, industrial gas and environmental performance summary 50
Figure 26: Case 3 capital cost estimate 51
Figure 27: Case 3 COE estimate. Contingency and Engineering costs reported here do not reflect contributions from the Cryogenic ASU or CPU equipment. 52
Figure 28: Advanced Power Cycle with WGCU for Sulfur containment 54
Figure 29: Case 4 Stream Summary 55
Figure 30: Case 4 power, industrial gas and environmental performance summary 56
Figure 31: Case 4 capital cost estimate 57
Figure 32: Case 4 COE estimate 58
Figure 33: Case 5 Stream Summary 59
Figure 34: Case 5 power, industrial gas and environmental performance summary 60
Figure 35: Case 5 capital cost estimate 61
Figure 36: Case 5 COE estimate 62
Figure 37: Case 6 Stream Summary 63
Figure 38: Case 6 power, industrial gas and environmental performance summary 64
Figure 39: Case 6 capital cost estimate 65
Figure 40: Case 6 COE estimate 66

Figure 41: Calculated COE for 6 OTM cases at various coal prices compared to the Air-PC reference case (no capture) 67
Figure 42: Percent increase in COE over the reference case for various coal prices. 68
Figure 43: Cost of CO2 avoided and removed for the 6 OTM cases at various coal prices. 69
Figure 44: COE vs fuel utilization for two membrane costs. 71

List of Acronyms

Adv-USC	Advanced Ultra Supercritical
ASU	Air Separation Unit
Aux	Auxiliary
BFW	Boiler Feedwater
BGL	British Gas-Lurgi (gasifier type)
Btu	British Thermal Unit
c	Cent
CCF	Capital Cost Factor
CCS	Carbon Capture and Sequestration
CF	Capacity Factor
CFB	Circulating Fluidized Bed
CM	Construction Management
COE	Cost of Electricity
CPU	Carbon Dioxide Processing Unit
Cryo	Cryogenic
DOE	Department of Energy
Eng'g	Engineering
EPC	Engineering Procurement and Construction
FCC	Fluidized Catalytic Cracker
FGD	Flue Gas Desulfurizer
FWH	Feedwater Heater
GE	General Electric
GT	Gas Turbine
Hg	Mercury
HHV	Higher Heating Value
IGCC	Integrated Gasification Combined Cycle
k	Thousand
kW	Kilowatt
kWh	Kilowatt-hour
LF	Levelization Factor
LMTD	Log Mean Temperature Difference
MM	Million
MU	Makeup
MW	Megawatt
MWh	Megawatt-hour
NETL	National Energy Technology Laboratory
NGCC	Natural Gas Combined Cycle
NOx	Nitrogen Oxides
O&M	Operations and Maintenance
OC	Operating Cost
OTM	Oxygen Transfer Membrane
PC	Pulverized Coal
PCC	Post Combustion Capture
PM	Particulate Matter
POX	Partial Oxidation
RTI	Research Triangle Institute

SC	Super Critical
scfh	Standard Cubic Foot per Hour
SECA	Solid State Energy Conversion Alliance
SOFC	Solid Oxide Fuel Cell
SOx	Sulfur Oxides
ston or ton	Short Ton
TPC	Total Plant Cost
tpd	Ton per Day
USC	Ultra Super Critical
WGCU	Warm Gas Cleanup
WT	Water Treatment

1. Introduction

There are three main technologies which can be used in the power generating industry for capturing CO_2 from power plants (in the relatively near term): pre-combustion (integrated gasification combined cycle, IGCC), oxy-combustion, and post-combustion capture (PCC). Praxair's Advanced Power Cycle concept represents a more efficient, although longer term, solution to this same situation that relies on OTM (oxygen transfer membranes) for oxy-combustion. In conventional oxy-combustion fuel is combusted with a mixture of oxygen and recycled flue gases to mimic the boiler temperatures and heat transfer profile of an air-fired scenario. Oxygen is supplied from a cryogenic air separation unit (cryo-ASU); this is currently the lowest cost technology for large scale oxygen supply. The goal of OTM technology is to make a step change reduction in the parasitic power required for oxygen supply and thus achieve a step change in efficiency improvement for a power plant.

The Advanced Power Cycle concept uses a gasifier to produce pressurized syngas which is heated with combustion reactions occurring on OTM membranes. The hot syngas is expanded to produce a portion of the plant gross power. The resulting near atmospheric pressure syngas is further combusted on the surface of OTM membranes in the OTM boiler. As the syngas is combusted in the OTM boiler, heat is transferred to steam and power is produced using a steam turbine. The flue gas is roughly equivalent to conventional oxy-combustion flue gas (but with a slightly higher CO_2 concentration) and is processed in the same manner for CO_2 purification and pressurization.

Compared to other power generation processes enabling CCS (pre-combustion, post combustion, and oxy-combustion), the OTM cycle has an energy efficiency advantage because

the power generation cycle contains both Brayton and Rankine cycles for. While this is similar to an IGCC cycle, the OTM case operates at an advantage to IGCC cycles with respect to the steam (Rankine) cycle because a higher pressure and temperature steam cycle can be used. This is because much of the fuel is combusted at atmospheric pressure and at around 1000C.

In comparison to conventional oxy-combustion, much of the electrical parasitic load associated with a large cryo-ASU is avoided due to the efficiency of the OTM membranes, also no flue gas recirculation is needed because the use of OTM membranes controls the rate of fuel combustion. When using OTM membranes the parasitic cost of oxygen production is essentially equal to the fan power needed to convey air through the OTM membrane assemblies. This is of course substantially less than the compressor power used in a cryogenic air separation plant (energy savings of ~70%). The flue gas is similar in composition to that from a conventional oxy-combustion power plant so in comparison to post-combustion capture technologies, there is no large thermal parasitic load associated with stripping CO_2 from an amine or other solution/absorbent.

The process mass and heat balance have been modeled together with Aspen Plus and Thermoflow's Steam Pro product. Thermoflow's Peace product was used for cost estimation of the steam turbine system, convective heat transfer surface, FGD, etc. BGL gasifier cost data was supplied by Allied Syngas and DOE reports while cryo-ASU, OTM and CPU capital cost is estimated by Praxair.

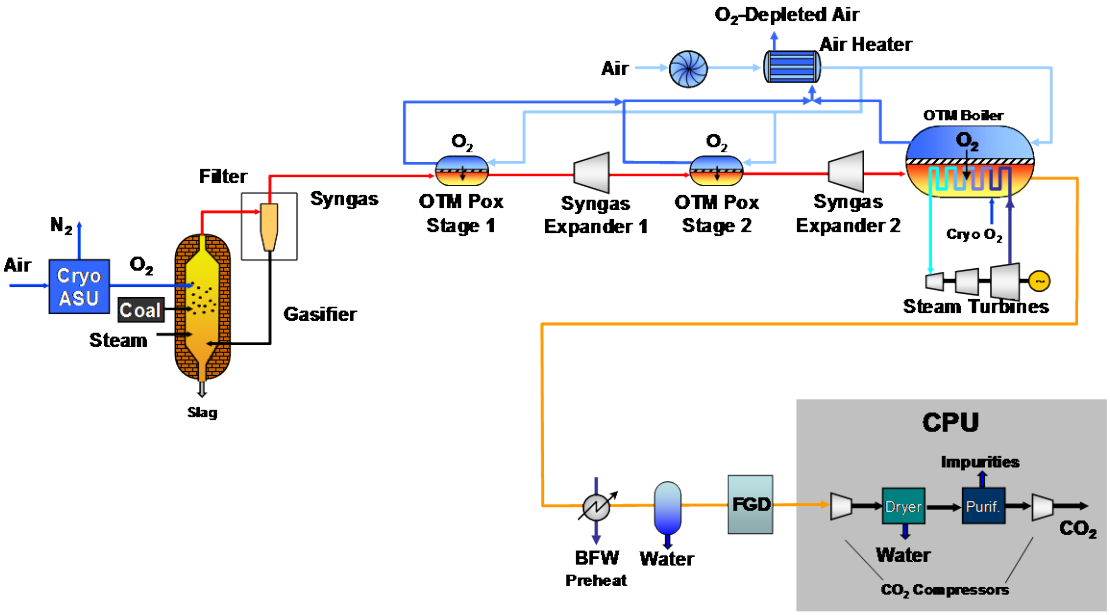

Figure 1: Advanced Power Cycle with FGD for sulfur recovery

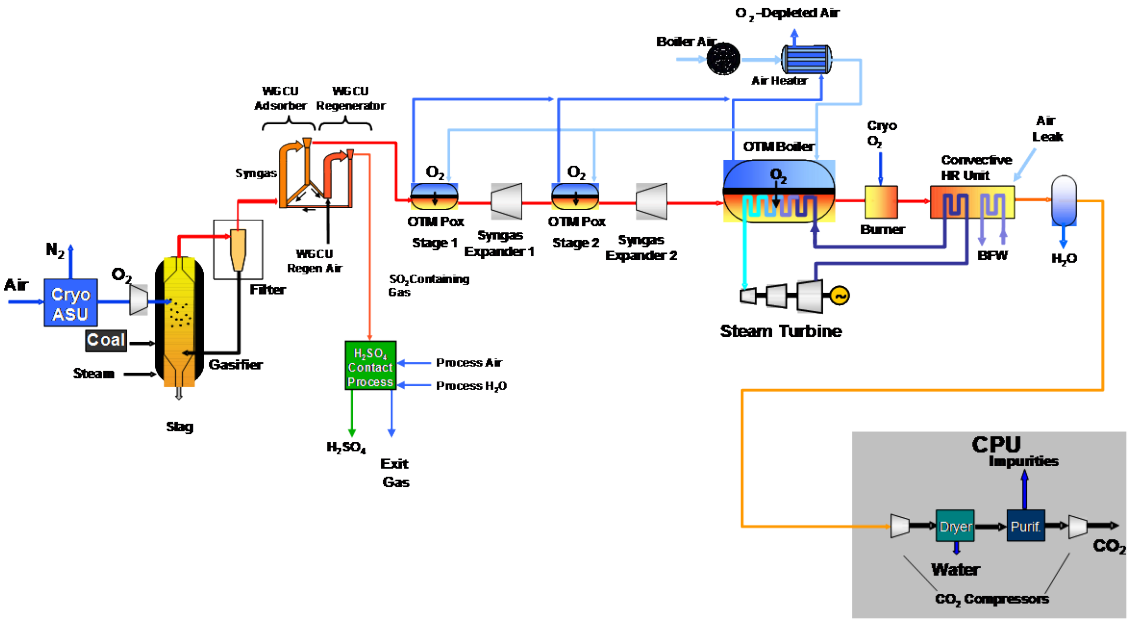

Figure 2: Advanced Power cycle using WGCU technology for sulfur removal

2. Design Basis and Assumptions

Six baseline OTM cases have been simulated. The list of originally agreed upon cases investigates the effect of 2 main parameters, steam cycle complexity and type of sulfur recovery unit. Three steam cycle options include a standard supercritical cycle, a currently available ultra-supercritical cycle as well as an advanced ultra-supercritical cycle. The two sulfur recovery options include a wet-FGD for SOx capture from the flue gas as well as a Warm Gas Cleanup (WGCU) option, using RTI's WGCU process, where sulfur species (H_2S and COS) are captured following the gasifier.

Case No.	Gasifier Type	OTM Pox Units	Expander Units	Steam Conditions	OTM Fuel Combustion	OTM Type	SRU	CO2 Purification	Suppl. Comb. Oxidant Source	Air Leak	Flue Gas Recycle
1	BGL	2	2	SC	90%	Tube	FGD	Yes	Cryo ASU	3%	No
2	BGL	2	2	USC-Comm	90%	Tube	FGD	Yes	Cryo ASU	3%	No
3	BGL	2	2	USC-Adv	90%	Tube	FGD	Yes	Cryo ASU	3%	No
4	BGL	2	2	SC	90%	Tube	WGCU	Yes	Cryo ASU	3%	No
5	BGL	2	2	USC-Comm	90%	Tube	WGCU	Yes	Cryo ASU	3%	No
6	BGL	2	2	USC-Adv	90%	Tube	WGCU	Yes	Cryo ASU	3%	No

Figure 3: Advanced Power Cycle Case List

The steam cycle conditions are shown in Figure 4. The ambient conditions and cooling water assumptions are show in Figure 5. Figure 6 shows the assumed characteristics of the OTM-ASU and Figure 7 shows the specifications for the CO_2 product.

Steam Cycle Conditions	
Cycle	**Steam Conditions**
Supercritical (SC):	3500psi, 1100/1100F
Ultra-Supercritical (USC):	4050psi, 1080/1100/1100F
Advanced Ultra-Supercritical (Adv-USC)	5075psi, 1292/1328F
Condenser Pressure	0.93 psia (99.3F)

Figure 4: Steam Cycle Conditions

Ambient Conditions	
temperature	59F
ambient pressure	14.7psia
relative humidity	60%
cooling water supply temperature	66.5F
cooling water return temperature	94.5F

Figure 5: Ambient and Cooling Water Conditions

OTM-ASU Operating Conditions	
operating temperature	1832 F (1000^{o}C)
O_2 recovery	70%
pressure drop in air circuit (pressure rise across air fan)	5 psi
approach temperature in regenerative heater	95 F

Figure 6: OTM-ASU Operating Assumptions

CO2 Product Specifications	
CO_2 Purity	>95%
CO_2 Pressure	2000 psia

Figure 7: CO2 Product Specifications

In addition to the originally agreed upon 6 cases above, a number of additional cases have been simulated to determine the optimal amount of fuel utilization in the OTM boiler for cost of electricity (COE) minimization. Between the limits of low and high OTM fuel utilization a minimum COE exists that is a tradeoff between high parasitic power (increased cryo-ASU power with low OTM fuel utilization) and high capital (increased OTM surface area at high OTM fuel utilization). To determine the optimal degree of OTM fuel utilization experimental data is gathered to determine the OTM membrane flux curve vs fuel utilization. OTM flux falls off with decreasing syngas concentration and the rate of this flux decrease helps determine what the optimal fuel utilization will be.

Coal Composition:

The coal composition for this study was taken to be the same as that used by the DOE in the report on "Pulverized Coal Oxycombustion Power Plants," (DOE/NETL-2007/1291).

Coal Characteristics:
Illinois #6 Coal

Proximate Analysis	As Received (%)	Dry (%)
Moisture	11.12	
Volatile Matter	34.99	39.37
Ash	9.70	10.91
Fixed Carbon	44.19	49.72

Ultimate Analysis	As Received (%)	Dry (%)
Carbon	63.75	71.73
Hydrogen	4.50	5.06
Nitrogen	1.25	1.41
Sulfur	2.51	2.82
Chlorine	0.29	0.33
Ash	9.70	10.91
Moisture	11.12	
Oxygen	6.88	7.74

HHV (btu/lb)	11666	13126
LHV (btu/lb)	11252	12660

Figure 8: Coal Composition

Capital Cost Estimation and COE Calculation Method:

The plant costing basis for the OTM power cycle plant was taken to be from 2008 because much of this analysis was performed in 2008 and because 2008 was the costing basis for the 2008 versions of Thermoflow's SteamPro and Peace software. Comparison cases from the DOE's report on "Pulverized Coal Oxycombustion Power Plants," (DOE/NETL-2007/1291) were updated from their 2007 costing basis to match the 2008 costing basis.

The DOE's reported plant cost values were updated from 2007 dollars to 2008 dollars by scaling the plant capital values ($/kw) found in the DOE/NETL-2007/1291 reference report using data from the SteamPro and Peace software. The Air Pulverized Coal based power plant, (DOE Case 1 with no CO_2 capture), was first simulated using the 2007 version of SteamPro. Both the plant performance and the capital cost values agree well between the DOE reported values and the SteamPro/Peace simulated values. After verifying good agreement, the same DOE reference plant (DOE's Case 1) was then simulated using the 2008 version of SteamPro/Peace software and the capital plant cost in 3/2008 dollars was taken as the basis for comparison going forward. Between 2007 and 2008 SteamPro/Peace predicted roughly a 22% escalation in capital cost. This 22% capital cost escalation was also applied to DOE's Case 3 (Air-Pulverized Coal with Post Combustion Capture) for comparison against the OTM cases.

From the estimated plant capital costs a 20 year levelized COE was estimated. The method for COE estimation was similar to that used by the DOE in DOE/NETL-2007/1291 where COE was estimated using capital cost factors (CCF) and levelization factors.

$$COE = \frac{CCF\ \ TPC}{CF\ \ kWh} + \sum \frac{OC\ \ LF}{CF\ \ kWh}$$

$$CCF = \frac{17.5\%}{yr}\ (High\ Risk)\ or\ \frac{16.4\%}{yr}\ (Low\ Risk)$$

$$LF \sim 116\%\ (General)\ or\ 120\%\ (Coal)$$

$$kWh : annual\ kWh\ power\ generated\ at\ 100\%\ capacity\ factor$$

$$CF :\ Capacity\ Factor$$

$$OC :\ Operating\ Cost$$

A levelization factor of 120% is used for fuel costs and 116% is used for all other operating expenses. These are similar to the factors used by the DOE in DOE/NETL-2007/1291. A 'low risk' capital cost factor of 16.4%/yr is used for the standard air blown pulverized coal

power plant while a 'high risk' CCF of 17.5%/yr is used for high risk processes such as OTM cases and the post-combustion capture reference case. These are the same values used by the DOE in the oxy-combustion report DOE/NETL-2007/1291.

Variable and fixed labor costs were assumed to be 30 and 40 $/(kw.yr) respectively. Variable labor expense scales with capacity factor while fixed labor costs do not. A capacity factor of 90% was used for all cases because an assumption is made that the cost comparison is for an nth of a kind plant with proven reliability.

Consumable and labor operating costs are shown below in comparison to DOE assumptions. Operating costs include gypsum disposal, ash disposal, limestone cost, water expense, and makeup & water reagent costs.

		Praxair OTM	OxyCombustion Cases DOE Report (DOE/NETL-2007/1291)
Variable Labor Cost	$/(kw.yr)	30	17.88
Fixed Labor Cost	$/(kw.yr)	40	16.43
Gypsum Disposal	$/ton	10	-
Ash Disposal	$/ton	16	15.45
Limestone Cost	$/ton	20	20.6
Water Cost	$/kgal	1	1.03
Makeup & Water Treatment cost	$/yr	$1.5MM	~$2.0MM
CCF	%/yr	17.5	17.5
Coal Levelization Factor	%	120.00	120.22
General O&M Levelization Factor	%	116.00	116.51

Figure 9: Power Cycle Operating Costs

Power Cycle		Praxair Air-PC (2008 SteamPro)		Praxair Air-PC (2007 SteamPro)	DOE Air-PC DOE/NETL-2007/1291	
CO2 sequestration		NO	YES	NO	NO	YES
Net Efficiency (HHV)		39.7	27.2	39.6	39.5	27.2
Cost Basis (Year)		3/2008	3/2008	2007	1/2007	1/2007
Plant Cost ($/kW)		$1,908	$3,488	$1,560	$1,563	$2,857
	Coal Price ($/MMbtu)					
COE ($/MWh)	1.8	$70.5	$115.2	$63.6	$63.0	$110
	3.0	$82.9	$133.2	$76.0		
	4.0	$93.2	$148.3	$86.3		

Figure 10: COE comparison basis

This COE comparison was performed for $1.8/MMBTU coal because this is the coal price used in the DOE report. Much of the analysis for this report was done in 2008 when there was a spike in coal prices. As a result COE's were calculated for coal prices from $1.8/MMBTU to $4/MMBTU. Going forward the basis for comparison against DOE goals is the left column in Figure 10 which is the Praxair/SteamPro simulated Air-Pulverized Coal power plant case (no capture). The coal cost was generally taken to be $3/MMBTU for comparison with OTM cases, again because this was a reasonable coal price in 2008.

Cost of CO_2 removed and avoided

Cost of CO_2 removed/avoided is calculated using a similar method as compared to the DOE in DOE/NETL-2007/1291. The reference case used to calculate the costs of CO_2 removed and avoided is the Praxair calculated analog of Case 1 from DOE/NETL-2007/1291. A cost of $4/ston CO_2 is also included in the COE of the sequestration case for the purpose of this calculation which is for CO_2 transport, storage and monitoring. The DOE OxyCombustion analysis presented in DOE/NETL-2007/1291 also assumes some penalty for CO_2 transport, storage and monitoring.

$$\text{Removal Cost} = \frac{COE_{with\ CCS} - COE_{w/o\ CCS}}{CO_2Total_{with\ CCS} - Emissions_{with\ CCS}}$$

$$\text{Avoided Cost} = \frac{COE_{with\ CCS} - COE_{w/o\ CCS}}{Emissions_{w/o\ CCS} - Emissions_{with\ CCS}}$$

3. Process Description

BGL gasifier and candle filters

The overall OTM boiler process starts with an oxygen blown BGL (British Gas-Lurgi) gasifier where O_2, coal, steam and limestone are used in the gasifier to produce syngas. The product syngas is filtered hot for removal of any entrained particulates. This process has been modeled using the BGL gasifier for coal to syngas conversion because this gasifier type is highly efficient and requires relatively little oxygen and steam compared to other gasification technologies. In typical BGL gasification applications the syngas is quenched for tar, oil, and particulate removal before the gas is used for it's ultimate purpose (synthetic fuels production for instance). In this project, hot syngas is advantageous (because any quenched syngas would otherwise have to be reheated) so it is assumed that candle filters and cyclones will enable the removal of any solid material from the raw syngas stream. It is also assumed that this filtered syngas can directly proceed on to the OTM Pox unit operations where any tars, oils, etc contained in the syngas stream will not pose a problem for the following OTM membranes or syngas turbines.

It is assumed that the gasifier lock system can be operated using the purified CO_2 product instead of air. A slipstream of purified CO_2 is extracted from the CPU pure product compression train and recycled back to the gasifier for use in the gasifier coal delivery system.

In addition to steam, coal, cryo-ASU O_2, and coal delivery gas, the gasifier is also operated with some other feeds as indicated in EPRI BGL gasification reports. This includes limestone (as a fluxing agent) and a small flow of natural gas and air used in the gasifier's tuyere system. These minor feeds were also included in the mass and energy balance simulation of the

Advanced Power Cycle system as well as in the economic analysis which includes limestone and natural gas expense.

Gasifier performance data was provided by Allied Syngas and through EPRI reports on the BGL gasification process. The gasifier system in this application includes 5 gasifiers with a single spare. The nominal capacity of each gasifer is 1100 tpd of coal which is consistent with the Schwartz Pumpe BGL gasifier size.

Syngas Turbines

Immediately following the gasifier and filter arrangement the syngas flows to a pressurized OTM Pox unit where OTM membranes combust only enough syngas to raise the temperature to 1000C. The syngas is then expanded to an intermediate pressure and flows through another OTM Pox stage, which again combusts only enough syngas to heat the stream to 1000C. The pressurized syngas then flows through the second syngas turbine and is expanded to near atmospheric pressure. Two expansion/POX stages, rather than one, are used to improve the efficiency of the overall Advanced Power Cycle. In this arrangement the OTM Pox unit operation is essentially a substitute for the combustor in a similar gas turbine type system.

Currently the syngas expansion turbine is not a commercially available product because there is no existing market for this equipment. However similar syngas/fuel expansion turbines are common in both the steel and refining industries (blast furnaces and fluidized catalytic crackers (FCC)). In both industries the turbines are of similar size to the one needed here and have proven reliable in their demanding, severe-service applications.

In the Advanced Power Cycle concept the expansion power of each turbine unit is similar to that of a GE Frame 5 Gas Turbine. Expansion performance was estimated to be similar to that of a GE Frame 5 GT with 88% isentropic expansion efficiency and 98% mechanical efficiency.

Boiler (Excluding OTM), Feedwater Heaters (FWH), Latent Heat Recovery

The non-standard OTM boiler arrangement differs significantly from the waterwall (or benson type once through boiler), radiative and convective sections in a standard pulverized coal or CFB power plant. Furthermore the arrangement of heat transfer area will be different with respect to the low temperature flue gas heat transfer because there is no air preheater in the flue gas duct.

A conventional Pulverized Coal boiler has a relatively standard arrangement of both convective and radiative heat transfer surface area. Figure 11 depicts a boiler temperature enthalpy diagram for a typical air blown pulverized coal power plant. In this diagram the upper line represents the flue gas stream cooling from right to left. As the flue gas cools this energy is used to heat water/steam in various radiative and convective heat exchangers including (from right to left) the 'waterwall', radiative superheater, convective superheater (CS2), convective reheater (CR2), convective superheater (CS1), convective reheater (CR1), economizer (ECO1) and lastly the air preheater.

Figure 11: Temperature Duty diagram for a traditional pulverized coal power plant. Diagram shows the traditional arrangement of heat transfer surface.

In this modern arrangement of boiler heat transfer surface area, the boiler feedwater is separately heated by steam extraction from various stages of the steam turbine. Figure 12 shows a temperature enthalpy diagram for the boiler feedwater train from a typical pulverized coal power cycle (air based combustion). The diagram shows boiler feedwater being heated (from right to left in blue) in 9 stages against extracted steam (magenta lines). Once heated to roughly 600F the preheated boiler feedwater flows to the boiler's economizer and on to other convective and radiative heat transfer sections.

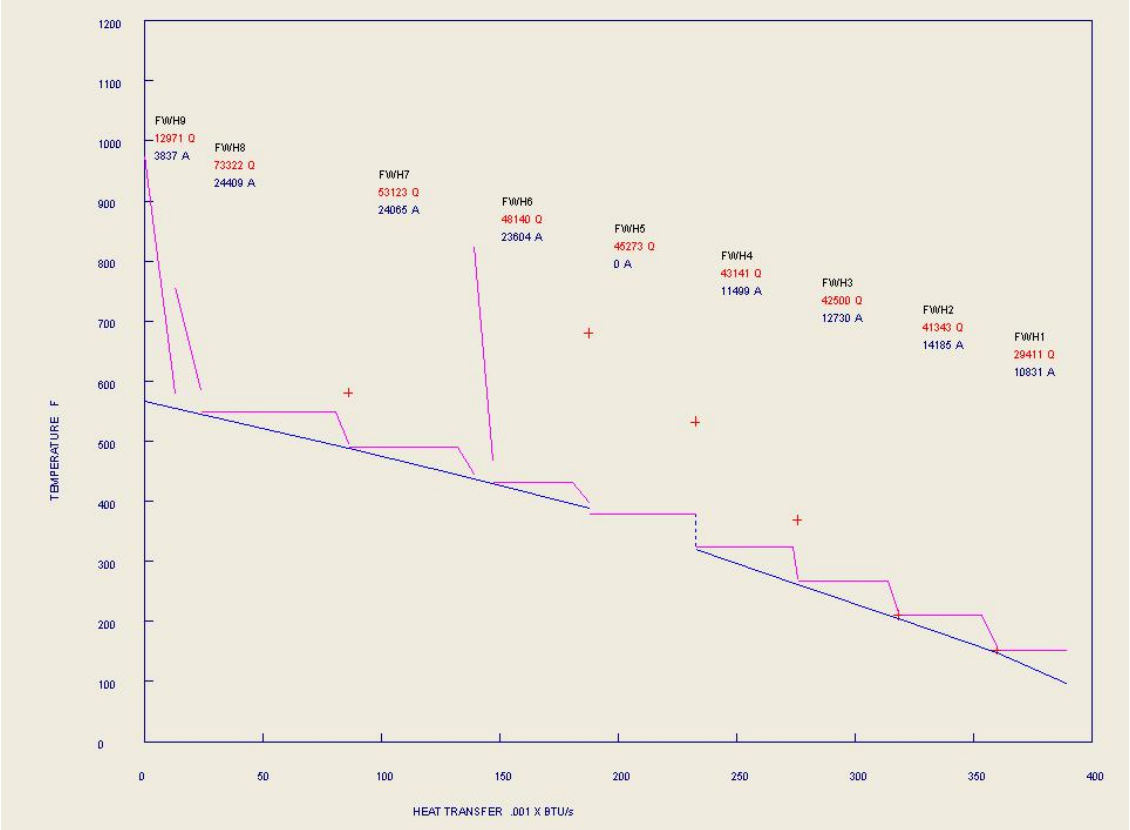

Figure 12: Temperature Duty diagram for a boiler feedwater preheat system of a traditional pulverized coal power plant.

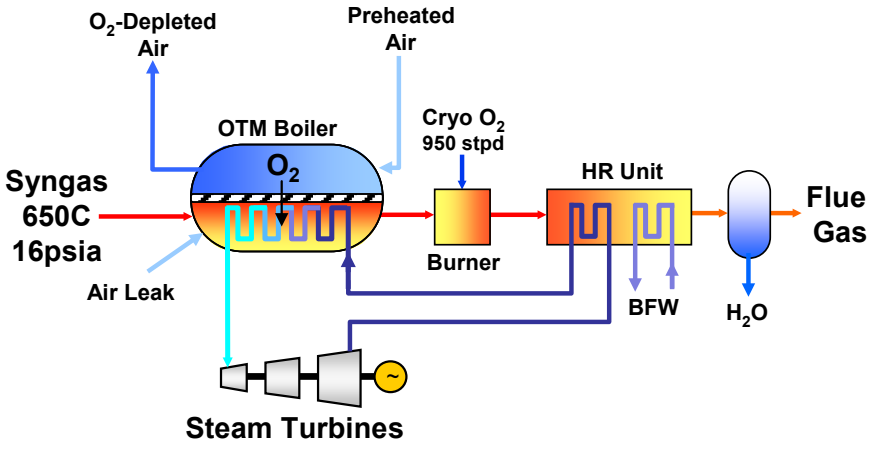

Figure 13: OTM boiler detail

Compared to the standard arrangement boiler and feedwater heat transfer surface, shown above in Figure 11 and Figure 12, the utility scale OTM system will have a different arrangement of heat transfer surface area because the OTM boiler system has a non-standard temperature profile. The operating temperature of the OTM boiler itself will be around 1000C (1832F). Following the OTM boiler a gas phase O_2 combustor is used to combust the remaining syngas using cryogenically supplied oxygen. Here the temperature will increase above 1000C. Following the gas phase combustor the flue gas is cooled by convective heat transfer and energy is transferred to high pressure water/steam as well as to low pressure boiler feedwater preheat. See Figure 13 for a schematic of the OTM boiler including the supplemental combustor and heat recovery unit. The absence of a traditional air preheater in this OTM system means that additional energy is available to supplement the preheating of boiler feed water. Figure 14 shows a representative temperature enthalpy diagram for the OTM boiler system.

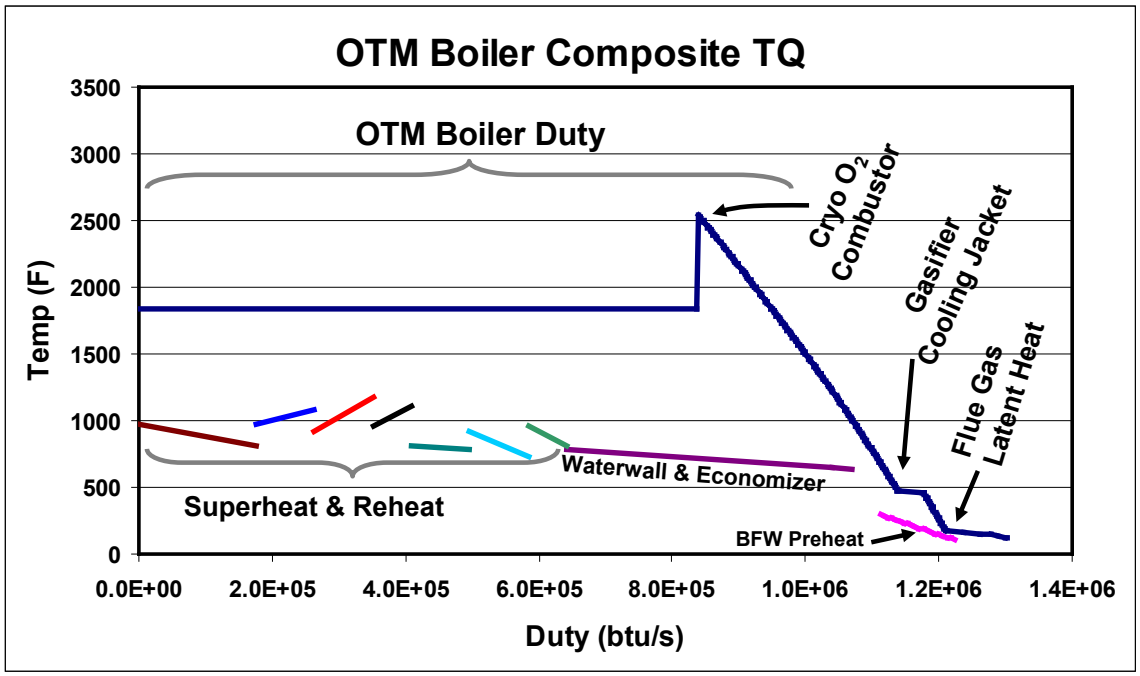

Figure 14: Representative Temperature Enthalpy Diagram for the Advanced Power Cycle

The boiler Syngas/Flue gas stream is indicated by the top blue line and flows from left to right. The syngas first enters the OTM boiler and is heated to 1832F (not shown) via syngas combustion on the OTM surface. Once the syngas reaches 1832F (1000C) it continues to be combusted in the OTM boiler while energy is removed via heat transfer to steam. In the OTM boiler section, energy is transferred to steam heaters, superheaters, and reheaters. In this entire section the gas temperature is maintained at around 1832F because this is the operating temperature of the OTM tubes.

Following the last OTM tubes some syngas still remains in the gas stream (5-20%) because it is uneconomical to combust all the syngas with OTM membrane area. Cryogenically supplied oxygen is used here to combust the remaining syngas, the flue gas temperature after the burner is increased due to this combustion (here to roughly 2500F). The flue gas is cooled first by radiative heat transfer and then via convective heat transfer against high pressure water in a section analogous to a standard economizer. Enough excess cryogenically supplied oxygen is used in the supplemental combustor to give a 1.2 mol% oxygen excess (wet basis) in the flue gas leaving the heat recovery section that follows the supplemental combustor.

Once the flue gas has cooled to sub-economizer temperatures the flue gas continues to cool against low pressure boiler feedwater (BFW). Due to the high moisture level in the flue gas some flue gas latent heat is transferable to the boiler feedwater stream. Some amount of moderate/low level energy is also available from the gasifier system because BGL gasifiers are operated with a water jacket. This gasifier energy is also used for BFW preheat. The remaining latent heat is transferred to the cooling water system and rejected to the environment.

In all cases the sensible flue gas energy, the recoverable flue gas latent heat and the gasifier steam jacket energy is enough to completely heat the boiler feedwater from the condenser outlet temperature to the temperature needed to enter the BFW deareator (about 300F).

The purpose of the analysis presented here is to investigate the heat and mass balance of the proposed OTM boiler at a high level. The specific design, arrangement, manifolding, etc of OTM surface, steam heat transfer surface, and OTM air flow is outside the scope of this analysis.

Steam Turbine, Condensers, Cooling Tower, Pumps, Tanks

Steam turbine and condenser performance is estimated using the Thermoflex SteamPro software. The software estimates the performance of individual steam turbine stages (including the boiler feed pump turbine), the steam seal system and steam turbine leakage. The SteamPro simulation also incorporates steam extractions used in the cryo-ASU and CPU.

The steam turbine condenser pressure is held at 0.93 psia (99.32F) and the condensed boiler feed water returns to the boiler feedwater preheat train. The condenser energy is rejected to a mechanical draft cooling tower. SteamPro calculates the power required for the mechanical draft cooling tower as well as for the cooling water forwarding pump. The SteamPro-simulated cooling water system also takes into account the cooling water needed for flue gas latent heat condensation as well as the cooling water required for the cryo-ASU and CPU islands. Other miscellaneous steam/water pumps, tanks, etc are included in the SteamPro peace simulation such as the condenser forwarding pump, FWH condensate forwarding pump, etc

FGD and WGCU

FGD

In cases 1, 2 and 3 a wet-FGD is used for SOx removal following the OTM boiler and flue gas cooling equipment. The FGD removes 98.0% of the SOx and uses a 2.0% excess of limestone. The CO_2 evolved in the FGD is contained in the flue gas stream. The FGD product is principally composed of calcium sulfite ($CaSO_3$) because no reaction with O_2 is considered. No excess O_2 (cryogenic or atmospheric air) is added to increase the production of gypsum.

WGCU

In cases 4, 5 and 6 the Warm Gas Cleanup process (WGCU) is used for H_2S and COS control following the gasifier and before the syngas flows to the first OTM Pox unit.

WGCU is a continuous process developed by RTI for removal of H_2S and COS from gas streams using a solid regenerable sorbent. In the WGCU unit syngas is processed immediately following the gasifier and candlefilters at a temperature of about 1000F and a pressure of about 340psia. The process involves the contact of the syngas with a solid metal oxide sorbent. The H_2S and COS in the gas stream react with recirculating solid metal oxide sorbent, typically ZnO, forming the metal sulfide, typically ZnS. This reaction occurs in the absorber portion of the WGCU unit. The solid sorbent continually circulates in the absorber portion of the WGCU unit.

A portion of the solid sorbent is continually withdrawn from the absorber, regenerated and re-introduced back to the absorber. In the regenerator portion of the WGCU process the spent solid sorbent is regenerated with air at near atmospheric pressure, producing ZnO and a SOx containing gas stream. The regenerated sorbent is then returned to the absorber portion of the WGCU unit while the SOx containing gas stream is processed for SOx control. The concentrated SOx containing gas stream has a significantly smaller molar flowrate as compared

to the raw syngas flow or the eventual flue gas flow and is therefore easier to process for control of sulfur emissions.

The SOx containing regenerator off-gas stream has a high concentration of SOx, >10mol%, and can be treated for removal of SOx in a few ways: 1) SOx can be further processed (oxidized) using the contact sulfuric acid process for recovery of the SOx as concentrated potentially saleable sulfuric acid (this is the method assumed in this report), 2) alternatively SOx can be reduced to elemental sulfur using a slipstream of cleaned syngas in a modified Claus process.

The SOx concentration in the regenerator off-gas stream is in the concentration range typically applicable for use in the contact process for conversion to H_2SO_4. As mentioned the alternative disposition of the sulfur in this gas stream is for conversion to elemental sulfur, however this method is disadvantaged and not used in this report because using this method requires a considerable slip stream of cleaned syngas (roughly 2% of the total syngas in the case of high sulfur Illinois coal) would be needed. The use of a syngas slipstream will reduce the efficiency of the overall power cycle, by roughly 2%, and will also reduce the carbon capture efficiency of the process by roughly 2% due to the carbon loss in the slipstream.

Cryogenic ASU

A cryogenic ASU is used to supply gaseous oxygen to the gasifier and the supplemental combustor. The oxygen purity delivered by the ASU is 95.5mol% oxygen. The cryogenic ASU design is assumed to be that of a currently commercially realizable low purity, low pressure ASU. The portion of the cryogenically supplied O_2 going to the gasifier is compressed to 517psia in a 5 stage compression train with each stage having 80% polytropic efficiency and 98% mechanical

efficiency. This cryogenically supplied oxygen accounts for roughly 33% of the total oxygen consumed by the process (with the other 67% supplied using OTM membranes). ASU power and utilities (regen steam, cooling water, auxiliary electrical power) are estimated by Praxair. It should be emphasized that the ASU specific power assumption is for a commercially realizable ASU design in 2008. As research continues on large scale, low purity ASU concepts, significant specific power and capital reductions are being made. Going forward these advances will further reduce the Cryo-ASU parasitic power demand and capital requirement.

OTM ASU (w/ air preheat, air fans/motors)

The OTM-ASU consists of air fans, air preheaters as well as the OTM-POX and OTM boiler unit operations that contain the actual OTM tube. The OTM tube contains two components: a porous support and an internal dense gas separation layer. The porous support provides mechanical strength to the OTM system. The internal gas separation layer facilitates the reduction of molecular oxygen (O_2) to oxygen ions (O^{2-}) on the surface of the air side of the OTM, the oxidation of fuel species on the surface of the fuel-side of the OTM, and transport of oxygen ions through the bulk of the membrane while preventing molecules in the air and fuel from crossing the membrane. Performance Improvement activities performed during Phase 1 of the OTM project yielded development of an advanced set of OTM Materials, selected to maximize the OTM's ability to transport O_2 from the air side of the OTM to the fuel side.

Praxair's OTM membranes are placed directly inside the furnace or partial oxidation unit operations where oxygen is consumed on the fuel-side of the membrane, where syngas is being combusted. Because the combustion reaction occurs on the surface of the membrane, an extremely low oxygen partial pressure is achieved. A driving force for oxygen ion transport from

the air-side to the fuel-side of the OTM membrane is established because air has a much higher oxygen partial pressure.

As air flows along the surface of the OTM tubes the air becomes depleted of oxygen. It is assumed that 70% of the air-side oxygen is transferred across the membrane for combustion with the remaining oxygen leaving in the O_2-depleted air stream. Hot oxygen depleted air leaving the OTM tubes is used to preheat the air entering the OTM tubes, via a regenerative air preheater.

OTM POX

The first of two OTM pox units are located immediately after the gasifier in cases 1, 2 and 3 and immediately after the WGCU sulfur removal process in Cases 4, 5 and 6. In all cases the second OTM Pox unit is located after the first syngas expander. The purpose of the OTM Pox units are to combust enough of the syngas to raise the gas temperature to 1000C. The OTM Pox units consist of a number of rows of OTM membrane (with no steam/water tubes) in a pressure vessel where oxygen transport occurs from the near-atmospheric pressure air-side to the high pressure syngas side. The high partial pressure of fuel on the syngas side (and resulting lower O_2 partial pressure on the membrane) actually serves to increase the rate of O_2 transfer across the membrane in comparison to the membranes in the OTM boiler.

OTM Boiler

Following the second expander, the still mostly un-combusted syngas flows to the OTM boiler where OTM tubes are used for combustion of up to 95% of the original syngas. In the OTM boiler, steam tubes are also arranged for removal of energy needed to keep the gas and OTM surface temperature at around 1000C. The degree of syngas combustion via OTM membranes is an important optimization variable. Depending on OTM flux and OTM "cost

allocation," 70-95% of the total syngas is combusted on the OTM membranes with the majority of the syngas combustion occurring in the OTM boiler.

Syngas flowing through the OTM boiler is combusted at atmospheric pressure and steam is used to remove energy. A non-traditional boiler arrangement will be required here to accommodate both the OTM surface and the steam tube surface. The section of the boiler containing OTM tubes should be maintained at between 900C and 1200C for optimal OTM performance. The OTM operating temperature was modeled as 1000C for the purpose of this report.

OTM Air Preheater

In the Advanced Power Cycle concept no standard flue gas to air preheater exists because air preheat/cooling for the OTM air is handled separately in a fixed bed regenerative heater. The fixed bed regenerative heater concept is similar to that of a cyclically operated blast furnace stove (iron ore refining) where solid ceramic media is used to store and transfer thermal energy between gas streams. This type of air preheater was chosen over other types of air preheaters because 1) the high 1000C temperature is within the current ability of such a heater (some modern hot blast stoves run at temperatures in excess of 1250C), 2) blast furnace stoves can be constructed at a large scale that as would be required in this application and 3) regenerative heat exchangers offer some of the highest thermal efficiencies of heat transfer equipment (modern hot blast stoves can operate with efficiencies on the order of 80%)

Because air can be supplied to all OTM membranes at the same pressure all of the air preheat can be integrated to a single system of regenerators. In other words it is assumed that separate air preheaters will not be necessary for each OTM Pox stage and for the OTM boiler.

The OTM air preheat system includes the fans and motors needed to convey air through the air preheater and OTM modules. A 5 psi pressure rise through the OTM air fan is assumed with an isentropic fan efficiency of 75% and mechanical efficiency of 95%.

CPU

The purpose of the Carbon Dioxide Processing Unit (CPU) is for compression and purification of the flue gas to a sequesterable CO2 product. The CPU takes the flue gas following the wet-FGD (if applicable) and latent heat removal operation. Flue gas is compressed to roughly 375 psi where it is treated for removal of mercury, water and some acid gases before the flue gas enters an auto-refrigerative process for inert removal. The raw flue gas is compressed in a 5 stage compression train with an average stage polytropic efficiency of ~85% and a mechanical efficiency of 98.5%.

In the auto-refrigerative process CO_2 is purified to a >95% CO_2 product with >97% recovery of CO_2. The cryogenic process also produces a vent stream which is enriched in atmospheric gases (N_2, O_2, Ar). Following the cryogenic portion of the CPU, the purified CO_2 stream is further compressed to 2000psi. The purified CO_2 is compressed in a multistage compressor train having an average stage efficiency of 77% polytropic and a 98.5% mechanical efficiency. CPU auxiliaries include electricity for compressor operation, electricity for chiller operation, steam for dryer bed regeneration, and cooling water utility for intercooler/aftercooler duty.

4. Major Equipment Capital Cost Estimation

BGL gasifier and candle filters

BGL gasifier costs were estimated by costing data provided by Allied Syngas. In early 2009 the estimated BGL gasifier costs were evaluated against gasifier costs in DOE reports for IGCC systems. The BGL gasifier costs were shown to be inline with gasifier costs reported in DOE report DOE/NETL-2007/1281 the gasifier cost estimate is around 450$/kw which is inline with other large scale gasifier systems not including the gas cleanup system. For all cases the gasifier cost is equivalent because the assumption is that in each case 5 gasifiers will be used plus one spare. Candle filter cost was estimated as roughly $1MM equipment cost per 1000 tpd coal usage (DOE/NETL-2007/1281 did not specifically separate cyclone/candle filter cost for the ConocoPhillips gasifier so the particulate removal equipment was estimated as roughly 5% of the "Gasifier, Syngas Cooler & Auxiliaries" equipment cost, which corresponds to roughly $1MM/1000tpd coal).

Syngas Turbines

The Syngas turbine cost was estimated to be the same as an entire GE Frame 5 Gas Turbine, with gas turbine cost data taken from the 2008 version of Thermoflex's GTPro and Peace softwares. The Costing basis for the Advanced Power Cycle power plant was assumed to be for an nth of a kind plant so the development costs associated with this type of equipment were not included. As previously mentioned other industrial processes use comparable syngas/fuel expansion turbines.

Boiler (Excluding OTM), Feedwater Heaters (FWH), Latent Heat Recovery

The convective and radiative heat transfer surface cost is estimated using information taken from a SteamPro design for a traditional gas fired boiler. However the areas (and costs) required for heat transfer were adjusted based on LMTD because the OTM boiler has a different temperature profile as compared to the SteamPro design case, as previously discussed in the Process Description section. Costs were taken and adjusted from a traditional gas fired boiler because the gas stream in the OTM boiler will be a clean gas stream with no particulates.

The SteamPro/Peace software estimates the performance and cost for each heat exchanger of a typical power plant. The SteamPro/Peace software estimates the area of each heat exchanger using the heat exchanger duty, LMTD, and calculated average heat transfer coefficient. Additionally SteamPro/Peace generates a heat exchanger cost and an approximate heat exchanger weight.

In the OTM case heat transfer surface is arranged differently because the boiler gas temperature profile is different; the heat transfer surface areas (and costs) must be adjusted from the SteamPro/Peace data. This adjustment is done by scaling the SteamPro/Peace area based on LMTD values, the cost of each heat exchanger is adjusted to match the adjusted area. It is assumed that SteamPro/Peace make reasonable assumptions for relative cost of high temperature/high pressure heat transfer area in the case of the advanced UltraSupercritical case. Although the Adv-USC steam cycle is not currently commercially realizable the assumption is that this cycle will be commercially available when the OTM membranes are ready for deployment on this large scale.

Costs for the boiler feedwater heaters are estimated using SteamPro and Peace softwares. Low temperature boiler feedwater preheat is achieved through heat transfer against cooling flue gas. This heat transfer surface is costed as expanded economizer surface relative to the SteamPro/Peace economizer estimated cost subject to the duty and LMTD of the heat exchanged. The cost of the latent heat recovery heat exchanger was estimated to be roughly the same per exchanger duty compared to the low temperature economizer heat exchanger.

The higher temperature boiler feedwater preheaters including the deaerator and high pressure boiler feedwater preheaters (following the boiler feed pump turbine) are costed directly by SteamPro and Peace software.

Steam Turbine, Condensers, Cooling Tower, Pumps, Tanks

Steam turbine cost is estimated using the SteamPro and Peace software. It is assumed that SteamPro and Peace make reasonable assumptions for relative steam turbine price in the Advanced UltraSupercritical case. The boiler feedpump and boiler feed pump turbine are also costed using information from the SteamPro and Peace software. The cooling system costs are taken from SteamPro and Peace. This includes costs for the steam turbine condenser, boiler feedpump condenser, cooling towers, cooling water forwarding pump, cooling water piping, etc.

FGD and WGCU

The wet-FGD unit cost was estimated using the SteamPro/Peace software. These costs include the wet-FGD absorber, slurry pumps, limestone processing equipment and gypsum dewatering equipment.

Costs for the WGCU unit were taken from the DOE's 2008 report on current and future gasification technologies (DOE/NETL-2008/1337) which included a cost estimate for the WGCU process. Costs for the Contact Process plant, used to convert SOx to H_2SO_4, was taken from a sulfuric acid book. Although the byproduct H_2SO_4 could be potentially sold in the H_2SO_4 market, no benefit (or disposal cost) was assumed for getting rid of the sulfuric acid byproduct. The sale price for sulfuric acid depends on geographical factors, acid purity, acid flowrte, etc and a net acid price of $0/ton is a conservative assumption. Even with a $0 sale price for acid the WGCU cases show a slight advantage over the FGD cases in terms of COE because there is no FGD limestone expense or FGD waste stream disposal expense.

Cryogenic ASU

Cryogenic ASU capital costs are estimated internally by Praxair. The Cryo-ASU costs were based on recently completed feasibility studies for 500+MW oxy-coal plants.

OTM ASU (w/ air preheat, air fans/motors)

There is still uncertainty regarding the OTM manufacturing, sealing, manifolding and installation cost, hence a "cost allocation" is used. The OTM "cost allocation" accounts for the installed cost of the OTM membranes in the OTM-Pox and OTM-boiler units, which includes:

- manufacturing the membrane surface
- installing the OTM surface inside the OTM-Pox and OTM boiler units
- OTM-Pox pressure vessels
- OTM boiler ducting
- Air ducting and manifolding to and from the air preheater
- Any necessary support structure for the OTM-Pox and OTM boiler equipment

For reference DOE's SECA (Solid State Energy Conversion Alliance) SOFC (solid oxide fuel cell) cost target is estimated to be about $\$110/ft^2$, including balance of plant. The OTM target 'Cost Allocation' values include OTM related vessels and air ducting, but does not include

balance of plant. In this report two 'Cost Allocation' values have been used: baseline 'Cost Allocation A' and a higher 'Cost Allocation B' (the $/ft2 values are not be disclosed here).

It is likely that in the near atmospheric pressure OTM boiler the OTM surface will be interspersed or in otherwise close proximity to boiler steam tubes. The particular arrangement, manifolding and spatial design of the OTM boiler is outside the scope of this analysis, but will be addressed in Phase II of the OTM project.

The cost of a regenerative preheater was estimated by a steel industry consultant with expertise in blast furnace stove design and costs. The bare erected cost of the OTM air fan and motors are estimated as roughly $510 per blower motor kW.

CPU

CPU cost has been determined by Praxair and includes the raw CO_2 compressors/motors, dryer beds, mercury removal, coldbox purification cycle, and purified CO_2 compressors/motors. The CPU costs were based on recently completed feasibility studies for 500+ MW oxy-coal plants.

5. Results

5.1. OTM cases with FGD

Cases 1,2 and 3 are the three cases where a wet-FGD is used for sulfur control from the flue gas following the OTM boiler. The three cases use different steam conditions as was previously mentioned. Refer to Figure 15 for the process schematic applying to these three cases. In each of these cases the OTM membranes are used to combust 90% of the syngas. The remaining portion of syngas is combusted using cryogenically supplied oxygen. In all of these cases the OTM Flux is lower in the OTM boiler (due to higher fuel utilization) and higher in the OTM Pox units. The OTM flux values used in this analysis are equal to actual laboratory-measured flux performance values of Praxair's advanced material OTM tubes, however the flux values are not disclosed here.

Case No.	Gasifier Type	OTM Pox Units	Expander Units	Steam Conditions	OTM Fuel Combustion	OTM Type	SRU	CO2 Purification	Suppl. Comb. Oxidant Source	Air Leak	Flue Gas Recycle
1	BGL	2	2	SC	90%	Tube	FGD	Yes	Cryo ASU	3%	No
2	BGL	2	2	USC-Comm	90%	Tube	FGD	Yes	Cryo ASU	3%	No
3	BGL	2	2	USC-Adv	90%	Tube	FGD	Yes	Cryo ASU	3%	No
4	BGL	2	2	SC	90%	Tube	WGCU	Yes	Cryo ASU	3%	No
5	BGL	2	2	USC-Comm	90%	Tube	WGCU	Yes	Cryo ASU	3%	No
6	BGL	2	2	USC-Adv	90%	Tube	WGCU	Yes	Cryo ASU	3%	No

For each of the three FGD cases (Case 1, Case 2, Case 3) the following performance information is given in Figure 16 to Figure 27:

- Stream Summary Table (corresponding to stream numbering in Figure 15)
- Performance Summary
- Capital Cost Summary for an OTM using "Cost Allocation A".
- Cost of Electricity breakdown for a coal price of $3/MMBTU

Figure 16 to Figure 19 refer to Case 1, Figure 20 to Figure 23 refers to Case 2 and Figure 24 to Figure 27 refers to Case 3.

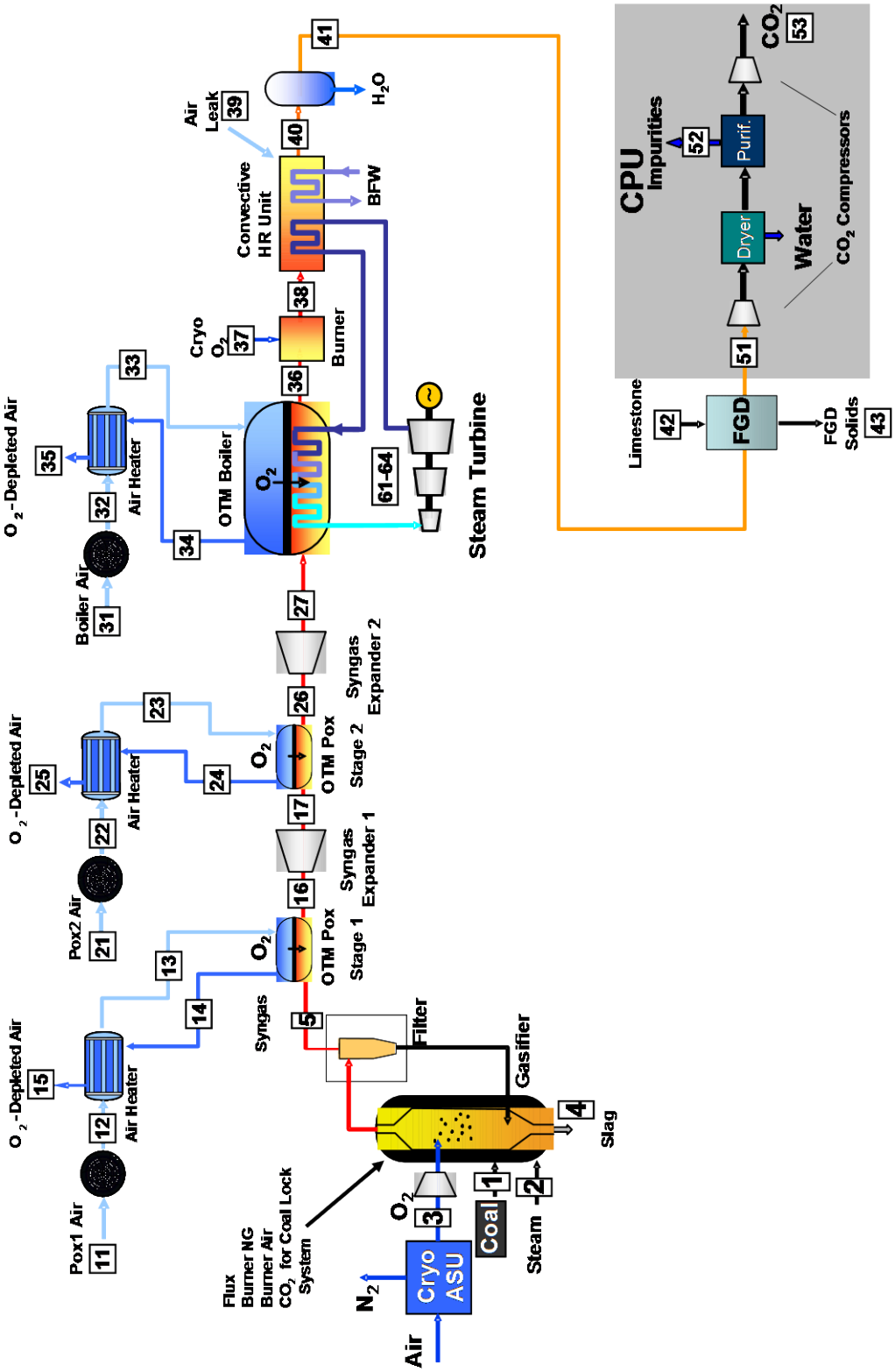

Figure 15: Advanced Power Cycle with FGD for Sulfur containment

Stream		Coal	Gasifier Steam	OTM Boiler Cold O2 Depleted	Gasifier Cryo O2	Residual Syngas	Gasifier Slag	Cyro O2 for Burner	Gasifier Syngas	Hot Flue Gas	Pox 1 Air	Air Leak	Pox 1 Air	Warm Flue Gas	Pox 1 Warm Air	Cold Flue Gas	Pox 1 Hot O2 Depleted	Lime-stone	Pox 1 Cold O2 Depleted	FGD Solids	Pox 1 Hot Syngas	Flue Gas to CPU	Pox 2 Warm Syngas	CPU Inerts	Pox 2 Air	CO2 Product	Pox 2 Air	HP Steam	Pox 2 Warm Air	Reheat 1 Steam	Pox 2 Hot O2 Depleted	Cond. Pump Out	Pox 2 Cold O2 Depleted	BFW to Boiler	Pox 2 Hot Syngas
Stream #		1	2	3	4	5	11	12	13	14	15	16	17	21	22	23	24	25	26															
Temperature	F	77	680	77	500	1000	75	137	1517	1832	232	1832	1238	75	137	1517	1832	232	1832															
Pressure	psia	-	510	20	396	340	14.7	19.7	18.7	18.7	17.7	338.5	75.34	14.7	19.7	18.7	18.7	17.7	73.84															
Flow	k lb/hr	443.2	128.7	223.2	6.36	807.3	430.6	430.6	430.6	359.9	359.9	876.0	878.0	251.9	251.9	251.9	210.6	210.6	919.4															
Flow	lbmol/hr	-	7,143	6,943	0	40,285	14,923	14,923	14,923	12,713	12,713	44,175	44,175	8,731	8,731	8,731	7,438	7,438	45,074															
Composition																																		
H_2	mol%					29.9%						32.7%	32.7%						31.4%															
CO	mol%					50.3%						46.7%	46.7%						44.6%															
CH_4	mol%					3.3%						1.1%	1.1%																					
CO_2	mol%					4.3%						8.1%	8.1%						10.1%															
H_2O	mol%		100.0%			9.4%						9.4%	9.4%						11.8%															
O_2	mol%			95.5%			21.2%	21.2%	21.2%	7.5%	7.5%			21.2%	21.2%	21.2%	7.5%	7.5%																	
N_2 + Ar	mol%			4.5%		1.2%	78.8%	78.8%	78.8%	92.5%	92.5%	1.3%	1.3%	78.8%	78.8%	78.8%	92.5%	92.5%	1.3%															
H_2S	mol%					0.8%						0.7%	0.7%						0.7%															
SOx	mol%																																	
Solids	k lb/hr	443.2			6.36																													

Stream		OTM Boiler Hot O2 Depleted	Hot Flue Gas	Air Leak	Warm Flue Gas	Cold Flue Gas	Lime-stone	FGD Solids	Flue Gas to CPU	CPU Inerts	CO2 Product	HP Steam	Reheat 1 Steam	Cond. Pump Out	BFW to Boiler
Stream #		34	38	39	40	41	42	43	51	52	53	61	62	63	64
Temperature	F	1832	2549	77	365	120	77	144.3	144	91	100	1100	1100	90	552.4

Figure 16: Case 1 Stream Summary

Case 1 Performance Summary

Power Production	
Steam Cycle (MW)	564.66
Expander 1	64.69
Expander 2	64.69
TOTAL GROSS POWER (MW)	**694.04**
AUX Load	
Cryo ASU + CPU	97.14
OTM ASU	17.14
Boiler Fuel Delivery	0.95
Flue Gas Desulfurization (FGD)	5.78
Condenser Circulation Pump	6.38
Cooling Tower Fan	4.73
Condensate Pump	0.93
Additional Auxilaries	5.26
Misc Plant Auxilaries	2.82
Gasifier and Slag Handling	2.79
Gas Liquor Separation	0.00
Gas Liquor Treatment	0.00
TOTAL AUX LOAD (MW)	**143.92**
Net Power (MW)	**550.12**
Net Efficiency (% HHV)	**36.30**
Coal Rate (tpd)	**5319**
Industrial Gases:	
O2 Cryogenic ASU (tpd)	3540
O2 OTM ASU (tpd)	7314
CO2 captured (tpd)	12334
CO2 emissions (tpd)	878
CO2 capture efficiency (%)	97.1%
CO2 Purity (%)	95.8%
Environmental Performance:	
SOx (lb/MMbtu)	1.1E-04
PM (lb/MMbtu)	negligible
CO2 (lb/MMbtu)	5.9
Hg (lb/MMbtu)	negligible

Figure 17: Case 1 power, industrial gas and environmental performance summary

OTM Case 1: FGD, SC		Equipment Cost	Installation Costs	Bare Erected Cost	Eng'g Fee, EPC Profit	Contingency	Total	$/kw
Gasifier Costs				$190,216,000	$15,707,000	$39,468,000	$245,391,000	$446
Candle Filter		$5,184,000	$3,629,000	$8,813,000	$881,000	$1,763,000	$11,457,000	$21
Syngas Turbines		$33,820,000	$23,674,000	$57,494,000	$5,749,000	$5,749,000	$68,992,000	$125
Boiler (Excluding OTM)		$56,361,000	$125,890,000	$182,251,000	$35,482,000	$12,639,000	$230,372,000	$419
Steam Turbine, FWH, Condensers		$93,789,000	$55,807,000	$149,596,000	$28,544,000	$10,563,000	$188,703,000	$343
FGD		$61,665,000	$68,953,000	$130,618,000	$25,430,000	$9,059,000	$165,107,000	$300
Cooling Tower, Pumps, Tanks, Misc		$36,171,000	$32,850,000	$69,021,000	$13,438,000	$4,787,000	$87,246,000	$159
Latent Heat Recovery		$10,368,000	$7,258,000	$17,626,000	$1,763,000	$1,763,000	$21,152,000	$38
Cryogenic ASU + CPU							$301,523,000	$548
OTM ASU				$210,009,000	$21,000,000	$41,121,000	$272,130,000	$495
						TOTAL	**$1,592,073,000**	**$2,894**

*Does not include "Owners Costs," Carrying Costs, Permit fees, owners CM expense, owners contingency, escalation during construction, etc

Figure 18: Case 1 capital cost estimate

Case 1 COE Calculation			
Net Power Produced	**550.1**	**MW**	
Capacity Factor	90.0%		
Coal Cost	3	$/MMbtu	
Heat Rate (including sequestration)	9,400	Btu/kwh	
Capital Investment	**$x1000**		**$/kw**
Bare Erected Capital Cost	$ 1,317,167		2,394
Engineering	$ 147,994		269
Contingency	$ 126,912		231
Total Plant Cost	**$ 1,592,073**		**2,894**
Operating & Maintenance Cost	**$x1000**		**$/kw-yr**
Fixed O&M	$ 22,005		40
Variable O&M	$ 16,504		30

COE Calculation	$x1000	factor	c/kwh
O&M Cost			
Fixed O&M	$ 22,005	1.16	0.589
Variable O&M	$ 16,504	1.16	0.397
Consumable Operating Costs (less Coal)			
Limestone	$ 3,655	1.16	0.098
Gypsum Disposal	$ 3,736	1.16	0.100
Ash Disposal	$ 3,112	1.16	0.083
Water	$ 788	1.16	0.021
MU & WT reagents	$ 1,500	1.16	0.040
Natural Gas	$ 1,591	1.2	0.044
Fuel Cost	$ 122,307	1.2	3.384
Total Capital	$ 1,592,073	0.175	6.424
TOTAL 20 Yr Levelized COE (c/kwh)			**11.18**

Figure 19: Case 1 COE estimate. Contingency and Engineering costs reported here do not reflect contributions from the Cryogenic ASU or CPU equipment.

Stream		Coal	Gasifier Steam	Gasifier Cryo O2	Gasifier Slag	Gasifier Syngas	Pox 1 Air	Pox 1 Air	Pox 1 Warm Air	Pox 1 Hot O2 Depleted	Pox 1 Cold O2 Depleted	Pox 1 Hot Syngas	Pox 2 Warm Syngas	Pox 2 Air	Pox 2 Air	Pox 2 Warm Air	Pox 2 Hot O2 Depleted	Pox 2 Cold O2 Depleted
Stream #		1	2	3	4	5	11	12	13	14	15	16	17	21	22	23	24	25
Temperature	F	77	680	77	500	1000	75	137	1517	1832	232	1832	1223	75	137	1517	1832	232
Pressure	psia	-	510	20	396	340	14.7	19.7	18.7	18.7	17.7	340	72.45	14.7	19.7	18.7	18.7	17.7
Flow	k lb/hr	427.5	124.1	215.3	6.14	778.6	415.3	415.3	415.3	347.1	347.1	846.8	846.8	248.2	248.2	248.2	207.4	207.4
Flow	lbmol/hr	-	6,889	6,696	0	38,851	14,391	14,391	14,391	12,260	12,260	42,601	42,601	8,601	8,601	8,601	7,327	7,327
Composition																		
H_2	mol%					29.9%						32.7%	32.7%					
CO	mol%					50.3%						46.7%	46.7%					
CH_4	mol%					3.3%						1.1%	1.1%					
CO_2	mol%					4.3%						8.1%	8.1%					
H_2O	mol%					9.4%						9.4%	9.4%					
O_2	mol%		100.0%				21.2%	21.2%	21.2%	7.5%	7.5%			21.2%	21.2%	21.2%	7.5%	7.5%
N_2 + Ar	mol%			95.5%		1.2%	78.8%	78.8%	78.8%	92.5%	92.5%	1.2%	1.2%	78.8%	78.8%	78.8%	92.5%	92.5%
H_2S	mol%			4.5%		0.8%						0.7%	0.7%					
SOx	mol%																	
Solids	k lb/hr	427.5			6.14													

Stream	OTM Boiler Hot O2	OTM Boiler Cold O2	Residual Syngas	Cyro O2 for Burner	Hot Flue Gas	Air Leak	Warm Flue Gas	Cold Flue Gas	Lime-stone	FGD Solids	Flue Gas to CPU	CPU Inerts	CO2 Product	HP Steam	Reheat 1 Steam	Reheat 2 Steam	Cond. Pump Out

Figure 20: Case 2 Stream Summary

Case 2 Performance Summary

Power Production	
Steam Cycle (MW)	562.34
Expander 1	63.21
Expander 2	63.21
TOTAL GROSS POWER (MW)	**688.76**
AUX Load	
Cryo ASU + CPU	94.93
OTM ASU	16.75
Boiler Fuel Delivery	0.93
Flue Gas Desulfurization (FGD)	5.78
Condenser Circulation Pump	3.90
Cooling Tower Fan	5.23
Condensate Pump	0.40
Additional Auxilaries	5.21
Misc Plant Auxilaries	2.81
Gasifier and Slag Handling	2.72
Gas Liquor Separation	0.00
Gas Liquor Treatment	0.00
TOTAL AUX LOAD (MW)	**138.66**
Net Power (MW)	**550.10**
Net Efficiency (% HHV)	**37.15**
Coal Rate (tpd)	**5197**
Industrial Gases:	
O2 Cryogenic ASU (tpd)	3460
O2 OTM ASU (tpd)	7147
CO2 captured (tpd)	12051
CO2 emissions (tpd)	859
CO2 capture efficiency (%)	97.1%
CO2 Purity (%)	95.8%
Environmental Performance:	
SOx (lb/MMbtu)	1.1E-04
PM (lb/MMbtu)	negligible
CO2 (lb/MMbtu)	5.9
Hg (lb/MMbtu)	negligible

Figure 21: Case 2 power, industrial gas and environmental performance summary

OTM Case 2: FGD, USC		Equipment Cost	Installation Costs	Bare Erected Cost	Eng'g Fee, EPC Profit	Contingency	Total	$/kw
Gasifier Costs				$190,216,000	$15,707,000	$39,468,000	$245,391,000	$446
Candle Filter		$5,066,000	$3,546,000	$8,612,000	$861,000	$1,722,000	$11,195,000	$20
Syngas Turbines		$33,678,000	$23,575,000	$57,253,000	$5,725,000	$5,725,000	$68,703,000	$125
Boiler (Excluding OTM)		$60,007,000	$126,300,000	$186,307,000	$37,268,000	$13,003,000	$236,578,000	$430
Steam Turbine, FWH, Condensers		$90,271,000	$60,174,000	$150,445,000	$29,372,000	$10,718,000	$190,535,000	$346
FGD		$59,857,000	$66,898,000	$126,755,000	$25,356,000	$8,846,000	$160,957,000	$293
Cooling Tower, Pumps, Tanks, Misc		$39,318,000	$34,241,000	$73,559,000	$14,715,000	$5,134,000	$93,408,000	$170
Latent Heat Recovery		$10,131,000	$7,092,000	$17,223,000	$1,722,000	$1,722,000	$20,667,000	$38
Cryogenic ASU + CPU							$294,647,000	$536
OTM ASU				$205,206,000	$20,520,000	$40,180,000	$265,906,000	$483
						TOTAL	**$1,587,987,000**	**$2,887**

*Does not include "Owners Costs," Carrying Costs, Permit fees, owners CM expense, owners contingency, escalation during construction, etc

Figure 22: Case 2 capital cost estimate

Case 2 COE Calculation

Net Power Produced		**550.1 MW**	
Capacity Factor		90.0%	
Coal Cost		3 $/MMbtu	
Heat Rate (including sequestration)		9,185 Btu/kwh	
Capital Investment		**$x1000**	**$/kw**
Bare Erected Capital Cost	$	1,015,576	1,846
Engineering	$	151,246	275
Contingency	$	126,518	230
Total Plant Cost	**$**	**1,587,987**	**2,887**
Operating & Maintenance Cost		**$x1000**	**$/kw-yr**
Fixed O&M	$	22,004	40
Variable O&M	$	16,503	30

COE Calculation		$x1000	factor	c/kwh
O&M Cost				
Fixed O&M	$	22,004	1.16	0.589
Variable O&M	$	16,503	1.16	0.397
Consumable Operating Costs (less Coal)				
Limestone	$	3,684	1.16	0.099
Gypsum Disposal	$	3,803	1.16	0.102
Ash Disposal	$	3,041	1.16	0.081
Water	$	788	1.16	0.021
MU & WT reagents	$	1,500	1.16	0.040
Natural Gas (Gasifier Auxiliary)	$	1,555	1.2	0.043
Fuel Cost	$	119,510	1.2	3.307
Total Capital	$	1,587,987	0.175	6.408
TOTAL 20 Yr Levelized COE (c/kwh)				**11.09**

Figure 23: Case 2 COE estimate. Contingency and Engineering costs reported here do not reflect contributions from the Cryogenic ASU or CPU equipment.

Stream		Coal	Gasifier Steam	Gasifier Cryo O2	Gasifier Slag	Gasifier Syngas	Pox 1 Air	Pox 1 Air	Pox 1 Warm Air	Pox 1 Hot O2 Depleted	Pox 1 Cold O2 Depleted	Pox 1 Hot Syngas	Pox 2 Warm Syngas	Pox 2 Air	Pox 2 Air	Pox 2 Warm Air	Pox 2 Hot O2 Depleted	Pox 2 Cold O2 Depleted
Stream #		1	2	3	4	5	11	12	13	14	15	16	17	21	22	23	24	25
Temperature	F	77	680	77	500	1000	75	137	1517	1832	232	1832	1238	75	137	1517	1832	232
Pressure	psia	-	510	20	396	340	14.7	19.7	18.7	18.7	17.7	338.5	75.32	14.7	19.7	18.7	18.7	17.7
Flow	k lb/hr	405.4	117.7	204.2	5.82	738.4	395.6	395.6	395.6	330.6	330.6	803.4	803.4	230.6	230.6	230.6	192.7	192.7
Flow	lbmol/hr	-	6,534	6,350	0	36,789	13,709	13,709	13,709	11,679	11,679	40,404	40,404	7,990	7,990	7,990	6,806	6,806
Composition																		
H_2	mol%					29.9%						32.6%	32.6%					
CO	mol%					50.2%						46.7%	46.7%					
CH_4	mol%					3.3%						1.0%	1.0%					
CO_2	mol%					4.4%						8.1%	8.1%					
H_2O	mol%		100.0%			9.5%						9.4%	9.4%					
O_2	mol%			95.5%			21.2%	21.2%	21.2%	7.5%	7.5%			21.2%	21.2%	21.2%	7.5%	7.5%
N_2 + Ar	mol%			4.5%		1.2%	78.8%	78.8%	78.8%	92.5%	92.5%	1.3%	1.3%	78.8%	78.8%	78.8%	92.5%	92.5%
H_2S	mol%					0.8%						0.7%	0.7%					
SOx	mol%																	
Solids	k lb/hr	405.4			5.82													

	OTM Boiler Warm Air	OTM Boiler Hot O2 Depleted	OTM Boiler Cold O2 Depleted	Residual Syngas	Cyro O2 for Burner	Hot Flue Gas	Air Leak	Warm Flue Gas	Cold Flue Gas	Lime-stone	FGD Solids	Flue Gas to CPU	CPU Inerts	CO2 Product	HP Steam	Reheat Steam	Cond. Pump Out	BFW to Boiler
Stream #	33	34	35	36	37	38	39	40	41	42	43	51	52	53	61	62	63	64
Temperature	1517	1832	232	1832	80	2547	77	365	120	77	144.3	144	91	100	1292	1328	89.64	576
Pressure	18.7	18.7	17.7	16	17	16.0	15.0	15.0	14.0	-	-	14.0	371.5	2000	5075	1200	220	5369
Flow	[illegible]	[illegible]	[illegible]	[illegible]	[illegible]	[illegible]	[illegible]	[illegible]	[illegible]	[illegible]	[illegible]	[illegible]	[illegible]	[illegible]	[illegible]	[illegible]	[illegible]	[illegible]

Figure 24: Case 3 Stream Summary

Case 3 Performance Summary

Power Production	
Steam Cycle (MW)	563.22
Expander 1	59.17
Expander 2	59.17
TOTAL GROSS POWER (MW)	**681.55**
AUX Load	
Cryo ASU + CPU	88.84
OTM ASU	15.68
Boiler Fuel Delivery	0.87
Flue Gas Desulfurization (FGD)	4.58
Condenser Circulation Pump	5.71
Cooling Tower Fan	4.26
Condensate Pump	1.08
Additional Auxilaries	5.19
Misc Plant Auxilaries	2.82
Gasifier and Slag Handling	2.55
Gas Liquor Separation	0.00
Gas Liquor Treatment	0.00
TOTAL AUX LOAD (MW)	**131.57**
Net Power (MW)	**549.98**
Net Efficiency (% HHV)	**39.68**
Coal Rate (tpd)	**4865**
Industrial Gases:	
O2 Cryogenic ASU (tpd)	3236
O2 OTM ASU (tpd)	6692
CO2 captured (tpd)	11281
CO2 emissions (tpd)	803
CO2 capture efficiency (%)	97.1%
CO2 Purity (%)	95.8%
Environmental Performance:	
SOx (lb/MMbtu)	1.1E-04
PM (lb/MMbtu)	negligible
CO2 (lb/MMbtu)	5.9
Hg (lb/MMbtu)	negligible

Figure 25: Case 3 power, industrial gas and environmental performance summary

OTM Case 3: FGD, Adv-USC		Equipment Cost	Installation Costs	Bare Erected Cost	Eng'g Fee, EPC Profit	Contingency	Total	$/kw
Gasifier Costs				$190,216,000	$15,707,000	$39,468,000	$245,391,000	$446
Candle Filter		$4,742,000	$3,319,000	$8,061,000	$806,000	$1,612,000	$10,479,000	$19
Syngas Turbines		$33,288,000	$23,302,000	$56,590,000	$5,659,000	$5,659,000	$67,908,000	$123
Boiler (Excluding OTM)		$60,627,000	$126,274,000	$186,901,000	$36,813,000	$13,332,000	$237,046,000	$431
Steam Turbine, FWH, Condensers		$94,001,000	$136,269,000	$230,270,000	$44,656,000	$16,632,000	$291,558,000	$530
FGD		$59,151,000	$66,006,000	$125,157,000	$24,652,000	$8,928,000	$158,737,000	$289
Cooling Tower, Pumps, Tanks, Misc		$34,984,000	$38,457,000	$73,441,000	$14,465,000	$5,239,000	$93,145,000	$169
Latent Heat Recovery		$9,483,000	$6,638,000	$16,121,000	$1,612,000	$1,612,000	$19,345,000	$35
Cryogenic ASU + CPU							$275,738,000	$501
OTM ASU				$192,101,000	$19,210,000	$37,614,000	$248,925,000	$453
						TOTAL	**$1,648,272,000**	**$2,997**

*Does not include "Owners Costs," Carrying Costs, Permit fees, owners CM expense, owners contingency, escalation during construction, etc

Figure 26: Case 3 capital cost estimate

Case 3 COE Calculation

Net Power Produced		**550.0**	**MW**
Capacity Factor		90.0%	
Coal Cost		3	$/MMbtu
Heat Rate (including sequestration)		8,600	Btu/kwh
Capital Investment		**$x1000**	**$/kw**
Bare Erected Capital Cost	$	1,354,596	2,463
Engineering	$	163,580	297
Contingency	$	130,096	237
Total Plant Cost	**$**	**1,648,272**	**2,997**
Operating & Maintenance Cost		**$x1000**	**$/kw-yr**
Fixed O&M	$	21,999	40
Variable O&M	$	16,499	30

COE Calculation		$x1000	factor	c/kwh
O&M Cost				
Fixed O&M	$	21,999	1.16	0.589
Variable O&M	$	16,499	1.16	0.397
Consumable Operating Costs (less Coal)				
Limestone	$	3,343	1.16	0.089
Gypsum Disposal	$	3,418	1.16	0.091
Ash Disposal	$	2,847	1.16	0.076
Water	$	788	1.16	0.021
MU & WT reagents	$	1,500	1.16	0.040
Natural Gas	$	1,455	1.2	0.040
Fuel Cost	$	111,868	1.2	3.096
Total Capital	$	1,648,272	0.175	6.652
TOTAL 20 Yr Levelized COE (c/kwh)				**11.09**

Figure 27: Case 3 COE estimate. Contingency and Engineering costs reported here do not reflect contributions from the Cryogenic ASU or CPU equipment.

5.2. OTM cases with WGCU

Cases 4,5 and 6 are the three cases where the WGCU option is used for sulfur control from the syngas following the gasifier. The three cases use different steam conditions as was previously mentioned. Refer to Figure 28 for the process schematic applying to these three cases. In each of these cases the OTM membranes are used to combust 90% of the syngas. The remaining portion of syngas is combusted using cryogenically supplied oxygen. In all of these cases the OTM Flux is lower in the OTM boiler (due to higher fuel utilization) and higher in the OTM Pox units. The OTM flux values used in this analysis are equal to actual laboratory-measured flux performance values of Praxair's advanced material OTM tubes, however the flux values are not disclosed here.

Case No.	Gasifier Type	OTM Pox Units	Expander Units	Steam Conditions	OTM Fuel Combustion	OTM Type	SRU	CO2 Purification	Suppl. Comb. Oxidant Source	Air Leak	Flue Gas Recycle
1	BGL	2	2	SC	90%	Tube	FGD	Yes	Cryo ASU	3%	No
2	BGL	2	2	USC-Comm	90%	Tube	FGD	Yes	Cryo ASU	3%	No
3	BGL	2	2	USC-Adv	90%	Tube	FGD	Yes	Cryo ASU	3%	No
4	BGL	2	2	SC	90%	Tube	WGCU	Yes	Cryo ASU	3%	No
5	BGL	2	2	USC-Comm	90%	Tube	WGCU	Yes	Cryo ASU	3%	No
6	BGL	2	2	USC-Adv	90%	Tube	WGCU	Yes	Cryo ASU	3%	No

For each of the three WGCU cases (Case 4, Case 5, and Case 6) the following performance information will be given in Figure 29 to Figure 40:

- Stream Summary Table (corresponding to stream numbering in Figure 28)
- Performance Summary
- Capital Cost Summary for an OTM using "Cost Allocation A".
- Cost of Electricity breakdown for a coal price of $3/MMBTU

Figure 29 to Figure 32 refers to Case 4, Figure 33 to Figure 36 refers to Case 5, and Figure 37 to Figure 40 refers to Case 6.

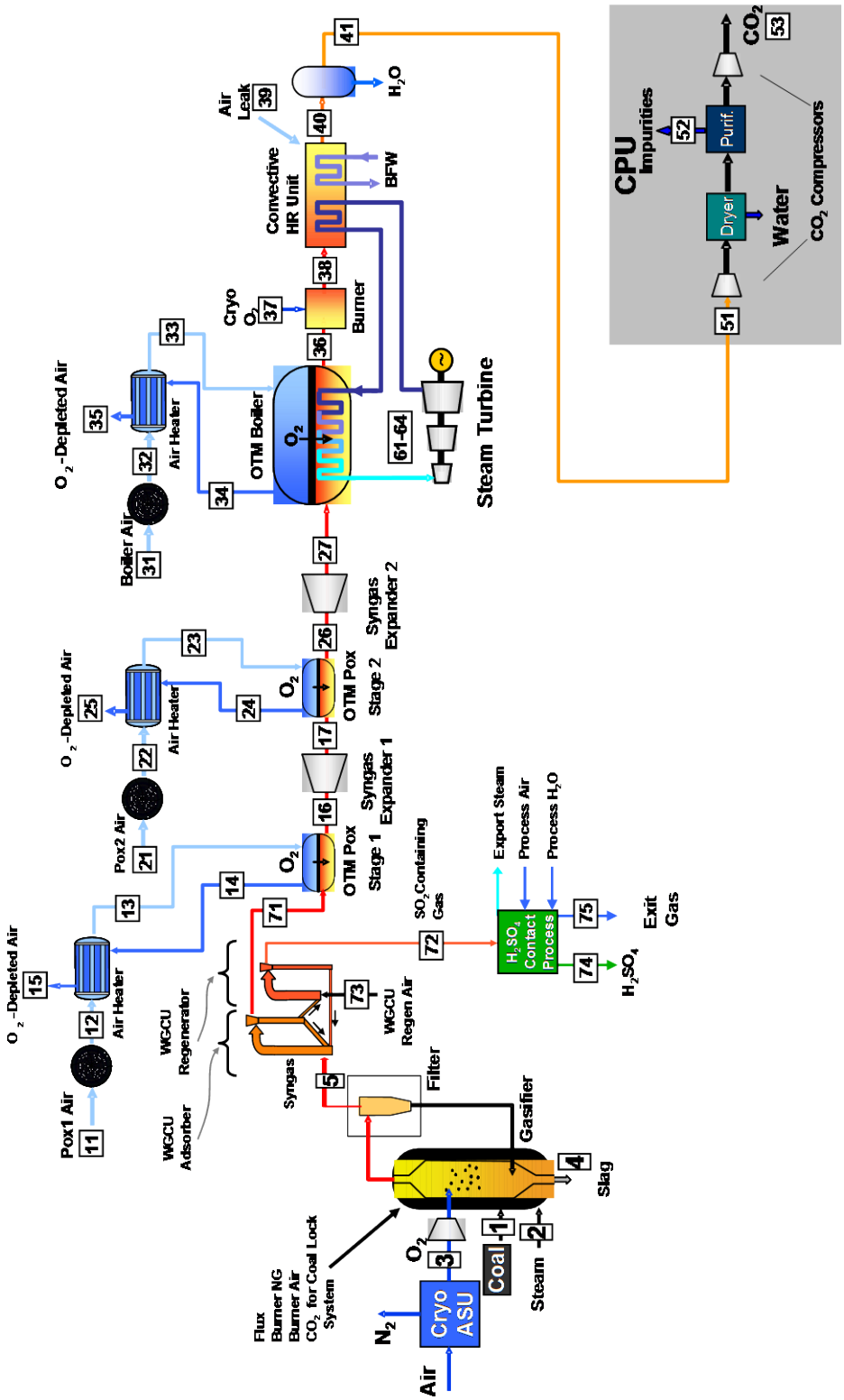

Figure 28: Advanced Power Cycle with WGCU for Sulfur containment

Figure 29: Case 4 Stream Summary

Case 4 Performance Summary

Power Production	
Steam Cycle (MW)	564.75
Expander 1	63.19
Expander 2	63.19
TOTAL GROSS POWER (MW)	**691.13**
AUX Load	
Cryo ASU + CPU	93.97
OTM ASU	17.05
Boiler Fuel Delivery	0.95
Flue Gas Desulfurization (FGD)	0.00
Condenser Circulation Pump	6.35
Cooling Tower Fan	4.70
Condensate Pump	0.92
Additional Auxilaries	5.25
Misc Plant Auxilaries	2.82
WGCU & Sulfur Recovery	5.91
Gasifier and Slag Handling	2.77
Gas Liquor Separation	0.00
TOTAL AUX LOAD (MW)	**140.70**
Net Power (MW)	**550.43**
Net Efficiency (% HHV)	**36.52**
Coal Rate (tpd)	**5290**
Industrial Gases:	
O2 Cryogenic ASU (tpd)	3324
O2 OTM ASU (tpd)	7275
CO2 captured (tpd)	12262
CO2 emissions (tpd)	703
CO2 capture efficiency (%)	97.1%
CO2 Purity (%)	95.8%
Environmental Performance:	
SOx (lb/MMbtu)	negligible
PM (lb/MMbtu)	negligible
CO2 (lb/MMbtu)	5.9
Hg (lb/MMbtu)	negligible

Figure 30: Case 4 power, industrial gas and environmental performance summary

OTM Case 4: WGCU, SC		Equipment Cost	Installation Costs	Bare Erected Cost	Eng'g Fee, EPC Profit	Contingency	Total	$/kw
Gasifier Costs				$190,216,000	$15,707,000	$39,468,000	$245,391,000	$446
Candle Filter		$5,156,000	$3,609,000	$8,765,000	$877,000	$1,753,000	$11,395,000	$21
Syngas Turbines		$33,675,000	$23,573,000	$57,248,000	$5,725,000	$5,725,000	$68,698,000	$125
Boiler (Excluding OTM)		$56,965,000	$125,517,000	$182,482,000	$35,525,000	$12,640,000	$230,647,000	$419
Steam Turbine, FWH, Condensers		$93,618,000	$55,383,000	$149,001,000	$28,474,000	$10,494,000	$187,969,000	$341
WGCU and Sulfur Recovery							$163,212,000	$297
Cooling Tower, Pumps, Tanks, Misc		$35,944,000	$32,755,000	$68,699,000	$13,374,000	$4,758,000	$86,831,000	$158
Latent Heat Recovery		$10,312,000	$7,218,000	$17,530,000	$1,753,000	$1,753,000	$21,036,000	$38
Cryogenic ASU + CPU							$293,683,000	$534
OTM ASU				$209,863,000	$20,987,000	$41,097,000	$271,947,000	$494
						TOTAL	**$1,580,809,000**	**$2,872**

*Does not include "Owners Costs," Carrying Costs, Permit fees, owners CM expense, owners contingency, escalation during construction, etc

Figure 31: Case 4 capital cost estimate

Case 4 COE Calculation

Net Power Produced		**550.4**	**MW**
Capacity Factor		90.0%	
Coal Cost		3	$/MMbtu
Heat Rate (including sequestration)		9,343	Btu/kwh
Capital Investment		**$x1000**	**$/kw**
Bare Erected Capital Cost	$	1,177,487	2,139
Engineering	$	122,422	222
Contingency	$	117,688	214
Total Plant Cost	**$**	**1,580,809**	**2,872**
Operating & Maintenance Cost		**$x1000**	**$/kw-yr**
Fixed O&M	$	22,017	40
Variable O&M	$	16,513	30

* Engineering & Contingency values shown do not include assumed values for Cryo ASU, CPU, WGCU

COE Calculation		**$x1000**	**factor**	**c/kwh**
O&M Cost				
Fixed O&M	$	22,017	1.16	0.589
Variable O&M	$	16,513	1.16	0.397
Consumable Operating Costs (less Coal)				
Limestone	$	890	1.16	0.024
Gypsum Disposal	$	-	1.16	-
Ash Disposal	$	3,095	1.16	0.083
Water	$	788	1.16	0.021
MU & WT reagents	$	1,500	1.16	0.040
Natural Gas	$	1,582	1.2	0.044
Acid Sale ($100/ton)	$	-	1.2	-
Fuel Cost	$	121,641	1.2	3.364
Total Capital	$	1,580,809	0.175	6.375
TOTAL 20 Yr Levelized COE (c/kwh)				**10.94**

Figure 32: Case 4 COE estimate

Figure 33: Case 5 Stream Summary

Case 5 Performance Summary

Power Production	
Steam Cycle (MW)	561.93
Expander 1	61.68
Expander 2	61.68
TOTAL GROSS POWER (MW)	**685.28**
AUX Load	
Cryo ASU + CPU	91.76
OTM ASU	16.65
Boiler Fuel Delivery	0.92
Flue Gas Desulfurization (FGD)	0.00
Condenser Circulation Pump	3.88
Cooling Tower Fan	5.20
Condensate Pump	0.40
Additional Auxilaries	5.17
Misc Plant Auxilaries	2.81
WGCU & Sulfur Recovery	5.77
Gasifier and Slag Handling	2.71
Gas Liquor Treatment	0.00
TOTAL AUX LOAD (MW)	**135.26**
Net Power (MW)	**550.02**
Net Efficiency (% HHV)	**37.37**
Coal Rate (tpd)	**5165**
Industrial Gases:	
O2 Cryogenic ASU (tpd)	3246
O2 OTM ASU (tpd)	7103
CO2 captured (tpd)	11976
CO2 emissions (tpd)	683
CO2 capture efficiency (%)	97.1%
CO2 Purity (%)	95.8%
Environmental Performance:	
SOx (lb/MMbtu)	negligible
PM (lb/MMbtu)	negligible
CO2 (lb/MMbtu)	5.9
Hg (lb/MMbtu)	negligible

Figure 34: Case 5 power, industrial gas and environmental performance summary

OTM Case 5: WGCU, USC	Equipment Cost	Installation Costs	Bare Erected Cost	Eng'g Fee, EPC Profit	Contingency	Total	$/kw
Gasifier Costs			$190,216,000	$15,707,000	$39,468,000	$245,391,000	$446
Candle Filter	$5,034,000	$3,524,000	$8,558,000	$856,000	$1,712,000	$11,126,000	$20
Syngas Turbines	$33,530,000	$23,471,000	$57,001,000	$5,700,000	$5,700,000	$68,401,000	$124
Boiler (Excluding OTM)	$60,311,000	$125,166,000	$185,477,000	$37,157,000	$12,930,000	$235,564,000	$428
Steam Turbine, FWH, Condensers	$90,093,000	$59,369,000	$149,462,000	$29,257,000	$10,626,000	$189,345,000	$344
WGCU and Sulfur Recovery						$159,355,000	$290
Cooling Tower, Pumps, Tanks, Misc	$38,871,000	$34,100,000	$72,971,000	$14,618,000	$5,087,000	$92,676,000	$168
Latent Heat Recovery	$10,068,000	$7,048,000	$17,116,000	$1,712,000	$1,712,000	$20,540,000	$37
Cryogenic ASU + CPU						$286,805,000	$521
OTM ASU			$204,905,000	$20,490,000	$40,126,000	$265,521,000	$483
					TOTAL	$1,574,724,000	$2,863

*Does not include "Owners Costs," Carrying Costs, Permit fees, owners CM expense, owners contingency, escalation during construction, etc

Figure 35: Case 5 capital cost estimate

Case 5 COE Calculation

Net Power Produced		**550.0**	**MW**
Capacity Factor		90.0%	
Coal Cost		3	$/MMbtu
Heat Rate (including sequestration)		9,129	Btu/kwh
Capital Investment		**$x1000**	**$/kw**
Bare Erected Capital Cost	$	885,706	1,610
Engineering *	$	125,497	228
Contingency *	$	117,361	213
Total Plant Cost	**$**	**1,574,724**	**2,863**
Operating & Maintenance Cost		**$x1000**	**$/kw-yr**
Fixed O&M	$	22,001	40
Variable O&M	$	16,501	30

* Engineering & Contingency values shown do not include assumed values for Cryo ASU, CPU, WGCU

COE Calculation		**$x1000**	**factor**	**c/kwh**
O&M Cost				
Fixed O&M	$	22,001	1.16	0.589
Variable O&M	$	16,501	1.16	0.397
Consumable Operating Costs (less Coal)				
Limestone	$	869	1.16	0.023
Gypsum Disposal	$	-	1.16	-
Ash Disposal	$	3,022	1.16	0.081
Water	$	788	1.16	0.021
MU & WT reagents	$	1,500	1.16	0.040
Natural Gas	$	1,545	1.2	0.043
Acid Sale	$	-	1.2	-
Fuel Cost	$	118,766	1.2	3.287
Total Capital	$	1,574,724	0.175	6.355
TOTAL 20 Yr Levelized COE (c/kwh)				**10.84**

Figure 36: Case 5 COE estimate

Figure 37: Case 6 Stream Summary

Case 6 Performance Summary

Power Production	
Steam Cycle (MW)	563.77
Expander 1	57.83
Expander 2	57.83
TOTAL GROSS POWER (MW)	**679.42**
AUX Load	
Cryo ASU + CPU	86.01
OTM ASU	15.61
Boiler Fuel Delivery	0.87
Flue Gas Desulfurization (FGD)	0.00
Condenser Circulation Pump	5.69
Cooling Tower Fan	4.24
Condensate Pump	1.07
Additional Auxilaries	5.19
Misc Plant Auxilaries	2.82
WGCU & Sulfur Recovery	5.41
Gasifier and Slag Handling	2.54
Gas Liquor Separation	0.00
TOTAL AUX LOAD (MW)	**129.44**
Net Power (MW)	**549.98**
Net Efficiency (% HHV)	**39.86**
Coal Rate (tpd)	**4842**
Industrial Gases:	
O2 Cryogenic ASU (tpd)	3042
O2 OTM ASU (tpd)	6659
CO2 captured (tpd)	11226
CO2 emissions (tpd)	641
CO2 capture efficiency (%)	97.1%
CO2 Purity (%)	95.8%
Environmental Performance:	
SOx (lb/MMbtu)	negligible
PM (lb/MMbtu)	negligible
CO2 (lb/MMbtu)	5.9
Hg (lb/MMbtu)	negligible

Figure 38: Case 6 power, industrial gas and environmental performance summary

Figure 39: Case 6 capital cost estimate

OTM Case 6: WGCU, Adv-USC		Equipment Cost	Installation Costs	Bare Erected Cost	Eng'g Fee, EPC Profit	Contingency	Total	$/kw
Gasifier Costs				$190,216,000	$15,707,000	$39,468,000	$245,391,000	$446
Candle Filter		$4,719,000	$3,303,000	$8,022,000	$802,000	$1,604,000	$10,428,000	$19
Syngas Turbines		$33,160,000	$23,212,000	$56,372,000	$5,637,000	$5,637,000	$67,646,000	$123
Boiler (Excluding OTM)		$60,630,000	$125,944,000	$186,574,000	$36,828,000	$13,308,000	$236,710,000	$430
Steam Turbine, FWH, Condensers		$93,931,000	$132,721,000	$226,652,000	$44,077,000	$16,362,000	$287,091,000	$522
WGCU and Sulfur Recovery							$149,389,000	$272
Cooling Tower, Pumps, Tanks, Misc		$34,809,000	$37,846,000	$72,655,000	$14,341,000	$5,182,000	$92,178,000	$168
Latent Heat Recovery		$9,439,000	$6,607,000	$16,046,000	$1,605,000	$1,605,000	$19,256,000	$35
Cryogenic ASU + CPU							$268,848,000	$489
OTM ASU				$192,071,000	$19,207,000	$37,612,000	$248,890,000	$453
						TOTAL	**$1,625,827,000**	**$2,956**

*Does not include "Owners Costs," Carrying Costs, Permit fees, owners CM expense, owners contingency, escalation during construction, etc

Case 6 COE Calculation

Net Power Produced		**550.0**	**MW**
Capacity Factor		90.0%	
Coal Cost		3	$/MMbtu
Heat Rate (including sequestration)		8,559	Btu/kwh
Capital Investment		**$x1000**	**$/kw**
Bare Erected Capital Cost	$	1,217,456	2,214
Engineering	$	138,204	251
Contingency	$	120,778	220
Total Plant Cost	**$**	**1,625,827**	**2,956**
Operating & Maintenance Cost		**$x1000**	**$/kw-yr**
Fixed O&M	$	21,999	40
Variable O&M	$	16,499	30

* Engineering & Contingency values shown do not include assumed values for Cryo ASU, CPU, WGCU

COE Calculation		**$x1000**	**factor**	**c/kwh**
O&M Cost				
Fixed O&M	$	21,999	1.16	0.589
Variable O&M	$	16,499	1.16	0.397
Consumable Operating Costs (less Coal)				
Limestone	$	814	1.16	0.022
Gypsum Disposal	$	-	1.16	-
Ash Disposal	$	2,833	1.16	0.076
Water	$	788	1.16	0.021
MU & WT reagents	$	1,500	1.16	0.040
Natural Gas	$	1,448	1.2	0.040
Acid Sale ($100/ton)	$	-	1.2	-
Fuel Cost	$	111,339	1.2	3.081
Total Capital	$	1,625,827	0.175	6.562
TOTAL 20 Yr Levelized COE (c/kwh)				**10.83**

Figure 40: Case 6 COE estimate

5.3. Cost Summary

The base case COE was calculated for a coal price of $3/MMBTU however the COE was calculated for other coal prices due to the volatility in coal prices in 2008. Figure 41 below shows COE for coal prices of 1.8, 3.0 and 4.0/MMBTU for OTM cases 1 thru 6. In all cases the installed OTM 'Cost Allocation A' was used and the OTM fuel utilization is 90%.

		OTM FGD Process CASES			OTM WGCU Process CASES			Air-PC Case
Case		1 SC	2 USC	3 AdvUSC	4 SC	5 USC	6 AdvUSC	Praxair/DOE No CCS SC
Net Efficiency (HHV)		36.3	37.2	39.7	36.6	37.4	39.9	39.7
Cost Basis (Year)		3/2008	3/2008	3/2008	3/2008	3/2008	3/2008	3/2008
Plant Cost ($/kW)		$2,894	$2,887	$2,997	$2,872	$2,863	$2,956	$1,908
	Coal Price ($/MMbtu)							
COE ($/MWh)	1.8	$98.3	$97.6	$98.5	$95.9	$95.2	$96.0	$70.5
	3	$111.8	$110.9	$110.9	$109.4	$108.4	$108.3	$82.9
	4	$123.1	$121.9	$121.2	$120.6	$119.3	$118.5	$93.2

Figure 41: Calculated COE for 6 OTM cases at various coal prices compared to the Air-PC reference case (no capture)

For reference also shown on the figure is the COE from the Praxair simulated version of the DOE's Supercritical Air-Pulverized Coal case which has been adjusted to match the 2008 capital basis for all the OTM cases. This reference case has been adjusted from Case 1 in the DOE oxy-combustion report DOE/NETL-2007/1291. This DOE-based reference case is the basis for calculating the % increase in COE for the OTM cases. The DOE goal for cost of electricity increase is <35% increase in COE for power cycles which enable CCS. Figure 42 shows the calculated increase in COE over the reference case for the 6 OTM cases at the three different coal prices. The areas shaded in green denote that the case satisfies the DOE requirement for an increase in COE of less than 35%.

		OTM FGD Process CASES			OTM WGCU Process CASES			Air-PC Case
Case		1 SC	2 USC	3 AdvUSC	4 SC	5 USC	6 AdvUSC	Praxair/DOE No CCS SC
Net Efficiency (HHV)		36.3	37.2	39.7	36.6	37.4	39.9	39.7
Cost Basis (Year)		3/2008	3/2008	3/2008	3/2008	3/2008	3/2008	3/2008
Plant Cost ($/kW)		$2,894	$2,887	$2,997	$2,872	$2,863	$2,956	$1,908
	Coal Price ($/MMbtu)							
Increase in COE over Reference	1.8	39.4%	38.4%	39.7%	36.0%	35.0%	36.2%	
	3.0	34.9%	33.8%	33.8%	32.0%	30.8%	30.6%	
	4.0	32.1%	30.8%	30.0%	29.4%	28.0%	27.1%	

Figure 42: Percent increase in COE over the reference case for various coal prices.

Cost of CO_2 avoided and cost of CO_2 removed is calculated as described in the Design Basis section. In all cases the cost of CO_2 avoided/removed reflects a $4/ton of CO_2 cost for transport, final sequestration, measurement, verification, etc. Cost of CO_2 avoided/removed are shown below in Figure 43. The relatively low cost of CO_2 avoided/removed for the Advanced Power Cycle of $30 to $40/ton CO_2 is due to the fact that the OTM based power cycle enables a high level of CO_2 capture with relatively low COE all while keeping a high net cycle HHV efficiency.

		OTM FGD Process CASES			OTM WGCU Process CASES			Air-PC Case
Power Cycle Case		1 FGD SC	2 FGD USC	3 FGD AdvUSC	4 WGCU SC	5 WGCU USC	6 WGCU AdvUSC	Praxair/DOE Air-PC no CCS
Plant Cost ($/kW)		$2,894	$2,887	$2,997	$2,872	$2,863	$2,956	$1,908
Net Efficiency (HHV)		36.3	37.2	39.7	36.6	37.4	39.9	39.7
Coal Price ($/MMbtu)								
1.8	Removal Cost ($/ton)	34.04	34.07	37.44	31.67	31.63	34.69	
	Avoided Cost ($/ton)	37.51	36.66	37.64	34.68	33.82	34.70	
3	Removal Cost ($/ton)	35.22	35.06	37.44	32.86	32.52	34.57	
	Avoided Cost ($/ton)	38.80	37.72	37.64	35.98	34.76	34.58	
4	Removal Cost ($/ton)	36.29	35.82	37.44	33.83	33.18	34.45	
	Avoided Cost ($/ton)	39.98	38.54	37.64	37.04	35.47	34.46	

Figure 43: Cost of CO_2 avoided and removed for the 6 OTM cases at various coal prices.

5.4. Optimum 'Extent of Combustion' with OTM

All previous results were evaluated assuming 90% OTM fuel utilization with 'Cost Allocation A' for the membrane area cost. Additional cases have been simulated from Case 2 to investigate the effect of two parameters on the COE value: 1) OTM fuel utilization and 2) OTM "cost allocation".

The OTM fuel utilization specification is an adjustable variable that determines the degree of syngas combustion in the OTM boiler before the remainder of the syngas is combusted in the supplemental combustor using cryogenically supplied oxygen. OTM membrane performance changes with H_2 and CO concentration meaning that at the end of the OTM boiler the OTM surface has lower flux as compared to the beginning of the OTM boiler. Practically this means that more OTM surface is needed to combust one mole of fuel at the end of the OTM boiler than at the beginning of the OTM boiler. Furthermore there is a degree of OTM fuel utilization beyond which it is more economical to combust the remaining syngas using cryogenically supplied oxygen because of the diminishing return of additional OTM surface.

Experimental data is gathered in the laboratory to determine a performance curve for specific oxygen flux vs fuel utilization. The shape of this curve is used to determine the minimal COE for the system. At low fuel utilization a large amount of supplemental oxidant is used (cryo-ASU supplied). In this case parasitic power increases and the cycle efficiency suffers, thus increasing COE. In the limit where fuel utilization is very high, ie >95%, significant membrane area must be added to combust the last 5-10% of fuel. Here the capital cost associated with the last bit of low flux OTM membranes increases and the COE again suffers. Between these two extremes of low cycle efficiency and high membrane area (cost) a minimum COE exists.

A number of variations of Case 2 have been simulated by varying the OTM fuel utilization from the default of 90%. Measured membrane performance from laboratory experiments at various syngas concentrations allows for prediction of a membrane flux profile as the syngas travels through the OTM boiler. This enables the determination of the optimal fuel utilization for the OTM system that gives a minimum in COE.

Figure 44 shows the COE results when varying the degree of fuel utilization between 50% and 85% for two different membrane costs, lower 'Cost Allocation A' and higher 'Cost Allocation B' (referred to as 'Cost Target 1' and 'Cost Target 2', respectively, in Figure 44. In both cases a minimum COE is achieved at or near 80% fuel utilization.

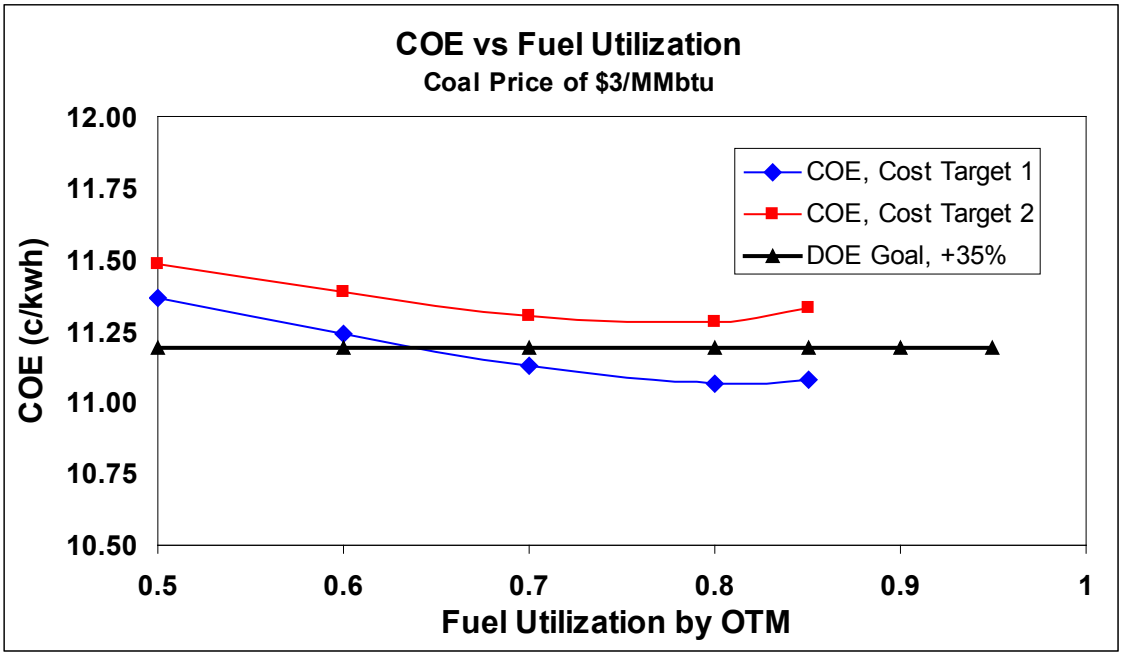

Figure 44: COE vs fuel utilization for two membrane costs.

The COE results shown here for 80% fuel utilization is slightly improved over the results shown in the previous chapter for the OTM Case 2 because 80% fuel utilization is more ideal

than 90% fuel utilization given the OTM membrane cost assumption and the performance profile of the laboratory-measured OTM membranes. Given any advancements in OTM performance (with fixed cost) or improvements in cost (with fixed performance) the optimal percentage of fuel utilization using OTM membranes will be higher than 80%.

6. Conclusions and Recommendations

The Advanced Power Cycle calculated COE satisfies the DOE goal of less than 35% increase in COE for a number of the cases analyzed. The effect of varying the price of coal was evaluated on the COE for all 6 base cases. Higher coal price decreases the % increase in COE due to the high efficiency of the Advanced Power Cycle.

The WGCU sulfur recovery option simulated in cases 4, 5 and 6 has a COE and efficiency advantage over cases where a wet-FGD is used for sulfur removal, simulated in cases 1-3. For a \$0/ton net H_2SO_4 price the COE advantage is essentially due to the plant's reduced limestone usage and eliminated cost for FGD byproduct disposal.

The Advanced Power Cycle has a low cost of CO_2 removed and avoided due to three factors: 1) relatively low COE which in many cases meets the DOE's goal of <35% increase in COE, 2) high net cycle HHV efficiency, and 3) high CPU CO_2 capture efficiency. The net CO2 capture efficiency of the CPU purification process is roughly 97% in all cases including the CO2 losses for purifying the flue gas to >95% CO_2 product because the flue gas CO_2 concentration is relatively high to begin with.

This high CO_2 recovery is achievable because of a few factors unique to the Advanced Power Cycle concept:

1) The OTM membranes effectively supply pure oxygen to the process with no other atmospheric gases as would be typical in an oxy-combustion power cycle where 'low purity' cryo-ASU oxygen is supplied to the boiler at between 95% and 97% purity.

2) The mechanism for oxygen transfer through the OTM membranes controls the rate of combustion in the boiler so flue gas recirculation is NOT necessary. The simulation results presented here assume an air ingress rate of 3%, however without boiler flue gas recirculation the impact of air ingress through the boiler is reduced by about 3 times because as compared to oxy-combustion cases because the flue gas does not have to travel through the boiler 3-4 times.

3) A traditional air preheater is not used in this system. A typical regenerative air preheater is responsible for a large amount of air to flue gas leakage in a traditional power plant due to poor sealing in the heat exchanger. In the Advanced Power Cycle air preheat is achieved without any flue gas contact; this eliminates any possible air leakage to the flue gas side.

The results of Section 5.4 show that further slight improvements in terms of COE can be made by adjusting the degree of fuel utilization in the OTM boiler as was demonstrated by making adjustments to the base Case 2. The optimal degree of fuel utilization depends on membrane flux performance and the OTM "cost allocation". With improvement in membrane performance and cost the optimal degree of fuel utilization will shift upward.

The results of this techno-economic evaluation show that the Advanced Power Cycle meets the DOE goals for COE increase given the current level of OTM membrane performance and the current assumption for OTM cost allocation. The economics of the OTM power cycle will be reevaluated based on this better estimate of OTM cost obtained during Phase II of the OTM project.

To expand on the techno-economic analysis performed to this point it is recommended that the Advanced Power Cycle is simulated with a different type of gasifier. Also going forward a detailed design of the OTM-Pox and OTM boiler units should be performed and a detailed OTM cost model should be developed for comparison against the OTM cost allocation used in this report. A cost sensitivity analysis is also recommended to determine impact of non-OTM equipment costs on the OTM cost target needed to achieve the DOE's COE goals. OTM membranes have potential applicability in other processes; the use of OTM membranes should be evaluated in a natural gas combined cycle (NGCC) process.

Appendix B

Shaw Energy & Chemical Reports

Appendix 16 rev 2.0

Mechanical Engineering Science Report

A16.0 Executive Summary

Three models were created to study the proposed prototype OTM furnace.

1. A Full Module 3D CFD model was created to determine the flow distribution quality to the OTM tubes in the proposed design. This model was a full 3D module of 10 OTM columns, designated as a macro- model. It includes the steam tubes and the manifolds in detail and the OTM columns are treated as porous zones for simplicity. The results of this model revealed a fairly good overall distribution based on peak to average velocity (1.7-1.8 times average velocity), but a relatively high mean steady state deviation in flow velocity (40-45% of average velocity). This means that the flow quality is likely to be improved by flow smoothing devices to reduce overall variations in velocity. Modifications to the design are recommended by adding flow straightening devices such as turning vanes, perforated plate or screens. These should flatten the velocity profile to obtain better overall performance of combustion and heat transfer. In addition, it may be an enhancement to add static mixers to the inlet of the OTM to control mixing and combustion of fuel species.

2. Two 3D CFD detailed sub-models were created for combustion CFD modeling and to determine the radiation view factors of the geometric design.

The first 3D CFD sub-model consisted of one OTM column in detail and adjacent half steam tubes. This model found a view factor of 0.33. No walls were included in this model.

Another CFD sub-model was created to determine the contribution to radiation view factor of the adjacent OTM columns and steam tubes. This 3D model consisted of 3 OTM columns. The results of this model revealed a view factor of 0.43 between the 3 OTM columns and two columns of steam tubes on each side of the center.

Using the results of the two sub-models, a radiation shape factor for the entire furnace can be estimated. This estimate is a module view factor of 0.45 for 10 columns of 65 OTMs. These estimates do not include the refractory wall effects.

3. Module Analytical Radiation Heat Transfer Model – Several Mathcad worksheets have been created using traditional radiation heat transfer network based methods. These were created as prerequisites to a 3D combustion CFD model anticipated for future work.

A. Gray gas model of the contribution of CO, CO2, and water vapor. This Mathcad worksheet uses the gray gas model of Beer, Foster, and Siddell to include the effects of CO on the gray gas emissivity. Most gray gas models do

not include the effects of CO gas. Based on average composition, the emissivity of the gray gas in the OTM furnace will be highly significant. This model can be used within a CFD combustion model, cell by cell.

The overall gray gas emissivity of the OTM module is estimated at about 0.3 for use in the network radiation model.

B. Radiation View Factor Analysis – This Mathcad worksheet allows quick study of geometry changes to the OTMs and steam tubes size and arrangement to optimize a module design. This model predicts that the current prototype design will have a view factor of about 0.4 from OTMs to steam tubes. Modifications to tube geometries and arrangements can be made to compare potential changes in view factor.

C. Radiation Heat Transfer Network Analysis of the OTM module. This Mathcad worksheet was created as a preliminary step to a verification and validation of a full CFD combustion model. It can be used to estimate and optimize the potential radiation heat transfer in the OTM module design. It uses a radiation network model of the OTMs, gray gas, and steam tubes. Variations in temperature of the gray gases, composition, and OTM coils has been explored with this model and compared to the bulk average method. The average result of heat transfer is only 3% lower than the variable temperature and components model.

Recommendations for Further CFD and Analytical Study

1. Determine the optimum prototype design for the OTM-steam tube size and arrangement using the Mathcad worksheets. Consider mean beam lengths from the gray gas model as well as manufacturing and other practical constraints.

2. With optimized modifications to tube size and arrangement from part one above, revise the Radiation Network Mathcad worksheet to include refractory walls in the network and determine the potential radiation heat transfer available from the optimized prototype design.

3. Create a simplified 3D transient CFD combustion model of the modified prototype design to uncover unknown flow and combustion factors, problems and constraints to the operation of the prototype. This model will include effects of fuel species flow, mixing, and combustion in an entire module column.

4. Investigate addition of straightening, static mixing and other devices to optimize the performance of the 3D CFD combustion model in 3 above.

A16.1 CFD Model for Flow Distribution Quality

Summary

Praxair Inc. has subcontracted The Shaw Group Inc. to provide a feasible design for a boiler and a partial oxidation unit based on the OTM (Oxygen Transport Membrane) technology. The objective of this study is to determine whether the proposed OTM tubes and steam pipes layout would provide an adequate fuel distribution quality to the core of the boiler module.

The OTM Boiler System consists of eight identical OTM modules that are fed rich fuel gas through two intake manifolds. For this study it was assumed that each module is fed an equal amount of fuel, i.e. one-eighth of the total mass flow rate. Each OTM module has geometrical symmetry with respect to a vertical plane contained in the centerline of the outlet steam pipe.

The CFD setup was simplified in order to reduce the model complexity. The set of assumptions and simplifications envelop both the geometry and the physical and chemical phenomena. Only the rich fuel stream flow was modeled for the present study. Some assumptions made for this model could introduce significant deviations from the real phenomena.

The ten rows of OTM tubes are not modeled in detail but as porous media with constant flow resistance. These porous regions are also used to “create” mass and heat inside the domain. Both volumetric mass and the heat sources are assumed to have constant values.

One flow case was modeled for an OTM boiler module. The process conditions are summarized in Table 1. The flow distribution quality was assessed at the entrance and at the exit of the OTM core section (the region where all the OTM tubes are located) and is summarized in Table 2. The Shaw’s maximum acceptable value for the flow distribution criteria for distillation trays are shown in Table 3. Using this criteria, the flow distribution quality found in this model is acceptable for the PAV criterion but it is outside the recommended limits for the standard deviation values.

Table 1. Rich fuel process conditions and inlet properties

	Units	Design Case
Mass flow rate	lbm/hr	1,015.375

Pressure	psia	20
Temperature	°F	400
Molecular weight	lbm/mol	20.32

Table 2. Flow distribution quality at the inlet and outlet of the OTM boiler core

	PAV	Std Dev (%)	Swirl number
Core inlet	**1.73**	**44.6**	**1.10**
Core exit	**1.83**	**41.7**	**1.01**

Table 3. Flow distribution quality indices (maximum acceptable values for distillation trays)

PAV	**2.0**
Standard deviation (non-dimensional)	**20%**
Swirl number	**1.50**

Definitions

PAV Ratio of maximum value of vertical velocity to area-weighted average vertical velocity

Standard deviation Ratio of standard deviation value of vertical velocity component to area-weighted average value of vertical velocity

Swirl number Area-weighted average ratio of local velocity magnitude to local vertical velocity component

1. Introduction

The current design for the Praxair's OTM Boiler System was modeled and analyzed for potential issues with regard to flow distribution quality. The focus of the study is on the core region of the OTM boiler module where all the oxygen transport, chemical reactions and most of the heat transfer takes place. However, due to the very complex nature of the phenomena and the complicated geometry there were a number of simplifications made, listed in a subsequent paragraph. This study shall provide a valuable starting point for the future, more detailed study of the rich fuel flow around OTM and steam tubes.

The air flowing inside the OTM tubes (left to right blue arrow in Figure 1) was not part of this study. The layout of the OTM boiler module and some dimensions are presented in Figure 1. The portion of the OTM boiler module included in the CFD model is also identified in this figure.

2. Conclusions

The PAV values for vertical velocity at the OTM core inlet and outlet are lower than the acceptable limits. At the same time the fuel gas distribution quality is lower than the recommended limits for a good distribution. However it is not clear at this point whether the current flow distribution quality criteria are applicable for this particular application.

The dynamic pressure of the fuel gas flow is extremely low and as a result the pressure loss inside the OTM module is virtually negligible (Fig. 4). At the outlet of the inlet duct, the flow cannot turn sharply upward and instead crosses the entire module. As a result the Figure 7 shows that more fuel gas flows on the opposite side of the inlet duct. This pattern persists all the way to the OTM core inlet elevation. The current assumptions and simplifications do not allow for a more in-depth analysis of the flue gas flow distribution.

3. Recommendations

a. Turning vanes could be used at the junction with the body of the OTM module for better vertical flow distribution at the OTM core inlet. It is very possible that the inlet flue gas manifold should have turning vanes in order to avoid flow mal-distribution in the fuel gas inlet duct.

b. Perforated plates or screens could help to improve the flatness of the flow distribution into the core of the OTM module.

c. Static mixers at the flue gas entrance to the OTM core could control mixing rate and enhance combustion and heat transfer.

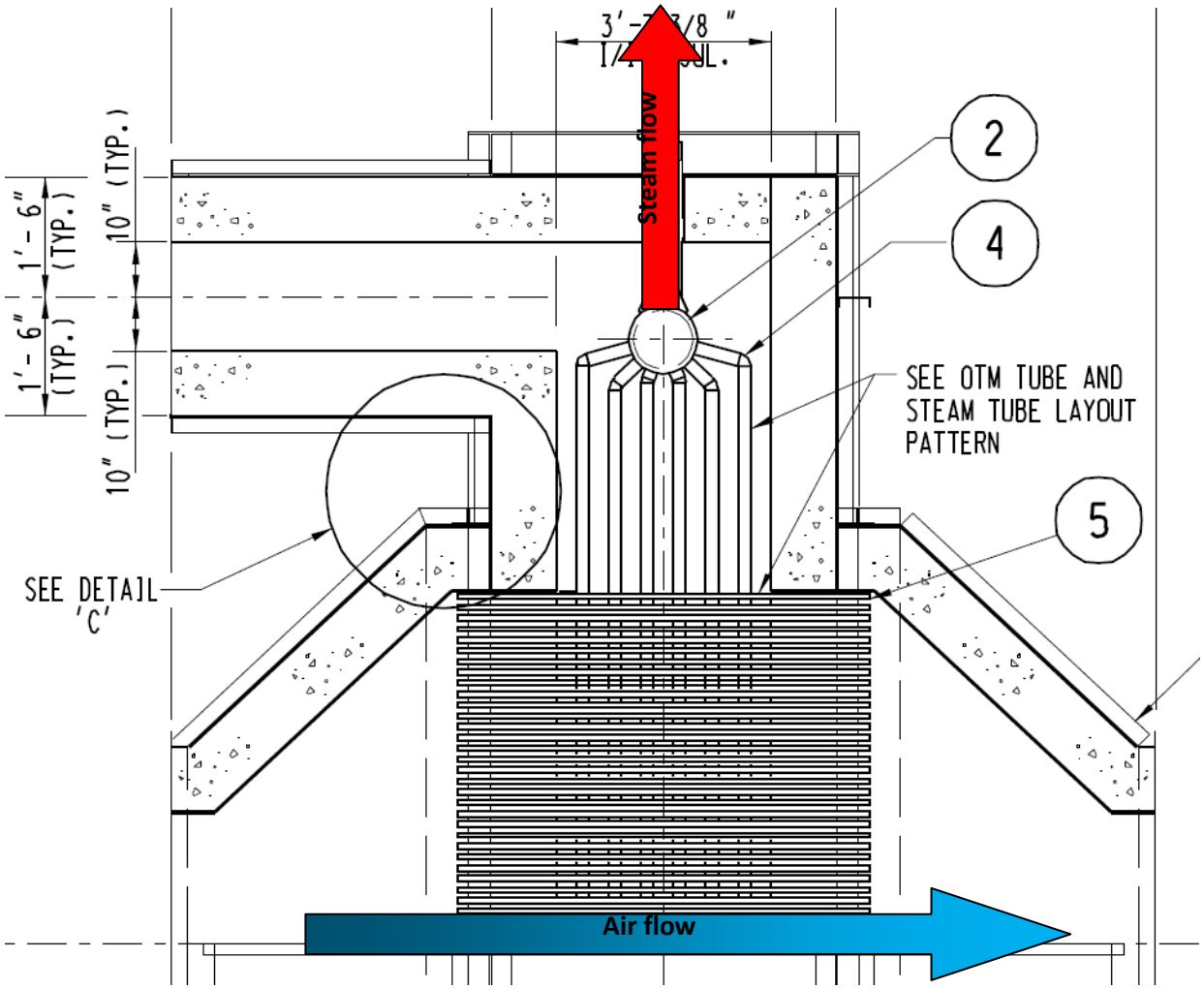

Figure 1. Praxair DOE OTM Boiler System layout (detail)

4. CFD Analysis

Model setup

This study is based upon numerical solution of the full Navier – Stokes equations with the Realizable K-ε model of turbulence, as available in ANSYS Fluent, Version 13. The computational domain was discretized using hybrid grid. The OTM boiler module exhibits geometrical and flow half-symmetry about a vertical plane which contains the inlet and outlet steam pipes centerlines. In order to reduce the grid size and the CPU run-time only half of the domain was modeled. Figure 2 shows the resolution of the mesh used to discretize the computational domain. Figure 3 displays three-dimensional views of the solid model where one can distinguish the steam tubes and headers and the five OTM volumes.

The following assumptions are used in the study and are based upon physics of the fluid flow and heat transfer in OTM module:

a) The flow is steady.
b) The flow has half-symmetry.
c) The velocity profile at the fuel gas inlet is uniform and normal to the boundary.
d) The OTM rows of tubes were modeled as porous media with constant resistance flow coefficients.
e) The heat of reaction is introduced inside the domain through uniform volumetric heat sources inside the porous media volumes.
f) The flux of oxygen transferred through the OTM tubes is modeled as a separate species and is introduced as uniform volumetric mass sources inside the porous media volumes.
g) The steam tubes are adiabatic. The added heat is only transferred to the gaseous species.
h) The chemical reactions that occur at the surface of the OTM are not modeled. As a result the flue gas composition and properties do not correspond to the design case.

The mass source value corresponds to the amount of oxygen combusted at the surface of the OTM tubes (521 lbm/hr/module) and it is equal to 0.07947 kg/m^3-s. The strength of the volumetric heat source was adjusted until the temperature at the outlet duct exit matched the process temperature value (1138°F).

Results

Below and above the core of the OTM module the flow streamlines are mostly vertical. Inside the core there are both heat and mass transfer and the streamlines are losing their vertical, ordered pattern. The OTM volumes offer a high resistance to vertical direction and very low resistance to both transversal and longitudinal directions. As a result all the mass flow generated inside these volumes will leave the volumes horizontally.

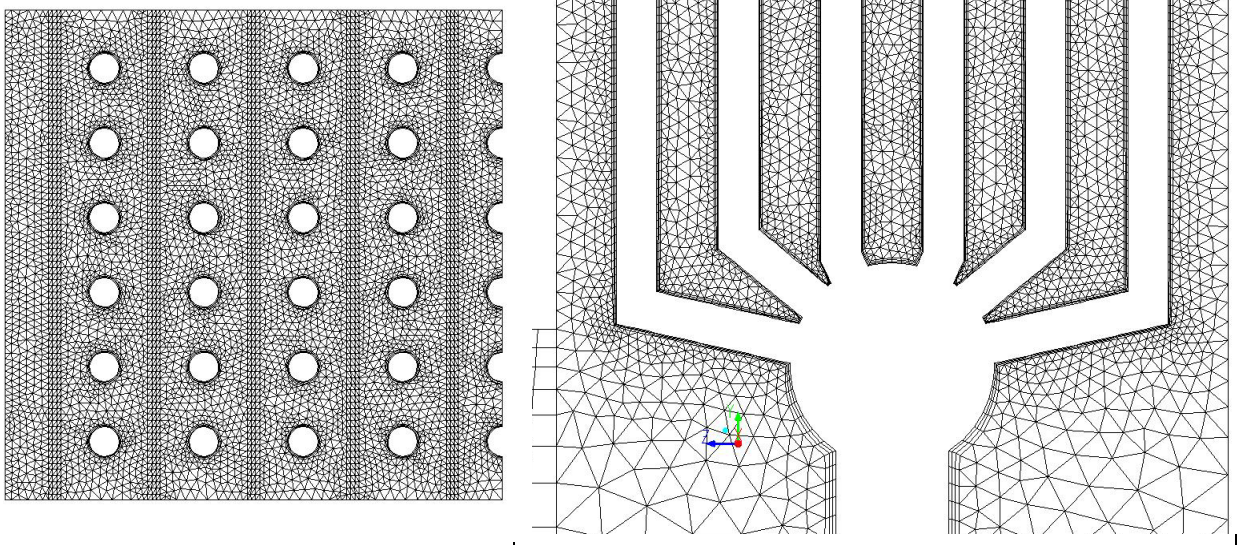

Fig.2 Mesh detail: horizontal cross-section (left) and vertical cross-section (right)

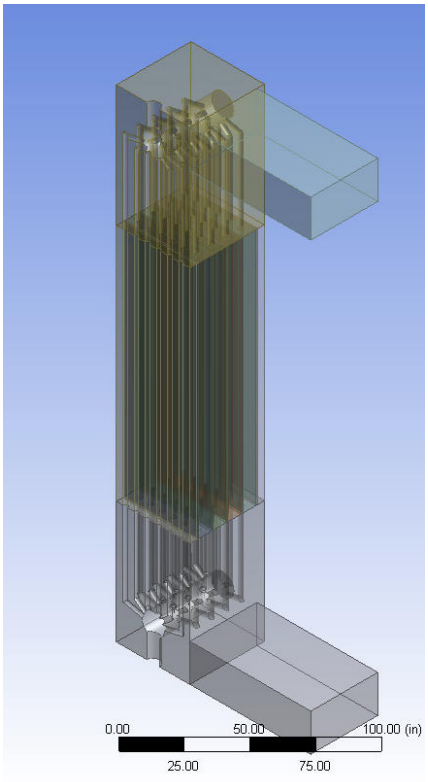

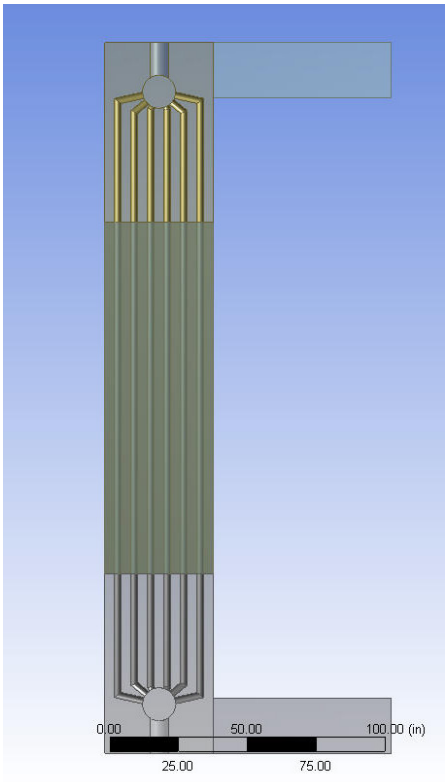

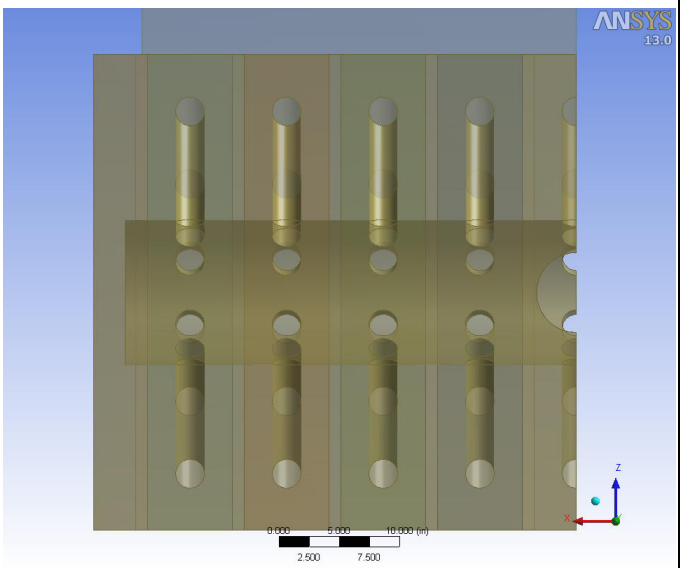

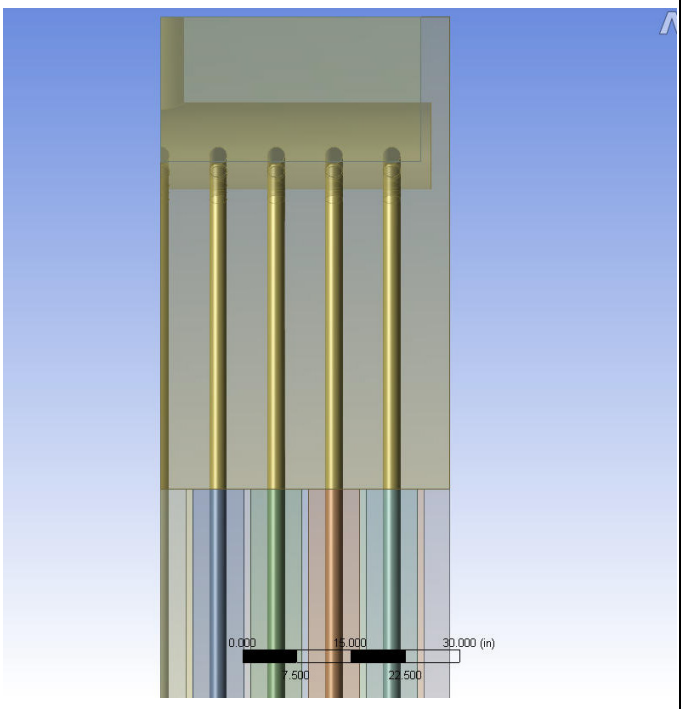

Fig. 3 Praxair DOE OTM solid model

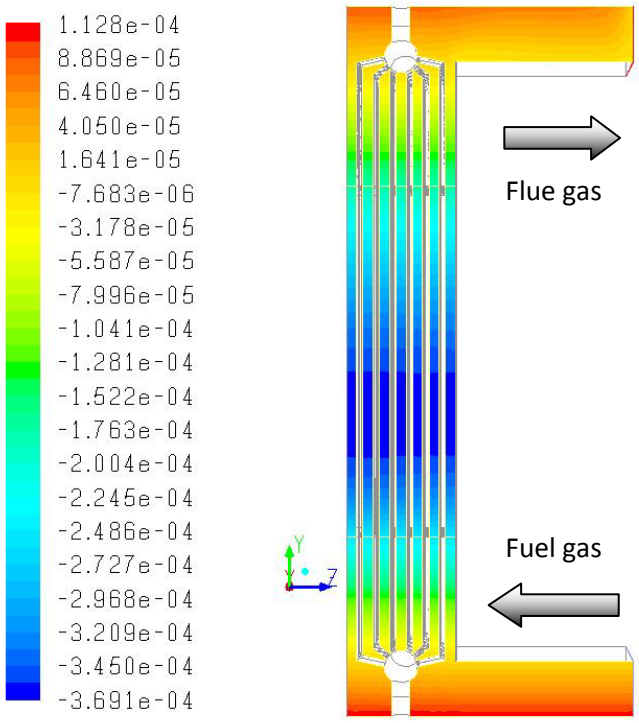

Fig. 4 Contours of static pressure (psi)

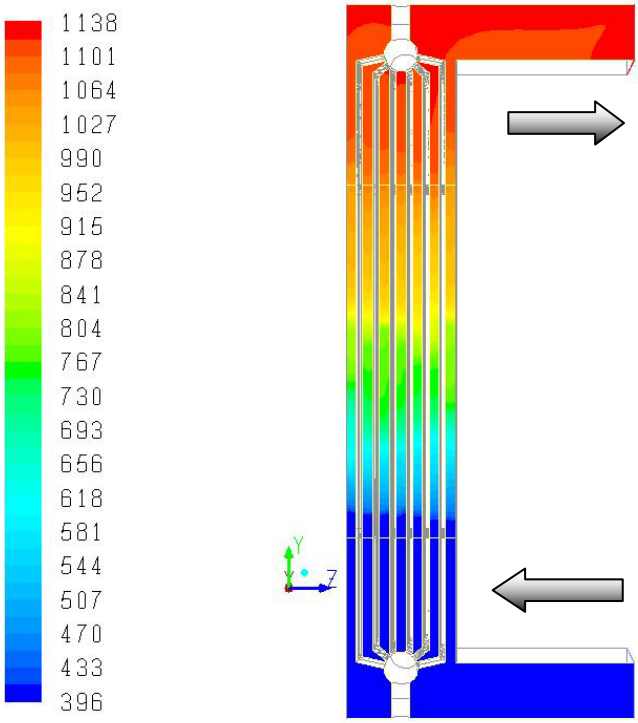

Fig.5 Contours of temperature (°F)

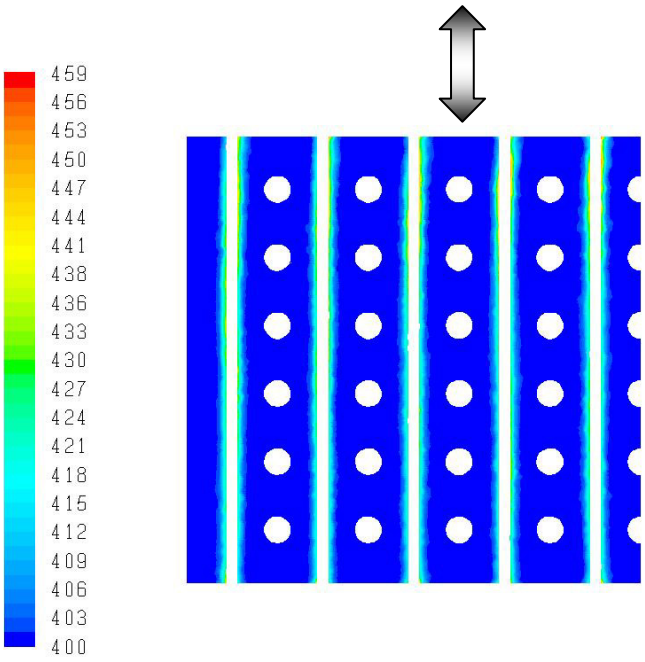

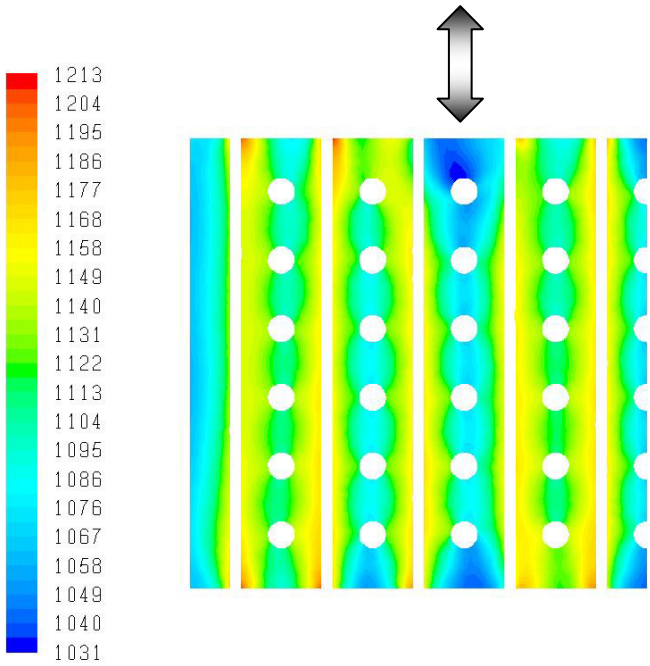

Fig. 6 Contours of temperature(°F): Core inlet (left) and core exit (right)

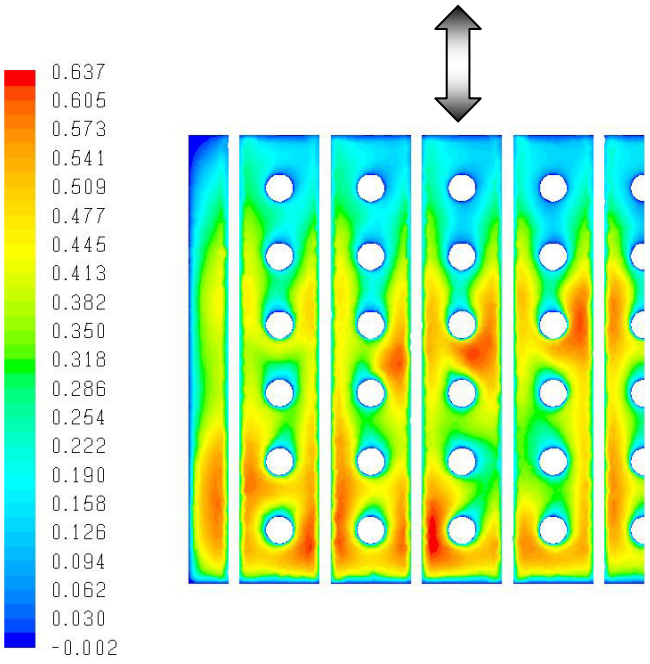

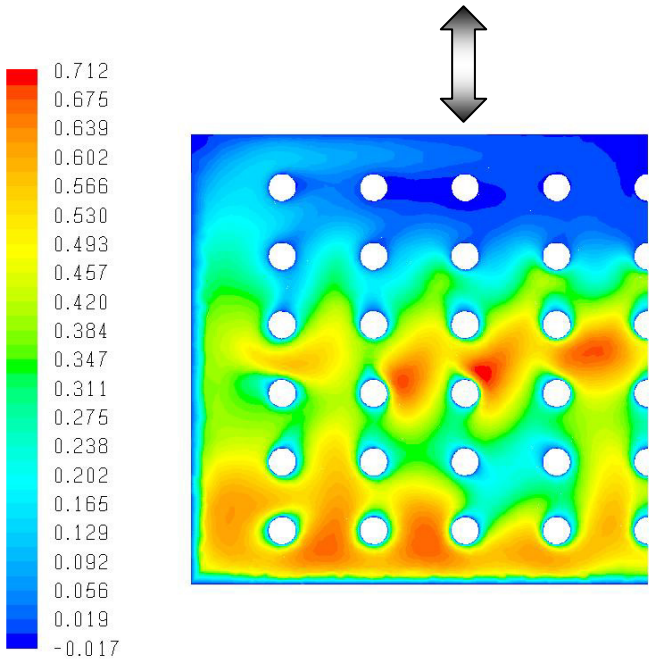

Fig. 7 Contours of vertical velocity (ft/s): Core inlet (left) and 1.5 ft below core inlet (right)

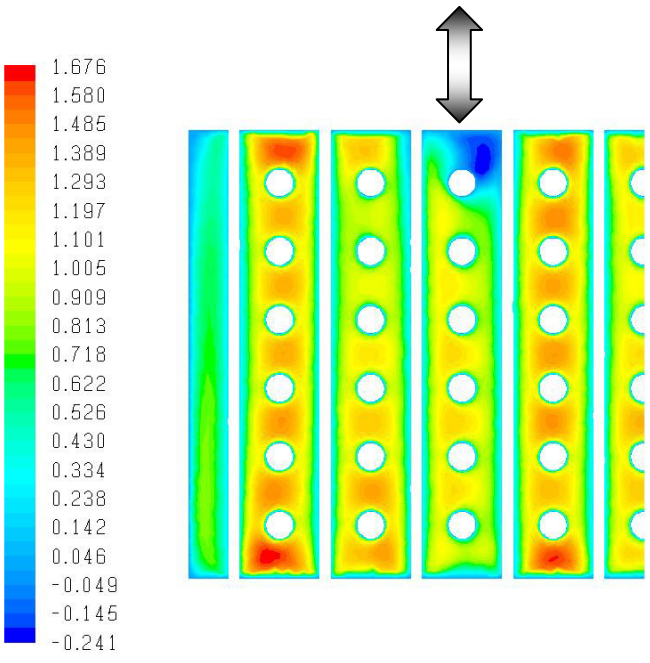

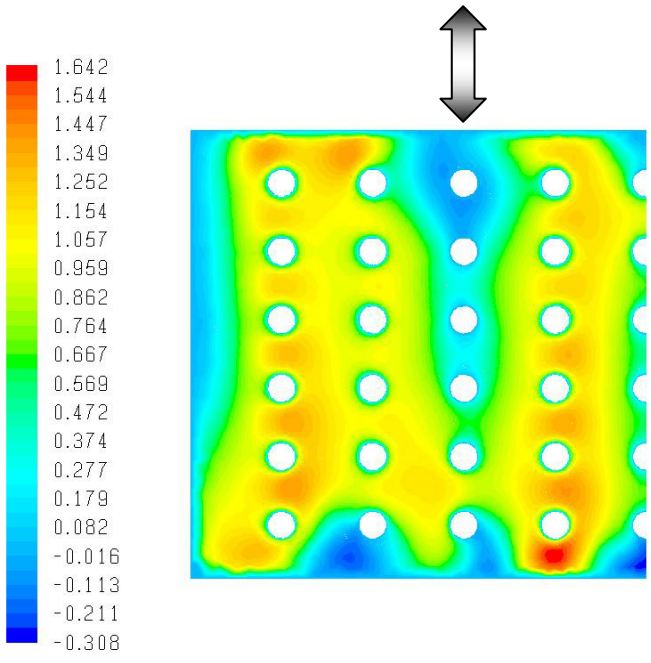

Fig. 8 Contours of vertical velocity (ft/s): Core exit (left) and 1.5 ft above core exit (right)

5. References and bibliography

Praxair OTM Boiler System Drawings
Process conditions, Flow diagrams, and Species temperature-dependent properties, Private communications from George Dabney
Handbook of hydraulic resistance, Idelchik, I. E.

A16.2 Gray Gas Emissivity Model

The radiation must be transmitted through the fuel gas and combustion products to reach the steam tubes. These gases have absorption, and diffusion coefficients that are used to determine how much heat energy is absorbed, transmitted and reflected. Carbon monoxide is present in relatively high concentrations. The Beer, et al. model includes CO.

The radiation must be transmitted through the fuel gas and combustion products to reach the steam tubes. These gases have absorption, and diffusion coefficients that are used to determine how much heat energy is absorbed, transmitted and reflected.

$Y_f := 0.5$ frac of furnace ht.

$$P_{tot} := -0.1077 \cdot Y_f^2 + 0.4323 \cdot Y_f + 0.9185 = 1.108$$

$T_{avgg} := 692$ K $\qquad T_{avg} := T_{avgg} \cdot \frac{9}{5} = 1.246 \times 10^3$

$a_1 := 0.4092 + 7.53 \cdot 10^{-5} \cdot T_{avgg} = 0.461 \qquad a_2 := 0.284 + 2.58 \cdot 10^{-5} \cdot T_{avgg} = 0.302$

$a_3 := 0.211 - 6.54 \cdot 10^{-5} \cdot T_{avgg} = 0.166 \qquad a_4 := 0.0958 - 3.57 \cdot 10^{-5} \cdot T_{avgg} = 0.071$

$k_1 := 0 \qquad k_2 := 0.91 \qquad k_3 := 9.4 \qquad k_4 := 130$

$L := 0.225$ m mean radiation beam length $\qquad L \cdot 39.38 = 8.861$ in

$PL := P_{tot} \cdot L = 0.249$

$$\varepsilon_g := a_1 \cdot \left[1 - e^{-(k_1 \cdot PL)}\right] + a_2 \cdot \left[1 - e^{-(k_2 \cdot PL)}\right] + a_3 \cdot \left[1 - e^{-(k_3 \cdot PL)}\right] + a_4 \cdot \left[1 - e^{-(k_4 \cdot PL)}\right] = 0.282$$

$\varepsilon_m := \varepsilon_g = 0.28217$ average emmisivity of the gray gaseous media

A16.3 CFD Discrete Ordinates Radiation View Factor

Two separate CFD models were created in order to determine the radiation view factor of the proposed OTM and steam tubes arrangement of the OTM Boiler. Both calculations were performed using the Discrete Ordinates Model available in ANSYS Fluent 13.0 and used the same geometry but with different boundary conditions.

The reported results represent the radiation view factors between the OTM tubes and steam tubes only. All other walls and/or model boundaries are “deactivated” for radiation heat transfer. All the walls (OTM tubes, steam tubes, refractory, inlet, and outlet) have an emissivity ε value of 1.0 which means they absorb all the incident radiation (black body behavior).

Methodology

The basic equation describing the radiation heat transfer (W) between two bodies is

$$Q = \varepsilon\sigma A F_{12}(T_1^4 - T_2^4)$$

where $\sigma = 5.669 \times 10^{-8}$ W/m^2-K^4 is the Stefan-Boltzmann constant.

The surfaces of interest (OTM tubes and the steam tubes) have imposed temperatures. The temperature of OTM tubes is $T_1 = 1300$ K and the temperature of the steam tubes is $T_2 = 0$ K. The gas present in the model does not participate to the radiation heat transfer. The heat flux q (W/m^2) value obtained from the simulation enables us to get an estimate for the view factor F_{12}. All other surfaces temperatures are set to a very low value (T = 1 K). These settings insure that only direct incident radiation is transmitted from the emitting hot surface (OTM tubes) to the cold receptor surface (steam tubes) and there is no reflected radiation from any surrounding walls.

$$F_{12} = \frac{q}{\sigma T_1^4}$$

Model with side surfaces set as walls with ε = 1

This model eliminates the radiation coming through the side surfaces from the adjacent rows of OTM tubes and therefore is expected to provide a lower value for the view factor. This setup provides a lower heat flux value radiated to the target surface (steam tubes) of 0.330 for F_{12} factor.

Model with side surfaces set as "symmetry" boundary conditions, sidewalls with ε = 1

This model is more representative for a vertical slice located in the middle of the OTM Boiler module since the "symmetry" BCs enables the radiation from adjacent (but not physically modeled) two rows of OTMs to penetrate into the model. Based on the heat flux radiated to the target surface (steam tubes) we obtained $F_{12} = 0.433$.

Validation

The CFD setup employed for view factor estimation was first calibrated on a simple geometry for which the view factor value can be found in the literature. The purpose of this sub-model was to determine the mesh resolution and the spatial discretization for the DO model along with the other settings which will generate a numerical value for the view factor value close to the analytical value.

For the discs modeled r = 0.5 and therefore the analytical value for $F_{12} = 0.172$. Our sub-model predicted a value of 0.170 which represents 1.2% relative error.

Case	View factor	Plot

View factor of the OTMs to steam tubes has been estimated using a geometrical analysis. The plan and elevation view factors provide a product which can estimate the view factor for optimization of the furnace design and verification of the CFD factor.

Between two identical coaxial discs of radius *R* and separation *H*, with *r=R/H*. 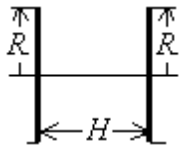	$F_{12} = 1 + \frac{1-\sqrt{4r^2+1}}{2r^2}$ (e.g. for *r*=1, F_{12}=0.382)	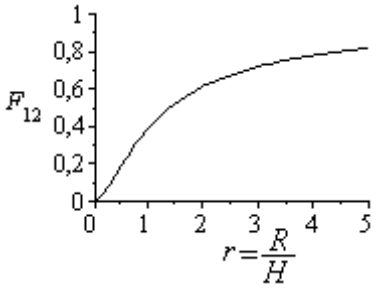

A16.4 Calculated Radiation View Factor

Elevation View Factor - F_{el}

Figure 1: Radiation view factor geometry for elevation view, OTMs to steam tubes

From the figure above it can be seen that the typical view of the steam tube by the OTM tube is a simple 2 x θ_c in the elevation direction.

$R_o := 0.5in$ $P_o := 2in$ radius and pitch of the otms

$\theta_c := \operatorname{acos}\left(\frac{R_o}{P_o}\right) = 75.522 \cdot deg$ half angle of direct radiation view

$F_{eld} := \frac{2 \cdot \theta_c}{\pi} = 0.839$ elevation direct view factor of all otms

$F_{elr} := \left(1 - F_{eld}\right) \cdot 0.9 = 0.145$ elevation view factor of OTM radiation reflected off of adjacent OTM

$F_{el} := F_{eld} + F_{elr} = 0.984$ elevation shape factor

From a pure elevation perspective, almost all of the radiation from the OTMs can be seen by the steam tubes.

Plan View Factor - F_p

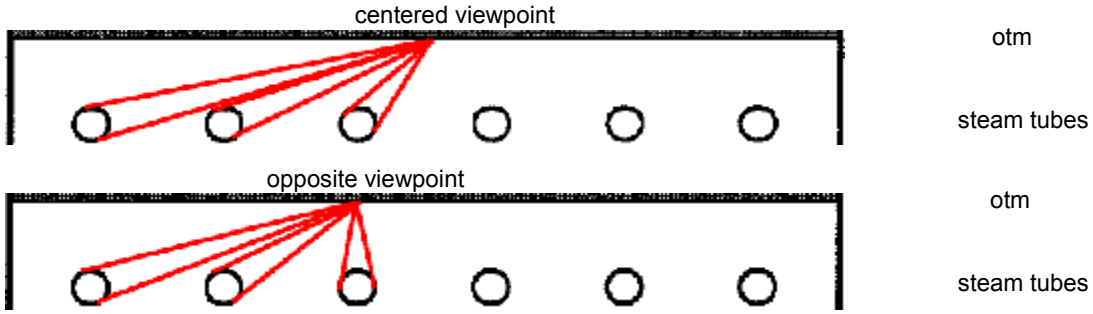

Figure 2: Radiation view factor geometry for plan view - OTMs to steam tubes- examples of types of viewpoints - centered and opposite.

From the figure above, it can be seen that the center and opposite viewpoints of the steam tubes from the surfaces of the OTM can be represented by the angle sweeps shown in the dashed lines.

$D_{st} := 2\,in \qquad P_{st} := 6\,in \qquad S := 4\,in$

Diameter, pitch and spacing of steam tube

$R_{st} := \frac{D_{st}}{2} \qquad R_o = 0.5 \cdot in$

Steam tube radius and distance from OTM surface to steam tube center

$C_c := (S - R_o) \qquad C := S - R_o - R_{st} = 2.5 \cdot in$

Clearance from OTM to steam tube

$$\theta_{p1} := 2\,\mathrm{atan}\left[\frac{R_{st}}{\sqrt{\left(\frac{1}{2}\cdot P_{st}\right)^2 + C_c^{\,2}}}\right] = 24.479 \cdot deg$$

Centered between tubes viewpoint angle of adjacent tubes

[minimum angle with blockage, angle with no blockage]

$$\theta_{p2} := \min\left[\mathrm{atan}\left(\frac{C}{0.5\cdot P_{st}}\right) - \mathrm{atan}\left(\frac{C}{1.5\cdot P_{st}}\right), 2\,\mathrm{atan}\left[\frac{R_{st}}{\sqrt{\left(1.5\cdot P_{st}\right)^2 + C_c^{\,2}}}\right]\right] = 11.825 \cdot deg$$

$$\theta_{p3} := \min\left[\mathrm{atan}\left(\frac{C}{1.5\cdot P_{st}}\right) - \mathrm{atan}\left(\frac{C}{2.5\cdot P_{st}}\right), 2\,\mathrm{atan}\left[\frac{R_{st}}{\sqrt{\left(2.5\cdot P_{st}\right)^2 + C_c^{\,2}}}\right]\right] = 6.062 \cdot deg$$

[minimum angle with blockage, angle with no blockage]

$$\theta_{p4} := \min\left[\mathrm{atan}\left(\frac{C}{2.5\cdot P_{st}}\right) - \mathrm{atan}\left(\frac{C}{3.5\cdot P_{st}}\right), 2\,\mathrm{atan}\left[\frac{R_{st}}{\sqrt{\left(3.5\cdot P_{st}\right)^2 + C_c^{\,2}}}\right]\right] = 2.673 \cdot deg$$

$$\theta_{p5} := \min\left[\operatorname{atan}\left(\frac{C}{3.5\cdot P_{st}}\right) - \operatorname{atan}\left(\frac{C}{4.5\cdot P_{st}}\right), 2\operatorname{atan}\left[\frac{R_{st}}{\sqrt{\left(4.5\cdot P_{st}\right)^2 + C_c{}^2}}\right]\right] = 1.499\cdot\text{deg}$$

$$\theta_{p6} := \min\left[\operatorname{atan}\left(\frac{C}{4.5\cdot P_{st}}\right) - \operatorname{atan}\left(\frac{C}{5.5\cdot P_{st}}\right), 2\operatorname{atan}\left[\frac{R_{st}}{\sqrt{\left(5.5\cdot P_{st}\right)^2 + C_c{}^2}}\right]\right] = 0.958\cdot\text{deg}$$

Viewpoint angles from position opposite a steam tube

$$\theta_{p1o} := \operatorname{atan}\left(\frac{D_{st}}{C_c}\right) = 29.745\cdot\text{deg}$$

$$\theta_{p2o} := \min\left[\operatorname{atan}\left(\frac{C}{R_{st}}\right) - \operatorname{atan}\left(\frac{C}{P_{st}}\right), 2\operatorname{atan}\left[\frac{R_{st}}{\sqrt{\left(1\cdot P_{st}\right)^2 + C_c{}^2}}\right]\right] = 16.384\cdot\text{deg}$$

$$\theta_{p3o} := \min\left[\operatorname{atan}\left(\frac{C}{P_{st}}\right) - \operatorname{atan}\left(\frac{C}{2P_{st}}\right), 2\operatorname{atan}\left[\frac{R_{st}}{\sqrt{\left(2\cdot P_{st}\right)^2 + C_c{}^2}}\right]\right] = 9.148\cdot\text{deg}$$

$$\theta_{p4o} := \min\left[\operatorname{atan}\left(\frac{C}{2\cdot P_{st}}\right) - \operatorname{atan}\left(\frac{C}{3\cdot P_{st}}\right), 2\operatorname{atan}\left[\frac{R_{st}}{\sqrt{\left(3\cdot P_{st}\right)^2 + C_c{}^2}}\right]\right] = 3.861\cdot\text{deg}$$

$$\theta_{p5o} := \min\left[\operatorname{atan}\left(\frac{C}{3\cdot P_{st}}\right) - \operatorname{atan}\left(\frac{C}{4\cdot P_{st}}\right), 2\operatorname{atan}\left[\frac{R_{st}}{\sqrt{\left(4\cdot P_{st}\right)^2 + C_c{}^2}}\right]\right] = 1.96\cdot\text{deg}$$

$$\theta_{p6o} := \min\left[\operatorname{atan}\left(\frac{C}{4\cdot P_{st}}\right) - \operatorname{atan}\left(\frac{C}{5\cdot P_{st}}\right), 2\operatorname{atan}\left[\frac{R_{st}}{\sqrt{\left(5\cdot P_{st}\right)^2 + C_c{}^2}}\right]\right] = 1.183\cdot\text{deg}$$

Viewpoint Shape Factors

$$F_{pdc} := 2\frac{\theta_{p1} + \theta_{p2} + \theta_{p3}}{180\text{deg}} = 0.471$$

Dead center viewpoint, 1 position

$$F_{po1} := \frac{\theta_{p1o} + 2\cdot\theta_{p2o} + 2\cdot\theta_{p3o} + \theta_{p4o}}{180deg} = 0.47$$

Opposite steam tube, next to center viewpoint, 2 positions

$$F_{pc23} := \frac{2\theta_{p1} + 2\theta_{p2} + \theta_{p3} + \theta_{p4}}{180deg} = 0.452$$

Centered between 2nd and 3rd tube viewpoint, 2 positions

$$F_{po2} := \frac{\theta_{p1o} + 2\cdot\theta_{p2o} + 1\cdot\theta_{p3o} + \theta_{p4o} + \theta_{p5o}}{180deg} = 0.43$$

Opposite the 2nd tube viewpoint, 2 positions

$$F_{pc12} := \frac{2\theta_{p1} + \theta_{p2} + \theta_{p3} + \theta_{p4} + \theta_{p5}}{180deg} = 0.395$$

Centered between 1st and 2nd tube viewpoint, 2 positions

$$F_{po3} := \frac{\theta_{p1o} + \theta_{p2o} + \theta_{p3o} + \theta_{p4o} + \theta_{p5o} + \theta_{p6o}}{180deg} = 0.346$$

Opposite the 1st tube viewpoint, 2 positions

$$F_{pe} := \frac{\theta_{p1} + \theta_{p2} + \theta_{p3} + \theta_{p4} + \theta_{p5} + \theta_{p6}}{180deg} = 0.264$$

End viewpoint, 2 positions

Total Average Plan View Factor

$$F_p := \frac{\left(F_{pdc} + 2F_{po1} + 2F_{pc23} + 2\cdot F_{po2} + 2\cdot F_{pc12} + 2F_{po3} + 2F_{pe}\right)}{13} = 0.399$$

Global Average View Factor

$$F_{os} := F_p\cdot F_{el} = 0.392$$

A16.5 Calculated Mean Beam Length

The mean beam length is necessary for determining the gas radiation emissivity. This length represents the average path of radiation from the gray gas. This has been determined by calculating from geometry.

Elevation beam length can be determined by the average beam length of the elevation view. This will equal the resultant of quarter angle of the elevation view.

Plan beam length is determined by the average beam length in the plan view. The vector sum of elevation and plan view, divided by two, is the calculated mean beam length.

Also included is a sample calculation using Hottel and Sarofim's method as well as the method of Wimpress. These give lower numbers perhaps because they are more simplified methods based on flat surfaces.

Mean Beam Length Calculation by Geometry

$C_L := C + 0.707R_{st} + 0.707 \cdot R_o = 3.56 \cdot in$ Average clearance between gray gas and tubes

$R_{Lavg} := \frac{C_L}{\cos\left(\frac{\theta_c}{2}\right)} = 4.504 \cdot in$ Elevation mean beam length

$L_{elavg} := R_{Lavg}$

Plan Beam length can be determined by averaging the beam length from all the OTM surfaces to all steam tube surfaces.

$L_{p1} := \sqrt{\left(\frac{1}{2} \cdot P_{st}\right)^2 + \left(C_L\right)^2} = 4.656 \cdot in$ Center beam length

$L_{p2} := \sqrt{\left(1.5 \cdot P_{st}\right)^2 + \left(C_L\right)^2} = 9.679 \cdot in$

$L_{p3} := \sqrt{\left(2.5 \cdot P_{st}\right)^2 + C_L^2} = 15.417 \cdot in$

$L_{p4} := \sqrt{\left(3.5 \cdot P_{st}\right)^2 + C_L^2} = 21.3 \cdot in$

$L_{p5} := \sqrt{\left(4.5 \cdot P_{st}\right)^2 + C_L^2} = 27.234 \cdot in$

$L_{p6} := \sqrt{\left(5.5 \cdot P_{st}\right)^2 + C_L^2} = 33.192 \cdot in$

$L_{p1o} := C_c$

$L_{p2o} := \sqrt{(1 \cdot P_{st})^2 + C_L^2} = 6.977\,in$

$L_{p3o} := \sqrt{(2 \cdot P_{st})^2 + C_L^2} = 12.517\,in$

$L_{p4o} := \sqrt{(3 \cdot P_{st})^2 + C_L^2} = 18.349\,in$

$L_{p5o} := \sqrt{(4 \cdot P_{st})^2 + C_L^2} = 24.263\,in$

$L_{p6o} := \sqrt{(5 \cdot P_{st})^2 + C_L^2} = 30.211\,in$

$$L_{plcavg} := \frac{2L_{p1} + 2 \cdot L_{p2} + 2 \cdot L_{p3} + 2L_{p4} + 2 \cdot L_{p5} + 2 \cdot L_{p6}}{12} = 18.579\,in$$

$$L_{ploavg} := \frac{2 \cdot L_{p1o} + 2 \cdot L_{p2o} + 2 \cdot L_{p3o} + 2 \cdot L_{p4o} + 2 \cdot L_{p5o} + 2 \cdot L_{p6o}}{12} = 15.969\,in$$

$$L_{plavg} := \frac{L_{plcavg} + L_{ploavg}}{2} = 17.274\,in$$

$$L_{geom} := \frac{\sqrt{L_{plavg}^2 + L_{elavg}^2}}{2} = 8.926\,in$$

Module mean beam length

Hottel and Sarofim Mean Beam Length

$H := 130in \quad W := 39.375in \quad D := 4in$ Height, width, depth of column of gg

$V := H \cdot W \cdot D$

$A_{tot} := (H \cdot W) \cdot 2 = 1.024 \times 10^{4}\,in^{2}$ Total radiation surface area

$C_{gg} := 0.9$ Hottel and Sarofim 0.9 c-factor

$L_{HS} := \frac{4 \cdot C_{gg} \cdot V}{A_{tot}} = 7.2\,in$ Viskanta and Menguc equation for gray gas mean beam length

Wimpress mean Beam Length

$H_{fr} := \frac{130}{130} = 1 \qquad W_{fr} := \frac{W}{H} = 0.303 \qquad D_{fr} := \frac{D}{H} = 0.031$

$322 - 10 - 1$ Characteristic ratio of dimension derives 1.8 factor of D

$L_{wimpress} := D \cdot 1.8 = 7.2\,in$ R.N. Wimpress formula

A16.6 Radiation Heat Transfer Model of the OTM Furnace

A radiation model of the OTM furnace has been created to:

1. Validate the Shaw/Wimpress Method

2. Compare with the CFD model.

3. Determine the sensitivity of temperature and gray gas changes through the OTM core.

The following assumptions are made:

Assumptions:

1. Temperatures of OTMs and Gray Gases vary linearly over module height.
2. Mass fractions of components vary linearly over module height.
3. Temperature of Steam tubes is constant = 836 R (464 K)
4. Average Fuel Utilization = 0.80
5. Beginning Fuel utilization = 0.70
6. Final Fuel utilization = 0.9

This model starts with specific temperature boundary conditions. The following temperatures profiles were assumed:

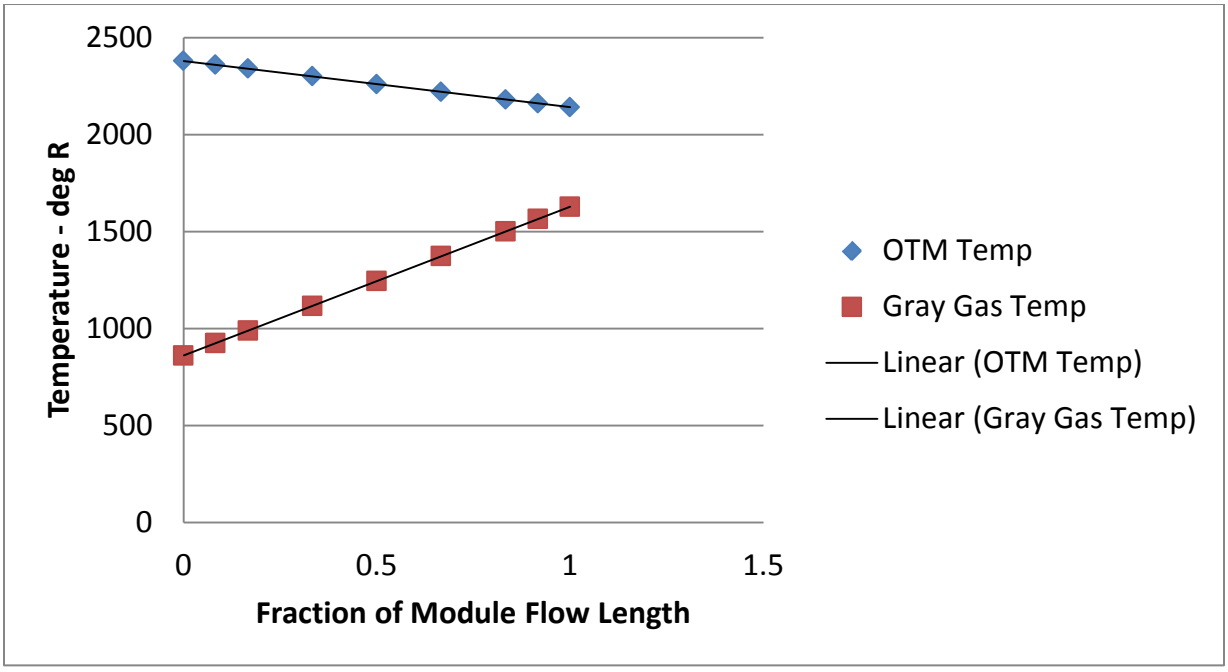

Figure A16.6 – 1: OTM and gray gas temperature assumptions

This model takes into account the changes in the temperature of the OTM core as well as temperature and components of the gray gases as they passes through the OTM module. Figure A16.6 – 2 shows the variation in mass fraction with OTM height. Figure A16.6 – 3 illustrates the changes in total partial pressure of the gray gases vs. module height.

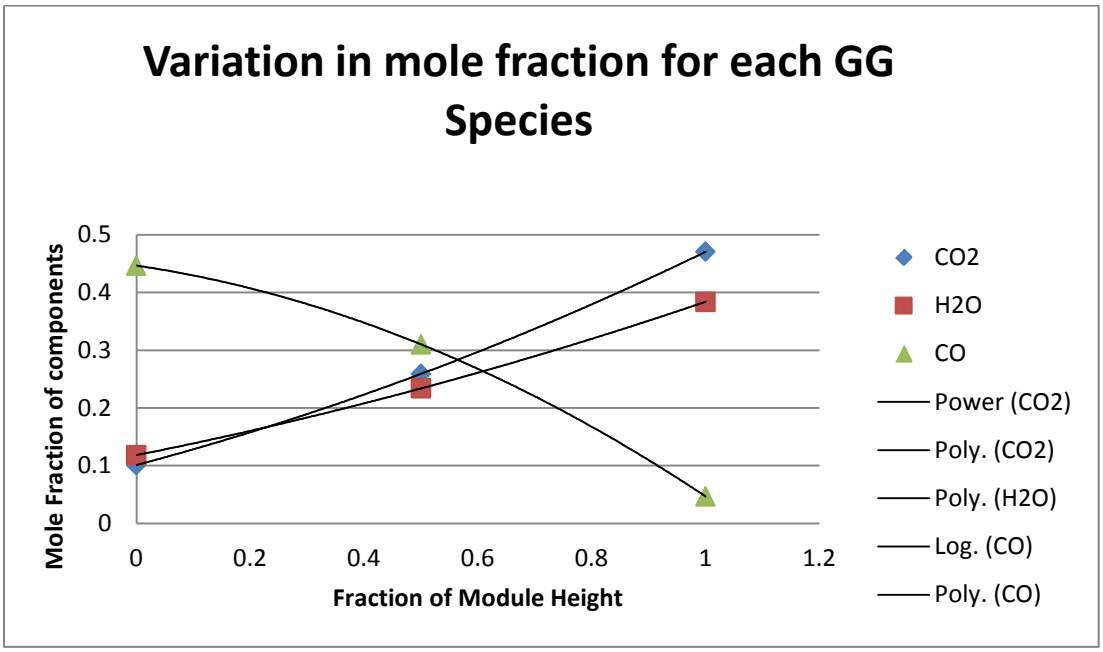

Figure A16.6 – 2: Variation in mole fraction of gray gas components as a function of module height

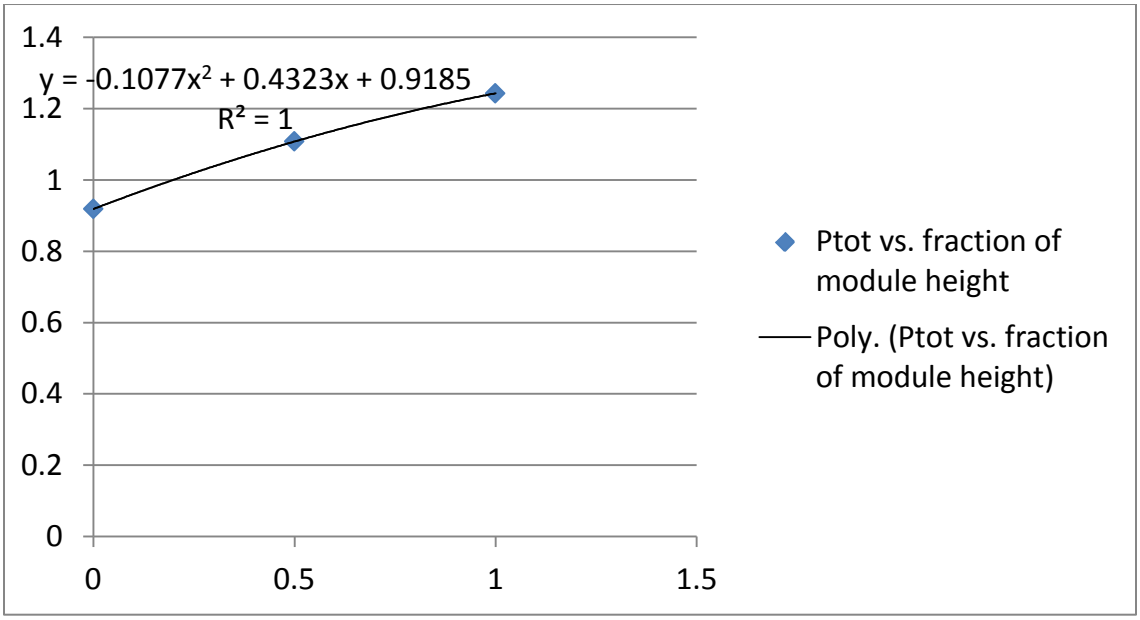

Figure A16.6 – 3: Variation in total partial pressure of gray gas components as a function of OTM core height.

Figure A16.6 – 4 illustrates the changes in the gray gas emissivity vs. OTM core height.

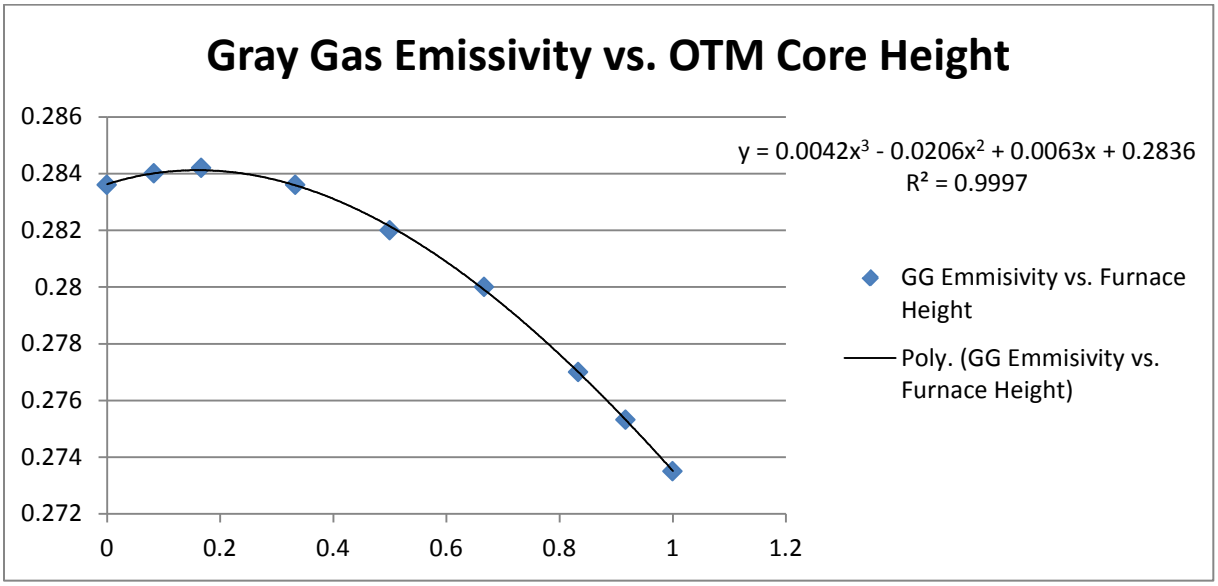

Figure A16.6 – 4: Variation in gray gas emissivity vs. OTM core height.

The Radiation Network Model

This model is a traditional radiation network model using the electrical analogy of J. P. Holman (Heat Transfer, 3rd Edition, McGraw Hill, 1972). Resistances are represented by the inverse of area, view factor, and emissivity. If the resistance of a surface is modeled, the view factor is equal to one. This

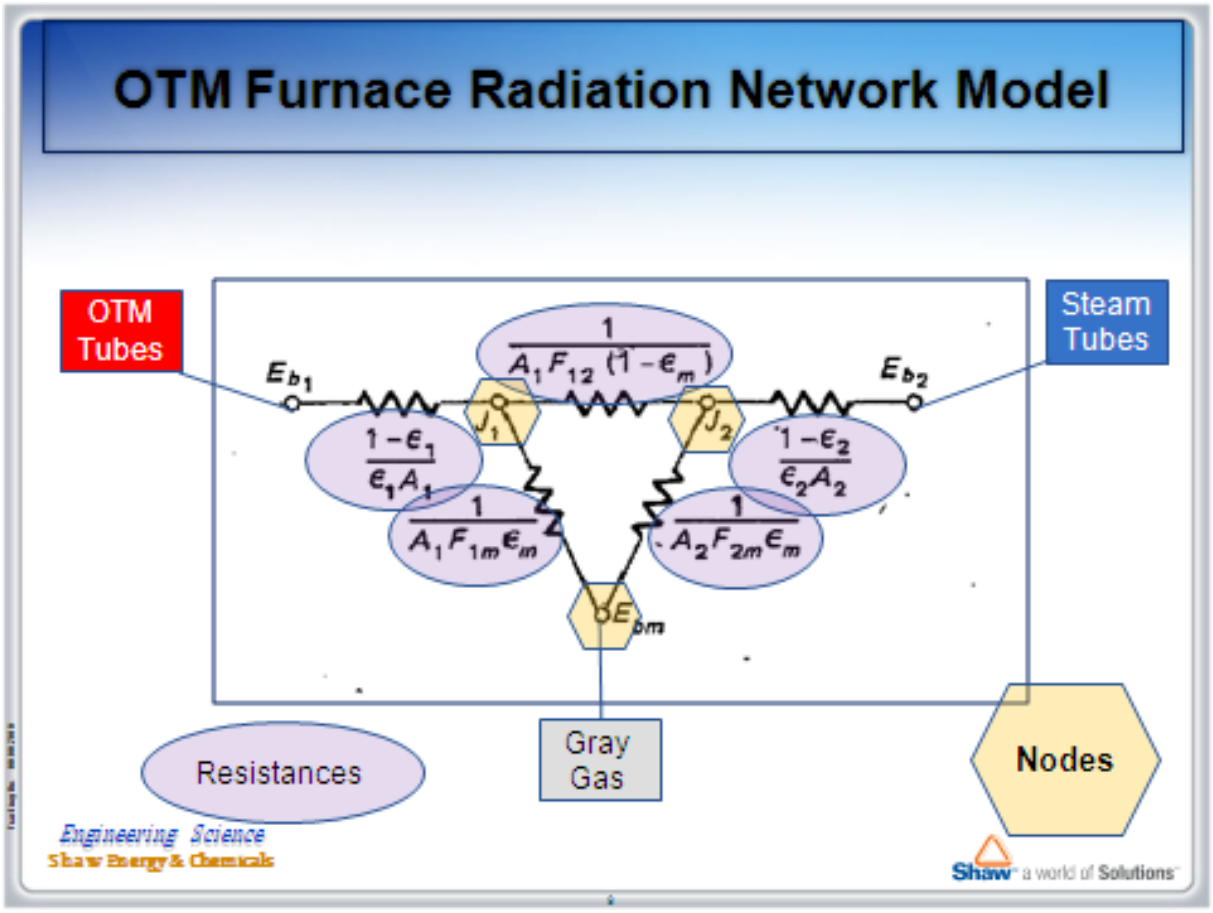

Figure A16.6 – 5: Radiation network model diagram.

model can take into account the many reflections of radiation between non-black bodies and gray gases, including the view factors between. This particular model includes the OTM tubes, steam tubes, and the gray gas medium. There are junctions at the nodes through which the radiant heat flows. These nodes or junctions form convenient points to calculate the heat flow by radiation using the electrical analogy with Kirchoff's law. Kirchoff's law stipulates that the sum of the radiation heat transfer entering and exiting a node must be equal. Therefore each node represents an equation of heat transfer flux that sums to zero. The results of this analysis are summarized below in Figure A16.6 – 6.

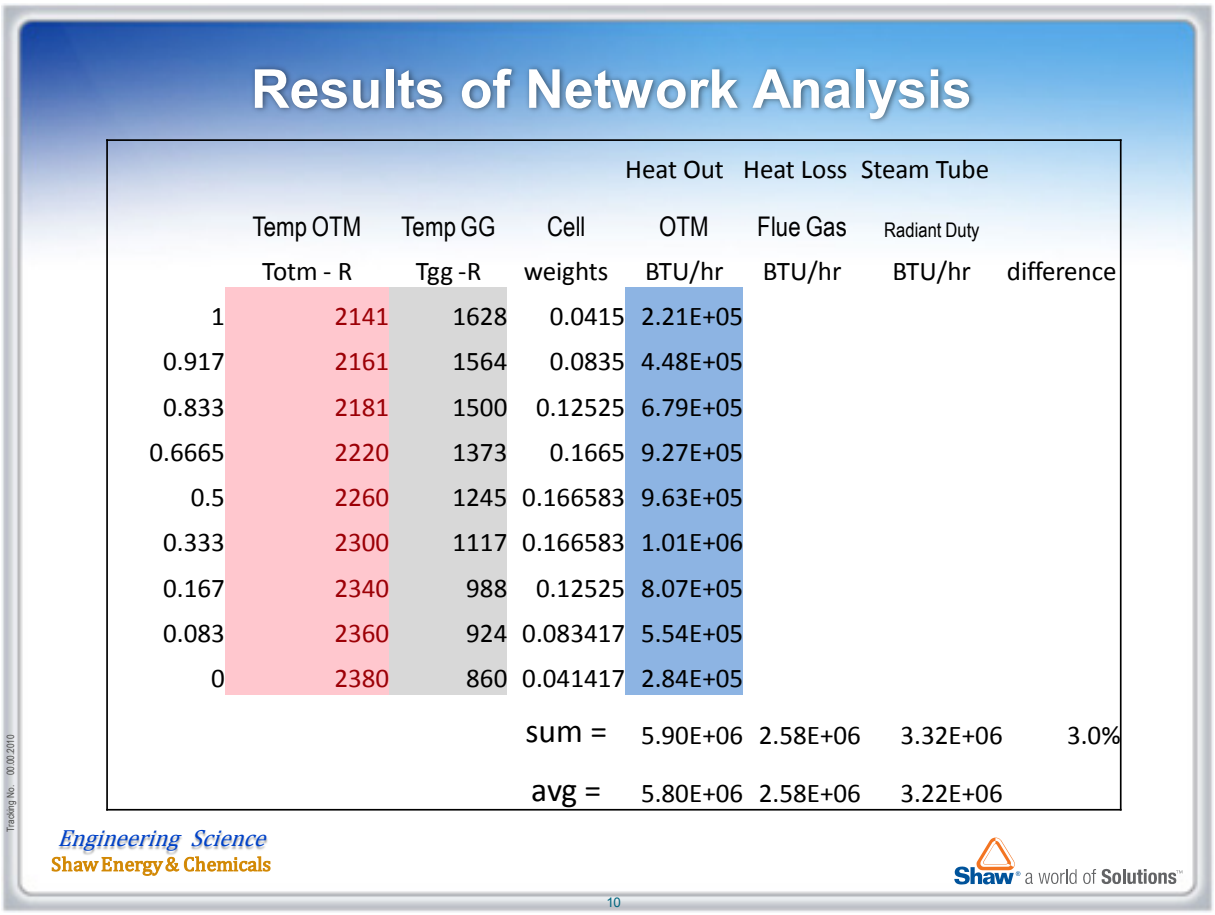

Results of Network Analysis

	Temp OTM	Temp GG	Cell	Heat Out OTM	Heat Loss Flue Gas	Steam Tube Radiant Duty	
	Totm - R	Tgg -R	weights	BTU/hr	BTU/hr	BTU/hr	difference
1	2141	1628	0.0415	2.21E+05			
0.917	2161	1564	0.0835	4.48E+05			
0.833	2181	1500	0.12525	6.79E+05			
0.6665	2220	1373	0.1665	9.27E+05			
0.5	2260	1245	0.166583	9.63E+05			
0.333	2300	1117	0.166583	1.01E+06			
0.167	2340	988	0.12525	8.07E+05			
0.083	2360	924	0.083417	5.54E+05			
0	2380	860	0.041417	2.84E+05			
			sum =	5.90E+06	2.58E+06	3.32E+06	3.0%
			avg =	5.80E+06	2.58E+06	3.22E+06	

Figure A16.6 – 6: Results of the radiation network model in conjunction with the variations in temperature and gray gas emissivity vs. OTM core height.

The results reveal the very small sensitivity of the OTM furnace to changes in the composition of the gray gases as they pass through the OTM module. The difference between the bulk average radiation heat transfer and the one dimensional model of temperature, and gray gas emissivity variation is only +3%. Therefore the sensitivity of the OTM furnace to these variations is not great.

A sample calculation of the radiation network model using bulk average temperatures and gray gas emissivity is included in the next section.

Sample Calculation of Radiant Heat Transfer

$\varepsilon_{st} := 0.8$ emissivity of the steam tubes

$\varepsilon_m = 0.282$ emissivity of the gray gases

$N_{otm} := 65$ number of otm tubes

$D_{otm} = 1 \cdot in$ diameter of otm tubes

$L_{otm} := 1m$ length of the OTM tubes

$a_{hotm} := D_{otm} \cdot \frac{\pi}{2} \cdot N_{otm} \cdot L_{otm} = 4.02 \times 10^3\ in^2$ half area of otm tubes in one column

$F_{os} := 0.45$ view factor for radiation ht from otm to steam tubes determined with discrete ordinates CFD

$a_{hst} := D_{st} \cdot \frac{\pi}{2} \cdot 6 \cdot 3250mm = 2.412 \times 10^3\ in^2$ half area of 6 steam tubes

$F_{sto} := \frac{F_{os} \cdot a_{hotm}}{a_{hst}} = 0.75$ view factor for radiation heat transfer from steam to OTM tubes by reciprocity.

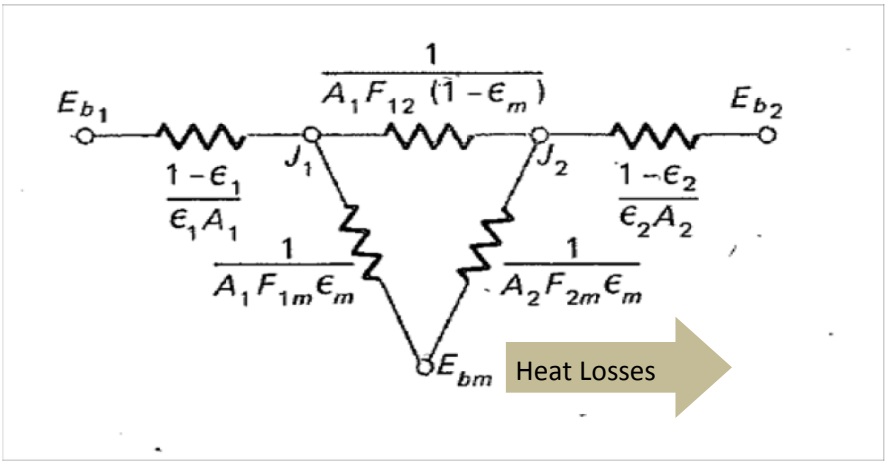

Figure 1: Radiation network for the otm furnace column. Subscript 1 is the otm and 2 is the steam tube, m is the gray gas medium. Eb is the black body emmissive power.

$F_{om} := 1.0$ $F_{stm} := 1.0$ view factors from otms and steam tubes to gray gas medium

Radiation Resistances

$$R_{11} := \frac{1 - \varepsilon_{otm}}{\varepsilon_{otm} \cdot a_{hotm}} = 2.764 \times 10^{-5} \frac{1}{in^2}$$ resistance of otm surfaces

$$R_{12} := \frac{1}{a_{hotm} \cdot F_{os} \cdot (1 - \varepsilon_m)} = 7.701 \times 10^{-4} \frac{1}{in^2}$$ resistance of the view between otm and steam tubes

$$R_{1m} := \frac{1}{a_{hotm} \cdot F_{om} \cdot \varepsilon_m} = 8.816 \times 10^{-4} \frac{1}{in^2}$$ resistance of the otm to the gray gas

$$R_{2m} := \frac{1}{a_{hst} \cdot F_{stm} \cdot \varepsilon_m} = 1.469 \times 10^{-3} \frac{1}{in^2}$$ resistance of the steam tubes to the gray gas

$$R_{22} := \frac{1 - \varepsilon_{st}}{a_{hst} \cdot \varepsilon_{st}} = 1.037 \times 10^{-4} \frac{1}{in^2}$$ resistance of the steam tubes surface

Kirchoff's Law at Each Node J

$$\frac{E_{b1} - J_1}{R_{11}} + \frac{J_2 - J_1}{R_{12}} + \frac{E_{bm} - J_1}{R_{1m}} = 0$$ Node J1

$$\frac{E_{b2} - J_2}{R_{22}} + \frac{J_1 - J_2}{R_{12}} + \frac{E_{bm} - J_2}{R_{2m}} = 0$$ Node J2

$$\sigma := 0.1714 \cdot 10^{-8} \frac{BTU}{hr \cdot ft^2 \cdot R^4}$$

$T_m := T_{avgg} \cdot K$ $\quad T_m = 1246 \cdot R$ temperature of the gray gas medium

$T_{otm} = 2.26 \times 10^3 R$ $\quad T_{st} = 836 R$ temperature of the otm and steam tubes

$$E_{b1} := \sigma \cdot T_{otm}^{\ 4} = 4.471 \times 10^4 \cdot \frac{BTU}{hr \cdot ft^2}$$

$$E_{b2} := \sigma \cdot T_{st}^{\ 4} = 837.213 \cdot \frac{BTU}{hr \cdot ft^2}$$

$$E_{bm} := \sigma \cdot T_m^{\ 4} = 4.126 \times 10^3 \cdot \frac{BTU}{hr \cdot ft^2}$$

Solving for J1 and J2:

Given

$J_1 := 1 \frac{lbm}{s^3}$ $\quad J_2 := 1 \frac{lbm}{s^3}$ Initial Guesses

$$\frac{E_{b1} - J_1}{R_{11}} + \frac{J_2 - J_1}{R_{12}} + \frac{E_{bm} - J_1}{R_{1m}} = 0$$ Equation 1

$$\frac{E_{b2} - J_2}{R_{22}} + \frac{J_1 - J_2}{R_{12}} + \frac{E_{bm} - J_2}{R_{2m}} = 0$$ Equation 2

$$\begin{pmatrix} J_1 \\ J_2 \end{pmatrix} := \text{Find}(J_1, J_2)$$ solver script

$J_1 = 293.111 \frac{1}{in^2} \cdot \frac{BTU}{hr}$ $J_2 = 39.237 \frac{1}{in^2} \cdot \frac{BTU}{hr}$ results

$\frac{E_{b1} - J_1}{R_{11}} + \frac{J_2 - J_1}{R_{12}} + \frac{E_{bm} - J_1}{R_{1m}} = -1.075 \times 10^{-4} \cdot \frac{BTU}{hr}$ check

$\frac{E_{b2} - J_2}{R_{22}} + \frac{J_1 - J_2}{R_{12}} + \frac{E_{bm} - J_2}{R_{2m}} = 1.571 \times 10^{-7} \cdot \frac{BTU}{hr}$ check

The heat absorbed by 1/2 column of steam tubes is:

$Q_{hst} := \frac{J_2 - E_{b2}}{R_{22}} = 3.224 \times 10^{5} \cdot \frac{BTU}{hr}$ radiant heat transfer for one column of the OTM and steam tube coils

$N_{hst} := 18$ number of 1/2 steam tubes

$Q_{otm} := Q_{hst} \cdot N_{hst} = 5.804 \times 10^{6} \frac{BTU}{hr}$ total heat radiated from OTMs as a result of temperatures boundary conditions

$Q_{fg} := 2.53 \cdot 10^{6} \frac{BTU}{hr}$ heat from radiation exiting with the flue gas and unburnt fuel + other heat losses of combustion.

$Q_{strad} := N_{hst} \cdot Q_{hst} \cdot 0.99 - Q_{fg} = 3.22 \times 10^{6} \cdot \frac{BTU}{hr}$ radiant heat transfered to the steam tubes

PRAXAIR

PRAXAIR OXYGEN TRANSPORT MEMBRANE CONFIGURATION OPTION SELECTION MEETING

Date: 7 June 2011

Praxair's Offices Tonawanda, New York

Executive Summary:

The option selection meeting to determine the most favorable configuration of the oxygen transport membranes developed by Praxair for both a boiler and a partial oxidation unit (POx) was convened in Praxair's offices in Tonawanda New York. The six (6) Shaw proposed configurations for the boiler were reviewed and their merits considered. It was determined that Boiler Concept 2, a tube-configured cross-flow concept with water in vertical tubes, air in horizontal tubes and gas in the annular space design, was the most favorable based on the agreed to selection criteria. The merits of this design included: vertical tubes (favorable orientation for steam generation with elevated steam drum) and an OTM tube design where the tubes will penetrate the tube sheets and seals will be developed to seal the penetration points. The POx unit was not individually evaluated as it was determined that the Advanced Power Cycle configuration will be revised to allow the POx unit to operate at low pressure by using a 'slip stream' approach. This low pressure approach allows the same configuration to be used as for the boiler.

The intent is that this configuration will now be progressed further into basic engineering to allow for a more accurate design and cost estimate.

1. CONCEPT DEVELOPMENT

1.1 Option Selection

An option selection meeting to determine the most favorable configuration of the oxygen transport membranes developed by Praxair for the OTM Boiler was convened in Praxair's offices in Tonawanda, New York. The seven (7) Shaw

proposed configurations for the boiler were reviewed and their merits considered. It was determined that Boiler Concept 2, a tube configured cross flow concept with water in vertical tubes, air in horizontal tubes and gas in the annular space design, was the most favorable based on the agreed to selection criteria. The merits of this design included: vertical tubes (favorable orientation for steam generation with elevated steam drum) and an OTM tube design where the tubes will penetrate the tube sheets and seals will be developed to seal the penetration points.

1.2 Planar vs. Tubular Option

Background:

The concept development phase of the project was important to this project as it was the catalyst to a technical solution as well as defining the basis for the cost estimate. Due to the unique features of the OTM membrane, conventional boiler design was deemed not suitable. In early meetings with Shaw, Praxair shared some results from their ongoing development for use of the OTM membrane within an Autothermal Reformer. Additionally, Praxair advised some key features and aspects of the OTM membrane that guided Shaw in the development of the concepts.

Key Features:

- OTM membrane can be applied on the support structure (advanced ceramic material with porous construction) on either the air or gas side.
- The support structure will be ceramic based, so welding and other typical joining convention may be limited.
- The support structure can be either in tubular or planar form. More later on the limitations of each form.
- OTM membrane's working temperature range required that there be continuous flow across the surface. The heat transfer cooling media needs to be uniform, to absorb and maintain the heat flux.

As a visual aid, the concept development phase was performed in 3D graphics. The modeling for these graphics also allowed the designer to extract the parts, make multiple view cuts, and to annotate descriptions in both 2D and 3D views. Below are the concepts that were taken to the selection stage. These concepts were discussed in detail during the review stage and more information can is available in the concept selection report. Descriptions and captions below provide a summary of these concepts.

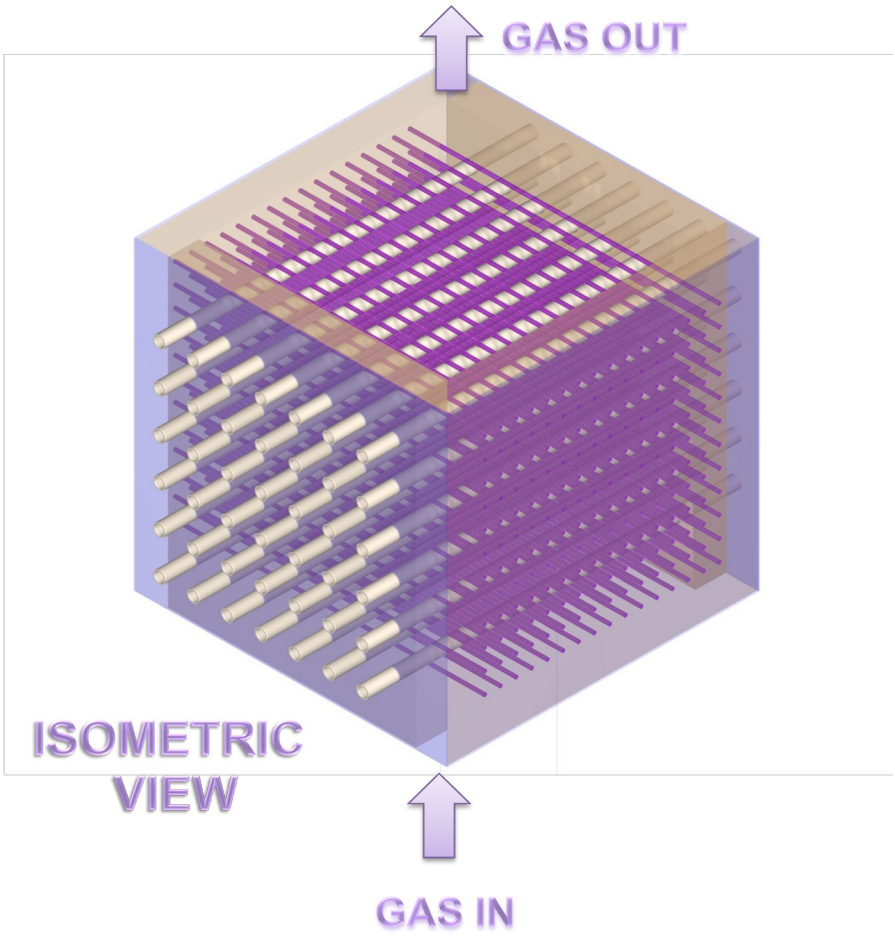

Boiler Concept – 1

Concept 1, above, was one of the tubular concepts where the OTM membrane is coated on the interior surface of ceramic tubes. The air passes on the inside, while the fuel passes on the OD of the tube. The water tubes run perpendicular to the OTM tubes.

This configuration had advantages of good overall view factor between the OTM tubes and the water tubes. All tubes would be enclosed in a metal plate structure with

refractory insulation to retain the heat. This is practical considering that both the air and gas streams operate at a relatively low pressure (5 psig or less).

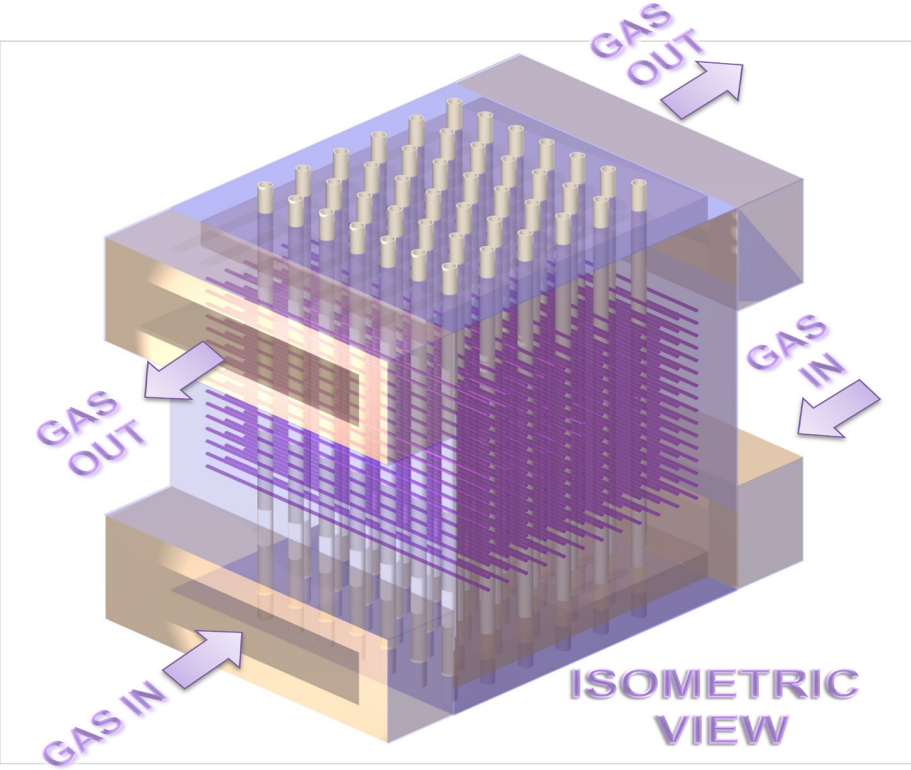

Boiler Concept - 2

Concept 2 is similar to Concept 1, however the fuel runs parallel to the direction of the steam/water tubes.

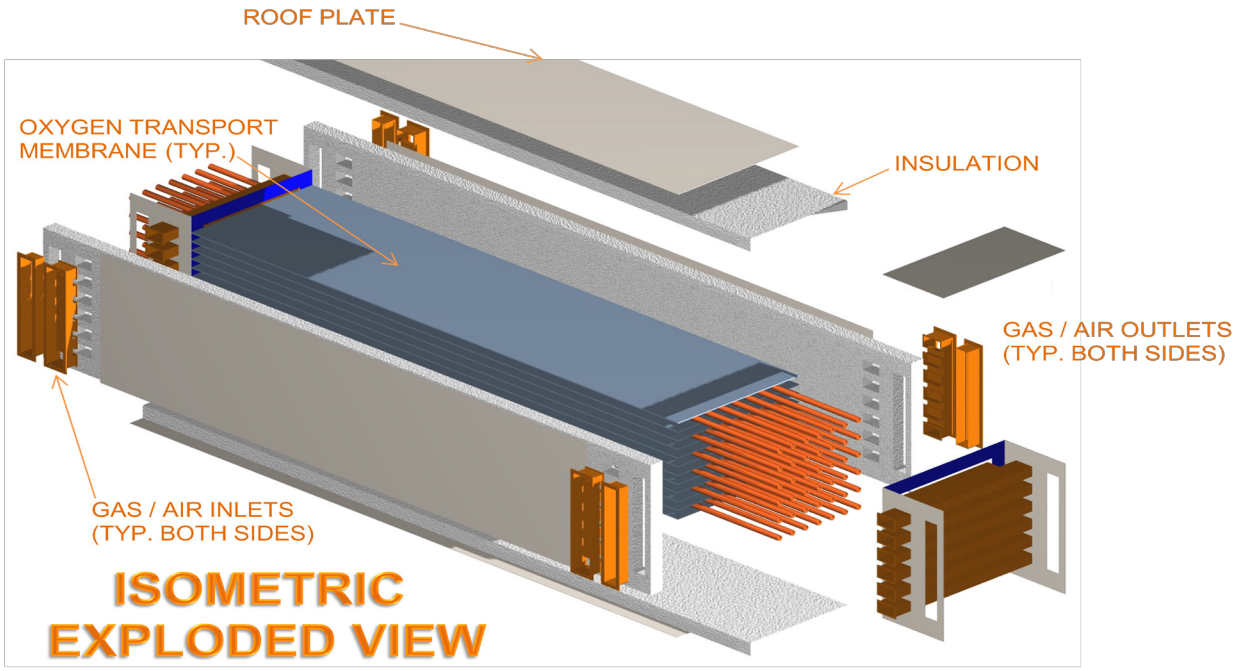

Boiler Concept – 3

Concept 3 was termed the "Planar Concept". The OTM membrane in this concept was applied to the surface of ceramic sheets or plates. Steam/water passes inside the orange metallic tubes in a convention manner, while being heated up by the planar OTM surfaces. The gas runs parallel to the steam tubes, while the air passes between layers of the OTM plate in alternating pattern.

This concept raised some interest as it was initially thought of as providing the best overall view factor between the OTM surface and the steam tubes. However, the complexity in the design, in addition to other factors resulted in elimination:

- The plate structure is not a proven manufacturing process for the special ceramic required for the support of the OTM membrane.
- If the plate structure was feasible, the consultant ceramics manufacturer advised that the size of the plate would be limited, perhaps no more than 1 square foot. This would require a “tile” design, leading to other issues, such as support of the ceramic tiles and sealing.
- The framing/support for the “tile” would also reduce the effective area of the OTM, thereby reducing the overall view factor.
- Safety was a greater concern with this concept, when considering the sealing aspect.

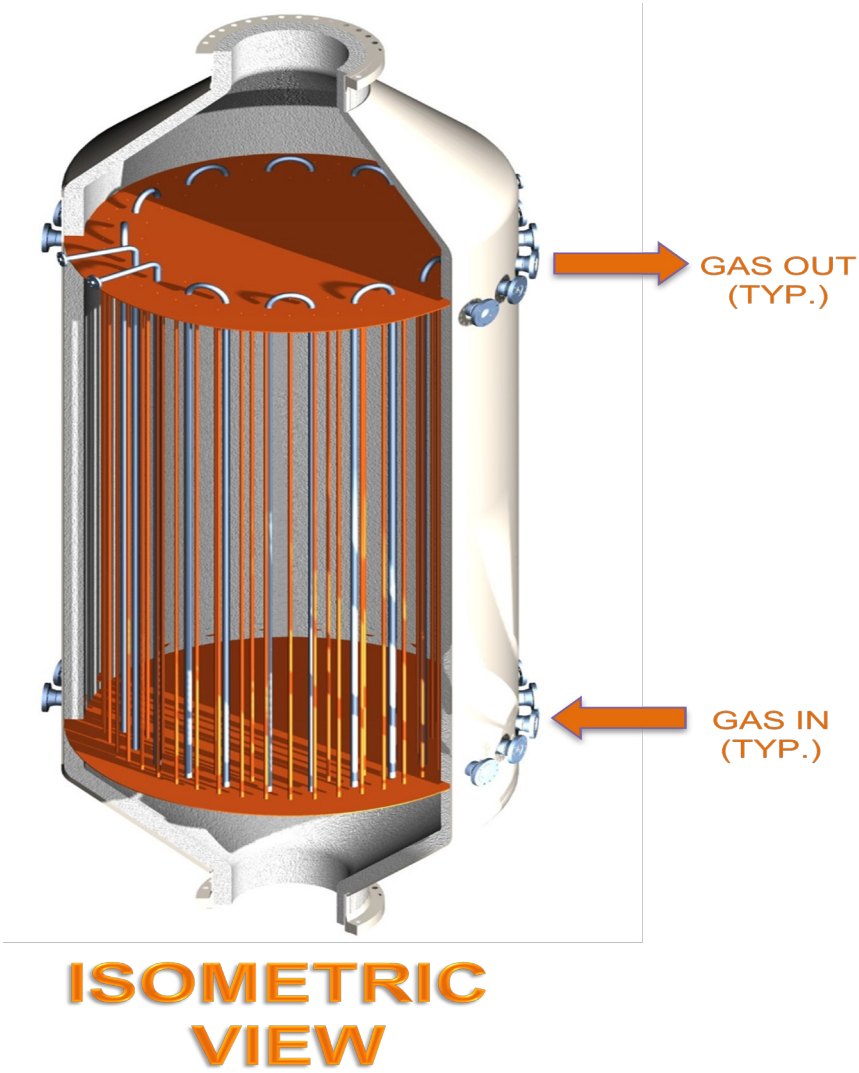

Boiler Concept – 4

Concept 4 was dismissed:

- The serpentine nature of the steam coils is not conducive to steam thermal siphon to the steam drum.
- The length of ceramic tube would likely be restrictive.

- Overall size of the exchanger would be prohibitive.

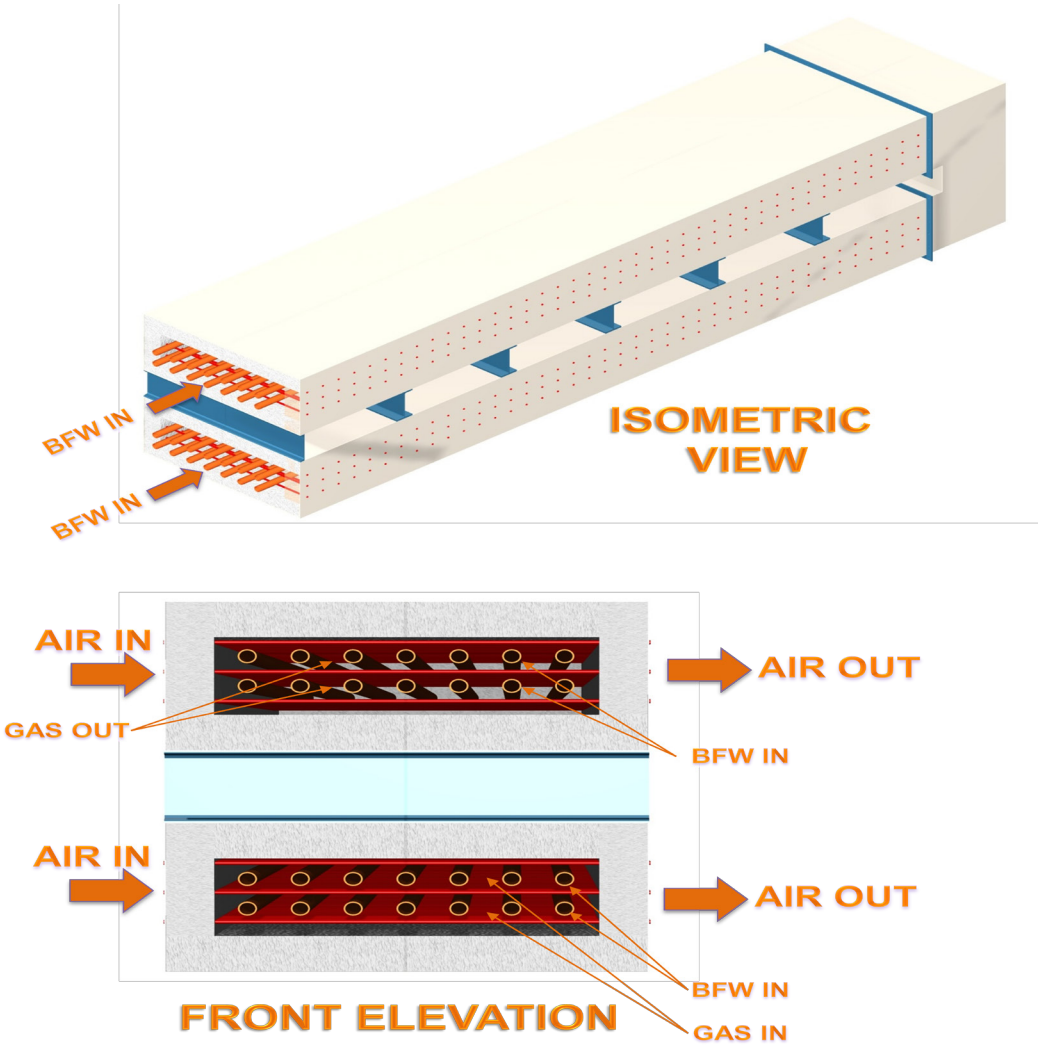

Boiler Concept – 5

Concept 5 is similar to Concept 2, with the added feature of an enclosure on the gas side to return the gas down a second pass against the OTM tubes.

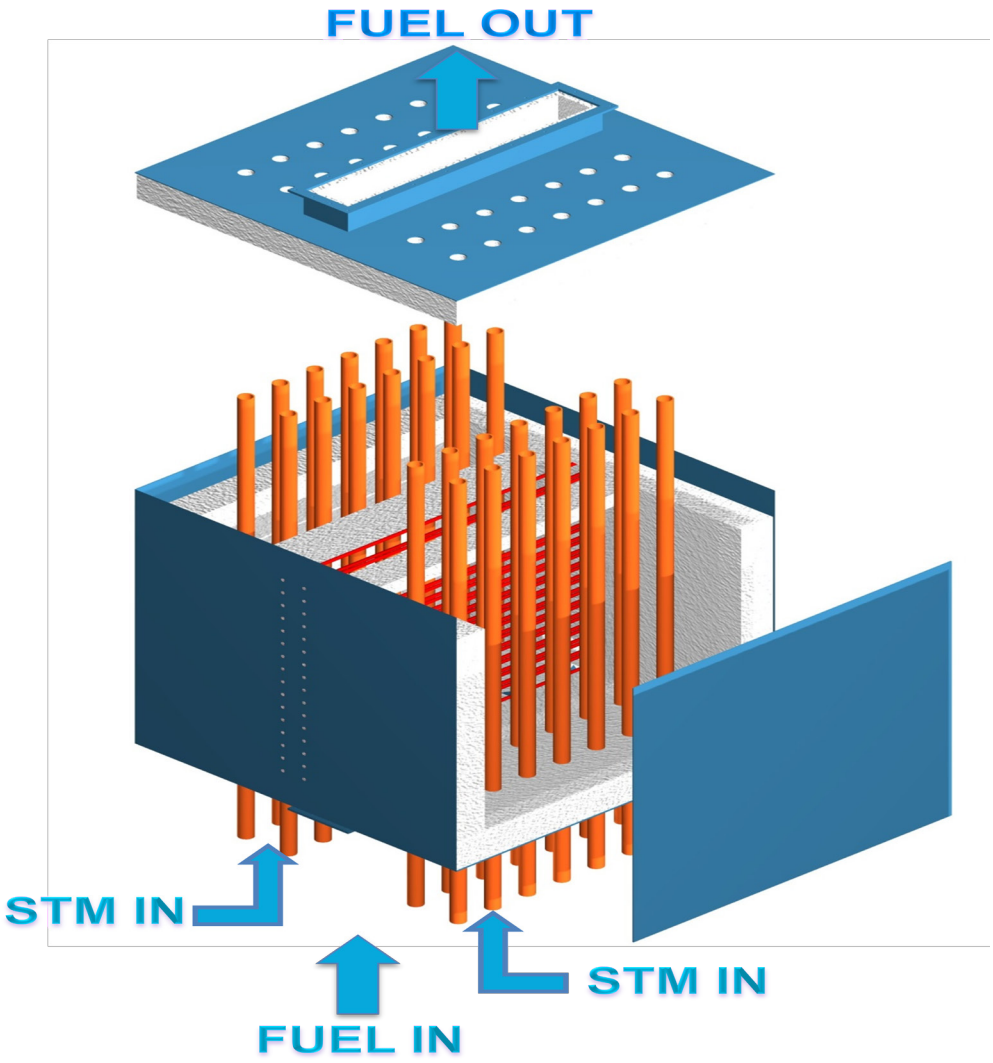

Boiler Concept – 6

Concept 6 had the steam/water tubes in separate chambers from the OTM tubes. The thought was that this configuration would make it easier to separate the OTM tubes from the steam/water tubes in case of maintenance and replacement.

However, the view factor for this concept was prohibitive to heat transfer. Also the proximity of the OTM tubes would likely result in local overheating.

2. CONCEPT SELECTION METHODOLOGY

The six boiler configuration options were reviewed and discussed to allow all team members to understand the approach for each design. A list of evaluation criteria was generated by the group and grouped into major categories with shared characteristics. The agreed upon criteria are listed below:

- **Ease/ Ability of Manufacture /Design Simplicity/Complexity/Cost**
  - Ceramic Membranes
  - Balance of Design
- **Technically Viable / Risk**
  - Ceramic Membranes
  - Balance of design

- **Safety**
  - Leak potential
  - Pressure Integrity
  - Deflagration Potential
- **Configuration Efficiency**
  - Air Side Pressure Drop
  - Fuel side pressure drop
  - Area Utilization for HT & Mass Transfer
- **Material Compatibility Risk(metallurgy, temperature)**
- **Flexibility**
  - Process
  - Boiler vs POx
- **Serviceability**
- **Scalability**

As part of the evaluation group discussion, a weighting scale was applied to the criteria using a three-point scale with 3 being characteristic of most important criteria, and 1 being characteristic of least relative importance.

The Pugh's analysis methodology was employed to rank the concepts relative to each other with respect to the criteria. In a Pugh's analysis, a case is identified as a base-case and all other concepts are evaluated as either "better than", "same as", or "worse than" the base-case. For simplicity Boiler option 1 was chosen as the base case, and a numerical designation was used to denote position relative to the base-case as follows:

PRAXAIR

0 = "same as"
-1 = "less favorable"
+1 = "more favorable"

Each of the criteria was examined for each boiler option by the group. A Pugh's ranking was given for each of the criteria through comparison with boiler 1, and the product of the selection criteria weighting and the concept relative Pugh's analysis rank was computed. For each boiler concept, the sum of the weighted ranking was used as a measure of design concept value. The highest positive sum corresponds to the highest ranked design concept.

3. RESULTS:

The results of the selection criteria ranking is shown in the table below. Each column corresponds to a boiler design concept and the criteria are evaluated in each row.

PRAXAIR

CRITERIA	WEIGHTING (WT)	Boiler 1 (Base)	Boiler 2	Boiler 2 - WT x Score	Boiler 3	Boiler 3 - WT x Score	Boiler 4	Boiler 4 - WT x Score	Boiler 5	Boiler 5 - WT x Score	Boiler 6	Boiler 6 - WT x Score
Ease/ Ability of Manufacture/Design Simplicity/complexity/Cost												
Ceramic	3	0	0	0	1	3	-1	-3	0	0	0	0
Balance of Reactor	2	0	0	0	-1	-2	-1	-2	-1	-2	-1	-2
seals	3	0	0	0	-1	-3	0	0	0	0	0	0
Technically Viable/Risk												
Ceramic	3	0	0	0	0	0	-1	-3	0	0	0	0
Balance of Reactor	2	0	0	0	0	0	-1	-2	0	0	-1	-2
seals	3	0	0	0	0	0	0	0	0	0	0	0
Safety												
Leak Potential	2	0	0	0	-1	-2	0	0	0	0	0	0
Pressure Integrity	2	0	0	0	-1	-2	1	2	0	0	0	0
Membrane Rupture Consequence	2	0	0	0	-1	-2	0	0	0	0	0	0
Configuration Efficiency												
Air Side Pressure Drop	1	0	0	0	1	1	0	0	0	0	0	0
Fuel side Pressure Drop	1	0	0	0	0	0	0	0	0	0	0	0
Area Utilization for HT & Mass Transfer	1	0	1	1	0	0	-1	-1	1	1	-1	-1
Material Compatibility	1	0	0	0	0	0	-1	-1	0	0	0	0
Flexibility												
Process	1	0	0	0	0	0	0	0	0	0	0	0
Boiler vs POx	2	0	0	0	0	0	0	0	0	0	0	0
Serviceability	2	0	0	0	-1	-2	-1	-2	0	0	-1	-2
Scalability	2	0	0	0	0	0	-1	-2	0	0	-1	-2
TOTAL		0		**1**		**-9**		**-14**		**-1**		**-9**

Boiler Design Evaluation Results

All of the concepts, save Boiler Concept 2, evaluated as lower quality than the baseline concept. The key factors in the evaluation proved to be risk, complexity, serviceability, and scalability. Boiler Concept 2, evaluated as slightly advantaged over the baseline concept, and this was based upon slightly better area utilization for heat transfer and flow. Boiler Concept 2 was chosen as the target configuration for the boiler design. In addition to being the highest ranked concept, it also has the following desirable characteristics.

- Best potential view factor between OTM tubes and steam coils
- Vertical alignment of steam coil tubes supporting integration into steam drum
- Manufacturing practicality for the module as well as OTM tube

- Scale-up was enabled in the modular concept
- Design can be serviced/repaired with straightforward access to membranes

Boiler Concept 2 was used by the Shaw Energy and Chemical Furnace Design Group as the basis to do a detailed OTM boiler module design. The resulting OTM boiler module in exploded assembly view detail is shown in the figure below. To produce a 7.5 MWth rated boiler for the scope of this project, eight such modules are required.

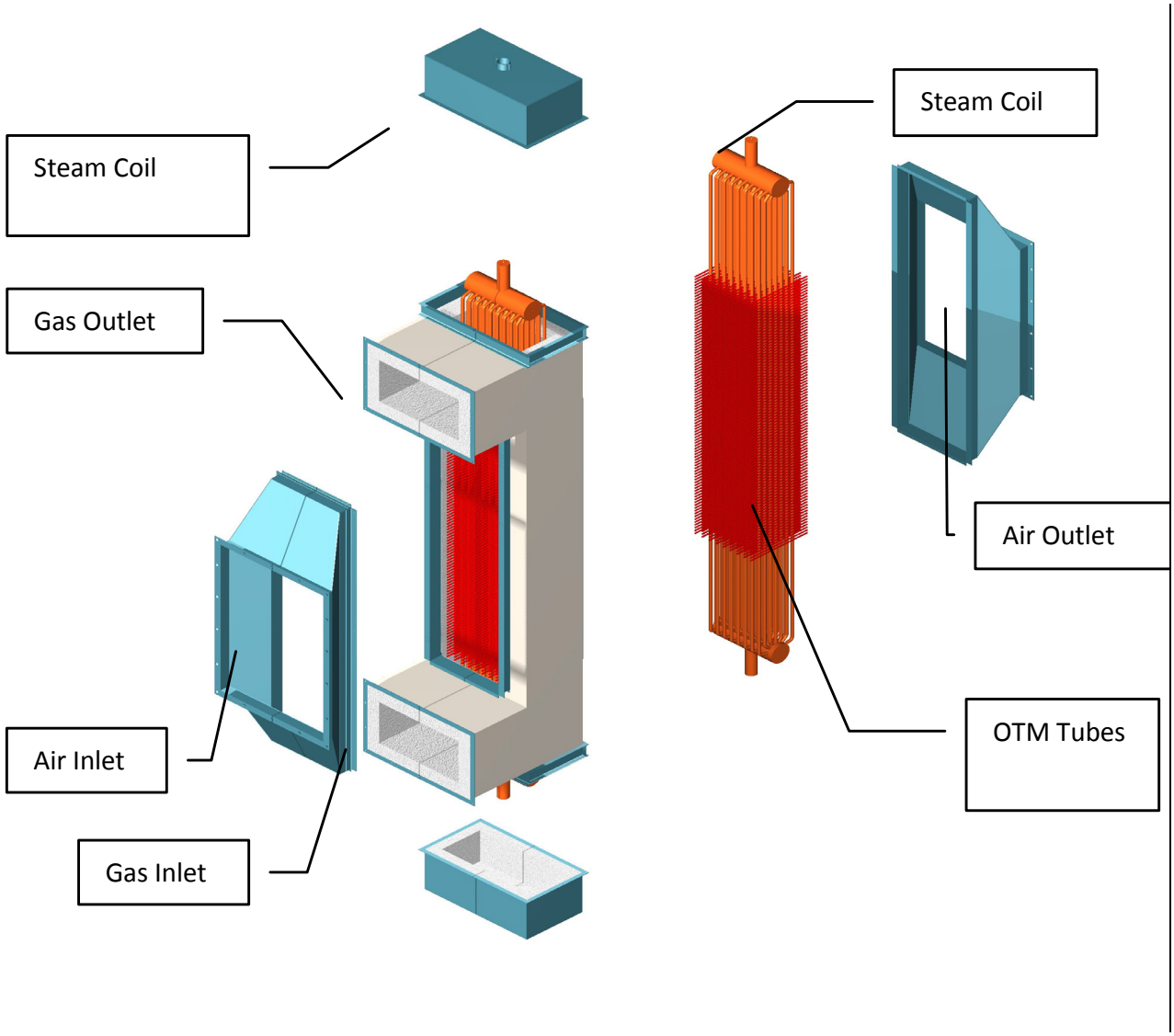

Exploded Isometric View – Tubular OTM Boiler Module

4. CONCLUSION:

The option selection exercise clearly indicated positive merit for the boiler configuration where the ceramic membranes were formed into tubes (Boiler 1, 2 and 5) and arrayed with water tubes with gas in the interstitial spaces. Out of these three options option 2 was considered the most favorable as the water tubes were vertical giving the correct

orientation for flow into an elevated steam drum. This configuration will be designed to manifold the steam tubes into a common header with one line running back and forth from the steam drum. For the OTM tubes distribution will be via a tubesheet and ducts. The OTM tubes will penetrate through the tubesheet and a seal will be developed for the penetration. The more innovative solution of using flat plate ceramic membranes did not result in an attractive score due to lack of experience in manufacture and concerns over the number of joints / seals required and dissimilar materials. The tubular design was considered to be much more feasible than the more complex, seal intensive design with the flat plates.

Appendix C

University of Utah Final Report

Oxy-Coal Combustion Using Oxygen Transport Membranes

Oxy-Coal Combustion Using Oxygen Transport Membranes

Final Report

To Praxair, Inc,

Submitted by

Joseph Adams

Eric Eddings

Department of Chemical Engineering

University of Utah

April 30, 2012

Executive Summary

A reactor was developed at the University of Utah to test the operation of a Praxair oxygen transport membrane (OTM) in a coal-generated syngas environment. A hot oxygen burner (HOB) gasifier, developed by Praxair, was utilized to provide rapid gasification of coal and subsequent generation of syngas for reaction with the OTM tubes. Testing campaigns were performed using a low sulfur coal blend and a high sulfur coal blend. Findings from these testing campaigns have determined that:

1. OTM tube performance was stable for ~80 hours of operation for each coal blend
2. Ash accumulation does not impose a restriction on the mass transfer of fuel to the OTM
3. The O_2 flux from the OTM increased with increases in OTM operating temperature and partial pressure of O_2 in the air side of the OTM
4. The percent of H_2 in the syngas fuel has a measurable impact on the O_2 flux performance.

In addition to these findings, measurements and calculations were made to characterize:

1. The coal fuel blends used with the HOB
2. Trace species present within the syngas
3. The difference between the temperature readings from different points on the OTM tube
4. The syngas flow rate leaving the HOB
5. The entrained solids flux flow rate from the HOB.

Oxygen Transport Membrane Reactor (OTMR)

A reactor was designed and developed to test the Praxair OTM tubes with a coal-derived syngas fuel. This reactor was designed, fabricated and modified over a 3.5 year period. A picture of the final reactor configuration is given in Figure 1. Component drawings of each of the 3 sections of the OTMR are given in Figures 2-4.

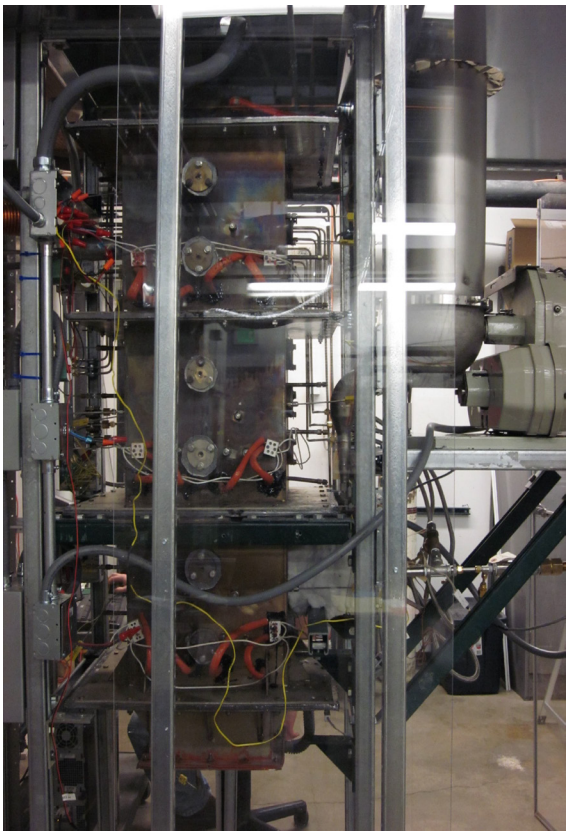

Figure 1: Oxygen Transport Membrane Reactor

The first section, or HOB section, houses the Praxair Hot Oxygen Burner (HOB) and is shown in Figure 2. The HOB is used to generate the coal syngas using a hot oxygen jet to quickly pyrolyze and gasify the coal. OTM tube access ports were included on the first section as well as all the other sections of the reactor. This was done to increase the versatility of the reactor to enable different OTM tube positions within the reactor to be tested. It was initially envisioned that OTM tubes could be tested at any point in the reactor. As the OTMR was developed, modifications were made that restricted the OTM tube to the second section or OTM section of the reactor (Figure 3). One of these modifications was the attachment of the HOB to the first section of the reactor.

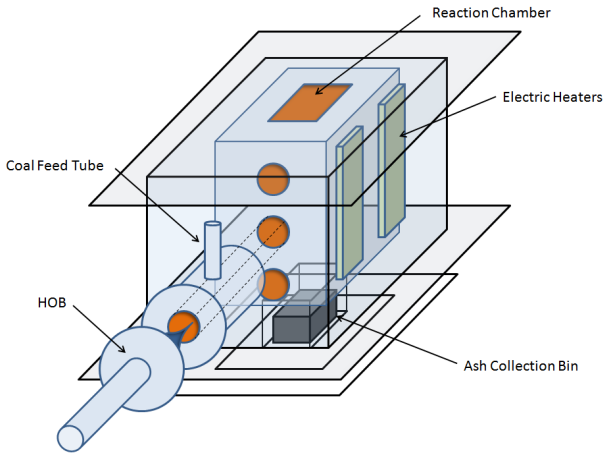

Figure 2: HOB Section of the OTMR

The second section, or OTM section, is where the OTM tube is housed. This section is shown in Figure 3. The OTM tube was typically positioned in the middle port or top port of this section. Included on the right side are two sampling ports. These ports were used to sample syngas before and after the OTM, when the OTM was positioned in the middle port.

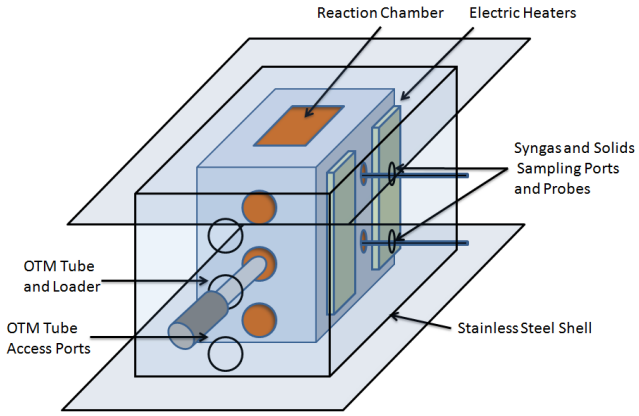

Figure 3: OTM Section of the OTMR

The third section of the OTMR is the Afterburner section of the reactor and is shown in Figure 4. The Afterburner section is used to burn off the excess fuel generated by the HOB. Much more fuel is generated in the HOB than can be burned by an OTM. The fuel is burned off by mixing O_2 with the syngas and then using a torch as an ignition source for the mixture. The auxiliary O_2 supply is not shown in Figure 4 because the line connects to the posterior surface of the Afterburner section, or the surface moving into the page.

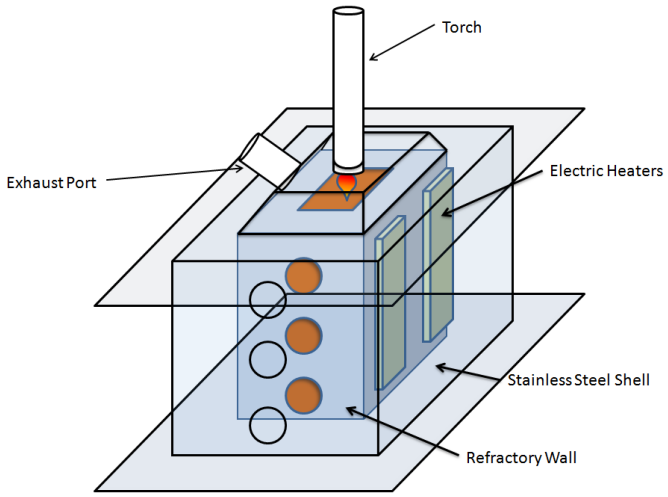

Figure 4: Afterburner Section of the OTMR

Analysis of Coals Used in Tests with OTM

The coal blends used in these tests with the Praxair OTM tubes were comprised of a low-sulfur bituminous Utah coal, a high-sulfur bituminous Illinois coal and a sub-bituminous low sulfur North Antelope Powder River Basin (PRB) coal. The low sulfur Utah coal was blended at 25 wt % to 75 wt % of the PRB coal. The high sulfur Illinois coal was blended at 50 wt % to 50 wt % of the PRB. As discussed in previous reports, the reason for using coal blends was to facilitate extended HOB operating time due to challenges with ash slagging, and plugging during feeding due to coal swelling.

The ultimate and proximate analysis of each coal is given in Table 1. Based upon this data, calculations were made to determine the respective coal blend properties. Ultimate and Proximate analysis measurements were then performed for each of the coal blends. The blended properties are compared with the calculated blend properties.

Table 1: Ultimate and Proximate Analysis of Coals Used in Testing Campaigns with Praxair OTM Tubes (wt%)

Coal Type	LOD (105°C)	Ash (705°C)	C	H	N	S	O (by diff)	Volatile Matter	Fixed Carbon	HHV (BTU/lb)
Utah	3.18	8.83	70.6	5.41	1.42	0.53	13.21	38.6	49.39	12606
Illinois	9.65	7.99	64.67	5.59	1.12	3.98	16.65	36.78	45.58	11598
PRB	23.69	4.94	53.72	6.22	0.78	0.23	34.11	33.36	38.01	9078
Utah/PRB Blend (Calc.)	18.5625	5.9125	57.94	6.02	0.94	0.31	28.89	34.67	40.855	9960
Utah/PRB Blend (measured)	10.68	6.23	61.78	5.38	0.86	0.3	25.45	37.63	45.46	10544

Ill./ PRB Blend (calc.)	13.44	6.89	62.16	5.82	1.1	0.38	23.66	35.98	43.7	10842
Ill./PRB Blend (measured)	7.88	7.68	64.00	5.29	0.97	2.09	19.97	37.17	47.27	11134
Indonesian	8.62	2.20	62.29	5.33	0.72	0.14	29.32	45.28	43.90	10458

The calculated contents of the Utah/PRB coal blend and the Illinois/PRB coal blend were made by using the following relationships.

$$N_{Utah/PRB\ Blend} = y_{Utah} * N_{Utah} + y_{PRB} N_{PRB}$$

$$N_{Illinois/PRB\ Blend} = y_{Illinois} * N_{Illinois} + y_{PRB} N_{PRB}$$

Where N refers to: LOD, Ash, C, H, N, S, O, Volatiles, Fixed Carbon and HHV with y_i referring to the mass fraction of the coal type in the blend.

Table 1 shows that there is a difference between the calculated blend properties and the measured blend properties. The largest deviation in composition is in the moisture content. For the Utah/PRB coal blend the moisture content varied 42.4 % from the calculated value to the measured value. For the Illinois/PRB blend the moisture content varied 41.4 %. This result indicates that the coals used had experienced some drying since the original tests were made with the individual Utah and Illinois coals on June 22, 2009. The analyses for the coal blends were made on March 22, 2012, and clearly there was a notable loss in the moisture content of the coal samples.

All of the sample analyses for the Utah/PRB and the Illinois/PRB coal blends were conducted by Huffman Laboratories, Inc. in Golden, Colorado. All of the percents reported are based upon the mass of the as-received sample. The loss on drying measurements was done by exposing the sample for 1 hour to an air stream at 105^{o}C. The ash for the ash analysis was generated by exposing the coal to air at 750^{o}C for 14-16 hours.

Analytical and Gas Chromatograph Sampling Results for HOB Syngas

Analytical samples of the syngas generated from the HOB for the Utah/PRB and Illinois/PRB blends were taken. The two syngas samples for the Illinois/PRB blend were collected on different days. The syngas samples collected for the Utah/PRB blend were collected on the same day but at different times in the run. The results of the sampling of the two coal blends are given in Table 2.

The compounds CH_4, C_2H_4, C_2H_6, H_2S, COS and CS_2 were taken using a 6 L summa canister. The canister is connected to the reactor and the valve is opened. The vacuum of the canister draws in the sample until the pressures between the reactor and the summa canister are at equilibrium.

The other three compounds, NH3, HCN and Cl are analyzed using a solid sorbent. The solid sorbent is packed into a glass tube which is sealed off at each end. Prior to testing the seal is broken and the tube is connected to a sampling line on one end and a pump on the other. The sample is drawn through the glass tube at a flow rate of 200 mL/min for 20 minutes. This exposes the sorbent to 4 L of sample gas.

Both the sampling equipment and the analysis of the samples are provided by ALS Environmental. The summa canister is analyzed on site in Utah while the solid sorbent samples are analyzed in a facility in Ohio.

Table 2: Trace Species Analysis of SynGas Generated from Two Different Coal Blends (ppm)

Coal Blend & Date	CH_4	C_2H_4	C_2H_6	H_2S	COS	CS_2	NH_3	HCN	Cl
Illinois/PRB 11/17	3900	470	51	1700	260	6.6	<0.43	<0.047	<0.086
Illinois/PRB 12/19	5600	1400	88	0.052	340	29	2.3	<0.063	<0.11
Utah/PRB (A) 1/6	7400	1300	66	<0.007	150	0.39	<0.57	<0.063	<0.11
Utah/PRB (B) 1/6	15000	3000	120	<0.007	110	0.88	130	<0.063	<0.11

It can be seen from Table 2 that there is a large discrepancy in the concentrations of some of the species. The most striking difference in concentration is between the first and second samples for H_2S, from the Illinois/PRB coal blend. For H_2S, the first measurement is 5 orders of magnitude higher than the second. It is possible that dilution effects may have influenced the first measurements on 11/17, which would explain why almost all the species have lower concentrations, but this does not account for the high difference in the concentration of H_2S. It is possible that an analytical error occurred in measuring H_2S. An equilibrium calculation was performed for the experimental conditions of these tests and provided an estimated H_2S concentration of 1600 ppm, which is very similar to the test performed on 11/17. This comparison suggests that the value obtained for H_2S on 12/19 might be in error.

A gas chromatograph was used to quantify gas concentrations for several major species. The data, which was collected using a Varian Micro GC, is given in Table 3. It should be noted that we were not able to determine the percent of CO with the samples on 11/17. The percent of CO is estimated based upon comparable samples with similar operating conditions and results. The comparison of the Micro GC results from the two different tests, with the Illinois/PRB blend, shows that the major syngas components are very comparable. This result indicates that the error in Table 2 for H_2S is likely an analytical error.

Table 3: GC Data Analysis (values in %)

	H_2	N_2	CO	CH_4	CO_2
11/17	18.78	1.04	~32	1.01	43.67
St. Dev.	0.4796	0.1567	-	0.093	1.6901
12/19	20	0.93	34.84	0.86	42.42
St. Dev.	1.60	0.62	3.41	0.08	5.54
1/6 (A) –	32.24	0.91	50.72	2.05	14.08

3 samples					
St. Dev.	1.93	0.03	1.61	0.04	3.51
1/6 (B) – 7 Samples	20.10	0.89	32.57	1.71	44.73
St. Dev.	2.22	0.14	3.23	0.25	4.61

It can also be seen in Table 3 that the fuel components of the syngas, meaning H_2, CO and CH_4, generated for sample set A for the Utah/PRB blend were higher than in sample set B. Sample set A was measured early in the run between 1:45 and 2:00 PM. Sample set B was measured later in the run between 5:08 and 5:47 PM. This data shows that the HOB syngas fuel is more concentrated with H_2, CO and CH_4 at the beginning of the run as compared to later in the run for this test. This represents a significant drop in the concentration of the fuel. The H_2 drops 37.7 dry vol. % and the CO drops 35.8 dry vol. %. The drop in fuel concentration is over a time period of ~3.5 hours. This measurement indicates that the concentration of the fuel was not constant during the operation of the run. It was found from analyzing the data used to get the numbers in Table 3 for the Utah/PRB analysis for samples A and B that fuel concentrations for H_2 and CO decreased over time. This data is given in Figure 5.

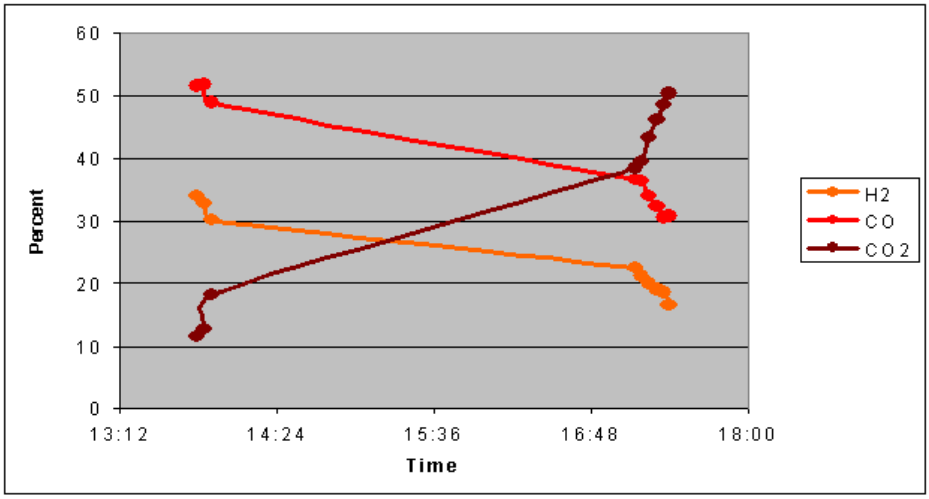

Figure 5: Change in H_2, CO and CO_2 Concentrations in the Utah/PRB Coal Blend Syngas

The trend in Figure 5 shows that not only did the overall fuel concentration for H_2 and CO decrease over time, but that the fuel concentration for H_2 and CO also decreased within the sample sets taken.

The drop in fuel concentration may be a product of the buildup of slag in the HOB. The buildup of slag decreases the volume within the HOB which causes the velocity of syngas to increase. The increase in the syngas velocity leads to lower residence times at the high temperature conditions within the HOB. This effectively reduces the residence time in which H_2 and CO can be generated within the HOB. The problem with this conclusion is that if the

buildup of slag in the HOB causes a decrease in fuel concentration of H_2 and CO, then the same result should be seen with the tests with the Illinois/PRB coal. A set of GC data was taken from a test with the Illinois/PRB coal and is presented in Figure 6. The data was taken over a time period of 2.5 hours.

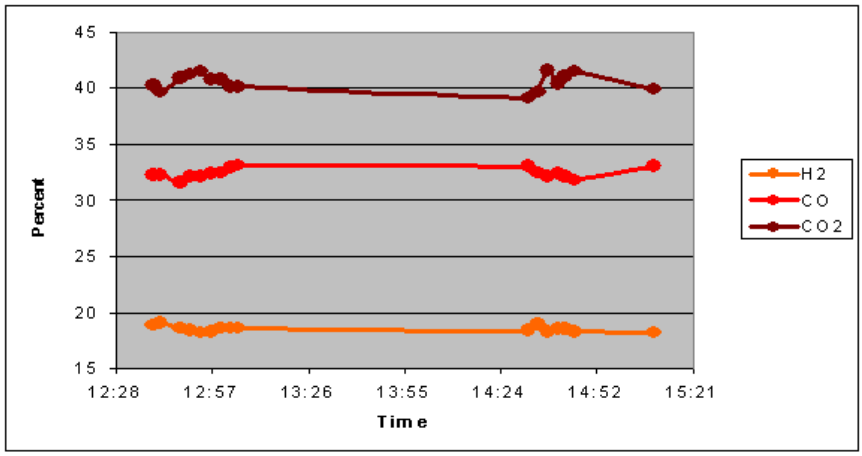

Figure 6: Change in H_2, CO and CO_2 Concentrations in the Illinois/PRB Coal Blend Syngas

From the data in Figure 6 it can be seen that there is only a slight decrease in the H_2 and a very slight increase in CO concentrations. The percent difference in the decrease of the initial to the final H_2 value is 3.2 %. The percent difference of the increase of CO is 2.2 %. This result indicates the syngas composition for this coal blend is not varying over time.

In comparing the data found in Figure 5 for the Utah/PRB case to Figure 6 for the Illinois/PRB case, it is concluded that the drop in fuel concentrations for H_2 and CO during the Utah/PRB case does not depend upon slag buildup in the HOB since there was also slag buildup for the Illinois/PRB case.

Utah/PRB Coal Blend Testing Campaign

A single OTM tube was used in the experiments with the Utah/PRB blend and was tested for 22 different runs. Each run requires a heat up and cool down cycle, which means that the OTM tube survived 22 different thermal cycles. The total numbers of hours tested with this tube was 81.2 hours.

The focus of the experiments of the OTM with the Utah/PRB coal blend were to shakedown the reactor, accumulate testing hours and to obtain the following data:

1. Effect of heating rate of the OTM on the O_2 flux performance
2. Comparison of thermocouple temperature readings at different points on the OTM
3. Effect of O_2 flux performance of the OTM as a function of inside OTM temperature
4. Effect of O_2 flux as a function of O_2 partial pressure within the OTM and temperature
5. Effect of prolonged exposure of the OTM to a syngas environment on the O_2 flux performance
6. Solid flux measurement of char and ash in the HOB

Testing Method of OTM Tube in Top Port

The initial tests of the Utah/PRB testing campaign focused on maximizing the OTM tube performance. Oxygen flux is dependent on tube temperature as well as fuel concentration surrounding the tube. To maximize temperature, the OTM tube was placed in the top port of the OTM section. A visual depiction of this arrangement is provided in Figures 7-9. Figure 7shows the OTM or second section of the oxygen transport membrane reactor (OTMR). Figure 8 shows the position of the OTM in the top port. The placing of the OTM in the top port was done to allow radiation from the torch to aid in the heat up the OTM tube to a predetermined maximum temperature limit. Based upon conversations with Praxair, it was determined to take the OTM tube to temperatures up to a maximum of ~1850°F. Temperatures above that threshold may degrade the membrane and lead to a reduction in oxygen flux.

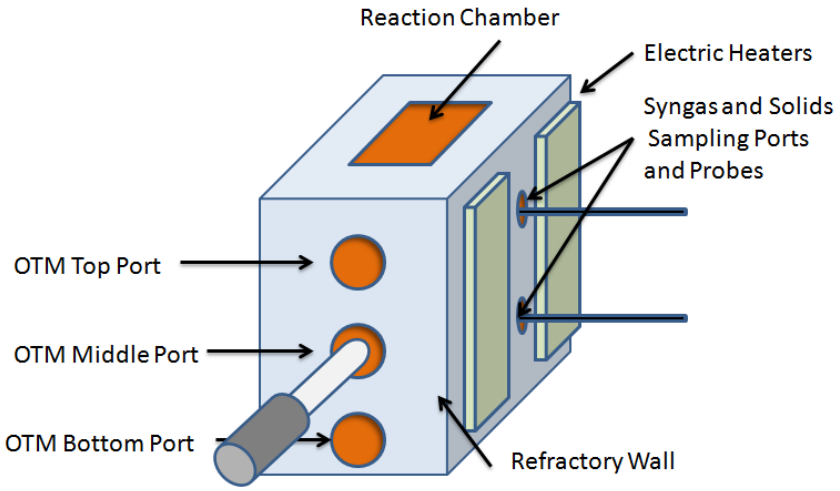

Figure 7: Inner Components of the OTM Section of the OTMR

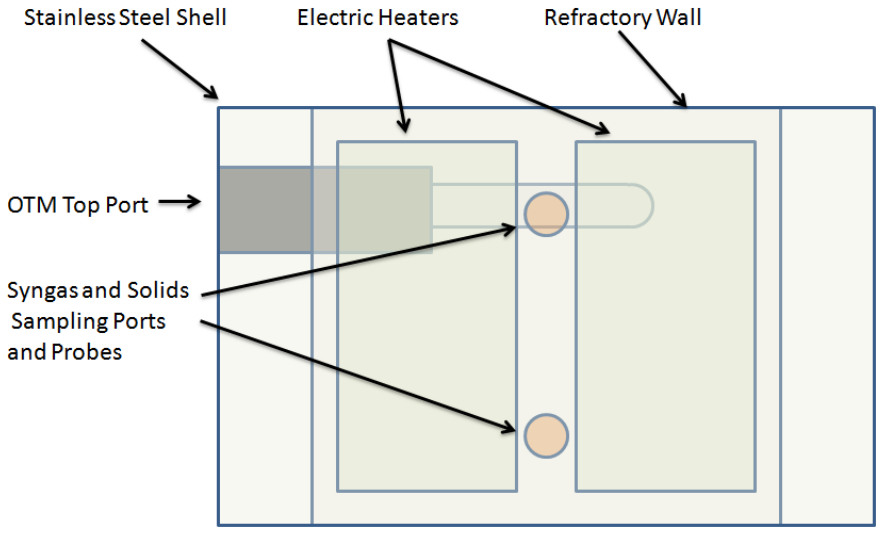

Figure 8: Location of OTM Tube in Top Port

The advantage of testing the OTM tube in this position is due to its proximity to the torch. Because the OTM tube is closer to the torch, it is possible to heat up the tube to operational conditions in a shorter amount of time. This also enables the tube to reach the peak temperature of 1850^{o}F. One drawback to having the OTM tube in such close proximity to the torch is that care must be taken to ensure the OTM tube does not experience rapid changes in temperature. An OTM tube can be thermally shocked when the tube is heated or cooled too quickly. Shocking the OTM tube can result in cracks, which develop within the porous support and leads to leaks.

The integrity of the OTM tube is ensured by adjusting the flow rate of air to the OTM tube. When the temperature of the tube is rising too quickly, the operator responds by increasing the flow of air to the OTM tube. The increase in air flow reduces the rate at which the tube heats up, leading to a better heat up rate for the OTM tube. A similar approach is taken if the OTM tube is cooling down too quickly. In this case air flow is restricted so that the tube cools down at a lower rate.

A disadvantage of testing the OTM tube in the top port is that fuel samples cannot be extracted before and after the OTM tube. Fuel samples are withdrawn from the reactor and analyzed using a Varian Micro-GC. There are two sampling ports for each section. When the tube is in the top port the fuel sampling line is right next to the OTM tube. Because there is insufficient distance from the tube at the sampling port, the fuel concentrations can only be sampled prior to the OTM tube or at the OTM tube surface. The sampling of the gas close to the tube surface is an interesting measurement, but it cannot account for the change in fuel gas composition before and after the OTM tube. Thus in this OTM tube configuration it is not possible to estimate what percent of the fuel was consumed by the OTM tube.

The general method for testing the OTM tube in the top port consisted of heat up, optimization, and cool down periods. The heat up portion of the run takes the longest amount of time. It involves bringing the OTM tube up to operating temperature. When the tube is at operating temperature, different parameters are adjusted to maintain the tube temperature close to 1850^{o}F. This involves making modifications to the flow rate of air and fuel to the torch, changes in the flow to the OTM tube, and changes in the flow of CO_2 to the HOB gasifier. Effects to the OTM tube from changing the first two parameters are fairly self explanatory. Decreasing the torch flow rates (both air and fuel) and increasing the flow of air to the OTM tube will lower the tube temperature. The third parameter is less intuitive and the mechanism for bringing down the tube temperature is less understood. By way of explanation, there is a supply of CO_2 provided to the coal feeder elbow to aid in the flow of coal to the HOB gasifier. In consultation with Praxair, it was suggested that supplying a flow of CO_2 to the flow of coal solids to the HOB would reduce the onset of clogging from the coal. This result was verified in experiments during the shakedown of the HOB.

If was found that an increase in the flow of CO_2 to the HOB caused a decrease in the temperature of the OTM tube. This decrease is likely due to fuel dilution and a subsequent reduction in the temperature of HOB.

Testing Method for OTM Tube in Middle Port

Tests were performed with the OTM tube placed in the middle port as shown in Figure 9. The advantage of having the OTM tube in the middle port is that it is between two reactor sampling ports. This allows the syngas from the HOB to be tested before and after the OTM tube. The disadvantage of this position is that it is not possible to maintain tube operating temperatures above ~1700^{o}F. This temperature limit restricts the amount of O_2 that can be generated by the OTM tube.

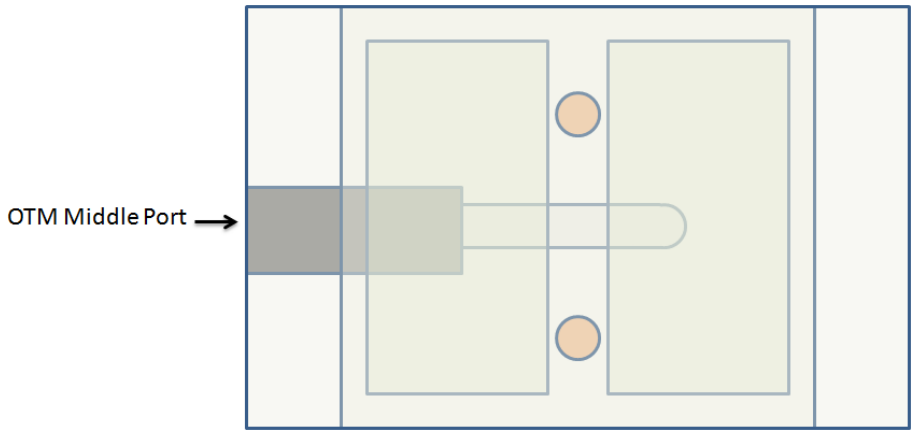

Figure 9: Location of OTM Tube in Middle Port

The main restriction in testing the OTM tube in this port is the slow heat up rate. Since the OTM tube is located lower in the OTM section, the tube is more shielded from the radiation of the torch. This results in the tube taking more time to heat up to operating temperatures.

The purpose of having the tube in this position is to be able to estimate the amount of fuel consumed by the OTM tube. By sampling the fuel concentration before and after the OTM tube, it is possible to estimate how much fuel has been consumed. Results of this analysis are given in the experimental results for the Illinois/PRB coal blend section of the report.

Effect of Heating Rate on OTM O_2 Flux Performance

The rate at which the OTM is heated is affected by the syngas fuel composition, the initial temperature of the OTM and the rate of heat transfer from the reactor walls. The relative percents of H_2 and CO in the syngas impact the performance of the OTM by the relative supply of fuel present at the OTM surface. The increase of fuel species at the membrane surface drives higher rates of O_2 flux and consequently increases the heating rate of the OTM. The initial temperature of the OTM reached prior to producing syngas from the HOB also has an effect of the performance of the OTM. The higher the starting temperature, the higher the relative O_2 flux, which causes higher heating rates. The reactor is given 12+ hours to heat such that the OTM is between 1450-1550^{o}F prior to turning on the HOB. The higher the initial temperature of the OTM prior to O_2 flux, the less time is needed to reach higher operating temperatures. The other factor that influences the heating rate of the OTM is the transport of heat from the reactor walls to the OTM. Heaters are used to heat the refractory of the reactor which in turn heat the OTM predominately through radiation.

There is a potential that the heating rate of the OTM may have an effect on the O_2 flux. Data was analyzed for two different runs with similar operating conditions but with different heating rates to determine if there is a measureable effect on the O_2 flux with respect to heating rate. The data used for this analysis is given in Figures 10-11.

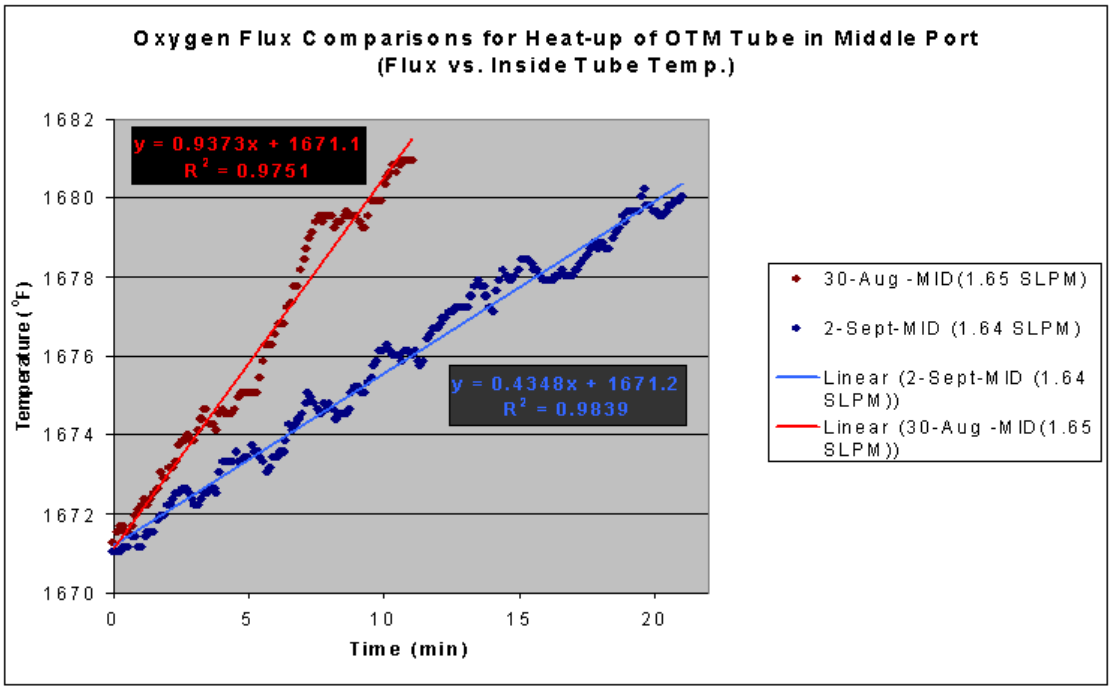

Figure 10: OTM Heating Rates

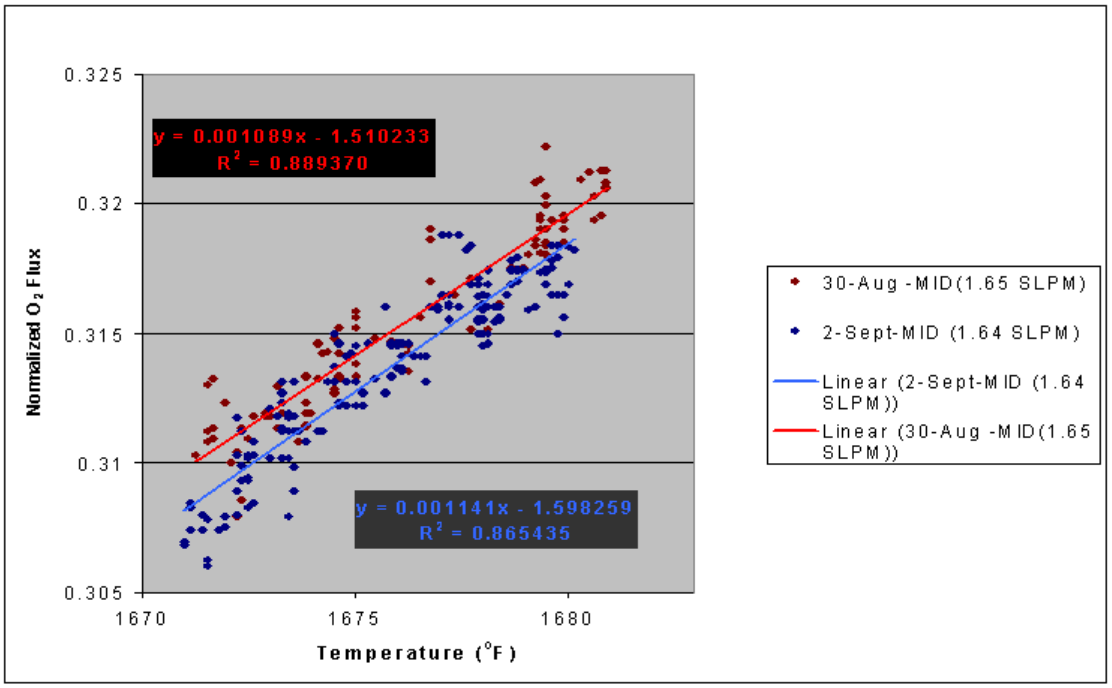

Figure 11: Changes in Performance for 30-Aug. and 2-Sep.

The two runs in Figures 10 and 11 were performed with a Utah/PRB coal blend with the flow rate of air to the OTM from 1.64-1.65 SLPM. In these experiments, the OTM tube is located in the middle port. As seen in Figure 10 the heating rate of 30-Aug is over two times higher than that of 2-Sep. This corresponds to a 53.61 % difference in the heating rates. With such a large difference between the heating rates, it is very possible that such a heating rate would have an effect on the O_2 flux of the OTM. The normalized O_2 fluxes for the same temperature range given in Figure 10 are compared in Figure 11. These results in Figure 11 show that there is a small change in the normalized O_2 flux between the two runs. If the slopes are assumed to be the same, then the intercept value can be compared for the two runs. The percent difference between the y intercept values of the two runs is 5 %. This is a very small degree of change between the two runs. Further, in Figure 11, it can be seen that much of the data between the two runs overlap, thus it is possible that the 5% difference between the tread line y-intercepts is a result of experimental error and cannot be attributed to the heating rate of the OTM. This leads to the conclusion that the heating rate of the OTM does not have an impact on the performance of the O_2 flux through the OTM.

Inside and Outside OTM Temperature Reading Comparisons for OTM in Top and Middle Port

The temperature readings from the OTM were measured in degrees Fahrenheit with the thermocouple positions depicted in Figure 12. Error is introduced into the measurement by the nature of the thermocouples used. Closed ungrounded 1/16 in. type K thermocouples were used on both the inside and outside temperature readings.

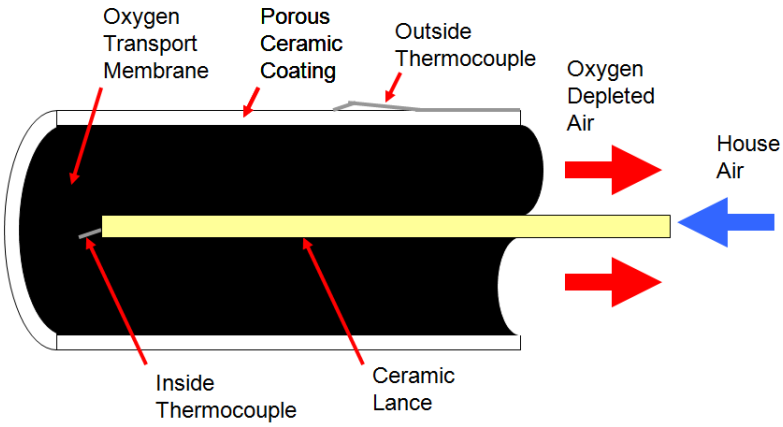

Figure 12: Cutaway View of a Praxair OTM

Presented in Figure 13 is the percent difference between the outside OTM temperature to the inside temperature. These experiments were conducted when the OTM was in the top port where the difference in the temperatures was most pronounced. Data was collected using the inside temperature as the reference. The inside temperatures considered ranged from 1560-1680°F in increments of 20°F. It is shown that as the flow rate of air to the OTM increases the percent difference increases. The percent difference in temperature also increases as the normalized flux of the OTM decreases. This means that the two temperatures on the OTM approach each other as the temperature and the normalized O_2 flux of the OTM increases.

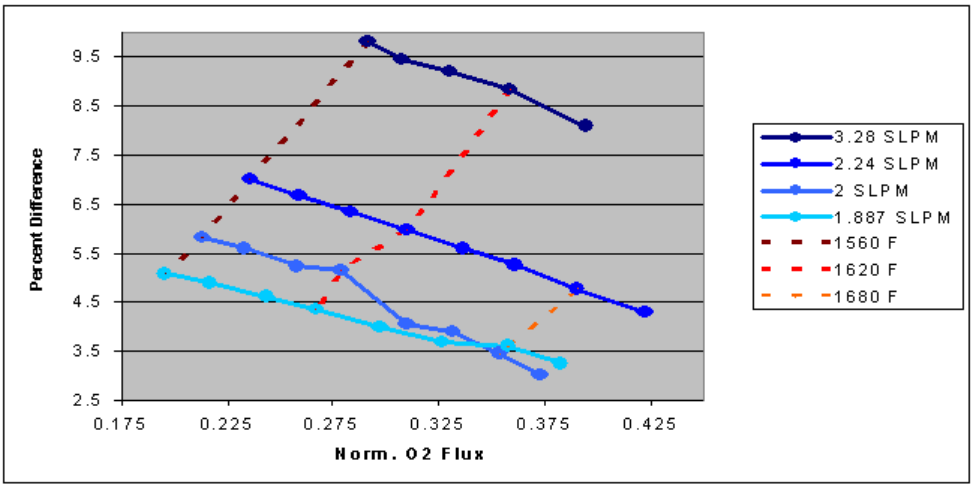

Figure 13: Percent Difference from the Outside to the Inside Temperature in the Top Port

The percent difference is calculated using the following expression:

$$Percent\ Difference = \frac{T_{outside} - T_{inside}}{T_{outside}} * 100 \qquad [1]$$

It can also be seen in Figure 13 that at 1.887 SLPM there is a point where the percent difference in the temperature crosses the trend for 2 SLPM. This result may indicate that there is a potential asymptotic minimum value for the percent difference in temperature.

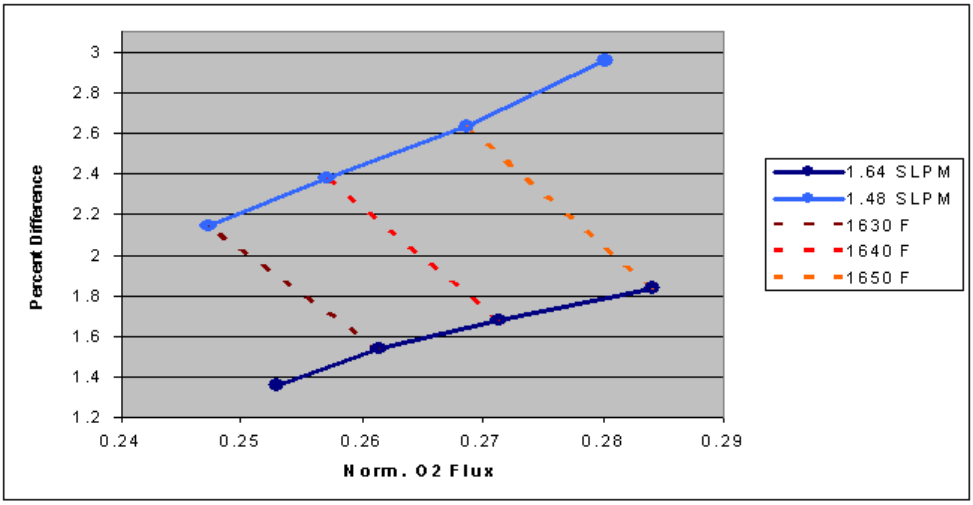

Figure 14: Percent Difference from the Outside to the Inside Temperature for the Middle Port

When the OTM was placed in the middle port the difference in temperature of the inside and outside thermocouples, as seen in Figure 14, had the opposite trend as compared to the data for the top port in Figure 10. As the flow rate of air to the OTM increased, the percent difference decreased. Also the percent difference increased as the temperature and normalized O_2 flux increased.

With the OTM in the middle port the percent difference is calculated using the following expression:

$$Percent\ Difference = \frac{T_{inside} - T_{outside}}{T_{inside}} * 100 \quad [2]$$

As in Figure 13, the isotherms are taken using the inside temperature as the reference. The temperature range considered is 1630-1650°F with increments of 10°F.

The comparison of the data given in Figures 13 and 14 illustrate the difference in operating conditions using the two different testing positions within the OTMR. When the OTM is in the top port, $T_{outside}>T_{inside}$. This may indicate that heat is transferred from the outside ceramic surface inward to the membrane surface. When the OTM is in the middle port $T_{inside}>T_{outside}$ which indicates that heat is transferred from the membrane to the outside ceramic surface. Note that for this condition, the temperature difference tends to be small, as illustrated below.

An additional two sets of experiments were analyzed with similar operating conditions, but with the OTM in the two different port positions. The flow rate of air to the OTM was 2.2 SLPM for the experiment of the OTM in the top port and 2.24 SLPM in the middle port. The raw data for this test is shown in Figure 15.

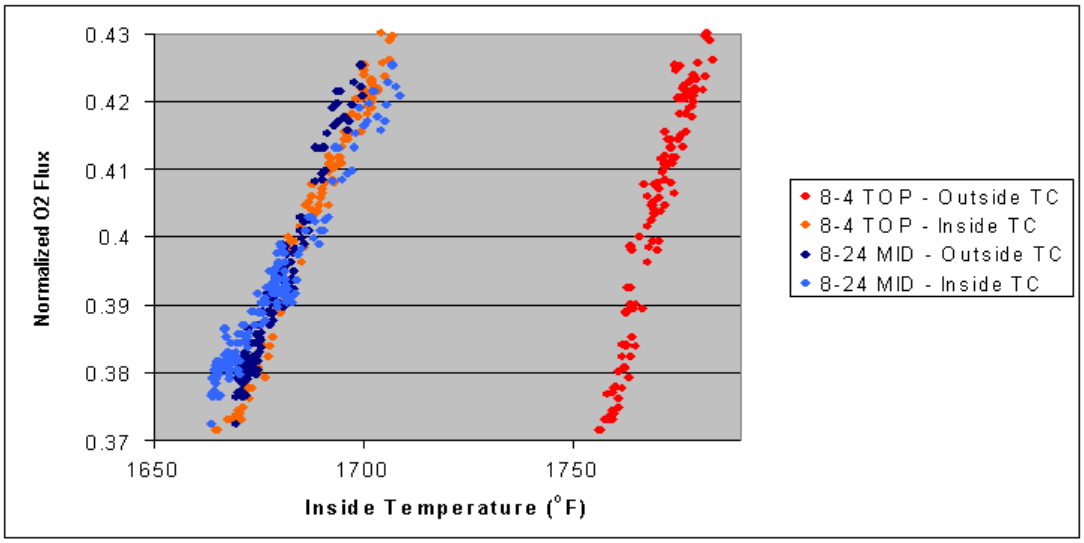

Figure 15: Raw Data Comparison for O_2 Flux vs. Temperature for Top and Middle Tube Positions

As seen in Figure 15 the temperature difference in $T_{outside}$ and T_{inside} is more pronounced when the OTM was in the top port. It is also interesting to note that the inside temperatures of the two tests were very comparable. This shows that the inside temperature of the OTM is consistent with tests conducted at different port locations.

Calculations were made using equation 1 on both the top and middle positions of the OTM using the raw data in Figure 15. The results are presented in Figure 16.

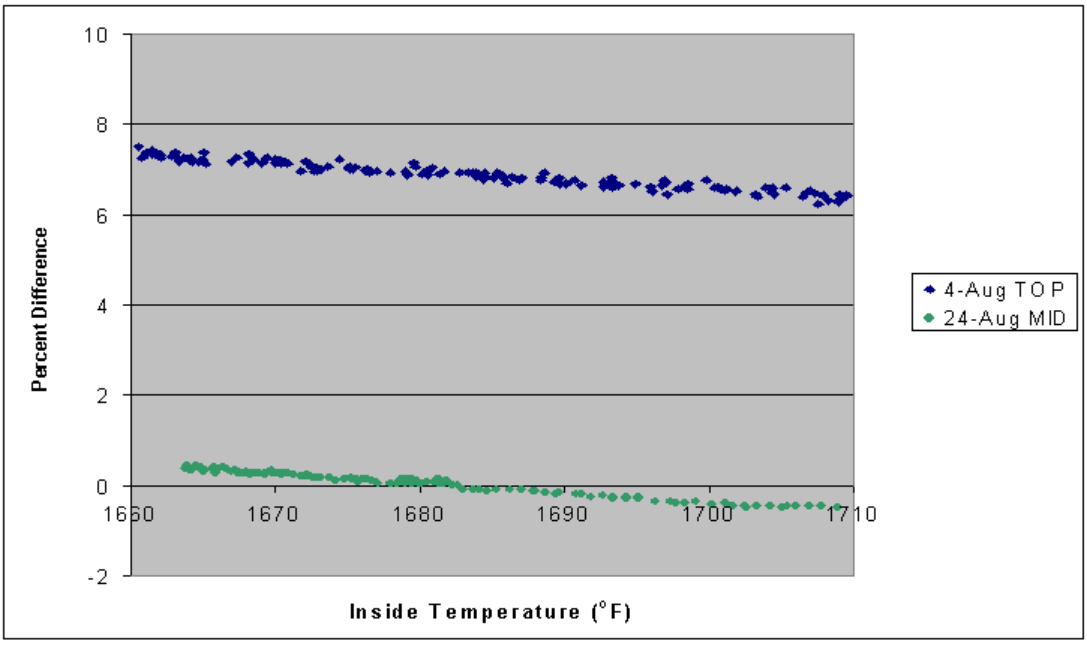

Figure 16: Raw Data Comparison for Percent Difference vs. Temperature for Top and Middle Tube Positions

The results in Figure 16 quantify the percent difference in the temperatures of the outside to the inside temperatures shown in Figure 15. Both the top and middle port tests show a decrease in the percent difference as the inside tube temperature increases. As expected, the percent difference is much higher for the top port, ranging from 7.5 to 6.2%, which corresponds to a differences in temperatures of 102.6 to 89.5°F respectively. The percent difference is almost negligible for the middle port which ranges from 0.32 to -0.52 % which corresponds to temperature differences of 5.8 to -7.6°F respectively. Negative values are reported for the percent difference because the absolute value of the difference is not taken. The transition of the percent difference from positive to negative indicates that the $T_{inside} > T_{outside}$.

Normalized O_2 Flux vs. O_2 Concentration and Temperature

In Figure 17 the change in the normalized O_2 flux through the OTM is plotted as a function of scaled O_2 concentration. Scaled O_2 concentrations were used to preserve the proprietary nature of the O_2 flux through the OTM. Three different isotherms are considered along with six different flow rates of air to the OTM. The different flow rates of air to the OTM allow for different O_2 concentrations leaving the OTM.

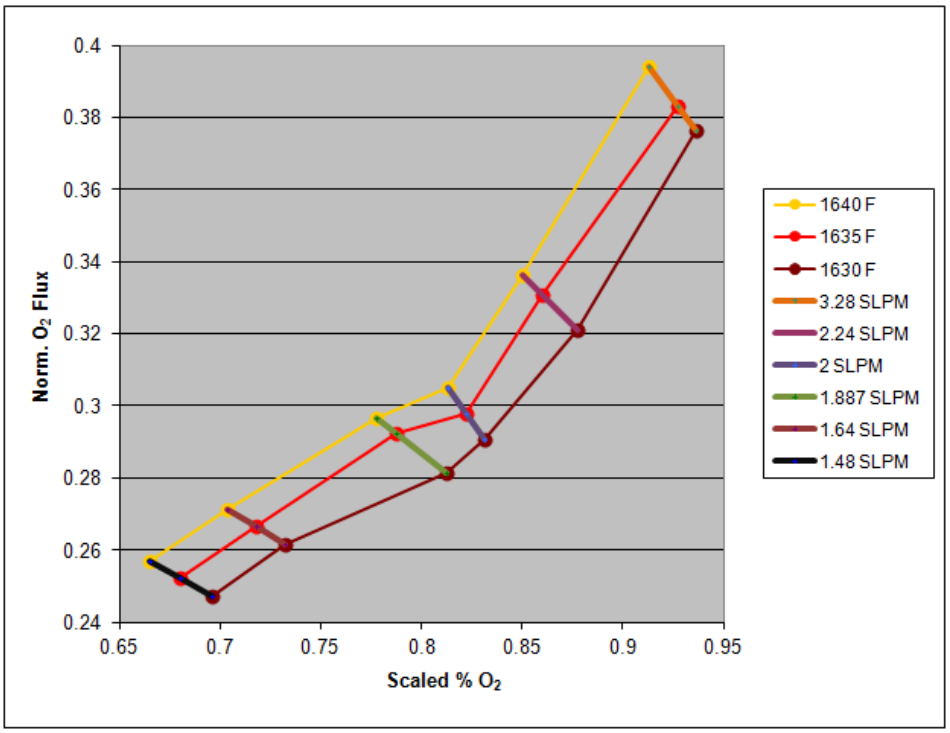

Figure 17: Normalized O_2 Flux vs. O_2 Concentration and Temperature

Effect of Prolonged Used of an OTM in the Utah/PRB Coal Blend

Data from five different runs were analyzed to determine if there was an effect of the prolonged use of the OTM, as shown in Figure 18. It is possible that the prolonged use of an OTM in a syngas envirionment may corrode the OTM and lead to a decrease in O_2 flux. Ideally, a single OTM would be tested for a very long time to determine corrosion issues of an OTM. Due to time constraints and operation restrictions with the reactor, only ~80 hours were accumulated for the Utah/PRB coal. Data were collected from runs with the OTM in both the top and middle ports.

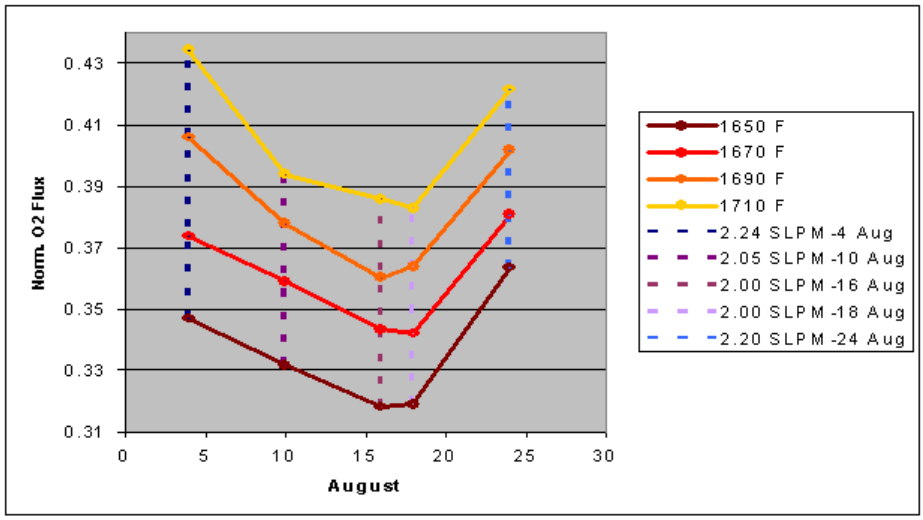

Figure 18: Change in Normalized O_2 Flux over Time for Utah/PRB Coal Blend Campaign.

This plot shows the change in OTM flux performance with time for the Utah/PRB coal blend. The campaign with the Utah/PRB coal blend was focused on optimizing the OTM tube performance. As a result, several different settings for air flow rate to the OTM were investigated. From this data, it is clear that determining the change in tube performance over a period of time was difficult to obtain. Figure 18 depicts a set of runs over a period of almost 3 weeks where the OTM was run at relatively similar conditions.

The y-axis data points represent the average of the 6 numerical values closest to the isothermal inner tube temperature considered for each of the dates sampled. The runs taken for the operating condition of ~2.2 SLPM are distinguised by blue scale colors. Two runs were taken at this condition and are comprised of the first and last test dates used for this figure. The runs taken for the operating condition of 2.0 SLPM are distinguished by purple scale colors which comprise of the middle three test dates used in this figure.

It can be seen from this graph that the flux of the OTM both decreases and increases with time. The change in flux is clearly dependent on the inner tube temperature, as shown by the isotherms considered. On closer inspection, it appears that the trends shown correlate reasonably well with the flowrate of air coming into the tubes, within some reasonable margin of experimental air. The highest values of O2 flux observed are for the flowrates of ~2.2 slpm (the first and last test dates). The intermediate test dates were at ~2.0 slpm, and may indicate a slight decrease in O_2 flux over time, but the changes are small. Also, since this test series was more exploratory in nature, primarily attempting to optimize overall performance, it is possible that other variables were not controlled as tightly to provide a truly accurate picture of this effect.

Thus, this data shows does not provide conclusive evidence of OTM flux degradation over time for the Utah/PRB coal blend testing campaign.

Ash Deposition on OTM Tube

During 58 hours of testing time, ash was not removed from the OTM tube. The presence of ash on the OTM tube may lead to a lower O_2 flux in the tube as a result of an added diffusional resistance for the syngas to reach the OTM surface. Figure 19shows the collection of ash on the tube. It should be noted that the surface facing the viewer is the surface with the most ash deposits and represents the downstream side of the tube. Deposits are greater downstream due to the recirculation zone that forms on the back side of the tube. In the reactor, this tube surface was downstream of the HOB gasifier and facing the torch. It should also be noted that patches of ash were present on all the surfaces of the OTM tube.

Figure 19: Accumulation of Ash Buildup on OTM Tube for Tests with Utah/PRB Coal Blend

Though only ash is present on the pictured OTM, in actual operation there will be both ash and char around the OTM. Both char and ash are entrained from the HOB and deposited on the OTM. This flow of char and ash through the OTMR has been measured and is reported later in the report.

Estimation of Syngas Flow Rate

A mass balance was performed on the HOB to estimate the molar flow rate of syngas leaving the HOB for the Utah/PRB coal blend. A diagram showing this mass balance is depicted in Figure 20. The molar flow rates (N_i) are shown in Table 5 for the gaseous streams and Table 6 for the solid coal stream.

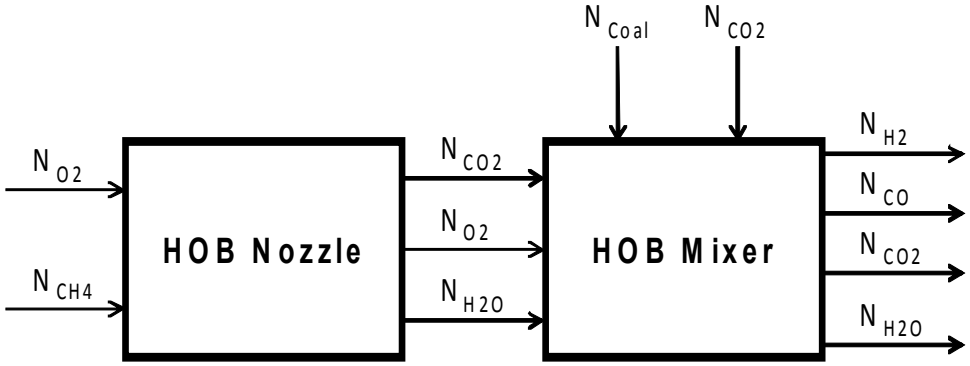

Figure 20: Mass Balance Diagram for Molar Flow Rates within the HOB

Table 5: HOB Molar Flow Rates for Utah/PRB Coal Blend (mol/min)			
	Nozzle Input Stream	Mixer Input Stream	HOB Syngas Stream

H_2	-	-	0.1060
CO	-	-	0.1578
O_2	0.1878	0.1502	-
CO_2	-	0.0188	0.2043
CH_4	0.0188	-	-
H_2O	-	0.0376	0.1094

Table 6: Molar Coal Feed Rates for N_{Coal} with the Utah/PRB Coal Blend		
Feeding Rate 13.41 g/min	**wt %**	**Mixer Input (mol/min)**
C	61.8	0.5311
H	5.4	0.5506
O	25.5	0.1641
S	0.3	0.00097
N	0.86	0.0063
Ash	6.23	N/A
H_2O	10.7	0.0685

The Chemical Equilibrium Applications (CEA) program developed by NASA was used to estimate the moisture content in the syngas stream leaving the HOB for the Utah/PRB coal blend. The calculation was performed using a calculated chemical composition of $C_1H_{1.04}O_{0.31}N_{0.01}S_{0.0018}$ for the Utah/PRB coal blend. The equilibrium calculation was performed at a constant temperature and pressure at conditions that mimic conditions within the HOB. The results are given in Table 7.

Table 7:Experimental Micro-GC Results Compared to Calculated Equilibrium Composition with NASA CEA Program				
	Experimental	CEA (dry)	Percent Difference	CEA (wet)
H_2	0.2471	0.2265	5.32	0.1828
CO	0.3192	0.3371	4.56	0.2721
CO_2	0.4165	0.4364	8.34	0.3522

H_2O	Not Available	-	-	0.1886
CH_4	0.0132	-	-	0

From Table 7 it can be seen that the equilibrium calculation results are in reasonable agreement with the experimental results. The highest percent difference was with CO_2 with 8.34%. Using this equilibrium calculation, the concentration of H_2O in the syngas can be estimated. This data also allows the calculation of the syngas flow rate based upon a mass balance for O_2. This calculation was made by assuming that oxygen is conserved in the system. Based upon the mass balance calculation, the flow rate of syngas was estimated to be 17.2 SLPM for the Utah/PRB coal blend. The dry flow rate of syngas is 13.88 SLPM or 0.4681 mol/min. This calculation was made by considering the O_2 that entered the HOB through the lean HOB nozzle flame, the supply of CO_2 into the coal feeder elbow and the O_2 present in the pulverized coal. It was also assumed that all the O_2 present in the coal reacts during the gasification process within the HOB, and that no tramp air leaks into the HOB.

Solids Flow Measurements

The flow of solids into the OTM zone of the reactor was measured using an isokinetic probe. Solids are collected through an opening in a stainless steel probe pictured in Figures 21 and 22.

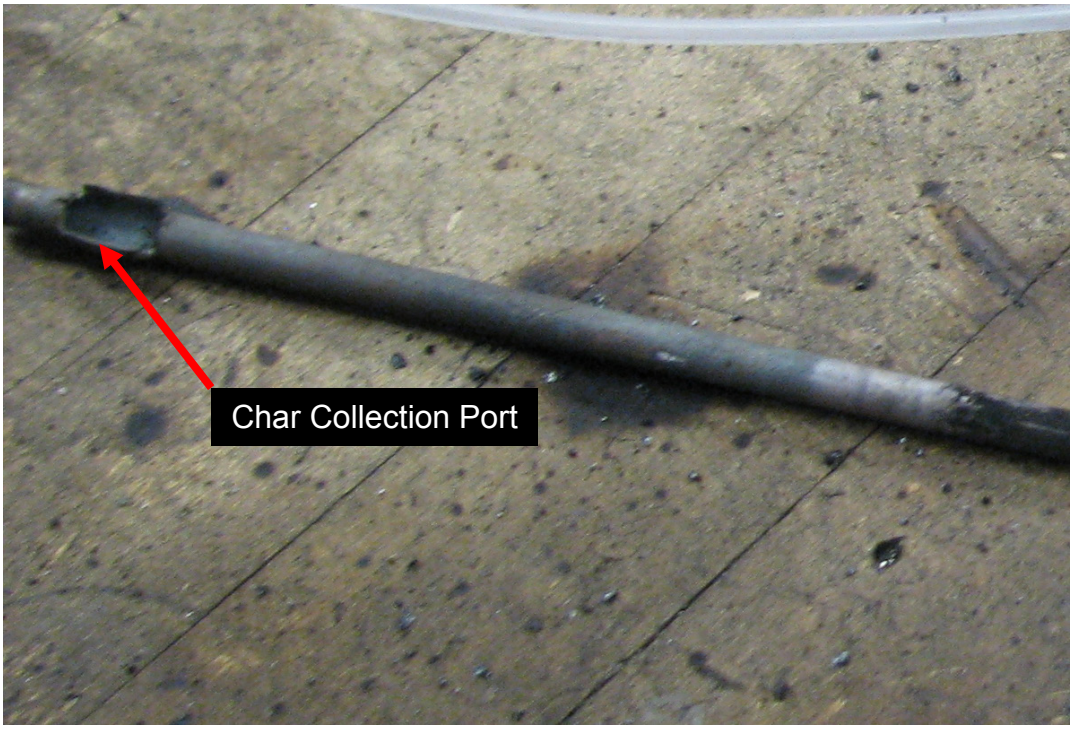

Figure 21: Char and Ash Collection Probe

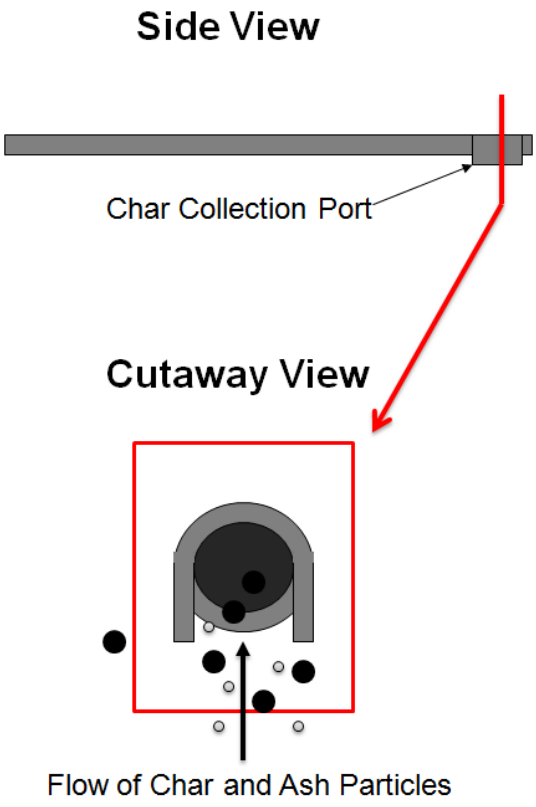

The solids collection probe draws in char and ash to a stainless steel collection container. Entrained particles are impacted into the container wall and drop out of the entrainment gas due to momentum loss of the impacted particles and the velocity drop of the entrainment gas. This process is depicted in Figure 23.

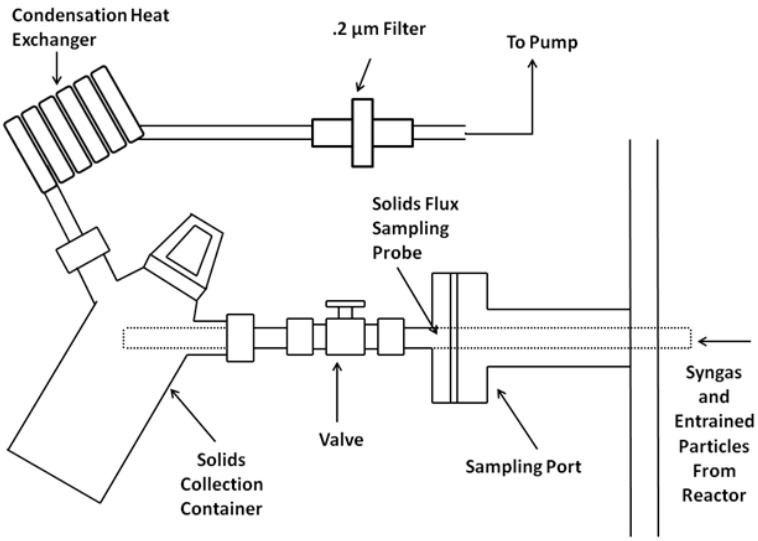

Figure 22: Char and Ash Collection Probe

As the sample is collected, char and ash form deposits on the solids sampling probe. These char and ash deposits eventually restrict the flow of solids in the probe. The buildup can be severe enough that flow of char and ash into the probe can be obstructed. It was found that sampling times of 90 seconds provided good results without the buildup of a char and ash obstructions in the sampling line.

The deposition of char and ash in the sampling line needs to be accounted for in the measured char and ash mass. The measured values of char and ash were corrected with the measured amount of char and ash in the collection probe.

Char and ash were sampled at two points in the reactor. The ports in the reactor used to sample the solids flux are the same as those used to sample the reactor syngas using the Micro GC. The top port of the HOB section was used along with the bottom port of the OTM section. The probe was positioned such that the sampling opening would be in the axial centerline of the reactor.

To ensure isokinetic sampling, the velocity of the syngas was calculated from the estimated syngas volumetric flow. A pump was used draw the samples with a rotameter to control the flow. The solids flux is calculated using equation 3.

$$\dot{m}'' = \frac{m_{sample}}{t\, A_{s,\,probe}} \qquad [3]$$

$\dot{m}''$ = the solids mass flux

m_{sample}= mass of collected char and ash from the solids collection probe

t = time in which sample was collected

$A_{s,probe}$ = cross sectional surface area of the probe

The solids flow is calculated using the solids flux calculation with the multiplication of equation 3 by the cross sectional surface area of the reactor space within the OTMR ($A_{s,OTMR}$). The results of this calculation are given in Figure 24.

$$\dot{m} = \frac{m_{sample} A_{s,\,OTMR}}{t\, A_{s,\,probe}} \qquad [4]$$

The results of the entrained char and ash particle sampling for the Utah/PRB Coal blend are given in Figure 24. The data in Figure 24 shows that the sampled solids flow is between 2.15 and 2.56 g/s based upon centerline sampling of the OTMR. The solids flux is based upon the open area of the solids collecting probe is 0.143 g/in^2/s and 0.170 g/in^2/s. The solid flux calculations were made using equation 3. The position of the solids sampling probe is measured as a downstream distance with respect to the HOB. This gives a position of the probe relative to the fuel source.

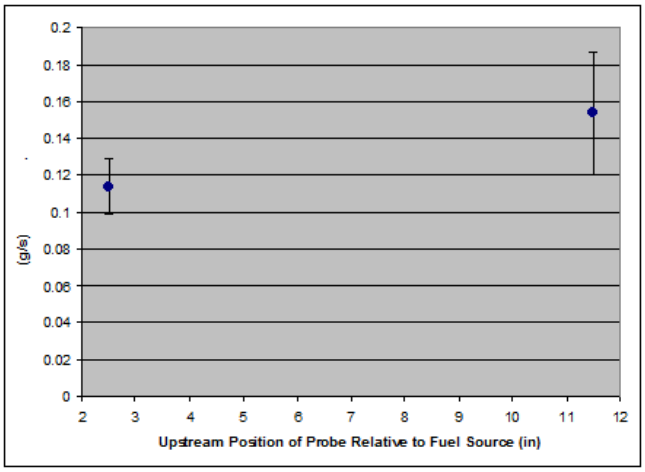

Figure 24: Diagram for Solids Collection Apparatus

The data in Figure 24 also shows that there is a significant degree of variability in the precision of the measurements, specifically at 11.5 inches. The high degree in variability is shown by the large standard deviation of the measurements as well as the change in the solids flow values from the two positions within the reactor. Three measurements were taken to obtain the average and the standard deviation was taken for the three data points.

Illinois/PRB Coal Blend Testing Campaign

The Illinois/PRB coal blend tests accumulated 78.5 hours of operation. These hours were accumulated over a total of 20 runs.

The tests conducted with the Illinois/PRB coal blend were designed to focus on getting repeatable measurements. Experimental operating conditions and methodology were refined to get consistent, repeatable data. In the process of performing these tests, some other experiments were conducted. These include:

7. Determination of the effect ash buildup on the O_2 flux through the OTM
8. Effect of O_2 flux performance of the OTM as a function of inside OTM temperature
9. Effect of percent O_2 leaving the OTM on the O_2 flux under isothermal conditions
10. Determination of minimum percent O_2 leaving the OTM to get normal performance
11. Sampling of the syngas before and after the OTM
12. Comparison of different temperature readings at different points on the OTM
13. Effect of prolonged exposure of OTM to syngas environment on O_2 flux performance
14. Measurement of char and ash solids flux within the OTMR

Ash Deposition on OTM Tube Surface

Three sets of experiments were used to determine the effect of that ash deposition on the OTM surface has on the O_2 flux performance. Unattached loose ash was collected on the top (downstream) surface of the OTM tube over the space of several weeks of operation. This loose ash was then removed through an air blower after the OTM had been cooled down. There is the possibility that some particles of ash fused to the ceramic support surface and remained after the loose ash was removed. The fusing of ash onto the surface of the tube will be referred to as fixed ash. It can be seen in Table 8 that the O_2 flux measurements with and without the loose ash are within the standard deviation of the O_2 flux from the OTM tube. This result shows that the collection of loose ash on the outside membranes surfaces does not add a significant resistance to the transport of H_2 and CO to the membrane

surface due to the low density and high permeability of the ash. It is not currently known if the accumulation of fixed ash affects the performance of the OTM tube.

Table 8: Normalized O_2 flux data analysis for tests prior to and after ash removal for the Illinois/PRB blend

Temperature (F)	**1550**	**1560**	**1570**	**1580**	**1590**	**1600**
11/9: With Ash	0.1165	0.1219	0.1283	0.1339	0.1416	0.1497
11/11: With Ash	0.1179	0.1226	0.1275	0.1346	0.1390	0.1468
11/14: Without Ash	0.1169	0.1222	0.1285	0.1343	0.1403	0.1482
AVG	**0.1171**	**0.1222**	**0.1343**	**0.1343**	**0.1403**	**0.1482**
St. Dev.	**0.0008**	**0.0004**	**0.0011**	**0.0004**	**0.0013**	**0.0014**

Normalized O_2 Flux Performance vs. Temperature

Data for the performance of an OTM tube vs. inside tube temperature in a high-sulfur Illinois/PRB blend is given in Figure 25. The oxygen flux in this graph is normalized and the error bars represent one standard deviation of the normalized flux values. This plots shows that the performance of the OTM tube is consistent and repeatable with a low degree of variability.

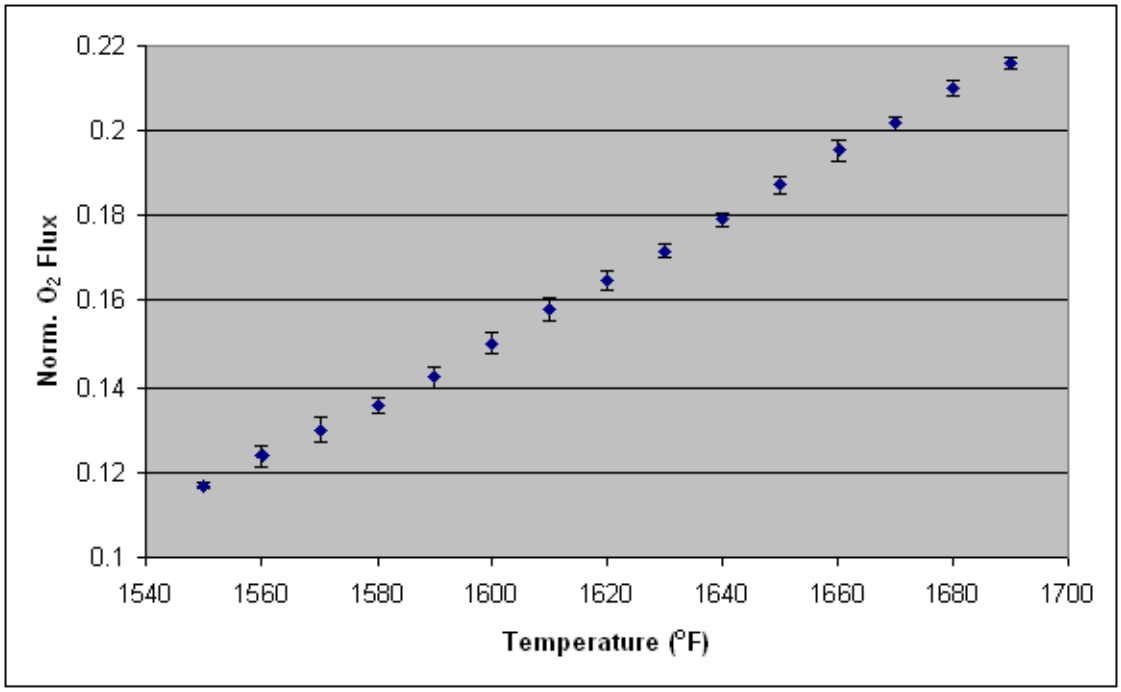

Figure 24: Measured Solid Flux for Utah/PRB Coal Blend vs. distance from the HOB.

It can be seen in Figure 26 that there is a linear relationship between the OTM tube performance and the temperature of the OTM tube. It should be noted, however, that this performance is restricted to the temperature range of 1550-1690°F.

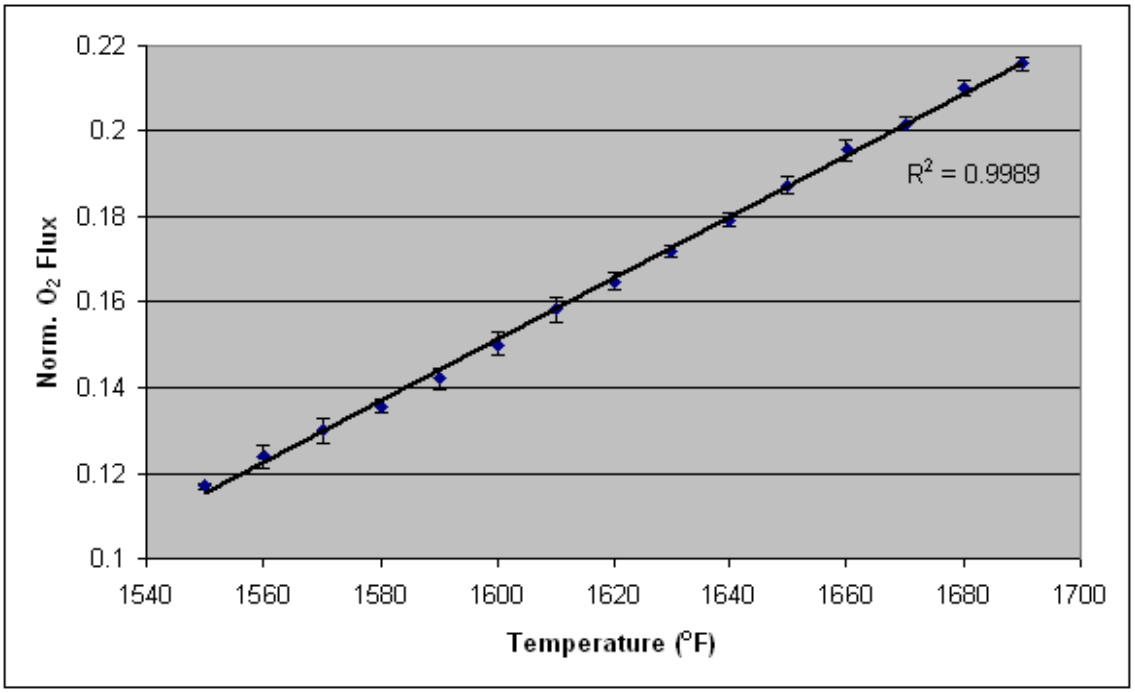

Figure 25: Performance plot for OTM tube with Illinois/PRB coal blend. Measured inside OTM tube temperature is plotted along the x-axis.

Effect of Diminishing O_2 Concentration within OTM on Normalized O_2 Flux Performance

Another observation from the data set is that at higher temperatures, the OTM tube performance departs from linearity, and this may be due to a reduction in the available oxygen concentration within the OTM tube. This limit can be visually seen in the data in Figure 27. It can be seen that the performance of the OTM tube follows a linear trend until the normalized oxygen flux of 0.24 is reached. At this point, the slope begins to decrease with increasing temperature. This phenomenon is due to the concentration of oxygen within the OTM tube as seen in Figure 28. Figure 28 suggests that there is a minimum oxygen concentration that must be maintained to ensure optimal OTM tube performance. This limit can be estimated to be 0.3 scaled % from the data in Figure 28.

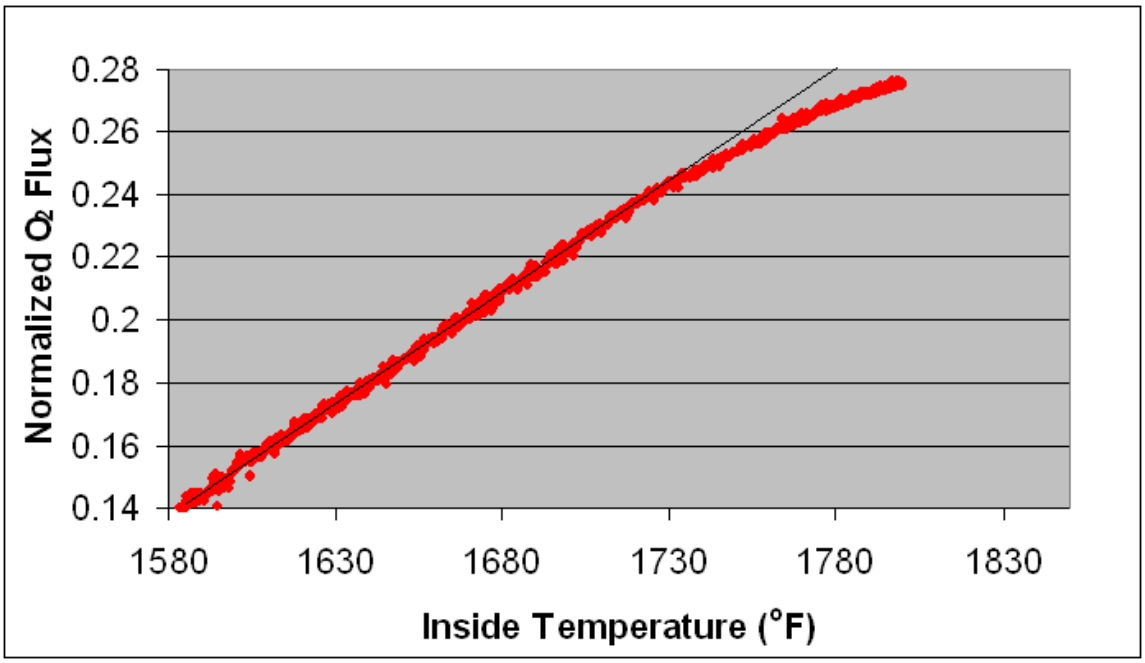

Figure 26: Performance plot for OTM Tube with Illinois/PRB Coal Blend with Tread Line.

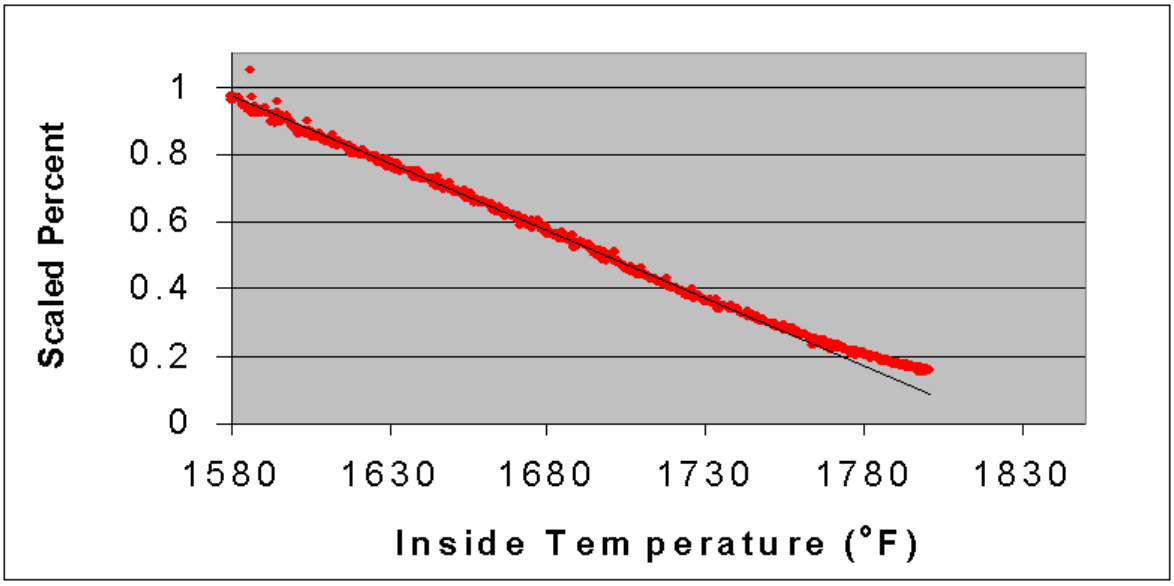

Figure 27: Reduction OTM Tube Performance at Higher Operating Temperatures.

Effect of O_2 Concentration within the OTM on Normalized O_2 Flux Performance

A single run was performed to analyze the effect oxygen concentration has on the normalized O_2 flux of the OTM tube. This data is presented in Figure 28 This figure shows that the partial pressure of oxygen within the OTM tube

increases the oxygen flux through a quadratic relationship. All of the data points in Figure 29 were taken at 1820°F to remove the effect of tube temperature on the O_2 flux.

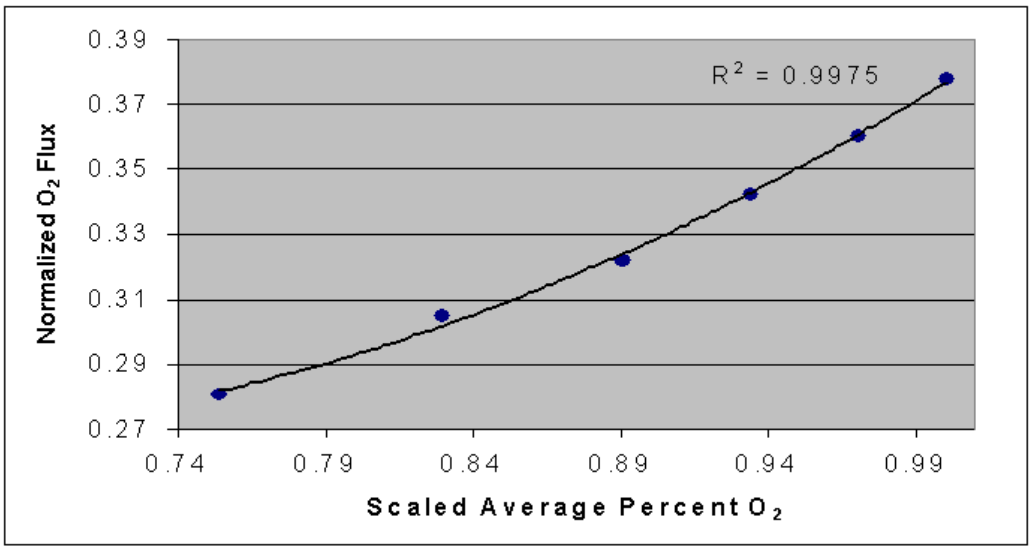

Figure 28: Relationship of the Reduction OTM Tube Performance due to Available Oxygen.

Point Calculation for OTM Flux and Fuel Consumption

Gas chromatograph measurements were taken before and after the OTM tube. As seen in Figure 9, there are Micro GC sampling ports available before and after the OTM tube. These ports were used to collect gas samples in order to estimate the fuel consumption efficiency of the OTM tube. The findings of these measurements are given in Table 9.

Table 9: Syngas Fuel Concentration (%) Before and After OTM Tube, 11/11/2011

	Before (Avg.)	Std Dev	After (Avg.)	Std Dev
H_2	17.98	0.34	17.58	0.12
CO	30.89	1.12	34.72	0.06
CO_2	49.77	0.96	46.4	0.19
CH_4	0.97	0.04	0.89	0.045
C_2H_4	0.18	0.01	0.14	0.02
C_2H_6	0.02	0.0003	0.006	0.006

The data in Table 9 suggests that H_2 was consumed in the process and that CO was generated. One potential explanation for the CO result is that some entrained char was gasified between the two

sampling ports to generate additional CO in the syngas. This observation could also explain why CO_2 decreased. It should be noted that the syngas was analyzed on a dry basis. It is possible to estimate the wet syngas composition based upon chemical equilibrium calculations; however, the estimated value will have at least a 3-6% difference between the estimated and the measured values based on earlier evaluations of the equilibrium calculations. This error would lead to additional uncertainty in drawing conclusions from the data because the difference in percents for some of the components is less than 1%. Thus, to estimate the wet syngas composition would not lead to any reliable conclusions.

It should also be noted that the residence time of the syngas between the two sampling ports is very low. With low gasification temperatures (~1650^{o}F) within the reactor, it is very unlikely that a measureable amount of syngas can be generated between the two sampling ports. The low syngas residence time and the low reactor temperature point to the conclusion that the reported data is an anomaly and cannot be used to estimate the percent of syngas consumed by the OTM.

Estimation of Syngas Concentration at Permeate Side of OTM Surface

A simplified approach to estimate the ratio of H_2 to CO fuel concentrations at the membrane surface was performed for the Illinois/PRB coal blend. This approach starts by determining the ratio of diffusivities of H_2 to CO through the ceramic porous support layer of the OTM. Using the Knudsen diffusivity model given by

$$D_{Kn,i} = \frac{2}{3} r \sqrt{\frac{8RT}{\pi MW_i}}, \qquad [5]$$

The ratio of the diffusivity of H_2 to CO can be calculated simply by taking the square root of the ratio of the molecular weight of CO to H_2, where the molecular weight of CO = 28.01 g/mol and H_2 is 1.008 g/mol.

$$\frac{D_{Kn,H_2}}{D_{Kn,CO}} = \sqrt{\frac{MW_{CO}}{MW_{H_2}}} = 3.73 \qquad [6]$$

Using this result, the relative mass flux of H_2 and CO across a porous membrane can be modeled using the thin film membrane model,

$$j = \frac{D}{l}\left(C_{syngas} - C_{OTM}\right) \qquad [7]$$

Where

j = molar flux [mol/cm^2/s]

D = diffusivity through pores [cm^2/s]

C = concentration of species on porous layer or OTM surface

This analysis assumes that a boundary layer does not exist at the porous membrane surface on the fuel side. The model also assumes that the diffusion of fuel through the pores can be modeled using Knudsen diffusion. Only H_2 and CO are accounted for in this analysis with CH_4, ethane and ethylene omitted.

$$j_{H_2} = \frac{D_{Kn,H_2}}{l}\left(C_{H_2,syngas} - C_{H_2,OTM}\right) \quad [8]$$

j_{H_2} = Flux of H_2 through the pores of the OTM ceramic porous support

D_{Kn,H_2} = Knudsen diffusivity of H_2 through the pores

$C_{H_2,syngas}$ = Concentration of H_2 in the syngas fuel stream

$C_{H_2,OTM}$ = Concentration of H_2 at the membrane surface

Similarly, the flux of CO through the porous ceramic support can be modeled using the following relationship.

$$j_{CO} = \frac{D_{Kn,CO}}{l}\left(C_{CO,syngas} - C_{CO,OTM}\right) \quad [9]$$

To simplify the analysis, it is further assumed that the concentrations of H_2 and CO at the membrane surface are much smaller than on the surface of the porous support.

$$C_{H_2,syngas} \gg C_{H_2,OTM}$$

$$C_{CO,syngas} \gg C_{CO,OTM}$$

Using this assumption, the ratio of the molar fluxes of H_2 and CO can be determined using the ratio of Knudsen diffusivities and the ratio of mole fractions of H_2 and CO.

$$\frac{j_{H_2}}{j_{CO}} = \frac{D_{Kn,H_2}}{D_{Kn,CO}}\frac{C_{H_2,syngas}}{C_{CO,syngas}} = 3.73\frac{x_{H_2,syngas}}{x_{CO,syngas}}$$

Where

$$\frac{D_{Kn,H_2}}{D_{Kn,CO}} = 3.73$$

A sample calculation can be performed using volume fractions from Table 9 to yield the following

$$x_{H_2,syngas} \approx 0.18$$

$$x_{CO,\,syngas} \approx 0.3$$

Using these values the ratio of the molar flux of H_2 to CO is given by

$$\frac{j_{H_2}}{j_{CO}} = 2.49$$

This indicates that 71.3% of the fuel consumed at the membrane surface is H_2, with 28.7% being CO. This conclusion is based on the assumption that the percent of the fuel consumed is dependent on the resistance to mass transfer of the fuel through the porous ceramic support on the OTM.

This result shows that the major species being consumed at the membrane surface is H_2. This is in spite of H_2 usually only accounting for less than 20 % of the total volume of syngas. The high permeability of H_2 through the pores of the ceramic porous support leads to the hypothesis that the H_2 content in the syngas has a large effect on the measured performance of the OTM. In a subsequent section, we will show that there is a significant difference in the measured flux of O_2 with the Utah/PRB blend and the Illinois/PRB blend. The hypothesis is that the difference in tube performance is a result of different concentrations of H_2 in the syngas fuel.

Calculating Syngas Flow Rate from HOB

Mass Balance Approach

Calculations were made using a mass balance and a chemical equilibrium calculation to estimate the flow rate of syngas leaving the HOB. Molar stream data are given in Tables 10 and 11. The same mass balance approach that was used for the Utah/PRB coal blend, was used for the Illinois/PRB coal blend.

Table 10: HOB Molar Flow Rates for Illinois/PRB Coal Blend (mol/min)

	Nozzle Input Stream	Mixer Input Stream	HOB Syngas Stream
H_2	-	-	0.0905
CO	-	-	0.1616
O_2	0.2367	0.2681	-
CO_2	-	0.0574	0.2155
CH_4	0.0237	-	-
H_2O	-	0.1073	0.1656

Table 11: Molar Coal Feed Rates for N_{Coal} with Illinois/PRB Coal Blend		
Feeding Rate 13.41 g/min	**wt %**	**Mixer Input (mol/min)**
C	64	.7146
H	5.3	.7038
O	20	.1673
S	2.1	.0087
N	1	.0093
Ash	7.7	N/A
H_2O	7.9	.0587

The CEA program was again used to estimate the moisture content in the syngas stream leaving the HOB for the Illinois/PRB coal blend. The calculation was performed using a calculated chemical composition of $C_1H_{1.11}O_{0.29}N_{0.015}S_{0.0023}$ for the Illinois/PRB coal blend. The equilibrium calculation was performed with a specified temperature and pressure which were chosen to mimic conditions within the HOB.

From Table 12 it can be seen that the equilibrium calculation results provide a reasonable representation of the experimental data. The highest percent difference was again with CO_2 with 5.324%. Based upon the mass balance of oxygen within the HOB system, the flow rate of syngas was calculated to be 18.88 SLPM for the Illinois/PRB coal blend. The dry flow rate of syngas is 13.87 SLPM or 0.4676 mol/min.

Table 12:Experimental Micro-GC Results Compared to Calculated Equilibrium Composition with NASA CEA Program				
	Experimental	CEA (dry)	Percent Difference	CEA (wet)
H_2	0.1938	0.1935	0.1548	0.1421
CO	0.3593	0.3457	3.785	0.2539
CO_2	0.4376	0.4609	5.324	0.3385
H_2O	Not Available	-	-	0.2602
CH_4	0.0132	-	-	0

<u>N_2 Tracer Approach</u>

Another approach was taken to estimate the flow rate of syngas into the HOB. This involved the use of a N_2 tracer of a known volumetric flow rate to estimate the dry syngas flow rate. During a run with a Praxair sparger tube, which is a porous support tube that did not have an imbedded oxygen transport membrane, N_2 was fed into the coal feeder elbow rather than CO_2. It was assumed that N_2 does not react to form NO_x species under those conditions and that tramp air was not feed into the HOB. Based upon the volumetric flow rate of N_2 to the HOB, it was calculated that the dry syngas flow rate is 15.61 SLPM or 0.5641 mol/min. This gives a percent difference of 11.14 % for the dry flow rate based on a comparison with a mass balance calculation to the calculated flow rate from the N_2 tracer.

Corrosion Issues with Using Illinois/PRB Coal Blend

The coupled effect of high sulfur content and moisture in the reactor resulted in corrosion issues with exposed thermocouples and heater connection wires. The corrosion has resulted in the reduction of the lifespan of these components.

Many of the reactor thermocouples are exposed directly to the syngas generated in the HOB. These includes thermocouples within the HOB, a single thermocouple located on the outside of the OTM tube, and the thermocouples located between the heaters and the refractory. All of these thermocouples have been replaced since tests have begun with the Illinois/PRB coal blend. Of all of the exposed thermocouples, the outside OTM thermocouple had the shortest life span within the reactor. The outside thermocouple on the OTM tube has been experimentally shown to last only 2-3 runs before corrosion corrupts the thermocouple reading or breaks the thermocouple entirely. Due to the short lifespan of this thermocouple, it was removed from operation.

The removal of the outside thermocouple on the OTM tube was done to increase testing time with the OTM tube and to allow ash to accumulate on the OTM tube. For this thermocouple to be replaced, the reactor required a cooling period of 2 days to reach temperatures where the OTM tube could be removed. The refractory lining within the reactor has a high heat capacity, which is helpful when running because the refractory serves to keep the reactor from experiencing extremes in temperature variation. The drawback is that it takes a long time for heat up and requires even more time to cool down. Typically, the OTMR is tested one day and then is serviced the next day. During reactor servicing the ash collection bin is emptied and the slag is drilled out of the mixing chamber of the HOB. During this servicing, the OTMR is maintained at a temperature between 300-500^{o}F. After servicing, the reactor is reheated for the next test on the following day. By keeping the reactor warm during servicing, the heat up schedule is reduced which allows tests to be performed every other day. The drawback of taking only one day to service the OTMR is that the OTM tube is not at a temperature where it can be safely removed from the reactor.

The second reason for taking the outside thermocouple out of service was to increase the time available for the OTM tube to collect ash. For the outside thermocouple to be replaced, the ash from the OTM tube would have to be removed from the outside surface. When replacing the outside thermocouple on the OTM tube, new support wires would need to be added and a new thermocouple attached. Because of this, the outside thermocouple was removed from operation.

The high sulfur content also reduced the lifespan of the heaters used to heat up and maintain the reactor operating temperature. These heaters are located on the outside of the refractory but are insulated from the reactor shell by Insboard insulation. A diagram illustrating the position of the heaters within the reactor is given in Figure 30.

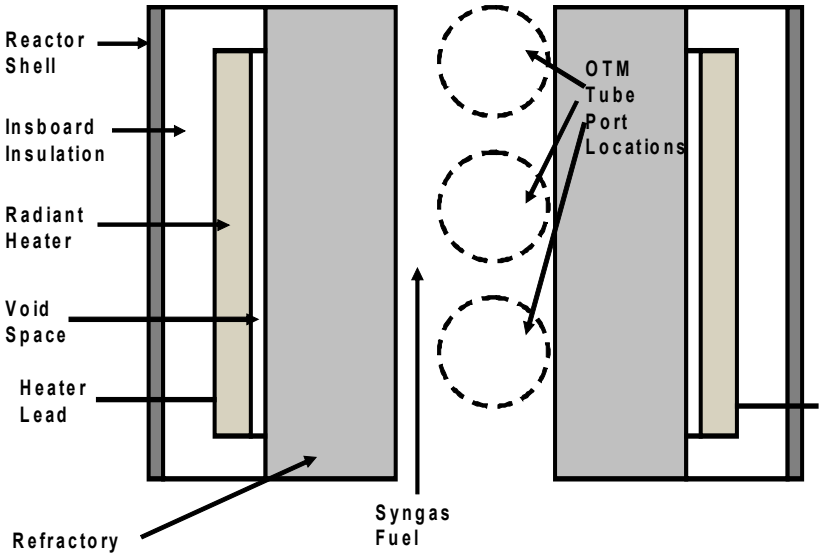

Figure 29: Isothermal Data taken at 1820^{o}F of O_2 flux as a function of inner tube O_2.

The pressure within the reactor is slightly positive to minimize air in-leakage, which leads to the possibility that the heater wires are exposed to sulfur and moisture from the reactor. During late November, the heaters had to be replaced due to the inability of the OTMR to reach the minimal operation temperature, which was indicative of the loss of one or more heaters. The OTMR was disassembled and the heaters were removed and replaced. Tests with the new heaters have shown that the heater replacement was successful. The replacement of the heaters increased the overall heater output, which allowed the OTMR to run at higher operating conditions. To maintain consistency with OTMR operation conditions prior to replacing the heaters, the power to the heaters was reduced by lowering the heater operating temperature set point. It has been found that this reduction in heater set point gives results consistent with OTM tube performance prior to the heaters being replaced.

Measured Temperature at Different Points on the OTM

It was decided to remove the outside thermocouple from service during the Illinois/PRB coal blend tests due to the short service life of the thermocouple in the high sulfur syngas environment. To illustrate the short service life of the thermocouple, and to get temperature readings from different points on the OTM, two thermocouples were added to the outside of the OTM tube. The thermocouples that were added were 1/32" type K thermocouples. One thermocouple was added to the top of the OTM and the other to the bottom. The purpose of this test was to determine the temperature difference between the top of the OTM, the bottom and the inside OTM temperature. Results of this test are given in Figures 31-33.

It was found that the two thermocouples (TC) did not last very long before the thermocouple degraded or detached from the OTM. In Figure 27 it can be seen that the outside top thermocouple started to show variance in the recorded temperature at ~1690°F. This variation leads to a significant drop in temperature at an inside temperature of ~1710°F. It was concluded that the thermocouple discontinued reading an accurate temperature after reaching 1690°F. The rationale for this conclusion is that the temperature profile did not continue a typical smooth trajectory that was present prior to this temperature.

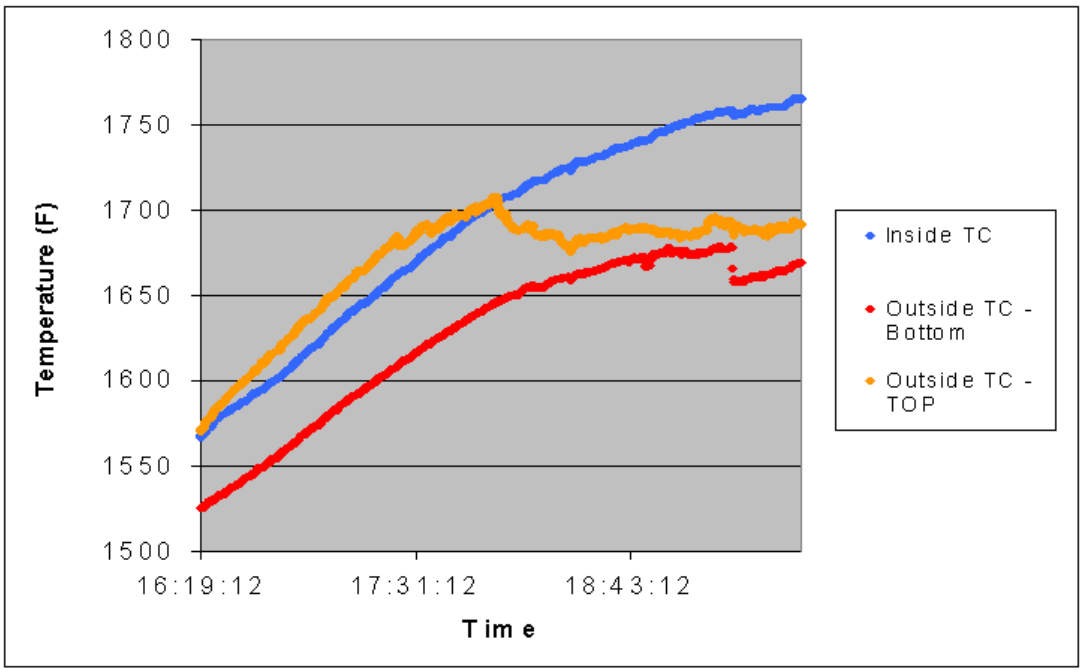

Figure 30: Heater Positions in a Section of the OTMR

There is a recorded sudden drop in temperature with the outside bottom thermocouple at ~1690°F. In this case, the thermocouple made a drastic jump from ~1680 to ~1650°F. This may have been due to a sudden change in temperature of the syngas from the HOB, or the detachment of the thermocouple from the OTM surface. The thermocouples are attached to the OTM using spent thermocouples. It has been found that they have the best resistance to the corrosive effects of the coal. High temperature wires have been used but they fail very quickly during a run. The advantage of using spent thermocouples is that the thermocouple is composed of both ceramic and inconel materials. It is speculated that the ceramic interior of the thermocouple prevents the inconel from stretching and fracturing under high temperatures. In contrast a high temperature Hastelloy wire was found to fracture under the tensile stresses put on the wire during operation.

In Figure 32 the temperatures shown in Figure 31 are contrasted with the temperature of the syngas leaving the HOB. From Figure 32 it can be seen that the temperature of the syngas is substantially lower than the measured temperatures of the OTM tube. From this data, it can be concluded that the syngas cools the OTM through convective heat transfer. The data suggests that the convective heat transfer is more effective at the bottom of the OTM than on the top due to the large temperature gradient between these two thermocouples. This may be explained as well by the presence of char and ash on the top of the OTM. As shown earlier, ash and char collect on the top of the OTM. This collection of char and ash may serve to insulate the outside top thermocouple from convective heat loss to the syngas.

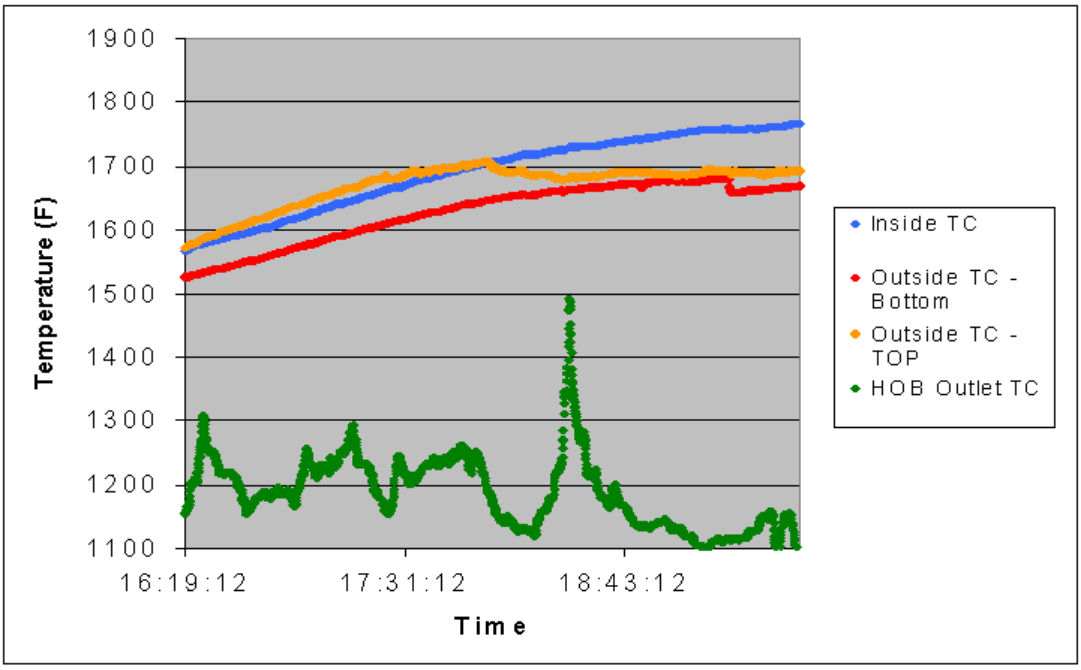

Figure 31: Temperature Profiles as a Function of Time

Another observation from Figure 32 is that large fluctuations in temperature of the syngas leaving the HOB do not have an impact on the measured OTM temperatures. This means that the performance of the OTM is not dependent on the temperature of the fuel supply as long as the OTM is able sustain operating temperatures. It also means that the OTM will not be damaged if there are sudden changes in the fuel temperature.

The three temperatures measured from the OTM are compared in Figure 33 prior to the degradation of the outside top thermocouple. From this graph it can be seen that the outside top thermocouple temperature range is closer in proximity to the inside temperature range of the OTM. The lowest temperature range is observed in the outside bottom thermocouple.

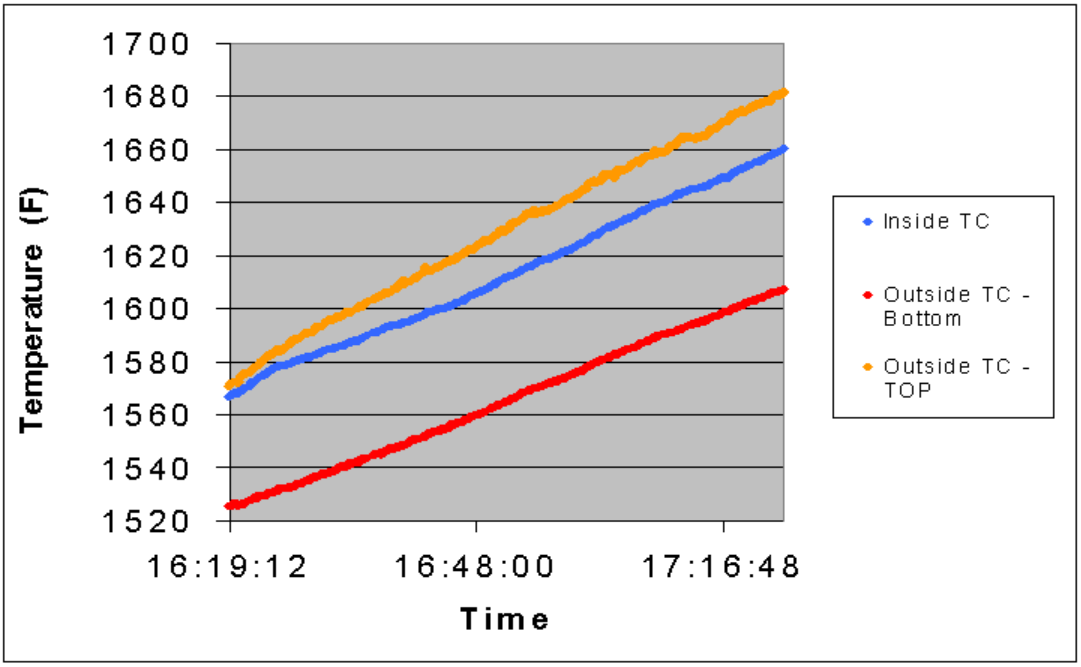

Figure 32: Temperature Profiles as a Function of Time

Using the outside top temperature as a reference point, the percent difference was calculated for the measured inside thermocouple temperature as well as the outside bottom temperature. The results are presented in Figure 34.

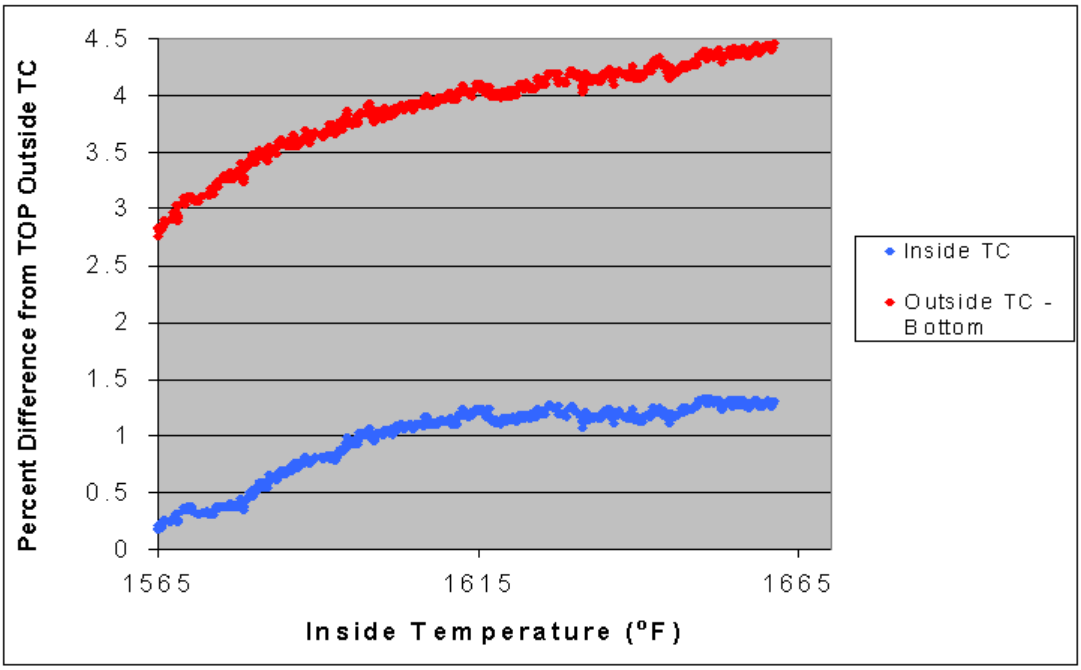

Figure 33: Temperature Profiles as a Function of Time Prior to Outside Thermocouple Degradation

The results of Figure 34 show that the percent difference between temperatures increases with the increase in the inside tube temperature. The percent difference is more pronounced with the outside bottom temperature than with the inside temperature.

The normalized O_2 flux performance of the OTM is measured as a function of temperature in Figure 35. This plot illustrates how the measured performance of the OTM can change with respect to temperature depending on which thermocouple the flux is compared to. If the bottom thermocouple is used as the temperature of the OTM, then the normalized O_2 flux performance increases by a significant amount. At 1608°F the reported normalized O_2 flux increases by 18.5%. The actual flux through the OTM doesn't change, but the reference temperature does.

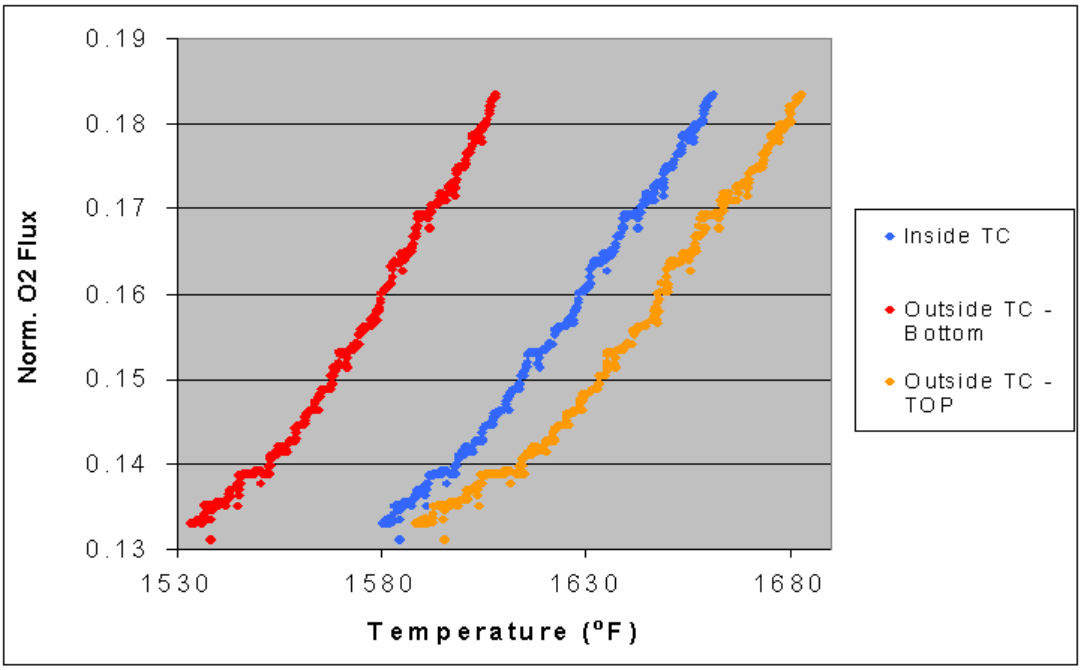

Figure 34: Percent Difference in Measured Thermocouple Readings

Analysis of O_2 Depleted Air Leaving the OTM

Gases leaving the OTM were analyzed to determine the flux of O_2 through the OTM tube. Data was collected for concentrations of O_2, H_2O and CO leaving the OTM. Using the data from the experiment cited in the previous section, these concentrations are presented in Figures 36-37.

The change in the scaled percent O_2 and scaled percent relative humidity concentrations leaving the OTM are plotted in Figure 36 as a function of the inside temperature of the OTM. It can be seen that as the inside temperature of the OTM increases, the scaled percent of O_2 leaving the OTM decreases. This result shows that the flux of the OTM increases with respect to temperature. The scaled percent relative humidity increases with respect to temperature indicting that the back diffusion of H_2 into the OTM increases with temperature.

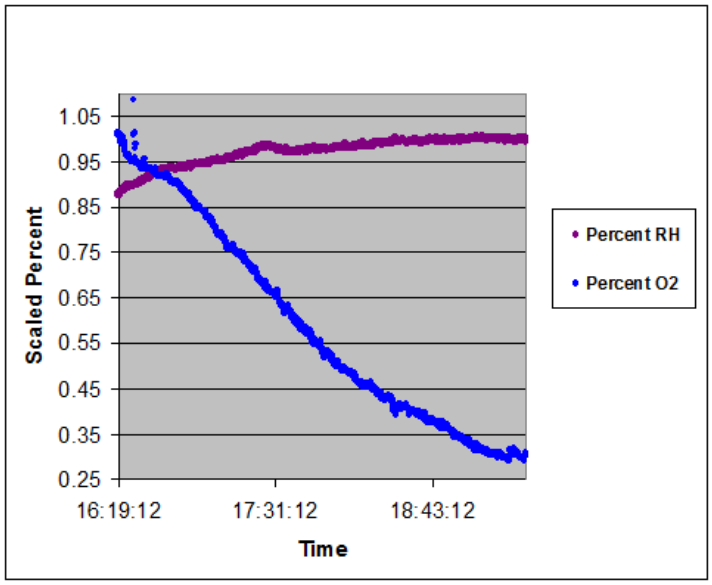

Figure 35: Effect of Reference Temperature on the Reported Normalized O_2 Flux

The measured ppm concentration of CO leaving the OTM is plotted as a function of time in Figure 37. It is shown that the concentration of CO increases with respect to time. This indicates that more CO back diffuses through the membrane as the temperature of the membrane increases since the OTM temperature increases with time. Another important conclusion of this data is that CO only exists in the ppm range. The maximum observed CO value was 81 ppm or 0.0081%. Though small, this concentration of CO shows that CO does indeed back diffuse through the OTM, but does so at a level that is difficult to account for. It was found that the measured percent of CO_2 from the depleted air stream leaving the OTM was much too small to measure for the analyzers available. Thus the concentration of CO and CO_2 leaving the OTM were not accounted for when calculating the flux of O_2 leaving the OTM.

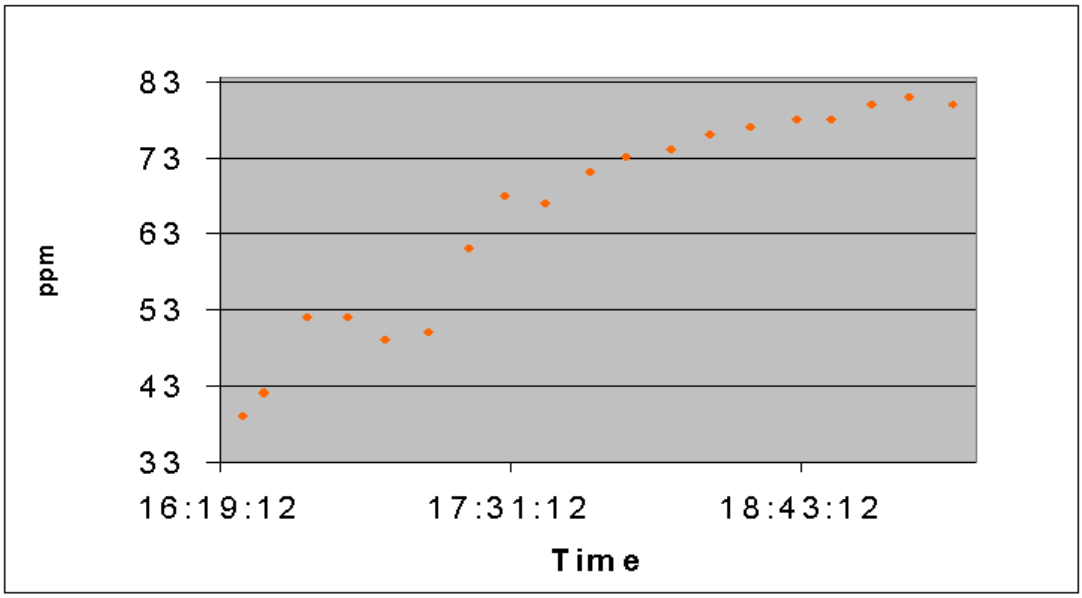

Figure 36: Scaled Percents for O_2 and Relative Humidity

Effect of Prolonged Exposure on OTM Flux Performance with Illinois/PRB Coal Blend

Changes in normalized O_2 flux was analyzed over time for the Illinois/PRB blend with the results presented in Figures 38-39 for low operating temperature conditions between 1570°F and 1600°F. This data also show the effect of the replacement of panel heaters in the OTMR. As explained earlier, the use of a high sulfur Illinois coal caused the corrosion of the heaters which resulted in the failure of multiple heaters. Enough heaters failed that the remaining heaters could not sustain the required wattage to heat the OTM tube to operating temperature. At that point, the reactor was taken apart and the heaters replaced. The heaters were replaced within the gap between the first three testing dates and the last three testing dates as shown in Figure 38. It can be seen in Figure 38 that the replacement of the heaters increased the performance of the OTM tube. The average percent increase in normalized O_2 flux performance was calculated to 2.5%. In looking at the dates after the heaters were replaced, the only isotherm that the normalized flux of O_2 decreased over time was at 1600°F. The other temperatures observed an increase in flux.

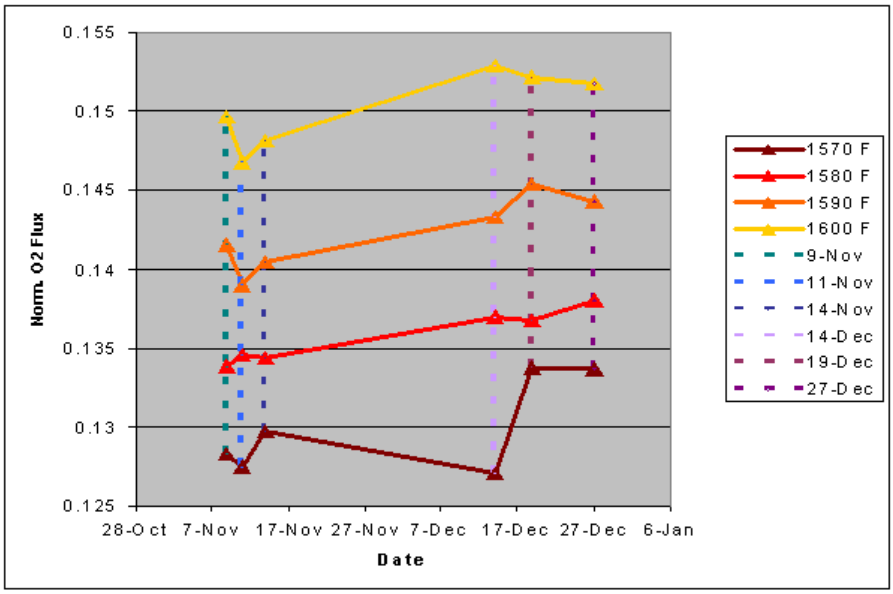

Figure 37: Measured concentration of CO Leaving the OTM

Figure 39 shows the change in normalized O_2 flux performance for the dates between 12/14 and 12/29/2011. This graph gives a higher range of temperatures observed for the OTM, ranging from 1620-1680°F. It can be observed that the difference between the initial flux value and the final flux value decreases with increasing temperature. This data was used to calculate the percent difference of the change in flux for each isotherm. The results are given in Figure 40.

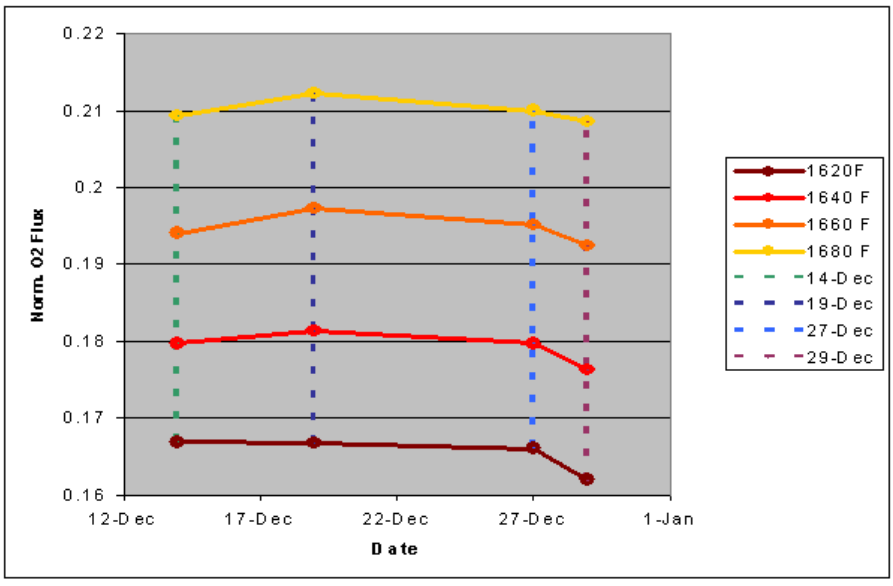

Figure 38: Effect of Heater Replacement and the Change in Normalized O_2 Flux over Time for Illinois/PRB Coal Blend Campaign.

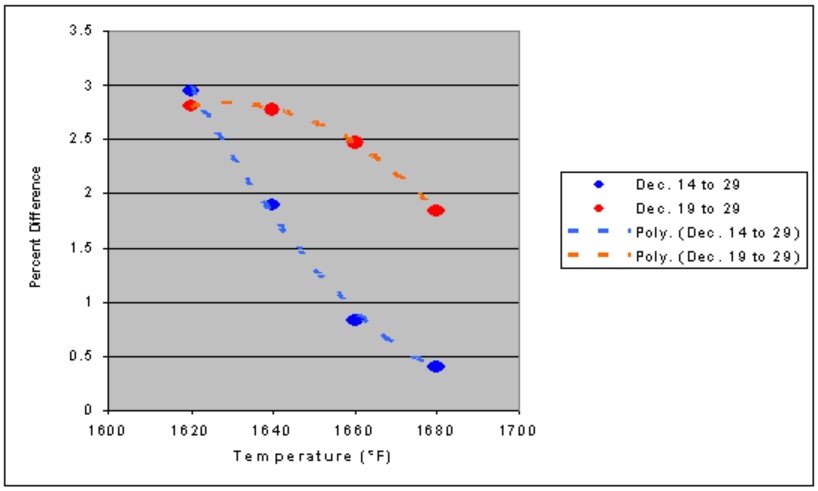

Figure 39: Change in Normalized O_2 Flux over Time for Illinois/PRB Coal Blend Campaign for the Temperature Range of 1620°F to 1680°F.

It is shown in Figure 40 that the percent difference of the normalized O_2 flux changes substantially depending on the date used as the reference. As seen in Figure 40 the normalized O_2 flux increased from December 14th to the 19th. Thus the percent difference will be higher if the 19th is used rather than the 14th.

The data in Figure 40 also show that the percent difference between the original normalized O_2 flux value and the final flux value decreases with temperature. This may suggest that degradation from the prolonged use of an OTM will have the most effect at lower temperatures. This trend is consistent for both the data sets considered.

Solid Flux Measurements

The flow of solids in the OTMR using the Illinois/PRB coal blend was measured using the isokinetic sampling system presented in Figures 21-23. The calculations were performed using the same process with the Utah/PRB coal blend. The solids were sampled along the axial centerline of the OTMR. The solids flow rate through the OTMR with respect to reactor position is given in Figure 41.

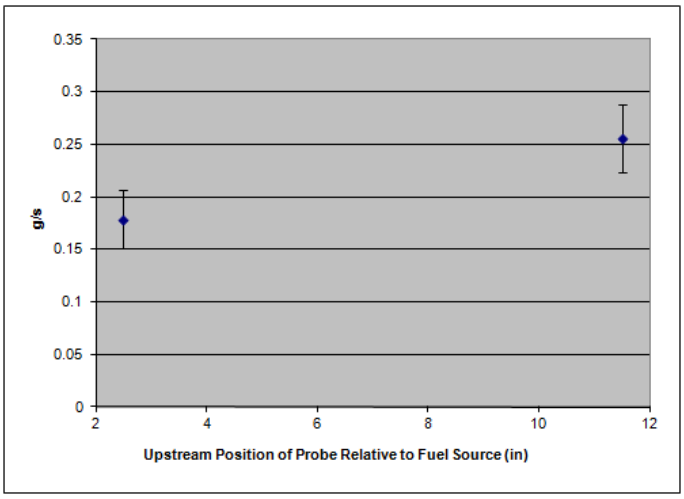

Figure 40: Percent Difference in the Normalized O_2 Flux over Time for Illinois/PRB Coal Blend Campaign using Data from the Temperature Range of 1620°F to 1680°F.

A comp en in Figure 42. The data show that the measured solids flow from the Illinois/PRB blend is higher than for the Utah/PRB blend. This result is not unexpected since the flow rate of coal with the Illinois/PRB coal blend (13.41 g/min) is higher than the flow rate of the Utah/PRB coal blend (11.55 g/min) The percent difference between these two flow rates is 13.9%. A comparison of this data shows that the average solids flow of the Illinois/PRB blend is 36.3 % higher than the Utah/PRB blend for the port located 2.5 inches from the HOB and is 39.8% at 11.5 inches from the HOB. Both of these values are much higher than the percent difference for the flow rates of the two coal blends to the HOB. The data also shows that the there is a consistent increase in the flow of solids with respect to an increase in the sampling positions.

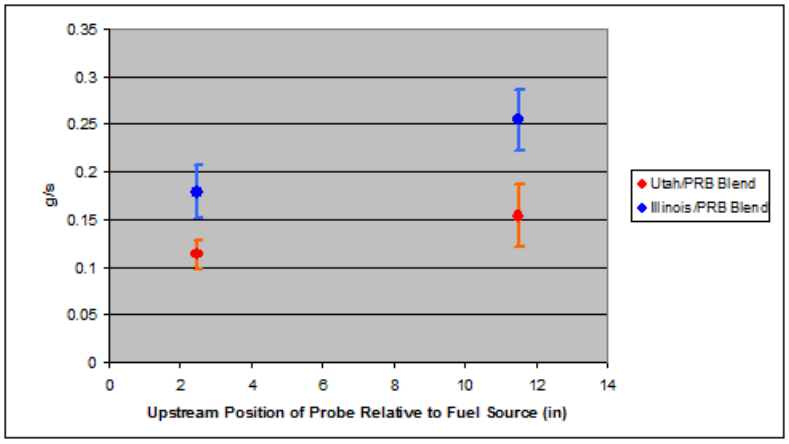

Figure 41: Solids Flow of Char and Ash in the OTMR Using Two Different Sampling Positions

OTM O_2 Flux Performance Comparison between Two Coal Blends

Tests have been performed with both the Utah/PRB and the Illinois/PRB blends. A separate OTM tube was used for the testing of each coal blend. From this data it was found that both tubes performed consistently with their

respective blend for ~80 hrs with no detectable loss of oxygen flux performance. It was discovered, however, that the two coal blends had significant differences in the O_2 flux performance. Figure 43 shows the difference in OTM tube performance between the two coal blends at similar operating conditions.

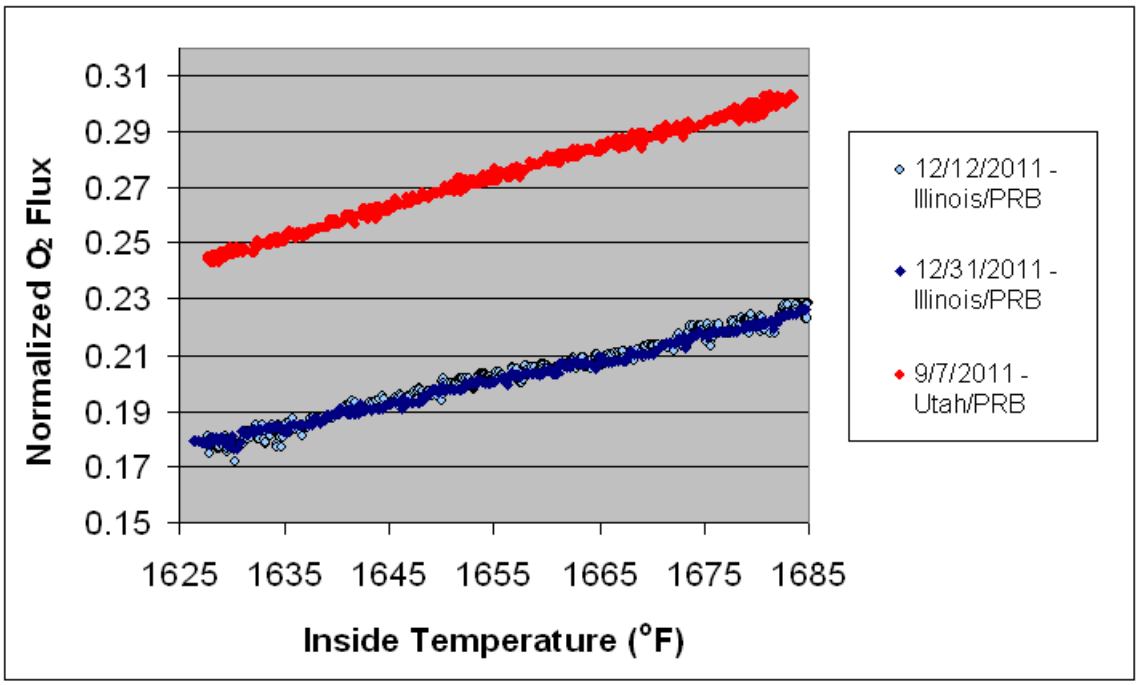

Figure 42: Comparison of Solids Flow of Char and Ash in the OTMR with the Utah/PRB and the Illinois/PRB Coal Blends

One test was performed with the Utah/PRB blend and two tests were performed with the Illinois/PRB blend. Two tests were performed with the Illinois coal to determine if there was an effect of the heater settings. The test on 12/31/2011 was conducted at a heater setting to mimic conditions prior to the heaters being replaced. The comparison of these tests shows that there is a significant difference in the performance of OTM tubes with different coal blends. The maximum percent difference between the normalized O_2 fluxes between the two runs is 25.1%.

In comparing these tests, there are many factors that need to be considered to assess the validity of the comparison. The flow of air to the OTM tube was the same for each test and was set at 1.48 SLPM. In all of the tests, the OTM tube was located in the middle port of the OTM section of the reactor. The major differences between the runs were the HOB settings, the weight percentage of PRB, the syngas fuel composition and the residence time of the syngas fuel. This data is given in Table 13.

Table 13: Operational Parameter Differences for Utah/PRB and Illinois/PRB Comparison Tests

	Utah/PRB	Illinois/PRB
Nozzle SR	5	5

Mixing SR	0.3	0.3
Blend (wt. %)	25/75	50/50
Coal Flow Rate (g/min)	11.55	13.41
HOB Methane Flow (SLPM)	0.557	0.702
HOB Oxygen Flow (SLPM)	5.57	7.02
Estimated Syngas Flow (SLPM)	17.2	17.9
Estimated Residence Time (sec)	3.71	3.57
Syngas Composition		
H_2	0.1828	0.1421
CO	0.2721	0.2531
CO_2	0.3522	0.3305
H_2O	0.1886	0.2602

From Table 13 it can be seen that the Utah/PRB coal blend has a higher residence time and a higher H_2 and CO fuel concentration in the syngas. It is proposed that the higher concentration of H_2 and CO fuel with the Utah/PRB coal blend can be used to explain the increase in performance of the O_2 flux. It is interesting to note that the percent difference between the H_2 concentrations in the syngas between the two coal blends is 22.3% which is very similar to the percent difference in the performance of the OTM tubes. This result illustrates the impact the H_2 content in the syngas has on the OTM performance. Based upon this result, it would appear that the higher the H_2 content in the syngas the higher the O_2 flux performance will be.

Conclusions

The OTMR developed at the University of Utah has been used to show that Praxair OTM tubes can operate for ~80 hours of cyclical operation in realistic coal syngas environment. In performing the two extended testing campaigns with different coal blends, it has been shown that the presence of ash does not create a resistance to the mass transfer of fuel to the OTM such that the O_2 flux would be impeded. It was also found that the flux of O_2 through the OTM is dependent on the temperature and the partial pressure of O_2 on the air side of the OTM. Another conclusion is that the concentration of H_2 in the syngas fuel has a significant impact on the performance of the OTM.

Appendix D

International Conference on Greenhouse Gas Control Technologies 2010 Paper. 'Development of oxygen transport membranes for coal-based power generation (Energy Procedia Volume 4, 2011 pp. 750-755)

ELSEVIER
Available online at www.sciencedirect.com
ScienceDirect
Energy Procedia 4 (2011) 750–755
Energy Procedia
www.elsevier.com/locate/procedia

GHGT-10

Development of Oxygen Transport Membranes for Coal-Based Power Generation

Lee Rosen[a*], Nick Degenstein[a], Minish Shah[a], Jamie Wilson[a]
Sean Kelly[a], John Peck[a] and Max Christie[a]

[a]*Praxair, Inc., 175 East Park Drive, Tonawanda, NY 14150, USA*

Abstract

Praxair is developing an Advanced Zero Emission Coal Fired Power Plant (Advanced Power Cycle) that enables carbon capture and sequestration (CCS) at a "levelized" cost of electricity below the U.S. Department of Energy's target for CO_2 capture from coal fired power plants. The power cycle utilizes a gasifier, partial oxidation units, power recovery turbines and an oxygen fired boiler to yield a process that meets the DOE's goal of <35% increase in cost of electricity with CCS. Through the use of Praxair's reactively driven Oxygen Transport Membrane (OTM) technology, the parasitic load of the oxygen supply system to both the partial oxidation reactors and boiler is reduced by approximately 75%. The Advanced Power Cycle [1] uses coal gasification to produce a gaseous fuel that is then combusted in an oxygen fired supercritical boiler. Low cost oxygen is made available by integrating Praxair's OTMs into the boiler and, depending on the gasifier selected, into a post gasification partial oxidation system to convert tars and methane to CO and hydrogen. Praxair has completed a detailed techno-economic analysis of the performance of the Advanced Power Cycle (APC) and achieved significant breakthroughs in the OTM architecture and gas separation layer chemistry to achieve the commercial flux targets under phase 1 of a cooperative research agreement [2] with the United States Department of Energy (DOE). Phase 2 of this agreement, currently underway, is focused on developing a detailed cost estimate of key components of the cycle as well as developing fabrication cost estimates of the membranes. While the APC is targeted at coal based CCS, the key components of the APC can offer benefits to integrated gasification fuel cell cycles, natural gas combined cycle plants as well as other processes. These additional processes represent opportunities to demonstrate key components of the APC prior to demonstrating the technology in its entirety. These opportunities not only allow investment dollars to be leveraged for additional benefits but also allow critical performance and reliability to be gained at commercial scale in an industrial environment – a critical hurdle that must be crossed for any new technology to be implemented at utility scale. Praxair is encouraged by the progress made to date and believes that great progress has been made in the area of materials and cycle development. The newly developed materials and membrane architecture have met commercial flux targets while demonstrating robust performance. The APC holds great promise to address the needs of CCS, while minimizing the cost of compliance.

* Corresponding author. Tel.: +1-716-879-2881; fax: +1-716-879-7931
E-mail address: lee_rosen@praxair.com

doi:10.1016/j.egypro.2011.01.115

L. Rosen et al. / Energy Procedia 4 (2011) 750–755
Rosen/ Energy Procedia 00 (2010) 000–000

Keywords: Oxyfuel combustion; power plants; near zero emissions; CO_2 purification; CO_2 capture.

1. Process Cycle

During the initial phase of the program, Praxair developed and evaluated a number of different process cycles. Through a series of feasibility and techno-economic analyses one cycle was selected to result in the smallest increase in the cost of electricity when compared with an air fired pulverized coal plant. The process cycle that was selected is illustrated in Figure 1. The concept utilizes a gasifier that is fed with oxygen from a conventional air separation unit (ASU). The gasifier is selected such that it achieves high carbon conversion with minimal oxygen. After particulate cleanup, the syngas is reacted in an OTM partial oxidation (POx) reactor to raise the temperature prior to expansion through a power recovery turbine (PRT). Figure 1 shows a series of two POx/PRTs to maximize the efficiency of power recovery. After expansion to slightly above atmospheric pressure the synthesis gas is fed to the OTM boiler. In the OTM boiler, synthesis gas reacts with oxygen separated from air via OTM devices. The conceptual design of the boiler has OTM elements interspersed with steam tubes such that the radiant heating from the OTM elements supplies the energy to the steam tubes. While the OTM provides low cost oxygen for the bulk of combustion, the incremental OTM area required to provide the final oxygen to complete combustion comes at a cost higher than that of conventional oxygen production. Therefore, the final 10 – 20% of the oxygen required to complete combustion is supplied from the conventional ASU (although not shown in Figure 1). This is due to the decrease in oxygen flux with lower concentrations of fuel species. The process as illustrated in Figure 1 is designed to allow the optimization of the overall cost of oxygen by balancing it between conventional cryogenic ASU and advanced OTM methods. After the fuel is completely oxidized with externally supplied O_2, the flue gas will pass through a convective section of the boiler for further steam generation and boiler feed water preheating. The flue gas exiting the FGD scrubber is compressed to >2000 psia and purified to >95% purity for sequestration or enhanced oil recovery (EOR).

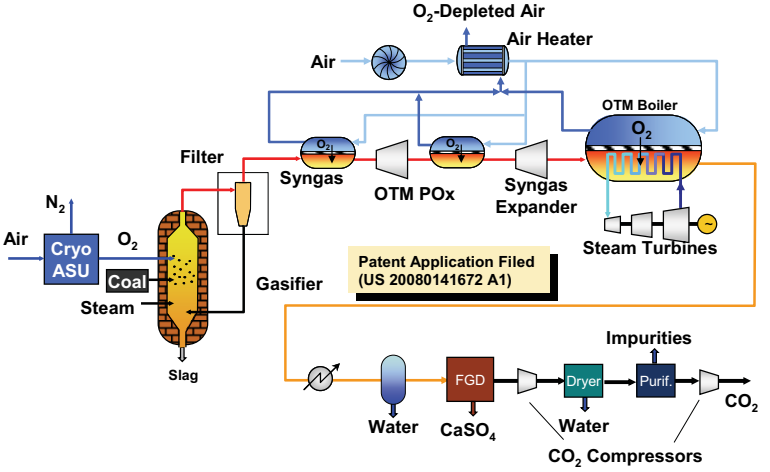

Figure 1. Process for Integration of OTM into Power Generation Cycle with CO_2 Capture

Although the OTM power cycle uses a gasifier at the front end of the process, its CO_2 capture characteristics are similar to an oxy-combustion process. Table 1 shows a comparison of the key features of the OTM power cycle, an IGCC power cycle and an oxyfuel fired boiler cycle. If CO_2 capture is required from an IGCC-based power plant, the syngas from the gasifier must be shifted to maximize the hydrogen concentration using water gas shift. The shifted syngas is cooled to near ambient temperature where an acid gas recovery unit removes sulfur compounds and CO_2 from the cooled syngas stream and hydrogen is sent to a combined cycle section for power generation. A significant amount of fuel energy is lost as the coal is transformed into hydrogen. A report published by DOE/NETL

[3] shows that the efficiency of an IGCC plant with CO_2 capture will range from 31.7% (HHV) to 32.5% (HHV) depending on the type of gasifier used.

Table 1: Comparison of features of APC, IGCC and Oxyfuel power cycles

	APC	IGCC	Oxyfuel
Gasifier	Yes	Yes	No
Syngas Expander	Yes	Yes/No	No
Shift Reactor	No	Yes	No
Acid Gas Recovery (e.g. Selexol)	No	Yes	No
H_2 Combustion Turbine	No	Yes	No
Steam Generation Unit	OTM Boiler	HRSG	Oxyfuel Boiler
Oxidant for Combustion	Oxygen	Air	Oxygen
Pre-Combustion CO_2 Capture	No	Yes	No
Oxy-Combustion CO_2 Capture	Yes	No	Yes
Power Production from Major Units			
Combustion Gas Turbine	0%	62%	0%
Syngas Expander	18%	1%	0%
Steam Cycle	82%	37%	100%

In the OTM process, there is no loss of energy associated with syngas conditioning for CO_2 and sulfur removal. Laboratory scale tests have demonstrated the ability of the membranes to survive in atmospheres with up to 1% of H_2S and COS. Overall, the OTM process is projected to achieve 37.2% (HHV) efficiency [4] when coupled with an ultra supercritical steam cycle. This is 4.7 to 5.5 percentage points higher than the efficiency of an IGCC plant with CO_2 capture [3] and within 2.5 percentage points of a conventional air fired PC Boiler without CO_2 capture. In the IGCC process, CO_2 must be separated using solvents such as selexol, rectisol or other amine. In the OTM process, the CO_2-rich stream is generated in the OTM boiler similar to a conventional oxygen-fired PC boiler. In IGCC, about two thirds of the power is generated by the combustion turbines with the remaining third generated in the steam cycle. In the OTM power cycle, more than 80% of the power is generated in the steam cycle and the balance of power is generated by syngas expanders. Final purification of CO_2 in the OTM process is similar to that of a conventional oxy-combustion process. Overall, the OTM power cycle shares more features with the conventional oxy-combustion process than that of an IGCC process.

2. Techno Economic Analysis

A detailed techno-economic evaluation of the APC was performed for 6 cases to determine the cycle efficiency and cost of electricity (COE) in 2008 dollars. The six simulated cases investigate the effect of 2 main parameters: steam cycle complexity (super critical, ultra-supercritical and advanced ultra-supercritical) and type of sulfur recovery unit (flue gas desulfurization and warm gas cleanup unit). For each of the 6 cases evaluated, the sensitivity of COE to coal price was evaluated using three coal prices. The results of this analysis are shown in Table 2. Thirteen of the eighteen scenarios satisfy the DOE goal of less than 35% increase in COE. These cases are highlighted in green in Table 2. Higher coal price favors the APC COE (relative to other processes, e.g. IGCC) due to the high efficiency enabled by utilization of OTM technology in the process cycle.

Table 2: Comparison of OTM cases with Air PC base case (cost basis for all cases March, 2008)

		OTM FGD Cases			OTM WGCU Cases			Air-PC Case
Case		1 SC	2 USC	3 Adv USC	4 SC	5 USC	6 Adv USC	Praxair/DOE No CCS SC
Net Efficiency (HHV) (%)		36.3	37.2	39.7	36.6	37.4	39.9	39.7
Plant Cost ($/kW)		2,894	2,887	2,997	2,872	2,863	2,956	1,908
	Coal Price ($/MMBtu)							
Increase in COE over Reference	1.8	39.4%	38.4%	39.7%	36.0%	35.0%	36.2%	
	3	34.9%	33.8%	33.8%	32.0%	30.8%	30.6%	
	4	32.1%	30.8%	30.0%	29.4%	28.0%	27.1%	

In comparison to other power cycles that enable carbon capture and sequestration (CCS), the APC has a uniquely low cost of CO_2 removed and avoided due to a relatively low COE, a high net cycle HHV efficiency, and high CO_2 capture efficiency. Additionally, the high net cycle HHV efficiency results in low operating cost making these units more likely to operate as base loaded units as opposed to other CCS equipped power plants with high operating costs that would be lower on the dispatch list.

3. Materials Development

The structural, chemical and mechanical stability of OTM materials at high temperatures and in reducing environments is critical to the reliability of the OTM system. In the 1998 – 2003 time frame, ceramic membrane failures were prevalent during heating, cooling, thermal cycling, and changes in fuel composition, due in part to mechanical strength deficiencies and to chemical and thermal expansion mechanisms associated with the single phase pervoskites that were utilized. Recognizing the importance of reliability and the challenges in managing this with a single phase perovskite system, Praxair redesigned the OTM architecture using a combination of layers and materials to address the known failure mechanisms and the functional requirements of the membranes. In 2005 a breakthrough in the materials development was achieved. With the new materials set, the failure rate in small laboratory scale reactors dropped to near zero. However, while the reliability of the system improved dramatically, the oxygen flux performance suffered. Techno-economic analyses indicated that a performance improvement of at least 2x was required to achieve economic targets. A detailed analysis of the rate limiting steps indicated that improvements in mass transfer through the porous support and fuel oxidation at the anode surface would have the biggest impact on membrane performance. Significant progress was made in both of these areas as illustrated in Figure 2 where the combination of improved mass transfer and improved fuel oxidation result in nearly a 4x improvement in oxygen flux. With the improvements in fuel oxidation and architecture of the porous support and the associated improvement in performance, some failures were initially observed when the fuel flow was turned off at the completion of a test. More recently, high performance, single tube OTM structures have been demonstrated to maintain performance and structural integrity after several full thermal and chemical cycles in laboratory scale reactors. Failure analysis has indicated that failures are more often related to the laboratory scale seal technology used in the test stands. Not withstanding this identified issue, the OTM tubes continue to be robust during heat up in air and rapid addition of fuel. These characteristics were not achieved with the original OTM material set (e.g. single phase perovskites) utilized in the 1998 – 2003 timeframe.

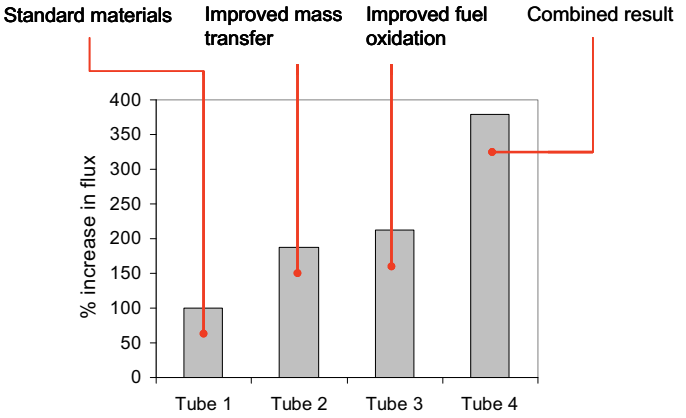

Figure 2: Membrane performance for individual and combined improvements in porous support and fuel oxidation (Tube 1: Standard support, Tube 2: Improved support, Tube 3: Improved fuel oxidation, Tube 4: Improved support & fuel oxidation).

4. Synergies with Other Technologies

While the focus of Praxair's efforts under the DOE cooperative agreement are on the advanced power cycle, key components of the process cycle have benefits in other areas as well. These areas include:

Integrated Gasification Fuel Cell (IGFC) power cycle

OTM devices could be utilized in multiple locations in the process cycle currently under consideration to reduce the parasitic load of the oxygen on the overall process. This would result in an increment boost in net power output and overall cycle efficiency.

Process heating furnaces in refineries and chemical plants (e.g. crude heaters, ethylene crackers, etc.)

The CO_2 Capture Project [5] is currently studying different solutions for capturing CO_2 emissions from process heaters within refineries. As CCS regulations extend beyond power production, the OTM boiler approach would facilitate oxyfuel combustion with a significantly lower cost of oxygen.

Natural gas combined cycle power plants

Based on a preliminary evaluation, the benefits of integrating OTM elements into a NGCC include < 35% increase in COE for CCS, 100% CO_2 capture; < 1ppm NOx emission and >20% reduction in cost of capturing CO_2 compared to post-combustion.

5. Development Roadmap

With the progress that has been made on materials and membrane performance, Praxair is in the process of forming strategic alliances with firms that will continue the development of the technology in a collaborative effort. The near term goal of the joint effort will be to develop an OTM module that is conceptually similar to an SOFC stack. The OTM module then becomes the building block for larger scale systems. It is anticipated that the next phase of the project will run through 2015 and will culminate in a robust, reliable, module design that has been proven in pilot scale test equipment in both a partial oxidation mode and a combustion mode. Follow on efforts will focus on scaling the system size thereby demonstrating the scalability of the system and positioning the technology for future commercial scale demonstrations.

6. Conclusions

Praxair is encouraged by the progress made to date and believes the APC holds great promise to address the needs of CCS while minimizing its cost. The work completed over the past 6 years under the DOE cooperative agreements has led to the development of a robust material set that is capable of surviving in an industrial environment. The materials have demonstrated the ability to survive transients with no special precautions. In addition to continuing to improve the performance of the materials, future work will focus on integrating and packaging the membranes into reactors and long term testing of these systems. We look forward to continuing our cooperation with the DOE to scale up this technology and deliver a cost effective solution for carbon capture and sequestration for fossil fuel fired power plants.

7. Disclaimer

This material is based upon work supported by the Department of Energy under Award Number DE-FE26-07NT43088. Neither the United States Government nor any agency thereof, nor any of their employees, makes any warranty, express or implied, or assumes any legal liability or responsibility for the accuracy, completeness, or usefulness of any information, apparatus, product, or process disclosed, or represents that its use would not infringe privately owned rights. Reference herein to any specific commercial product, process, or service by trade name, trademark, manufacturer, or otherwise does not necessarily constitute or imply its endorsement, recommendation, or favoring by the United States Government or any agency thereof. The views and options of authors expressed herein do not necessarily state or reflect those of the United States government or any Agency thereof.

8. References

[1] Shah, M.M, Jamal, A., Drnevich, R.F., van Hassel, B.A., Christie, G.M., Kobayashi, H., Bool, L.E., “Electric Power Generation Method”, U.S. Patent Application 2008/0141672, June 19, 2008.
[2] DE-FC26-07NT43088 “OTM Based Oxycombustion for CO2 Capture from Coal Power Plants.”
[3] Woods,M.C., Capicotto, P.J., Haslbeck, J.L., Kuehn, N.J., Matuszewski, M., Pinkerton, L.L., Rutkowski, M.D., Schoff, R.L., Vaysman, V., “Cost and Performance Baseline for Fossil Energy Plants”, DOE/NETL Report 2007/1281, Rev. 1, August 2007.
[4] Shah, M.M., Christie, G.M., Degenstein, N., Wilson, J., “Oxycombustion on Oxygen Transport Membranes,” 1st International Oxycoal Combustion Conference, Cottbus, Germany, Sept. 8 – 10, 2009.
[5] www.co2captureproject.org

Appendix E

Clearwater Papers 2007 - 2010

Publication Year		Page
2007 Publication	……	E2
2008 Publication	……	E8
2009 Publication	……	E18
2010 Publication	…….	E30

2007: **OTN based Oxycombustion for CO_2 Capture from Coal Power Plants**

2008: **Progress towards the Demonstration of OTM Integration with Coal Combustion**

2009: **OTM Based Oxy-fuel Combustion for CO2 Capture**

2010**: OTM Based Oxy-fuel Combustion for CO2 Capture**

OTM BASED OXYCOMBUSTION FOR CO_2 CAPTURE FROM COAL POWER PLANTS

Maxwell Christie, Bart van Hassel, Juan Li, Minish Shah

Praxair, Inc.
175 East Park Drive, Tonawanda, NY 14150.
Tel: (716) 879-7739, email: max_christie@praxair.com

Abstract

Praxair and The United States Department of Energy (DOE) have recently signed a new Cooperative Agreement (DE-FC26-07NT43088) to develop Oxygen Transport Membrane (OTM) based oxygen combustion process for carbon dioxide (CO_2) capture from coal power plants. The economics of oxygen combustion processes for coal power plants are currently limited by the parasitic power that is required for cryogenic oxygen production in conventional air separation units (ASU). When thermally integrated in a coal power plant, Praxair's OTM technology has the potential to reduce the parasitic power consumption required for oxygen production is reduced by 70-80% as compared to cryogenic oxygen production. A successful outcome of the new project shall be to develop an OTM based oxygen combustion process that meets DOE goals for CO_2 capture and to drive the OTM manufacturing technology to a level where it is ready for pilot-testing.

Introduction

Oxycombustion, or burning fuel in oxygen to generate flue gas consisting of primarily CO_2 and H_2O, is established as a credible means to facilitate CO_2 capture from coal power plants. The economics of conventional oxycombustion processes are currently limited by the parasitic power that is required for cryogenic oxygen production in conventional air separation units (ASU). A further limitation of oxycombustion is the requirement that a portion of the CO_2 in the exhaust must be cooled and recycled in order to maintain the temperature in the combustion chamber within practical limits.

Praxair is developing novel OTM technology that has the potential to solve both of these issues. OTMs can be integrated such that there is minimal need for air compression and the parasitic power consumption required for oxygen production is reduced by 70-80% as compared to cryogenic ASU.

OTM development at Praxair for oxyfuel combustion applications has previously been funded through cooperative agreements with DOE under agreement DE-FC26-01NT41147 and recently some significant milestones have been achieved. Novel OTM materials exhibiting high reliability and tolerance for repeated chemical and thermal cycling have been demonstrated. More than 18,000 cumulative hours of failure-free operation in a combustion environment has been achieved. In the new agreement with DOE Praxair shall continue the development and scale-up OTM technology in order to drive the technology status to a level where it is ready for pilot-testing. Praxair shall also work to down select an optimum process for integration of the membranes in a coal power plant through process and economic modeling and technical feasibility assessments. Assuming success in the early phases of the project Praxair shall develop basic engineering design and cost of key pieces of OTM-based equipment and develop a plan for pilot testing.

Process

The proposed process for integration of OTM in a coal power plant is a hybrid of gasification and oxy-fuel combustion. The key aspect of this process is to use a high efficiency gasifier to convert coal into relatively clean syngas and then deliver the gaseous fuel to an OTM Partial Oxidation (POx) reactor and OTM boiler for oxy-fuel combustion. This process is designed such that the majority of the components with the exception of the OTM equipment are well known and commercially available.

A simplified process schematic is presented in Figure 1. Coal is gasified and fines are removed by a cyclone or a candle filter and recycled back to the gasifier. The resulting syngas containing small quantities of tars and oils is then fed to an OTM POx unit with sulfur-tolerant membranes to partially oxidize syngas to raise its temperature and to convert tars and oils to syngas. The hot pressurized syngas is expanded to generate power before combustion is completed in an OTM Boiler. The OTM Boiler contains OTM and steam tubes, interspersed such that the fuel stream passes through alternating combustion and heat transfer zones. Feed-air to the OTM is preheated using the oxygen depleted air stream exiting OTM manifolds.

In the OTM boiler, combustion is limited by the oxygen flux through the membrane and therefore oxygen supply for combustion is distributed over a long section of the boiler. This results in a unique temperature profile in the OTM boiler (as compared to a conventional boiler where all the fuel and oxidant are delivered at burner tips) and no flue gas recirculation is required. Approximately 75% of the total O_2 requirement for the process is supplied by OTM (65% in boiler and 10% in POx). The remainder is provided by high-purity (99.5%) O_2 from a cryogenic air separation unit (ASU).

The flue gas exiting the OTM Boiler is at ~1770ºF, and consists of ~ 52% H_2O, 46% CO_2, with a balance N_2, SO_2, and O_2. The economizer and the boiler feed water heater recover heat from this flue gas. The flue gas is further cooled and then sent to a wet flue gas desulphurization (FGD) scrubber to remove >98% SO_2. The FGD unit will be much smaller than for an air fired boiler due to the smaller flue gas volume. The flue gas exiting the FGD scrubber consists mainly of CO_2, with residual H_2O, Ar, N_2, O_2 and trace amounts of SO_2. The flue gas is compressed in a multistage inter-cooled compressor to 350 psia, dried and further compressed to 2204 psia (152 bars) for transport to the sequestration site. Since CO_2 purity is >95%, there is no need for further purification, which normally causes CO_2 loss.

Economics

Table 1 compares the performance of two oxy-fuel technologies: 1. Oxy-PC boiler based on oxygen supplied from a cryogenic ASU and 2. OTM process that supplies a majority of oxygen needed for the process through OTM and the remainder of oxygen from cryogenic ASU. Air-fired PC boiler with 39% (HHV) efficiency is used as a reference case. The nominal net output was kept at 600 MW for all the cases. For the oxy-PC case, it is assumed that flue gas recirculation is used so that oxy-firing operation mimics the air-fired boiler operation. Oxygen with 95% purity is supplied from a cryogenic ASU and is mixed with re-circulated flue gas before feeding it to the boiler. Air leak is assumed to be 3% of the total flue gas volume and the resulting flue gas contains ~80% CO_2 on a dry basis. This flue gas stream is compressed and purified to obtain 96% CO_2 stream at 1500 psia. In the purification system, the CO_2 recovery is 90%.

In the OTM process, solid fuel is first reacted in a BGL gasifier with oxygen supplied from a cryogenic ASU to produce a syngas stream at 1000 ^{o}F. The syngas stream is processed in an OTM POx reactor to raise its temperature to 1800 ^{o}F. The hot syngas stream is expanded to recover power. The expanded syngas stream is fed to an OTM boiler for oxy-fuel combustion and to raise steam for a supercritical steam cycle.

The overall efficiency of the oxy-PC system is 29.9% (HHV). Parasitic power consumed in air separation unit and CO_2 processing plant account for the bulk of the efficiency penalty compared to the air-fired PC case. The overall efficiency of the OTM process is much higher at 34.5% (HHV). In the OTM process, ~75% of oxygen requirement is met by oxygen supplied through OTM. Due to significantly lower air compression requirements in the OTM process, parasitic power consumption drops significantly. In addition, power recovery from the syngas expander contributes to further efficiency improvement. Another benefit of the OTM process is that there is no need for flue gas recirculation and oxygen supplied for combustion is inherently high purity oxygen. As a result, flue gas with much higher CO_2 concentration is obtained from the boiler. Therefore, it is possible to recover 98% of CO_2 from the CO_2 purification system.

Percent CO_2 avoided is calculated as (specific CO_2 emission in the reference case in t/MWh - specific CO_2 emission in the oxy-fuel case in t/MWh)/ specific CO_2 emission in the reference case in t/MWh x 100%. Due to higher CO_2 recovery and lower parasitic power consumption, % CO_2 avoided is much higher for the OTM process compared to the conventional oxy-fuel case.

Technical Feasibility

Praxair has been engaged in OTM development since 1994. Early in the OTM program, membrane materials were developed that had a high oxygen flux but were not sufficiently reliable and mechanically robust for commercial application. In late 2004 Praxair embarked on a new OTM materials approach with the aim of developing first developing a highly robust membrane and then working to drive up oxygen transport rates. The robustness and reliability of the new membrane materials is evidenced by >18,000 hrs of failure free operation in single tube reactors with multiple thermal and chemical cycles. By prioritizing membrane strength and reliability in OTM membrane development, oxygen transport fluxes initially suffered. However since the conception of the new materials system a significant and continuous improvement in oxygen transport flux has been demonstrated (see Figure 2). A further highlight of the recent OTM combustion work at Praxair is demonstration of complete oxidation of natural gas in a laboratory scale OTM reactor with no air compression (see Figure 3). The dried flue gas composition from the laboratory scale demonstration contained >90% CO_2, the balance being predominantly excess O_2 and N_2 present in the natural gas fuel and introduced from air leaks. The reactor was run for >1000 hrs with no observed degradation in OTM performance before being intentionally shut down for modifications. Future tests in this laboratory scale reactor shall include the addition of H_2S and COS to the fuel stream.

The materials that are used in Praxair's OTMs have been selected such that they are not likely to form corrosion products with the sulfur-containing impurities in the coal synthesis gas. Tars, fines and fly ash can be expected to be present in the synthesis gas from the coal gasifier despite precautionary measures like cyclones and candle filters. It is expected that tars and fines will be converted to gaseous products when given a sufficient resident time in the high pressure OTM POx unit, but this needs to be verified. The influence of all these and other contaminants like HCl and NH_3 is yet unknown and Praxair will study the feasibility of

combustion of combustion of coal fines and tar vapors at the Utah Clean Coal Center who are sub-contracted to Praxair in the recent DOE Cooperative Agreement.

In Figure 1 the OTM tubes in the partial oxidation unit in front of the hot gas expander operate at high temperature and under a high differential pressure, which raises the concerns for mechanical stability of the membrane. The porous support structure of the OTM provides the mechanical support for the membrane and the material selected for this component has a very low creep rates so as to avoid creep induced buckling issues. The porous support thickness could be increased in order to make the membranes even more robust in the high pressure environment. The ability of the OTM to perform at elevated pressures shall also be verified experimentally in laboratory scale reactors in Tonawanda.

Summary

Praxair has proposed a novel method of integrating Oxygen Transport Membranes in a Coal Power Plant with CO_2 capture such that the energy penalty for oxyfuel combustion is substantially reduced. In a preliminary analysis the efficiency of the proposed OTM oxy-combustion power cycle is 4 to 5 points higher than an oxy-combustion pulverized coal power cycle with CO_2 capture. Praxair has recently entered into a Coopereative Agreement with the United States Department of Energy in which the technical and economic feasibility of the proposed power cycle will be further evaluated. A successful outcome to this project will result in a development plan for pilot testing of the OTM technology.

Acknowledgements

This work was prepared with the support of the U.S. Department of Energy, under Award Numbers DE-FC26-01NT41147 and DE-FC26-07NT43088. However, any opinions, findings, conclusions, or recommendations expressed herein are those of the authors and do not necessarily reflect the views of the DOE.

Figures and Tables

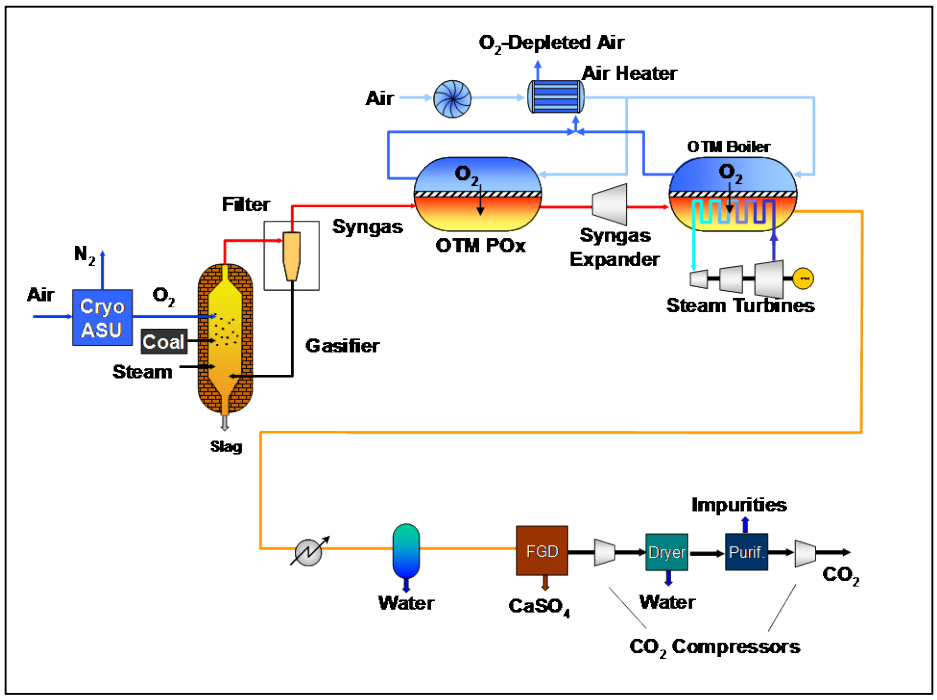

Figure 1: OTM Integrated Coal Power Plant with CO_2 Capture (Patent Application Filed)

	Air Fired PC Boiler	Oxy-PC w/ CO_2 Capture	OTM Process w/ CO_2 Capture
Net Output, MW	600	600	600
Efficiency % HHV	39.1%	29.9%	34.5%
CO_2 Emissions, t/MWh	0.88	0.12	0.016
Purity of Captured CO_2, %	-	96%	96%
% CO_2 Captured	-	90%	98.4%
% CO_2 Avoided	-	86%	98.2%

Table 1: Preliminary Performance Comparison of Air and Oxyfuel Pulverized Coal Boiler Power Plants and Proposed Oxygen Transport Membrane Process with CO_2 Capture.

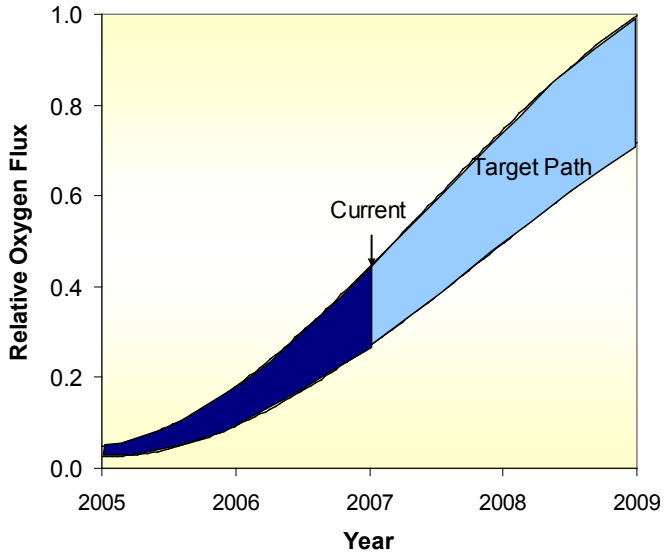

Figure 2: Progress in Oxygen Transport Membrane Flux with Robust Membrane Materials

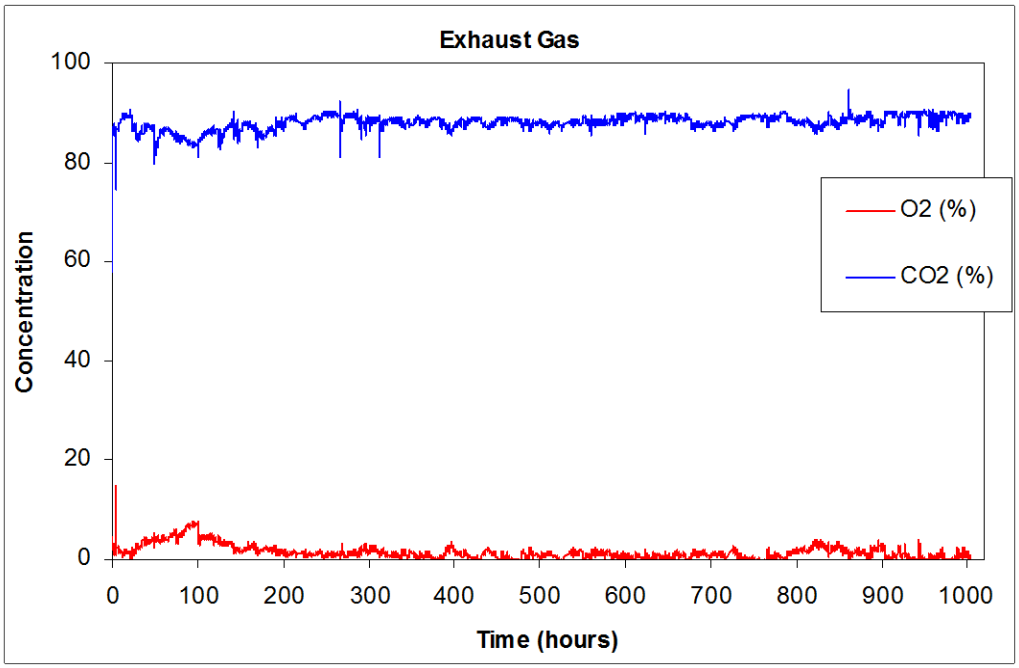

Figure 3: Dry Exhaust Gas Composition from OTM Combustion of Natural Gas in a Laboratory Scale Reactor

Progress towards the Demonstration of OTM Integration with Coal Combustion

Juan Li, Jamie Wilson, Nick Degenstein, Minish Shah, Bart A. van Hassel,
Maxwell Christie,
Praxair, Inc., Tonawanda, NY 14151
V. Venkateswaran, ENrG Inc., Buffalo, NY 14207

E-mail: bart_vanhassel@praxair.com

ABSTRACT

Praxair, Inc. and the United States Department of Energy (DOE) are developing an Oxygen Transport Membrane (OTM) based oxygen combustion process for Carbon Dioxide (CO_2) capture from coal power plants under a three year Cooperative Agreement (DE-FC26-07NT43088). The project has two phases. Phase I has a duration of two years and started April 1st of 2007. The primary focus of Phase I is OTM development. A further objective of Phase I is to down-select an optimum process integration cycle for the OTM membranes with CO_2 capture and to provide a full system and economic analysis of that cycle.

OTM development focuses on performance improvement while maintaining a high reliability; this requires a good understanding of the rate limiting steps. A performance improvement plan has been developed. An advanced porous support is being developed in collaboration with ENrG, Inc. (Buffalo, NY) in a project funded by NYSERDA (agreement number: 10080) and work continues to focus on improving the rate of fuel oxidation.

The performance of the OTM elements will be characterized in three types of reactors. Low pressure membrane reactors are being used to characterize the performance and robustness of OTM elements when exposed to synthesis gas in the OTM boiler of the proposed process. A high pressure test facility was constructed in order to characterize the performance and robustness of OTM tubes in the partial oxidation reactor of the proposed process. OTM tubes will first be tested with a simulated synthesis gas from the coal gasifier that does not contain H_2S and COS. Testing in the presence of those impurities will be conducted when suitable materials have been identified for the pressure vessel so that it can

withstand the highly corrosive atmosphere. The third reactor is being developed at the Utah Center for Ultra-Clean Coal Utilization in a Carbon- Constrained Environment (UC^3) and allows us to perform explorative research about burning coal with oxygen supplied by oxygen transport membranes.

Working towards down selection of the process integration cycle, the process and economic analysis approach and basis have been established. Progress is being made in developing the process simulation cases and the conceptual design of the OTM boiler.

Keywords: o*xygen transport membrane, oxy-fuel combustion, oxycombustion, OTM boiler, OTM POx, syngas, partial oxidation, gasification, auxiliary power*

1. INTRODUCTION

In the oxycombustion process, coal or another fossil fuel is burned with a mixture of pure oxygen and recycled flue gas. Due to the elimination of N_2 and thus a high CO_2 concentration in the flue gas, oxycombustion is established as a credible means to facilitate CO_2 capture from coal power plants. In a retrofit situation on an existing air-coal PC plant this may be conventionally achieved by supplying all the oxygen needed for combustion from a cryogenic air separation unit (ASU). A portion of the CO_2 rich flue gas must then be recirculated for furnace temperature control. Although the parasitic power requirement of the ASU will be large, both the overall plant efficiency is expected to be higher as compared to the air-coal case with post-combustion CCS (MEA).

Praxair is developing a novel OTM technology that has the potential to keep the CO_2 sequestration rate above 90% while eliminating the need for flue gas recycle and reducing the parasitic power requirement for the ASU. The OTM utilizes the combustion reaction with fuel to create a very low oxygen partial pressure on the fuel side to drive oxygen transport through the membrane, therefore there is minimal need for air compression and the parasitic power consumption required for oxygen production is reduced by 70-80% as compared to a cryogenic ASU [1].

Recently some significant milestones have been achieved in the OTM development at Praxair for oxycombustion applications. Novel OTM materials exhibiting high reliability and tolerance for repeated chemical and thermal cycling have been demonstrated. In a new Cooperative Agreement with DOE (DE-FC26-07NT43088) Praxair continues the development and scale-up OTM technology in order to drive the technology status to a level where it is ready for pilot-testing. The project has two phases. Phase I focuses on the OTM materials development and the selection of an optimum process to integrate the membranes in a coal power plant through process and economic modeling and technical feasibility assessment. Assuming success in the first phase of the project, Praxair will develop basic engineering design and cost of key pieces of OTM-based equipment and develop a plan for pilot testing of the technology.

2. PROCESS AND SYSTEM ENGINEERING

The proposed process for integration of OTM in a coal power plant is a hybrid of gasification and oxycombustion. The key aspect of this process is to use a high efficiency gasifier to convert coal into relatively clean syngas and then deliver the gaseous fuel to an OTM Partial Oxidation (POx) reactor and an OTM boiler for oxy-fuel combustion. This process is designed such that the majority of the components with the exception of the OTM equipment are well known and commercially available.

A simplified process schematic is presented in Figure 1. Coal is gasified and fines are removed by a cyclone or a candle filter and recycled back to the gasifier. The resulting syngas, containing small quantities of tars and oils, is then fed to an OTM POx unit with sulfur-tolerant membranes. In the OTM POx, partial oxidation of syngas occurs, which raises the syngas temperature, allowing conversion of tars and oils to syngas. The hot pressurized syngas is expanded to generate power before combustion is completed in an OTM Boiler. The OTM Boiler contains OTM and steam tubes, interspersed such that the fuel stream passes through alternating combustion and heat transfer zones [2,7]. Feed-air to the OTM is preheated using the oxygen depleted air stream exiting OTM manifolds.

In the OTM boiler, combustion is limited by the oxygen flux through the membrane and therefore oxygen supply for combustion is distributed over a long section of the boiler. This results in a unique temperature profile in the OTM boiler as compared to a conventional boiler where all the fuel and oxidant are delivered at burner tips. The result of the distributed combustion is that no flue gas recirculation is required. Approximately 75% of the total O_2 requirement for the process is supplied by OTM (65% in boiler and 10% in POx). The remainder is provided by high-purity (99.5%) O_2 from a cryogenic air separation unit (ASU).

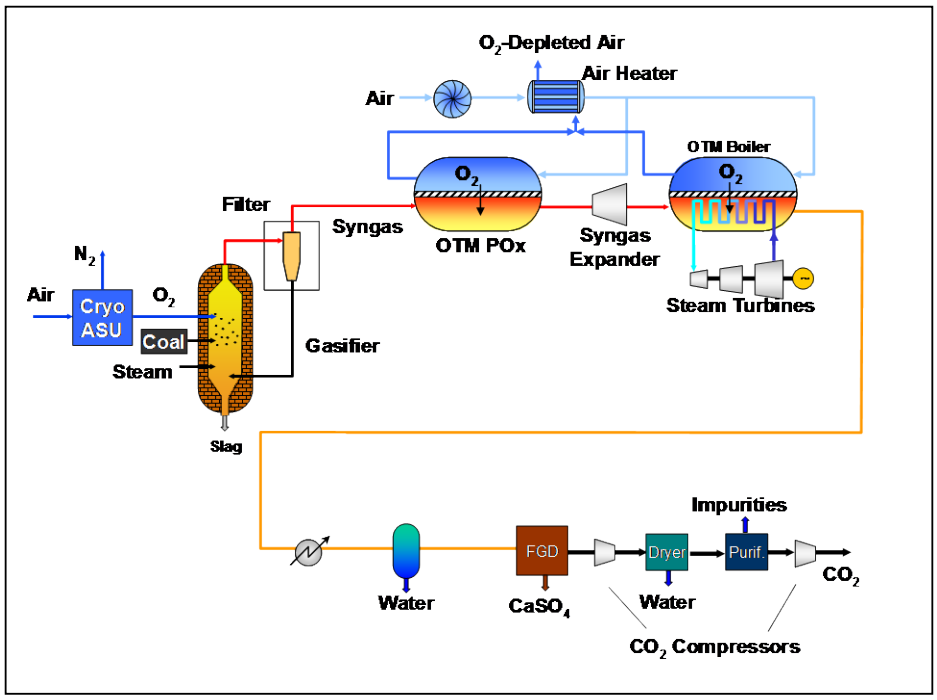

Figure 1, OTM integrated coal power plant with CO_2 capture (patent application filed).

The flue gas exiting the OTM boiler is at ~1770ºF, and consists of ~ 45% H_2O, 52% CO_2, with a balance of N_2, SO_2, and O_2. The economizer and the boiler feed water heater recover heat from the flue gas before it being further cooled and sent to a wet flue gas desulphurization (FGD) scrubber to remove SO_2. The FGD unit will be much smaller than for an air fired boiler due to the smaller flue gas volume. The flue gas exiting the FGD scrubber consists mainly of CO_2, with residual H_2O, Ar, N_2, O_2 and trace amounts of SO_2. The flue gas is compressed in a multistage compressor to >2000 psia for transport to the sequestration site.

Since CO_2 purity is >95%, there is no need for further purification, which normally causes CO_2 loss.

Preliminary economic analysis has been performed to compare the performance of two oxy-fuel technologies with CO_2 capture, a traditional oxycombustion pulverized coal (Oxy-PC) boiler with oxygen supplied from a cryogenic ASU and the OTM process proposed above that supplies majority of oxygen through OTM and the remainder from cryogenic ASU [8]. The economic analysis shows that the overall efficiency (HHV) of the OTM process is higher (34.5%) than the oxy-PC system (29.9%) due to significantly lower air compression requirements as well as the power recovery in the syngas expander of the OTM process. The higher overall efficiency results in an about 10% higher percentage of CO_2 avoided in the OTM process in comparison to conventional oxycombustion.

3. OTM MATERIALS DEVELOPMENT

The OTM tube consists of a robust inert porous support coated with an internal dense gas separation layer. Air flows through the inside the tube where molecular oxygen reacts with oxygen vacancies and electrons on the gas separation surface to form oxygen ions, which transport through the separation layer. Fuel species, typically a combination of CO, H_2 and CO_2, are fed to the outside of the tube where they transport through the support and react with oxygen ions at the separation layer surface to form oxidation products (H_2O, CO_2) and oxygen vacancies and electrons in the crystalline lattice structure of the separation layer.

In order to improve the mass transport through the porous support, the development of new porous supports is being explored in collaboration with ENrG, Inc. (Buffalo, NY) in a project supported by NYSERDA.

A number of different chemistries and architectures have been explored to attempt to improve the rate of fuel oxidation. Recent work has uncovered several materials that yielded a lower resistance to fuel oxidation in independent measurements, but have not yet led to an increase in overall oxygen flux in OTM tubes.

Figure 2 shows normalized oxygen flux results obtained from tubes measured in a H_2/CO_2 gas environment without sulfur impurities in an atmospheric pressure

reactor as a function of development time. Initial work carried out to modify materials and composite architectures yielded improved oxygen flux, but recent work has yielded little change in OTM performance. There are significant challenges ahead in meeting the targeted O_2 flux, given the processing and operating conditions.

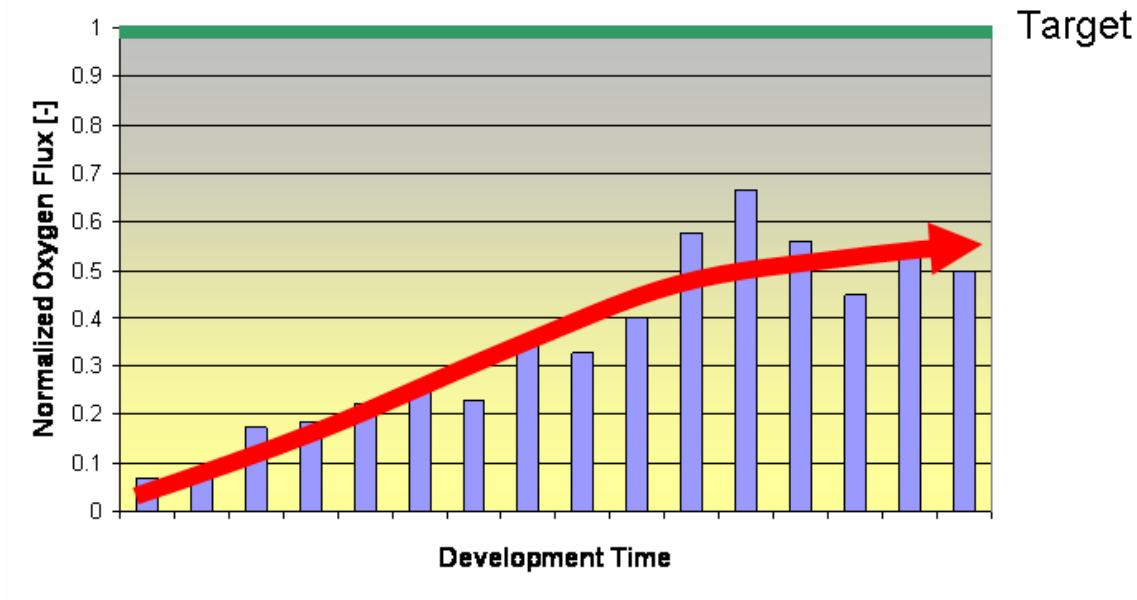

Figure 2, Normalized oxygen flux in OTM tubes at an operating temperature of 900°C and with fuel gas composition 2 (a H_2 /CO_2 mixture).

4. LABORATORY SCALE COMBUSTION TESTS

Laboratory scale combustion tests are being conducted in order to determine the OTM tube performance in the OTM boiler and the POx unit. The OTM tubes in the OTM boiler operate near atmospheric pressure and a large fraction of the fuel needs to be combusted. It is expected that complete oxidation of the fuel will be achieved with oxygen that will be supplied from the cryogenic air separation unit. The current performance of OTM tubes under conditions of the OTM boiler is shown in Figure 2. More development work is required in order to reach the target oxygen flux.

The OTM tubes in the partial oxidation unit of Figure 1 operate at high temperature and high differential pressure but only a small fraction of the fuel will need to be combusted. The operating conditions are severe and raise concerns about the chemical and mechanical stability of the membranes. The ability of the OTM to perform at elevated pressures needs therefore to be verified experimentally. A high pressure test facility (Figure 3) has been constructed and utilized at Praxair to characterize the performance and robustness of the OTM tubes. The tubes are first tested with a simulated synthesis gas from the coal gasifier that does not contain H_2S and COS. Tests in the presence of those impurities will be conducted in the sulfur resistant pressure vessels that were received recently.

Tests using simulated synthesis gas without sulfur impurities have been conducted in the high pressure reactor under elevated fuel pressure (up to 200 psig) and ambient OTM air pressure. As shown in the Figures 4 and 5, the OTM oxygen flux increases with increasing fuel pressure as well as with increasing operation temperature, and the oxygen flux levels off at high pressures. The OTM tubes tested in the reactor experienced a number of thermal cycles, pressure cycles, and changes in fuel composition. The OTM tubes have been demonstrated to be robust during the entire test period.

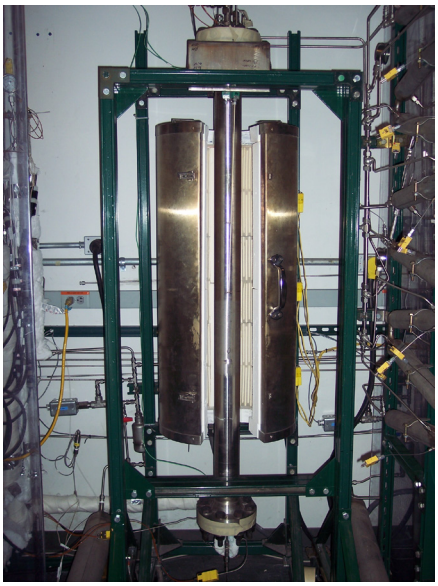

Figure 3, High-pressure reactor for testing OTM tubes at high temperatures and pressures at Praxair, Tonawanda, NY.

Praxair's OTM materials have been selected to limit the formation of corrosion products with the sulfur-containing impurities in the coal synthesis gas. Tars, fines and fly ash will be present in the synthesis gas from the coal gasifier despite precautionary measures like cyclones and candle filters. It is expected that tars and fines will be converted to gaseous products when given a sufficient resident

time in the high pressure OTM POx unit, but this needs to be verified. The influence of all these and other contaminants like HCl and NH_3 is yet unknown.

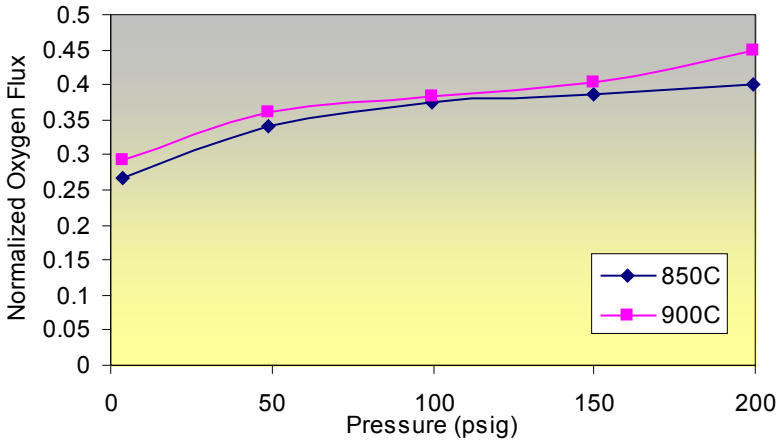

Figure 4, Change of oxygen flux of an OTM tube with the pressure of fuel with gas composition 1 (a CO/CO_2 mixture) at 850°C and 900°C.

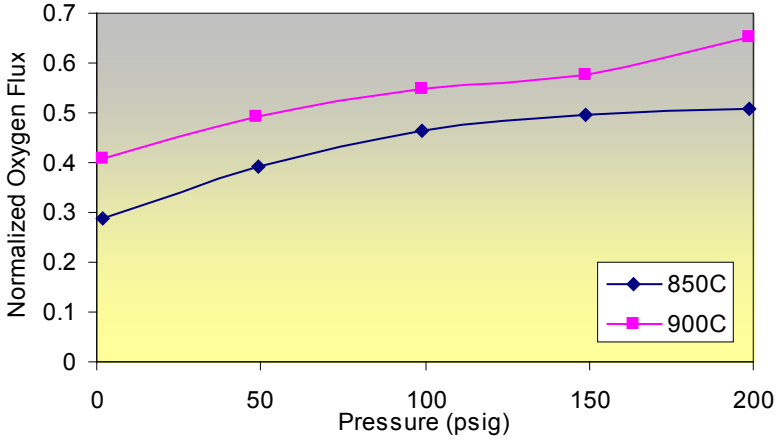

Figure 5, Change of oxygen flux of an OTM tube with the pressure of fuel with gas composition 2 (a H_2/CO_2 mixture) at 850°C and 900°C.

The unit power for oxygen production with OTM elements that have been integrated with a combustion process is significantly lower than the unit power of a cryogenic air separation unit. It is therefore advantageous to use oxygen from

the OTM elements wherever the operating conditions are appropriate and oxygen is required.

The Utah Center for Ultra-Clean Coal Utilization in a Carbon- Constrained Environment (UC^3) has been subcontracted to study the feasibility of coal combustion with oxygen that permeates through OTM tubes. In this advanced concept, O_2 from OTM tubes directly combusts coal providing a more efficient process design. UC^3 has finished the design of a multi-tube laboratory scale combustion apparatus. UC^3 is now in the process of fabricating this reactor.

5. SUMMARY

Praxair proposes a novel method of integrating Oxygen Transport Membranes in a Coal Power Plant with CO_2 capture such that the energy penalty for oxycombustion is substantially reduced. A successful outcome of this project will be the development of OTM tubes that reach the oxygen flux target while maintaining reliability at high pressure and in the presence of contaminants, and the completion of a development plan for pilot testing of the OTM technology. An OTM performance improvement plan has been developed and a high pressure reactor was constructed to characterize the performance and robustness of OTM tubes in the partial oxidation reactor of the proposed process. Tests illustrated an increase of the performance of the OTM tubes with an increase in pressure and temperature. A multi-tube reactor has been designed and is currently being constructed at the Utah Center for Ultra-Clean Coal Utilization in a Carbon-Constrained Environment (UC^3), where combustion of coal directly with oxygen supplied by OTM tubes will be studied.

6. ACKNOWLEDGEMENTS

This work was prepared with the support of the U.S. Department of Energy, under Award Number DE-FC26-07NT43088 and the New York State Energy Research and Development Authority (NYSERDA) under agreement number 10080. However, any opinions, findings, conclusions, or recommendations expressed herein are those of the authors and do not necessarily reflect the views of the DOE or NYSERDA.

7. REFERENCE

[1] J. Li, L. Switzer, B. Van Hassel, and M. Christie, "Thermally Integrated Oxy-Fuel Boiler", 30th International Technical Conference on Coal Utilization & Fuel Systems, Clearwater, FL, 2005.

[2] R. Prasad, C.G. Gottzmann, N.R. Keskar, Reactive Purge for Solid Electrolyte Membrane Gas Separation, US 5,837,125

[3] R. Prasad, C.F. Gottzmann, R.F. Drnevich, N.R. Keskar and H. Kobayashi, Process for Enriched Combustion Using Solid Electrolyte Ionic Conductor Systems, US 5,888,272

[4] L.E. Bool, III and H. Kobayashi, Air Separation Method and System for Producing Oxygen to Support Combustion in a Heat Consuming Device, US 6,382,958

[5] L.E. Bool, III and H. Kobayashi, Oxygen Separation and Combustion Apparatus and Method, US 6,394,043

[6] R. Prasad, H. Kobayashi and P.J. Cook, Integration of Ceramic Oxygen Transport Membrane Combustor with Boiler Furnace

[7] L.E. Bool, III, H. Kobayashi, Method and System for Combusting a Fuel, US 6,562,104

[8] M. Christie, B. van Hassel, J. Li, and M. Shah, "OTM Based Oxycombustion for CO_2 Capture from Coal Power Plants", 32nd International Technical Conference on Coal Utilization & Fuel Systems, Clearwater, FL, 2007.

OTM Based Oxy-fuel Combustion for CO_2 Capture

Jamie Wilson, Maxwell Christie, Nick Degenstein, Minish Shah, Juan Li
Praxair, Inc., Tonawanda, NY 14151
V. Venkateswaran, ENrG Inc., Buffalo, NY 14207
Eric Eddings and Joseph Adams, University of Utah, Salt Lake City, UT 84112

E-mail: max_christie@praxair.com

ABSTRACT

Praxair, Inc. and the United States Department of Energy (DOE) are developing an optimum process configuration for integrating Oxygen Transport Membranes (OTMs) into a power generation process allowing for high efficiency Carbon Dioxide (CO_2) capture from coal power plants under a three year Cooperative Agreement (DE-FC26-07NT43088). The main objective of Phase I is to develop OTM technology that meets commercial targets for oxygen flux, strength and reliability. A second objective of Phase I is to down-select an optimum process integration cycle for the OTM membranes with CO_2 capture and to provide a full system and economic analysis of that cycle.

An advanced porous support for the membrane separation layers was developed in collaboration with ENrG, Inc. (Buffalo, NY) in a project funded by NYSERDA (agreement number: 10080), preliminary tests revealed that this advanced support allowed significantly higher oxygen flux than the standard support material. When combined with further improvements to the fuel oxidation layer, oxygen transport rates that approach commercial targets were demonstrated at the laboratory scale.

Three types of reactors have been constructed to characterize the performance of OTM elements. A high pressure reactor was constructed to characterize the performance of OTM tubes under partial oxidation conditions at high pressure (up to 200 psig). Simulated synthesis gas from a coal gasifier with and without H_2S and COS is used as the fuel in this partial oxidation reactor. Tests show that the oxygen flux increases with fuel pressure and that the

membranes can tolerate high levels of sulfur impurities. Low pressure membrane reactors are used to characterize the performance and robustness of OTM elements when exposed to synthesis gas in the OTM boiler of the proposed process. The third reactor, which will allow testing of the OTM tubes with solid fuel has been developed and constructed at the Utah Clean Coal Center.

Process simulations have been performed for the overall OTM process with power generation at a scale of 550 MWe net. Approximate capital costs have been determined for cost of electricity (COE) comparison against other technologies for CO_2 sequestration. Sensitivity around OTM membrane cost and delivered coal price has been determined to understand how these variables affect the total COE.

Keywords: o*xygen transport membrane, oxy-fuel combustion, oxycombustion, OTM boiler, OTM POx, synthesis gas, partial oxidation, gasification, auxiliary power*

1. INTRODUCTION

The oxycombustion process is one of several proposed methods to capture CO_2 from coal-fired power plants. In a retrofit situation, pure oxygen would replace air required for combustion, and the oxygen would likely be supplied via a cryogenic air separation unit (ASU). An advantage of oxycombustion is the high available CO_2 concentration in the flue gas, available in part because pure O_2 is used for combustion instead of air. However, the parasitic power requirement of the ASU poses a significant energy penalty to the process.

An Oxygen Transport Membrane (OTM) technology being developed by Praxair has the potential to reduce the parasitic power requirement for the ASU, while maintaining a high (>95%) CO_2 capture rate. The OTM utilizes the large gradient in oxygen partial pressure between the fuel and airside of the OTM system to drive oxygen transport through the membrane. By utilizing a chemical driving force for air separation, very little power is consumed for air compression

and the parasitic power consumption required for oxygen production is reduced by 70-80% as compared to a cryogenic ASU [1].

In a Cooperative Agreement with DOE (DE-FC26-07NT43088) Praxair is developing and scaling-up the OTM technology in order to drive the technology status to a level where it is ready for pilot-testing. The project has two phases. In phase I, Praxair will work on OTM materials development and through process and economic modeling along with technical feasibility studies, Praxair will select an optimum process configuration for OTM integration into a coal power plant. Phase II of this project will involve developing basic engineering design and costing of key pieces of OTM-based equipment. Phase II will also involve the development of a plan for pilot testing of the technology. Praxair is currently working on the first phase of this project.

2. PROCESS AND SYSTEM ENGINEERING

Process concepts incorporating ceramic oxygen transport membranes (OTM) into coal-fired power plants in order to facilitate carbon dioxide capture have undergone technical and economic evaluation. Figure 1 depicts a simplified schematic of the first process concept, in which coal is reacted in an oxygen-blown gasifier to generate synthesis gas. A cyclone or a candle filter removes fines from the synthesis gas, before the synthesis gas is fed to an OTM partial oxidation reactor (OTM POx). In the POx unit, the reaction between oxygen generated by the OTM tubes and synthesis gas provides heat, increasing the temperature of the synthesis gas. Power is then recovered by expanding the hot synthesis gas. After expansion, the synthesis gas, at slightly above the ambient pressure, is fed to the OTM boiler.

In the OTM boiler, synthesis gas reacts with oxygen produced from the OTM tubes. The OTM system will be used to supply oxygen to the fuel side until 80 – 90% fuel utilization is achieved. The OTM tubes produce oxygen by using a gradient in chemical potential to drive oxygen ions across the ceramic material of the OTM. Because oxidized synthesis gas provides less of driving

force for oxygen ion transport than the starting synthesis gas, OTM derived oxygen is an inefficient source for the final 10 – 20% of oxygen, and therefore oxygen supplied from the cryogenic air separation unit will be used to complete combustion. The exiting flue gas at ~1770ºF and consisting of ~ 45% H_2O, 52% CO_2, with a balance of N_2, SO_2, and O_2 will pass through a convective section of the boiler for further steam generation and boiler feed water preheating. The flue gas exiting the FGD scrubber consists mainly of CO_2 (>95%) and is compressed in a multistage compressor to >2000 psia for transport to the sequestration site.

Basic conceptual engineering design of the OTM Boiler will take place during Phase II of this project. The design is currently envisaged to include steam tubes interspersed with OTM tubes such that the thermal energy released from reactions on the OTM tubes will heat the steam tubes, and OTM temperatures across the boiler will be maintained at a level which will allow optimum and stable membrane performance.

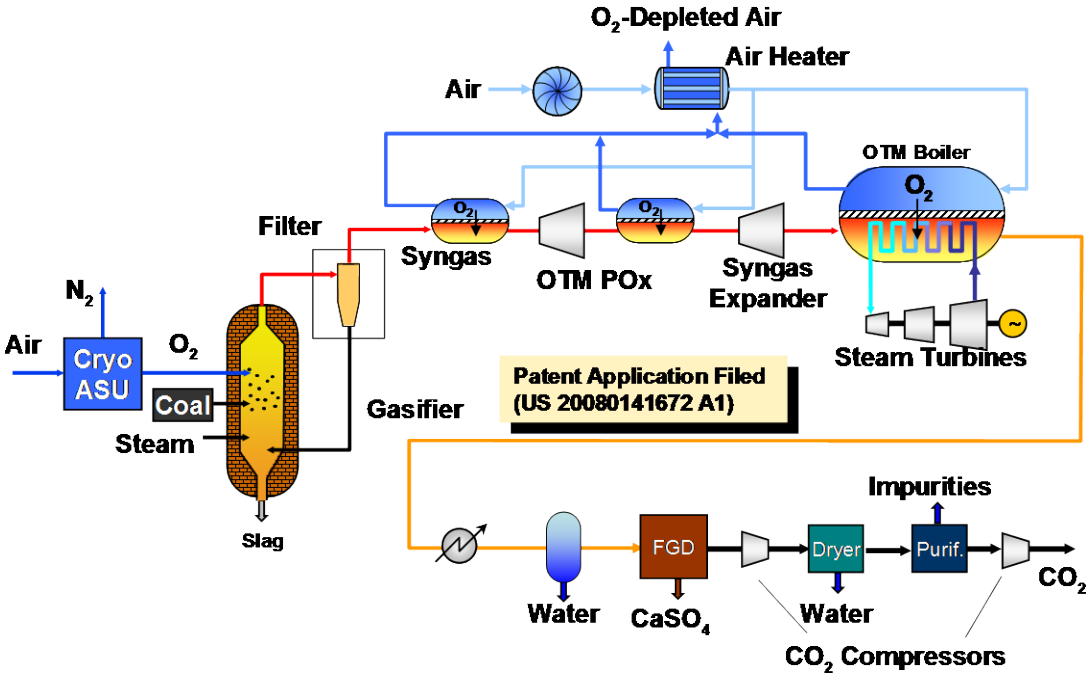

Figure 1, Process for Integration of OTM into Power Generation Cycle with CO_2 Capture

A summary of recently completed techno-economic analysis is presented in Table 1, which shows that given a coal price of $3/MMBTU the cost of electricity is expected to increase < 35% when compared with the Air fired PC case.

Table 1 Cost and Performance Summary of OTM Process

	Air fired PC	OTM Process
Efficiency, %HHV	39.7%	37.2%
CO2 purity, %		96%
CO2 recovery, %		96.7%
Coal Price $1.8/MMBtu		
Cost of electricity, $/MWh	$70	$97
Cost of electricity increase over base, %		38%
Cost of CO2 capture, $/ton		$29
Cost of CO2 avoided, $/ton		$31
Coal Price $3.0/MMBtu		
Cost of electricity, $/MWh	$83	$110
Cost of electricity increase over base, %		33%
Cost of CO2 capture, $/ton		$30
Cost of CO2 avoided, $/ton		$32

3. OTM MATERIALS DEVELOPMENT

In the OTM tubes, air enters the inside of the tube, and fuel (typically consisting of CO, H_2, CO_2, CH_4, and H_2O, along with dilute quantities of impurities such as H_2S, COS, etc.) is in contact with the outside of the tubes. Molecular oxygen in the air reacts on the inside of the tube and dissociates into oxygen ions that are transported through the tube to the fuel-side where they oxidize the fuel species. Oxygen depleted air exits the inside of the OTM tubes and is used to preheat the inlet air. The oxidized syngas, i.e. flue gas, exits the OTM system and is also used for further heat integration.

The OTM tube contains two components: a porous support and an internal dense gas separation layer. The porous support provides mechanical strength to the OTM system. The internal gas separation layer facilitates the reduction of molecular oxygen (O_2) to oxygen ions (O^{2-}) on the surface of the air

side, the oxidation of fuel species on the surface of the fuel-side, and transport of oxygen ions through the bulk of the membrane while preventing molecules in the air and fuel from crossing the membrane.

Mass transport through the porous support and fuel oxidation on the internal gas separation layer were identified as co-contributors to performance losses. In order to improve mass transport through the porous support, the development of an advanced porous support was explored in collaboration with ENrG, Inc. (Buffalo, NY) in a project supported by NYSERDA; this work has demonstrated a breakthrough in oxygen flux performance on laboratory scale samples. In addition, a modification to the chemistry of the fuel-oxidation surface was employed which yielded a significant improvement in the rate of fuel oxidation, and once incorporated in the OTM system provided a further increase in oxygen flux.

Figure 2 shows normalized oxygen flux results obtained from OTM laboratory samples in a synthesis gas environment as a function of fuel utilization. Samples prepared with the standard porous support and standard fuel oxidation surface are represented as blue symbols. A physical model describing the mass transport and kinetic phenomena occurring in the OTM system was used to predict performance of the OTM over the full range of fuel utilization, and is shown to compare well with experimental data. At the commercial target of ~80-90% fuel utilization, predictions from the physical model and experimental data indicate that the current OTM architecture will not achieve a normalized flux of 1. Green symbols represent performance of OTM samples prepared with the "advanced support" and improved fuel oxidation surface, and the physical model was updated with improved OTM characteristics of the new materials. OTM samples prepared with the improved support and fuel oxidation surface show ~2X improvement in performance at ~10% fuel utilization when compared to the previous OTM system, and performance is predicted to approach the flux target at high fuel utilization (~80-90%). Work is currently being performed in collaboration with ENrG, Inc. (Buffalo, NY) in a project supported by NYSERDA to prepare samples with the upgraded material system that will be

capable of supporting higher fuel utilizations and to scale-up the OTM system with the "advanced support" to pilot scale.

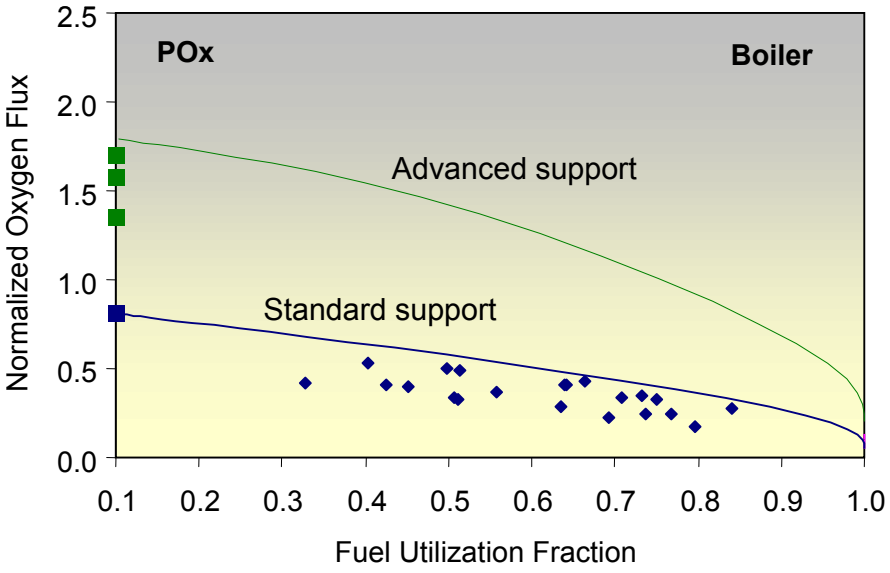

Figure 2, Normalized average oxygen flux versus fuel utilization of OTM laboratory samples. OTM samples with the standard support and standard fuel oxidation surface represented as blue squares at low fuel utilization and with blue diamonds at high fuel utilization. OTM samples with the "advanced support" and advanced fuel oxidation surface represented as green squares at low fuel utilization. Blue and green lines represent performance predicted by a physical model.

4. LABORATORY SCALE COMBUSTION TESTS

Laboratory scale combustion tests are being conducted in order to determine the OTM tube performance in the OTM boiler and the POx unit. The OTM tubes in the OTM boiler operate near atmospheric pressure and ~ 80 – 90% of the fuel needs to be combusted. The OTM tubes in the partial oxidation unit of Figure 1 operate at high temperature and high differential pressure and only a small fraction of the fuel will need to be combusted. The fuel composition, which contains trace impurities such as H_2S and COS, along with a high differential pressure, raises concerns about the chemical and mechanical stability of the membranes. A high-pressure test facility was constructed at Praxair, as shown in

Figure 3. OTM tubes were tested in this facility under appropriate pressure gradient conditions and with a simulated synthesis gas from the coal gasifier that contained H_2S and COS. Results from these tests are presented in Figure 4. An increase in performance was observed under the pressure gradient conditions and with the inclusion of sulfur containing impurities. OTM tubes were tested for a period of seven hours, and showed stable performance during testing. The facility has been modified to allow for longer test runs to gain a greater understanding of stability under long operating times. The POx unit operates at relatively low fuel utilization (~ 25%), and is expected to yield higher performances than the OTM Boiler unit.

Figure 3, High-pressure reactor for testing OTM tubes at high temperatures, high pressures, and with sulfur containing impurities at Praxair, Tonawanda, NY.

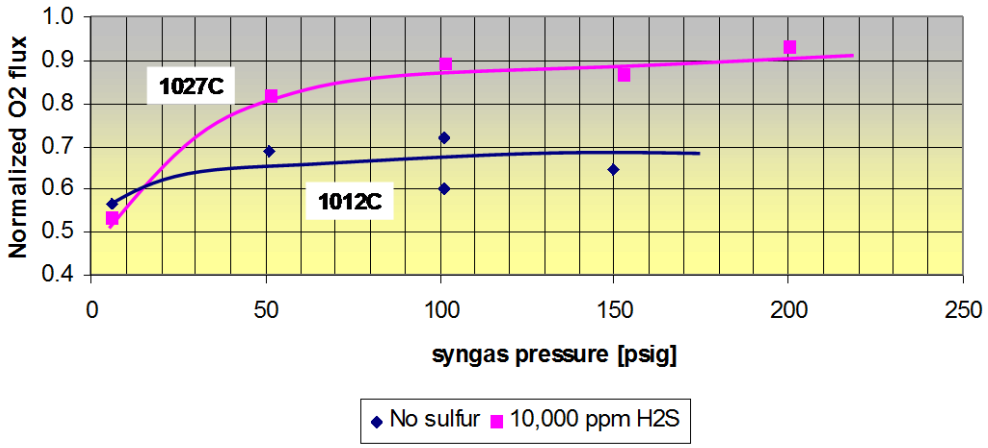

Figure 4, Oxygen flux of an OTM tube as a function of the pressure of fuel with a simulated synthesis gas with no impurities [blue symbols] and with 1% H_2S [pink symbols]. This OTM tube was prepared with the standard porous support and the standard fuel oxidation surface of the dense gas separation layer.

The Utah Clean Coal Center (UC^3) has been subcontracted to study the feasibility of operating the OTM tubes in a coal environment. UC^3 has finished construction of a multi-tube laboratory scale combustion reactor, consisting of three distinct modules, as shown in Figure 5. The reactor can be operated either as a fluidized bed reactor or as a fixed bed reactor. In the fixed bed reactor design, coal can be partially oxidized with molecular oxygen in one module to form synthesis gas, and the generated synthesis gas can be combusted with the OTM tubes in a separate module, generating heat and flue gas. The fixed bed reactor configuration represents the current process design and will allow testing in a real coal derived synthesis gas, with tars, fines, fly-ash, HCl, NH_3, and other impurities present in the fuel. Preliminary testing has recently begun in the facility.

Figure 5, Multi-tube reactor for testing multiple OTM tubes in a coal environment at the University of Utah, Salt Lake City, UT.

5. SUMMARY

Praxair has developed an Oxygen Transport Membrane (OTM) technology and has proposed a method for integrating these membranes into a Coal Power Plant to allow for CO_2 capture with a reduced parasitic power penalty, and a cost of electricity increase compared to an Air fired PC estimated to approach the DOE's targets. A successful outcome of Phase I of this project will be the development and scale-up of OTM tubes that reach the oxygen flux target while maintaining reliability at high pressure and in the presence of contaminants. Improving the porous support microstructure and modifying the chemistry of the gas separation layer has yielded significant progress towards approaching the oxygen flux performance targets on laboratory scale samples. Tests illustrated an increase of the performance of the OTM tubes with an increase in pressure and in the presence of sulfur impurities. A multi-tube reactor has been constructed at the Utah Clean Coal Center (UC^3), where the performance of OTM tubes in a real coal-derived synthesis gas with oxygen supplied by OTM tubes will be studied.

6. ACKNOWLEDGEMENTS

This work was prepared with the support of the U.S. Department of Energy, under Award Number DE-FC26-07NT43088 and the New York State Energy Research and Development Authority (NYSERDA) under agreement number 10080 and 10080-1.

7. DISCLAIMER

This material is based upon work supported by the Department of Energy under Award Number DE-FE26-07NT43088. Neither the United States Government nor any agency thereof, nor any of their employees, makes any warranty, express or implied, or assumes any legal liability or responsibility for the accuracy, completeness, or usefulness of any information, apparatus, product, or process disclosed, or represents that its use would not infringe privately owned rights. Reference herein to any specific commercial product, process, or service by trade name, trademark, manufacturer, or otherwise does not necessarily constitute or imply its endorsement, recommendation, or favoring by the United States Government or any agency thereof. The views and options of authors expressed herein do not necessarily state or reflect those of the United States government or any Agency thereof.

The material is also based upon work supported by NYSERDA under agreement number 10080 and 10080-1. NYSERDA has not reviewed the information contained herein, and the opinions expressed in this report do not necessarily reflect those of NYSERDA or the State of New York.

8. REFERENCES

[1] J. Li, L. Switzer, B. Van Hassel, and M. Christie, "Thermally Integrated Oxy-Fuel Boiler", 30th International Technical Conference on Coal Utilization & Fuel Systems, Clearwater, FL, 2005.

[2] R. Prasad, C.G. Gottzmann, N.R. Keskar, Reactive Purge for Solid Electrolyte Membrane Gas Separation, US 5,837,125

[3] R. Prasad, C.F. Gottzmann, R.F. Drnevich, N.R. Keskar and H. Kobayashi, Process for Enriched Combustion Using Solid Electrolyte Ionic Conductor Systems, US 5,888,272

[4] L.E. Bool, III and H. Kobayashi, Air Separation Method and System for Producing Oxygen to Support Combustion in a Heat Consuming Device, US 6,382,958

[5] L.E. Bool, III and H. Kobayashi, Oxygen Separation and Combustion Apparatus and Method, US 6,394,043

[6] R. Prasad, H. Kobayashi and P.J. Cook, Integration of Ceramic Oxygen Transport Membrane Combustor with Boiler Furnace

[7] L.E. Bool, III, H. Kobayashi, Method and System for Combusting a Fuel, US 6,562,104

[8] M. Christie, B. van Hassel, J. Li, and M. Shah, "OTM Based Oxycombustion for CO_2 Capture from Coal Power Plants", 32nd International Technical Conference on Coal Utilization & Fuel Systems, Clearwater, FL, 2007.

[9] J. Li, J. Wilson, N. Degenstein, M. Shah, B. van Hassel, M. Christie. 33rd International Technical Conference on Coal Utilization & Fuel Systems, Clearwater, FL, 2008.

OTM Based Oxy-fuel Combustion for CO_2 Capture

Jamie Wilson, Maxwell Christie, Nick Degenstein, Minish Shah, Juan Li, Lee Rosen, John Peck
Praxair, Inc., Tonawanda, NY 14151
V. Venkateswaran, K. Helmer, A. Urban and J. Newkirk,
ENrG Inc., Buffalo, NY 14207
Eric Eddings and Joseph Adams, University of Utah, Salt Lake City, UT 84112

E-mail: max_christie@praxair.com

ABSTRACT

Oxygen transport membrane (OTM) based Oxy-fuel Combustion is a technology that integrates ceramic OTMs into coal-fired power plants to allow for efficient carbon dioxide capture. Due to high efficiencies and low parasitic power requirements, this technology has the potential to meet the United States Department of Energy (DOE) cost of electricity goals for power plants with carbon capture and compression. Under a Cooperative Agreement (DE-FC26-07NT43088), Praxair, Inc. and the DOE are working on a multiple phase project that is focused on the development of an optimum process configuration for OTM based Oxy-fuel Combustion, and preparation for pilot scale testing.

Phase I of this project, concluding at the end of 2009, involved development of a robust OTM technology that met commercial performance targets and provision of an optimized process integration cycle for the OTM membranes with CO_2 capture along with a full system and economic analysis of that cycle. Phase II of this project, initiating at the start of 2010 will result in delivery of a detailed plan for pilot testing that will include basic engineering design and cost estimation of key pieces of OTM-based equipment.

Phase I of this project ended with the selection of an optimum process integration cycle. The OTM cycle includes a gasifier, which produces pressurized synthesis gas. In contact with OTM elements, the synthesis gas is heated and partially oxidized. Next, the partially oxidized synthesis gas is expanded, producing a portion of the plant gross power. Post expansion, the partially

oxidized synthesis gas is combusted to near completion on the surface of OTM membranes in an OTM boiler. In the boiler, heat generated from combustion is transferred to steam, and energy is produced using a steam turbine.

Membrane development work completed during Phase I yielded advancements in both the porous support material and fuel activation layer, providing significantly higher oxygen flux values (scfh/ft^2) across a broad range of operating conditions and meeting oxygen flux targets required for commercial application in OTM integrated oxyfuel combustion applications. OTM performance is not the only variable influencing the Cost of Electricity (COE) of OTM based power cycles with Carbon Capture and Sequestration (CCS). The COE is also dependent on variables such as fuel price and the capital cost of OTM integrated equipment. A portion of the work to be performed in Phase II is focused on OTM equipment design and developing a better understanding of capital costs.

Three types of reactors that characterize performance of OTM elements are currently operational (1) reactors that allow testing single elements under near atmospheric pressure and in simulated fuel gases without the presence of contaminants, (2) a reactor that allows testing under partial oxidation conditions at high pressure (up to 200 psig) and in simulated fuel gases with and without H_2S and COS contaminants, and (3) a reactor constructed at the Utah Clean Coal Center at the University of Utah that allows testing of multiple OTM elements in a coal derived synthesis gas at atmospheric pressure. Performance characteristics of OTM elements derived from these three reactors will be presented. Progress towards demonstration of a pilot-scale OTM reactor will also be presented.

Keywords: o*xygen transport membrane, oxy-fuel combustion, oxycombustion, OTM boiler, OTM POx, synthesis gas, partial oxidation, gasification, auxiliary power*

1. INTRODUCTION

The oxycombustion process is one of several proposed methods to capture CO_2 from coal-fired power plants. In a retrofit situation, pure oxygen would replace air required for combustion, and the oxygen would be supplied via a cryogenic air separation unit (ASU). An advantage of oxycombustion is the high available CO_2 concentration in the flue gas, available in part because pure O_2 is used for combustion instead of air. However, the parasitic power requirement of the ASU poses a significant energy penalty to the process.

An Oxygen Transport Membrane (OTM) technology being developed by Praxair has the potential to reduce the parasitic power requirement for the ASU, while maintaining a high (>95%) CO_2 capture rate. The OTM utilizes the large gradient in oxygen partial pressure between the fuel and airside of the OTM system to drive oxygen transport through the membrane. By utilizing a chemical driving force for air separation, very little power is consumed for air compression and the parasitic power consumption required for oxygen supply is reduced by 70-80% as compared to a cryogenic ASU [1-4].

In a Cooperative Agreement with DOE (DE-FC26-07NT43088) Praxair is developing and scaling-up the OTM technology in order to drive the technology status to a level where it is ready for pilot-testing. The project consists of two phases. Praxair has completed the first phase of this project, and is currently working on the second phase of the project. In Phase I, OTM performance improvement was achieved through materials development. Also in Phase I, process and economic modeling along with technical feasibility studies were performed that allowed Praxair to down select an optimum process configuration for OTM integration into a coal power plant that predicts a < 35% increase in COE over an air fired PC plant with post combustion carbon capture and compression. Phase II of this project involves developing basic engineering design and costing of key pieces of OTM-based equipment. Phase II also involves the development of a plan for pilot testing of the technology.

2. PROCESS AND SYSTEM ENGINEERING

During the initial phase of the program, Praxair developed and evaluated several process cycles. The process scheme that was selected is illustrated in Fig. 1. The concept utilizes a gasifier that is fed with oxygen from a conventional air separation unit (ASU). The gasifier is selected such that it achieves high carbon conversion with minimal oxygen. After particulate cleanup, the syngas is reacted in an OTM partial oxidation (POx) reactor to raise the temperature prior to expansion through a power recovery turbine (PRT). The process cycle illustrated in Fig. 1 shows a series of two POx/PRTs to maximize the efficiency of power recovery. After expansion to slightly above atmospheric pressure, the synthesis gas is fed to the OTM boiler.

In the OTM boiler, synthesis gas reacts with oxygen separated from air via OTM devices. The conceptual design of the boiler has OTM elements interspersed with steam tubes such that the radiant heating from the OTM elements supplies the energy to the steam tubes [5-10]. The final 10 – 20% of the oxygen required to complete combustion is supplied from the conventional ASU. This is due to the decrease in oxygen flux in the OTM with lower concentrations of fuel species. The incremental OTM area required to provide the final oxygen to complete combustion comes at a cost higher than that of conventional oxygen production. The process as illustrated in Fig. 1 is designed to allow the optimization of the overall cost of oxygen by balancing it between conventional production methods and advanced OTM methods.

After the fuel is completely oxidized with externally supplied O_2, the flue gas will pass through a convective section of the boiler for further steam generation and boiler feed water preheating. The flue gas exiting the FGD scrubber consists mainly of CO_2 and is compressed in a multistage compressor to >2000 psia for transport to the sequestration site.

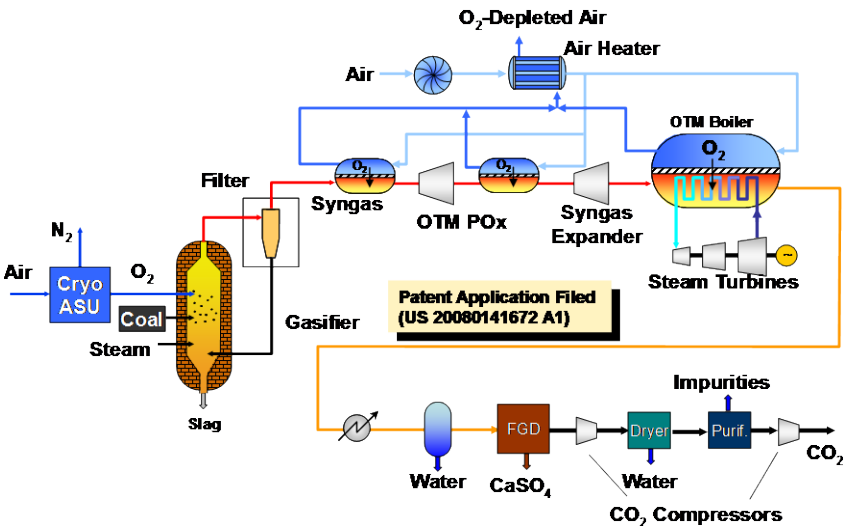

Figure 1: Process for Integration of OTM into Power Generation Cycle with CO_2 Capture

A techno-economic evaluation of the OTM process illustrated in Fig. 1 was performed to determine the cycle efficiency and cost of electricity (COE) of the OTM process. Originally this evaluation was run with a target OTM flux (scfh/ft^2) performance. After experimental performance improvement, the techno-economic evaluation was updated to reflect the observed oxygen flux results over a range of OTM fuel utilization values. This model also incorporates an estimated OTM cost allocation ($/ft^2). A better OTM cost estimate will be determined for manufacturing cost after completion of OTM boiler equipment conceptual design during Phase II.

Table 1 presents a summary of recently updated techno-economic analysis with an OTM fuel utilization of 80%. Table 1 shows that given a coal price of $3/MMBTU the cost of electricity is expected to increase < 35% when compared with the air fired PC case. The COE for the air-fired PC case was taken from a DOE oxy-combustion report (DOE/NETL-2007-1291) and adjusted to 2008 capital dollars [11].

Table 1: Comparison of OTM case with Air PC base case (cost basis for all cases March, 2008)

	Air fired PC	**OTM Process**

Efficiency, %HHV	39.7%	37.2%
CO2 purity, %		95.8%
CO2 recovery, %		97.1%
Coal Price $1.8/MMBtu		
Cost of electricity, $/MWh	$70	$97.6
Cost of electricity increase over base, %		38.4%
Cost of CO2 removal, $/ton		$34.07
Cost of CO2 avoided, $/ton		$36.66
Coal Price $3.0/MMBtu		
Cost of electricity, $/MWh	$83	$110.9
Cost of electricity increase over base, %		33.8%
Cost of CO2 removal, $/ton		$35.06
Cost of CO2 avoided, $/ton		$37.72

3. OTM MATERIALS DEVELOPMENT

The OTM tube is composed of a porous support, an internal gas-separation layer, and two activation layers. Air is exposed to one side of the OTM tube, while fuel (CO, H_2, CO_2, CH_4, and H_2O along with dilute quantities of impurities such as H_2S, COS, etc.) is exposed to the opposing side of the OTM tube. On the air side of the separation layer, an activation layer promotes reduction of molecular oxygen to oxygen ions. The gas separation membrane transports oxygen ions from the air-side activation layer of the OTM tube to the fuel-side activation layer. The gradient in partial pressure of oxygen between the fuel-side and air-side of the separation layer drives transportation of oxygen ions across the membrane. Between the support and the separation membrane, a second activation layer (the fuel-side activation layer) promotes fuel oxidation.

During Phase I, material development activities yielded identification of two methods of improving oxygen transport across the OTM over a range of fuel utilization conditions. Firstly, the architecture of the porous support was modified to reduce fuel diffusion limitations. Secondly, the fuel-side activation layer material set was modified to enhance the fuel oxidation kinetics. Fig. 2 shows the relative improvements in membrane performance.

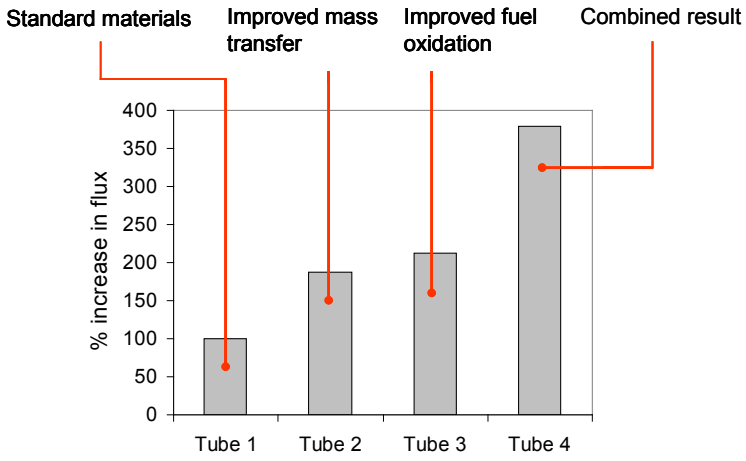

Figure 2: Relative membrane performance for OTM tubes, combining improvements in porous support and fuel oxidation (Tube 1: Standard support, Tube 2: Improved support, Tube 3: Improved fuel oxidation, Tube 4: Improved support & fuel oxidation).

4. LABORATORY SCALE COMBUSTION TESTS

Laboratory scale combustion tests were conducted in order to determine the OTM tube performance in the OTM boiler and the POx unit. The POx unit operates at up to 300-350 psig and relatively low fuel utilization (~ 25%), while the OTM boiler operates at near atmospheric pressure and at relatively high fuel utilization (~80-90%). Three facilities have been constructed at Praxair that allow testing of OTM elements in simulated synthesis gas; a facility can test a single OTM element at a time. Each test facility only allowed measurement over a narrow fuel utilization range (Reactor 1 - 10% fuel utilization, Reactor 2 –20%-55% fuel utilization, and Reactor 3 – 55%-90% fuel utilization). Fig. 3 shows "average" oxygen flux performance levels as a function of fuel utilization obtained from the three reactors for laboratory scale OTM samples prepared with the standard material set (blue triangles) and with several iterations of the advanced material set (green triangles). All results shown in Fig. 3 were obtained from tests performed under near atmospheric pressure, and in simulated synthesis gas compositions that did not include sulfur impurities. Fig. 3 shows performance

levels improving 2X-3X across a broad range of fuel utilization when implementing the advanced material set.

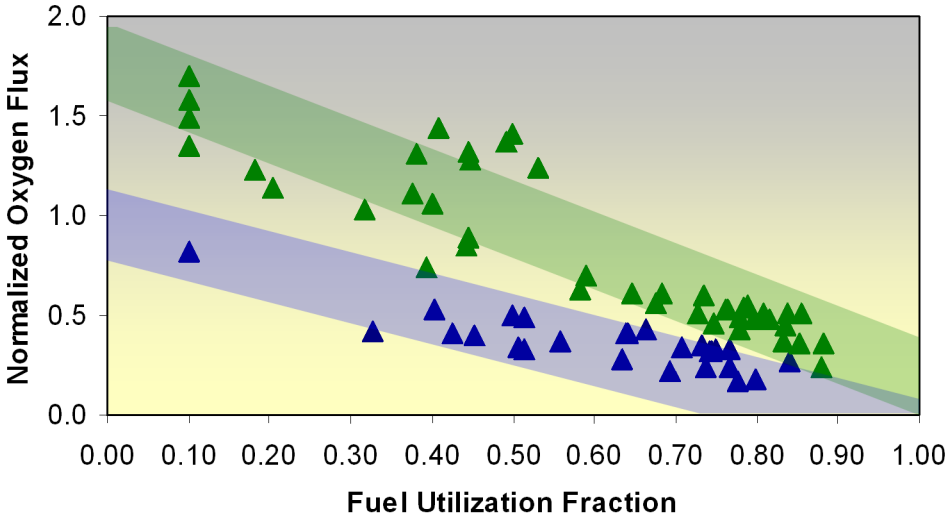

Figure 3: Average oxygen flux versus fuel utilization of OTM laboratory samples. OTM samples with the 'standard' materials represented as blue triangles. OTM samples with the 'advanced' materials are represented as green triangles.

Several ambiguities led to challenges in data interpretation. Firstly, only Reactor 2 was constructed to allow feed of a simulated synthesis gas that included all key fuel constituents including methane and steam, whereas tests performed in Reactor 1 and 3 were run without inclusion of methane and steam in the inlet. Also, Reactor 2 was constructed so that it could be operated in an optimized flow configuration. Therefore of the data presented in Fig. 3, we had significantly higher confidence in the data presented in the 25-55% fuel utilization range. Therefore the OTM performance in the range of fuel utilization anticipated in the OTM boiler (80-90%) was not well understood.

A new testing protocol was developed to allow Reactor 2 to probe a broader range of fuel utilization. The fuel flow rate was increased significantly, so that only a small fraction of the fuel could combust, and therefore the fuel composition was approximately the same over the length of the reactor. A series of ten tests were performed on a single tube where the fuel inlet composition for the first test was the intended entrant synthesis gas composition, but for each of

the following tests the fuel inlet composition was set to the outlet gas composition of the preceding test. These tests provided a set of "instantaneous oxygen flux" values over a broad fuel utilization range (18% - 85%). This data was then integrated, converting it to a set of average oxygen flux data, displayed as red triangles in Fig. 4.

Fig. 4 also presents a commercial target for oxygen flux as a function of fuel utilization obtained from an economic analysis of the OTM-based process for power generation with CO_2 capture, assuming a coal price of $3/MMBTU, and an estimate for the OTM cost allocation ($/ft^2). Meeting the target O_2 flux shown in Fig. 4 allows achievement of a 35% COE increase over the Air fired PC case with post combustion CO_2 capture and compression, while exceeding the target allows achievement of a < 35% COE increase over the Air fired PC case. Fig. 4 shows that given this set of assumptions, the experimental oxygen flux values exceed the target at fuel utilizations > 65%, and further analysis indicated that an optimum OTM fuel utilization of 80% allows the lowest COE increase.

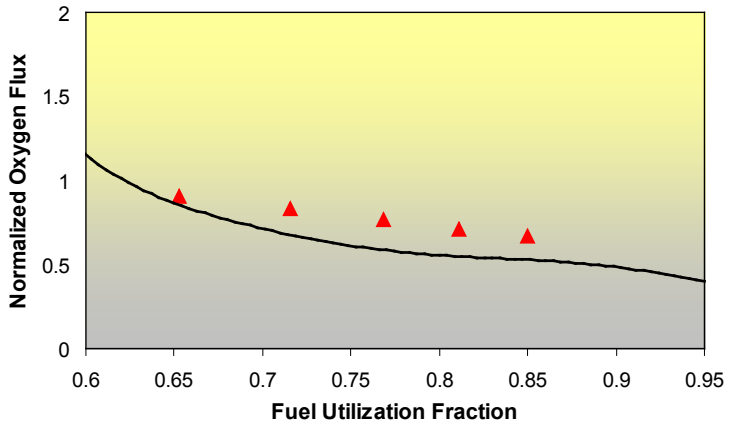

Figure 4: Average oxygen flux versus fuel utilization of OTM laboratory samples. OTM sample prepared with advanced materials tested in Reactor 2 (red triangles), and target oxygen flux assuming a coal price of $3/MMBTU (black line).

Reactor 2 was also upgraded to enable testing of OTM tubes at pressures up to 200 psig and in sulfur containing fuel environments, in order to better simulate the conditions of the POx reactor. OTM tubes prepared with the 'standard' materials were tested under pressure and in simulated synthesis gas that

contained H_2S and COS contaminants. Test results indicated an increase in oxygen flux in the presence of sulfur containing fuel species; i.e., no performance degradation was observed. In addition, an increase in performance is observed when the fuel-side of the OTM tube is pressurized [3,4]. The Utah Clean Coal Center (UC^3) is continuing to work with Praxair to expose OTM tubes to synthesis gas derived from solid coal, containing tars, fines, fly-ash, HCl, NH_3, and other impurities. Results from this work will provide an understanding of OTM compatibility and performance in actual coal derived synthesis gas.

5. SUMMARY/PATH FORWARD

Praxair has developed an Oxygen Transport Membrane (OTM) technology and has proposed a method for integrating these membranes into a Coal Power Plant to allow for CO_2 capture with a reduced parasitic power penalty. In comparison to other power cycles that enable carbon capture and sequestration (CCS), the OTM process has a low cost of CO_2 removed and avoided due to a relatively low COE, a high net cycle HHV efficiency, and high CO_2 capture efficiency.

Praxair is currently executing work to scale-up the OTM tubes. During the initial part of Phase II, the length of the OTM tube was has been increased, and work is currently underway to determine the size of OTM tube/module that would be appropriate for pilot tests. Phase II will also involve development of a preliminary engineering design and cost estimate of a pilot facility. The cost estimates will be used to further refine the economic analysis of the OTM process cycle. Furthermore, as the program transitions from a heavy focus on materials development and process design to system design and scale up, we are engaging strategic industrial partners with proven competencies in critical areas to aid in the development of a detailed plan (as part of the phase II work) for pilot scale testing of the OTM technology.

6. ACKNOWLEDGEMENTS

This work was prepared with the support of the U.S. Department of Energy, under Award Number DE-FC26-07NT43088 and the New York State Energy Research and Development Authority (NYSERDA) under agreement number 10080 and 10080-1.

7. DISCLAIMER

This material is based upon work supported by the Department of Energy under Award Number DE-FE26-07NT43088. Neither the United States Government nor any agency thereof, nor any of their employees, makes any warranty, express or implied, or assumes any legal liability or responsibility for the accuracy, completeness, or usefulness of any information, apparatus, product, or process disclosed, or represents that its use would not infringe privately owned rights. Reference herein to any specific commercial product, process, or service by trade name, trademark, manufacturer, or otherwise does not necessarily constitute or imply its endorsement, recommendation, or favoring by the United States Government or any agency thereof. The views and options of authors expressed herein do not necessarily state or reflect those of the United States government or any Agency thereof.

The material is also based upon work supported by NYSERDA under agreement number 10080 and 10080-1. NYSERDA has not reviewed the information contained herein, and the opinions expressed in this report do not necessarily reflect those of NYSERDA or the State of New York.

8. REFERENCES

[1] J. Li, L. Switzer, B. Van Hassel, and M. Christie, "Thermally Integrated Oxy-Fuel Boiler", 30th International Technical Conference on Coal Utilization & Fuel Systems, Clearwater, FL, 2005.

[2] M. Christie, B. van Hassel, J. Li, and M. Shah, "OTM Based Oxycombustion for CO_2 Capture from Coal Power Plants", 32nd International Technical Conference on Coal Utilization & Fuel Systems, Clearwater, FL, 2007.

[3] J. Li, J. Wilson, N. Degenstein, M. Shah, B. van Hassel, and M. Christie. 33rd International Technical Conference on Coal Utilization & Fuel Systems, Clearwater, FL, 2008.

[4] J. Wilson, M. Christie, N. Degenstein, M. Shah, and J. Li, "OTM Based Oxy-fuel Combustion for CO_2 Capture", 34th International Technical Conference on Coal Utilization & Fuel Systems, Clearwater, FL, 2009.

[5] R. Prasad, C.G. Gottzmann, N.R. Keskar, Reactive Purge for Solid Electrolyte Membrane Gas Separation, US 5,837,125

[6] R. Prasad, C.F. Gottzmann, R.F. Drnevich, N.R. Keskar and H. Kobayashi, Process for Enriched Combustion Using Solid Electrolyte Ionic Conductor Systems, US 5,888,272

[7] L.E. Bool, III and H. Kobayashi, Air Separation Method and System for Producing Oxygen to Support Combustion in a Heat Consuming Device, US 6,382,958

[8] L.E. Bool, III and H. Kobayashi, Oxygen Separation and Combustion Apparatus and Method, US 6,394,043

[9] R. Prasad, H. Kobayashi and P.J. Cook, Integration of Ceramic Oxygen Transport Membrane Combustor with Boiler Furnace

[10] L.E. Bool, III, H. Kobayashi, Method and System for Combusting a Fuel, US 6,562,104

[11] U.S. Dept of Energy, "Pulverized Coal Oxycombustion Power Plants, Vol. 1 : Bituminous Coal to Electricity," Publication No. DOE/NETL-2007/1291, Revision 2, DOE Office of Fossil Energy's National Energy Technology Laboratory, Pittsburgh, PA (Aug. 2008).

Appendix F

Clean Coal Today Publication (2008)

"NETL EMPHASIZES CO_2 CAPTURE FROM EXISTING PLANTS"

OFFICE OF FOSSIL ENERGY, U.S. DEPARTMENT OF ENERGY • DOE/FE-0519 • ISSUE NO. 75, SPRING 2008

Office of Fossil Energy, U.S. Department of Energy • DOE/FE-0519 • Issue No. 75, Spring 2008

CLEAN COAL TODAY

A Newsletter About Innovative Technologies for Coal Utilization

News Bytes

On January 30, 2008, the **Department of Energy (DOE) issued a "Request for Information on the Department of Energy's Plan to Restructure FutureGen."** Comments were due March 3, 2008, and are to be followed by a competitive solicitation. The FutureGen concept announced in 2003 planned the creation of a near-zero emissions, 275-MW power plant that would produce hydrogen and electricity from coal, and serve as a laboratory for commercial development. DOE considers the restructured approach an all-around better investment. Under this strategy, DOE would join industry in its efforts to build commercial-scale power plants utilizing Integrated Gasification Combined Cycle. DOE would provide funding for the addition of carbon capture and

See "News Bytes" on page 7...

Inside This Issue

NETL CO_2 Capture Program.....1
News Bytes.....1
R&D 100 Awards.....4
Water Recovery Technologies.....6
Fabricating Boiler Components....8
Upcoming Events.....9
RTI's Warm Gas Cleanup.....10
International Initiatives 11
Status Report.....14

NETL Emphasizes CO_2 Capture from Existing Plants

Over the past two decades, the Department of Energy's (DOE) Innovations for Existing Plants (IEP) Program has played a crucial role in moving advanced emission control technologies from concept to commercial reality. The successes from the program have been many. In recent years, several advanced NO_x control technologies, such as Praxair's oxygen-enhanced combustion and REI's ALTA NO_x technology, have been commercially deployed on the existing fleet of coal-fired power plants. In addition, as a direct result of the IEP program, more than 40 gigawatts of an advanced mercury control technology — activated carbon injection — will be installed on new and existing pulverized coal plants, with more orders anticipated.

SRI's Combustion Research Facility will be retrofitted for oxycombustion operation

The IEP program is now positioned to take on the critical challenge of climate change. In response to Congressional language in the Fiscal Year 2008 budget, the IEP program will shift focus to R&D on CO_2 capture technologies that can be retrofitted to existing pulverized coal-fired power plants. To implement this new program focus, DOE's National Energy Technology Laboratory issued a Funding Opportunity Notice on February 13, 2008, seeking applications for advanced concepts in post-combustion capture (membranes, solvents, and solid sorbents); various aspects of oxycombustion, and chemical looping combustion to be carried out through laboratory, bench-scale, and pilot-scale R&D. Technologies must be capable of achieving at least 90 percent CO_2 capture at less than a 20 percent increase in the cost of electricity. Applications are due April 10, with multiple awards anticipated to be made by the end of September 2008.

See "CO_2 Capture" on page 2...

... *"CO_2 Capture" continued*

The new research will build on a portfolio of advanced CO_2 capture projects that were awarded under a 2005 solicitation directed toward a broader range of capture technologies. A brief description of several projects follows.

Sorbents for Post-Combustion Capture

Post-combustion CO_2 capture technologies deal with the removal of CO_2 from power plant flue gas. Removal can be accomplished through the use of solvents, sorbents, membranes, and other gas removal technologies. *RTI International* is heading a research team tasked with continuing development and scale-up of its innovative process utilizing a dry, regenerable, carbonate-based sorbent. The sorbent captures CO_2 in the presence of water to form bicarbonate. Upon heating, the bicarbonate decomposes into a CO_2/steam mixture that can be converted into a pure CO_2 gas stream suitable for industrial use or for sequestration. RTI has started process engineering work to design a "pre-pilot" system based on the novel process design concept. The design basis is a system that can capture 1–2 tons of CO_2 per day from a coal-fired flue gas stream.

Another CO_2 capture sorbent system is being investigated by *UOP LLC*. The company is developing novel microporous metal organic frameworks (MOFs) and an associated process for the removal of CO_2 from coal-fired power plant flue gas. Significant progress has been made on the synthesis of MOF materials, with more than 20 MOFs prepared to date. The MOF materials have been characterized to ultimately enhance the understanding of relationships among material properties and CO_2 capture performance. Studies to investigate the adsorptive behavior of CO_2 on MOFs have been initiated, while increasingly rigorous testing of thermal and contaminant effects will be applied to optimize the MOF materials. As the three-year project progresses, MOF materials that demonstrate the best performance and stability will be selected for optimization and scale-up to quantities needed for pilot-scale testing.

Ionic Solvents

The *University of Notre Dame* and its partners are working to develop a process using novel ionic liquids (a solvent-based system) for the removal of CO_2 from coal-fired power plant flue gas. Researchers have initiated a synthesis program for ionic liquids having functional groups capable of complexing with CO_2, thereby increasing absorption capacity. To date, 13 new ionic liquids have been synthesized. Nuclear magnetic resonance characterization and measurement of impurities in these ionic liquids has also been completed. In a related effort, researchers have undertaken atomistic-level classical and quantum calculations to engineer ionic liquid structures that maximize CO_2 carrying capacity while minimizing regeneration costs. Also, research efforts have been initiated to measure or accurately estimate all physical properties of the ionic liquids that are essential for detailed engineering and design calculation. During the three-year project, researchers will refine development efforts for the optimal absorbent and use this information to complete a detailed systems and economic analysis study.

Membrane-Based Capture

Carbozyme is developing membrane-based technologies for CO_2

capture, specifically the contained-liquid membrane (CLM) system that leverages a highly efficient CO_2 catalyst, carbonic anhydrase (CA). The main objective of this project is to demonstrate and evaluate, at pre-pilot scale, the ability of the enzyme-based CLM permeator to capture CO_2 from a variety of combusted coal rank flue gas streams. In order to maintain membrane life, a flue-gas pretreatment system has been installed at the *University of North Dakota Energy and Environmental Research Center's* combustion test furnace (CTF). CLM modules will be evaluated using flue gases produced by the CTF. Enzymes capable of operating in an industrial gas environment have also been produced by *Novozymes* for testing on the CLM. Future work will focus on the scale-up of the hollow fiber CLM permeator and engineering and economic analysis of the technology as it relates to retrofit and greenfield installations.

Progress in Oxycombustion

Oxycombustion involves the combustion of coal or another fossil fuel with a mixture of pure oxygen and recycled flue gas. This eliminates the presence of N_2 in the flue gas and results in much higher CO_2 concentrations. The oxycombustion flue gas will then only require a minor purification step prior to sequestration. *The Babcock and Wilcox Company (B&W)* is leading a project team to further develop the oxycombustion technology for commercial retrofit in existing wall-fired and cyclone boilers by 2012. To meet this goal, a two-phase research project is planned that includes pilot-scale testing and a full-scale engineering and economic analysis. Progress has been made in defining the requirements for combustion, purification, transportation and sequestration of CO_2 in the oxycombustion process. In addition, the design, fabrication, and installation activities for oxygen testing at the B&W test facility continue. The new 6 MBtu/h pilot facility is expected to begin start up operations in June 2008. As part of the research effort, Air Liquide has simulated several CO_2 purification techniques that substantially reduce moisture, nitrogen and oxygen, and increase CO_2 concentration.

An oxycombustion retrofit with CO_2 recycle is being evaluated in a project with the *Southern Research Institute (SRI)*. Under this effort, SRI's 6 MBtu/h Combustion Research Facility (CRF) will be retrofitted for oxycombustion operation. An oxycombustion burner has been designed by MAXON specifically for the CRF and coal-based oxycombustion. The initial design of the retrofit system and the construction of the burner have been completed. An existing computational fluid dynamics model of the CRF has been updated to include the effects of oxycombustion with flue gas recycle, and the model will be validated against the results of detailed experiments. Testing will include operation with different coal types, oxygen and recycled flue gas flow configurations, and oxygen purity.

In order to produce the large amounts of oxygen that would be required by a pulverized coal oxycombustion system, cryogenic air separation systems would be necessary. These systems use large amounts of electricity for refrigeration. Thus, the IEP program also is conducting research on technologies that aim to reduce air separation costs in conjunction with the oxycombustion process. *The BOC Group, Inc.* (a member of the Linde Group) is currently developing a process that utilizes the oxygen storage capacity of perovskite materials at high temperatures. The Ceramic Autothermal Recovery (CAR) involves oxygen sorption and oxygen release. Air is passed through one bed to allow sorption and storage of oxygen, followed by a sweep gas (such as flue gas or steam), which is passed through the other bed to release the stored oxygen. The process operation is made continuous by operating two or more beds in a cyclic mode. Current work focuses on the testing of CAR bed material performance in the presence of coal-based flue gas contaminants.

Praxair is also developing oxygen transport membranes (OTM) for integration into coal-based power production systems to reduce the costs

See "CO_2 Capture" on page 9...

Praxair's high pressure reactor

Appendix G

Florida Turbine Technologies 2012 Report

Table of Contents

Introduction 1
Turbine Aerodynamic Conceptual Design 3
Heat Transfer 10
Materials and Coatings 12
Summary 13

Introduction

This report summarizes work done by Florida Turbine Technologies (FTT) in support of the Praxair Cooperative Agreement (DE-FC26-07NT43088) to integrate the Praxair Oxygen Transport Membrane (OTM) technology into a carbon-capture advanced power cycle. In this cycle (Figure 1), Syngas from a coal gasifier is reheated in OTM partial oxidation reactors then expanded through turbines which drive electrical generators. For the demonstration of this power cycle, it is desirable to modify existing turbomachinery for the Syngas expander application.

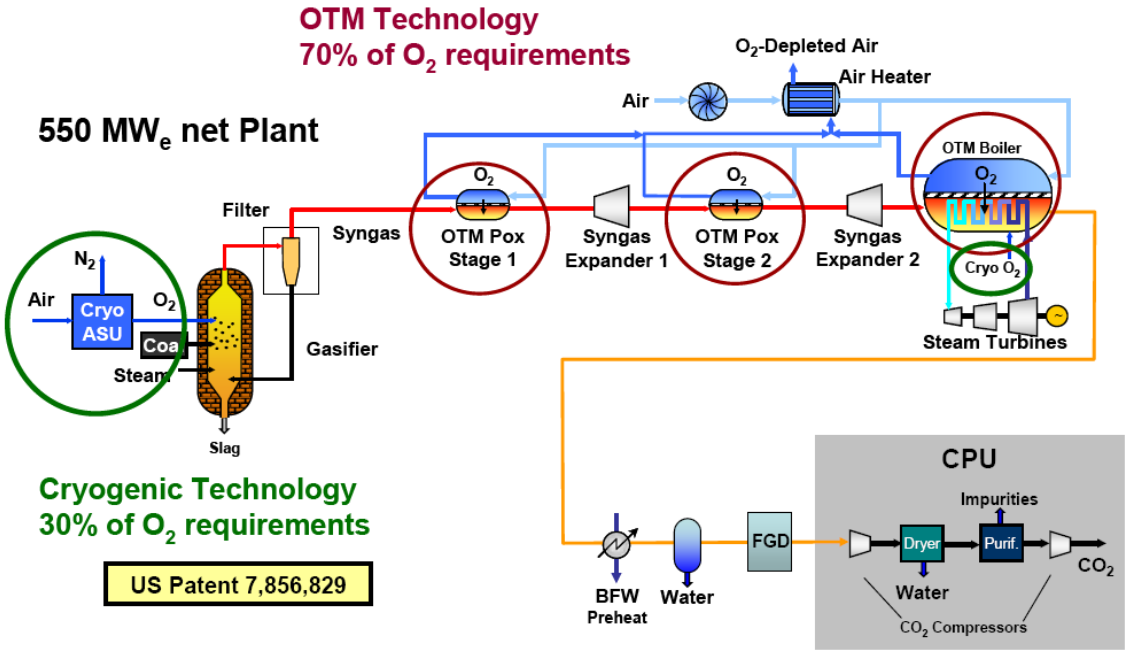

Figure 1: OTM Advanced Power Cycle

Based upon the OTM power cycle requirements provided in Tables 1 and 2, conceptual aerodynamic designs have been prepared for the two expander turbines (POX-1 and POX-2 in Figure 1) using FTT's proprietary Huberline 1-D meanline analysis

software. Table 1 details the molar composition of the drive gas. Table 2 shows the turbine inlet mass flow rate, the inlet and exit temperatures and pressures.

FTT's deliverables include conceptual aerodynamic design specifications for each Syngas expander turbine. Both direct coupling to electrical generators (RPM=3600) and coupling through a speed reduction gearbox have been investigated. The aerodynamic meanline results for the Syngas turbine application include basic design parameters such as the flowpath elevations, number of stages, airfoil chord lengths, stage Mach numbers, airfoil turning, predicted efficiency and power output. These Syngas turbine conceptual designs have also been analyzed for operational characteristics in a conventional air-breathing gas turbine engine, in order to identify the basic attributes sought from existing turbines which may be candidates for the proposed modification.

Table 1: OTM Syngas Properties

OTM Syngas Primary Constituents	**%MOL**
Carbon Monoxide (CO)	50.703
Hydrogen (H_2)	30.203
Water (H_2O)	9.449
Carbon Dioxide (CO_2)	4.350
Methane (CH_4)	3.339
OTM Syngas Avg Properties:	
Average Molecular Weight	19.90
Gas Constant, R	77.77
Specific Heat Ratio, γ	1.31
Compressibility, Z	1.00
Specific Heat, C_p (BTU/lbm)	0.42

The properties of the working fluid affect the aerodynamic and thermodynamic performance of the turbine. For example, water has a significantly higher specific heat (C_p) than air. Therefore, increasing the percentage of steam in the working fluid increases

the output power for a given mass flow. The specific heat of the OTM Syngas products of combustion is ~ 45% higher than products of natural gas combustion. However, the effect of increased C_p is partially offset by the reduced ratio of specific heats (γ) and the difference in average molecular weight. With typical OTM Syngas combustion products, the flow per unit area in the turbine decreases by ~ 16% due to the molecular weight/density of this fluid relative to natural gas combustion.

Table 2: Turbine Boundary Conditions

Boundary Conditions	POX-1	POX-2
Turbine Inlet Temperature (°F)	1650	1700
Turbine Inlet Total Pressure (psia)	335.3	106.3
Mass Flow Rate (lbm/s)	212.9	212.9
Turbine Pressure Ratio (total-to-total)	2.806	2.73

Turbine Aerodynamic Conceptual Design

Before detailing the results of the turbine aerodynamic conceptual design, a brief background on the meanline tool and its calibration is given. The axial turbine meanline is a one-dimensional analysis tool that is used early in the aerodynamic design process to calculate gas conditions, velocity triangles, approximate airfoil counts, and to predict the performance of candidate flow paths. The code uses empirical performance loss models that have been calibrated to existing rotating rig data. As illustrated in Figure 2, meanline predicted turbine efficiency is within 1% of measurements for 13 of the 16 rigs that have been evaluated. The turbine meanline code can handle various gas conditions using NIST real gas properties, and can be used for cooled or uncooled turbines.

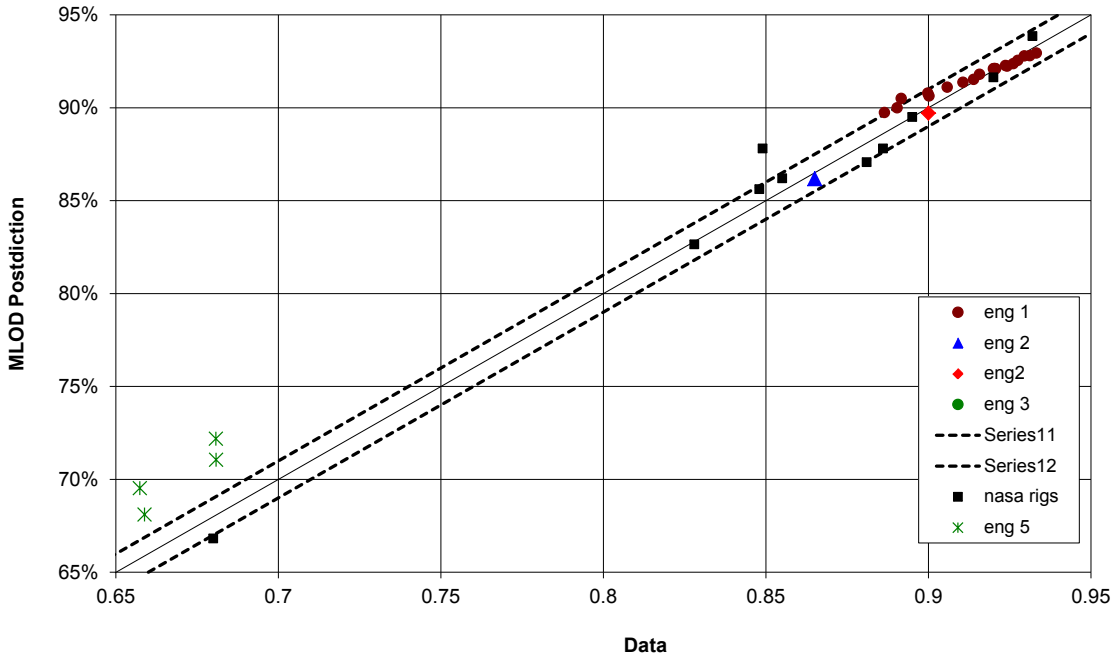

Figure 2: FTT's Turbine Meanline Calibration: Predicted vs. Measured Efficiency

The following aerodynamic trade studies were performed assuming a "clean-sheet" design of the turbines, to provide a range of the highest power outputs available. Note that running an existing industrial gas turbine (IGT) off-design will result in a performance degradation of anywhere from 2-4 percentage points in efficiency (which can translate to ~3% less power). In other words, running a given fixed geometry with a different drive gas, at the same inlet boundary conditions, will result in different incidence on the initial rotor blades, because the drive gas density is different due to the difference in average molecular weight. This rotor blade incidence, analogous to angle of attack on an airfoil, will cause additional losses due to increased leading edge flow velocities and subsequent deceleration. As shown later, adjusting the inlet boundary conditions can reduce the resulting incidence when running on OTM Syngas.

POX-1 Aerodynamics

The results of the speed and diameter trade studies for the POX-1 Expander are shown in Figure 3. The powers for 5000RPM and 9000RPM have been debited 1.5% to approximate transmission losses due to a speed reducing gearbox. Depending on the complexity of the desired mechanical system, a 3-Stage turbine at 3600RPM performs on par with a 2-Stage turbine at 5000RPM, so a trade between the added complexity of a gearbox vs. the added cost of a third turbine stage would need to be assessed for the cycle cost as a whole.

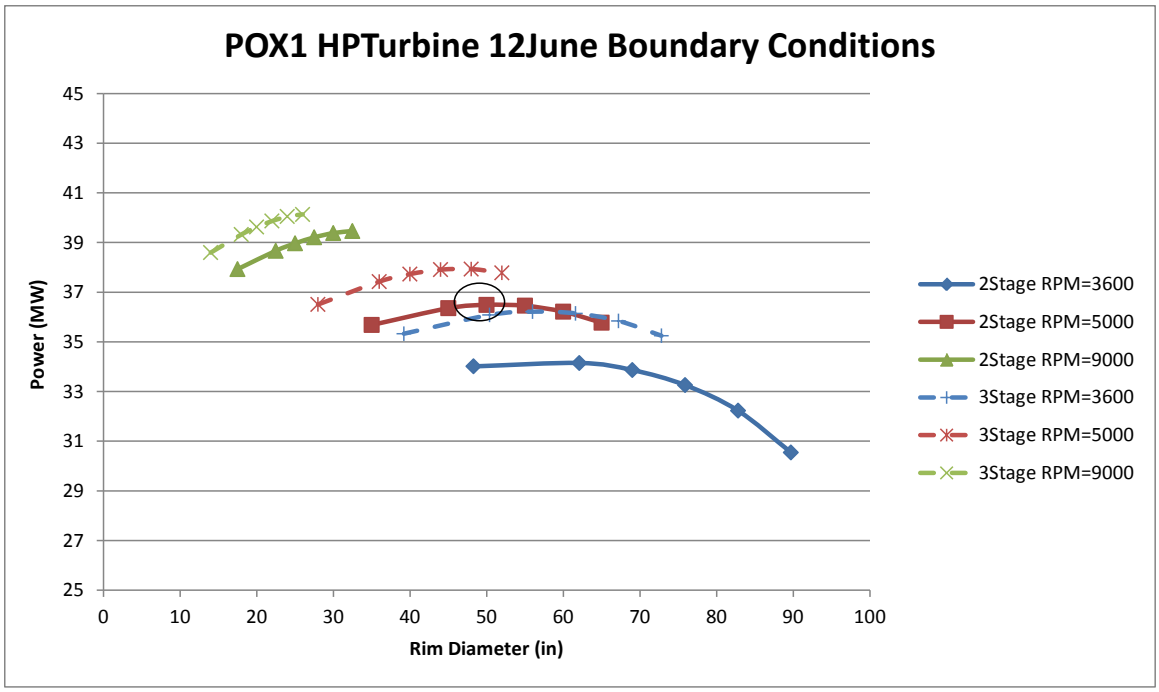

Figure 3: POX-1 Speed & Diameter Trade Study

A sample flow path for a 2-Stage POX-1 at 5000RPM is shown in Figure 4, along with detailed aerodynamic parameters per station in Table 3. The rim speed is well within existing IGT capabilities (up to ~1250 ft/s max), and the gas turnings are all below 120°.

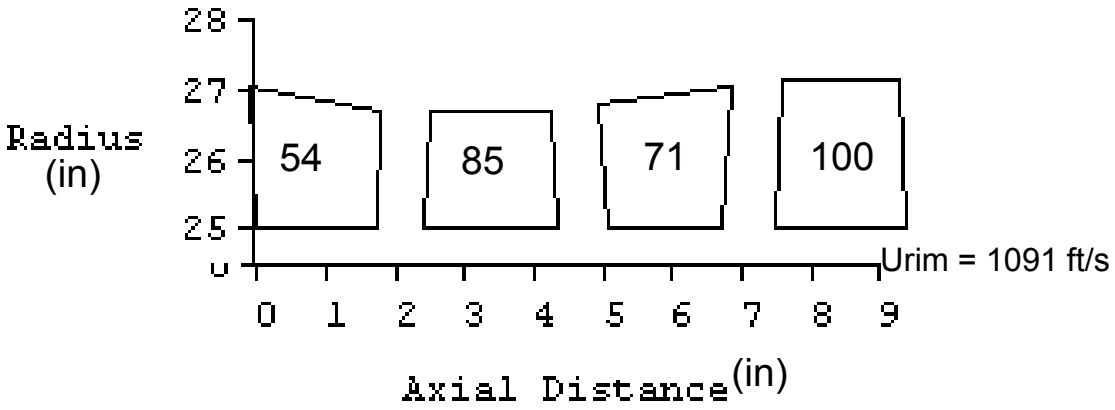

Figure 4: Sample Flow Path for POX-1 @ 5000RPM, Power = 36.5 MW

Table 3: Sample Flow Path for POX-1 @ 5000RPM, Aero Parameters per Stage

	Vane1	Blade1	Vane2	Blade2	Turbine Exit (Absolute)
~Airfoil LE Gas Temp (°F)	1650	1540	1470	1340	1237
Gas Turning	74°	114°	95°	112°	Swirl = 23°
Exit Mach #	0.65	0.6	0.79	0.67	0.31

The next step was to evaluate a fixed geometry with the same inlet boundary conditions and different drive gases. The sample flow-path from above was run "off-design" using natural gas products of combustion. Table 4 summarizes the results of this analysis, showing that for the same size geometry, a natural gas turbine has a higher mass flow rate but less output power because of the reduced specific heat. Therefore for a given turbine size, turbine power with OTM Syngas working fluid will typically increase by ~ 20%. Additionally, running an existing turbine designed for natural gas with the OTM Syngas would result in a *positive* incidence to the numbers shown in the table. By searching for a natural gas turbine with a higher inlet temperature, the incidence is reduced.

Table 4: Sample POX-1 @ 5000RPM Syngas vs. Natural Gas "Off-Design"

	OTM Syngas	Natural Gas	Natural Gas
Turbine Inlet Temperature (°F)	1650	1650	1850
Mass Flow (lbm/s)	213	255	243
Specific Heat, C_p (BTU/lbm)	0.42	0.29	0.30
2Stg Power (MW)	36.9	31.2	32.7
2Stg ~Incidence (°)		-20	-12
3Stg Power (MW)	38.5	32.3	33.8
3Stg ~Incidence (°)		-30	-20

Note the power in Table 4 has not been adjusted for transmission loss (~1.5% less). As mentioned earlier, there is an additional penalty on OTM Syngas power for running a Natural Gas (NG) turbine off-design (~3% less).

Industrial gas turbines running on natural gas products of combustion with turbine inlet flow parameter (see Equation 1) of ~ 35 are the correct "flow size" to meet POX-1 expander requirements. To avoid potential structural issues with casings, turbine inlet pressure should be ~330 psia or higher. Turbine inlet temperature should be ~1650°F, or higher. Using an existing gas turbine with higher gas temperatures reduces the OTM positive airfoil incidence. Increased NG turbine inlet temperature also offsets the reduction in temperature drop through the turbine with OTM gas. Another option to reduce OTM airfoil incidence would be increased RPM, but this is typically not feasible due to structural limitations.

$$Turbine\ FP = \frac{\dot{m}_{in}\sqrt{T_{t\_in}}}{P_{t\_in}}$$

Equation 1: Turbine Flow Parameter, units are (lbm/s) (°R)$^{0.5}$ / (psia)

As a general rule, turbine power is approximately twice the net power of the engine, in order to drive the compressor. Therefore, if all the existing turbine stages were to be used for the OTM POX-1 expander, existing engines with a net power of ~15 MW would be investigated. To meet the POX-1 pressure ratio and power requirements, it is likely not all the turbine stages will be required. Existing turbine engines with output power of ~25-40 MW should be near the correct flow/power range to meet POX-1 requirements by utilizing the initial 2 or 3 stages of the turbine. Industrial turbines in this class may have some level of dedicated airfoil cooling depending on materials used and life requirements. Steam flow could be used to provide this cooling in the OTM cycle if desired. This would change power output slightly, and decrease turbine exit temperature.

The POX turbine requirements include the ability to increase flow by 10%. One way to do this is to increase inlet pressure by 10%. The other way to increase flow is to re-stagger stage 1 turbine vane open ~2° to increase flow while maintaining inlet pressure. Increasing pressure is feasible if this is considered in the turbine and casing mechanical design. The main aerodynamic change with this option is increased turbine exit swirl and Mach number. Therefore, this must be considered in the expander exhaust system design used in this option. The stage 1 vane can be opened if the stage 1 blade is designed to handle the resulting airfoil negative incidence. Note, running OTM Syngas on an existing NG turbine will result in blade 1 running with positive incidence, so opening a NG stage 1 vane to increase flow is a very good option if the existing airfoil castings have the material required to do this built into the casting.

POX-2 Aerodynamics

Similarly to the conceptual design work done for POX-1, trade studies were run on diameters and rotor speeds for POX-2, with the results shown in Figure 5. It is worthwhile to note at the upper speed investigated, 9000RPM, there is no added benefit in going from a 2-Stage turbine to a 3-Stage turbine. As a result of this trend, a 1-Stage design at 9000RPM was investigated. Such a design is considered "advanced technology" structurally because the average rim speed for max power output is 1500 ft/s or greater, which is outside the existing range of IGTs.

Figure 6 shows an example flow path for a 2-Stage POX-2 turbine at 9000RPM, along with detailed aerodynamic parameters per station in Table 5. Once again the rim speed is well within existing IGT capabilities (up to ~1250 ft/s max), and the gas turnings are all well below 120°. Due to the lower inlet pressure of the POX-2 expander, its annulus area is increased relative to POX-1. Running at a speed of 9000RPM, the AN^2 (blade annulus area * RPM^2) value is towards the upper limits of existing industrial turbines. If this is a problem with selected life requirements and materials, the design RPM can be reduced with a small performance loss.

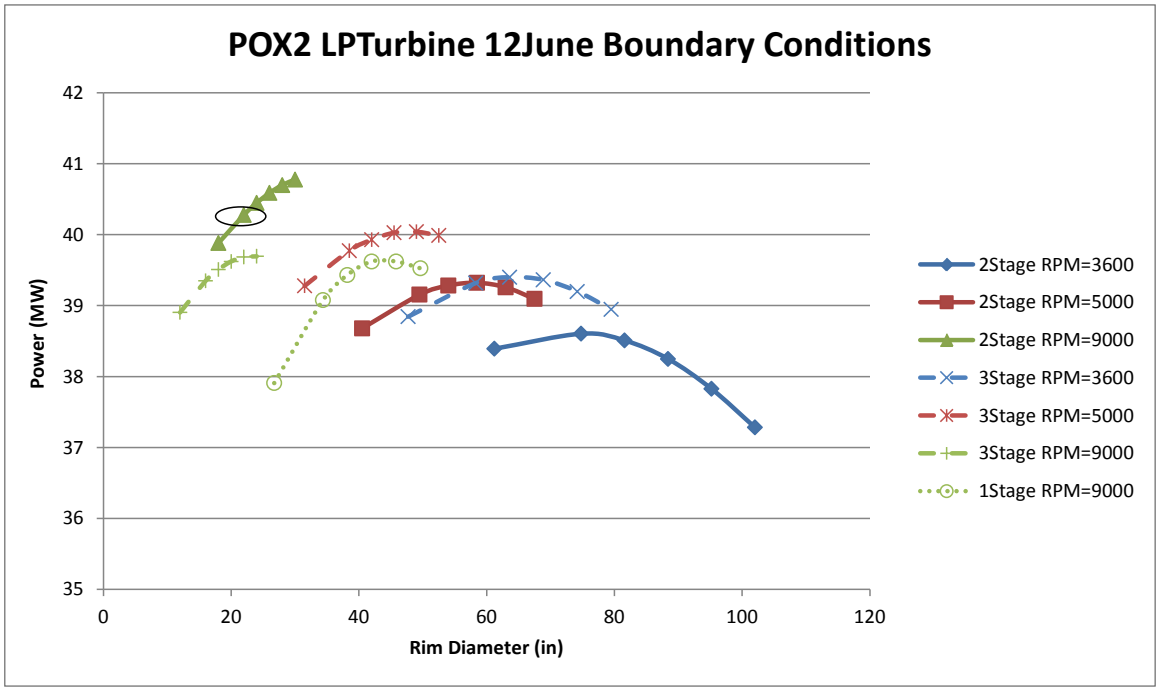

Figure 5: POX-2 Speed & Diameter Trade Study

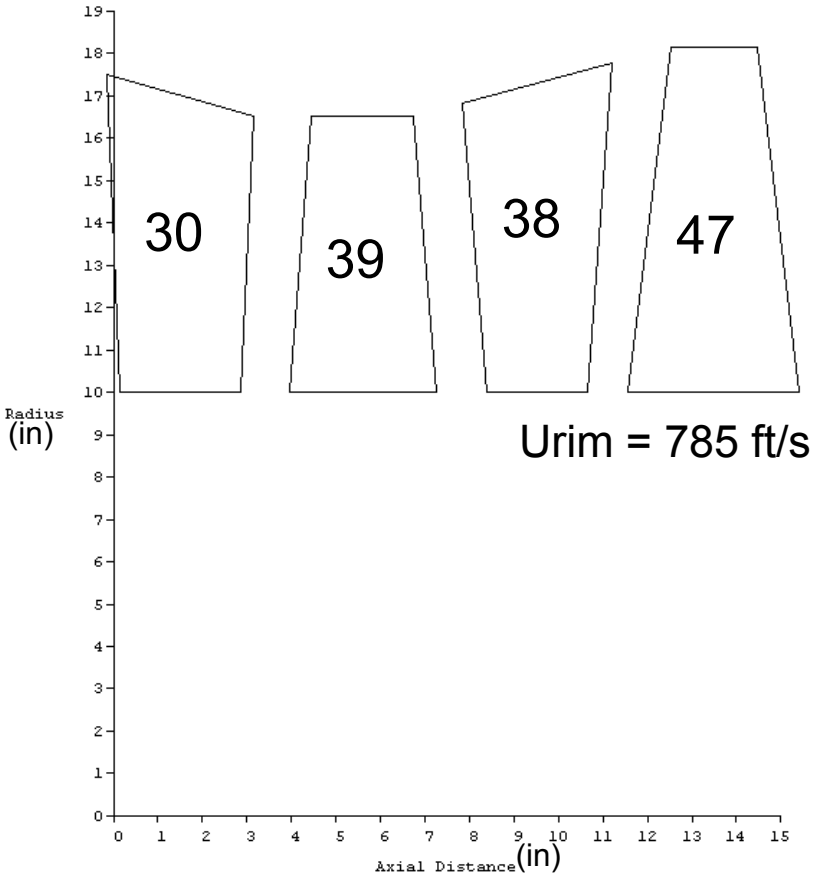

Figure 6: Sample Flow Path for POX-2 @ 9000RPM, Power = 40MW

Table 5: Sample Flow Path for POX-2 @ 9000RPM, Aero Parameters per Stage

	Vane1	Blade1	Vane2	Blade2	Turbine Exit (Absolute)
~Airfoil LE Gas Temp (°F)	1700	1604	1506	1379	1250
Gas Turning	63°	90°	91°	90°	Swirl = 20°
Exit Mach #	0.66	0.73	0.87	0.83	0.53

As done previously with POX-1, the sample POX-2 flow path was run "off-design" with natural gas products of combustion. The results of the off-design analysis are shown in Table 6. The initial incidence on the POX-2 turbine is less, which is attributed to the increased annulus area due to the lower turbine inlet pressure. (In other words, a larger area to push the increased mass flow through, resulting in less drastic change of Vane 1 exit angle.) The prior results for the POX-1 off-design analysis also hold here - looking for a turbine designed with a higher inlet temperature than required for the OTM cycle will decrease the incidence.

Table 6: Sample POX-2 @ 9000RPM Syn Gas vs. Natural Gas "Off-Design"

	OTM Syn Gas	Natural Gas	Natural Gas
Turbine Inlet Temperature (°F)	1700	1700	1900
Mass Flow (lbm/s)	213	251	240
Specific Heat, Cp (BTU/lbm)	0.43	0.298	0.303
2Stg Power (MW)	40.6	34.04	35.6
2Stg ~Incidence (°)		-15	-10

Once again, the powers have not been adjusted for transmission loss (~1.5% less) and there also remains a (~3%) penalty on the OTM Syngas power for running a natural gas turbine off-design.

Industrial gas turbines running on natural gas products of combustion with turbine inlet flow parameters of ~110 are the correct "flow size" to meet POX-2 expander requirements. To avoid potential structural issues with casings, the turbine inlet pressure should be ~106 psia or higher. Additionally, the turbine inlet temperature should be ~1700°F, or higher. Use of the aft turbine stages from an existing gas turbine used to meet POX-1 requirements is likely not an option. While these stages could be near the correct flow parameter size, they would have been designed for a lower gas temperature.

Heat Transfer

For an industrial gas turbine engine which is expected to run for extended periods of time at base load conditions, whenever the turbine inlet temperature exceeds about 800°C (1472°F), cooling should be considered, or at least secondary flows to maintain the integrity of static support structures and rotating disks. The POX-1 turbine inlet temperature is 1650°F (899°C) and the POX-2 turbine inlet temperature is 1700°F (927°C), so both of these turbines will require first vane cooling.

For the hotter inlet temperature, POX-2 turbine, the estimated average cooling effectiveness (Equation 2) requirement is 0.161, assuming steam coolant could be supplied to the vane with 200°F (93°C) superheat (at the turbine inlet pressure). The assumptions include implementing a cooling circuit into the vane to produce 40% thermal efficiency, and that thermal barrier coating (TBC) would not be used. Under these circumstances, the required heat load parameter is 0.48.

$$Average\ Cooling\ Effectivenes = \frac{\left(T_{gas} - T_{avg\_external\_metal}\right)}{\left(T_{gas} - T_{coolant}\right)}$$

Equation 2: Average Cooling Effectiveness

The first blade AN^2 ($157x10^8$ in^2-rpm^2) is quite low, which should keep the P/A stress at the root below 20ksi (138MPa) with just a little bit of taper in the blade. At this stress, creep (50,000 hours using conventionally cast (CM247) material) becomes a concern if the part temperature exceeds 850°C (1562°F). Since the blade inlet relative gas temperature is 1601°F (872°C), the first stage blade in the POX-2 turbine will probably also require some cooling. The first stage blade in the POX-1 turbine is quite a bit cooler ~1540°F (838°C), and thus could probably get along without any cooling. However, some disk purge/leakage flow will likely be required to keep the disk and attachment areas cool enough.

Determining the required magnitude of cooling is beyond the initial scope of this effort, because the complexity involved considering the difference between the hot gas working fluid (51% CO, 30% H_2, 13% steam and 7% CO_2) while the cooling fluid is assumed to be pure steam. Additionally, basic information about the geometry is needed in order to get an estimate of the amount of surface area to be cooled.

An initial turbine meanline analysis, with assumed cooling flows, has been run to illustrate the effect of added cooling flow on the overall performance, in Table 7.

Table 7: Effect of Steam Cooling on Turbine Performance

	POX-1 uncooled	POX-1 cooled	POX-2 uncooled	POX-2 cooled
Efficiency (t-t)	85.40%	84.95%	93.45%	91.94%
Power (MW)	37.09	37.25	40.57	40.50
Exit Mass flow (lbm/s)	212.9	221.4	212.9	225.7
Vane1 Exit Temp (°F)	1650	1605	1700	1654
Blade1 Exit Temp (°F)	1542	1491	1605	1522
Vane2 Exit Temp (°F)	1470	1414	1506	1421
Blade2 Exit Temp (°F)	1340	1280	1379	1293

There is an efficiency penalty for cooling, however since the cooling mass flow is added to the flow path from an outside source, the overall power change is small. There

will be a reduction in turbine exhaust temperature due to cooling that should be considered in system calculations.

Materials and Coatings

The selection of materials for conventional industrial gas turbine engine components is largely a balance between maximizing the cycle efficiency through the use of high temperature capable materials, and minimizing the component cost by using the least expensive alloys and processing to obtain the required durability. The performance of the proposed Syngas expander turbines, derived from an existing gas turbine engine, will be prescribed by the existing component designs operating in a different working fluid (air vs. Syngas). In addition to the aerodynamics and thermodynamic changes previously discussed, however, the durability of the components may be substantially different due to the potential for environmental degradation of the base alloy or coating system.

Table 8 lists the major gas turbine engine component types that are likely to be reused in the conversion to a Syngas expander turbine for demonstration of the OTM advanced power cycle, in addition to some of the materials typically used in the gas turbine component.

Table 8: Typical Gas Turbine Materials

Syngas Expander Turbine Components	Typical Gas Turbine Engine Materials
Outer Casings	1.25Cr & 2.25Cr Alloy Steels, 410SS, A216
Rotor	4340, 3.5Ni Alloy Steel, Inconel 706
Rotor Tiebolts	422SS, Inconel 718
Combustor Transitions	Inconel 617, Hastelloy X, MCrAlY & TBC Coatings
Vanes - Cooled	ECY768, Alloy 247, Inconel 939, Rene 80, MCrAlY & TBC Coatings
Vanes - Uncooled	Inconel 939, Rene 80, X45, MCrAlY Coatings
Blades - Cooled	Inconel 738, Alloy 247, MCrAlY & TBC Coatings
Blades - Uncooled	U520, Alloy 247, Inconel 738, MCrAlY Coatings
Gaspath Seals (Ring Segments)	310SS, X45, Hastelloy X, Alloy 247, MCrAlY Coatings
Exhaust Gaspath	2.25Cr Alloy Steel, 410SS, 347SS, 18-8

This listing is provided to give initial guidance for material investigations into the potentially damaging effects of operation in the hot Syngas environment.

Summary

In conclusion, OTM Syngas driven turbines are aerodynamically and structurally consistent with existing IGT designs and therefore feasible. When selecting an existing design, consideration of flow and performance effects due to gas properties needs to be considered. An IGT designed for a higher gas temperature than required for OTM Syngas should be considered; this will reduced the incidence when running on OTM Syngas.

The stage 1 vanes for both the POX-1 and POX-2 turbines will require some cooling fluid and the POX-2 stage 1 blade will likely also require some cooling, assuming typical existing IGT materials are used. Additionally, some secondary flows will likely also be required to cool disks. The results of an initial turbine meanline analysis show the effect of added cooling flow on power will be small.

These aerodynamic effects on gas turbine performance and durability of the modified natural gas turbine must be considered to select the proper turbine inlet pressure and inlet temperature for a modified gas turbine. In addition, other low risk items that would be addressed in future work include material corrosion and adapting of cooling schemes. The results from this study can be used to determine the approximate flow size of existing gas turbines to investigate.

Appendix H

Patents

Patent Title	Inventors	Application Date Filed	Patent Date Issued	Appplication No	US Patent No	Page
Composite Oxygen Ion Transport Membrane	Nagendra Nagabhushushana	August 22, 2006	July 7, 2009	11/507,486	US 7,556,676	H-1
	Jonathan Lane					
	Max Christie					
	Bart van Hassel					
Electrical Power Generation Method	Minish Shah	December 15, 2006	December 28, 2010	11/639,459	US 7,856,829	H-9
	Aqil Jamal					
	Ray Drnevich					
	Max Christie					
	Bart van Hassel					
	Hisashi Kobayashi					
	Lawrence Bool					
Electrical Power Generation Apparatus	Minish Shah	November 17, 2010	June 12, 2012	12/948,128	US 8,196,387	H-29
	Aqil Jamal					
	Ray Drnevich					
	Max Christie					
	Bart van Hassel					
	Hisashi Kobayashi					
	Lawrence Bool					
Catalyst Containing Oxygen Transport Membrane	Max Christie,	December 15, 2010	December 4, 2012	12/968,699	US 8,323,463	H-50
	Jamie Wilson,					
	Bart van Hassel					
Catalyst Containing Oxygen Transport Membrane	Max Christie,	November 8, 2012		13/671,835		H-60
	Jamie Wilson,					
	Jonathan Lane					

(12) **United States Patent**
Nagabhushana et al.

(10) **Patent No.: US 7,556,676 B2**
(45) **Date of Patent: Jul. 7, 2009**

(54) **COMPOSITE OXYGEN ION TRANSPORT MEMBRANE**

(75) Inventors: **Nagendra Nagabhushana**, Williamsville, NY (US); **Jonathan Andrew Lane**, Amherst, NY (US); **Gervase Maxwell Christie**, Buffalo, NY (US); **Bart Antonie van Hassel**, Getzville, NY (US)

(73) Assignee: **Praxair Technology, Inc.**, Danbury, CT (US)

(*) Notice: Subject to any disclaimer, the term of this patent is extended or adjusted under 35 U.S.C. 154(b) by 526 days.

(21) Appl. No.: **11/507,486**

(22) Filed: **Aug. 22, 2006**

(65) **Prior Publication Data**

US 2008/0047431 A1 Feb. 28, 2008

(51) **Int. Cl.**
B01D 53/22 (2006.01)

(52) **U.S. Cl.** **96/11**; 96/4; 95/54

(58) **Field of Classification Search** 95/45, 95/54; 96/4, 7, 11; 502/4; 429/19, 33
See application file for complete search history.

(56) **References Cited**

U.S. PATENT DOCUMENTS

5,240,480	A	8/1993	Thorogood et al.	96/4
5,306,411	A	4/1994	Mazanec et al.	204/265
5,569,633	A *	10/1996	Carolan et al.	95/54
5,702,999	A *	12/1997	Mazanec et al.	95/54
5,714,091	A	2/1998	Mazanec et al.	252/373
5,747,184	A	5/1998	Kurbjuhn et al.	
5,817,597	A *	10/1998	Carolan et al.	95/54
5,958,304	A	9/1999	Khandkar et al.	252/519.15
6,056,807	A *	5/2000	Carolan et al.	96/4
6,332,968	B1 *	12/2001	Mazanec et al.	205/334
6,488,739	B1	12/2002	Mazanec et al.	95/54

(Continued)

FOREIGN PATENT DOCUMENTS

EP 0 438 902 A2 7/1991

(Continued)

OTHER PUBLICATIONS

Vlajic, M. D., et al., "Synthesis, Sintering and Properties of Doped LaSrCrO3", Database accession No. E2003037326893 Abstract and Materials Science Forum, 2002, vol. 413, pp. 121-128.

(Continued)

Primary Examiner—Jason M Greene
(74) *Attorney, Agent, or Firm*—David M. Rosenblum

(57) **ABSTRACT**

A composite oxygen ion transport membrane having a dense layer, a porous support layer, an optional intermediate porous layer located between the porous support layer and the dense layer and an optional surface exchange layer, overlying the dense layer. The dense layer has electronic and ionic phases. The ionic phase is composed of scandia doped, yttrium or cerium stabilized zirconia. The electronic phase is composed of a metallic oxide containing lanthanum, strontium, chromium, manganese and vanadium and optionally cerium. The porous support layer is composed of zirconia partially stabilized with yttrium, scandium, aluminum or cerium or mixtures thereof. The intermediate porous layer, if used, contains the same ionic and electronic phases as the dense layer. The surface exchange layer is formed of an electronic phase of a metallic oxide of lanthanum and strontium that also contains either manganese or iron and an ionic phase of scandia doped zirconia stabilized with yttrium or cerium.

10 Claims, 1 Drawing Sheet

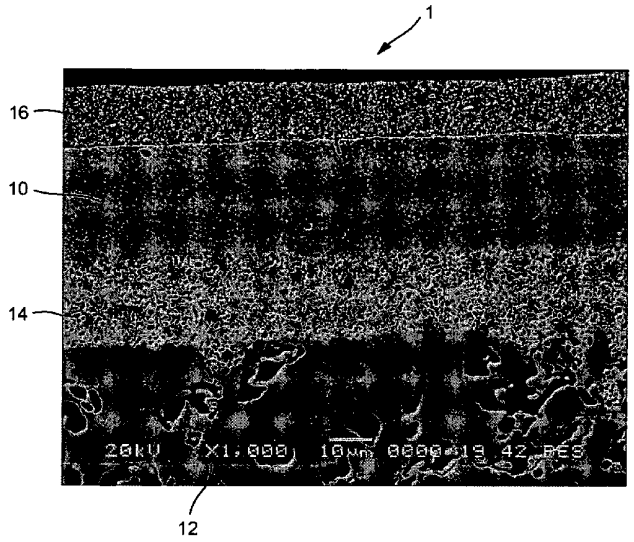

U.S. PATENT DOCUMENTS

6,537,465	B2 *	3/2003	Gottzmann et al.	95/54
6,537,514	B1 *	3/2003	Prasad et al.	423/437.1
6,539,719	B2 *	4/2003	Prasad et al.	95/54
6,544,404	B1 *	4/2003	Mazanec et al.	95/54
6,565,632	B1 *	5/2003	van Hassel et al.	95/54
6,730,808	B2 *	5/2004	Bitterlich et al.	502/4
6,786,952	B1 *	9/2004	Risdal et al.	95/54
7,332,108	B2 *	2/2008	Chartier et al.	429/33

FOREIGN PATENT DOCUMENTS

EP	399833	1/1996
EP	1 202 370 A1	5/2002

OTHER PUBLICATIONS

Zhenwei Wang et al., "Anode-supported SOFC with 1Ce10ScZr Modified Cathode/Electrolyte Interface", Journal of Power Sources 156, 2006, pp. 306-310.

* cited by examiner

U.S. Patent Jul. 7, 2009 US 7,556,676 B2

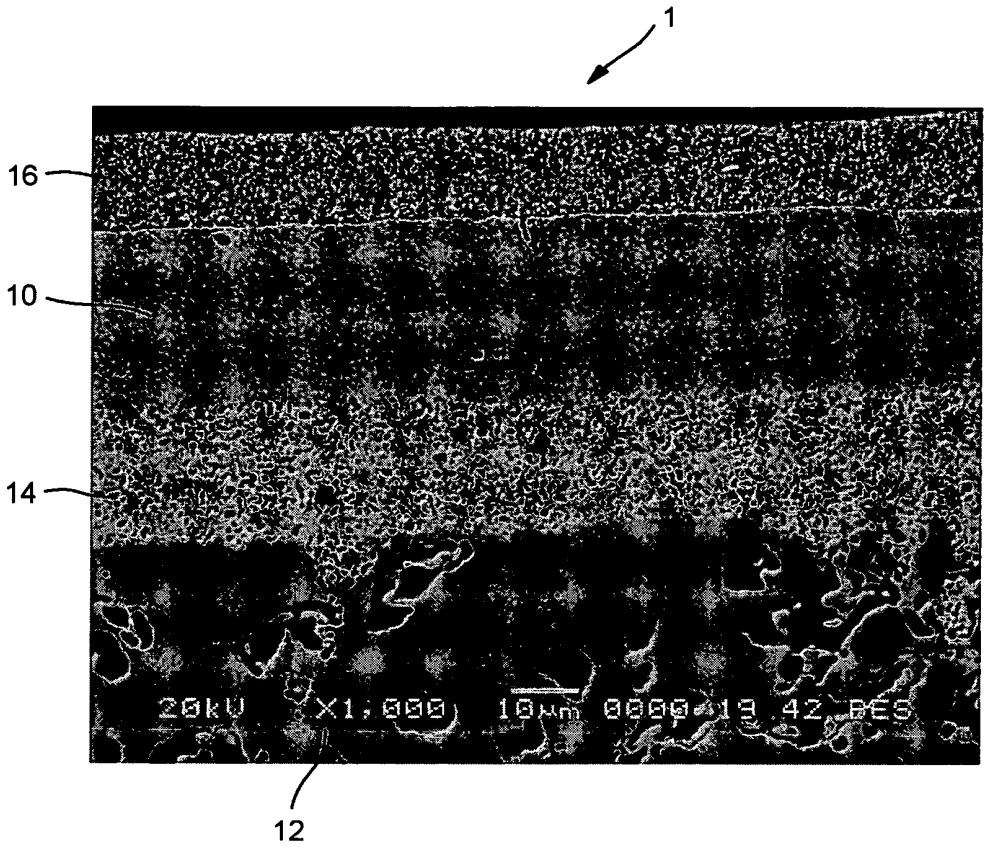

FIG.

US 7,556,676 B2

COMPOSITE OXYGEN ION TRANSPORT MEMBRANE

FIELD OF THE INVENTION

The present invention relates to a composite oxygen ion transport membrane in which a dense layer having electronic and ionic conducting phases is supported on a porous support layer. More particularly, the present invention relates to such a composite oxygen ion transport membrane in which the electronic phase is a vanadium containing perovskite-like metallic oxide, the ionic phase is a stabilized zirconia and the porous support layer is formed of a partially stabilized zirconia.

BACKGROUND OF THE INVENTION

Composite oxygen ion transport membranes have been proposed for a variety of uses that involve the production of essentially pure oxygen by separation of oxygen from an oxygen containing feed through oxygen ion transport through such membrane. For example, each membrane can be used in combustion devices to support oxy-fuel combustion or for partial oxidation reactions involving the production of a synthesis gases.

In such membranes, the oxygen ion transport principally occurs within a dense layer that allows both oxygen ions and electronic transport at elevated temperatures. The oxygen from an oxygen containing feed ionizes on one surface of the membrane and the resultant oxygen ions are driven through the dense layer and emerge on the opposite side thereof to recombine into elemental oxygen. In the recombination, electrons are liberated and are transported back through the membrane to ionize the oxygen.

Such membranes can employ two phases, an ionic phase to conduct the oxygen ions and an electronic phase to conduct the electrons. In order to minimize the resistance of the membrane to the ionic transport, such membranes are made as thin as practical and are supported on porous support layers. The resulting composite oxygen transport membrane can be fabricated as a planar element or as a tube in which the dense layer is situated either on the inside or the outside of the tube.

An example of a composite oxygen ion transport membrane is disclosed in U.S. Pat. No. 5,240,480 that has a dense layer supported on two porous layers. The dense layer can be formed of an ionic conducting phase that contains yttrium stabilized zirconia and an electronic conducting phase that is formed from platinum or another noble metal. The porous layer adjacent to the dense layer is active and is capable of conducting oxygen ions and electrons. The other porous layer can be yttrium stabilized zirconia or calcium-stabilized zirconia.

U.S. Pat. No. 5,478,444 discloses a two-phase material capable of transporting oxygen ions and electrons. The oxygen ion conducting phase can be a metallic cerium oxide incorporating a yttrium stabilizer and a dopant that can be iron or cobalt. The electronic conducting phase can be a perovskite that contains lanthanum, strontium, magnesium and cobalt or lanthanum, strontium cobalt and iron.

U.S. Pat. No. 5,306,411 discloses a dual-phase membrane having an ionic conducting phase formed from Sc_2O_3-stabilized zirconia. The electronically conducting phase can be a perovskite material containing, for example lanthanum strontium, iron, chromium and vanadium. The resultant dense layer can be supported on atria-stabilized zirconia.

The problem that exists with all composite oxygen ion transport membranes is one of strength and durability. This problem arises in part due to the high temperatures that occur when such membranes are used in connection with oxygen-fuel combustion and in reactors. Since the dense layer is very thin it must be supported. As a result, there must be a close match between the thermal expansion of the dense layer, its porous support and any intermediate active porous layer. Additionally, a further problem exists when such membranes are subjected to high oxygen partial pressures. High oxygen partial pressures are produced in combustion devices because as soon as the oxygen emerges from the membrane, it is consumed by reaction with the fuel. This results in chemical expansion due to the high reducing environment. Additionally, perovskites, when used as supports, are particularly susceptible to a phenomenon known as "creep" in which the material will fail under prolonged thermal and mechanical stresses.

As will be discussed, the present invention provides a composite oxygen ion transport membrane element that is more robust than the prior art composite membranes discussed above and that is particularly suitable to environments of high temperature and chemical expansion.

SUMMARY OF THE INVENTION

The present invention provides a composite oxygen ion transport membrane comprising a dense layer having an electronic phase and an ionic phase. As used herein and in the claims, the term "dense" layer means a layer in which the ceramic layer has no connected through porosity.

In accordance with the present invention, the electronic phase is $(La_uSr_vCe_{1-u-v})_wCr_xMn_yV_zO_{3-5}$ where u is from about 0.7 to about 0.9, v is from about 0.1 to about 0.3 and (1−u−v) is greater than or equal to zero, w is from about 0.94 to about 1, x is from about 0.67 to about 0.77, y is from about 0.2 to about 0.3, z is from about 0.015 to about 0.03, and x+y+z=1. The ionic phase is $Zr_{x'}Sc_{y'}A_{z'}O_{2-\delta}$, where y' is from about 0.08 to about 0.15, z' is from about 0.01 to about 0.03, x'+y'+z'=1 and A is Y or Ce or mixtures of Y and Ce.

The dense layer is supported by a porous support layer. The porous support layer is formed of $Zr_{x''}A_{y''}O_{2-\delta}$, where y" is from about 0.03 to about 0.05, x"+y"=1, A is Y or Sc or Al or Ce or mixtures of Y, Sc, Al and Ce.

There are many advantages of the materials used in the present invention over the prior art. A principal advantage of the present invention is that all materials have a very close thermal expansion match in that they all possess a very low linear expansion. Furthermore, all materials have limited chemical expansion and this is particularly important for the perovskite chosen for the electronic phase of the dense layer. In this regard, the use of such perovskite is particularly advantageous as opposed to a metal in that a noble metal would have to be used to prevent oxidation. The obvious problem with the use of a noble metal is one of expense. At the same time, the vanadium containing perovskite is a particularly difficult material to sinter. However, as will be discussed below, the inventors herein have solved such problem allowing its use in the oxygen transport membrane. Furthermore, the support is particularly robust due to the use of partially stabilized zirconia.

A porous intermediate layer can be provided between the dense layer and the porous support layer. Such porous intermediate layer can be composed of the electronic phase and the ionic phase of the dense layer. Furthermore, a surface exchange layer, overlying the dense layer can be provided so that the dense layer is located between the surface exchange layer and the porous intermediate layer. The surface exchange layer can incorporate a further electronic conductor com-

posed of $(La_{x'''}Sr_{1-x'''})_{y'''}MO_{3-\delta}$, where x''' is from about 0.2 to about 0.8, y''' is from about 0.95 to 1, M=Mn, Fe and a further ionic conductor composed of $Zr_x^{iv}Sc_y^{iv}A_z^{iv}O_{2-\delta}$, where y^{iv} is from about 0.08 to about 0.15, z^{iv} is from about 0.01 to about 0.03, $x^{iv}+y^{iv}+z^{iv}=1$ and A=Y, Ce.

Preferably, the ionic phase constitutes between about 35 percent and 65 percent by volume of each of the dense layer and the intermediate porous layer, remainder the electronic phase and the further ionic conductor constitutes between about 35 percent and about 65 percent by volume of the surface exchange layer, remainder the further electronic conductor. Preferably, the ionic phase constitutes about 50 percent by volume of each of the dense layer and the intermediate porous layer, remainder the electronic phase and the further ionic conductor constitutes between about 50 percent by volume of the surface exchange layer, remainder the electronic conductor.

Preferably, in the dense layer, the electronic phase is $(La_{0.825}Sr_{0.175})_{0.97}Cr_{0.76}Mn_{0.225}V_{0.015}O_{3-\delta}$ and the ionic phase is $Zr_{0.89}Sc_{0.1}Y_{0.01}O_{2-\delta}$. The porous support layer is preferably formed of $Zr_{0.97}Y_{0.03}O_{2-\delta}$. In the surface exchange layer, if used, the further ionic conductor is $Zr_{0.89}Sc_{0.1}Y_{0.01}O_{2-\delta}$ and the further electronic conductor is $La_{0.8}Sr_{0.2}FeO_{3-\delta}$. In a particularly preferred embodiment of the present invention, the porous intermediate layer has a first thickness of between about 20 micron and about 60 micron, a first average pore size of between about 0.1 micron and about 0.5 micron and a first porosity of between about 40 percent and about 60 percent. In such embodiment, the porous support layer can preferably have a second thickness of between about 1 mm and about 2.5 mm, a second average pore size of between about 2 micron and about 5 micron and a second porosity of between about 40 percent and about 60 percent. The overlying porous support layer can have a third thickness of between about 10 micron and about 25 micron, a third average pore size of between about 0.1 micron and about 0.5 micron and a third porosity of between about 40 percent and about 60 percent.

It is to be noted, that as used herein and in the claims, the term "pore size" means average pore diameter as determined by quantitative stereological line intersection analysis, a technique well known in the art.

BRIEF DESCRIPTION OF THE DRAWING

While the specification concludes with claims distinctly pointing out the subject matter that Applicants regard as their invention, it is believed that the invention would be better understood when taken in connection with the accompanying drawing in which the sole FIGURE is a scanning electron micrograph of a composite oxygen ion transport membrane of the present invention.

DETAILED DESCRIPTION

With reference to the sole FIGURE an oxygen ion transport membrane **1** of the present invention is illustrated. Oxygen ion transport membrane **1** has a dense layer **10** supported on a porous support **12**. Optional intermediate porous layer **14** and a surface exchange layer **16** can be provided.

Dense layer **10** functions to separate oxygen from an oxygen containing feed exposed to one surface of the oxygen ion transport membrane **10** and contains an electronic and ionic conducting phases. As discussed above, the electronic phase of $(La_uSr_vCe_{1-u-v})_wCr_xMn_yV_zO_{3-5}$, where u is from about 0.7 to about 0.9, v is from about 0.1 to about 0.3 and (1−u−v) is greater than or equal to zero, w is from about 0.94 to about 1, x is from about 0.67 to about 0.77, y is from about 0.2 to about 0.3, z is from about 0.015 to about 0.03, and x+y+z=1. The ionic phase is $Zr_{x'}Sc_{y'}A_{z'}O_{2-\delta}$, where y' is from about 0.08 to about 0.15, z' is from about 0.01 to about 0.03, x'+y'+z'=1 and A is Y or Ce or mixtures of Y and Ce. It is to be noted, that since the quantity (1−u−v) can be equal to zero, cerium may not be present within an electronic phase of the present invention.

The porous support layer **12** is formed of $Zr_{x''}A_{y''}O_{2-\delta}$, where y'' is from about 0.03 to about 0.05, x''+y''=1, A is Y or Sc or Al or Ce or mixtures of Y, Sc, Al and Ce.

Oxygen ion transport membrane **1** is specifically designed to be used in connection with oxy-fuel combustion applications as well as applications involving chemical reactions. The application of the present invention is not, however, limited to such uses. However, where the application involves fuel combustion, the use of intermediate porous layer **14** enhances the rate of fuel oxidation at that interface by providing a high surface area where fuel can react with oxygen or oxygen ions under the formation of partial or complete oxidation products. The oxygen ions diffuse through the mixed conducting matrix of this porous layer towards the porous support **12** and react with the fuel that diffuses inward from the porous support **12** into this porous intermediate layer **14**. Preferably, porous intermediate layer **14** is formed from the same electronic and ionic phases as dense layer **10**.

Any embodiment of the present invention can advantageously incorporate a surface exchange layer **16** that overlies the dense layer opposite to the porous intermediate layer if the same is used. Surface exchange layer **16** enhances the surface exchange rate by enhancing the surface area of the dense layer **10** while providing a path for the resulting oxygen ions to diffuse through the mixed conducting oxide phase to the dense layer **10** and for oxygen molecules to diffuse through the open pore space to the same. The surface exchange layer **16** therefore, reduces the loss of driving force in the surface exchange process and thereby increases the achievable oxygen flux. As indicated above, it also can be a two-phase mixture containing an electronic conductor composed of $(La_{x'''}Sr_{1-x'''})_{y'''}MO_{3-\delta}$, where x''' is from about 0.2 to about 0.8, y''' is from about 0.95 to 1, M=Mn, Fe and an ionic conductor composed of $Zr_x^{iv}Sc_y^{iv}A_z^{iv}O_{2-\delta}$, where y^{iv} is from about 0.08 to about 0.15, z^{iv} is from about 0.01 to about 0.03, $x^{iv}+y^{iv}+z^{iv}=1$ and A=Y, Ce.

In a particularly preferred embodiment of the present invention, the dense layer **10** incorporates an electronic phase composed of $(La_{0.825}Sr_{0.175})_{0.97}Cr_{0.76}Mn_{0.225}V_{0.015}O_{3-\delta}$ and an ionic phase composed of $Zr_{0.89}Sc_{0.1}Y_{0.01}O_{2-\delta}$. In such embodiment, the porous support layer **12** is formed of $Zr_{0.97}Y_{0.03}O_{2-\delta}$ and the surface exchange layer incorporates an ionic conductor composed of $Zr_{0.89}Sc_{0.1}Y_{0.01}O_{2-\delta}$ and an electronic conductor composed of $La_{0.8}Sr_{0.2}FeO_{3-\delta}$. Preferably, the porous intermediate layer **14** has a thickness of between about 20 micron and about 60 micron, an average pore size of between about 0.1 microns and about 0.5 microns and a first porosity of between about 40 percent and about 60 percent. Porous support layer **12** has a thickness of between about 1 mm and about 2.5 mm, an average pore size of between about 2 micron and about 5 micron and a porosity of between about 40 percent and about 60 percent. The surface exchange layer **16** has a thickness of between about 10 microns and about 25 microns, an average pore size of between about 0.1 microns and about 0.5 microns and a porosity of between about 40 percent and about 60 percent.

As an example of fabricating an oxygen transport membrane element of the present invention, a porous support layer **12** is first fabricated from spray granulated yttrium stabilized

zirconia powder having a chemical formula of $Zr_{0.97}Y_{0.03}O_{2-\delta}$ (hereinafter, "YSZ Powder".) The particle size of such powder is d50=0.6 μm (about a 50 percentile of the particles have a particle size of below 0.6 μm.) The powder is then wet mixed with glassy carbon having a particle size of a d50 of from about 0.4 to about 12 μm and starch having a particle size of a d50 of about 34 μm. The mixture contains about 10 percent glassy carbon, 15 percent starch and a remainder of the yttrium stabilized zirconia powder. It is desirable that the oxygen transport membrane element be non-porous at the ends for sealing purposes. As such, the YSZ Powder is mixed with a binder such as PVB (Poly Vinyl Butyrl) that can be obtained from Sigma-Aldrich, 3050 Spruce Street, St. Louis, Mo. 63103 and then poured into an isopressing mold. The isopressing mold can be a 20 mm thick flexible tube having an inner diameter of about 24.75 mm and an internal 17.75 mm diameter mandrel. Thereafter, the mixture of YSZ Powder, carbon starch and the binder is poured into the mold and a further amount of the mixture of YSZ Powder and binder alone is then poured into the mold. As a result, the ends of the support layer **12** will be non-porous and a central section will be porous.

The mold is then subjected to a hydrostatic pressure of about 20 ksi to form a green tube. After the green tube is formed, the tube can then be fired at 1000° C. for 4 hours to achieve reasonable strength for further handling. After firing, the resulting tube can be checked for porosity, permeability/tortuosity and stored in a dry oven at about 60° C.

After forming the green tube, intermediate porous layer **14** is then formed. A mixture of about 34 grams of powders having electronic and ionic phases and the chemical formulas, $(La_{0.825}Sr_{0.175})_{0.97}Cr_{0.76}Mn_{0.225}V_{0.015}O_{3-\delta}$ ("LSCMV") and $Zr_{0.89}Sc_{0.1}Y_{0.01}O_{2-\delta}$ ("YScZ"), respectively, is prepared so that the mixture contains equal proportions by volume of LSCMV and YScZ. To the mixture, 100 grams of toluene, 20 grams of the binder of the type mentioned above, 400 grams of 1.5 mm diameter YSZ grinding media are added. The mixture is then milled for about 6 hours to form a slurry (d_{50} of about 0.34 μm). About 6 grams of carbon black having a particle size of about d50=0.8 μm is then added to the slurry and milled for additional 2 hours. An additional 10 grams of toluene and about 10 grams of additional binder were added to the slurry and mixed for between about 1.5 and about 2 hours. The inner wall of the green tube formed above is then coated by pouring the slurry, holding once for 5 seconds and pouring out the residual back to the bottle. The coated green tube is then dried and fired at 850° C. for 1 hour in air for binder burnout.

The dense layer **10** is then applied. A mixture weighing about 40 grams is prepared that contains the same powders as used in forming the intermediate porous layer **14**, discussed above, except that the ratio between LSCMV and YScZ is about 40/60 by volume, 2.4 grams of cobalt nitrate $\{Co(NO_3)_2.6H_2O\}$, 95 grams of toluene, 5 grams of ethanol, 20 grams of the binder identified above, 400 grams of 1.5 mm diameter YSZ grinding media are then added to the mixture and the same is milled for about 10 hours to form a slurry (d_{50}~0.34 μm). Again, about 10 grams of toluene and about 10 grams of binder are added to the slurry and mixed for about 1.5 and about 2 hours. The inner wall of the tube is then coated by pouring the slurry, holding once for 10 seconds and pouring out the residual back to the bottle. The tube is then stored dry prior to firing the layers in a controlled environment.

The coated green tube is then placed on a C-setter in a horizontal tube furnace and porous alumina tubes impregnated with chromium nitrate are placed close to the coated tube to saturate the environment with chromium vapor. The tubes are heated in static air to about 800° C. for binder burnout and the environment is switched to an atmosphere of a saturated nitrogen mixture (nitrogen and water vapor) that contains about 4 percent by volume of hydrogen to allow the vanadium containing electronic conducting perovskites to properly sinter. The tube is held at 1400° C. for 8 hours and then cooled in nitrogen to complete the sintering of the materials. The sintered tube is checked for helium leak rates that should be lower than 10^{-7} Pa.

Surface exchange layer **16** is then applied. A mixture of powders is prepared that contains about 35 of equal amounts of ionic and electronic phases having chemical formulas of $Zr_{0.89}Sc_{0.1}Y_{0.01}O_{2-\delta}$ and $La_{0.8}Sr_{0.2}FeO_{3-\delta}$, respectively. To this mixture, about 100 grams of toluene, 20 grams of the binder identified above, about 400 grams of 1.5 mm diameter YSZ grinding media are added and the resultant mixture is milled for about 14 hours to form a slurry (d_{50}~0.4 μm). About six grams of carbon black are added to the slurry and milled for additional 2 hours. A mixture of about 10 grams of toluene and about 10 grams of the binder are then added to the slurry and mixed for between about 1.5 and about 2 hours. The inner wall of the tube is then coated by pouring the slurry, holding twice for about 10 seconds and then pouring out the residual back to the bottle. The coated tube is then dried and fired at 1100° C. for two hours in air.

The resultant tubes have the preferred thickness, pore size and porosity within the ranges outlined above, namely, the porous intermediate layer **14** has a thickness of about 25 microns, an average pore size of between about 0.1 to about 0.5 microns and a porosity of between about 40 percent and about 60 percent. Porous support layer **12** has a thickness of about 2.1 mm, an average pore size of between about 2 and about 5 microns and a porosity of about 45 percent. The surface exchange layer **16** has a thickness of about 14 microns, an average pore size of between about 0.1 and about 0.5 microns and a porosity of between about 40 percent and about 60 percent. Such tubes have been found to be able to withstand operational cycles involving cool down to a temperature of about 25° C. and heating to a temperature of about 1000° C. of 20-40 cycles over 1512 hours of operation.

It is to be noted that in any embodiment of the present invention, the particle size of the chromite/zirconia slurry for deposition of the intermediate and dense separation layers **14** and **10** should be in a range of between about 0.3 and about 0.35 μm. Membranes fabricated from such slurries indicated minimal reactivity between the two phases and with shrinkage matching the porous zirconia support.

Cobalt nitrate is preferably utilized as a sintering aid to the densification of the dense layer **10**. Preferably, the porous alumina tubes have a pore size of about 0.5 mm and a porosity of about 60 percent, a diameter of about 12.75 mm, and a thickness of about 2 mm. Each of the alumina tubes contains about 10 percent by weight of chromium nitrate.

While the invention has been described with respect to a preferred embodiment, as will occur to those skilled in the art, numerous changes, additions and omissions may be made without departing from the spirit and scope of the present invention provided for in the appended claims.

We claim:

1. A composite oxygen ion transport membrane comprising:

a dense layer having an electronic phase and an ionic phase;

said electronic phase is $(La_uSr_vCe_{1-u-v})_wCr_xMn_yV_zO_{3-5}$, where u is from about 0.7 to about 0.9, v is from about 0.1 to about 0.3 and (1−u−v) is greater than or equal to zero, w is from about 0.94 to about 1, x is from about

0.67 to about 0.77, y is from about 0.2 to about 0.3, z is from about 0.015 to about 0.03, and x+y+z=1;

said ionic phase is $Zr_{x'}Sc_{y'}A_{z'}O_{2-\delta}$, where y' is from about 0.08 to about 0.15, z' is from about 0.01 to about 0.03, x'+y'+z'=1 and A is Y or Ce or mixtures of Y and Ce;

a porous support layer, said porous support layer formed of $Zr_{x''}A_{y''}O_{2-\delta}$, where y" is from about 0.03 to about 0.05, x"+y"=1, A is Y or Sc or Al or Ce or mixtures of Y, Sc, Al and Ce.

2. The composite ion transport membrane of claim **1**, further comprising:

a porous intermediate layer between the dense layer and the porous support layer; and

the porous intermediate layer composed of the electronic phase and the ionic phase.

3. The composite ion transport membrane of claim **2**, further comprising:

a surface exchange layer, overlying the dense layer so that the dense layer is located between the surface exchange layer and the porous intermediate layer;

said surface exchange layer composed of a further electronic conductor composed of $(La_{x'''}Sr_{1-x'''})_{y'''}MO_{3-\delta}$, where x'" is from about 0.2 to about 0.8, y'" is from about 0.95 to 1, M=Mn, Fe and a further ionic conductor composed of $Zr_x^{iv}Sc_y^{iv}A_z^{iv}O_{2-\delta}$, where y^{iv} is from about 0.08 to about 0.15, z^{iv} is from about 0.01 to about 0.03, $x^{iv}+y^{iv}+z^{iv}=1$ and A=Y, Ce.

4. The composite ion transport membrane of claim **3**, wherein:

the ionic phase constitutes between about 35 percent and 65 percent by volume of each of the dense layer and the intermediate porous layer, remainder the electronic phase; and

the further ionic conductor constitutes between about 35 percent and about 65 percent by volume of the surface exchange layer, remainder the further electronic conductor.

5. The composite ion transport membrane of claim **4**, wherein:

the ionic phase constitutes about 50 percent by volume of each of the dense layer and the intermediate porous layer, remainder the electronic phase; and

the further ionic conductor constitutes between about 50 percent by volume of the surface exchange layer, remainder the electronic conductor.

6. The composite ion transport membrane of claim **1**, wherein:

the electronic phase is $(La_{0.825}Sr_{0.175})_{0.97}Cr_{0.76}Mn_{0.225}V_{0.015}O_{3-\delta}$; and

the ionic phase is $Zr_{0.89}Sc_{0.1}Y_{0.01}O_{2-\delta}$.

7. The composite ion transport membrane of claim **2**, wherein:

the electronic phase is $(La_{0.825}Sr_{0.175})_{0.97}Cr_{0.76}Mn_{0.225}V_{0.015}O_{3-\delta}$; and the ionic phase is $Zr_{0.89}Sc_{0.1}Y_{0.01}O_{2-\delta}$.

8. The composite ion transport membrane of claim **6** or claim **7**, wherein said porous support layer is formed of $Zr_{0.97}Y_{0.03}O_{2-\delta}$.

9. The composite ion transport membrane of claim **5**, wherein:

the electronic phase is $(La_{0.825}Sr_{0.175})_{0.97}Cr_{0.76}Mn_{0.225}V_{0.015}O_{3-\delta}$; the ionic phase is $Zr_{0.89}Sc_{0.1}Y_{0.01}O_{2-\delta}$;

said porous support layer is formed of $Zr_{0.97}Y_{0.03}O_{2-\delta}$; the further ionic conductor is $Zr_{0.89}Sc_{0.1}Y_{0.01}O_{2-\delta}$; and the further electronic conductor is $La_{0.8}Sr_{0.2}FeO_{3-\delta}$.

10. The composite ion transport membrane of claim **9**, wherein:

the porous intermediate layer has a first thickness of between about 20 micron and about 60 micron, a first average pore size of between about 0.1 mic and about 0.5 mic and a first porosity of between about 40 percent and about 60 percent;

the porous support layer has a second thickness of between about 1 mm and about 2.5 mm, a second average pore size of between about 2 micron and about 5 micron and a second porosity of between about 40 percent and about 60 percent; and

said overlying porous support layer has a third thickness of between about 10 micron and about 25 micron, a third average pore-size of between about 0.1 micron and about 0.5 micron and a third porosity of between about 40 percent and about 60 percent.

* * * * *

(12) **United States Patent**
Shah et al.

(10) **Patent No.: US 7,856,829 B2**
(45) **Date of Patent: Dec. 28, 2010**

(54) **ELECTRICAL POWER GENERATION METHOD**

(75) Inventors: **Minish Mahendra Shah**, E. Amherst, NY (US); **Aqil Jamal**, Grand Island, NY (US); **Raymond Francis Drnevich**, Clarence Center, NY (US); **Bart Antonie van Hassel**, Getzville, NY (US); **Gervase Maxwell Christie**, Buffalo, NY (US); **Hisashi Kobayashi**, Putnam Valley, NY (US); **Lawrence E. Bool, III**, E. Aurora, NY (US)

(73) Assignee: **Praxair Technology, Inc.**, Danbury, CT (US)

(*) Notice: Subject to any disclaimer, the term of this patent is extended or adjusted under 35 U.S.C. 154(b) by 1034 days.

(21) Appl. No.: **11/639,459**

(22) Filed: **Dec. 15, 2006**

(65) **Prior Publication Data**

US 2008/0141672 A1 Jun. 19, 2008

(51) **Int. Cl.**
F02C 6/18 (2006.01)

(52) **U.S. Cl.** **60/780**

(58) **Field of Classification Search** 60/780, 60/781, 39.12, 39.182, 39.461, 39.464, 39.465, 60/39.47

See application file for complete search history.

(56) **References Cited**

U.S. PATENT DOCUMENTS

3,868,817	A *	3/1975	Marion et al.	60/781
4,261,167	A *	4/1981	Paull et al.	60/781
4,322,389	A *	3/1982	Schmid	422/187
5,467,722	A *	11/1995	Meratla	110/345
5,570,578	A *	11/1996	Saujet et al.	60/647
5,820,654	A	10/1998	Gottzman et al.	95/54
5,820,655	A	10/1998	Gottzmann et al.	95/54
5,927,103	A	7/1999	Howard	62/620
5,964,922	A	10/1999	Keskar et al.	
6,035,662	A	3/2000	Howard et al.	62/617
6,070,471	A	6/2000	Westphal et al.	73/766
6,139,810	A	10/2000	Gottzmann et al.	422/197
6,382,958	B1	5/2002	Bool, III et al.	431/2
6,394,043	B1	5/2002	Bool, III et al.	122/488
6,562,104	B2	5/2003	Bool, III et al.	95/54
6,702,570	B2	3/2004	Shah et al.	431/11
7,008,967	B2 *	3/2006	Keyser et al.	518/702
2002/0073938	A1 *	6/2002	Bool et al.	122/451.1

(Continued)

FOREIGN PATENT DOCUMENTS

DE 10330859 A1 2/2004

(Continued)

OTHER PUBLICATIONS

Babcock & Wilcox, Steam 40, "Sulfur Dioxide Control"(1992).

(Continued)

Primary Examiner—William H Rodriguez
Assistant Examiner—Andrew Nguyen
(74) *Attorney, Agent, or Firm*—David M. Rosenblum

(57) **ABSTRACT**

A method of generating electrical power in which a synthesis gas stream generated in a gasifier is combusted in an oxygen transport membrane system of a boiler. The combustion generates heat to raise steam to in turn generate electricity by a generator coupled to a steam turbine. The resultant flue gas can be purified to produce a carbon dioxide product.

13 Claims, 8 Drawing Sheets

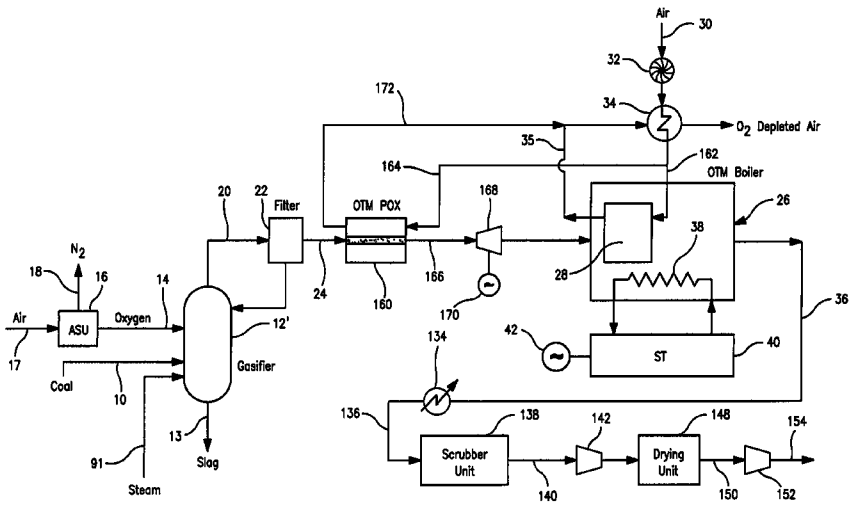

U.S. PATENT DOCUMENTS

2002/0194849	A1*	12/2002	Saviharju et al.	60/670
2006/0112696	A1*	6/2006	Lynghjem et al.	60/772

FOREIGN PATENT DOCUMENTS

DE	102004038435	A1	2/2006
EP	1717420	A1	11/2006
GB	713553		11/1951

OTHER PUBLICATIONS

Okawa et al., Trial Design of a CO_2 Recovery Power Plant by Burning Pulverized Coal in O_2/CO_2, Energy Convers. Mgmt., vol. 38, supplemental (1997) pp. S123-S127.

U.S. Department of Energy—Office of Fossil Energy and U.S. Department of Energy/NETL, "Evaluation of Innovative Fossil Fuel Power Plants with CO_2 Removal", Interim Report (2000).

U.S. Department of Energy, "Evaluation of Fossil Fuel Power Plants with CO_2 Recovery", Final Report (2002).

Holt, "Gasification Process Selection—Trade-offs and Ironies", Presented at the Gasification Technologies Conference (2004).

Switzer et al., "Cost and Feasibility Study on the Praxair Advanced Boiler for the CO_2 Capture Project's Refinery Scenario", Carbon Dioxide Capture for Deep Geologic Formations—Results from the CO_2 Capture Project, vol. 2, Elsevier Science Publishing Company (2005) pp. 1-26.

Dyer et al., "Ion Transport Membrane Technology for Oxygen Separation and Syngas Production", Solid State Ionics 134 (2000) p. 21-33.

Radtke et al., "Renaissance of Gasification based on Cutting Edge Technologies", VGB PowerTech (2005).

* cited by examiner

U.S. Patent Dec. 28, 2010 Sheet 1 of 8 US 7,856,829 B2

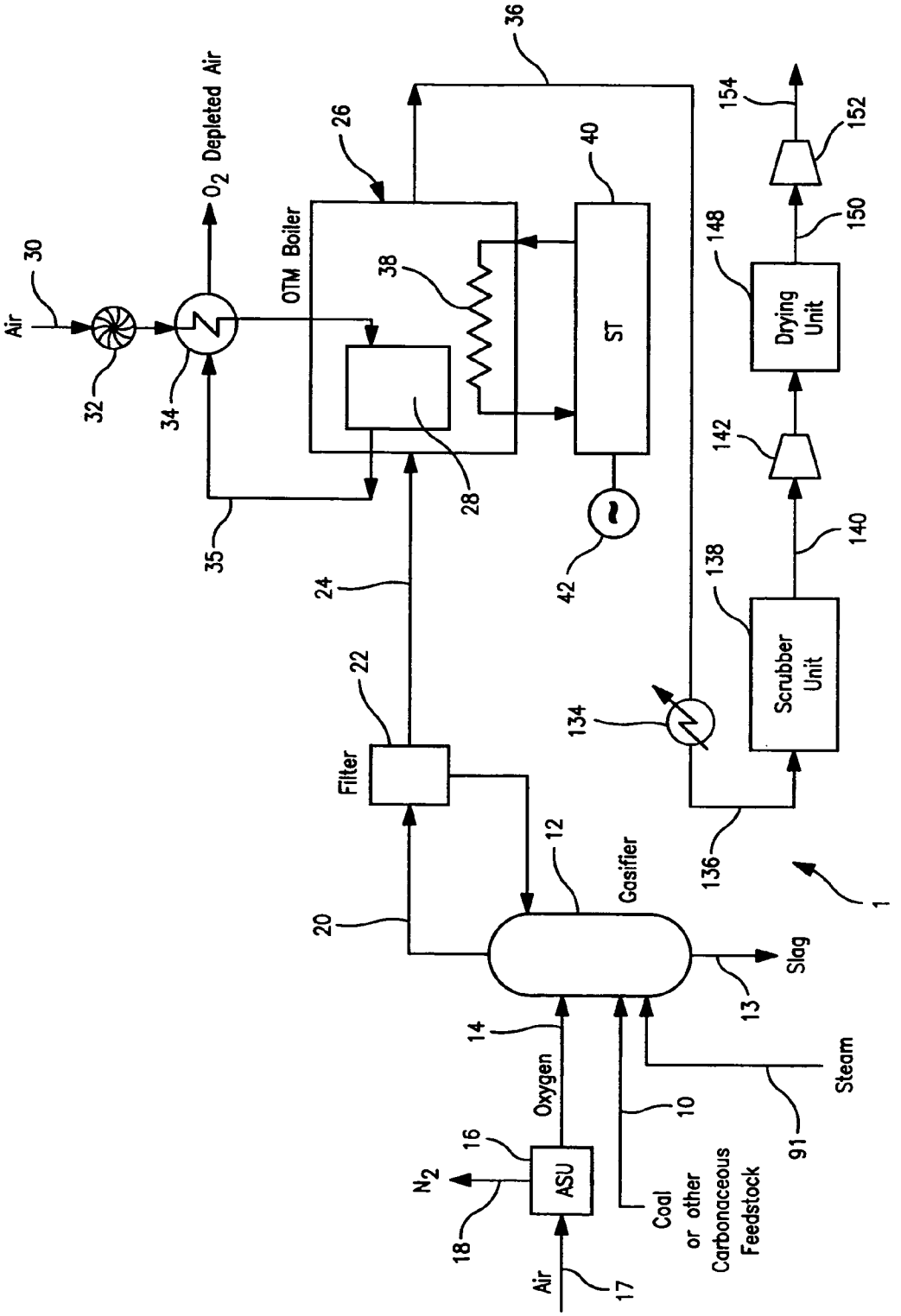

FIG. 1

U.S. Patent Dec. 28, 2010 Sheet 2 of 8 US 7,856,829 B2

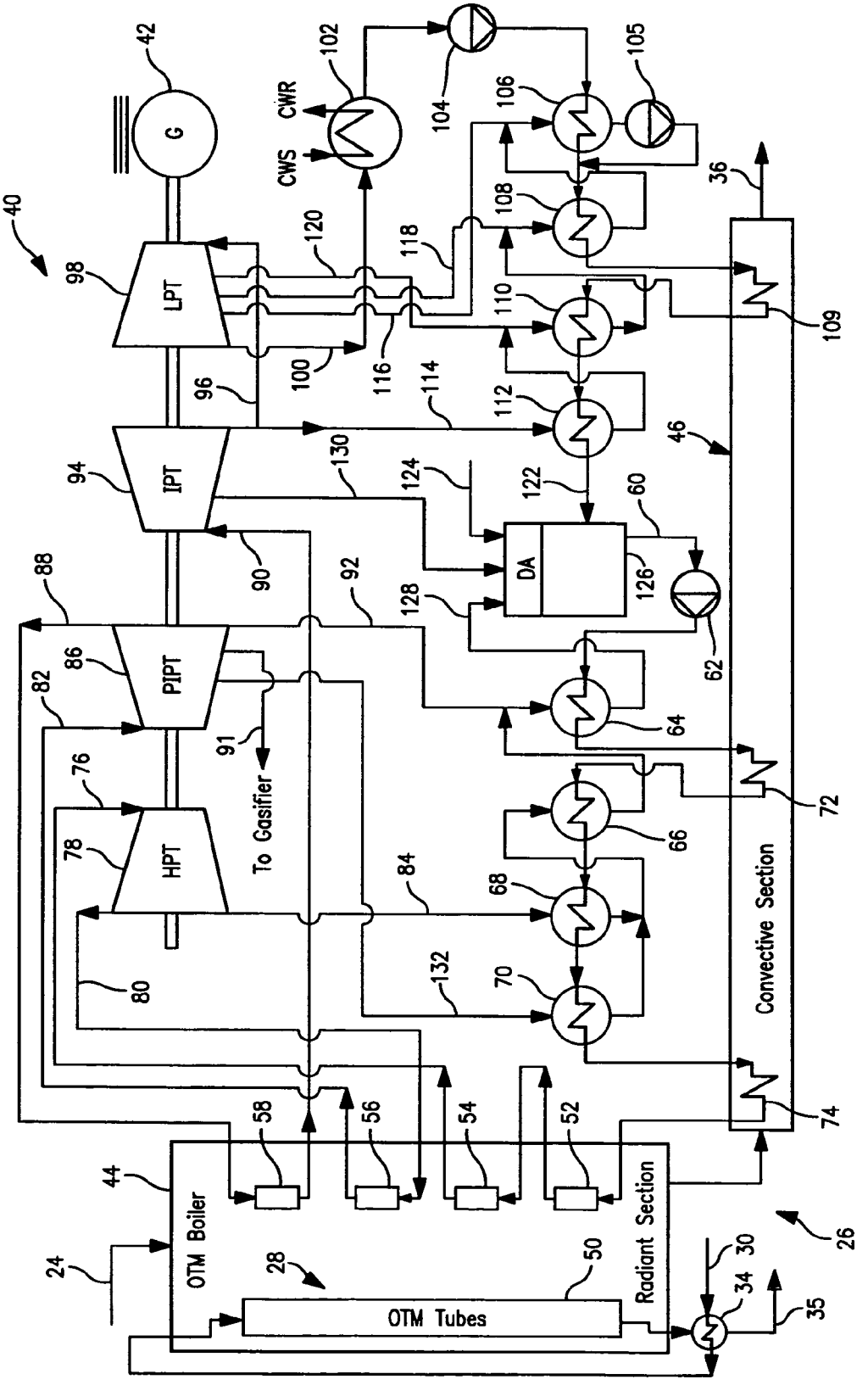

FIG. 2

U.S. Patent Dec. 28, 2010 Sheet 3 of 8 US 7,856,829 B2

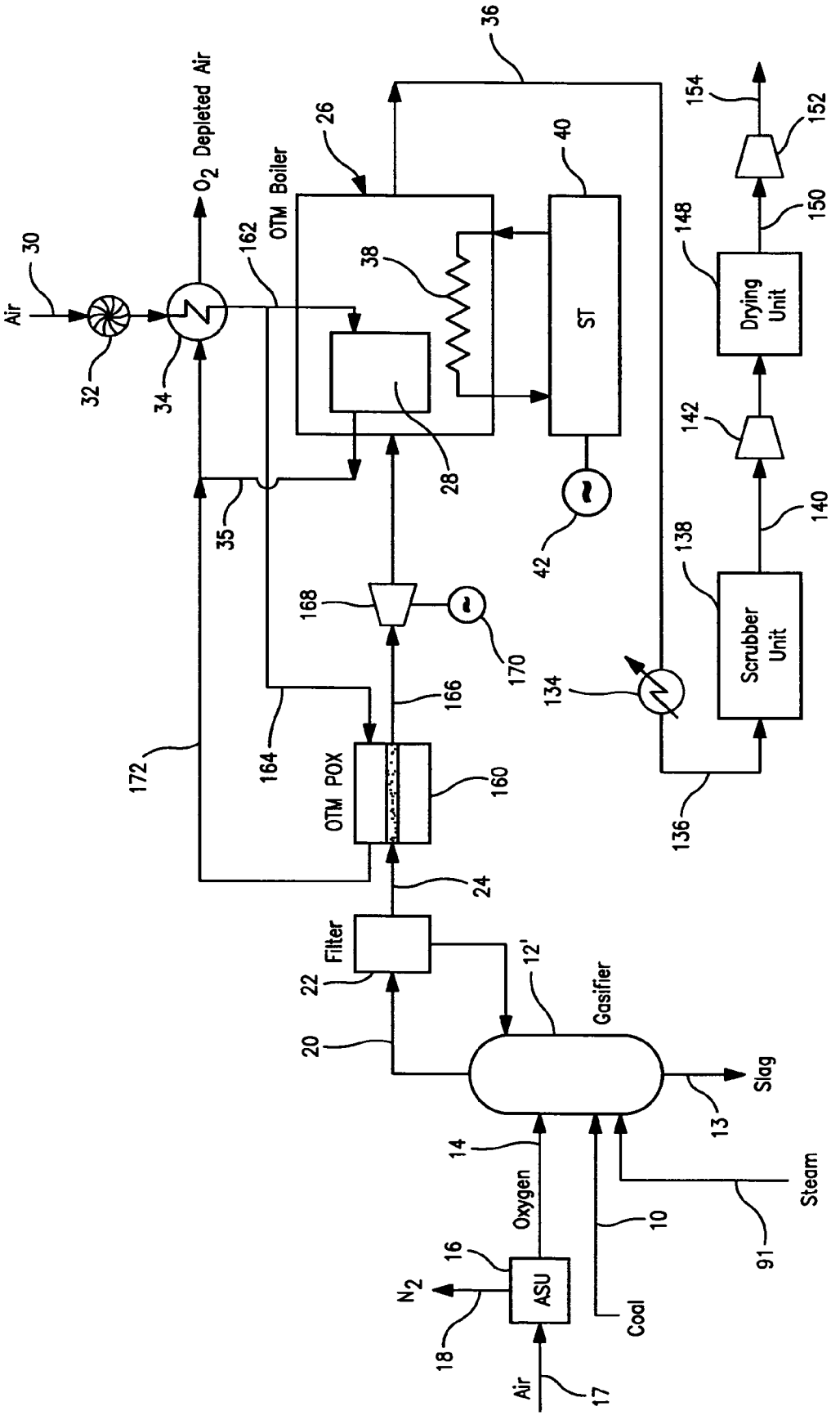

FIG. 3

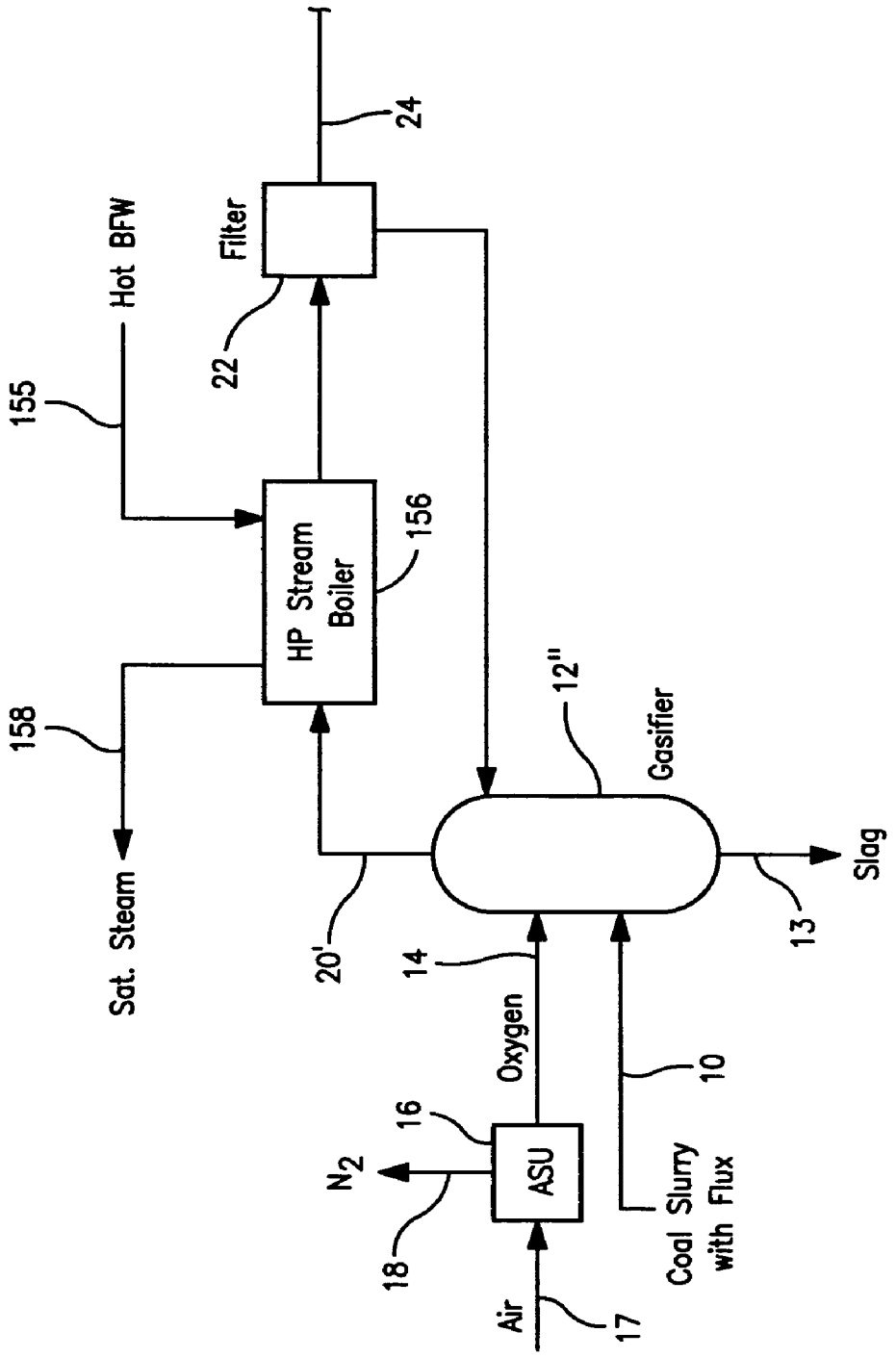
24
Filter
22
Hot BFW
155
HP Stream Boiler
156
158
Sat. Steam
12"
Gasifier
Slag
13
20'
14
Oxygen
10
16
N_2
ASU
Coal Slurry with Flux
18
Air
17

FIG. 4

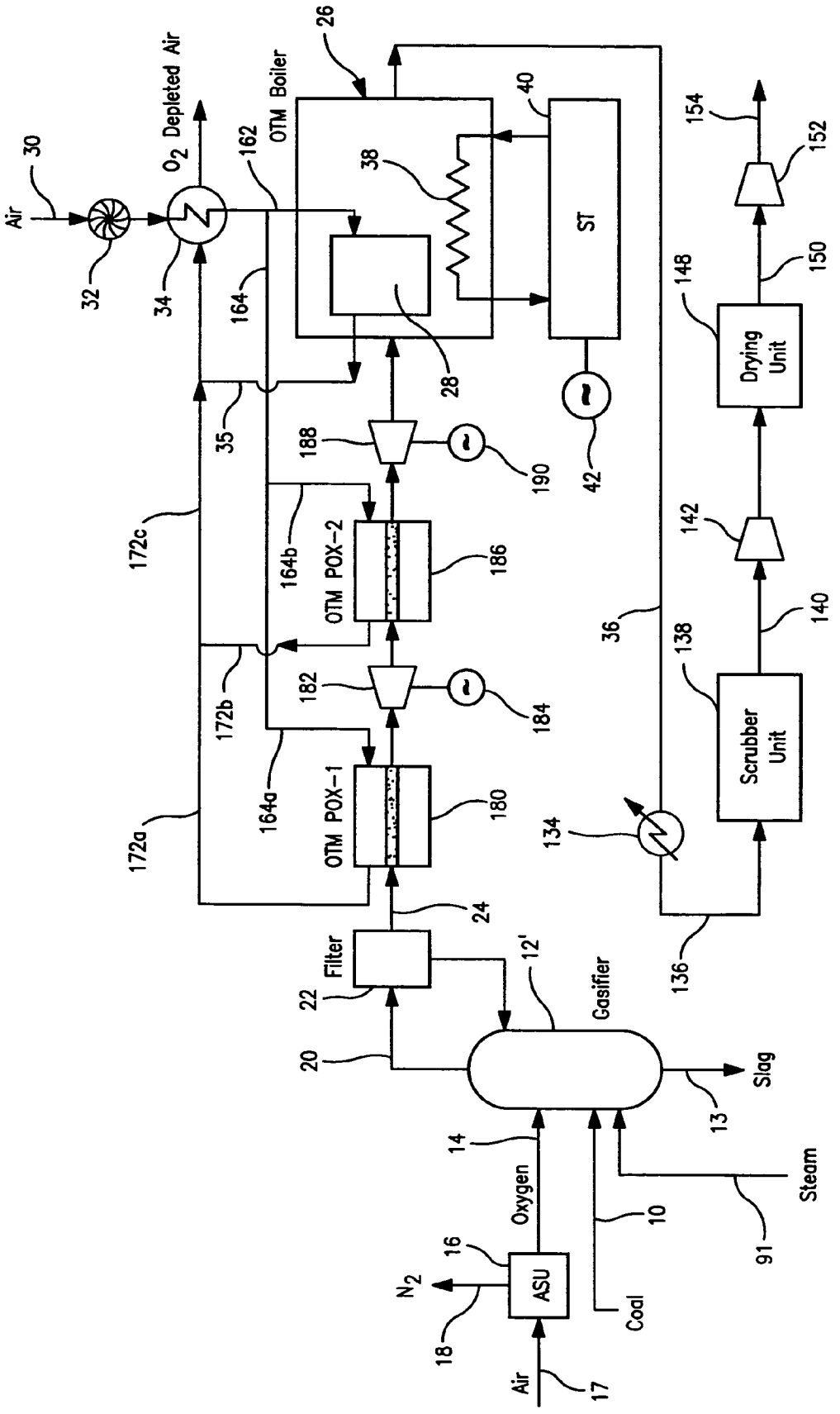
Air
30
32
34
O_2 Depleted Air
OTM Boiler
162
164
26
28
38
40
ST
42
35
188
190
172c
164b
OTM POX-2
186
172b
182
184
164a
OTM POX-1
180
172a
24
Filter
22
20
12'
Gasifier
Slag
13
14
Oxygen
16
N_2
ASU
18
Air
17
Coal
10
Steam
91
36
134
138
Scrubber Unit
140
142
136
148
Drying Unit
150
152
154

FIG. 5

U.S. Patent Dec. 28, 2010 Sheet 6 of 8 US 7,856,829 B2

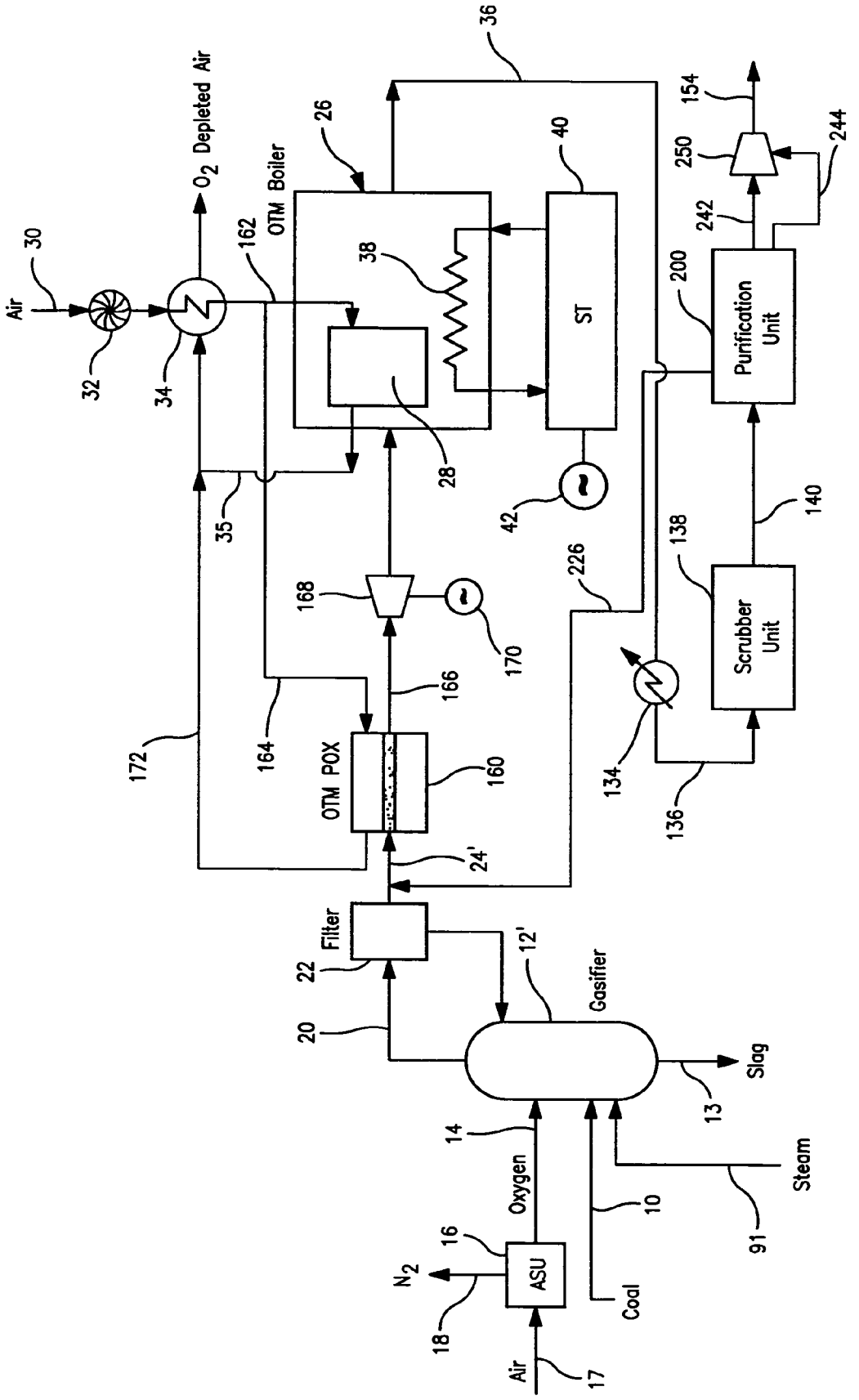

FIG. 6

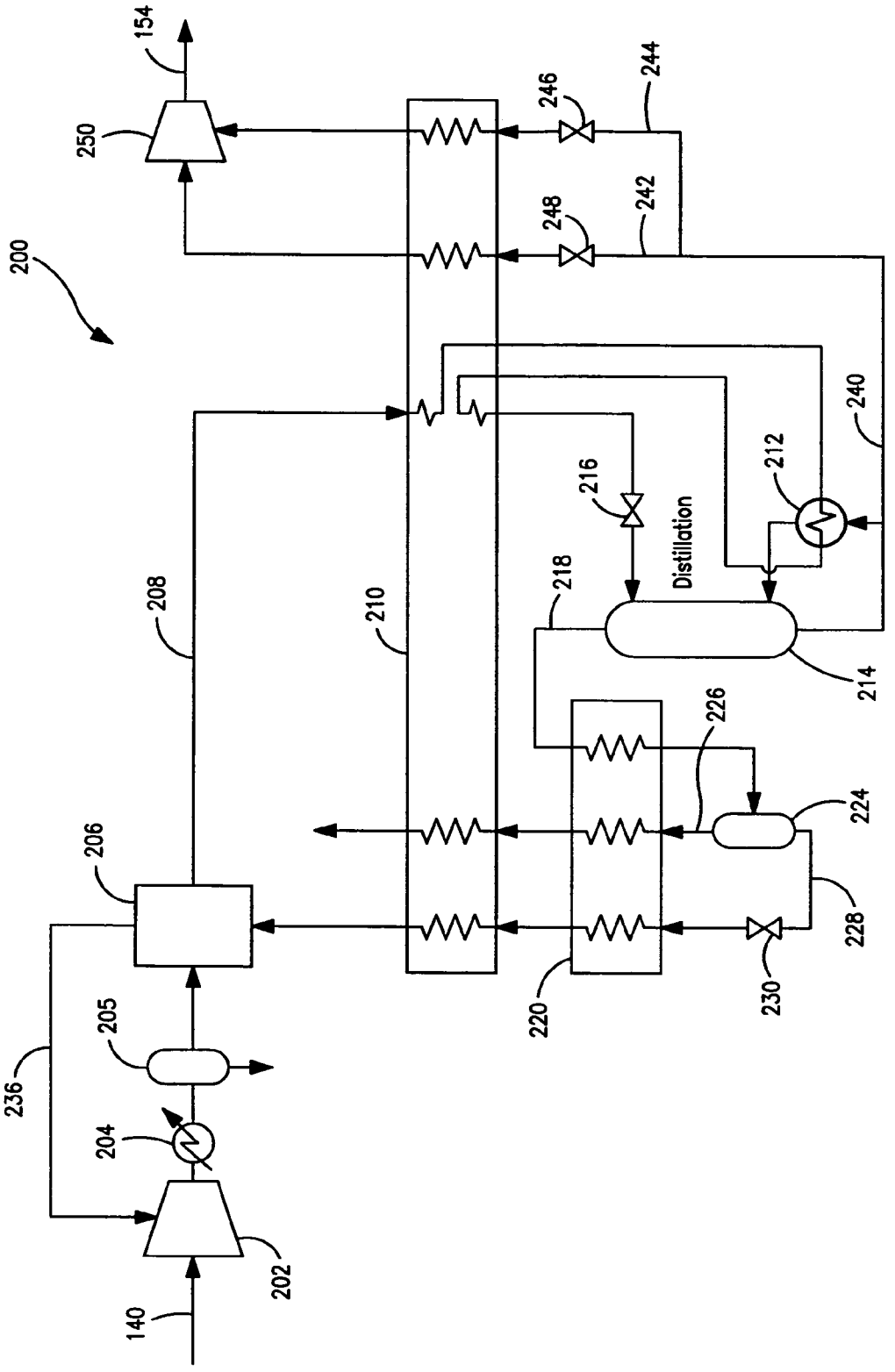
154
250
246
244
248
242
200
240
212
216
Distillation
218
208
210
214
226
224
206
228
205
230
220
236
204
202
140

FIG. 7

U.S. Patent Dec. 28, 2010 Sheet 8 of 8 US 7,856,829 B2

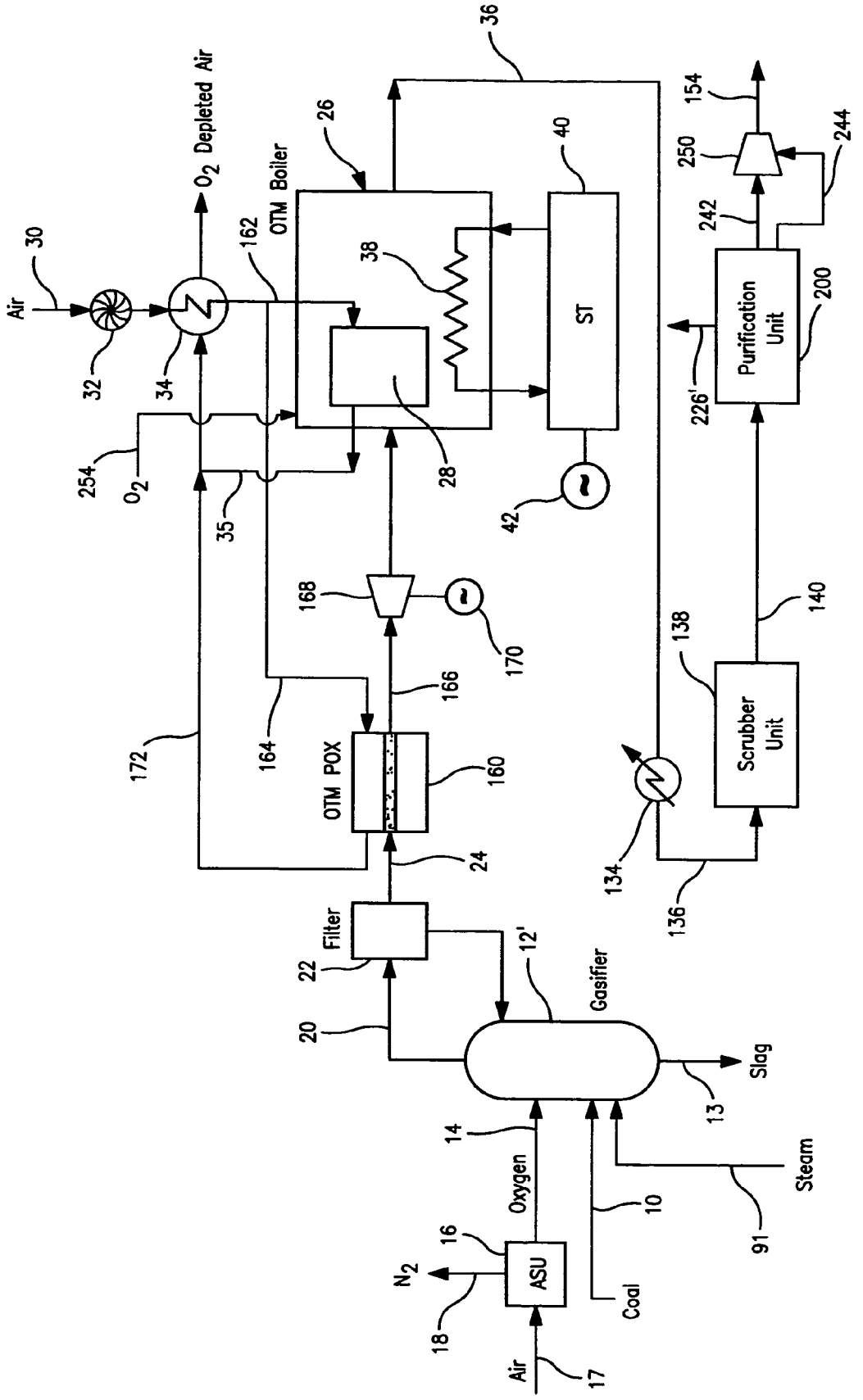

FIG. 8

US 7,856,829 B2

ELECTRICAL POWER GENERATION METHOD

FIELD OF THE INVENTION

The present invention relates to a method of generating electrical power in which a synthesis gas stream, produced in a gasifier, is combusted to generate heat that is used to raise steam and that is in turn used in a steam turbine to generate electrical power. More particularly, the present invention relates to such a method in which the synthesis gas stream is combusted in a boiler that employs an oxygen transport membrane to supply oxygen to support the combustion and that has provision for the purification of the resultant flue gases to produce a carbon dioxide-rich stream for further utilization or sequestration.

BACKGROUND OF THE INVENTION

Coal-fired power plants are utilized throughout the world to generate electricity. Typically, the coal is either in a pulverized form or within a slurry is combusted to generate heat within a boiler to raise steam. The steam is passed into a steam turbine to generate electrical power.

There has been recent interest in capturing carbon dioxide from power plants that use coal and other carbonaceous feed stock such as asphalt, heavy oil, petroleum coke, biomass or natural gas. An integrated gasification and combined cycle (IGCC) is proposed as a preferred method of power generation when carbon dioxide capture is required. In IGCC, gasification of fuel produces a synthesis gas containing mainly hydrogen, carbon monoxide and carbon dioxide with some amount of methane and sulfur and chloride containing impurities. In a typical gasifier the carbonaceous feed is reacted with steam and oxygen to produce the synthesis gas. Typically, the oxygen is provided to the gasifier by a cryogenic rectification plant in which air is rectified within distillation columns at low temperatures to produce the oxygen.

In an integrated gasification combined cycle, the synthesis gas produced as a result of the gasification is cooled to a temperature suitable for its further processing in a water-gas shift reactor to increase the hydrogen and carbon dioxide content of the synthesis gas. The water-gas shift reactor also hydrolyzes most of the carbonyl sulfide into hydrogen sulfide. The synthesis gas is then further cooled for carbon dioxide and hydrogen sulfide separation within a solvent scrubbing plant employing physical or chemical absorption for separation of the carbon dioxide and hydrogen sulfides and carbonyl sulfide from the synthesis gas. This allows for the capture and sequestration of the carbon dioxide which is present within the synthesis gas. The resulting hydrogen-rich gas is then fed to a gas turbine that is coupled to an electrical generator to generate electricity. Heat is recovered from the cooling of the raw synthesis gas stream, from cooling the heated discharge from the water-gas shift reactor, and cooling the exhaust from the gas turbine to raise steam and to generate additional electrical power from a steam turbine.

As can be appreciated, the integrated gasification combined cycle is environmentally very advantageous in that a clean burning synthesis gas stream is used to power the gas turbine while at the same time, the carbon dioxide produced by the gasification can be captured for use in other industrial processes, for enhanced oil recovery or for sequestration. The disadvantage of such a cycle is the high energy penalty associated with the air separation and solvent scrubbing plants. Additionally, the recovery of heat energy in several stages is inherently inefficient in that such heat recovery always involves loss and in any case, the heat is recovered at a low temperature. Lastly, the use of solvent scrubbing plants, water-gas shift reactors and gas turbines is an expensive proposition given their acquisition costs.

It has been suggested to supply the oxygen to the gasification process in lieu of a cryogenic air separation plant with the use of oxygen transport membranes. In such membranes, oxygen is separated from the air with the use of a gas tight membrane formed of the ceramic material that is capable of oxygen ion transport at elevated temperatures. The oxygen ionizes on one surface of the membrane by gaining electrons to form the oxygen ions. Under a driving force of a partial pressure differential, the oxygen ions pass through the membrane and either react with a fuel or recombine to elemental oxygen liberating the electrons used in the ionization of the oxygen.

Where the membrane material is a mixed conductor, the electrons are transported through the membrane. In a membrane that uses an ionic conductor, that is, capable only of conducting oxygen ions, the electrons are transported with the use of an external electric circuit.

The use of ceramic membrane systems have also been contemplated in connection with boilers to generate product steam that has value as a feed to a refinery or to a steam methane reformer as opposed to a combined cycle incorporating a steam turbine. In such boilers, the combustion of a fuel such as natural gas is supported by oxygen separated within the membrane system. Since such combustion will produce a flue gas rich in carbon dioxide and water, the production of a carbon dioxide-rich stream can be accomplished by condensing the water out of the flue gas and then compressing the stream.

An example of a study of such a boiler with carbon dioxide capture appears in a paper entitled, "Cost and Feasibility Study on the Praxair Advanced Boiler for CO_2 Capture Project's Refinery Scenario", Switzer et al. (2005) published by Elsevier. In this paper, a boiler is disclosed in which fuel and recirculated flue gas is passed through a housing having a heat recovery steam generator to exchange heat from a retentate produced by the membrane system with boiler feed water to raise saturated steam. The fuel and flue gas mixture then passes to the membrane system for combustion and generation of the flue gas. Intermingled with the membrane system is another heat recovery steam generator to superheat the saturated steam and thereby to produce the product steam. Heat is recovered from the flue gas to preheat the air and the boiler feed water. Other boiler designs that incorporate oxygen transport membranes and that are capable of producing product steam are disclosed in U.S. Pat. Nos. 6,394,043; 6,382,958 and 6,562,104.

As will be discussed, the present invention provides a method of generating electrical power in which a synthesis gas stream is produced by gasification is then combusted in an oxygen transport membrane to generate heat and in turn raise steam for a steam turbine. As will become apparent, a method of the present invention generates the power in a more thermally efficient manner than an integrated gasification combined cycle with carbon dioxide capture and does not require the use of expensive gas turbines, water-gas shift reactors and solvent recovery units for carbon dioxide capture.

SUMMARY OF THE INVENTION

The present invention provides a method of generating electrical power in which a synthesis gas stream is generated in a gasifier. The synthesis gas stream is combusted to generate heat and a flue gas. The synthesis gas stream is combusted

while at an elevated temperature and the flue gas contains carbon dioxide. As used herein and in the claims, the term "elevated temperature" means a temperature that is at least about 50° F. above the dew point of the synthesis gas stream. In this regard, at lower temperatures, excess fuel would be required for its combustion and in any event, water condensation is to be avoided because of potential mechanical and corrosion issues that could be appreciated by those well skilled in the art. The combustion of the synthesis gas stream is supported by separating oxygen from an oxygen containing stream within an oxygen transport membrane system that is operatively associated with a boiler. Steam is produced within the boiler by indirectly transferring the heat to the boiler feed water. Energy is extracted from the steam by a steam turbine system of a steam cycle operatively associated with the oxygen transport membrane boiler. The energy is converted to electrical power by an electrical generator coupled to the steam turbine system. The flue gas stream can then be purified to produce a carbon dioxide-rich stream.

As is apparent from the above description of the invention, since the synthesis gas stream is combusted while at an elevated temperature, the method of the present invention does not have the built-in thermal inefficiency that can be found in prior art integrated gasification combined cycles with carbon dioxide capture. This thermal inefficiency is due to the fact that the carbon dioxide is removed from the synthesis gas in a solvent system that requires the synthesis gas to be cooled to near ambient temperatures and the energy input that is required to operate the solvent system. As will also be discussed, the flue gas stream can be directly purified in a manner that will be discussed in more detail below that does not involve the use of solvent scrubbing units.

Advantageously, in a particularly preferred embodiment, the synthesis gas stream can be expanded within an expander having at least one expansion stage prior to the combusting of the synthesis gas stream and the synthesis gas stream can be partially oxidized prior to expanding the synthesis gas stream in at least one partial oxidation stage. The partial oxidation will act to oxidize a volatile content of the synthesis gas stream and will further heat the synthesis gas stream. The expander can be coupled to another electrical generator to generate the additional electrical power.

Preferably, the partial oxidation stage is formed by an oxygen transport membrane rector generating oxygen to support the oxidation of the synthesis gas stream. In an alternative embodiment of the present invention, the at least one expansion stage and the at least one partial oxidation stage can be a first partial oxidation stage followed by a first expansion stage, a second partial oxidation stage following the first expansion stage and then a second expansion stage following the second partial oxidation stage.

Combustion of the synthesis gas stream in the oxygen transport membrane boiler can be incomplete resulting in fuel species being present within the flue gas stream. In such case, the fuel species can be separated from the flue gas stream and recycled to the at least one partial oxidation stage. Another variation is to conduct the process such that the combustion of the synthesis gas stream supported by separating oxygen from an oxygen containing stream within an oxygen transport membrane system is not complete. In such case, the combustion of the synthesis gas stream can be completed by addition of an oxygen containing stream. The advantage of such embodiments is to conserve the amount of material used from the oxygen transport membranes within the oxygen transport membrane system.

Advantageously, the carbon dioxide can be purified by cooling the flue gas stream to produce a cooled flue gas stream. After removing sulfur dioxide, the flue gas stream can be compressed and then dried within a dryer to produce a carbon dioxide containing stream having a purity of no less than about 90% by volume. The carbon dioxide containing stream can be further compressed to produce a carbon dioxide product stream. The carbon dioxide product stream has further known industrial uses such as enhanced oil recovery. In any case, the carbon dioxide product stream can be further distributed by a pipeline.

Where the combustion of the synthesis gas stream results in fuel species being present within the flue gas stream, the fuel species can be separated from the flue gas stream after having been dried and prior to being further compressed.

Although there are a variety of different gasifiers and different feed stocks that are possible, the gasifier can generate the synthesis gas stream through the gasification of coal. In this regard, the gasification of the coal can be conducted in a moving bed gasifier utilizing steam generated by the steam cycle. In any embodiment of the present invention, the steam cycle can be an ultra-supercritical steam cycle.

The gasifier can be an entrained flow gasifier. In such case, the synthesis gas stream is cooled by indirect heat exchange with a heated boiler feed water stream to produce a steam stream. The steam stream can then be combined with steam produced within the boiler.

BRIEF DESCRIPTION OF THE DRAWINGS

While the specification concludes with claims distinctly pointing out the subject matter that Applicants regard as their invention, it is believed that the invention will be better understood when taken in connection with the accompanying drawings in which:

FIG. **1** is a process flow diagram of a method for generating electrical power in accordance with the present invention;

FIG. **2** is a schematic of a boiler incorporating an oxygen transport membrane system integrated with a steam cycle;

FIG. **3** is an alternative embodiment of FIG. **1**;

FIG. **4** is a fragmentary view of an alternative embodiment of FIG. **3**;

FIG. **5** is an alternative embodiment of FIG. **3**;

FIG. **6** is an alternative embodiment of FIG. **3**;

FIG. **7** is an embodiment of the purification unit used in FIG. **6**; and

FIG. **8** is an alternative embodiment of FIG. **7**.

DETAILED DESCRIPTION

With reference to FIG. **1**, the present invention illustrates an apparatus **1** for carrying out a method in accordance with the present invention in which coal is gasified. This is for exemplary purposes because as indicated above, feed stock to be gasified could be other substances such as coal, asphalt, heavy oil, petroleum coke, biomass or natural gas.

In accordance with FIG. **1**, a prepared coal feed stream **10** is gasified within a gasifier **12** with the addition of a gasifying agent such as an oxygen stream **14**. Oxygen stream **14** is created by the cryogenic rectification of air within a cryogenic rectification unit **16**. In some gasifiers such as moving bed gasifiers high pressure steam as a steam stream **91**, to be discussed, is also injected into the gasifier.

Cryogenic rectification unit **16** ("ASU") consists of a compressor to compress an air stream **17** and a purifier to remove the higher boiling contaminants such as carbon dioxide, water and hydrocarbons. The resultant purified and compressed stream is then cooled within a main heat exchanger against return streams consisting of the fractionated components of

the air, namely, nitrogen and oxygen. The oxygen is discharged as oxygen stream **14** and the nitrogen is discharged as a nitrogen stream **18**. If necessary, the oxygen stream **14** can be compressed to suitable pressure for injection into gasifier **12**.

In a typical cryogenic rectification unit **16**, the air is cooled within the main heat exchanger to a temperature suitable for its rectification, generally in a double distillation column having a high pressure column that is operatively associated with the low pressure column by a condenser-reboiler. The high pressure column will typically operate at a pressure of about 5 bar absolute to produce a nitrogen-rich overhead and an oxygen-rich, column bottoms. An oxygen-rich column bottoms is further refined within the low pressure column that generally operates at a pressure of about 1.2 bar absolute. The column bottoms of the lower pressure column is enriched in the oxygen. The oxygen is vaporized against condensing a nitrogen-rich tower overhead produced in the higher pressure column. The resulting condensate of the higher pressure column is valve expanded and used to reflux the lower pressure column.

Other alternatives for generation of the oxygen stream **14** are possible. For example, an oxygen transport membrane reactor in which the compressed air can be partially combusted within a combustor and introduced into the oxygen transport membrane reactor for separation of oxygen in a manner known in the art.

Gasifier **12** incorporates any of the numerous commercially available gasification technologies. For example, in the counter-current "fixed" (or moving) bed type of gasifier, a downward flowing bed of carbonaceous fuel is contacted with gasification products generated by steam and oxygen that enter at the bottom of the moving bed. The gasification products flow in a counter-current configuration relative to the carbonaceous bed. The slag or ash **13** will be removed in all gasifiers. For example, in a counter-current fixed bed gasifier the reference number **13** would designate a slag for removal. In a fluid bed gasifier the fuel particles are fluidized as a result of injection of oxygen and steam at or near the bottom of the bed. In the entrained flow gasifier dry pulverized solids such as pulverized coal or a fuel slurry is gasified with oxygen in a co-current flow.

Within gasifier **12**, known reactions involving the coal and the oxygen produces a synthesis gas stream **20** which contains hydrogen, carbon monoxide, methane, carbon dioxide, steam, sulphur compounds and small quantities of higher hydrocarbons. The temperature of synthesis gas stream **20** will depend on the type of gasifier used. In the entrained flow gasifier of gasifier **12**, the synthesis gas exits the gasification section of the process at a temperature of between about 1600° F. and about 3500° F. It is to be noted, however, that other types of gasifiers could be used in an integration in accordance with the present invention and as such, it is worth mentioning that in other types of the gasifiers, the synthesis gas stream will be produced at other temperature ranges. For example, in fixed bed gasifiers, the synthesis gas will be produced at temperatures of between about 900° F. and about 1000° F.

Particulate removal from the synthesis gas stream **20** can be carried over by known techniques that include a cyclone or a candle filter **22**. Candle filter **22** can be ceramic or metallic candle filters which are used for removing such particulate matter from a synthesis gas stream **20**. Candle filter **22** should in any case preferably operate about 700° F. and more preferably above 1000° F. It is to be noted that filtering is optional in that it is generally present to protect an expander from erosion. In some gasifiers, the stream is recycled to the front end thereof to improve carbon conversion.

The resultant filtered syngas stream **24** contains a synthesis gas that is then sent to an oxygen transport membrane boiler **26**. Although there is no particular oxygen transport membrane boiler that is preferred, in any such device the filtered synthesis gas stream **24** is introduced into an oxygen transport membrane system **28** that can comprise a plurality of tubes made of a ceramic material that can be a mixed conductor or a dual-phase conductor, such as described above. It is understood that oxygen transport membrane system **28** could employ oxygen transport membrane elements in forms other than tubes, for instance, planar elements also known in the art. An oxygen containing gas, for example air is introduced into the tubes as an air stream **30** with the use of a blower **32**. Air stream **30** is preheated by means of a waste heat recovery heat exchanger **34** prior to being introduced into the oxygen transport membrane tubes. The oxygen ions permeate through the membrane and immediately combine with the filtered synthesis gas stream **24** to support combustion of the filtered synthesis gas stream **24**. The oxygen depleted retentate, as a retentate stream **35**, is passed through the waste heat recovery heat exchanger **34** for recovery of heat and discharge.

In the illustrated oxygen transport membrane boiler **26**, combustion of the filtered synthesis gas stream **24** provides the driving force for the oxygen separation within the oxygen transport membrane system **28**. As such, air stream **30** is not appreciably compressed. However, while it is possible to integrate an oxygen transport membrane boiler that does utilize compression for the oxygen containing gas in accordance with the present invention, such integration is not preferred due to the power penalty involved in such compression.

Preferably, the surface temperature of the OTM tubes is maintained at between about 1600° F. and about 2000° F. throughout the oxygen transport membrane boiler **26**. A flue gas stream **36** is discharged from the oxygen transport membrane boiler **26** in a temperature of preferably between about 1600° F. and about 2000° F. It consists predominately of water and carbon dioxide with small amounts of nitrogen, argon and sulphur dioxide and potentially residual oxygen.

The heat generated by the combustion occurring within the oxygen transport membrane boiler **26** is recovered by a heat exchange network, generally indicated by reference numeral **38** in which steam is generated and utilized in a steam cycle ("ST") generally indicated by block **40** that incorporates a steam turbine system to generate power that can be applied to driving an electrical generator **42**. There are many steam cycles that are possible for use in connection with the present invention and in fact the design of the steam cycle is a routine matter that is often carried out by computer programs that are specifically capable of generating such designs. As will be discussed, ultra-supercritical steam cycles are preferred. However, sub-critical and supercritical steam cycles are also possible. Moreover, there are many possible designs for oxygen transport membrane boiler **26**. Having said this, as an example, a more detailed description of a suitable design that can be used in connection with oxygen transport membrane boiler **26** and the associated steam cycle **40** is illustrated in FIG. **2**.

With specific reference now to FIG. **2**, oxygen transport membrane boiler **26** is based upon a conventional commercially available unit that has been modified in a manner that will be discussed hereinafter. Oxygen transport membrane boiler **26** generally consists of a radiant section **44** in which radiant heat transfer predominates and a convective section

46 in which heat transfer is accomplished by convective heat transfer. Oxygen transport membrane boiler **26** is integrated with a steam cycle **40**.

Radiant section **44** is modified with the provision of oxygen transport membrane tubes **50** that form the oxygen transport membrane system **28** of oxygen transport membrane boiler **26**. Oxygen transport membrane tubes **50** are connected in parallel to receive air stream **30** and alternate with a series of steam tubes **52**, **54**, **56** and **58** forming part of the heat exchange network **38** to raise steam and for the steam cycle **40**. In the illustrated embodiment, steam tubes **52**, **54**, **56** and **58** are in series. However, in practice they could be positioned anywhere in the radiant section **44** in that such section has a uniform temperature. Although not specifically illustrated, each of the steam tubes **52**, **54**, **56** and **58** would be part of larger alternating arrays in which all steam tubes of an array, for example, steam tubes **52** would be connected in parallel. Furthermore, as also not illustrated, saturated steam produced within steam tubes **52** can be collected in a steam drum prior to introduction into steam tubes **54**.

With respect to the steam cycle **40**, an ultra-supercritical steam cycle is preferred and as used herein and in the claims means a cycle that employs steam at a temperature of at least about 1000° F. and at a pressure of at least 4000 psia. The following discussion of steam cycle **40** utilizes temperatures and pressures that are applicable to examples 1 and 2 discussed below.

In accordance with steam cycle **40**, a boiler feed water stream **60** is pressurized by being pumped by a pump **62** and preheated within preheaters **64**, **66**, **68** and **70** and heat exchangers **72** and **74** within convective section **46** to a temperature of about 650° F. and a pressure of about 4366 psia that has been imparted through the pressurization less piping losses. It is to be noted, that heat exchangers **72**, **74** and **109**, to be discussed and the steam tubes **52**, **54**, **56** and **58** form the heat exchange network **38** of oxygen transport membrane boiler **26**.

The boiler feed water stream **60**, thereafter, enters steam tubes **52** that act as a steam generator and then to steam tubes **54** to superheat the generated steam to produce a steam stream **76** at a temperature of about 1080° F. and a pressure of about 4050 psia. Steam stream **76** is then introduced into high pressure steam turbine **78** ("HPT") where it is expanded to 1226 psia. About 2725 klb/hr of expanded steam, that constitutes about 90% of stream **76**, as a stream **80** is passed through steam tubes **56** that serve as a reheater where stream **80** is reheated to a temperature of about 1111° F. to produce a stream **82** having a pressure of about 1170 psia. The remaining part **84** is introduced into preheater **68**.

Reheated stream **82** is then introduced into a primary intermediate pressure turbine **86** ("PIPT") to be expanded to about 505 psia and a temperature of about 822° F. About 2328 klb/hr of this steam as a stream **88**, that constitutes about 85% of stream **80**, is introduced into steam tubes **58** that serve as a second reheater to produce a reheated stream **90** having a temperature of about 1111° F. The remainder of the expanded steam is introduced as a stream **92** to preheater **64**.

Reheated stream **90** is then introduced into intermediate pressure steam turbine **94** ("IPT"). A stream **96** is then expanded in low pressure turbine **98** ("LPT") to a pressure of about 0.75 psia. The resulting stream **100** is then passed into a condenser **102** and then pumped by pump **104** to a series of low pressure boiler-feed water heaters **106**, **108**, **109**, **110** and **112** to be heated to about 210° F. using extracted steam streams **114**, **116**, **118** and **120** taken from intermediate pressure steam turbine **94** and low pressure turbine **98**. All of the extracted streams are combined, pumped to pressure by pump **105** and combined with stream **100**. The resultant heated feed water stream **122** is mixed with feed water stream **124** in deairator **126** along with a stream **128** and a stream **130** extracted from intermediate pressure steam turbine **94** and used to strip volatile gases from the water. Stream **128** is made up of stream **92**, stream **84** and a stream **132** extracted from primary intermediate pressure steam turbine **86**. Stream **60** from deairator **126** is pumped by pump **62** to a pressure of about 4452 psia.

Referring again to FIG. **1**, flue gas stream **36** is then purified by first being cooled within a water-cooler **134** to a temperature of between about 160° F. and about 300° F. Cooled stream **136** is then sent to a flue gas desulphurization scrubber unit **138** well known in the art and that is capable of removing more than about 98% by volume of the sulphur dioxide. Flue gas desulphurization scrubber unit **138** is a known system that can be obtained from a variety of manufacturers, for example, Babcock & Wilcox Company, 20 S. Van Buren Avenue Barberton, Ohio, U.S.A 44203-0351. Typically, a flue gas desulphurization scrubber unit **138** will typically comprise three parts, namely, limestone handling and reagent preparation, where limestone is received, stored and grinded in a ball mill to prepare an aqueous slurry. A second part is a scrubber where the limestone slurry is brought into contact with a flue gas which in the illustrated embodiment would be cooled stream **136** in a counter-current mode in a spray-tower column. This is followed by by-product dewatering where the bleed slurry from the flue gas desulphurizor absorber is dewatered and gypsum is separated and stored. The resulting partly purified flue gas stream **140** consists mainly of carbon dioxide and about 10 to 15 mole percent of water with some residual argon and nitrogen, oxygen and trace amounts of sulphur dioxide.

Partly purified flue gas stream **140** is then compressed in a base load compressor **142** to a pressure of between about 300 psia and about 500 psia and then dried within a drying unit **148** to remove moisture. The drying unit is a glycol system that is a known system that is typically used for drying natural gas. Preferably, although not illustrated, partly purified flue gas stream **140** is first cooled to about 110° F. prior to such compression and any condensate removed to conserve on the energy of compression. It is also understood that base load compressor **142** is generally a multistage, inter-cooled compression system with knock-put drums to remove additional water. Glycol systems can be obtained from a variety of sources including NATCO Group Inc. 2950 North Loop West, Suite 750 Houston, Tex. 77092. In a typical glycol system, partly purified flue gas stream **140** after compression is contacted in a counter-current manner within a glycol solution in an absorption column. The dried gas leaves the top of the absorption column. The glycol solution containing absorbed water is sent to a connected distillation column. Heat is supplied to separate the water and the regenerated glycol solution is circulated back to the absorption column using a pump. A heat exchanger is used to exchange heat between the glycol solutions flowing between the two columns. The removal of water prevents the formation of carbonic acid in the carbon dioxide product that could corrode pipelines. Normally, the water level should be reduced below about 600 ppm by volume for this purpose.

Additionally, reducing the water content will prevent freezing when used in downstream processing such as sub-ambient purification processes. Although not illustrated, a dryer for such purpose could be based on adsorption using molecular sieves. In such case, the dryer can comprise a multi-bed molecular sieve dryer system in which half of the beds process the feed to be dried and the other half undergo

regeneration. A product portion of the product gas is used as a regenerating gas which is heated to about 450° F. with a heater to remove moisture from the beds. After the beds are free to moisture the regeneration gas at near-ambient temperature is passed through the beds to cool them down. The regeneration gas can then be recycled to a base load carbon dioxide compressor **142** at an appropriate point upstream of the last stage that is utilized for such purpose.

The dried stream **150** from drying unit **148** is then passed to a booster compressor **152** to produce a product stream **154** that can be passed to a pipeline or for enhanced oil recovery or sequestration purposes. Booster compressor **152** is a multi-stage, inter-cooled machine. The product stream **154** preferably has a carbon dioxide content of at least about 90% by volume and as indicated in the examples, the carbon dioxide content can be about 92% or about 95% by volume.

With reference to FIG. **3**, another embodiment is illustrated that utilizes an oxygen transport membrane partial oxidation reactor **160**. This feature has particular applicability to where the coal is gasified in a moving bed gasifier that utilizes less oxygen than other types of gasifiers. In such embodiment, synthesis gas stream **20** produced by a moving bed gasifier **12'** at a temperature of between 900° F. and about 1000° F. and contains volatile substances such as tars and oils. Steam is also utilized in such gasifier and is obtained, as indicated in FIG. **2**, by way of stream **91** extracted from an intermediate stage of intermediate pressure steam turbine **94** or possibly other sources not shown. Partial oxidation reactor **160** partially oxidizes the syngas to raise its temperature from between about 1600° F. and about 1800° F. to remove such volatile substances such as tars, oils and phenols that are oxidized to hydrogen, carbon monoxide, methane and carbon dioxide. Partial oxidation reactor **160** employs one or more oxygen transport membrane elements that are typically mixed conductors in tubular form. At about 1800° F., partial oxidation reactions will proceed in the absence of a catalyst. In this regard, the synthesis gas stream **20** will often contain sulfur that is a known catalyst poison and if a catalytic reactor were used, upstream treatment or a sulfur tolerant catalyst would be required. Typical examples of partial oxidation reactors are well known and are illustrated in U.S. Pat. Nos. 5,820,654; 5,820,655 and 6,139,810.

In such embodiment as illustrated in FIG. **3**, the air stream **30** is divided into first and second subsidiary oxygen containing streams **162** and **164**. First subsidiary oxygen containing stream **162** is fed to oxygen transport membrane boiler **26**. Second subsidiary oxygen containing stream **164** is supplied to the inside of the oxygen transport membrane elements of partial oxidation reactor **160**. The filtered synthesis gas stream **24** is supplied to the exterior to the shell of such reactor and the oxygen ions react with the volatiles to produce the reaction products mentioned above. Alternatively, separate air supplies along with blowers and heat exchangers analogous to units **32** and **34** can be used to supply the oxidant to units **26** and **160**.

The resultant synthesis gas stream **166**, after having the volatiles reacted in the oxygen transport membrane partial oxidation reactor **160**, has a pressure of between about 300 and about 1200 psia. Synthesis gas stream is then expanded within an expander **168** coupled to an electrical generator **170** to generate additional electrical power. Between about 60% and about 80% of the total oxygen requirement for apparatus **1** will typically be supplied by the oxygen transport membranes contained within oxygen transport membrane partial oxidation reactor **160** and the oxygen transport membrane boiler **26**. The remainder is supplied by cryogenic air separation unit **16** and to the gasifier **12'**. A retentate stream **172** joins retentate stream **35** and the combined stream is fed to heat recovery heat exchanger **34**.

With brief reference to FIG. **4**, an alternative embodiment of FIG. **3** is illustrated that utilizes an entrained flow or fluid bed type of gasifier **12"**. Since the temperature of synthesis gas stream **20'** produced by such a gasifier is about 1800° F., a high pressure steam boiler **156** is provided to produce a steam stream **158** from hot boiling feed water stream **155**. Steam stream **158** can be combined with the steam entering steam tube **54** located within oxygen transport membrane boiler **26** and shown in more detail in FIG. **2**. The boiler **156** decreases the temperature of stream **20'** to facilitate the use of high temperature filters which are currently limited to operating temperatures below about 1000° F. These filters are used to minimize erosion in hot gas expanders as has been mentioned above.

With reference to FIG. **5**, stages of partial oxidation and expansion are illustrated in which the filtered synthesis gas stream **24** is introduced into a first partial oxidation stage produced by a first partial oxidation reactor **180** followed by expansion within expansion stage provided by an expander **182** coupled to an electrical generator **184** to generate additional electricity. Thereafter, the treated filtered synthesis gas stream **24** after expander **182** is then introduced into a second partial oxidation stage provided by a second partial oxidation reactor **186** followed by a second expansion stage provided by a second expander **188** coupled to an additional electrical generator **190** for generating yet additional electrical power. In such embodiment, second subsidiary oxygen containing stream **164** is divided into portions **164***a* and **164***b* that are fed into the first partial oxidation reactor **180** and the second partial oxidation reactor **186**. The resultant oxygen depleted retentate streams **172***a* and **172***b* are combined to produce a combined stream **172**c that is further combined with retentate stream **35** and passed through heat recovery heat exchanger **34**. Again, independent air supply systems are also possible as have been discussed above.

With reference to FIG. **6**, an embodiment is illustrated in which combustion is not completed within oxygen transport membrane system **28** of boiler **26**. Typically, the area required for oxygen transport that would be necessary for complete combustion would be quite high. In order to avoid excessive costs, combustion may be completed only to the extent of between about 80% and about 90% of the fuel species contained within synthesis gas stream **20**. In such a situation, flue gas stream **36** will contain small amounts of fuel species such as hydrogen and carbon monoxide. Carbon dioxide stream could then be further purified within a purification unit **200** that incorporates cryogenic distillation. Alternative methods of purification including distillation processes with external refrigeration can be used to form purification unit **200**. Well known purification processes are illustrated in U.S. Pat. Nos. 5,927,103; 6,035,662 and 6,070,471.

With reference to FIG. **7**, a specific embodiment of purification unit **200** is illustrated that purifies partly purified flue gas stream **140**. Partly purified flue gas stream **140** is compressed in a compressor **202** to a pressure of between about 150 psia and about 1000 psia. The amount of carbon dioxide that can be recovered is a function of the feed pressure supplied to the cold box. As can be appreciated, carbon dioxide recovery can be increased by increasing this pressure. However, such increase in pressure will result in greater production costs. After having been cooled within water cooled chiller **204**, partly purified flue gas stream **140** is then introduced into a phase separator **205** to disengage water that has

been condensed within partly purified flue gas stream **140** by virtue of its having been cooled in water cooled chiller **204**.

The partly purified flue gas stream **140** is then introduced into a dryer **206**. Dryer **206** is preferably an adsorption system that can contain beds of molecular sieve adsorbent operating out a phase to adsorb moisture and other impurities such as heavy hydrocarbons that will boil at a higher temperature than the partly purified flue gas stream **140**. The beds of molecular sieve adsorbent operate out a phase so that as one bed is adsorbing such higher boiling impurities the other bed is being regenerated. Even number of beds numbering greater than two can also be used for large flows with half of beds performing adsorption while the other half of beds undergoing regeneration. A bed is regenerated by lowering its pressure and/or by increasing its temperature to desorb the adsorbed component and then purging the bed with a stream that is lean in the adsorbed component. In a system that employs temperature swing, the bed is regenerated by heating a stream lean in the adsorbed component and then introducing it into the bed to be regenerated to cause desorption and to carry away desorbed components. These systems vary but there are many examples of the same known that are well known in the art. In this regard, non-adsorbent based systems are possible such as by the use of reversing heat exchangers that are well known in the art of distillation.

The resultant dried feed stream **208**, that consists of partly purified flue gas stream **140** after having been compressed by compressor **202** and dried, is then introduced into a main heat exchanger **210** in which it is partly cooled and then introduced into a reboiler **212** that serves to produce boil up or initiate an ascending vapor phase within a stripping column **214**. Dried feed stream **208** is then again introduced into main heat exchanger **210** in which it is fully cooled to at least partially liquefy the dried feed stream **208**. The dried feed stream **208** is then introduced into an expansion valve **216** into stripping column **214** to initiate a descending liquid phase within such column.

As well known in the art, stripping column **214** preferably has structured packing to contact the ascending vapor phase flowing up through the packing with a descending liquid film of the liquid phase. Other vapor-liquid contacting elements known in the art could be used such as sieve trays. As a result of the contact, the descending liquid phase becomes evermore rich in carbon dioxide, the less volatile component and the ascending vapor phase becomes evermore rich in impurities that have a higher volatility than the carbon dioxide. Within stripping column **214**, the remaining uncombusted constituents of the filtered synthesis gas stream **24**, namely, hydrogen, carbon monoxide and methane, and any inert constituents that may arise from air ingress into combustion zone, namely, nitrogen and argon, all being more volatile than the carbon dioxide, will be stripped from the descending liquid to produce a carbon dioxide-lean column overhead and a carbon dioxide-rich, liquid column bottoms.

A column overhead stream **218** can be extracted from stripping column **214** that is composed of the carbon dioxide-lean column overhead and then introduced into an auxiliary heat exchanger **220** so that the carbon dioxide overhead stream **218** is at least partially liquefied. The carbon dioxide overhead stream **218** is then introduced into a phase separator **224** to produce a carbon dioxide-depleted vapor stream **226** and a carbon dioxide-rich liquid stream **228**. Carbon dioxide-rich liquid stream **228** is expanded within an expansion valve **230** and then passed together with the carbon dioxide-depleted vapor stream **226** into auxiliary heat exchanger **220**. Expansion valve **230** provides refrigeration for the partial liquefaction of carbon dioxide overhead stream **218**.

Carbon dioxide-depleted vapor stream **226** can be passed into main heat exchange **210** and then recycled and combined with filtered synthesis gas stream **24** to provide a synthesis gas feed stream **24'** to oxygen transport membrane partial oxidation reactor **160**. As would be understood by those skilled in the art, if the gasifier used operates at a higher pressure than carbon dioxide-depleted vapor stream **226**, a recycle compressor would have to be provided to accomplish the recycle. A small amount of stream **226** can be purged from the process as a fuel stream to avoid the build up of inerts such as nitrogen and argon in the loop. The purge gas may require incineration or catalytic oxidation or other treatment to manage carbon monoxide, methane, or other emissions.

Carbon dioxide-rich liquid stream **228** after having passed through main heat exchanger **210** will be vaporized and as such can be used to regenerate dryer **206**, for example, such stream can be heated and then introduced into an adsorption bed for regeneration purposes and thereafter, be reintroduced as a recycle stream **236** into an appropriate stage of compressor **202** to enhance carbon dioxide recovery.

A carbon dioxide product stream **240** as a liquid can be extracted from stripping column **214** that is composed of carbon dioxide-rich liquid column bottoms. The carbon dioxide product stream can then be expanded in an expansion valve to generate refrigeration for the process. Advantageously, carbon dioxide product stream **240** is split into subsidiary streams **242** and **244** and at least the subsidiary stream **244** is expanded to lower pressure by the use of expansion valve **246**, optionally both streams **242** and **244** are simultaneously expanded to lower and the higher pressures by the use of expansion valves **246** and **248**, respectively. Both subsidiary streams **242** and **244** are then vaporized in main heat exchanger **210**. The resultant lower pressure subsidiary stream **242** is introduced into the inlet of product compressor **250**. The lower pressure subsidiary stream **244** is introduced into an intermediate stage of product compressor **250**. The product compressor **250** could be a multi-stage compressor with interstage cooling. It is to be noted, that, although not illustrated, some of the carbon dioxide product could be taken as a liquid from carbon dioxide product stream.

With reference to FIG. **8**, another variation of FIG. **6** is to inject supplemental oxygen containing stream **254** within the radiant section **44** of the oxygen transport membrane boiler **26** to complete the combustion of the fuel. Supplemental oxygen stream **254** is an oxygen containing stream that contains at least about 40% oxygen to prevent the build-up of nitrogen in the carbon dioxide to be captured. A disadvantage of such a process is that inerts are introduced into the flue gas stream **36** and the purity of the carbon dioxide will thereby suffer. In such embodiment, stream **226'** can be produced containing the more volatile components of the partly purified flue gas stream that will simply be treated or vented depending on the characteristics of the constituents. The stream **226'** could also contain oxygen. Therefore, although not illustrated, catalytic oxidation could be incorporated at the end of the radiant section or the convective section of the oxygen transport membrane boiler **26**. This would also reduce the amount of oxygen required to achieve complete combustion. In this regard, to the extent that there exists any excess oxygen in any embodiment of the present invention, such catalytic oxidation could be incorporated together with purification.

The apparatus shown in FIGS. **3**, **4** and **5** were modeled using computer programs to assess the predicted performance of such illustrated embodiment. Guidelines set forth in the Carbon Capture and Sequestration Systems Analysis Guidelines, U.S. Department of Energy, Office of Fossil Energy,

National Energy Technology Laboratory, April 2005 were used along with the assumptions contained in the EPRI reports, Holt, N., Updated Cost and Performance Estimates for Fossil Fuel Power Plants with CO_2 Removal, EPRI Report to DOE-NETL No. 1004483, December (2002), U.S.DOE/NETL, Pittsburgh and Holt, N., Evaluation of Innovative Fossil Fuel Power Plants with CO_2 Removal, EPRI Report to DOE-NETL No. 1000316, December (2000), U.S. DOE/NETL, Pittsburgh, Pa. The specific assumption listed in Table 1 are used in the examples and may differ from such guidelines.

Tables 4, 5 and 6 present the key streams for processes shown in FIGS. **3**, **5** and **4**, respectively. The performance comparison for the three cases is summarized in Table 7.

TABLE 1

Process Assumptions
1. IL # 6 Coal
2. ASU oxygen purity: 95%
3. Pressure with BGL Gasifier: 400 psig
4. Pressure with E-gas Gasifier: 800 psig
5. Sulfur removal using wet-FGD
6. Supercritical steam cycle with double reheat: 4050 psia, 1080° F./1111° F./1111° F.
7. CO_2 compressed to 2204 psia
8. Air-leak to the boiler: 1% of the flue gas

As to the design of the oxygen transport membrane system **28** within oxygen transport membrane boiler **26**, for a given size boiler, the surface area and the number of the oxygen transport membrane tubes, such as oxygen transport membrane tubes **50** of FIG. **2**, that will be required depends on the oxygen flux per unit area of a tube and the length and diameter of a single tube. By way of example, in order to design an oxygen transport membrane boiler **26** that produces net electric power of about 500 MWe, the amount of coal can be computed. For 500 MWe, 4838 tpd of Illinois number 6 coal will be required. Then, using any of a number of known programs that will simulate the operation of a gasifier, the amount of synthesis gas that will be produced can also be calculated along with the amount of oxygen that will be required. Once the amount of synthesis gas produced from the gasifier is known, a calculation can be formed as to the amount of oxygen required for complete combustion. Assuming only 70% of the oxygen in the feed air will be transferred through the oxygen transport membrane tube, and further assuming that there will be about 0.2 and about 0.4 mol percent of oxygen left in the flue gas. From this the actual amount of oxygen and the amount of feed air that will be required can also be computed. Once the amount of oxygen needed to be transferred through the oxygen transport membrane tube is known the required surface area of the oxygen transport membrane tubes can be calculated provided that the amount of oxygen flux through the oxygen transport membrane tube is known. An assumed oxygen flux for exemplary purposes is about 20 scf/ft^2/hr. The exact oxygen flux would of course depend upon membrane material performance. Hence, for low oxygen flux systems, a greater membrane area will be required to achieve the exemplary results set forth below. This would increase capital costs but not decrease efficiency. Using this flux, the surface area requirements can be calculated and samples of such calculation are shown in Table 2 below.

TABLE 2

Example No.	O_2 Requirement (tpd)	O_2 Requirement (MM scf/hr)	O_2 Flux From OTM Tubes Scf/ft^2/hr	OTM Tube Surface (ft^2)
1	7051	6.97	20	348395.8
2	7051	6.97	20	348395.8
3	6335	6.26	20	312979.2

The actual number of oxygen transport membrane tubes will depend on the outer diameter and the length of the tubes. Based on two different tube lengths, the required numbers of tubes for the three examples are given in Table 3.

TABLE 3

Example No.	No of OTM Tubes (OD = 1 inch Length = 5 ft.)	No. of OTM Tubes (OD = 1 inch Length = 20 ft.)
1	266048	66512
2	266048	66512
3	239002	59751

TABLE 4

(See FIG. 3):

Parameters/ Components	Units	IL No. 6 Coal (St. 10)	O_2 to Gasifier (St. 14)	Steam to Gasifier (St. 91)	Feed Air to OTM-Sys (St. 30)	O_2 Depleted Air (St. 35)	Fuel Gas to OTM POX (St. 24)	Fuel Gas to Expander (St. 166)	Fuel Gas to OTM Boiler (Exiting 168)	Flue Gas to FGD (St. 136)	Crude CO_2 to Drying & Comp. (St. 140)	CO_2 to EOR or Seq. Site (St. 154)
Temp.	F.	77.0	254.0	600.0	77.0	215.0	1000.0	1799.8	705.2	163.3	154.0	110.0
Pressure	psia	414.7	500.0	514.7	14.7	14.7	410.0	410.0	16.0	14.8	14.7	2204.6
Molar Flow	MMscfd		65.2		1150.0	982.8	345.7	376.5	376.5	314.6	270.2	208.2
Mass Flow	klb/hr	403.2	230.6	120.9	3656.6	3069.0	763.4	820.0	820.0	1208.6	1105.5	982.7
Hydrogen	mol %						25.53	32.62	32.62	0.00	0.00	0.00
CO	"						46.96	40.96	40.96	0.00	0.00	0.00
CO2	"						2.93	9.30	9.30	61.37	71.47	92.75
Nitrogen	"		1.40		78.17	91.47	2.80	2.70	2.70	3.88	4.52	5.86
Argon	"		3.60		0.93	1.09	0.68	0.63	0.63	0.75	0.87	1.13
Methane	"						3.88	1.02	1.02	0.00	0.00	0.00
Ethane	"						0.12	0.00	0.00	0.00	0.00	0.00
Propane	"						0.09	0.00	0.00	0.00	0.00	0.00
n-Butane	"						0.07	0.00	0.00	0.00	0.00	0.00
Phenols	"						0.06	0.00	0.00	0.00	0.00	0.00
Naphtha	"						0.07	0.00	0.00	0.00	0.00	0.00

TABLE 4-continued

(See FIG. 3):

Parameters/ Components	Units	IL No. 6 Coal (St. 10)	O_2 to Gasifier (St. 14)	Steam to Gasifier (St. 91)	Feed Air to OTM-Sys (St. 30)	O_2 Depleted Air (St. 35)	Fuel Gas to OTM POX (St. 24)	Fuel Gas to Expander (St. 166)	Fuel Gas to OTM Boiler (Exiting 168)	Flue Gas to FGD (St. 136)	Crude CO_2 to Drying & Comp. (St. 140)	CO_2 to EOR or Seq. Site (St. 154)
H2O	"			100.00			15.60	11.91	11.91	32.83	22.94	0.00
H2S	"						0.77	0.76	0.76	0.00	0.00	0.00
COS	"						0.06	0.00	0.00	0.00	0.00	0.00
SO2	"						0.00	0.00	0.00	0.91	0.00	0.00
NH3	"						0.25	0.01	0.01	0.00	0.00	0.00
HCN	"						0.06	0.00	0.00	0.00	0.00	0.00
HCl	"						0.09	0.08	0.08	0.09	0.00	0.00
Oxygen	"		95.00		20.90	7.44	0.00	0.00	0.00	0.17	0.19	0.25

TABLE 5

(See FIG. 5):

Parameters/ Components	Units	IL No. 6 Coal (St. 10)	O_2 to Gasifier (St. 14)	Steam to Gasifier (St. 91)	Feed Air to OTM-Sys (St. 30)	O_2 Depleted Air (St. 35)	Fuel Gas to OTM POX (St. 24)	Fuel Gas to Expander-1 (Exiting 180)
Temp.	F.	77.0	254.0	600.0	77.0	215.0	1000.0	1799.8
Pressure	psia	414.7	500.0	514.7	14.7	15.0	410.0	410.0
Molar Flow	MMscfd		65.2		1150.0	982.7	345.7	376.5
Mass Flow	klb/hr	403.2	230.6	120.9	3656.6	3068.8	763.4	820.0
Hydrogen	mol %						25.53	32.62
CO	"						46.96	40.96
CO2	"						2.93	9.30
Nitrogen	"		1.40		78.17	91.47	2.80	2.70
Argon	"		3.60		0.93	1.09	0.68	0.63
Methane	"						3.88	1.02
Ethane	"						0.12	0.00
Propane	"						0.09	0.00
n-Butane	"						0.07	0.00
Phenols	"						0.06	0.00
Naphtha	"						0.07	0.00
H2O	"			100.00			15.60	11.91
H2S	"						0.77	0.76
COS	"						0.06	0.00
SO2	"						0.00	0.00
NH3	"						0.25	0.01
HCN	"						0.06	0.00
HCl	"						0.09	0.08
Oxygen	"		95.00		20.90	7.43	0.00	0.00

Parameters/ Components	Fuel Gas to OTM POX-2 (Exiting 182)	Fuel Gas to Expander-2 (Exiting 186)	Fuel Gas to OTM Boiler (Exiting 188)	Flue Gas to FGD (St. 136)	Crude CO_2 to Drying & Comp. (St. 140)	CO_2 to EOR or Seq. Site (St. 154)
Temp.	1199.9	1802.6	1134.6	163.3	154.0	110.0
Pressure	90.0	90.0	16.0	14.8	14.7	2204.6
Molar Flow	376.5	384.0	384.0	314.7	270.2	208.2
Mass Flow	820.0	856.4	856.4	1208.8	1105.7	982.9
Hydrogen	32.62	31.41	31.41	0.00	0.00	0.00
CO	40.96	39.24	39.24	0.00	0.00	0.00
CO2	9.30	11.01	11.01	61.36	71.46	92.72
Nitrogen	2.70	2.66	2.66	3.88	4.52	5.86
Argon	0.63	0.61	0.61	0.75	0.87	1.13
Methane	1.02	0.03	0.03	0.00	0.00	0.00
Ethane	0.00	0.00	0.00	0.00	0.00	0.00
Propane	0.00	0.00	0.00	0.00	0.00	0.00
n-Butane	0.00	0.00	0.00	0.00	0.00	0.00
Phenols	0.00	0.00	0.00	0.00	0.00	0.00
Naphtha	0.00	0.00	0.00	0.00	0.00	0.00
H2O	11.91	14.21	14.21	32.83	22.94	0.00
H2S	0.76	0.75	0.75	0.00	0.00	0.00
COS	0.00	0.00	0.00	0.00	0.00	0.00
SO2	0.00	0.00	0.00	0.91	0.00	0.00

TABLE 5-continued

	(See FIG. 5):					
NH3	0.01	0.00	0.00	0.00	0.00	0.00
HCN	0.00	0.00	0.00	0.00	0.00	0.00
HCl	0.08	0.08	0.08	0.09	0.00	0.00
Oxygen	0.00	0.00	0.00	0.18	0.22	0.28

TABLE 6

(See FIG. 4):

Parameters/ Components	Units	IL No. 6 Coal (St. 10)	O_2 to Gasifier (St. 14)	Feed Air to OTM-Sys (St. 30)	O_2 Depleted Air (St. 35)	Raw Syngas from 12" (St. 20)	Fuel Gas to OTM POX (St. 24)	Fuel Gas to Expander (St. 166)	Fuel Gas to OTM Boiler (Exiting 168)	Flue Gas to FGD (St. 136)	Crude CO_2 to Drying & Comp. (St. 140)	CO_2 to EOR or Seq. Site (St. 154)
Temp.	F.	77.0	274.2	77.0	215.0	1850.0	996.6	1801.5	590.9	163.3	154.0	110.0
Pressure	psia	814.7	978.0	14.7	15.0	810.0	800.0	800.0	16.0	14.8	14.7	2204.6
Molar Flow	MMscfd		82.7	1025.0	874.8	367.8	367.8	364.9	364.9	303.6	260.6	200.8
Mass Flow	klb/hr	403.2	292.7	3259.1	2731.2	802.4	802.4	839.3	839.3	1177.5	1077.4	958.9
Hydrogen	mol %					32.74	32.74	28.78	28.78	0.00	0.00	0.00
CO	"					40.65	40.65	37.80	37.80	0.00	0.00	0.00
CO2	"					10.20	10.20	13.01	13.01	63.26	73.70	95.65
Nitrogen	"		1.40	78.17	91.60	0.76	0.76	0.91	0.91	1.75	2.04	2.65
Argon	"		3.60	0.93	1.09	0.81	0.81	0.81	0.81	0.98	1.14	1.48
Methane	"					1.29	1.29	1.82	1.82	0.00	0.00	0.00
Ethane	"					0.00	0.00	0.00	0.00	0.00	0.00	0.00
Propane	"					0.00	0.00	0.00	0.00	0.00	0.00	0.00
n-Butane	"					0.00	0.00	0.00	0.00	0.00	0.00	0.00
Phenols	"					0.00	0.00	0.00	0.00	0.00	0.00	0.00
Naphtha	"					0.00	0.00	0.00	0.00	0.00	0.00	0.00
H2O	"					12.41	12.41	16.00	16.00	32.83	22.95	0.00
H2S	"					0.74	0.74	0.78	0.78	0.00	0.00	0.00
COS	"					0.03	0.03	0.00	0.00	0.00	0.00	0.00
SO2	"					0.00	0.00	0.00	0.00	0.94	0.00	0.00
NH3	"					0.23	0.23	0.01	0.01	0.00	0.00	0.00
HCN	"					0.06	0.06	0.00	0.00	0.00	0.00	0.00
HCl	"					0.08	0.08	0.08	0.08	0.10	0.00	0.00
Oxygen	"		95.00	20.90	7.31	0.00	0.00	0.00	0.00	0.14	0.17	0.22

TABLE 7

Parameters	Units	Example 1 BGL with 1 OTM-POX FIG. 3	Example 2 BGL with 2 OTM POX FIG. 5	Example 3 E-Gas with 1 OTM-POX FIG. 4
Coal Feed	tpd	4,838	4,838	4,838
Heat Input as Coal (HHV)	MMbtu/hr	4,703	4,703	4,703
Heat Input as Coal (LHV)	MMbtu/hr	4,486	4,486	4,486
Gross Power Summary				
Steam Turbine	MW	514.3	500.0	506.0
Fuel Gas Expander-1	MW	111.4	62.8	123.5
Fuel Gas Expander-2	MW	0.0	71.2	
Generator Loss	MW	6.3	6.3	6.3
Gross Plant Power	MW	619.4	627.7	623.2
Power Consumptions				
ASU	MW	35.0	35.0	58.0
CO2 Capture & Compression	MW	51.4	51.4	49.2
Air Blowers	MW	22.5	22.5	20.0
Other Plant Aux.	MW	21.0	21.0	29.9
Total Auxillary Power	MW	129.9	129.9	157.1
Net Power	MW	489.5	497.8	466.1
HHV Efficiency	%	35.5	36.1	33.8
LHV Efficiency	%	37.2	37.9	35.5

As is apparent from Table 7, the embodiment of FIG. **5** provided the most net power and was also the most efficient.

While the present invention has been described to a preferred embodiment, as will be understood by those skilled in the art, numerous changes and omissions can be made without departing from the spirit and the scope of the present invention which is set forth in the presently pending claims.

We claim:

1. A method of generating electrical power comprising:

generating a synthesis gas stream in a gasifier;

partially oxidizing the synthesis gas stream in at least one partial oxidation stage to oxidize a volatile content of the synthesis gas stream and to heat the synthesis gas stream, the at least one partial oxidation stage formed by an oxygen transport membrane reactor generating oxygen to support the partial oxidation of the synthesis gas stream;

expanding the synthesis gas stream in an expander of at least one expansion stage after having been heated in the at least one partial oxidation stage and generating electrical power from a generator coupled to the expander;

combusting the synthesis gas stream, after having been expanded, within an oxygen transport membrane boiler to generate heat and a flue gas, the synthesis gas stream being combusted while at an elevated temperature;

the flue gas containing carbon dioxide;

the combusting of the synthesis gas stream supported by separating additional oxygen from an oxygen containing stream within an oxygen transport membrane system operatively associated with a boiler within the oxygen transport membrane boiler;

producing steam within the boiler by indirectly transferring the heat to boiler feed water;

extracting energy from the steam by a steam turbine system of a steam cycle operatively associated with the oxygen transport membrane boiler and converting the energy to additional electrical power by an additional electrical generator coupled to the steam turbine system; and

purifying the flue gas stream to produce a carbon dioxide-rich stream.

2. The method of claim **1**, wherein the at least one expansion stage and the at least one partial oxidation stage is a first partial oxidation stage followed by a first expansion stage, a second partial oxidation stage following the first expansion stage and a second expansion stage following the second partial oxidation stage.

3. The method of claim **1**, wherein:

the combusting of the synthesis gas stream is incomplete resulting in fuel species being present within the flue gas stream; and

the fuel species are separated from the flue gas stream and recycled to the at least one partial oxidation stage.

4. The method of claim **1** or claim **2** or claim **3**, wherein the carbon dioxide is purified by:

cooling the flue gas stream to produce a cooled flue gas stream;

removing sulfur dioxide from the cooled flue gas stream;

after removing the sulfur dioxide from the flue gas stream, compressing the flue gas stream and then drying the flue gas stream in a dryer to produce a carbon dioxide containing stream having a purity of no less than about 90% by volume; and

further compressing the carbon dioxide containing stream to produce a carbon dioxide product stream.

5. The method of claim **3**, wherein:

the combusting of the synthesis gas stream is incomplete resulting in fuel species being present within the flue gas stream;

the carbon dioxide is purified by: cooling the flue gas stream to produce a cooled flue gas stream;

removing sulfur dioxide from the cooled flue gas stream;

after removing the sulfur dioxide from the flue gas stream, compressing the flue gas stream and then drying the flue gas stream in a dryer to produce a carbon dioxide containing stream having a purity of no less than about 90% by volume;

further compressing the carbon dioxide containing stream to produce a carbon dioxide product stream; and

the fuel species are separated from the flue gas stream after having been dried and prior to having been further compressed and recycled to the at least one partial oxidation stage.

6. The method of claim **4**, wherein the gasifier generates the synthesis gas stream through gasification of coal supported by further oxygen.

7. The method of claim **6**, wherein the gasification of the coal is conducted in a moving bed gasifier utilizing steam generated by the steam cycle.

8. The method of claim **4**, wherein the steam cycle is an ultra-supercritical steam cycle.

9. The method of claim **1**, wherein the gasifier generates the synthesis gas stream through gasification of coal supported by oxygen.

10. The method of claim **9**, wherein the gasification of the coal is conducted in a moving bed gasifier utilizing steam generated by the steam cycle.

11. The method of claim **10**, wherein the steam cycle is an ultra-supercritical steam cycle.

12. The method of claim **1**, wherein:

the gasifier is an entrained flow gasifier;

the synthesis gas stream is cooled by indirect heat exchange with a heated boiler feed water stream to produce a steam stream; and

the steam stream is combined with steam produced within the boiler.

13. The method of claim **1**, wherein:

the combustion of the synthesis gas stream supported by separating the additional oxygen from an oxygen containing stream within an oxygen transport membrane system is not complete; and

the combustion of the synthesis gas stream is completed by addition of an additional oxygen containing stream.

* * * * *

(12) **United States Patent**
Shah et al.

(10) **Patent No.: US 8,196,387 B2**
(45) **Date of Patent: Jun. 12, 2012**

(54) **ELECTRICAL POWER GENERATION APPARATUS**

(75) Inventors: **Minish Mahendra Shah**, E. Amherst, NY (US); **Aqil Jamal**, Grand Island, NY (US); **Raymond Francis Dmevich**, Clarence Center, NY (US); **Bart Antonie van Hassel**, Getzville, NY (US); **Gervase Maxwell Christie**, Buffalo, NY (US); **Hisashi Kobayashi**, Putnam Valley, NY (US); **Lawrence E. Bool, III**, E. Aurora, NY (US)

(73) Assignee: **Praxair Technology, Inc.**, Danbury, CT (US)

(*) Notice: Subject to any disclaimer, the term of this patent is extended or adjusted under 35 U.S.C. 154(b) by 104 days.

(21) Appl. No.: **12/948,128**

(22) Filed: **Nov. 17, 2010**

(65) **Prior Publication Data**

US 2011/0061361 A1 Mar. 17, 2011

Related U.S. Application Data

(63) Continuation of application No. 11/639,459, filed on Dec. 15, 2006, now Pat. No. 7,856,829.

(51) **Int. Cl.**
F02C 3/26 (2006.01)

(52) **U.S. Cl.** **60/39.464**; 60/780

(58) **Field of Classification Search** 60/780, 60/781, 39.182, 39.461, 39.464, 39.465, 60/39.47, 39.12

See application file for complete search history.

(56) **References Cited**

U.S. PATENT DOCUMENTS

4,261,167	A *	4/1981	Paull et al.	60/781
5,820,654	A	10/1998	Gottzman et al.	
5,820,655	A	10/1998	Gottzmann et al.	
5,927,103	A	7/1999	Howard	
5,964,922	A	10/1999	Keskar et al.	
6,035,662	A	3/2000	Howard et al.	
6,070,471	A	6/2000	Westphal et al.	
6,139,810	A	10/2000	Gottzmann et al.	
6,382,958	B1	5/2002	Bool, III et al.	

FOREIGN PATENT DOCUMENTS

DE	10330859	A1	2/2004
DE	102004038435	A1	2/2006
EP	1717420	A1	11/2006
GB	713553		11/1951

OTHER PUBLICATIONS

Babcock & Wilcox, Steam 40, "Sulfur Dioxide Control" (1992).
Okawa et al., Trial Design of a CO_2 Recovery Power Plant by Burning Pulverized Coal in O_2/CO_2, Energy Convers. Mgmt., vol. 38, Supplemental (1997) pp. S123-S127.

(Continued)

Primary Examiner — Ehud Gartenberg
Assistant Examiner — Andrew Nguyen
(74) *Attorney, Agent, or Firm* — David M. Rosenblum

(57) **ABSTRACT**

An apparatus for generating electrical power in which a synthesis gas stream generated in a gasifier is partially oxidized, expanded and thereafter, is combusted in an oxygen transport membrane system of a boiler. The combustion generates heat to raise steam to in turn generate electricity by a generator coupled to a steam turbine. The resultant flue gas can be purified to produce a carbon dioxide product.

17 Claims, 8 Drawing Sheets

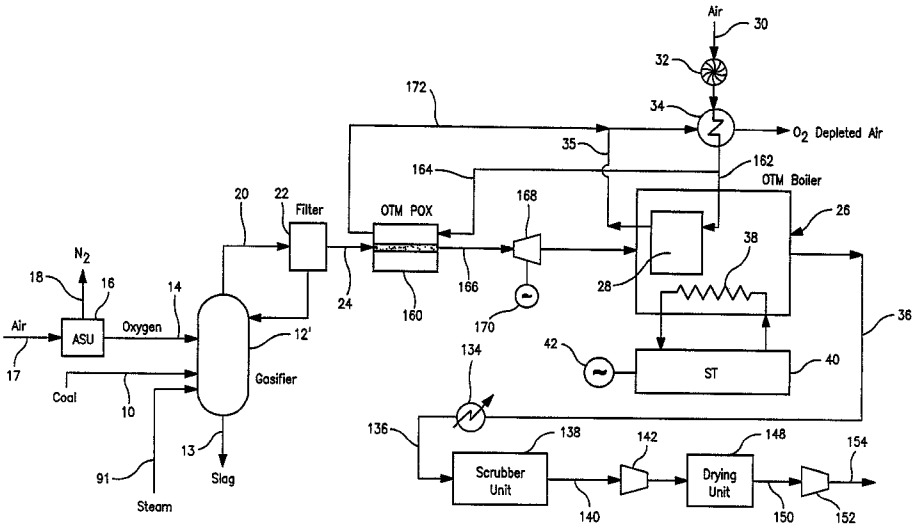

OTHER PUBLICATIONS

U.S. Department of Energ —Office of Fossil energy and U.S. Department of Energy/NETL, "Evaluation of Innovative Fossil Fuel Power Plants with C_2 Removal", Interim Report (2000).

Dyer et al., "Ion Transport Membrane Technology for Oxygen Separation and Syngas Production", Solid State Ionics 134 (2000) p. 21-33.

U.S. Department of Energy, "Evaluation of Fossil Fuel Power Plants with CO_2 Recovery", Final Report (2002).

Holt, "Gasification Process Selection—Trade-offs and Ironies", Presented at the Gasification Technologies Conference (2004).

Switzer et al., "Cost and Feasibility Study on the Praxair Advanced Boiler for the CO_2 Capture Project's Refinery Scenario", Carbon Dioxide Capture for Deep Geologic Formations—Results from the CO_2 Capture Project, vol. 2, Elsevier Science Publishing Company (2005) pp. 1-26.

Radtke et al., "Renaissance of Gasification based on Cutting Edge Technologies", VGB PowerTech (2005).

* cited by examiner

U.S. Patent Jun. 12, 2012 Sheet 1 of 8 US 8,196,387 B2

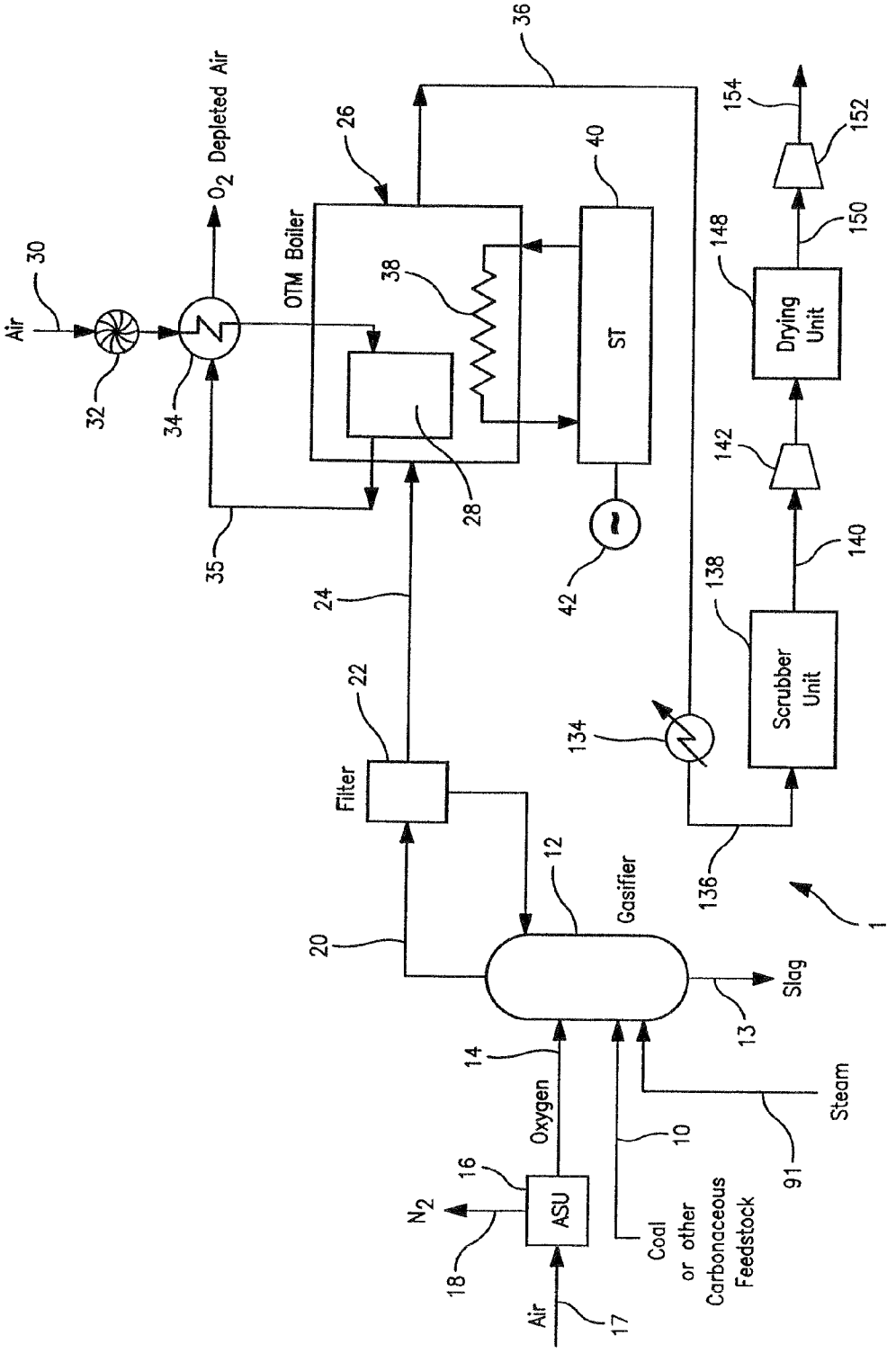

FIG. 1

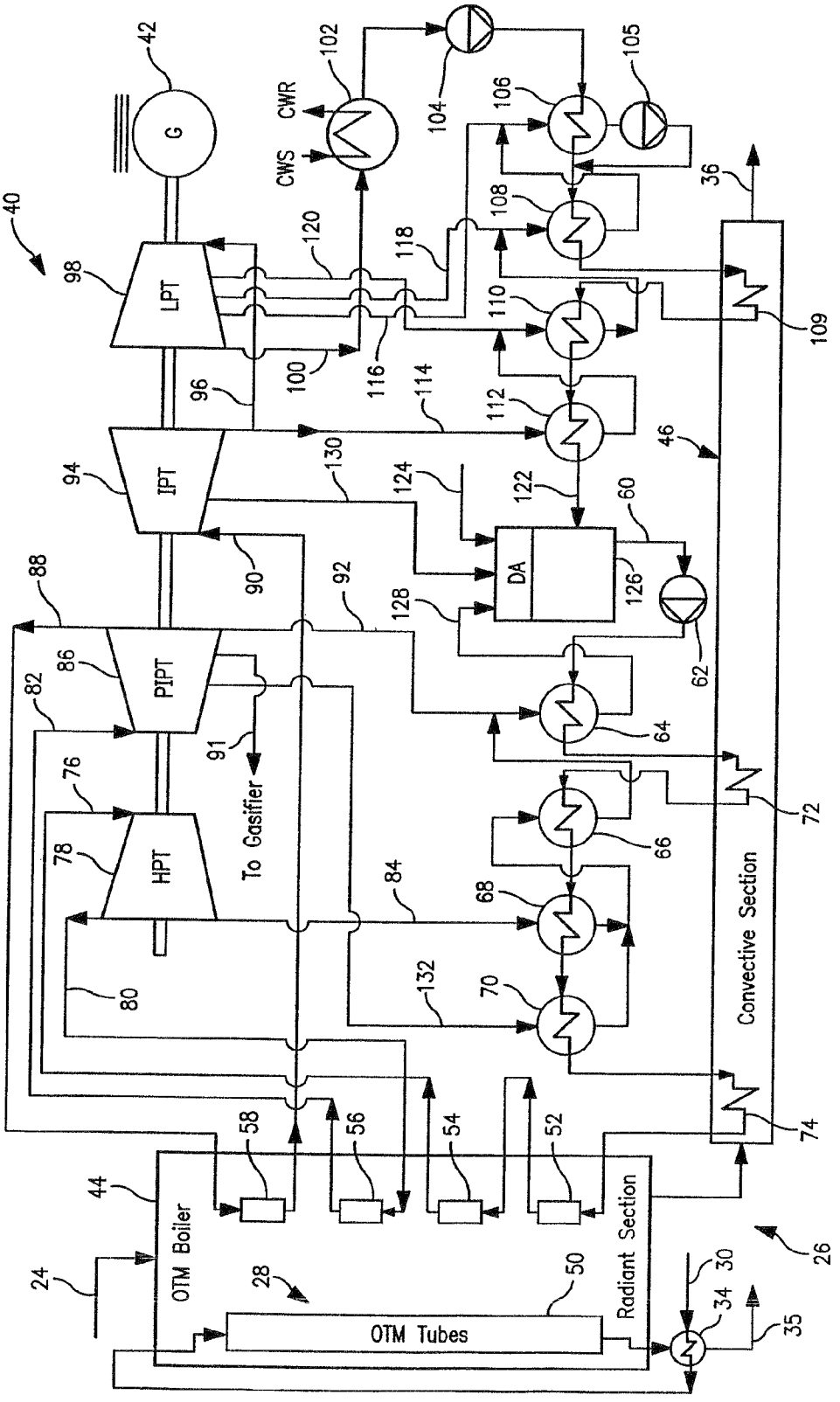
G
LPT
IPT
PIPT
HPT
DA
To Gasifier
OTM Boiler
OTM Tubes
Radiant Section
Convective Section
CWS
CWR
40
42
44
46
24
26
28
30
34
35
36
50
52
54
56
58
60
62
64
66
68
70
72
74
76
78
80
82
84
86
88
90
91
92
94
96
98
100
102
104
105
106
108
109
110
112
114
116
118
120
122
124
126
128
130
132

FIG. 2

U.S. Patent Jun. 12, 2012 Sheet 3 of 8 US 8,196,387 B2

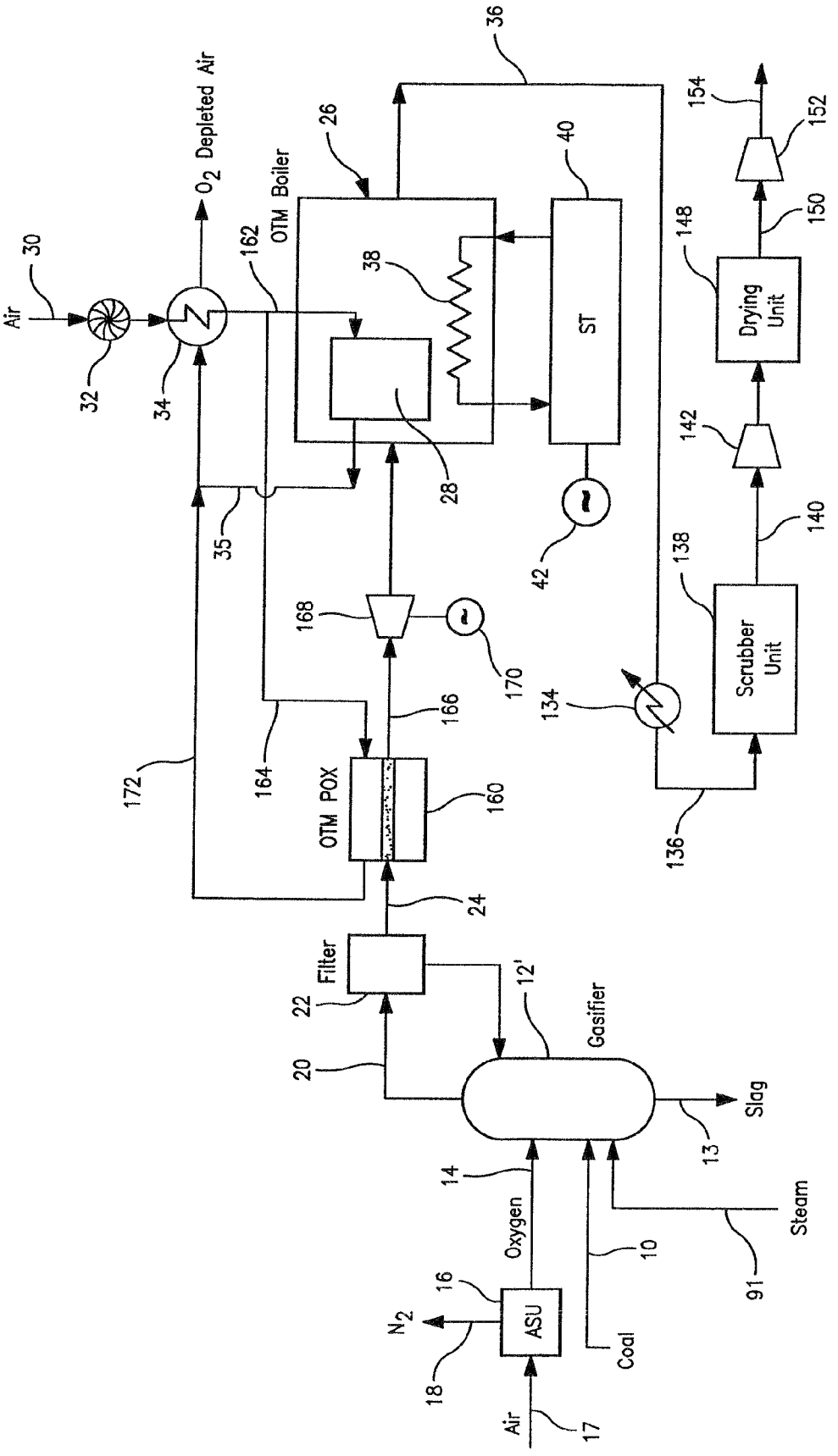

FIG. 3

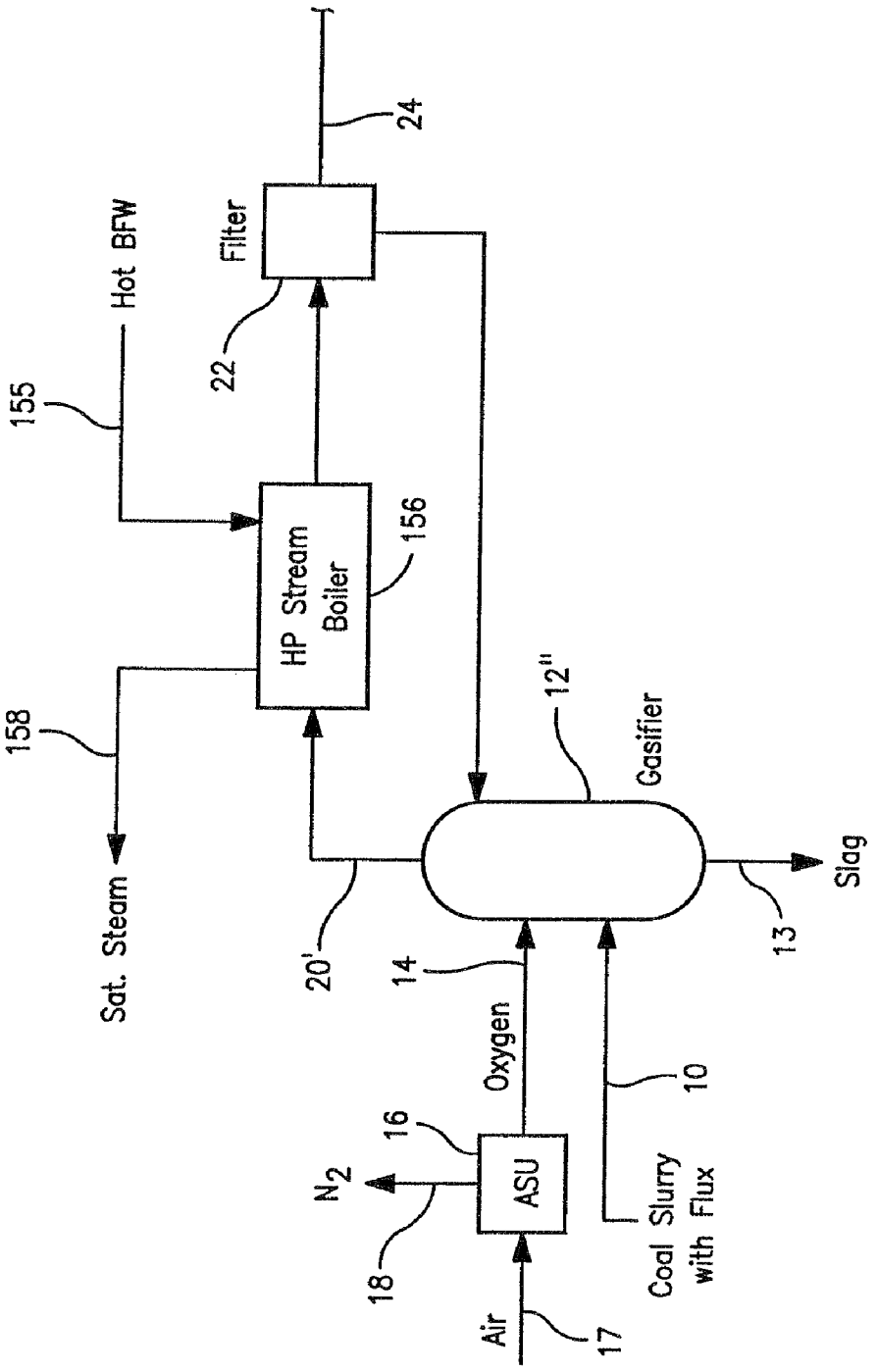
24
Filter
22
Hot BFW
155
HP Stream Boiler
156
158
Sat. Steam
12"
Gasifier
Slag
13
20'
14
Oxygen
10
16
N_2
ASU
Coal Slurry with Flux
18
Air
17

FIG. 4

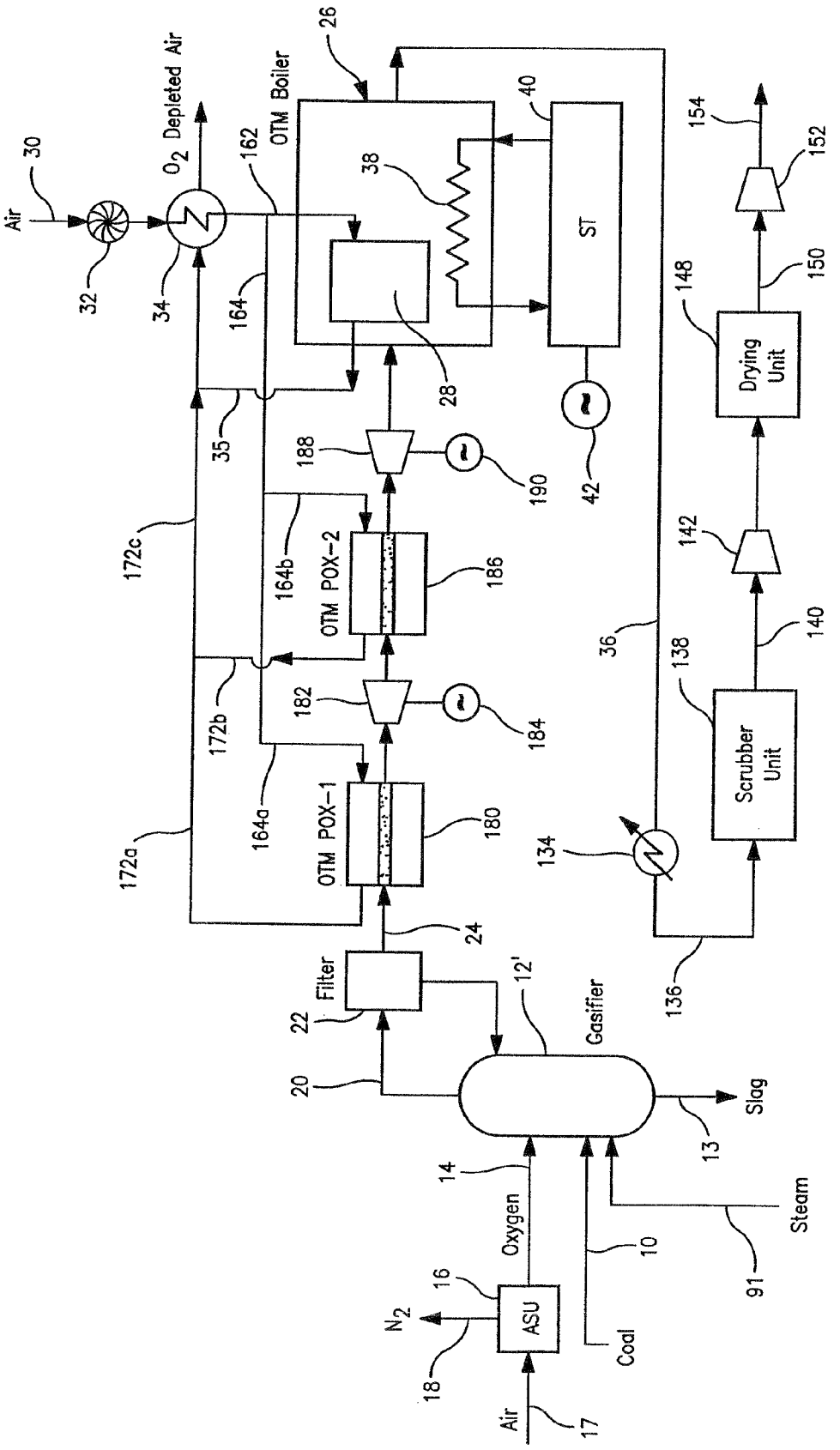
Air
30
32
34
O_2 Depleted Air
OTM Boiler
162
164
26
28
38
40
ST
42
35
188
190
172c
164b
OTM POX-2
186
172b
182
184
164a
OTM POX-1
180
172a
24
Filter
22
20
12'
Gasifier
Slag
13
14
Oxygen
16
N_2
ASU
18
Air
17
Coal
10
Steam
91
36
134
136
138
Scrubber Unit
140
142
Drying Unit
148
150
152
154

FIG. 5

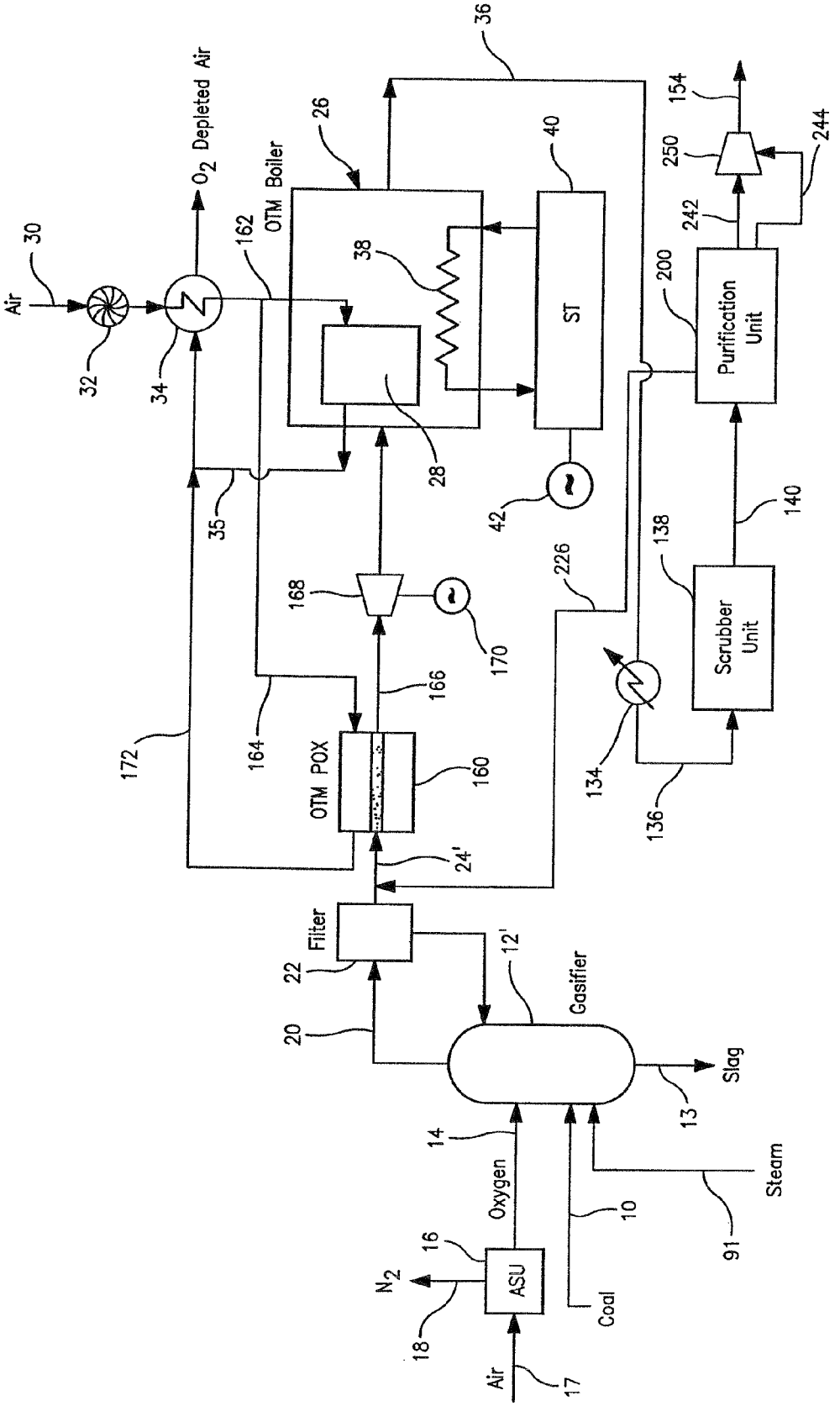
Air
30
32
34
O_2 Depleted Air
OTM Boiler
162
26
36
38
40
ST
28
42
35
154
250
244
242
200
Purification Unit
140
138
Scrubber Unit
226
168
170
166
164
172
OTM POX
160
134
136
24'
Filter
22
12'
Gasifier
20
Slag
13
14
Oxygen
Steam
91
10
16
N_2
ASU
Coal
18
Air
17

FIG. 6

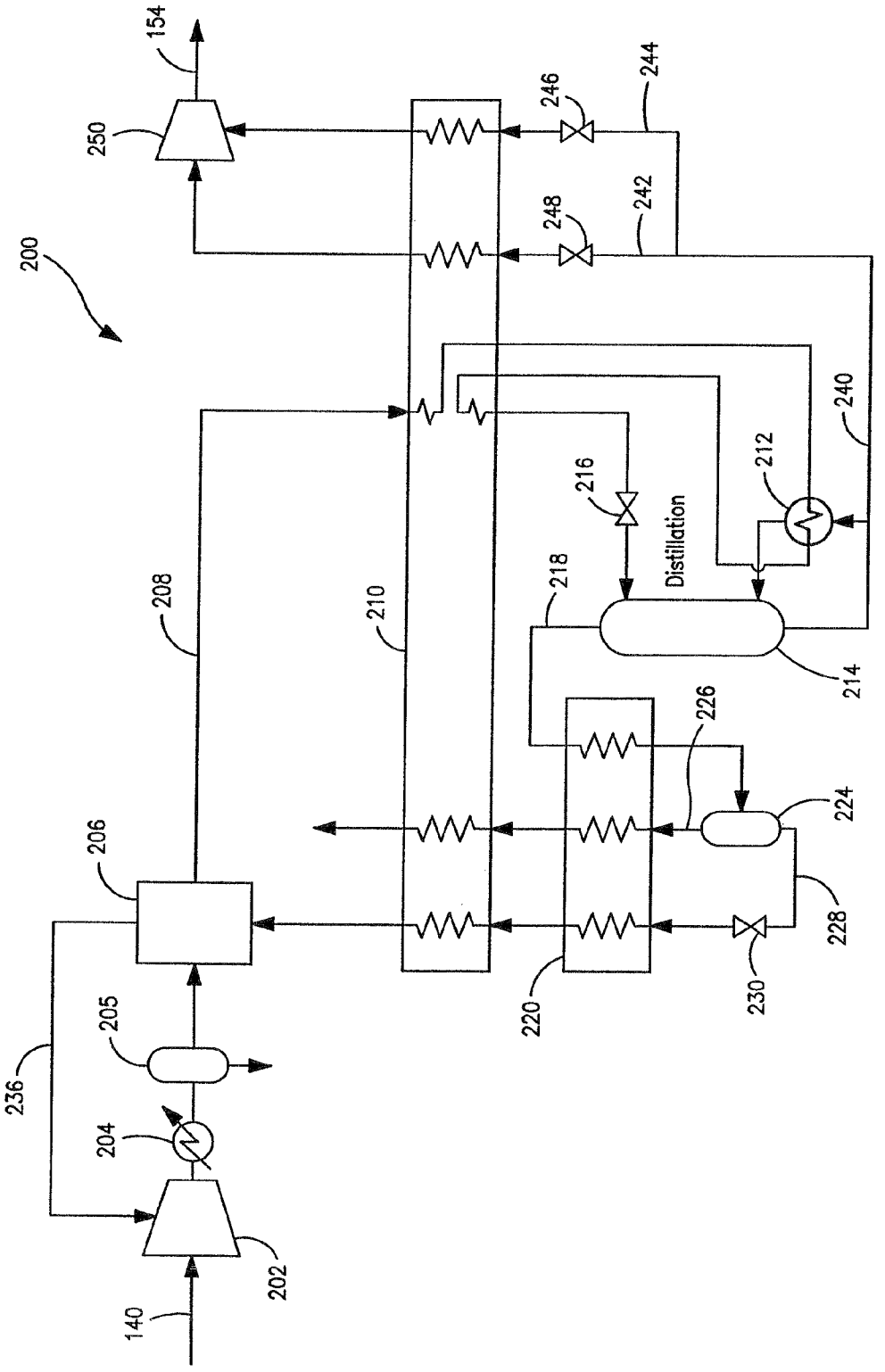
154
250
246
244
248
242
200
240
212
216
Distillation
218
208
210
214
226
224
206
228
205
230
220
236
204
202
140

FIG. 7

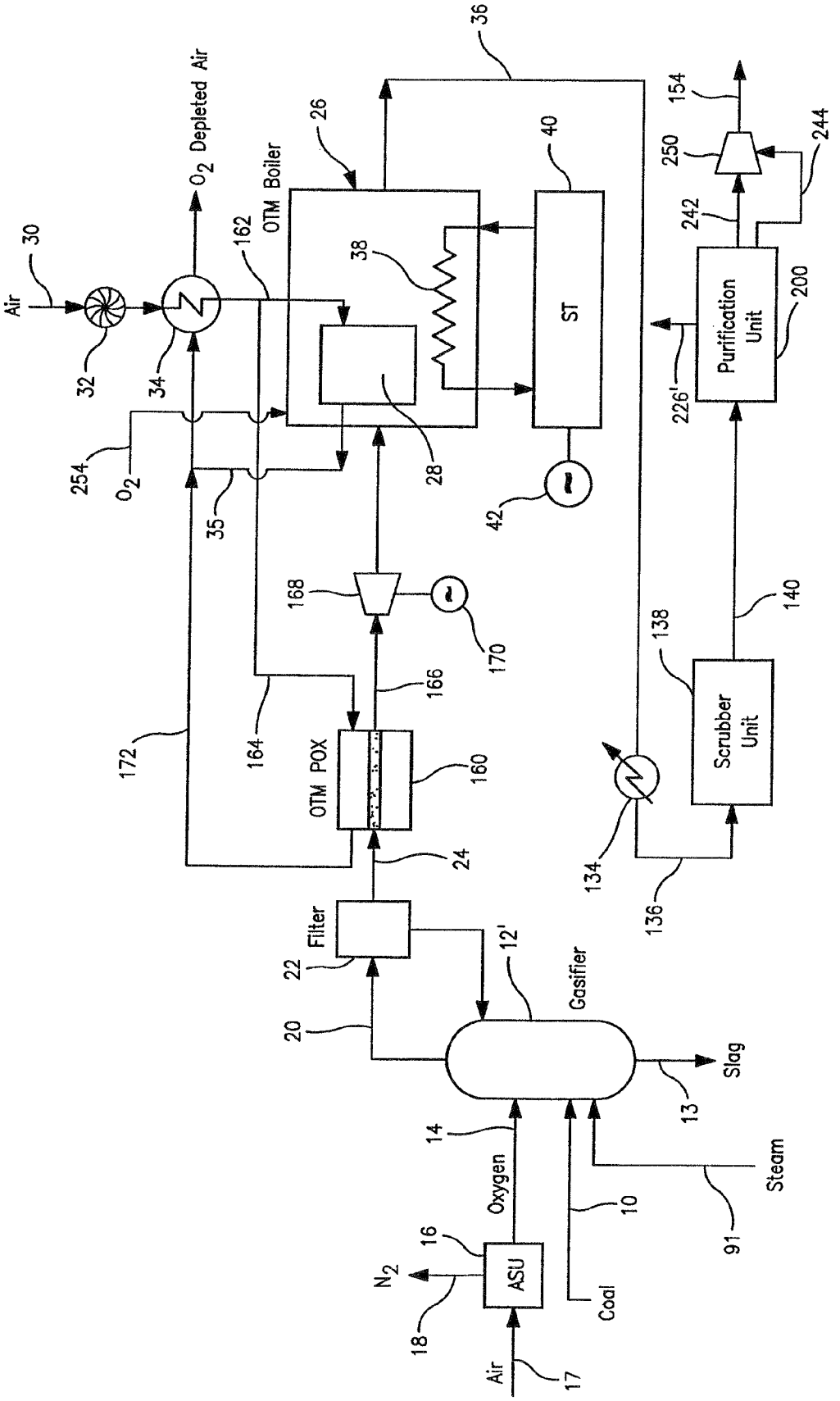
Air
30
32
34
O_2 Depleted Air
OTM Boiler
162
26
36
38
40
ST
28
42
254
O_2
35
168
170
166
164
172
OTM POX
160
24
Filter
22
20
12'
Gasifier
Slag
13
14
Oxygen
16
ASU
N_2
18
Air
17
Coal
10
Steam
91
154
250
244
242
Purification Unit
200
226'
138
Scrubber Unit
140
134
136

FIG. 8

ELECTRICAL POWER GENERATION APPARATUS

RELATED APPLICATION

This application is a continuation of prior U.S. application Ser. No. 11/639,459 filed Dec. 15, 2006 now U.S. Pat. No. 7,856,829.

FIELD OF THE INVENTION

The present invention relates to an apparatus for generating electrical power in which a synthesis gas stream, produced in a gasifier, is combusted to generate heat that is used to raise steam and that is in turn used in a steam turbine to generate electrical power. More particularly, the present invention relates to such an apparatus in which the synthesis gas stream is combusted in a boiler that employs an oxygen transport membrane to supply oxygen to support the combustion and that has provision for the purification of the resultant flue gases to produce a carbon dioxide-rich stream for further utilization or sequestration.

BACKGROUND OF THE INVENTION

Coal-fired power plants are utilized throughout the world to generate electricity. Typically, the coal is either in a pulverized form or within a slurry is combusted to generate heat within a boiler to raise steam. The steam is passed into a steam turbine to generate electrical power.

There has been recent interest in capturing carbon dioxide from power plants that use coal and other carbonaceous feed stock such as asphalt, heavy oil, petroleum coke, biomass or natural gas. An integrated gasification and combined cycle (IGCC) is proposed as a preferred method of power generation when carbon dioxide capture is required. In IGCC, gasification of fuel produces a synthesis gas containing mainly hydrogen, carbon monoxide and carbon dioxide with some amount of methane and sulfur and chloride containing impurities. In a typical gasifier the carbonaceous feed is reacted with steam and oxygen to produce the synthesis gas. Typically, the oxygen is provided to the gasifier by a cryogenic rectification plant in which air is rectified within distillation columns at low temperatures to produce the oxygen.

In an integrated gasification combined cycle, the synthesis gas produced as a result of the gasification is cooled to a temperature suitable for its further processing in a water-gas shift reactor to increase the hydrogen and carbon dioxide content of the synthesis gas. The water-gas shift reactor also hydrolyzes most of the carbonyl sulfide into hydrogen sulfide. The synthesis gas is then further cooled for carbon dioxide and hydrogen sulfide separation within a solvent scrubbing plant employing physical or chemical absorption for separation of the carbon dioxide and hydrogen sulfides and carbonyl sulfide from the synthesis gas. This allows for the capture and sequestration of the carbon dioxide which is present within the synthesis gas. The resulting hydrogen-rich gas is then fed to a gas turbine that is coupled to an electrical generator to generate electricity. Heat is recovered from the cooling of the raw synthesis gas stream, from cooling the heated discharge from the water-gas shift reactor, and cooling the exhaust from the gas turbine to raise steam and to generate additional electrical power from a steam turbine.

As can be appreciated, the integrated gasification combined cycle is environmentally very advantageous in that a clean burning synthesis gas stream is used to power the gas turbine while at the same time, the carbon dioxide produced by the gasification can be captured for use in other industrial processes, for enhanced oil recovery or for sequestration. The disadvantage of such a cycle is the high energy penalty associated with the air separation and solvent scrubbing plants. Additionally, the recovery of heat energy in several stages is inherently inefficient in that such heat recovery always involves loss and in any case, the heat is recovered at a low temperature. Lastly, the use of solvent scrubbing plants, water-gas shift reactors and gas turbines is an expensive proposition given their acquisition costs.

It has been suggested to supply the oxygen to the gasification process in lieu of a cryogenic air separation plant with the use of oxygen transport membranes. In such membranes, oxygen is separated from the air with the use of a gas tight membrane formed of the ceramic material that is capable of oxygen ion transport at elevated temperatures. The oxygen ionizes on one surface of the membrane by gaining electrons to form the oxygen ions. Under a driving force of a partial pressure differential, the oxygen ions pass through the membrane and either react with a fuel or recombine to elemental oxygen liberating the electrons used in the ionization of the oxygen.

Where the membrane material is a mixed conductor, the electrons are transported through the membrane. In a membrane that uses an ionic conductor, that is, capable only of conducting oxygen ions, the electrons are transported with the use of an external electric circuit.

The use of ceramic membrane systems have also been contemplated in connection with boilers to generate product steam that has value as a feed to a refinery or to a steam methane reformer as opposed to a combined cycle incorporating a steam turbine. In such boilers, the combustion of a fuel such as natural gas is supported by oxygen separated within the membrane system. Since such combustion will produce a flue gas rich in carbon dioxide and water, the production of a carbon dioxide-rich stream can be accomplished by condensing the water out of the flue gas and then compressing the stream.

An example of a study of such a boiler with carbon dioxide capture appears in a paper entitled, "Cost and Feasibility Study on the Praxair Advanced Boiler for CO_2 Capture Project's Refinery Scenario", Switzer et al. (2005) published by Elsevier. In this paper, a boiler is disclosed in which fuel and recirculated flue gas is passed through a housing having a heat recovery steam generator to exchange heat from a retentate produced by the membrane system with boiler feed water to raise saturated steam. The fuel and flue gas mixture then passes to the membrane system for combustion and generation of the flue gas. Intermingled with the membrane system is another heat recovery steam generator to superheat the saturated steam and thereby to produce the product steam. Heat is recovered from the flue gas to preheat the air and the boiler feed water. Other boiler designs that incorporate oxygen transport membranes and that are capable of producing product steam are disclosed in U.S. Pat. Nos. 6,394,043; 6,382,958 and 6,562,104.

As will be discussed, the present invention provides an apparatus for generating electrical power in which a synthesis gas stream is produced by gasification is then combusted in an oxygen transport membrane to generate heat and in turn raise steam for a steam turbine. As will become apparent, an apparatus of the present invention generates the power in a more thermally efficient manner than an integrated gasification combined cycle with carbon dioxide capture and does not require the use of expensive gas turbines, water-gas shift reactors and solvent recovery units for carbon dioxide capture.

SUMMARY OF THE INVENTION

The present invention provides an apparatus for generating electrical power. The apparatus has a gasifier for generating a synthesis gas stream. At least one partial oxidation stage is configured to partially oxidize the synthesis gas stream and thereby oxidize a volatile content of the synthesis gas stream and to heat the synthesis gas stream. The at least one partial oxidation stage has an oxygen transport membrane reactor configured to generate oxygen to support the partial oxidation of the synthesis gas stream. At least one expansion stage is provided having an expander for expanding the synthesis gas stream after having been heated in the at least one partial oxidation stage and a generator coupled to the expander for generating electrical power. An oxygen transport membrane boiler is in flow communication with the at least one expansion stage and is configured to generate: heat from combustion of the synthesis gas stream while at an elevated temperature; a flue gas containing carbon dioxide from the combustion of the synthesis gas stream; and steam through indirect heat transfer of the heat to boiler feed water. The oxygen transport membrane boiler has an oxygen transport membrane system operatively associated with a boiler. The oxygen transport membrane system is configured to separate additional oxygen from an oxygen containing stream and support the combustion of the synthesis gas stream with the additional oxygen and the boiler is configured to produce the steam by the indirect transfer of the heat to the boiler feed water. A steam cycle is operatively associated with the oxygen transport membrane boiler and has a steam turbine system to extract energy from the steam and an additional electrical generator is coupled to the steam turbine system to convert the energy to additional electrical power. A purification system is configured to purify the flue gas stream to produce a carbon dioxide-rich stream.

As is apparent from the above description of the invention, since the synthesis gas stream is combusted while at an elevated temperature, the method of the present invention does not have the built-in thermal inefficiency that can be found in prior art integrated gasification combined cycles with carbon dioxide capture. This thermal inefficiency is due to the fact that the carbon dioxide is removed from the synthesis gas in a solvent system that requires the synthesis gas to be cooled to near ambient temperatures and the energy input that is required to operate the solvent system. As will also be discussed, the flue gas stream can be directly purified in a manner that will be discussed in more detail below that does not involve the use of solvent scrubbing units.

The at least one partial oxidation stage can be a first partial oxidation stage and a second partial oxidation stage and the at least one expansion stage can be a first expansion stage and a second expansion stage. The first expansion stage is connected to the first partial oxidation stage, the second partial oxidation stage is connected to the first expansion stage, the second expansion stage is connected to the second partial oxidation stage and the oxygen transport membrane boiler is connected to the second expansion stage.

The apparatus can be designed such that combustion of the synthesis gas stream is incomplete resulting in fuel species being present within the flue gas stream. In such case, the purification system is configured to also separate the fuel species from the flue gas stream. The purification system is connected to the at least one partial oxidation stage such that the fuel species separated from the flue gas stream is recycled to the at least one partial oxidation stage.

In an embodiment of the present invention, the purification system can be provided with a water-cooler that is configured to cool the flue gas stream and thereby to produce a cooled flue gas stream. A flue gas desulphurization scrubber unit is connected to the water-cooler to remove sulfur dioxide from the cooled flue gas stream. A compressor connected to the sulfur dioxide removal unit to compress the flue gas stream and a drying unit connected to the compressor to produce a carbon dioxide containing stream having a purity of no less than about 90% by volume. Additionally, a further compressor is connected to the drying unit to further compress the carbon dioxide containing stream to produce a carbon dioxide product stream. In another embodiment, a purification unit is positioned between the flue gas desulphurization scrubber unit and the compressor. The purification unit is configured to separate the fuel species from the partly purified flue gas stream through distillation to produce the carbon dioxide containing stream having a purity of no less than about 90% by volume.

The gasifier can be configured to generate the synthesis gas stream through gasification of coal supported by further oxygen. The steam cycle can be configured to generate a steam stream and the gasifier can be a moving bed gasifier connected to the steam cycle to receive the steam stream. The steam cycle can be an ultra-supercritical steam cycle.

In any embodiment of the present invention, the gasifier can be configured to generate the synthesis gas stream through gasification of coal supported by an oxygen containing stream generated by an air separation unit.

The gasifier can be an entrained flow gasifier. Further, a high pressure steam boiler can be positioned between such gasifier and a filter configured to filter the synthesis gas stream produced by the gasifier. The high pressure steam boiler is configured to cool the synthesis gas stream through indirect heat exchange with a heated boiler feed water stream to produce a saturated steam stream and the high pressure steam boiler is connected to the boiler of the oxygen transport membrane boiler such that the steam stream is introduced into the boiler.

In any embodiment of the present invention, the oxygen transport membrane boiler can be provided with an inlet configured to receive an injected supplemental oxygen containing stream and to supply the injected supplemental oxygen containing stream to help support the combustion of the synthesis gas stream. However, where the supplemental oxygen containing stream is used, the purification system can be of the type, discussed above, that is provided with a water-cooler configured to cool the flue gas stream and thereby to produce a cooled flue gas stream and a flue gas desulphurization scrubber unit connected to the water-cooler to remove sulfur dioxide from the cooled flue gas stream and thereby produce a partly purified flue gas stream. A purification unit is configured to separate inerts from the partly purified flue gas stream through distillation and thereby to produce a carbon dioxide containing stream having a purity of no less than about 90% by volume and a product compressor connected to the purification unit to compress the carbon dioxide containing stream and thereby produce a carbon dioxide product stream. Further, the gasifier can be configured to generate the synthesis gas stream through gasification of coal supported by an oxygen containing stream generated by an air separation unit. The steam cycle can be configured to generate a steam stream and the gasifier can be a moving bed gasifier connected to the steam cycle to receive the steam stream. The steam cycle utilized can be an ultra-supercritical steam cycle.

BRIEF DESCRIPTION OF THE DRAWINGS

While the specification concludes with claims distinctly pointing out the subject matter that Applicants regard as their

invention, it is believed that the invention will be better understood when taken in connection with the accompanying drawings in which:

FIG. **1** is a process flow diagram of an apparatus for carrying out a method for generating electrical power in accordance with the present invention;

FIG. **2** is a schematic of a boiler incorporating an oxygen transport membrane system integrated with a steam cycle;

FIG. **3** is an alternative embodiment of FIG. **1**;

FIG. **4** is a fragmentary view of an alternative embodiment of FIG. **3**;

FIG. **5** is an alternative embodiment of FIG. **3**;

FIG. **6** is an alternative embodiment of FIG. **3**;

FIG. **7** is an embodiment of the purification unit used in FIG. **6**; and

FIG. **8** is an alternative embodiment of FIG. **6**.

DETAILED DESCRIPTION

With reference to FIG. **1**, the present invention illustrates an apparatus **1** for carrying out a method in accordance with the present invention in which coal is gasified. This is for exemplary purposes because as indicated above, feed stock to be gasified could be other substances such as coal, asphalt, heavy oil, petroleum coke, biomass or natural gas.

In accordance with FIG. **1**, a prepared coal feed stream **10** is gasified within a gasifier **12** with the addition of a gasifying agent such as an oxygen stream **14**. Oxygen stream **14** is created by the cryogenic rectification of air within a cryogenic rectification unit **16**. In some gasifiers such as moving bed gasifiers high pressure steam as a steam stream **91**, to be discussed, is also injected into the gasifier.

Cryogenic rectification unit **16** ("ASU") consists of a compressor to compress an air stream **17** and a purifier to remove the higher boiling contaminants such as carbon dioxide, water and hydrocarbons. The resultant purified and compressed stream is then cooled within a main heat exchanger against return streams consisting of the fractionated components of the air, namely, nitrogen and oxygen. The oxygen is discharged as oxygen stream **14** and the nitrogen is discharged as a nitrogen stream **18**. If necessary, the oxygen stream **14** can be compressed to suitable pressure for injection into gasifier **12**.

In a typical cryogenic rectification unit **16**, the air is cooled within the main heat exchanger to a temperature suitable for its rectification, generally in a double distillation column having a high pressure column that is operatively associated with the low pressure column by a condenser-reboiler. The high pressure column will typically operate at a pressure of about 5 bar absolute to produce a nitrogen-rich overhead and an oxygen-rich, column bottoms. An oxygen-rich column bottoms is further refined within the low pressure column that generally operates at a pressure of about 1.2 bar absolute. The column bottoms of the lower pressure column is enriched in the oxygen. The oxygen is vaporized against condensing a nitrogen-rich tower overhead produced in the higher pressure column. The resulting condensate of the higher pressure column is valve expanded and used to reflux the lower pressure column.

Other alternatives for generation of the oxygen stream **14** are possible. For example, an oxygen transport membrane reactor in which the compressed air can be partially combusted within a combustor and introduced into the oxygen transport membrane reactor for separation of oxygen in a manner known in the art.

Gasifier **12** incorporates any of the numerous commercially available gasification technologies. For example, in the counter-current "fixed" (or moving) bed type of gasifier, a downward flowing bed of carbonaceous fuel is contacted with gasification products generated by steam and oxygen that enter at the bottom of the moving bed. The gasification products flow in a counter-current configuration relative to the carbonaceous bed. The slag or ash **13** will be removed in all gasifiers. For example, in a counter-current fixed bed gasifier the reference number **13** would designate a slag for removal. In a fluid bed gasifier the fuel particles are fluidized as a result of injection of oxygen and steam at or near the bottom of the bed. In the entrained flow gasifier dry pulverized solids such as pulverized coal or a fuel slurry is gasified with oxygen in a co-current flow.

Within gasifier **12**, known reactions involving the coal and the oxygen produces a synthesis gas stream **20** which contains hydrogen, carbon monoxide, methane, carbon dioxide, steam, sulphur compounds and small quantities of higher hydrocarbons. The temperature of synthesis gas stream **20** will depend on the type of gasifier used. In the entrained flow gasifier of gasifier **12**, the synthesis gas exits the gasification section of the process at a temperature of between about 1600° F. and about 3500° F. It is to be noted, however, that other types of gasifiers could be used in an integration in accordance with the present invention and as such, it is worth mentioning that in other types of the gasifiers, the synthesis gas stream will be produced at other temperature ranges. For example, in fixed bed gasifiers, the synthesis gas will be produced at temperatures of between about 900° F. and about 1000° F.

Particulate removal from the synthesis gas stream **20** can be carried over by known techniques that include a cyclone or a candle filter **22**. Candle filter **22** can be ceramic or metallic candle filters which are used for removing such particulate matter from a synthesis gas stream **20**. Candle filter **22** should in any case preferably operate about 700° F. and more preferably above 1000° F. It is to be noted that filtering is optional in that it is generally present to protect an expander from erosion. In some gasifiers, the stream is recycled to the front end thereof to improve carbon conversion.

The resultant filtered syngas stream **24** contains a synthesis gas that is then sent to an oxygen transport membrane boiler **26**. Although there is no particular oxygen transport membrane boiler that is preferred, in any such device the filtered synthesis gas stream **24** is introduced into an oxygen transport membrane system **28** that can comprise a plurality of tubes made of a ceramic material that can be a mixed conductor or a dual-phase conductor, such as described above. It is understood that oxygen transport membrane system **28** could employ oxygen transport membrane elements in forms other than tubes, for instance, planar elements also known in the art. An oxygen containing gas, for example air is introduced into the tubes as an air stream **30** with the use of a blower **32**. Air stream **30** is preheated by means of a waste heat recovery heat exchanger **34** prior to being introduced into the oxygen transport membrane tubes. The oxygen ions permeate through the membrane and immediately combine with the filtered synthesis gas stream **24** to support combustion of the filtered synthesis gas stream **24**. The oxygen depleted retentate, as a retentate stream **35**, is passed through the waste heat recovery heat exchanger **34** for recovery of heat and discharge.

In the illustrated oxygen transport membrane boiler **26**, combustion of the filtered synthesis gas stream **24** provides the driving force for the oxygen separation within the oxygen transport membrane system **28**. As such, air stream **30** is not appreciably compressed. However, while it is possible to integrate an oxygen transport membrane boiler that does utilize compression for the oxygen containing gas in accordance

with the present invention, such integration is not preferred due to the power penalty involved in such compression.

Preferably, the surface temperature of the OTM tubes is maintained at between about 1600° F. and about 2000° F. throughout the oxygen transport membrane boiler **26**. A flue gas stream **36** is discharged from the oxygen transport membrane boiler **26** in a temperature of preferably between about 1600° F. and about 2000° F. It consists predominately of water and carbon dioxide with small amounts of nitrogen, argon and sulphur dioxide and potentially residual oxygen.

The heat generated by the combustion occurring within the oxygen transport membrane boiler **26** is recovered by a heat exchange network, generally indicated by reference numeral **38** in which steam is generated and utilized in a steam cycle ("ST") generally indicated by block **40** that incorporates a steam turbine system to generate power that can be applied to driving an electrical generator **42**. There are many steam cycles that are possible for use in connection with the present invention and in fact the design of the steam cycle is a routine matter that is often carried out by computer programs that are specifically capable of generating such designs. As will be discussed, ultra-supercritical steam cycles are preferred. However, sub-critical and supercritical steam cycles are also possible. Moreover, there are many possible designs for oxygen transport membrane boiler **26**. Having said this, as an example, a more detailed description of a suitable design that can be used in connection with oxygen transport membrane boiler **26** and the associated steam cycle **40** is illustrated in FIG. **2**.

With specific reference now to FIG. **2**, oxygen transport membrane boiler **26** is based upon a conventional commercially available unit that has been modified in a manner that will be discussed hereinafter. Oxygen transport membrane boiler **26** generally consists of a radiant section **44** in which radiant heat transfer predominates and a convective section **46** in which heat transfer is accomplished by convective heat transfer. Oxygen transport membrane boiler **26** is integrated with a steam cycle **40**.

Radiant section **44** is modified with the provision of oxygen transport membrane tubes **50** that form the oxygen transport membrane system **28** of oxygen transport membrane boiler **26**. Oxygen transport membrane tubes **50** are connected in parallel to receive air stream **30** and alternate with a series of steam tubes **52**, **54**, **56** and **58** forming part of the heat exchange network **38** to raise steam and for the steam cycle **40**. In the illustrated embodiment, steam tubes **52**, **54**, **56** and **58** are in series. However, in practice they could be positioned anywhere in the radiant section **44** in that such section has a uniform temperature. Although not specifically illustrated, each of the steam tubes **52**, **54**, **56** and **58** would be part of larger alternating arrays in which all steam tubes of an array, for example, steam tubes **52** would be connected in parallel. Furthermore, as also not illustrated, saturated steam produced within steam tubes **52** can be collected in a steam drum prior to introduction into steam tubes **54**.

With respect to the steam cycle **40**, an ultra-supercritical steam cycle is preferred and as used herein and in the claims means a cycle that employs steam at a temperature of at least about 1000° F. and at a pressure of at least 4000 psia. The following discussion of steam cycle **40** utilizes temperatures and pressures that are applicable to examples 1 and 2 discussed below.

In accordance with steam cycle **40**, a boiler feed water stream **60** is pressurized by being pumped by a pump **62** and preheated within preheaters **64**, **66**, **68** and **70** and heat exchangers **72** and **74** within convective section **46** to a temperature of about 650° F. and a pressure of about 4366 psia that has been imparted through the pressurization less piping losses. It is to be noted, that heat exchangers **72**, **74** and **109**, to be discussed and the steam tubes **52**, **54**, **56** and **58** form the heat exchange network **38** of oxygen transport membrane boiler **26**.

The boiler feed water stream **60**, thereafter, enters steam tubes **52** that act as a steam generator and then to steam tubes **54** to superheat the generated steam to produce a steam stream **76** at a temperature of about 1080° F. and a pressure of about 4050 psia. Steam stream **76** is then introduced into high pressure steam turbine **78** ("HPT") where it is expanded to 1226 psia. About 2725 klb/hr of expanded steam, that constitutes about 90% of stream **76**, as a stream **80** is passed through steam tubes **56** that serve as a reheater where stream **80** is reheated to a temperature of about 1111° F. to produce a stream **82** having a pressure of about 1170 psia. The remaining part **84** is introduced into preheater **68**.

Reheated stream **82** is then introduced into a primary intermediate pressure turbine **86** ("PIPT") to be expanded to about 505 psia and a temperature of about 822° F. About 2328 klb/hr of this steam as a stream **88**, that constitutes about 85% of stream **80**, is introduced into steam tubes **58** that serve as a second reheater to produce a reheated stream **90** having a temperature of about 1111° F. The remainder of the expanded steam is introduced as a stream **92** to preheater **64**.

Reheated stream **90** is then introduced into intermediate pressure steam turbine **94** ("IPT"). A stream **96** is then expanded in low pressure turbine **98** ("LPT") to a pressure of about 0.75 psia. The resulting stream **100** is then passed into a condenser **102** and then pumped by pump **104** to a series of low pressure boiler-feed water heaters **106**, **108**, **109**, **110** and **112** to be heated to about 210° F. using extracted steam streams **114**, **116**, **118** and **120** taken from intermediate pressure steam turbine **94** and low pressure turbine **98**. All of the extracted streams are combined, pumped to pressure by pump **105** and combined with stream **100**. The resultant heated feed water stream **122** is mixed with feed water stream **124** in deaerator **126** along with a stream **128** and a stream **130** extracted from intermediate pressure steam turbine **94** and used to strip volatile gases from the water. Stream **128** is made up of stream **92**, stream **84** and a stream **132** extracted from primary intermediate pressure steam turbine **86**. Stream **60** from deaerator **126** is pumped by pump **62** to a pressure of about 4452 psia.

Referring again to FIG. **1**, flue gas stream **36** is then purified by first being cooled within a water-cooler **134** to a temperature of between about 160° F. and about 300° F. Cooled stream **136** is then sent to a flue gas desulphurization scrubber unit **138** well known in the art and that is capable of removing more than about 98% by volume of the sulphur dioxide. Flue gas desulphurization scrubber unit **138** is a known system that can be obtained from a variety of manufacturers, for example, Babcock & Wilcox Company, 20 S. Van Buren Avenue Barberton, Ohio, U.S.A 44203-0351. Typically, a flue gas desulphurization scrubber unit **138** will typically comprise three parts, namely, limestone handling and reagent preparation, where limestone is received, stored and grinded in a ball mill to prepare an aqueous slurry. A second part is a scrubber where the limestone slurry is brought into contact with a flue gas which in the illustrated embodiment would be cooled stream **136** in a counter-current mode in a spray-tower column. This is followed by by-product dewatering where the bleed slurry from the flue gas desulphurizor absorber is dewatered and gypsum is separated and stored. The resulting partly purified flue gas stream **140** consists mainly of carbon dioxide and about 10 to 15 mole

percent of water with some residual argon and nitrogen, oxygen and trace amounts of sulphur dioxide.

Partly purified flue gas stream **140** is then compressed in a base load compressor **142** to a pressure of between about 300 psia and about 500 psia and then dried within a drying unit **148** to remove moisture. The drying unit is a glycol system that is a known system that is typically used for drying natural gas. Preferably, although not illustrated, partly purified flue gas stream **140** is first cooled to about 110° F. prior to such compression and any condensate removed to conserve on the energy of compression. It is also understood that base load compressor **142** is generally a multistage, inter-cooled compression system with knock-put drums to remove additional water. Glycol systems can be obtained from a variety of sources including NATCO Group Inc. 2950 North Loop West, Suite 750 Houston, Tex. 77092. In a typical glycol system, partly purified flue gas stream **140** after compression is contacted in a counter-current manner within a glycol solution in an absorption column. The dried gas leaves the top of the absorption column. The glycol solution containing absorbed water is sent to a connected distillation column. Heat is supplied to separate the water and the regenerated glycol solution is circulated back to the absorption column using a pump. A heat exchanger is used to exchange heat between the glycol solutions flowing between the two columns. The removal of water prevents the formation of carbonic acid in the carbon dioxide product that could corrode pipelines. Normally, the water level should be reduced below about 600 ppm by volume for this purpose.

Additionally, reducing the water content will prevent freezing when used in downstream processing such as sub-ambient purification processes. Although not illustrated, a dryer for such purpose could be based on adsorption using molecular sieves. In such case, the dryer can comprise a multi-bed molecular sieve dryer system in which half of the beds process the feed to be dried and the other half undergo regeneration. A product portion of the product gas is used as a regenerating gas which is heated to about 450° F. with a heater to remove moisture from the beds. After the beds are free to moisture the regeneration gas at near-ambient temperature is passed through the beds to cool them down. The regeneration gas can then be recycled to a base load carbon dioxide compressor **142** at an appropriate point upstream of the last stage that is utilized for such purpose.

The dried stream **150** from drying unit **148** is then passed to a booster compressor **152** to produce a product stream **154** that can be passed to a pipeline or for enhanced oil recovery or sequestration purposes. Booster compressor **152** is a multi-stage, inter-cooled machine. The product stream **154** preferably has a carbon dioxide content of at least about 90% by volume and as indicated in the examples, the carbon dioxide content can be about 92% or about 95% by volume.

With reference to FIG. **3**, another embodiment is illustrated that utilizes an oxygen transport membrane partial oxidation reactor **160**. This feature has particular applicability to where the coal is gasified in a moving bed gasifier that utilizes less oxygen than other types of gasifiers. In such embodiment, synthesis gas stream **20** produced by a moving bed gasifier **12'** at a temperature of between 900° F. and about 1000° F. and contains volatile substances such as tars and oils. Steam is also utilized in such gasifier and is obtained, as indicated in FIG. **2**, by way of stream **91** extracted from an intermediate stage of intermediate pressure steam turbine **94** or possibly other sources not shown. Partial oxidation reactor **160** partially oxidizes the syngas to raise its temperature from between about 1600° F. and about 1800° F. to remove such volatile substances such as tars, oils and phenols that are oxidized to hydrogen, carbon monoxide, methane and carbon dioxide. Partial oxidation reactor **160** employs one or more oxygen transport membrane elements that are typically mixed conductors in tubular form. At about 1800° F., partial oxidation reactions will proceed in the absence of a catalyst. In this regard, the synthesis gas stream **20** will often contain sulfur that is a known catalyst poison and if a catalytic reactor were used, upstream treatment or a sulfur tolerant catalyst would be required. Typical examples of partial oxidation reactors are well known and are illustrated in U.S. Pat. Nos. 5,820,654; 5,820,655 and 6,139,810.

In such embodiment as illustrated in FIG. **3**, the air stream **30** is divided into first and second subsidiary oxygen containing streams **162** and **164**. First subsidiary oxygen containing stream **162** is fed to oxygen transport membrane boiler **26**. Second subsidiary oxygen containing stream **164** is supplied to the inside of the oxygen transport membrane elements of partial oxidation reactor **160**. The filtered synthesis gas stream **24** is supplied to the exterior to the shell of such reactor and the oxygen ions react with the volatiles to produce the reaction products mentioned above. Alternatively, separate air supplies along with blowers and heat exchangers analogous to units **32** and **34** can be used to supply the oxidant to units **26** and **160**.

The resultant synthesis gas stream **166**, after having the volatiles reacted in the oxygen transport membrane partial oxidation reactor **160**, has a pressure of between about 300 and about 1200 psia. Synthesis gas stream is then expanded within an expander **168** coupled to an electrical generator **170** to generate additional electrical power. Between about 60% and about 80% of the total oxygen requirement for apparatus **1** will typically be supplied by the oxygen transport membranes contained within oxygen transport membrane partial oxidation reactor **160** and the oxygen transport membrane boiler **26**. The remainder is supplied by cryogenic air separation unit **16** and to the gasifier **12'**. A retentate stream **172** joins retentate stream **35** and the combined stream is fed to heat recovery heat exchanger **34**.

With brief reference to FIG. **4**, an alternative embodiment of FIG. **3** is illustrated that utilizes an entrained flow or fluid bed type of gasifier **12"**. Since the temperature of synthesis gas stream **20'** produced by such a gasifier is about 1800° F., a high pressure steam boiler **156** is provided to produce a steam stream **158** from hot boiling feed water stream **155**. Steam stream **158** can be combined with the steam entering steam tube **54** located within oxygen transport membrane boiler **26** and shown in more detail in FIG. **2**. The boiler **156** decreases the temperature of stream **20'** to facilitate the use of high temperature filters which are currently limited to operating temperatures below about 1000° F. These filters are used to minimize erosion in hot gas expanders as has been mentioned above.

With reference to FIG. **5**, stages of partial oxidation and expansion are illustrated in which the filtered synthesis gas stream **24** is introduced into a first partial oxidation stage produced by a first partial oxidation reactor **180** followed by expansion within expansion stage provided by an expander **182** coupled to an electrical generator **184** to generate additional electricity. Thereafter, the treated filtered synthesis gas stream **24** after expander **182** is then introduced into a second partial oxidation stage provided by a second partial oxidation reactor **186** followed by a second expansion stage provided by a second expander **188** coupled to an additional electrical generator **190** for generating yet additional electrical power. In such embodiment, second subsidiary oxygen containing stream **164** is divided into portions **164***a* and **164***b* that are fed into the first partial oxidation reactor **180** and the second

partial oxidation reactor **186**. The resultant oxygen depleted retentate streams **172***a* and **172***b* are combined to produce a combined stream **172***c* that is further combined with retentate stream **35** and passed through heat recovery heat exchanger **34**. Again, independent air supply systems are also possible as have been discussed above.

With reference to FIG. **6**, an embodiment is illustrated in which combustion is not completed within oxygen transport membrane system **28** of boiler **26**. Typically, the area required for oxygen transport that would be necessary for complete combustion would be quite high. In order to avoid excessive costs, combustion may be completed only to the extent of between about 80% and about 90% of the fuel species contained within synthesis gas stream **20**. In such a situation, flue gas stream **36** will contain small amounts of fuel species such as hydrogen and carbon monoxide. Carbon dioxide stream could then be further purified within a purification unit **200** that incorporates cryogenic distillation. Alternative methods of purification including distillation processes with external refrigeration can be used to form purification unit **200**. Well known purification processes are illustrated in U.S. Pat. Nos. 5,927,103; 6,035,662 and 6,070,471.

With reference to FIG. **7**, a specific embodiment of purification unit **200** is illustrated that purifies partly purified flue gas stream **140**. Partly purified flue gas stream **140** is compressed in a compressor **202** to a pressure of between about 150 psia and about 1000 psia. The amount of carbon dioxide that can be recovered is a function of the feed pressure supplied to the cold box. As can be appreciated, carbon dioxide recovery can be increased by increasing this pressure. However, such increase in pressure will result in greater production costs. After having been cooled within water cooled chiller **204**, partly purified flue gas stream **140** is then introduced into a phase separator **205** to disengage water that has been condensed within partly purified flue gas stream **140** by virtue of its having been cooled in water cooled chiller **204**.

The partly purified flue gas stream **140** is then introduced into a dryer **206**. Dryer **206** is preferably an adsorption system that can contain beds of molecular sieve adsorbent operating out a phase to adsorb moisture and other impurities such as heavy hydrocarbons that will boil at a higher temperature than the partly purified flue gas stream **140**. The beds of molecular sieve adsorbent operate out a phase so that as one bed is adsorbing such higher boiling impurities the other bed is being regenerated. Even number of beds numbering greater than two can also be used for large flows with half of beds performing adsorption while the other half of beds undergoing regeneration. A bed is regenerated by lowering its pressure and/or by increasing its temperature to desorb the adsorbed component and then purging the bed with a stream that is lean in the adsorbed component. In a system that employs temperature swing, the bed is regenerated by heating a stream lean in the adsorbed component and then introducing it into the bed to be regenerated to cause desorption and to carry away desorbed components. These systems vary but there are many examples of the same known that are well known in the art. In this regard, non-adsorbent based systems are possible such as by the use of reversing heat exchangers that are well known in the art of distillation.

The resultant dried feed stream **208**, that consists of partly purified flue gas stream **140** after having been compressed by compressor **202** and dried, is then introduced into a main heat exchanger **210** in which it is partly cooled and then introduced into a reboiler **212** that serves to produce boil up or initiate an ascending vapor phase within a stripping column **214**. Dried feed stream **208** is then again introduced into main heat exchanger **210** in which it is fully cooled to at least partially liquefy the dried feed stream **208**. The dried feed stream **208** is then introduced into an expansion valve **216** into stripping column **214** to initiate a descending liquid phase within such column.

As well known in the art, stripping column **214** preferably has structured packing to contact the ascending vapor phase flowing up through the packing with a descending liquid film of the liquid phase. Other vapor-liquid contacting elements known in the art could be used such as sieve trays. As a result of the contact, the descending liquid phase becomes evermore rich in carbon dioxide, the less volatile component and the ascending vapor phase becomes evermore rich in impurities that have a higher volatility than the carbon dioxide. Within stripping column **214**, the remaining uncombusted constituents of the filtered synthesis gas stream **24**, namely, hydrogen, carbon monoxide and methane, and any inert constituents that may arise from air ingress into combustion zone, namely, nitrogen and argon, all being more volatile than the carbon dioxide, will be stripped from the descending liquid to produce a carbon dioxide-lean column overhead and a carbon dioxide-rich, liquid column bottoms.

A column overhead stream **218** can be extracted from stripping column **214** that is composed of the carbon dioxide-lean column overhead and then introduced into an auxiliary heat exchanger **220** so that the carbon dioxide overhead stream **218** is at least partially liquefied. The carbon dioxide overhead stream **218** is then introduced into a phase separator **224** to produce a carbon dioxide-depleted vapor stream **226** and a carbon dioxide-rich liquid stream **228**. Carbon dioxide-rich liquid stream **228** is expanded within an expansion valve **230** and then passed together with the carbon dioxide-depleted vapor stream **226** into auxiliary heat exchanger **220**. Expansion valve **230** provides refrigeration for the partial liquefaction of carbon dioxide overhead stream **218**.

Carbon dioxide-depleted vapor stream **226** can be passed into main heat exchange **210** and then recycled and combined with filtered synthesis gas stream **24** to provide a synthesis gas feed stream **24'** to oxygen transport membrane partial oxidation reactor **160**. As would be understood by those skilled in the art, if the gasifier used operates at a higher pressure than carbon dioxide-depleted vapor stream **226**, a recycle compressor would have to be provided to accomplish the recycle. A small amount of stream **226** can be purged from the process as a fuel stream to avoid the build up of inerts such as nitrogen and argon in the loop. The purge gas may require incineration or catalytic oxidation or other treatment to manage carbon monoxide, methane, or other emissions.

Carbon dioxide-rich liquid stream **228** after having passed through main heat exchanger **210** will be vaporized and as such can be used to regenerate dryer **206**, for example, such stream can be heated and then introduced into an adsorption bed for regeneration purposes and thereafter, be reintroduced as a recycle stream **236** into an appropriate stage of compressor **202** to enhance carbon dioxide recovery.

A carbon dioxide product stream **240** as a liquid can be extracted from stripping column **214** that is composed of carbon dioxide-rich liquid column bottoms. The carbon dioxide product stream can then be expanded in an expansion valve to generate refrigeration for the process. Advantageously, carbon dioxide product stream **240** is split into subsidiary streams **242** and **244** and at least the subsidiary stream **244** is expanded to lower pressure by the use of expansion valve **246**, optionally both streams **242** and **244** are simultaneously expanded to lower and the higher pressures by the use of expansion valves **246** and **248**, respectively. Both subsidiary streams **242** and **244** are then vaporized in main heat exchanger **210**. The resultant lower pressure subsidiary

stream **242** is introduced into the inlet of product compressor **250**. The lower pressure subsidiary stream **244** is introduced into an intermediate stage of product compressor **250**. The product compressor **250** could be a multi-stage compressor with interstage cooling. It is to be noted, that, although not illustrated, some of the carbon dioxide product could be taken as a liquid from carbon dioxide product stream.

With reference to FIG. **8**, another variation of FIG. **6** is to inject supplemental oxygen containing stream **254** within the radiant section **44** of the oxygen transport membrane boiler **26** to complete the combustion of the fuel. Supplemental oxygen stream **254** is an oxygen containing stream that contains at least about 40% oxygen to prevent the build-up of nitrogen in the carbon dioxide to be captured. A disadvantage of such a process is that inerts are introduced into the flue gas stream **36** and the purity of the carbon dioxide will thereby suffer. In such embodiment, stream **226'** can be produced containing the more volatile components of the partly purified flue gas stream that will simply be treated or vented depending on the characteristics of the constituents. The stream **226'** could also contain oxygen. Therefore, although not illustrated, catalytic oxidation could be incorporated at the end of the radiant section or the convective section of the oxygen transport membrane boiler **26**. This would also reduce the amount of oxygen required to achieve complete combustion. In this regard, to the extent that there exists any excess oxygen in any embodiment of the present invention, such catalytic oxidation could be incorporated together with purification.

The apparatus shown in FIGS. **3**, **4** and **5** were modeled using computer programs to assess the predicted performance of such illustrated embodiment. Guidelines set forth in the Carbon Capture and Sequestration Systems Analysis Guidelines, U.S. Department of Energy, Office of Fossil Energy, National Energy Technology Laboratory, April 2005 were used along with the assumptions contained in the EPRI reports, Holt, N., Updated Cost and Performance Estimates for Fossil Fuel Power Plants with CO_2 Removal, EPRI Report to DOE-NETL No. 1004483, Dec. (2002), U.S. DOE/NETL, Pittsburgh and Holt, N., Evaluation of Innovative Fossil Fuel Power Plants with CO_2 Removal, EPRI Report to DOE-NETL No. 1000316, Dec. (2000), U.S. DOE/NETL, Pittsburgh, Pa. The specific assumption listed in Table 1 are used in the examples and may differ from such guidelines.

Tables 4, 5 and 6 present the key streams for processes shown in FIGS. **3**, **5** and **4**, respectively. The performance comparison for the three cases is summarized in Table 7.

TABLE 1

Process Assumptions
1. IL # 6 Coal
2. ASU oxygen purity: 95%
3. Pressure with BGL Gasifier: 400 psig
4. Pressure with E-gas Gasifier: 800 psig
5. Sulfur removal using wet-FGD
6. Supercritical steam cycle with double reheat: 4050 psia, 1080° F./1111° F./1111° F.
7. CO_2 compressed to 2204 psia
8. Air-leak to the boiler: 1% of the flue gas

As to the design of the oxygen transport membrane system **28** within oxygen transport membrane boiler **26**, for a given size boiler, the surface area and the number of the oxygen transport membrane tubes, such as oxygen transport membrane tubes **50** of FIG. **2**, that will be required depends on the oxygen flux per unit area of a tube and the length and diameter of a single tube. By way of example, in order to design an oxygen transport membrane boiler **26** that produces net electric power of about 500 MWe, the amount of coal can be computed. For 500 MWe, 4838 tpd of Illinois number 6 coal will be required. Then, using any of a number of known programs that will simulate the operation of a gasifier, the amount of synthesis gas that will be produced can also be calculated along with the amount of oxygen that will be required. Once the amount of synthesis gas produced from the gasifier is known, a calculation can be formed as to the amount of oxygen required for complete combustion. Assuming only 70% of the oxygen in the feed air will be transferred through the oxygen transport membrane tube, and further assuming that there will be about 0.2 and about 0.4 mol percent of oxygen left in the flue gas. From this the actual amount of oxygen and the amount of feed air that will be required can also be computed. Once the amount of oxygen needed to be transferred through the oxygen transport membrane tube is known the required surface area of the oxygen transport membrane tubes can be calculated provided that the amount of oxygen flux through the oxygen transport membrane tube is known. An assumed oxygen flux for exemplary purposes is about 20 scf/ft^2/hr. The exact oxygen flux would of course depend upon membrane material performance. Hence, for low oxygen flux systems, a greater membrane area will be required to achieve the exemplary results set forth below. This would increase capital costs but not decrease efficiency. Using this flux, the surface area requirements can be calculated and samples of such calculation are shown in Table 2 below.

TABLE 2

Example No.	O_2 Requirement (tpd)	O_2 Requirement (MM scf/hr)	O_2 Flux From OTM Tubes Scf/ft^2/hr	OTM Tube Surface (ft^2)
1	7051	6.97	20	348395.8
2	7051	6.97	20	348395.8
3	6335	6.26	20	312979.2

The actual number of oxygen transport membrane tubes will depend on the outer diameter and the length of the tubes. Based on two different tube lengths, the required numbers of tubes for the three examples are given in Table 3.

TABLE 3

Example No.	No of OTM Tubes (OD = 1 inch Length = 5 ft.)	No. of OTM Tubes (OD = 1 inch Length = 20 ft.)
1	266048	66512
2	266048	66512
3	239002	59751

TABLE 4

(See FIG. 3):

		Parameters										
Components	Units	IL No. 6 Coal (St. 10)	O_2 to Gasifier (St. 14)	Steam to Gasifier (St. 91)	Feed Air to OTM-Sys (St. 30)	O_2 Depleted Air (St. 35)	Fuel Gas to OTM POX (St. 24)	Fuel Gas to Expander (St. 166)	Fuel Gas to OTM Boiler (Exiting 168)	Flue Gas to FGD (St. 136)	Crude CO_2 to Drying & Comp. (St. 140)	CO_2 to EOR or Seq. Site (St. 154)
Temp.	F	77.0	254.0	600.0	77.0	215.0	1000.0	1799.8	705.2	163.3	154.0	110.0
Pressure	psia	414.7	500.0	514.7	14.7	14.7	410.0	410.0	16.0	14.8	14.7	2204.6
Molar Flow	MMscfd		65.2		1150.0	982.8	345.7	376.5	376.5	314.6	270.2	208.2
Mass Flow	klb/hr	403.2	230.6	120.9	3656.6	3069.0	763.4	820.0	820.0	1208.6	1105.5	982.7
Hydrogen	mol %						25.53	32.62	32.62	0.00	0.00	0.00
CO	"						46.96	40.96	40.96	0.00	0.00	0.00
CO2	"						2.93	9.30	9.30	61.37	71.47	92.75
Nitrogen	"		1.40		78.17	91.47	2.80	2.70	2.70	3.88	4.52	5.86
Argon	"		3.60		0.93	1.09	0.68	0.63	0.63	0.75	0.87	1.13
Methane	"						3.88	1.02	1.02	0.00	0.00	0.00
Ethane	"						0.12	0.00	0.00	0.00	0.00	0.00
Propane	"						0.09	0.00	0.00	0.00	0.00	0.00
n-Butane	"						0.07	0.00	0.00	0.00	0.00	0.00
Phenols	"						0.06	0.00	0.00	0.00	0.00	0.00
Naphtha	"						0.07	0.00	0.00	0.00	0.00	0.00
H2O	"			100.00			15.60	11.91	11.91	32.83	22.94	0.00
H2S	"						0.77	0.76	0.76	0.00	0.00	0.00
COS	"						0.06	0.00	0.00	0.00	0.00	0.00
SO2	"						0.00	0.00	0.00	0.91	0.00	0.00
NH3	"						0.25	0.01	0.01	0.00	0.00	0.00
HCN	"						0.06	0.00	0.00	0.00	0.00	0.00
HCl	"						0.09	0.08	0.08	0.09	0.00	0.00
Oxygen	"		95.00		20.90	7.44	0.00	0.00	0.00	0.17	0.19	0.25

TABLE 5

(See FIG. 5):

		Parameters						
Components	Units	IL No. 6 Coal (St. 10)	O_2 to Gasifier (St. 14)	Steam to Gasifier (St. 91)	Feed Air to OTM-Sys (St. 30)	O_2 Depleted Air (St. 35)	Fuel Gas to OTM POX (St. 24)	Fuel Gas to Expander-1 (Exiting 180)
Temp.	F	77.0	254.0	600.0	77.0	215.0	1000.0	1799.8
Pressure	psia	414.7	500.0	514.7	14.7	15.0	410.0	410.0
Molar Flow	MMscfd		65.2		1150.0	982.7	345.7	376.5
Mass Flow	klb/hr	403.2	230.6	120.9	3656.6	3068.8	763.4	820.0
Hydrogen	mol %						25.53	32.62
CO	"						46.96	40.96
CO2	"						2.93	9.30
Nitrogen	"		1.40		78.17	91.47	2.80	2.70
Argon	"		3.60		0.93	1.09	0.68	0.63
Methane	"						3.88	1.02
Ethane	"						0.12	0.00
Propane	"						0.09	0.00
n-Butane	"						0.07	0.00
Phenols	"						0.06	0.00
Naphtha	"						0.07	0.00
H2O	"			100.00			15.60	11.91
H2S	"						0.77	0.76
COS	"						0.06	0.00
SO2	"						0.00	0.00
NH3	"						0.25	0.01
HCN	"						0.06	0.00
HCl	"						0.09	0.08
Oxygen	"		95.00		20.90	7.43	0.00	0.00

TABLE 5-continued

(See FIG. 5):

		Parameters					
Components	Units	Fuel Gas to OTM POX-2 (Exiting 182)	Fuel Gas to Expander-2 (Exiting 186)	Fuel Gas to OTM Boiler (Exiting 188)	Flue Gas to FGD (St. 136)	Crude CO_2 to Drying & Comp. (St. 140)	CO_2 to EOR or Seq. Site (St. 154)
Temp.	F	1199.9	1802.6	1134.6	163.3	154.0	110.0
Pressure	psia	90.0	90.0	16.0	14.8	14.7	2204.6
Molar Flow	MMscfd	376.5	384.0	384.0	314.7	270.2	208.2
Mass Flow	klb/hr	820.0	856.4	856.4	1208.8	1105.7	982.9
Hydrogen	mol %	32.62	31.41	31.41	0.00	0.00	0.00
CO	"	40.96	39.24	39.24	0.00	0.00	0.00
CO2	"	9.30	11.01	11.01	61.36	71.46	92.72
Nitrogen	"	2.70	2.66	2.66	3.88	4.52	5.86
Argon	"	0.63	0.61	0.61	0.75	0.87	1.13
Methane	"	1.02	0.03	0.03	0.00	0.00	0.00
Ethane	"	0.00	0.00	0.00	0.00	0.00	0.00
Propane	"	0.00	0.00	0.00	0.00	0.00	0.00
n-Butane	"	0.00	0.00	0.00	0.00	0.00	0.00
Phenols	"	0.00	0.00	0.00	0.00	0.00	0.00
Naphtha	"	0.00	0.00	0.00	0.00	0.00	0.00
H2O	"	11.91	14.21	14.21	32.83	22.94	0.00
H2S	"	0.76	0.75	0.75	0.00	0.00	0.00
COS	"	0.00	0.00	0.00	0.00	0.00	0.00
SO2	"	0.00	0.00	0.00	0.91	0.00	0.00
NH3	"	0.01	0.00	0.00	0.00	0.00	0.00
HCN	"	0.00	0.00	0.00	0.00	0.00	0.00
HCl	"	0.08	0.08	0.08	0.09	0.00	0.00
Oxygen	"	0.00	0.00	0.00	0.18	0.22	0.28

TABLE 6

(See FIG. 4):

		Parameters										
Components	Units	IL No. 6 Coal (St. 10)	O_2 to Gasifier (St. 14)	Feed Air to OTM-Sys (St. 30)	O_2 Depleted Air (St. 35)	Raw Syngas from 12" (St. 20)	Fuel Gas to OTM POX (St. 24)	Fuel Gas to Expander (St. 166)	Fuel Gas to OTM Boiler (Exiting 168)	Flue Gas to FGD (St. 136)	Crude CO_2 to Drying & Comp. (St. 140)	CO_2 to EOR or Seq. Site (St. 154)
Temp.	F	77.0	274.2	77.0	215.0	1850.0	996.6	1801.5	590.9	163.3	154.0	110.0
Pressure	psia	814.7	978.0	14.7	15.0	810.0	800.0	800.0	16.0	14.8	14.7	2204.6
Molar Flow	MMscfd		82.7	1025.0	874.8	367.8	367.8	364.9	364.9	303.6	260.6	200.8
Mass Flow	klb/hr	403.2	292.7	3259.1	2731.2	802.4	802.4	839.3	839.3	1177.5	1077.4	958.9
Hydrogen	mol %					32.74	32.74	28.78	28.78	0.00	0.00	0.00
CO	"					40.65	40.65	37.80	37.80	0.00	0.00	0.00
CO2	"					10.20	10.20	13.01	13.01	63.26	73.70	95.65
Nitrogen	"		1.40	78.17	91.60	0.76	0.76	0.91	0.91	1.75	2.04	2.65
Argon	"		3.60	0.93	1.09	0.81	0.81	0.81	0.81	0.98	1.14	1.48
Methane	"					1.29	1.29	1.82	1.82	0.00	0.00	0.00
Ethane	"					0.00	0.00	0.00	0.00	0.00	0.00	0.00
Propane	"					0.00	0.00	0.00	0.00	0.00	0.00	0.00
n-Butane	"					0.00	0.00	0.00	0.00	0.00	0.00	0.00
Phenols	"					0.00	0.00	0.00	0.00	0.00	0.00	0.00
Naphtha	"					0.00	0.00	0.00	0.00	0.00	0.00	0.00
H2O	"					12.41	12.41	16.00	16.00	32.83	22.95	0.00
H2S	"					0.74	0.74	0.78	0.78	0.00	0.00	0.00
COS	"					0.03	0.03	0.00	0.00	0.00	0.00	0.00
SO2	"					0.00	0.00	0.00	0.00	0.94	0.00	0.00
NH3	"					0.23	0.23	0.01	0.01	0.00	0.00	0.00
HCN	"					0.06	0.06	0.00	0.00	0.00	0.00	0.00
HCl	"					0.08	0.08	0.08	0.08	0.10	0.00	0.00
Oxygen	"		95.00	20.90	7.31	0.00	0.00	0.00	0.00	0.14	0.17	0.22

TABLE 7

Parameters	Units	Example 1 BGL with 1 OTM-POX FIG. 3	Example 2 BGL with 2 OTM POX FIG. 5	Example 3 E-Gas with 1 OTM-POX FIG. 4
Coal Feed	tpd	4,838	4,838	4,838
Heat Input as Coal (HHV)	MMbtu/hr	4,703	4,703	4,703
Heat Input as Coal (LHV)	MMbtu/hr	4,486	4,486	4,486
Gross Power Summary				
Steam Turbine	MW	514.3	500.0	506.0
Fuel Gas Expander-1	MW	111.4	62.8	123.5
Fuel Gas Expander-2	MW	0.0	71.2	
Generator Loss	MW	6.3	6.3	6.3
Gross Plant Power	MW	619.4	627.7	623.2
Power Consumptions				
ASU	MW	35.0	35.0	58.0
CO2 Capture & Compression	MW	51.4	51.4	49.2
Air Blowers	MW	22.5	22.5	20.0
Other Plant Aux.	MW	21.0	21.0	29.9
Total Auxillary Power	MW	129.9	129.9	157.1
Net Power	MW	489.5	497.8	466.1
HHV Efficiency	%	35.5	36.1	33.8
LHV Efficiency	%	37.2	37.9	35.5

As is apparent from Table 7, the embodiment of FIG. **5** provided the most net power and was also the most efficient.

While the present invention has been described to a preferred embodiment, as will be understood by those skilled in the art, numerous changes and omissions can be made without departing from the spirit and the scope of the present invention which is set forth in the presently pending claims.

We claim:

1. An apparatus for generating electrical power comprising:

a gasifier for generating a synthesis gas stream;

at least one partial oxidation stage configured to partially oxidize the synthesis gas stream and thereby oxidize a volatile content of the synthesis gas stream and to heat the synthesis gas stream, the at least one partial oxidation stage having an oxygen transport membrane reactor configured to generate oxygen to support the partial oxidation of the synthesis gas stream;

at least one expansion stage having an expander for expanding the synthesis gas stream after having been heated in the at least one partial oxidation stage and a generator coupled to the expander for generating electrical power;

an oxygen transport membrane boiler in flow communication with the at least one expansion stage and configured to generate: heat from combustion of the synthesis gas stream while at an elevated temperature; a flue gas containing carbon dioxide from the combustion of the synthesis gas stream; and steam through indirect heat transfer of the heat to boiler feed water;

the oxygen transport membrane boiler having an oxygen transport membrane system operatively associated with a boiler, the oxygen transport membrane system configured to separate additional oxygen from an oxygen containing stream and support the combustion of the synthesis gas stream with the additional oxygen and the boiler configured to produce the steam by the indirect transfer of the heat to the boiler feed water;

a steam cycle operatively associated with the oxygen transport membrane boiler and having a steam turbine system to extract energy from the steam;

an additional electrical generator coupled to the steam turbine system to convert the energy to additional electrical power; and

a purification system configured to purify the flue gas stream to produce a carbon dioxide-rich stream.

2. The apparatus of claim **1**, wherein:

the at least one partial oxidation stage is a first partial oxidation stage and a second partial oxidation stage;

the at least one expansion stage is a first expansion stage and a second expansion stage;

the first expansion stage is connected to the first partial oxidation stage;

the second partial oxidation stage is connected to the first expansion stage;

the second expansion stage is connected to the second partial oxidation stage; and

the oxygen transport membrane boiler is connected to the second expansion stage.

3. The apparatus of claim **1**, wherein:

the combustion of the synthesis gas stream is incomplete resulting in fuel species being present within the flue gas stream; and

the purification system is configured to also separate the fuel species from the flue gas stream; and

the purification system is connected to the at least one partial oxidation stage such that the fuel species separated from the flue gas stream is recycled to the at least one partial oxidation stage.

4. The apparatus of claim **1** or claim **2**, wherein the purification system has:

a water-cooler configured to cool the flue gas stream and thereby to produce a cooled flue gas stream;

a flue gas desulphurization scrubber unit connected to the water-cooler to remove sulfur dioxide from the cooled flue gas stream;

a compressor connected to the sulfur dioxide removal unit to compress the flue gas stream;

a drying unit connected to the compressor to produce a carbon dioxide containing stream having a purity of no less than about 90% by volume; and

a further compressor connected to the drying unit to further compress the carbon dioxide containing stream to produce a carbon dioxide product stream.

5. The apparatus of claim 3, wherein the purification system comprises:

a water-cooler configured to cool the flue gas stream and thereby to produce a cooled flue gas stream;

a flue gas desulphurization scrubber unit connected to the water-cooler to remove sulfur dioxide from the cooled flue gas stream and thereby produce a partly purified flue gas stream;

a purification unit configured to separate the fuel species from the partly purified flue gas stream through distillation and thereby to produce a carbon dioxide containing stream having a purity of no less than about 90% by volume; and

a product compressor connected to the purification unit to compress the carbon dioxide containing stream and thereby produce a carbon dioxide product stream.

6. The apparatus method of claim 5, wherein the gasifier is configured to generate the synthesis gas stream through gasification of coal supported by further oxygen.

7. The apparatus of claim 6, wherein:

the steam cycle is configured to generate a steam stream; and

the gasifier is a moving bed gasifier connected to the steam cycle to receive the steam stream.

8. The apparatus of claim 4, wherein the steam cycle is an ultra-supercritical steam cycle.

9. The apparatus of claim 1, wherein the gasifier is configured to generate the synthesis gas stream through gasification of coal supported by an oxygen containing stream generated by an air separation unit.

10. The apparatus of claim 9, wherein:

the steam cycle is configured to generate a steam stream; and

the gasifier is a moving bed gasifier connected to the steam cycle to receive the steam stream.

11. The apparatus of claim 10, wherein the steam cycle is an ultra-supercritical steam cycle.

12. The apparatus of claim 1, wherein:

the gasifier is an entrained flow gasifier;

a high pressure steam boiler is positioned between the gasifier and a filter configured to filter the synthesis gas stream produced by the gasifier;

the high pressure steam boiler is configured to cool the synthesis gas stream through indirect heat exchange with a heated boiler feed water stream to produce a saturated steam stream; and

the high pressure steam boiler is connected to the boiler of the oxygen transport membrane boiler such that the steam stream is introduced into the boiler of the oxygen transport membrane boiler.

13. The apparatus of claim 1 or claim 2, wherein the oxygen transport membrane boiler has an inlet configured to receive an injected supplemental oxygen containing stream and to supply the injected supplemental oxygen containing stream to help support the combustion of the synthesis gas stream.

14. The apparatus of claim 13, wherein the purification system comprises:

a water-cooler configured to cool the flue gas stream and thereby to produce a cooled flue gas stream;

a flue gas desulphurization scrubber unit connected to the water-cooler to remove sulfur dioxide from the cooled flue gas stream and thereby produce a partly purified flue gas stream;

a purification unit configured to separate inerts from the partly purified flue gas stream through distillation and thereby to produce a carbon dioxide containing stream having a purity of no less than about 90% by volume; and

a product compressor connected to the purification unit to compress the carbon dioxide containing stream and thereby produce a carbon dioxide product stream.

15. The apparatus of claim 14, wherein the gasifier is configured to generate the synthesis gas stream through gasification of coal supported by an oxygen containing stream generated by an air separation unit.

16. The apparatus of claim 15, wherein:

the steam cycle is configured to generate a steam stream; and

the gasifier is a moving bed gasifier connected to the steam cycle to receive the steam stream.

17. The apparatus of claim 16, wherein the steam cycle is an ultra-supercritical steam cycle.

* * * * *

(12) **United States Patent**
Christie et al.

(10) **Patent No.: US 8,323,463 B2**
(45) **Date of Patent: Dec. 4, 2012**

(54) **CATALYST CONTAINING OXYGEN TRANSPORT MEMBRANE**

(75) Inventors: **Gervase Maxwell Christie**, Williamsville, NY (US); **Jamie Robyn Wilson**, Arlington, MA (US); **Bart Antonie van Hassel**, Weatgue, CT (US)

(73) Assignee: **Praxair Technology, Inc.**, Danbury, CT (US)

(*) Notice: Subject to any disclaimer, the term of this patent is extended or adjusted under 35 U.S.C. 154(b) by 168 days.

(21) Appl. No.: **12/968,699**

(22) Filed: **Dec. 15, 2010**

(65) **Prior Publication Data**

US 2011/0180399 A1 Jul. 28, 2011

Related U.S. Application Data

(60) Provisional application No. 61/291,221, filed on Jan. 22, 2010.

(51) **Int. Cl.**

C25B 13/04	(2006.01)
C25C 7/04	(2006.01)
B01D 53/22	(2006.01)
H01M 8/10	(2006.01)
H01M 8/12	(2006.01)

(52) **U.S. Cl.** **204/295**; 204/283; 205/159; 205/161; 205/162; 205/163; 205/634; 95/45; 95/54; 96/4; 429/481; 429/482; 429/483; 429/486; 429/488; 429/489; 429/491; 429/495; 429/496; 429/534

(58) **Field of Classification Search** 204/283, 204/295; 205/159, 161, 162, 163, 165, 634; 95/45, 54; 96/4; 429/481, 482, 483, 486, 429/488, 489, 491, 495, 496, 497, 532, 533, 429/534

See application file for complete search history.

(56) **References Cited**

U.S. PATENT DOCUMENTS

5,569,633	A *	10/1996	Carolan et al.	502/4
6,296,686	B1	10/2001	Prasad et al.	
6,641,626	B2 *	11/2003	Van Calcar et al.	48/198.2
6,811,904	B2	11/2004	Gorte et al.	

(Continued)

FOREIGN PATENT DOCUMENTS

WO	WO 2007/086949	A2	8/2007

(Continued)

OTHER PUBLICATIONS

Sylvain DeVille; "Freeze-Casting of Porous Ceramics: A Review of Current Achievements and Issues"; Advanced Engineering Materials 2008, 10, No. 3, pp. 155-169.

Primary Examiner — Bruce Bell
(74) *Attorney, Agent, or Firm* — David M. Rosenblum

(57) **ABSTRACT**

A composite oxygen transport membrane having a dense layer, a porous support layer and an intermediate porous layer located between the dense layer and the porous support layer. Both the dense layer and the intermediate porous layer are formed from an ionic conductive material to conduct oxygen ions and an electrically conductive material to conduct electrons. The porous support layer has a high permeability, high porosity, and a high average pore diameter and the intermediate porous layer has a lower permeability and lower pore diameter than the porous support layer. Catalyst particles selected to promote oxidation of a combustible substance are located in the intermediate porous layer and in the porous support adjacent to the intermediate porous layer. The catalyst particles can be formed by wicking a solution of catalyst precursors through the porous support toward the intermediate porous layer.

18 Claims, 2 Drawing Sheets

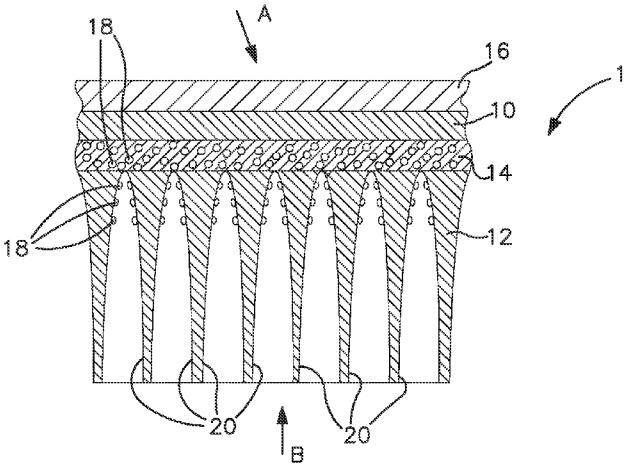

U.S. PATENT DOCUMENTS

6,846,511	B2	1/2005	Visco et al.	
7,125,528	B2	10/2006	Besecker et al.	
7,229,537	B2	6/2007	Chen et al.	
7,351,488	B2 *	4/2008	Visco et al.	429/486
7,534,519	B2	5/2009	Cable et al.	
7,556,676	B2 *	7/2009	Nagabhushana et al.	96/11
7,588,626	B2 *	9/2009	Gopalan et al.	95/45
7,901,837	B2 *	3/2011	Jacobson et al.	429/535
2005/0061663	A1	3/2005	Chen et al.	
2005/0214612	A1 *	9/2005	Visco et al.	429/30
2006/0127656	A1	6/2006	Gallo et al.	
2006/0191408	A1 *	8/2006	Gopalan et al.	95/55
2010/0015014	A1 *	1/2010	Gopalan et al.	422/187
2010/0143824	A1 *	6/2010	Tucker et al.	429/483
2011/0143255	A1 *	6/2011	Jain et al.	429/489

FOREIGN PATENT DOCUMENTS

WO	WO 2008/024405	A2	2/2008

* cited by examiner

U.S. Patent Dec. 4, 2012 Sheet 1 of 2 US 8,323,463 B2

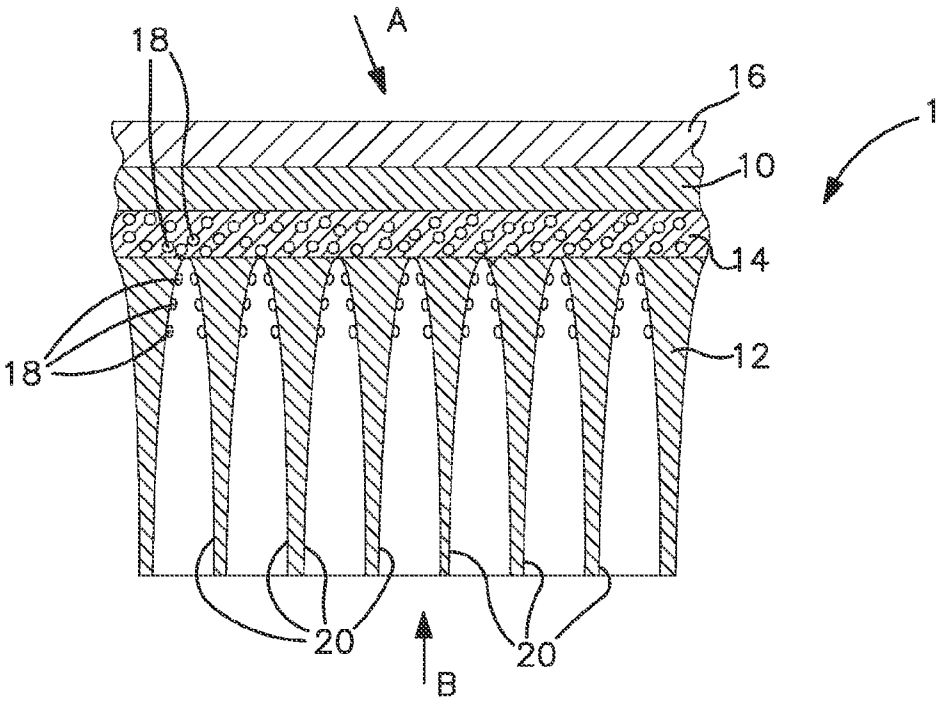

FIG. 1

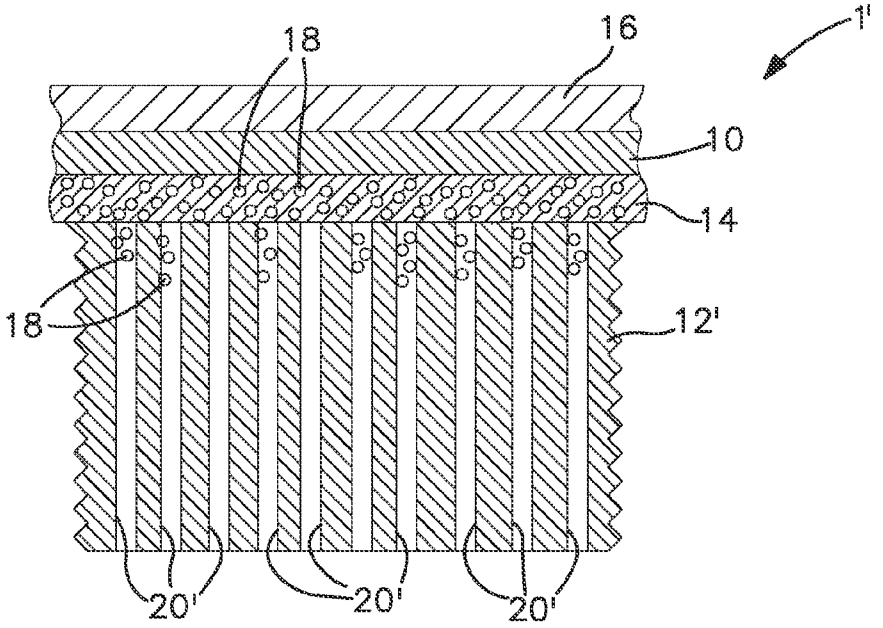

FIG. 2

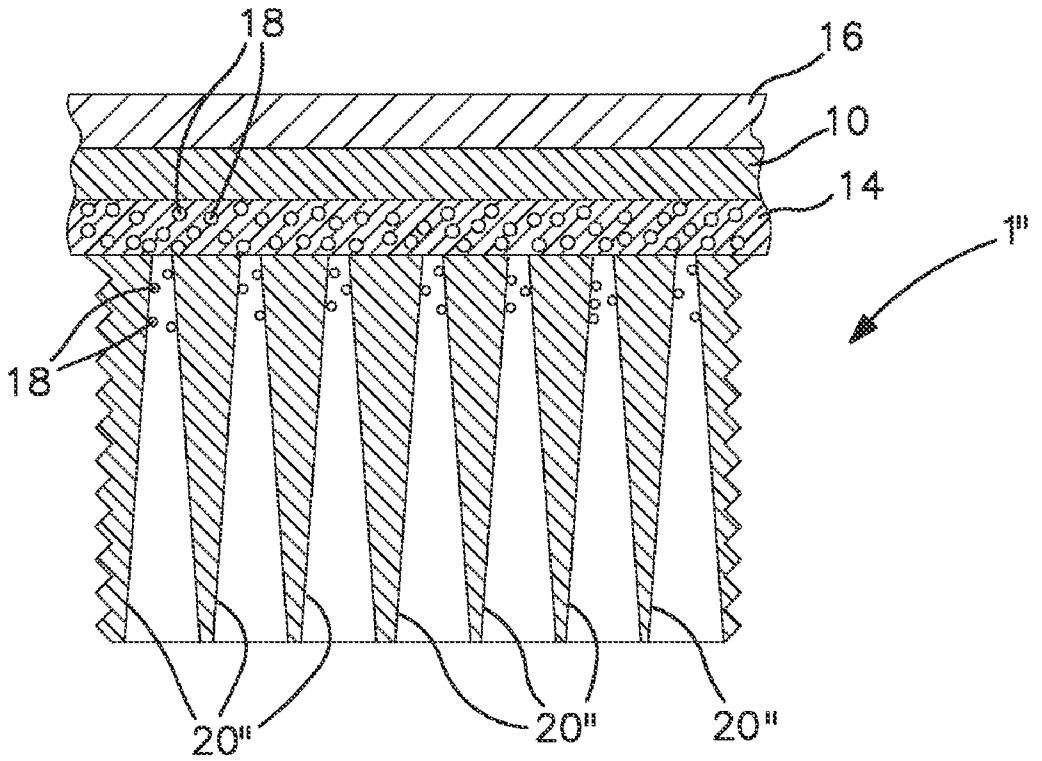

FIG. 3

CATALYST CONTAINING OXYGEN TRANSPORT MEMBRANE

RELATED APPLICATIONS

The present application claims priority from U.S. Application Ser. No. 61/291,221, filed Jan. 22, 2010, which is incorporated by reference herein in its entirety.

U.S. GOVERNMENT RIGHTS

This invention was made with Government support under. Cooperative-Agreement No. DE-FC26-07NT43088, awarded by the United States Department of Energy. The Government has certain rights in this invention.

FIELD OF THE INVENTION

The present invention relates to a composite oxygen transport membrane in which catalyst particles, selected to promote oxidation of a combustible substance, are located within an intermediate porous layer that is in turn located between a dense layer and a porous support layer and within the porous support and a method of applying the catalyst to the intermediate porous layer and the porous support layer through wicking of catalyst precursors through the porous support layer to the intermediate porous layer.

BACKGROUND OF THE INVENTION

Oxygen transport membranes function by transporting oxygen ions through a material that is capable of conducting oxygen ions and electrons at elevated temperatures. Such materials can be mixed conducting in that they conduct both oxygen ions and electrons or a mixture of materials that include an ionic conductor capable of primarily conducting oxygen ions and an electronic conductor with the primary function of transporting the electrons. Typical mixed conductors are formed from doped perovskite materials. In case of a mixture of materials, the ionic conductor can be yttrium or scandium stabilized zirconia and the electronic conductor can be a perovskite that will transport electrons, a metal or metal alloy or a mixture of the perovskite, the metal or metal alloy.

When a partial pressure difference of oxygen is applied on opposite sides of such a membrane, oxygen ions will ionize on one surface of the membrane and emerge on the opposite side of the membrane and recombine into elemental oxygen. The free electrons resulting from the combination will be transported back through the membrane to ionize the oxygen. The partial pressure difference can be produced by providing the oxygen containing feed to the membrane at a positive pressure or by supplying a combustible substance to the side of the membrane opposing the oxygen containing feed or a combination of the two methods.

Typically, oxygen transport membranes are composite structures that include a dense layer composed of the mixed conductor or the two phases of materials and one or more porous supporting layers. Since the resistance to oxygen ion transport is dependent on the thickness of the membrane, the dense layer is made as thin as possible and therefore must be supported. Another limiting factor to the performance of an oxygen transport membrane concerns the supporting layers that, although can be active, that is oxygen ion or electron conducting, the layers themselves can consist of a network of interconnected pores that can limit diffusion of the oxygen or fuel or other substance through the membrane to react with the oxygen. Therefore, such support layers are typically fabricated with a graded porosity in which the pore size decreases in a direction taken towards the dense layer or are made highly porous throughout. The high porosity, however, tends to weaken such a structure.

U.S. Pat. No. 7,229,537 attempts to solve such problems by providing a support with cylindrical or conical pores that are not connected and an intermediate porous layer located between the dense layer and the support that distributes the oxygen to the pores within the support. Porous supports can also be made by freeze casting techniques, as described in 10, No. 3, Advanced Engineering Materials, "Freeze-Casting of Porous Ceramics: A Review of Current Achievements and Issues" (2008) by Deville, pp. 155-169. In freeze casting, a liquid suspension is frozen. The frozen liquid phase is then sublimated from a solid to a vapor under reduced pressure. The resulting structure is sintered to consolidate and densify the structure. This leads to a porous structure having pores extending in one direction and that have a low toruosity. Such supports have been used to form electrode layers in solid oxide fuel cells. In addition to the porous support layers, a porous surface exchange layer can be located on the opposite side of the dense layer to enhance reduction of the oxygen into oxygen ions. Such a composite membrane is illustrated in U.S. Pat. No. 7,556,626 that utilizes two phase materials for the dense layer, the porous surface exchange layer and the intermediate porous layer. These layers are supported on a porous support that can be formed of zirconia.

As mentioned above, the oxygen partial pressure difference can be created by combusting a fuel or other combustible substance with the separated oxygen. The resulting heat will heat the oxygen transport membrane up to operational temperature and excess heat can be used for other purposes, for example, heating a fluid, for example, raising steam in a boiler or in the combustible substance itself. While perovskite materials will exhibit a high oxygen flux, such materials tend to be very fragile under operational conditions such as in the heating of a fluid. This is because the perovskite will have a variable stoichiometry with respect to oxygen. In air it will have one value and in the presence of a fuel that is undergoing combustion it will have another value. The end result is that at the fuel side, the material will tend to expand relative to the air side and a dense layer will therefore, tend to fracture. In order to overcome this problem, a mixture of materials can be used in which an ionic conductor is provided to conduct the oxygen ions and an electronic conductor is used to conduct the electrons. Where the ionic conductor is a fluorite, this chemical expansion is restrained, and therefore the membrane will be less susceptible to structural failure. However, the problem with the use of a fluorite, such as a stabilized zirconia, is that such a material has a lower oxygen ion conductivity. As a result, far more oxygen transport membrane elements are required for such a dual phase type of membrane as compared with one that is formed from a single phase perovskite.

As will be discussed, the present invention provides a robust oxygen transport membrane that utilizes a fluorite as an ionic conductor and that incorporates a deposit of a catalyst in an intermediate porous layer located between a dense layer and a porous support to promote oxidation of the combustible substance and thereby increase the oxygen flux that would otherwise have been obtained with the use of a fluorite as an ionic conductor.

SUMMARY OF THE INVENTION

The present invention provides a composite oxygen transport membrane that comprises a membrane element having a plurality of layers that comprise a dense layer, a porous sup-

port and an intermediate porous layer located between the dense layer and the porous support. Each of the dense layer and the intermediate porous layer are capable of conducting oxygen ions and electrons at an elevated operational temperature to separate oxygen from an oxygen containing feed. The dense layer and the intermediate porous layer comprising a mixture of an ionic conductive material and an electrically conductive material to conduct oxygen ions and electrons, respectively. The ionic conductive material is composed of a fluorite. The intermediate porous layer has a lower permeability and a smaller average pore size than the porous support layer to distribute the oxygen separated by the dense layer towards the porous support layer. Catalyst particles or a solution containing precursors of the catalyst particles are located in the intermediate porous layer and in the porous support adjacent to the intermediate porous layer. The catalyst particles contain a catalyst selected to promote oxidation of the combustible substance in the presence of the oxygen when the combustible substance is introduced into the pores of the porous support, on a side thereof opposite to the intermediate porous layer. The membrane element as described above will exhibit an increase in oxygen flux as compared to a membrane employing a dual phase conductor in which the ionic conductor is composed of a fluorite.

The porous support layer can have a permeability of between 0.25 Darcy and about 0.5 Darcy and an average porosity of greater than about 20 percent to inhibit diffusion resistance of a combustible substance through the porous support layer and the combustion products produced through combustion of the combustible substance. Standard procedures for measuring the permeability of a substrate in terms of Darcy number are outlined in ISO 4022.

It is to be noted that the term "combustible substance" as used herein and in the claims means any substance that is capable of being oxidized, including, but not limited, to a fuel in case of a boiler, a hydrocarbon containing substance for purposes of oxidizing such substance for producing a hydrogen and carbon monoxide containing synthesis gas or the synthesis gas itself for purposes of supplying heat to, for example, a reformer. As such the term, "oxidizing" as used herein and in the claims encompasses both partial and full oxidation of the substance.

The porous support layer can be a freeze cast substance. Another possibility is to fabricate the porous support layer with cylindrical or conical pores. The catalyst can be gadolinium doped ceria. Further, the plurality of layers can also comprise a porous surface exchange layer in contact with the dense layer opposite to the intermediate porous layer and the catalyst is gadolinium doped ceria. The support layer is preferably formed from a fluorite, for example 3 mol % yttria stabilized zirconia, or 3YSZ.

In a specific embodiment of the present invention, the intermediate porous layer can have a thickness of between about 10 microns and about 40 microns, a porosity of between about 25 percent and about 40 percent and an average pore diameter of between about 0.5 microns and about 3 microns. The dense layer can have a thickness of between about 10 microns and about 30 microns. The porous surface exchange layer can be provided with a thickness of between about 10 microns and about 40 microns, a porosity of between about 30 percent and about 60 percent and a pore diameter of between about 1 microns and about 4 microns and the support layer can have a thickness of between about 0.5 mm and about 4 mm and a pore size no greater than 50 microns. The intermediate porous layer can contain a mixture of about 60 percent by weight of $(La_{0.825}Sr_{0.175})_{0.96}Cr_{0.76}Fe_{0.225}V_{0.015}O_{3-\delta}$, remainder 10Sc1YSZ, the dense layer can be formed of a mixture of about 40 percent by weight of $(La_{0.825}Sr_{0.175})_{0.94}Cr_{0.72}Mn_{0.26}V_{0.02}O_{3-\delta}$, remainder 10Sc1YSZ and the porous surface exchange layer can be formed by a mixture of about 50 percent by weight of $(La_{0.8}Sr_{0.2})_{0.98}MnO_{3-\delta}$, remainder 10Sc1YSZ. In such case, the support layer is formed from 3YSZ. The support layer can be formed of a freeze cast material that has a permeability of between about 0.25 Darcy and about 0.5 Darcy and pores that are about 3 microns in diameter at a side of the porous support layer that is adjacent to the intermediate porous support and about 10 microns in diameter at the opposite side of the porous support layer.

In another aspect, the present invention provides a method of applying a catalyst to a composite oxygen transport membrane. In accordance with such method, a composite oxygen transport membrane is formed in a sintered state. The composite oxygen transport membrane has a plurality of layers comprising a dense layer, a porous support layer and an intermediate porous layer located between the dense layer and the porous support layer, each of the dense layer and the intermediate porous layer capable of conducting oxygen ions and electrons at an elevated operational temperature to separate oxygen from an oxygen containing feed. The dense layer and the intermediate porous layer comprising a mixture of an ionic conductive material and electrically conductive materials to conduct oxygen ions and electrons, respectively; the ionic conductive material being a fluorite. A solution containing catalyst precursors is applied to the porous support layer on a side thereof opposite to the intermediate porous layer. The catalyst precursors are selected to produce a catalyst upon applying heat to the solution and the catalyst is capable of promoting oxidation of the combustible substance in the presence of the oxygen. Pores within the porous support layer are infiltrated with the solution so that the solution penetrates the pores and also, at least partially infiltrates the intermediate porous layer. The infiltration of the pores is conducted, at least in part, from the solution wicking through the pores, from one side of the porous support layer located opposite to the intermediate porous layer to the other side of the intermediate porous layer located adjacent to the intermediate porous layer. The composite oxygen transport membrane is heated after infiltrating the pores and the intermediate porous layer such that the catalyst is formed from the catalyst precursors.

The porous support layer can have a permeability of between 0.25 Darcy and about 0.5 Darcy and an average porosity of greater than about 20 percent. The porous support layer can be formed by freeze casting. The solution can be an aqueous metal ion solution containing 20 mol % $Gd(NO_3)_3$ and 80 mol % $Ce(NO_3)_3$ that when sintered forms $Gd_{0.8}Ce_{0.2}O_{2-\delta}$. A pressure can be established on the side of the support layer to assist in the infiltration of the solution or the pores can first be evacuated of air using a vacuum to further assist in wicking of the solution and prevent the opportunity of trapped air in the pores preventing wicking of the solution all the way through the support structure to the intermediate layer. The composite oxygen transport membrane can be heated in service or alternatively, can be heated prior to being placed in service. The term "service" as used herein and in the claims means contacting the composite oxygen transport membrane with an oxygen containing substance and a combustible substance and oxidizing the combustible substance with oxygen transported through the membrane to generate the heat.

BRIEF DESCRIPTION OF THE DRAWINGS

While the specification concludes with claims distinctly pointing out the subject matter that Applicants regard as their

invention, it is believed that the invention will be better understood when taken in connection with the accompanying drawings in which:

FIG. **1** is a cross-sectional schematic view of a composite oxygen transport membrane element of the present invention that is fabricated in accordance with a method of the present invention;

FIG. **2** is an alternative embodiment of FIG. **1**; and

FIG. **3** is an alternative embodiment of FIG. **1**.

DETAILED DESCRIPTION

With reference to FIG. **1**, a sectional view of a composite oxygen transport membrane element **1** in accordance with the present invention is illustrated. As could be appreciated by those skilled in the art, such composite oxygen transport membrane element **1** could be in the form of a tube or a flat plate. Such composite oxygen transport membrane element **1** would be one of a series of such elements situated within a device to heat a fluid such as a boiler or other reactor having such a requirement.

Composite oxygen transport membrane element **1** is provided with a dense layer **10**, a porous support layer **12** and an intermediate porous layer **14** located between the dense layer **10** and the porous support layer **12**. A preferable option is, as illustrated, to also include a porous surface exchange layer **16** in contact with the dense layer **10**, opposite to the intermediate porous layer **14**. Catalyst particles **18** are located in the intermediate porous layer **14** that are formed of a catalyst selected to promote oxidation of a combustible substance in the presence of oxygen separated by the composite membrane element **1**.

Operationally, air or other oxygen containing fluid is contacted on one side of the composite oxygen transport membrane element **1** and more specifically, against the porous surface exchange layer **16** in the direction of arrowhead "A". The porous surface exchange layer **16** is porous and is capable of mixed conduction of oxygen ions and electrons and functions to ionize some of the oxygen. The oxygen that is not ionized at and within the porous surface exchange layer **16**, similarly, also ionizes at the adjacent surface of the dense layer **10** which is also capable of such mixed conduction of oxygen ions and electrons. The oxygen ions are transported through the dense layer **10** to intermediate porous layer **14** to be distributed to pores **20** of the porous support layer **12**. Some of the oxygen ions, upon passage through the dense layer will recombine into elemental oxygen. The recombination of the oxygen ions into elemental oxygen is accompanied by the loss of electrons that flow back through the dense layer to ionize the oxygen at the opposite surface thereof.

At the same time, a combustible substance, for example a hydrogen and carbon monoxide containing synthesis gas, is contacted on one side of the porous support layer **12** that is located opposite to the intermediate porous layer **14** as indicated by arrowhead "B". The combustible substance enters pores **20**, contacts the oxygen and burns through combustion supported by the oxygen. The combustion is promoted by the catalyst that is present by way of catalyst particles **18**.

The presence of combustible fuel on the side of the composite oxygen ion transport membrane element **1**, specifically the side of the dense layer **10** located adjacent to the intermediate porous layer **14** provides a lower partial pressure of oxygen. This lower partial pressure drives the oxygen ion transport as discussed above and also generates heat to heat the dense layer **10**, the intermediate porous layer **14** and the porous surface exchange layer **16** up to an operational temperature at which the oxygen ions will be conducted. In specific applications, the incoming oxygen containing stream can also be pressurized to enhance the oxygen partial pressure difference between opposite sides of the composite oxygen ion transport membrane element **1**. Excess heat that is generated by combustion of the combustible substance will be used in the specific application, for example, the heating of water into steam within a boiler or for heating the combustible substance itself for later partial oxidation reactions.

As indicated above, the use of a single phase mixed conducting material such as a perovskite has the disadvantage of exhibiting chemical expansion, or in other words, one side of a layer, at which the oxygen ions recombine into elemental oxygen, will expand relative to the opposite side thereof. This resulting stress can cause failure of such a layer or separation of the layer from adjacent layers. In order to avoid this, the dense layer **10**, the intermediate porous layer **14** and the porous surface exchange layer **16** were all formed of a two phase system comprising a fluorite in one phase as the ionic conductor of the oxygen ions and an electronic conducting phase that in the illustrated embodiment is a perovskite. In the illustrated embodiment, the porous support layer **12** was formed of the fluorite only and as such does not exhibit significant mixed conduction. However, as will be discussed, other materials for a porous support layer are possible such as oxide disbursed strengthened metals or other high strength ceramic materials. The material used in forming the porous support layer **12** preferably has a thermal expansion coefficient in the range 9×10^{-6} cm/cm$\times K^{-1}$ and 12×10^{-6} cm/cm$\times K^{-1}$ in the temperature range of 20° C. to 1000° C.; where "K" is the temperature in Kelvin.

As discussed above, dense layer **10** functions to separate oxygen from an oxygen containing feed exposed to one surface of the oxygen ion transport membrane **10** and contains an electronic and ionic conducting phases. As discussed above, the electronic phase of $(La_uSr_vCe_{1-u-v})_wCr_xMn_yV_zO_{3-\delta}$ ("LSCMV"), where u is from about 0.7 to about 0.9, v is from about 0.1 to about 0.3 and (1-u-v) is greater than or equal to zero, w is from about 0.94 to about 1, x is from about 0.67 to about 0.77, y is from about 0.2 to about 0.3, z is from about 0.015 to about 0.03, and x+y+z=1. The ionic phase is $Zr_{x'}Sc_{y'}A_{z'}O_{2-\delta}$ ("YScZ"), where y' is from about 0.08 to about 0.15, z' is from about 0.01 to about 0.03, x'+y'+z'=1 and A is Y or Ce or mixtures of Y and Ce. The variable "δ" as used in the formulas set forth below for the indicated substances, as would be known in the art would have a value that would render such substances charge neutral. It is to be noted, that since the quantity (1-u-v) can be equal to zero, cerium may not be present within an electronic phase of the present invention. In fact, preferably, the dense layer **10** contains a mixture of about 40 percent by weight of $(La_{0.825}Sr_{0.175})_{0.94}Cr_{0.72}Mn_{0.26}V_{0.02}O_{3-\delta}$, remainder 10Sc1YSZ. As also mentioned above, in order to reduce the resistance to oxygen ion transport, the dense layer should be made as thin as possible and in the illustrated embodiment has a thickness of between about 10 microns and about 30 microns.

Porous surface exchange layer **16** enhances the surface exchange rate by enhancing the surface area of the dense layer **10** while providing a path for the resulting oxygen ions to diffuse through the mixed conducting oxide phase to the dense layer **10** and for oxygen molecules to diffuse through the open pore space to the same. The porous surface exchange layer **16** therefore, reduces the loss of driving force in the surface exchange process and thereby increases the achievable oxygen flux. As indicated above, it also can be a two-phase mixture containing an electronic conductor composed of $(La_{x'''}Sr_{1-x'''})_{y'''}MO_{3-\delta}$, where x''' is from about 0.2 to about 0.9, y''' is from about 0.95 to 1, M=Mn, Fe and an ionic

conductor composed of $Zr_x^{iv}Sc_y^{iv}A_z^{iv}O_{2-\delta}$, where y^{iv} is from about 0.08 to about 0.15, z^{iv} is from about 0.01 to about 0.03, $x^{iv}+y^{iv}+z^{iv}=1$ and A=Y, Ce. In the illustrated embodiment, porous surface exchange layer **16** is formed of a mixture of about 50 percent by weight of $(La_{0.8}Sr_{0.2})_{0.98}MnO_{3-\delta}$, remainder 10Sc1YSZ. The porous surface exchange layer is a porous layer and preferably has a thickness of between about 10 microns and about 40 microns, a porosity of between about 30 percent and about 60 percent and a pore diameter of between about 1 microns and about 4 microns.

The intermediate porous layer **14** is formed of the same mixture as the dense layer **10** and preferably has a thickness of between about 10 microns and about 40 microns, a porosity of between about 25 percent and about 40 percent and an average pore diameter of between about 0.5 microns and about 3 microns. In addition, incorporated within the intermediate porous layer **14** are catalyst particles **18**. Catalyst particles **18** are preferably gadolinium doped ceria ("CGO") that have a size of between about 0.1 and about 1 microns. Preferably, the intermediate porous layer **14** contains a mixture of about 60 percent by weight of $(La_{0.825}Sr_{0.175})_{0.96}Cr_{0.76}Fe_{0.225}V_{0.015}O_{3-\delta}$, remainder 10Sc1YSZ. It is to be noted that intermediate porous layer **14** as compared with the dense layer **10** contains Iron in place of Manganese, a lower A-site deficiency, a lower transition metal (Iron) content on the B-site, and a slightly lower concentration of vanadium on the B-site. It has been found by the inventors herein that the presence of Iron aids combustion in the intermediate porous layer, also that the presence of Manganese at higher concentration and a higher A-site deficiency in the dense layer improves electronic conductivity and sintering kinetics. A higher concentration of vanadium is present in the dense layer because vanadium is a sintering aid, and is required for densification of the dense layer. Vanadium is required in lesser extent in the intermediate porous layer to match shrinkage and expansion characteristics with the dense layer.

The porous support layer **12** can be formed by known freeze casting techniques. Although pores **20** are indicated as being a regular network of non-interconnected pores, in fact there exists some degree of connection between pores **20** towards the intermediate porous layer **14**. Consequently, intermediate porous layer **14** has a tortuosity of greater than 1. However, as indicated previously, the open porous network provided by the porous support layer should be selected so as to promote diffusion of the combustible substance to the intermediate porous layer **14** and the flow of combustion products such as steam and carbon dioxide from the pores **20** in a direction opposite to that of arrowhead "B". The porosity of porous support layer **14** should be greater than about 20 percent both for the embodiment illustrated in FIG. **1** as well as other possible embodiments of the present invention. The porous support layer **12** preferably has a permeability of between about 0.25 Darcy and about 0.5 Darcy. Porous support layer **12** preferably has a thickness of between about 0.5 mm and about 4 mm and a pore size of no greater than 50 microns, again, in any embodiment. This being said, for the freeze cast porous support layer **14**, the permeability preferably between about 0.25 Darcy and about 0.5 Darcy and the pores vary in diameter from about 3 microns at the size of porous support layer **12** adjacent to the intermediate porous layer **14** and about 10 microns at the opposite side of the porous support layer **12**. Porous support layer **12** is fabricated from 3YSZ. Additionally, porous support layer **12** also has catalyst particles **18** located adjacent to the intermediate porous layer **14** within pores **20** for purposes of also promoting combustible substance oxidation. The presence of the catalyst particles **18** both within the intermediate porous layer and within the porous support layer **12** provides enhancement of oxygen flux and therefore generation of more heat that can be obtained by either providing catalyst particles within solely the intermediate porous layer **14** or the porous support layer **12** alone. It is to be noted that to a lesser extent, catalyst particles **18** can also be located in region of the pores **20** that are more remote from the intermediate porous layer **14**, and therefore do not participate in promoting fuel oxidation. However, the bulk of catalyst in a composite oxygen transport element of the present invention is, however, located in the intermediate porous layer **14** and within the pores **20**, adjacent the intermediate porous layer **14**.

With brief reference to FIGS. **2** and **3**, the porous support layers **12'** and **12"** illustrated in such Figures can have cylindrical pores **20'** or conical pores **20"**. Such pores could be formed from E-beam drilling or laser cutting techniques and as such the tortuosity would be equal to 1. Further, such supporting structure could be fabricated from materials such as oxide disbursed strengthened metals or other high strength ceramic materials.

In forming a composite oxygen transport membrane element in accordance with the present invention, the porous support (**12** or **12'** or **12"**) is first formed in a manner known in the art and as set forth in the references discussed above. For example, a freeze cast supporting structure could be formed in the manner discussed in "Freeze-Casting of Porous Ceramics: A Review of Current Achievements and Issues" (2008) by Deville, pp. 155-169 and a porous support having cylindrical or conical pores could be formed as discussed in U.S. Pat. No. 7,229,537. In either of such cases, the porous support could be formed into a tube in a green state and then subjected to a bisque firing at 1050° C. for 4 hours to achieve reasonable strength for further handling. After firing, the resulting tube can be checked for porosity and permeability and stored in a dry oven at about 60° C.

After forming the green tube, intermediate porous layer **14** is then formed. A mixture of about 34 grams of powders having electronic and ionic phases, LSCMV and 10Sc1YSZ, respectively, is prepared so that the mixture contains equal proportions by volume of LSCMV and 10Sc1YSZ. Prior to forming the mixture, the catalyst particles of **18** that can be CGO are so incorporated into the electronic phase LSCMV by forming deposits of such particles on the electronic phase, for example, by precipitation. However, it is more preferable to form the catalyst particles **18** within the intermediate porous layer by wicking a solution containing catalyst precursors through the porous support layer **12** towards the intermediate porous layer **14** as described below. As such, there is no requirement to deposit particles of catalyst on the electronic phase. The electronic phase particles are each about 0.3 microns prior to firing and the catalyst particles are about 0.1 microns or less and are present in a ratio by weight of 10 wt %. To the mixture, 100 grams of toluene, 20 grams of the binder of the type mentioned above, 400 grams of 1.5 mm diameter YSZ grinding media are added. The mixture is then milled for about 6 hours to form a slurry (d_{50} of about 0.34 μm). About 6 grams of carbon black having a particle size of about d50=0.8 μm is then added to the slurry and milled for additional 2 hours. An additional 10 grams of toluene and about 10 grams of additional binder were added to the slurry and mixed for between about 1.5 and about 2 hours. The inner wall of the green tube formed above is then coated by pouring the slurry, holding once for 5 seconds and pouring out the residual back to the bottle. The coated green tube is then dried and fired at 850° C. for 1 hour in air for binder burnout.

The dense layer **10** is then applied. A mixture weighing about 40 grams is prepared that contains the same powders as

used in forming the intermediate porous layer **14**, discussed above, except that the ratio between LSCMV and 10Sc1YSZ is about 40/60 by volume, 2.4 grams of cobalt nitrate {$Co(NO_3)_2.6H_2O$}, 95 grams of toluene, 5 grams of ethanol, 20 grams of the binder identified above, 400 grams of 1.5 mm diameter YSZ grinding media are then added to the mixture and the same is milled for about 10 hours to form a slurry (d_{50}~0.34 μm). Again, about 10 grams of toluene and about 10 grams of binder are added to the slurry and mixed for about 1.5 and about 2 hours. The inner wall of the tube is then coated by pouring the slurry, holding once for 10 seconds and pouring out the residual back to the bottle. The tube is then stored dry prior to firing the layers in a controlled environment.

The coated green tube is then placed on a C-setter in a horizontal tube furnace and porous alumina tubes impregnated with chromium nitrate are placed close to the coated tube to saturate the environment with chromium vapor. The tubes are heated in static air to about 800° C. for binder burnout and the environment is switched to an atmosphere of a saturated nitrogen mixture (nitrogen and water vapor) that contains about 4 percent by volume of hydrogen to allow the vanadium containing electronic conducting perovskites to properly sinter. The tube is held at about 1350° C. to 1400° C. for 8 hours and then cooled in nitrogen to complete the sintering of the materials. The sintered tube is checked for helium leak rates that should be lower than 10^{-7} Pa.

Surface exchange layer **16** is then applied. A mixture of powders is prepared that contains about 35 g of equal amounts of ionic and electronic phases having chemical formulas of $Zr_{0.89}Sc_{0.1}Y_{0.01}O_{2-\delta}$ and $La_{0.8}Sr_{0.2}FeO_{3-\delta}$, respectively. To this mixture, about 100 grams of toluene, 20 grams of the binder identified above, about 400 grams of 1.5 mm diameter YSZ grinding media are added and the resultant mixture is milled for about 14 hours to form a slurry (d_{50}~0.4 μm). About six grams of carbon black are added to the slurry and milled for additional 2 hours. A mixture of about 10 grams of toluene and about 10 grams of the binder are then added to the slurry and mixed for between about 1.5 and about 2 hours. The inner wall of the tube is then coated by pouring the slurry, holding twice for about 10 seconds and then pouring out the residual back to the bottle. The coated tube is then dried and fired at 1100° C. for two hours in air.

The structure formed in the manner described above is in a fully sintered state and the catalyst is then further applied by wicking a solution containing catalyst precursors in the direction of arrowhead B at the side of the porous support **12** opposite to the intermediate porous layer **14**. The solution can be an aqueous metal ion solution containing 20 mol % $Gd(NO_3)_3$ and 80 mol % $Ce(NO_3)_3$. A pressure can be established on the side of the support layer to assist in the infiltration of the solution or the pores can first be evacuated of air using a vacuum to further assist in wicking of the solution and prevent the opportunity of trapped air in the pores preventing wicking of the solution all the way through the support structure to the intermediate porous layer **14**. The resulting composite oxygen transport membrane **1** in such state can be directly placed into service or further fired prior to being placed into service so that the particles **18**, in this case $Ce_{0.8}Gd_{0.2}O_{2-\delta}$, are formed in the porous support **12** adjacent to the intermediate porous layer **14** and as described above, within the intermediate porous layer **14** itself. The firing to form $Ce_{0.8}Gd_{0.2}O_{2-\delta}$ would take place at a temperature of about 850° C. and would take about 1 hour to form the particles **18**.

Although the present invention has been described with reference to a preferred embodiment, as will occur to those skilled in the art, changes and additions to such embodiment can be made without departing from the spirit and scope of the present invention as set forth in the appended claims.

We claim:

1. A composite oxygen transport membrane, said composite oxygen transport membrane comprising:

a membrane element having a plurality of layers;

the plurality of layers comprising a dense layer, a porous support layer and an intermediate porous layer located between the dense layer and the porous support layer, each of the dense layer and the intermediate porous layer capable of conducting oxygen ions and electrons at an elevated operational temperature to separate oxygen from an oxygen containing feed;

the dense layer and the intermediate porous layer comprising a mixture of an ionic conductive material and electrically conductive materials to conduct oxygen ions and electrons, respectively, the ionic conductive material being a fluorite;

the intermediate porous layer having a smaller average pore size than the porous support layer to distribute the oxygen separated by the dense layer towards the porous support layer; and

catalyst particles or a solution containing precursors of the catalyst particles located in the intermediate porous layer and in the porous support adjacent to the intermediate porous layer, the catalyst particles containing of a catalyst selected to promote oxidation of a combustible substance in the presence of the oxygen when the combustible substance is introduced into the pores of the porous support, on a side thereof opposite to the intermediate porous layer.

2. The composite oxygen transport membrane element of claim **1**, wherein said porous support layer has a permeability of between 0.25 Darcy and 0.5 Darcy, an average porosity of greater than about 20 percent.

3. The composite oxygen transport membrane of claim **2**, wherein said porous support layer is a freeze cast substance.

4. The composite oxygen transport membrane of claim **1**, wherein said porous support layer has cylindrical or conical pores.

5. The composite oxygen transport membrane of claim **1** or claim **2** or claim **3** or claim **4**, wherein the catalyst is gadolinium doped ceria.

6. The composite oxygen transport membrane of claim **1**, wherein the plurality of layers also comprise a porous surface exchange layer in contact with the dense layer opposite to the intermediate porous layer and the catalyst is gadolinium doped ceria.

7. The composite oxygen transport membrane of claim **6**, wherein the support layer is formed from a flourite.

8. The composite oxygen transport membrane of claim **6**, wherein:

the intermediate porous layer has a thickness of between about 10 microns and about 40 microns, a porosity of between about 25 percent and about 40 percent and an average pore diameter of between about 0.5 microns and about 3 microns;

the dense layer has a thickness of between about 10 microns and about 30 microns;

the porous surface exchange layer has a thickness of between about 10 microns and about 40 microns, a porosity of between about 30 percent and about 60 percent and a pore diameter of between about 1 microns and about 4 microns; and

the porous support layer has a thickness of between about 0.5 mm and about 4 mm and a pore size no greater than 50 microns.

9. The composite oxygen transport membrane of claim 8, wherein:

the intermediate porous layer contains a mixture of about 60 percent by weight of $(La_{0.825}Sr_{0.175})_{0.96}Cr_{0.76}Fe_{0.225}V_{0.015}O_{3-\delta}$, remainder 10Sc1YSZ;

the dense layer contains a mixture of about 40 percent by weight of $(La_{0.825}Sr_{0.175})_{0.94}Cr_{0.72}Mn_{0.26}V_{0.02}O_{3-\delta}$, remainder 10Sc1YSZ;

the porous surface exchange layer is formed by a mixture of about 50 percent by weight of $(La_{0.8}Sr_{0.2})_{0.98}MnO_{3-\delta}$, remainder 10Sc1YSZ; and

the support layer is formed from 3YSZ.

10. The composite oxygen transport membrane of claim 9, wherein the porous support layer is formed of a freeze cast substance that has a ratio of the permeability of between 0.25 Darcy and about 0.5 Darcy and pores that are about 3 microns in diameter at a side of the porous support layer adjacent to the intermediate porous layer and about 10 microns in diameter at the opposite side of the porous support layer.

11. A method of applying a catalyst to a composite oxygen transport membrane, said method comprising:

forming a composite oxygen transport membrane in a sintered state, said composite oxygen transport membrane having a plurality of layers comprising a dense layer, a porous support layer and an intermediate porous layer located between the dense layer and the porous support layer, each of the dense layer and the intermediate porous layer capable of conducting oxygen ions and electrons at an elevated operational temperature to separate oxygen from an oxygen containing feed;

the dense layer and the intermediate porous layer comprising a mixture of an ionic conductive material and an electrically conductive materials to conduct oxygen ions and electrons, respectively, the ionic conductive material being a fluorite;

applying a solution containing catalyst precursors to the porous support layer on a side thereof opposite to the intermediate porous layer, the catalyst precursors selected to produce a catalyst, upon applying heat to the solution and the catalyst capable of promoting oxidation of the combustible substance in the presence of the oxygen;

infiltrating pores within the porous support layer with the solution so that the solution penetrates the pores and also, at least partially infiltrates the intermediate porous layer;

the infiltrating of the pores being conducted, at least in part, from the solution wicking through the pores, from one side of the porous support layer located opposite to the intermediate porous layer to the other side of the porous support layer located adjacent to the intermediate porous layer; and

heating the composite oxygen transport membrane after infiltrating the pores and the intermediate porous layer such that the catalyst is formed from the catalyst precursors.

12. The method of claim 11, wherein said porous support layer having a permeability of between 0.25 Darcy and about 0.5 Darcy and an average porosity of greater than about 20 percent.

13. The method of claim 11, wherein the support layer is formed by freeze casting.

14. The method of claim 11, wherein the pores of the support layer are of cylindrical or conical configuration.

15. The method of claim 12 or claim 13, wherein the solution is an aqueous metal ion solution containing 20 mol % $Gd(NO_3)_3$ and 80 mol % $Ce(NO_3)_3$ that when sintered forms $Gd_{0.8}Ce_{0.2}O_{2-\delta}$.

16. The method of claim 14, wherein a pressure is established on the second side of the support layer to assist in the infiltration of the solution or the pores can first be evacuated of air using a vacuum to further assist in wicking of the solution and prevent the opportunity of trapped air in the pores preventing wicking of the solution all the way through the support structure to the intermediate layer.

17. The method of claim 11, wherein the composite oxygen transport membrane is heated in service.

18. The method of claim 11, wherein the composite oxygen transport membrane is heated prior to being placed in service.

* * * * *

CATALYST CONTAINING OXYGEN TRANSPORT MEMBRANE

Cross Reference to Related Applications

[0001] The present application is a continuation-in part application of U.S. Patent Application Serial Number 12/968,699; filed December 15, 2010, which is incorporated by reference herein in its entirety.

U.S. Government Rights

[0002] The invention disclosed and claimed herein was made with United States Government support under Cooperative Agreement number DE-FC26-07NT43088 awarded by the U.S. Department of Energy. The United States Government has certain rights in this invention.

Field of the Invention

[0003] The present invention relates to a composite oxygen transport membrane in which catalyst particles, selected to promote oxidation of a combustible substance, are located within an intermediate porous layer that is in turn located between a dense layer and a porous support layer and within the porous support and a method of applying the catalyst to the intermediate porous layer and the porous support layer through wicking of catalyst precursors through the porous support layer to the intermediate porous layer.

Background

[0004] Oxygen transport membranes function by transporting oxygen ions through a material that is capable of conducting oxygen ions and electrons at elevated temperatures. Such materials can be mixed conducting in that they conduct both oxygen ions and electrons or a mixture of materials that include an ionic conductor capable of primarily conducting oxygen ions and an electronic conductor with the primary function of transporting the electrons. Typical mixed conductors are formed from doped perovskite structured materials. In case of a mixture of materials, the ionic conductor can be yttrium or scandium stabilized

zirconia and the electronic conductor can be a perovskite structured material that will transport electrons, a metal or metal alloy or a mixture of the perovskite type material, the metal or metal alloy.

[0005] When a partial pressure difference of oxygen is applied on opposite sides of such a membrane, oxygen ions will ionize on one surface of the membrane and emerge on the opposite side of the membrane and recombine into elemental oxygen. The free electrons resulting from the combination will be transported back through the membrane to ionize the oxygen. The partial pressure difference can be produced by providing the oxygen containing feed to the membrane at a positive pressure or by supplying a combustible substance to the side of the membrane opposing the oxygen containing feed or a combination of the two methods.

[0006] Typically, oxygen transport membranes are composite structures that include a dense layer composed of the mixed conductor or the two phases of materials and one or more porous supporting layers. Since the resistance to oxygen ion transport is dependent on the thickness of the membrane, the dense layer is made as thin as possible and therefore must be supported. Another limiting factor to the performance of an oxygen transport membrane concerns the supporting layers that, although can be active, that is oxygen ion or electron conducting, the layers themselves can consist of a network of interconnected pores that can limit diffusion of the oxygen or fuel or other substance through the membrane to react with the oxygen. Therefore, such support layers are typically fabricated with a graded porosity in which the pore size decreases in a direction taken towards the dense layer or are made highly porous throughout. The high porosity, however, tends to weaken such a structure.

[0007] U.S. Patent No. 7,229,537 attempts to solve such problems by providing a support with cylindrical or conical pores that are not connected and an intermediate porous layer located between the dense layer and the support that distributes the oxygen to the pores within the support. Porous supports can also be made by freeze casting techniques, as described in 10, No. 3, Advanced Engineering Materials, “Freeze-Casting of Porous Ceramics: A Review of

Current Achievements and Issues" (2008) by Deville, pp. 155-169. In freeze casting, a liquid suspension is frozen. The frozen liquid phase is then sublimated from a solid to a vapor under reduced pressure. The resulting structure is sintered to consolidate and densify the structure. This leads to a porous structure having pores extending in one direction and that have a low toruosity. Such supports have been used to form electrode layers in solid oxide fuel cells. In addition to the porous support layers, a porous surface exchange layer can be located on the opposite side of the dense layer to enhance reduction of the oxygen into oxygen ions. Such a composite membrane is illustrated in US Patent No. 7,556,676 that utilizes two phase materials for the dense layer, the porous surface exchange layer and the intermediate porous layer. These layers are supported on a porous support that can be formed of zirconia.

[0008] As mentioned above, the oxygen partial pressure difference can be created by combusting a fuel or other combustible substance with the separated oxygen. The resulting heat will heat the oxygen transport membrane up to operational temperature and excess heat can be used for other purposes, for example, heating a fluid, for example, raising steam in a boiler or in the combustible substance itself. While perovskite structured materials will exhibit a high oxygen flux, such materials tend to be very fragile under operational conditions such as in the heating of a fluid. This is because the perovskite type materials will have a variable stoichiometry with respect to oxygen. In air it will have one value and in the presence of a fuel that is undergoing combustion it will have another value. The end result is that at the fuel side, the material will tend to expand relative to the air side and a dense layer will therefore, tend to fracture. In order to overcome this problem, a mixture of materials can be used in which an ionic conductor is provided to conduct the oxygen ions and an electronic conductor is used to conduct the electrons. Where the ionic conductor is a fluorite structured material, this chemical expansion is restrained, and therefore the membrane will be less susceptible to structural failure. However, the problem with the use of a fluorite structure material, such as a stabilized zirconia, is that such a material has lower oxygen ion conductivity. As a result, far more oxygen transport membrane

elements are required for such a dual phase type of membrane as compared with one that is formed from a single phase perovskite type material.

[0009] As will be discussed, the present invention provides a robust oxygen transport membrane that utilizes a material having a fluorite structure as an ionic conductor and that incorporates a deposit of a catalyst in an intermediate porous layer located between a dense layer and a porous support to promote oxidation of the combustible substance and thereby increase the oxygen flux that would otherwise have been obtained with the use of a fluorite structured material as an ionic conductor.

Summary of the Invention

[0010] The present invention may be characterized as a composite oxygen transport membrane comprising (i) a porous support layer comprised of an fluorite structured ionic conducting material having a porosity of greater than 20 percent and a microstructure exhibiting substantially uniform pore size distribution throughout the porous support layer; (ii) an intermediate porous layer often referred to as a fuel oxidation layer disposed adjacent to the porous support layer and capable of conducting oxygen ions and electrons to separate oxygen from an oxygen containing feed and comprising a mixture of a fluorite structured ionic conductive material and electrically conductive materials to conduct the oxygen ions and electrons, respectively; (iii) a dense separation layer capable of conducting oxygen ions and electrons to separate oxygen from an oxygen containing feed, the dense layer adjacent to the intermediate porous layer and also comprising a mixture of a fluorite structured ionic conductive material and electrically conductive materials to conduct the oxygen ions and electrons, respectively; and (iv) catalyst particles or a solution containing precursors of the catalyst particles located in pores of the porous support layer and intermediate porous layer, the catalyst particles containing a catalyst selected to promote oxidation of a combustible substance in the presence of the separated oxygen transported through the dense layer and the intermediate porous layer to the porous support layer. The catalyst is preferably gadolinium doped ceria but may

also be other catalysts that promote fuel oxidation. The composite oxygen transport membrane may also include a porous surface exchange layer or an air activation layer disposed or applied to the dense separation layer on the side opposite to the intermediate porous layer or the fuel oxidation layer. If used, the porous surface exchange layer or an air activation layer preferably has a thickness of between 10 and 40 microns and a porosity of between about 30 and 60 percent.

[0011] The intermediate porous layer or fuel oxidation layer preferably has a thickness of between about 10 and 40 microns and a porosity of between about 20 and 50 percent whereas the dense layer has a thickness of between 10 and 50 microns. The porous support layer may be formed from a mixture comprising 3mol% yttria stabilized zirconia, or 3YSZ and a polymethyl methacrylate based pore forming material or a mixture comprising 3YSZ having a bi-modal or multimodal particle size distribution. In either embodiment, the porous support layer has a preferred thickness of between about 0.5 and 4 mm and porosity between about 20 and 40 percent.

[0012] Broadly characterizing the preferred embodiments of the composite oxygen transport membrane, the intermediate porous layer comprises a mixture of about 60 percent by weight of $(La_uSr_vCe_{1-u-v})_wCr_xM_yV_zO_{3-\delta}$ with the remainder $Zr_{x'}Sc_{y'}A_{z'}O_{2-\delta}$. Similarly, the dense separation layer comprises a mixture of about 40 percent by weight of $(La_uSr_vCe_{1-u-v})_wCr_xM_yV_zO_{3-\delta}$ with the remainder $Zr_{x'}Sc_{y'}A_{z'}O_{2-\delta}$. In the above formulations, u is from 0.7 to 0.9, v is from 0.1 to 0.3 and (1-u-v) is greater than or equal to zero, w is from 0.94 to 1, x is from 0.5 to 0.77, M is Mn or Fe, y is from 0.2 to 0.5, z is from 0 to 0.03, and x+y+z =1, where y' is from 0.08 to 0.3, z' is from 0.01 to 0.03, x'+y'+z'=1 and A is Y or Ce or mixtures of Y and Ce. The porous surface exchange layer or air activation layer, if employed, can be is formed by a mixture of about 50 percent by weight of $(La_{x'''}Sr_{1-x'''})_{y'''}MO_{3-\delta}$, where x''' is from 0.2 to 0.9, y''' is from 0.95 to 1, M is Mn or Fe, with the remainder $Zr_x^{iv}Sc_y^{iv}A_z^{iv}O_{2-\delta}$, where y^{iv} is from 0.08 to 0.3, z^{iv} is from 0.01 to 0.03, $x^{iv}+y^{iv}+z^{iv}=1$ and A is Y, Ce or mixtures thereof.

[0013] More specifically, one of the preferred embodiments of the composite oxygen transport membrane includes an intermediate porous layer or fuel oxidation layer that comprises about 60 percent by weight of $(La_{0.825}Sr_{0.175})_{0.96}Cr_{0.76}Fe_{0.225}V_{0.015}O_{3-\delta}$ or $(La_{0.8}Sr_{0.2})_{0.95}Cr_{0.7}Fe_{0.3}O_{3-\delta}$ with the remainder 10Sc1YSZ or 10Sc1CeSZ. Similarly, the dense separation layer comprises about 40 percent by weight of $(La_{0.825}Sr_{0.175})_{0.94}Cr_{0.72}Mn_{0.26}V_{0.02}O_{3-\delta}$ or $(La_{0.8}Sr_{0.2})_{0.95}Cr_{0.5}Fe_{0.5}O_{3-\delta}$, with the remainder 10Sc1YSZ or 10Sc1CeYSZ. The porous surface exchange layer or air activation layer is formed by a mixture of about 50 percent by weight of $(La_{0.8}Sr_{0.2})_{0.98}MnO_{3-\delta}$ or $La_{0.8}Sr_{0.2}FeO_{3-\delta}$, remainder 10Sc1YSZ or 10Sc1CeSZ.

[0014] The present invention may also be characterized as a product by process wherein the product is a composite oxygen transport membrane. The process comprises: (i) fabricating a porous support layer comprised of an fluorite structured ionic conducting material, the fabricating step including pore forming enhancement step such that the porous support layer has a porosity of greater than about 20 percent and a microstructure exhibiting substantially uniform pore size distribution throughout the porous support layer; (ii) applying an intermediate porous layer or fuel oxidation layer on the porous support layer, (iii) applying a dense separation layer on the intermediate porous layer; and (iv) introducing catalyst particles or a solution containing precursors of the catalyst particles to the porous support layer and intermediate porous layer, the catalyst particles containing a catalyst selected to promote oxidation of a combustible substance in the presence of the separated oxygen transported through the dense layer and the intermediate porous layer to the porous support layer.

[0015] Both the intermediate porous layer and dense separation layer are capable of conducting oxygen ions and electrons to separate oxygen from an oxygen containing feed. Both layers comprise a mixture of a fluorite structured ionic conductive material and electrically conductive materials to conduct the oxygen ions and electrons, respectively.

[0016] The pore forming enhancement process involves several alternative techniques including mixing a polymethyl methacrylate based pore forming

material with the fluorite structured ionic conducting material of the porous support layer. In addition or alternatively, the pore forming enhancement process may further involve use of bi-modal or multi-modal particle sizes of the polymethyl methacrylate based pore forming material and/or the fluorite structured ionic conducting material of the porous support layer.

[0017] The step of introducing catalyst particles or a solution containing precursors of the catalyst particles to the porous support layer and intermediate porous layer may further comprise either: (a) adding catalyst particles directly to the mixture of materials used in the intermediate porous layer; or (b) applying a solution containing catalyst precursors to the porous support layer on a side thereof opposite to the intermediate porous layer so that the solution infiltrates or impregnates the pores within the porous support layer and the intermediate porous layer with the solution containing catalyst precursors and heating the composite oxygen transport membrane after the solution containing catalyst precursors infiltrates the pores and to form the catalyst from the catalyst precursors.

[0018] Finally, the present invention may also be characterized as a method of producing a catalyst containing composite oxygen transport membrane comprising the steps of: (i) forming a composite oxygen transport membrane in a sintered state, said composite oxygen transport membrane having a plurality of layers comprising a dense separation layer, a porous support layer, and an intermediate porous layer (i.e. fuel oxidation layer) located between the dense separation layer and the porous support layer; (ii) applying a solution containing catalyst precursors to the porous support layer on a side thereof opposite to the intermediate porous layer, the catalyst precursors selected to produce a catalyst capable of promoting oxidation of the combustible substance in the presence of the separated oxygen; (iii) infiltrating or impregnating the porous support layer with the solution so that the solution wicks through the pores of the porous support layer and at least partially infiltrates or impregnates the intermediate porous layer (i.e. fuel oxidation layer), and (iv) heating the composite oxygen transport membrane after infiltrating the pores within the porous support layer and the intermediate porous layer such that the catalyst is formed from the catalyst

precursors. Preferably, the catalyst is gadolinium doped ceria and the solution is an aqueous metal ion solution containing about 20 mol% $Gd(NO_3)_3$ and 80 mol% $Ce(NO_3)_3$ that when sintered forms $Gd_{0.8}Ce_{0.2}O_{2-\delta}$.

[0019] Each of the dense layer and the intermediate porous layer capable of conducting oxygen ions and electrons at an elevated operational temperature to separate oxygen from an oxygen containing feed. The dense layer and the intermediate porous layer comprising mixtures of a fluorite structured ionic conductive material and electrically conductive materials to conduct oxygen ions and electrons, respectively.

[0020] The porous support layer comprising a fluorite structured ionic conducting material having a porosity of greater than about 20 percent and a microstructure exhibiting substantially uniform pore size distribution throughout the porous support layer. Pores are formed within the porous support layer using a polymethyl methacrylate based pore forming material mixed with the 3YSZ material of the porous support layer. In addition or alternatively, the pores may be formed using bi-modal or multi-modal particle sizes of the polymethyl methacrylate based pore forming material and/or the 3YSZ material of the porous support layer.

[0021] To aid in the infiltration or impregnation process, a pressure may be established on the second side of the porous support layer or the pores of the porous support layer and fuel oxidation layer may first be evacuated of air using a vacuum to further assist in wicking of the solution and prevent the opportunity of trapped air in the pores preventing wicking of the solution all the way through the support structure to the intermediate layer.

Brief Description of the Drawings

[0022] While the specification concludes with claims distinctly pointing out the subject matter that Applicants regard as their invention, it is believed that the invention will be better understood when taken in connection with the accompanying drawings in which:

[0023] Fig. 1 is a cross-sectional schematic view of a composite oxygen transport membrane element of the present invention that is fabricated in accordance with a method of the present invention;

[0024] Fig. 2 is an alternative embodiment of Fig. 1;

[0025] Fig. 3 is an alternative embodiment of Fig. 1;

[0026] Fig. 4 is an SEM micrograph image at 1000x magnification showing a porous support layer comprised of 3YSZ with walnut shells as the pore forming material;

[0027] Fig. 5 is an SEM micrograph image at 1000x magnification showing a porous support layer comprised of 3YSZ with a polymethyl methacrylate (PMMA) based pore forming material in accordance with the present invention;

[0028] Fig. 6 is another SEM micrograph image at 2000x magnification showing a porous support layer comprised of 3YSZ with a polymethyl methacrylate (PMMA) based pore forming material in accordance with the present invention; and

[0029] Fig. 7 is an SEM micrograph image at 2000x magnification showing a porous support layer comprised of 3YSZ with multi-modal particle sizes in accordance with the present invention.

Detailed Description

[0030] With reference to Fig. 1, a sectional view of a composite oxygen transport membrane element 1 in accordance with the present invention is illustrated. As could be appreciated by those skilled in the art, such composite oxygen transport membrane element 1 could be in the form of a tube or a flat plate. Such composite oxygen transport membrane element 1 would be one of a series of such elements situated within a device to heat a fluid such as in a boiler or other reactor having such a heating requirement.

[0031] Composite oxygen transport membrane element 1 is provided with a dense layer 10, a porous support layer 12 and an intermediate porous layer 14 located between the dense layer 10 and the porous support layer 12. A preferable option is, as illustrated, to also include a porous surface exchange layer 16 in contact

with the dense layer 10, opposite to the intermediate porous layer 14. Catalyst particles 18 are located in the intermediate porous layer 14 that are formed of a catalyst selected to promote oxidation of a combustible substance in the presence of oxygen separated by the composite membrane element 1. It is to be noted that the term "combustible substance" as used herein and in the claims means any substance that is capable of being oxidized, including, but not limited, to a fuel in case of a boiler, a hydrocarbon containing substance for purposes of oxidizing such substance for producing a hydrogen and carbon monoxide containing synthesis gas or the synthesis gas itself for purposes of supplying heat to, for example, a reformer. As such the term, "oxidizing" as used herein and in the claims encompasses both partial and full oxidation of the substance.

[0032] Operationally, air or other oxygen containing fluid is contacted on one side of the composite oxygen transport membrane element 1 and more specifically, against the porous surface exchange layer 16 in the direction of arrowhead "A". The porous surface exchange layer 16 is porous and is capable of mixed conduction of oxygen ions and electrons and functions to ionize some of the oxygen. The oxygen that is not ionized at and within the porous surface exchange layer 16, similarly, also ionizes at the adjacent surface of the dense layer 10 which is also capable of such mixed conduction of oxygen ions and electrons. The oxygen ions are transported through the dense layer 10 to intermediate porous layer 14 to be distributed to pores 20 of the porous support layer 12. It should be noted that in Figs. 1-3, the pores 20 within the porous support layer 12 are shown in an exaggerated manner. Some of the oxygen ions, upon passage through the dense layer will recombine into elemental oxygen. The recombination of the oxygen ions into elemental oxygen is accompanied by the loss of electrons that flow back through the dense layer to ionize the oxygen at the opposite surface thereof.

[0033] At the same time, a combustible substance, for example a hydrogen and carbon monoxide containing synthesis gas, is contacted on one side of the porous support layer 12 located opposite to the intermediate porous layer 14 as indicated by arrowhead "B". The combustible substance enters pores 20, contacts the

oxygen and burns through combustion supported by oxygen. The combustion is promoted by the catalyst that is present by way of catalyst particles 18.

[0034] The presence of combustible fuel on the side of the composite oxygen ion transport membrane element 1, specifically the side of the dense layer 10 located adjacent to the intermediate porous layer 14 provides a lower partial pressure of oxygen. This lower partial pressure drives the oxygen ion transport as discussed above and also generates heat to heat the dense layer 10, the intermediate porous layer 14 and the porous surface exchange layer 16 up to an operational temperature at which the oxygen ions will be conducted. In specific applications, the incoming oxygen containing stream can also be pressurized to enhance the oxygen partial pressure difference between opposite sides of the composite oxygen ion transport membrane element 1. Excess heat that is generated by combustion of the combustible substance will be used in the specific application, for example, the heating of water into steam within a boiler or to meet the heating requirements for other endothermic reactions.

[0035] In the embodiments described with reference to Figs. 1-3, the use of a single phase mixed conducting material such as a perovskite structured materials has the disadvantage of exhibiting chemical expansion, or in other words, one side of a layer, at which the oxygen ions recombine into elemental oxygen, will expand relative to the opposite side thereof. This resulting stress can cause failure of such a layer or separation of the layer from adjacent layers. In order to avoid this, the dense layer, the intermediate porous layer, and the porous surface exchange layer were all formed of a two phase system comprising a fluorite structured material in one phase as the ionic conductor of the oxygen ions and an electronic conducting phase that in the illustrated embodiment is a perovskite type material. In the described embodiments, the porous support layer 12, 12', 12'' have a thickness of between about 0.5 mm and about 4.0 mm, and more preferably about 1.0 mm and are preferably formed of a fluorite structured material only with a PMMA based pore former material. As such, the porous support layers 12; 12' and 12'' preferably do not exhibit significant mixed conduction. The material used in forming the porous support layer preferably

have a thermal expansion coefficient in the range 9 x 10^{-6} cm/cm x K^{-1} and 12 x 10^{-6} cm/cm x K^{-1} in the temperature range of 20ºC to 1000ºC; where "K" is the temperature in Kelvin.

[0036] As discussed above, dense layers 10, 10', 10'' or dense separation layers function to separate oxygen from an oxygen containing feed exposed to one surface of the oxygen ion transport membrane 10 and contains an electronic and ionic conducting phases. The dense separation layer also serves as a barrier of sorts to prevent mixing of the fuel on one side of the membrane with the air or oxygen containing feed stream on the other side of the membrane. As discussed above, the electronic phase in the dense layer is $(La_uSr_vCe_{1-u-v})_wCr_xM_yV_zO_{3-\delta}$ where u is from about 0.7 to about 0.9, v is from about 0.1 to about 0.3 and (1-u-v) is greater than or equal to zero, w is from about 0.94 to about 1, x is from about 0.5 to about 0.77, M is Mn or Fe, y is from about 0.2 to about 0.5, z is from about 0 to about 0.03, and x+y+z =1 ("LSCMV"). The ionic phase is $Zr_{x'}Sc_{y'}A_{z'}O_{2-\delta}$ ("YScZ"), where y' is from about 0.08 to about 0.3, z' is from about 0.01 to about 0.03, x'+y'+z'=1 and A is Y or Ce or mixtures of Y and Ce. The variable "δ" as used in the formulas set forth below for the indicated substances, as would be known in the art would have a value that would render such substances charge neutral. It is to be noted, that since the quantity (1-u-v) can be equal to zero, cerium may not be present within an electronic phase of the present invention. Preferably, the dense separation layer contains a mixture of 40 percent by weight $(La_{0.8}Sr_{0.2})_{0.95}Cr_{0.5}Fe_{0.5}O_{3-\delta}$, remainder 10Sc1CeYSZ; or alternatively about 40 percent by weight of $(La_{0.825}Sr_{0.175})_{0.94}Cr_{0.72}Mn_{0.26}V_{0.02}O_{3-\delta}$, remainder 10Sc1YSZ. As also mentioned above, in order to reduce the resistance to oxygen ion transport, the dense layer should be made as thin as possible and in the described embodiment has a thickness of between about 10 microns and about 50 microns.

[0037] Porous surface exchange layers 16, 16', 16'' or air activation layers are designed to enhance the surface exchange rate by enhancing the surface area of the dense layers 10, 10', 10'' while providing a path for the resulting oxygen ions to diffuse through the mixed conducting oxide phase to the dense layer and for oxygen molecules to diffuse through the open pore spaces to the same. The

porous surface exchange layer 16, 16', 16'' therefore, reduces the loss of driving force in the surface exchange process and thereby increases the achievable oxygen flux. As indicated above, it also can be a two-phase mixture containing an electronic conductor composed of $(La_{x'''}Sr_{1-x'''})_{y'''}MO_{3-\delta}$, where x''' is from about 0.2 to about 0.9, y''' is from about 0.95 to 1, M is Mn or Fe; and an ionic conductor composed of $Zr_x^{iv}\,Sc_y^{iv}A_z^{iv}O_{2-\delta}$, where y^{iv} is from about 0.08 to about 0.3, z^{iv} is from about 0.01 to about 0.03, $x^{iv}+y^{iv}+z^{iv}=1$ and A is Y, Ce or mixtures of Y and Ce. In the described embodiments, porous surface exchange layer is formed of a mixture of about 50 percent by weight of $(La_{0.8}Sr_{0.2})_{0.98}MnO_{3-\delta}$, remainder 10Sc1YSZ. The porous surface exchange layer is a porous layer and preferably has a thickness of between about 10 microns and about 40 microns, a porosity of between about 30 percent and about 60 percent and an average pore diameter of between about 1 microns and about 4 microns.

[0038] The intermediate porous layer 14, 14', 14'' is a fuel oxidation layer and is a preferably formed of the same mixture as the dense layer 10, 10', 10'' and preferably has an applied thickness of between about 10 microns and about 40 microns, a porosity of between about 25 percent and about 40 percent and an average pore diameter of between about 0.5 microns and about 3 microns.

[0039] In addition, incorporated within the intermediate porous layer 14, 14', 14'' are catalyst particles 18, 18', 18''. The catalyst particles 18, 18', 18'' in the described embodiments are preferably gadolinium doped ceria ("CGO") that have a size of between about 0.1 and about 1 microns. Preferably, the intermediate porous layers contain a mixture of about 60 percent by weight of $(La_{0.825}Sr_{0.175})_{0.96}Cr_{0.76}Fe_{0.225}V_{0.015}O_{3-\delta}$, remainder 10Sc1YSZ. It is to be noted that intermediate porous layer as compared with the dense layer preferably may contain iron in lieu of or in place of manganese, a lower A-site deficiency, a lower transition metal (iron) content on the B-site, and a slightly lower concentration of vanadium on the B-site. It has been found that the presence of iron in the intermediate porous layer aids the combustion process and that the presence of manganese at higher concentration and a higher A-site deficiency in the dense layer improves electronic conductivity and sintering kinetics. If needed, a higher

concentration of vanadium should be present in the dense layer because vanadium functions as a sintering aid, and is required to promote densification of the dense layer. Vanadium, if any, is required in lesser extent in the intermediate porous layer in order to match the shrinkage and thermal expansion characteristics with the dense layer.

[0040] The porous support layer 12, 12', 12'' can be formed from a past mixture by known forming techniques including extrusion techniques and freeze casting techniques. Although pores 20, 20', 20'' in the porous support layer are indicated as being a regular network of non-interconnected pores, in fact there exists some degree of connection between pores towards the intermediate porous layer. In any event, the porous network and microstructure of the porous support layer should be controlled so as to promote or optimize the diffusion of the combustible substance to the intermediate porous layer and the flow of combustion products such as steam and carbon dioxide from the pores in a direction opposite to that of arrowhead "B". The porosity of porous support layers 14, 14', 14'' should preferably be greater than about 20 percent for the described embodiment as well as other possible embodiments of the present invention.

[0041] The porous support layers 12, 12', 12'' are preferably fabricated from 3YSZ material commercially available from various suppliers including Tosoh Corporation and its affiliates, including Tosoh USA, with an address at 3600 Gantz Road, Grove City, Ohio. Advancements in the performance of the porous support layers have been realized when combining the Tosoh 3YSZ materials with fugitive organic pore former materials, specifically polymethyl methacrylate (PMMA). In the preferred embodiments, the porous support layer 12, 12', 12'' are preferably fabricated from 67wt% 3YSZ mixed together with 33wt% of a PMMA based pore forming material. The pore forming material is preferably a mixture comprising 30wt% carbon black with an average particle size less than or equal to about 1 micron combined with 70wt% PMMA pore formers having a narrow particle size distribution and an average particle size of between about 0.8 microns and 5.0 microns Although use of the PMMA pore formers with a narrow particle size distribution have shown promising results, further pore optimization

and microstructure optimization may be realized using hollow, spherical particles as well as bi-modal or multi-modal particle size distributions of either or both of the 3YSZ materials and the PMMA based pore formers. For example, bi-modal or multimodal particle size distribution of PMMA pore formers, including PMMA particles with average particle diameters of 0.8 microns, 1.5 microns 3.0 microns and 5.0 microns are contemplated.

[0042] As described in more detail below, the preferred fabrication process of the oxygen transport membrane is to form the porous support via an extrusion process and subsequently bisque firing of the extruded porous support. The porous support is then coated with the active membrane layers, including the intermediate porous layer and the dense layer, after which the coated porous support assembly is dried and fired. The coated porous support assembly is then co-sintered at a final optimized sintering temperature and conditions.

[0043] An important aspect or characteristic of the materials or combination of materials selected for the porous support is its ability to mitigate creep while providing enough strength to be used in the oxygen transport membrane applications, which can reach temperatures above 1000°C and very high loads. It is also important to select porous support materials that when sintered will demonstrate shrinkages that match or closely approximate the shrinkage of the other layers of the oxygen transport membrane, including the dense separation layer, and intermediate porous layer.

[0044] In a preferred embodiment, the final optimized sintering temperature and conditions are selected so as to match or closely approximate the shrinkage profiles of the porous support to the shrinkage profiles of the dense separation layer while minimizing any chemical interaction between the materials of the active membrane layers, the materials in the porous support layer, and the sintering atmosphere. Too high of a final optimized sintering temperature tends to promote unwanted chemical interactions between the membrane materials, the porous support, and surrounding sintering atmosphere. Reducing atmospheres during sintering using blends of hydrogen and nitrogen gas atmosphere can be used to reduce unwanted chemical reactions but tend to be more costly techniques

compared to sintering in air. Thus, an advantage to the oxygen transport membrane of the disclosed embodiments is that some may be fully sintered in air. For example, a dense separation layer comprising $(La_{0.8}Sr_{0.2})_{0.95}Cr_{0.5}Fe_{0.5}O_{3-\delta}$ and 10Sc1CeSZ appears to sinters to full density in air at about 1400°C to1430°C.

[0045] As shown in Fig. 5, the use of PMMA pore former produced oxygen transport membranes with both high porosity and a substantially uniform pore size distribution throughout the porous support layer. Helium leak rates were consistently lower for coated porous supports comprised of 3YSZ with PMMA based pore forming materials (i.e. as low as 4×10^{-9} atm·cc/sec) compared to helium leak rates for prior art coated porous supports comprised of 3YSZ and walnut shell pore formers. Figs. 4 and 5 are SEM micrographs (1000x magnification) which show greater pore uniformity and overall porous support layer microstructure uniformity when using a porous support comprised of 3YSZ with PMMA based pore forming material (Fig. 5) than a porous support comprised of 3YSZ and walnut shell pore formers (Fig. 4).

[0046] Fig. 6 and Fig. 7 also show SEM micrographs (2000x magnification) of a porous support microstructure comprised of a single average particle size 3YSZ material with PMMA based pore forming material of 1.5 micron particle size (Fig. 6) and a porous support comprised of 3YSZ having different (e.g. bi-modal or multi-modal) average particle sizes (Fig. 7). Both porous support microstructures shown in Figs. 6 and 7 exhibited higher strength, lower creep, and improved diffusion efficiency compared to a 3YSZ porous support having a single average particle size 3YSZ particle size and larger size walnut shell pore formers (see Fig. 4).

[0047] It has also been observed that the disclosed porous support layers 12, 12', 12'' preferably have a permeability of between about 0.25 Darcy and about 0.5 Darcy. Standard procedures for measuring the permeability of a substrate in terms of Darcy number are outlined in ISO 4022. Porous support layers 12, 12', 12'' also preferably have a thickness of between about 0.5 mm and about 4 mm and an average pore size diameter of no greater than about 50 microns. Additionally, the porous support layers also have catalyst particles 18, 18', 18'' located within pores 20, 20', 20'' and preferably adjacent to the intermediate

porous layer for purposes of also promoting combustible substance oxidation. The presence of the catalyst particles both within the intermediate porous layer and within the porous support layer provides enhancement of oxygen flux and therefore generation of more heat via combustion that can be obtained by either providing catalyst particles within solely the intermediate porous layer or the porous support layer alone. It is to be noted that to a lesser extent, catalyst particles can also be located in region of the pores that are more remote from the intermediate porous layer, and therefore do not participate in promoting fuel oxidation. However, the bulk of catalyst in a composite oxygen transport element of the present invention is, however, preferably located in the intermediate porous layer and within the pores adjacent or proximate to the intermediate porous layer.

[0048] In forming a composite oxygen transport membrane element in accordance with the present invention, the porous support 12, 12',12'' is first formed in a manner known in the art and as set forth in the references discussed above. For example, standard ceramic extrusion techniques can be employed to produce a porous support layer or structure in a tube configuration in a green state and then subjected to a bisque firing at 1050ºC for about 4 hours to achieve reasonable strength for further handling. After bisque firing, the resulting tube can be checked or tested for targeted porosity, strength, creep resistance and, most importantly, diffusivity characteristics. Alternatively, a freeze cast supporting structure could be formed as discussed in "Freeze-Casting of Porous Ceramics: A Review of Current Achievements and Issues" (2008) by Deville, pp. 155-169.

[0049] After forming the green tube, intermediate porous layer 14, 14', 14'' is then formed. A mixture of about 34 grams of powders having electronic and ionic phases, LSCMV and 10Sc1YSZ, respectively, is prepared so that the mixture contains generally equal proportions by volume of LSCMV and 10Sc1YSZ. Prior to forming the mixture, the catalyst particles, such as CGO, are so incorporated into the electronic phase LSCMV by forming deposits of such particles on the electronic phase, for example, by precipitation. However, it is more preferable to form the catalyst particles within the intermediate porous layer by wicking a solution containing catalyst precursors through the porous support layer towards

the intermediate porous layer after application of the membrane active layers as described in more detail below. As such, there is no requirement to deposit particles of catalyst on the electronic phase. The electronic phase particles are each about 0.3 microns prior to firing and the catalyst particles are about 0.1 microns or less and are present in a ratio by weight of about 10wt%. To the mixture, 100 grams of toluene, 20 grams of the binder of the type mentioned above, 400 grams of 1.5 mm diameter YSZ grinding media are added. The mixture is then milled for about 6 hours to form a slurry (d_{50} of about 0.34μm). About 6 grams of carbon black having a particle size of about d50 = 0.8μm is then added to the slurry and milled for additional 2 hours. An additional 10 grams of toluene and about 10 grams of additional binder is added to the slurry and mixed for between about 1.5 and about 2 hours. The inner wall of the green tube formed above is then coated by pouring the slurry, holding once for about 5 seconds and pouring out the residual back to the bottle. The coated green tube is then dried and fired at 850ºC for 1 hour in air.

[0050] The dense layer 10, 10', 10'' is then applied. A mixture weighing about 40 grams is prepared that contains the same powders as used in forming the intermediate porous layer, discussed above, except that the ratio between LSCMV and 10Sc1YSZ is about 40/60 by volume, 2.4 grams of cobalt nitrate $\{Co(NO_3)_2.6H_2O\}$, 95 grams of toluene, 5 grams of ethanol, 20 grams of the binder identified above, 400 grams of 1.5 mm diameter YSZ grinding media are then added to the mixture and the same is milled for about 10 hours to form a slurry (d_{50} ~ 0.34μm). Again, about 10 grams of toluene and about 10 grams of binder are added to the slurry and mixed for about 1.5 and about 2 hours. The inner wall of the tube is then coated by pouring the slurry, holding once for about 10 seconds and pouring out the residual back to the bottle. The coated green tube is then stored dry prior to firing the layers in a controlled environment.

[0051] The coated green tube is then placed on a C-setter in a horizontal tube furnace and porous alumina tubes impregnated with chromium nitrate are placed close to the coated tube to saturate the environment with chromium vapor. The tubes are heated in static air to about 800ºC for binder burnout and, if necessary,

the sintering environment is switched to an atmosphere of a saturated nitrogen mixture (nitrogen and water vapor) that contains about 4 percent by volume of hydrogen to allow the vanadium containing electronic conducting perovskite structured materials to properly sinter. The tube is held at about 1350°C to 1430ºC for about 8 hours and then cooled in nitrogen to complete the sintering of the materials. The sintered tube is then checked for leaks wherein the helium leak rates should be lower than 10^{-7} Pa.

[0052] Surface exchange layer 16 is then applied. A mixture of powders is prepared that contains about 35g of equal amounts of ionic and electronic phases having chemical formulas of $Zr_{0.80}Sc_{0.18}Y_{0.02}O_{2-\delta}$ and $La_{0.8}Sr_{0.2}FeO_{3-\delta}$, respectively. To this mixture, about 100 grams of toluene, 20 grams of the binder identified above, about 400 grams of 1.5 mm diameter YSZ grinding media are added and the resultant mixture is milled for about 14 hours to form a slurry (d_{50} ~ 0.4μm). About six grams of carbon black are added to the slurry and milled for additional 2 hours. A mixture of about 10 grams of toluene and about 10 grams of the binder are then added to the slurry and mixed for between about 1.5 and about 2 hours. The inner wall of the tube is then coated by pouring the slurry, holding twice for about 10 seconds and then pouring out the residual back to the bottle. The coated tube is then dried and fired at 1100ºC for two hours in air.

[0053] The structure formed in the manner described above is in a fully sintered state and the catalyst is then further applied by wicking a solution containing catalyst precursors in the direction of arrowhead B at the side of the porous support opposite to the intermediate porous layer. The solution can be an aqueous metal ion solution containing about 20 mol% $Gd(NO_3)_3$ and 80 mol% $Ce(NO_3)_3$. A pressure can be established on the side of the porous support layer to assist in the infiltration of the solution. In addition, the pores can first be evacuated of air using a vacuum to further assist in wicking of the solution and prevent the opportunity of trapped air in the pores preventing wicking of the solution all the way through the porous support layer to the intermediate porous layer. The resulting composite oxygen transport membrane 1 in such state can be directly placed into service or further fired prior to being placed into service so that the

catalyst particles, in this case $Ce_{0.8}Gd_{0.2}O_{2-\delta}$ are formed in the porous support layer adjacent to the intermediate porous layer and as described above, within the intermediate porous layer itself. The firing to form $Ce_{0.8}Gd_{0.2}O_{2-\delta}$ would take place at a temperature of about 850°C and would take about 1 hour to form the catalyst particles.

[0054] Although the present invention has been described with reference to a preferred embodiment, as will occur to those skilled in the art, changes and additions to such embodiment can be made without departing from the spirit and scope of the present invention as set forth in the appended claims.

Claims

1. A composite oxygen transport membrane, said composite oxygen transport membrane comprising:

a porous support layer comprised of an fluorite structured ionic conducting material having a porosity of greater than 20 percent and a microstructure exhibiting substantially uniform pore size distribution throughout the porous support layer;

an intermediate porous layer capable of conducting oxygen ions and electrons to separate oxygen from an oxygen containing feed, the intermediate porous layer applied adjacent to the porous support layer and comprising a mixture of a fluorite structured ionic conductive material and electrically conductive materials to conduct the oxygen ions and electrons, respectively;

a dense layer capable of conducting oxygen ions and electrons to separate oxygen from an oxygen containing feed, the dense layer applied adjacent to the intermediate porous layer and also comprising a mixture of a fluorite structured ionic conductive material and electrically conductive materials to conduct the oxygen ions and electrons, respectively; and

catalyst particles or a solution containing precursors of the catalyst particles located in pores of the porous support layer and intermediate porous layer, the catalyst particles containing a catalyst selected to promote oxidation of a combustible substance in the presence of the separated oxygen transported through the dense layer and the intermediate porous layer to the porous support layer.

2. The composite oxygen transport membrane of claim 1, wherein the catalyst is gadolinium doped ceria.

3. The composite oxygen transport membrane of claim 1, further comprising a porous surface exchange layer applied to the dense layer opposite to the intermediate porous layer.

4. The composite oxygen transport membrane of claim 1, wherein:

the intermediate porous layer has a thickness of between 10 and 40 microns, a porosity of between 20 percent and 50 percent and an average pore diameter of between 0.5 and 3 microns;

the dense layer has a thickness of between 10 and 50 microns;

the porous surface exchange layer has a thickness of between 10 and 40 microns, a porosity of between 30 percent and 60 percent and a pore diameter of between 1 and 4 microns; and

the porous support layer has a thickness of between 0.5 and 4 mm.

5. The composite oxygen transport membrane of claim 1, wherein:

the intermediate porous layer contains a mixture of about 60 percent by weight of $(La_{0.825}Sr_{0.175})_{0.96}Cr_{0.76}Fe_{0.225}V_{0.015}O_{3-\delta}$ or $(La_{0.8}Sr_{0.2})_{0.95}Cr_{0.7}Fe_{0.3}O_{3-\delta}$ with the remainder 10Sc1YSZ or 10Sc1CeSZ;

the dense layer contains a mixture of about 40 percent by weight of $(La_{0.825}Sr_{0.175})_{0.94}Cr_{0.72}Mn_{0.26}V_{0.02}O_{3-\delta}$ or $(La_{0.8}Sr_{0.2})_{0.95}Cr_{0.5}Fe_{0.5}O_{3-\delta}$, with remainder 10Sc1YSZ or 10Sc1CeYSZ;

the porous surface exchange layer is formed by a mixture of about 50 percent by weight of $(La_{0.8}Sr_{0.2})_{0.98}MnO_{3-\delta}$ or $La_{0.8}Sr_{0.2}FeO_{3-\delta}$, remainder 10Sc1YSZ or 10Sc1CeSZ;

the porous support layer has a thickness of between 0.5 and 4 mm and is formed from a mixture comprising 3YSZ and a polymethyl methacrylate based pore forming material.

6. The composite oxygen transport membrane of claim 1, wherein:

the intermediate porous layer contains a mixture of about 60 percent by weight of $(La_uSr_vCe_{1-u-v})_wCr_xM_yV_zO_{3-\delta}$ where u is from 0.7 to 0.9, v is from 0.1 to 0.3 and (1-u-v) is greater than or equal to zero, w is from 0.94 to 1, x is from 0.5 to 0.77, M is Mn or Fe, y is from 0.2 to 0.5, z is from 0 to 0.03, and x+y+z =1, with the remainder $Zr_{x'}Sc_{y'}A_{z'}O_{2-\delta}$, where y' is from 0.08 to 0.3, z' is from 0.01 to

0.03, x'+y'+z'=1 and A is Y or Ce or mixtures of Y and Ce, and the intermediate porous layer has a thickness of between 10 and 40 microns, and a porosity of between 25 percent and 40 percent;

the dense layer contains a mixture of about 40 percent by weight of $(La_uSr_vCe_{1-u-v})_wCr_xM_yV_zO_{3-\delta}$ where u is from 0.7 to 0.9, v is from 0.1 to 0.3 and (1-u-v) is greater than or equal to zero, w is from 0.94 to 1, x is from 0.5 to 0.77, M is Mn or Fe, y is from 0.2 to 0.5, z is from 0 to 0.03, and x+y+z =1, with the remainder $Zr_{x'}Sc_{y'}A_{z'}O_{2-\delta}$, where y' is from 0.08 to 0.3, z' is from 0.01 to 0.03, x'+y'+z'=1 and A is Y or Ce or mixtures of Y and Ce, and the dense layer has a thickness of between 10 and 50 microns;

the porous surface exchange layer is formed by a mixture of about 50 percent by weight of $(La_{x'''}Sr_{1-x'''})_{y'''}MO_{3-\delta}$, where x''' is from 0.2 to 0.9, y''' is from 0.95 to 1, M is Mn or Fe, with the remainder $Zr_x^{iv}Sc_y^{iv}A_z^{iv}O_{2-\delta}$, where y^{iv} is from 0.08 to 0.3, z^{iv} is from 0.01 to 0.03, $x^{iv}+y^{iv}+z^{iv}=1$ and A is Y, Ce or mixtures of Y and Ce; and

the porous support layer has a thickness of between 0.5 and 4 mm and is formed from 3YSZ having bi-modal or multi-modal particle sizes.

7. A composite oxygen transport membrane made by the process comprising:

fabricating a porous support layer comprised of an fluorite structured ionic conducting material, the fabricating step including pore forming enhancement step such that the porous support layer has a porosity of greater than about 20 percent and a microstructure exhibiting substantially uniform pore size distribution throughout the porous support layer;

applying an intermediate porous layer on the porous support layer, the intermediate porous layer capable of conducting oxygen ions and electrons to separate oxygen from an oxygen containing feed, the intermediate porous layer comprising a mixture of a fluorite structured ionic conductive material and electrically conductive materials to conduct the oxygen ions and electrons, respectively;

applying a dense layer on the intermediate porous layer, the dense layer capable of conducting oxygen ions and electrons to separate oxygen from an oxygen containing feed, the dense layer also comprising a mixture of a fluorite structured ionic conductive material and electrically conductive materials to conduct the oxygen ions and electrons, respectively; and

introducing catalyst particles or a solution containing precursors of the catalyst particles to the porous support layer and intermediate porous layer, the catalyst particles containing a catalyst selected to promote oxidation of a combustible substance in the presence of the separated oxygen transported through the dense layer and the intermediate porous layer to the porous support layer.

8. The composite oxygen transport membrane of claim 7, wherein the pore forming enhancement process comprises mixing a polymethyl methacrylate based pore forming material with the fluorite structured ionic conducting material of the porous support layer.

9. The composite oxygen transport membrane of claim 7, wherein the pore forming enhancement process comprises use of bi-modal or multi-modal particle sizes of the fluorite structured ionic conducting material of the porous support layer.

10. The composite oxygen transport membrane of claim 9, wherein the pore forming enhancement process comprises use of hollow spherical particles of the fluorite structured ionic conducting material of the porous support layer.

11. The composite oxygen transport membrane of claim 7, further comprising the step of applying a porous surface exchange layer to the dense layer opposite to the intermediate porous layer.

12. The composite oxygen transport membrane of claim 7, wherein the step of introducing catalyst particles or a solution containing precursors of the catalyst particles to the porous support layer and intermediate porous layer further

comprises adding catalyst particles to the mixture of fluorite structured ionic conductive material and electrically conductive materials in the intermediate porous layer.

13. The composite oxygen transport membrane of claim 7, wherein the step of introducing catalyst particles or a solution containing precursors of the catalyst particles to the porous support layer and intermediate porous layer further comprises:

applying a solution containing catalyst precursors to the porous support layer on a side thereof opposite to the intermediate porous layer so that the solution infiltrates pores within the porous support layer and the intermediate porous layer with the solution containing catalyst precursors; and

heating the composite oxygen transport membrane after the solution containing catalyst precursors infiltrates the pores and to form the catalyst from the catalyst precursors.

14. A method of producing a catalyst containing composite oxygen transport membrane, said method comprising:

forming a composite oxygen transport membrane in a sintered state, said composite oxygen transport membrane having a plurality of layers comprising a dense separation layer, a porous support layer, and an intermediate porous layer located between the dense separation layer and the porous support layer;

applying a solution containing catalyst precursors to the porous support layer on a side thereof opposite to the intermediate porous layer, the catalyst precursors selected to produce a catalyst capable of promoting oxidation of the combustible substance in the presence of the separated oxygen;

infiltrating or impregnating the porous support layer with the solution containing catalyst precursors so that the solution containing catalyst precursors wicks through the pores of the porous support layer and at least partially infiltrates or impregnates the intermediate porous layer; and

heating the composite oxygen transport membrane after infiltrating or impregnating the porous support layer and the intermediate porous layer such that the catalyst is formed from the catalyst precursors

wherein each of the dense separation layer and the intermediate porous layer are capable of conducting oxygen ions and electrons at an elevated operational temperature to separate oxygen from an oxygen containing feed;

wherein the dense separation layer and the intermediate porous layer comprising mixtures of a fluorite structured ionic conductive material and electrically conductive materials to conduct oxygen ions and electrons, respectively;

wherein the porous support layer comprises a fluorite structured ionic conducting material having a porosity of greater than about 20 percent and a microstructure exhibiting substantially uniform pore size distribution throughout the porous support layer.

15. The method of claim 14, wherein the solution containing catalyst precursors is an aqueous metal ion solution containing 20 mol% $Gd(NO_3)_3$ and 80 mol% $Ce(NO_3)_3$ that when sintered forms $Gd_{0.8}Ce_{0.2}O_{2-\delta}$.

16. The method of claim 14, wherein the catalyst is gadolinium doped ceria.

17. The method of claim 14, wherein a pressure is established on the second side of the support layer to assist in the infiltration or impregnation of porous support layer and intermediate porous layer with the solution containing catalyst precursors or wherein the pores can first be evacuated of air using a vacuum to further assist in wicking of the solution containing catalyst precursors and prevent the opportunity of trapped air in the pores preventing or inhibiting wicking of the solution containing catalyst precursors through the porous support layer to the intermediate porous layer.

18. The method of claim 14, wherein the pores in the porous support layer are formed using a polymethyl methacrylate based pore forming material mixed with the fluorite structured ionic conducting material of the porous support layer.

19. The method of claim 14, wherein the pores in the porous support layer are formed using bi-modal or multi-modal particle sizes of the polymethyl methacrylate based pore forming material or the fluorite structured ionic conducting material of the porous support layer.

20. The method of claim 14, wherein the pores in the porous support layer are formed using of hollow spherical particles of the polymethyl methacrylate based pore forming material or the fluorite structured ionic conducting material of the porous support layer.

CATALYST CONTAINING OXYGEN TRANSPORT MEMBRANE

Abstract of the Disclosure

A composite oxygen transport membrane having a dense layer, a porous support layer and an intermediate porous layer located between the dense layer and the porous support layer. Both the dense layer and the intermediate porous layer are formed from an ionic conductive material to conduct oxygen ions and an electrically conductive material to conduct electrons. The porous support layer has a high permeability, high porosity, and a microstructure exhibiting substantially uniform pore size distribution as a result of using PMMA pore forming materials or a bi-modal particle size distribution of the porous support layer materials. Catalyst particles selected to promote oxidation of a combustible substance are located in the intermediate porous layer and in the porous support adjacent to the intermediate porous layer. The catalyst particles can be formed by wicking a solution of catalyst precursors through the porous support toward the intermediate porous layer.

09-3030-CIP2-US 1/3

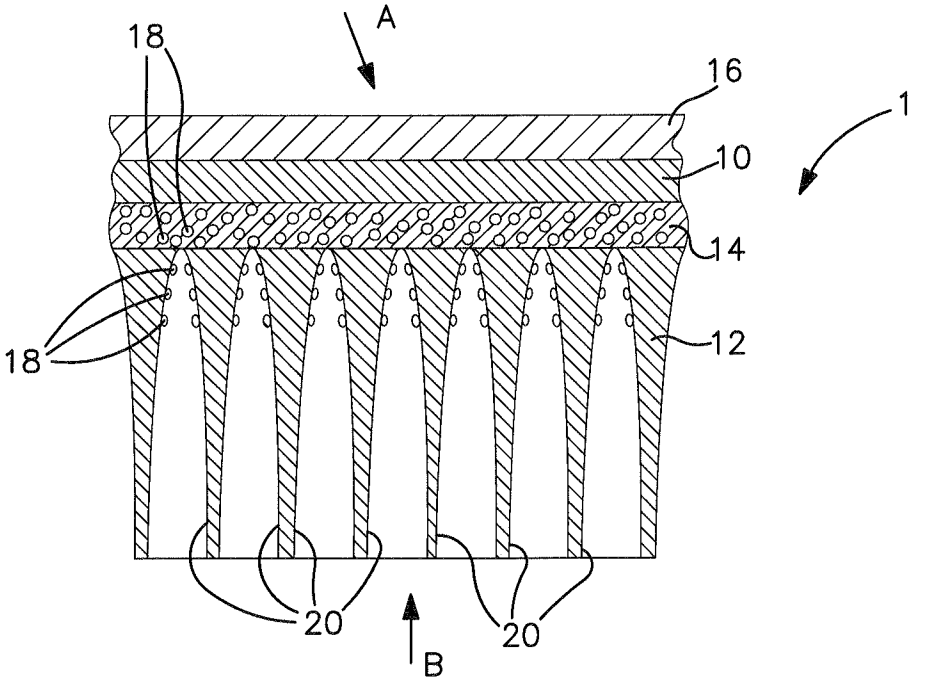

FIG. 1

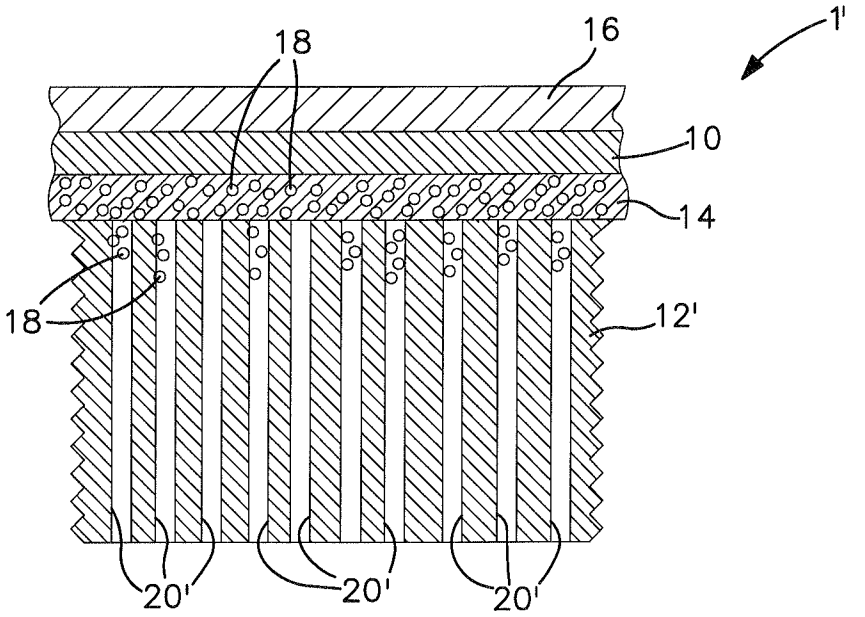

FIG. 2

09-3030-CIP2-US 2/3

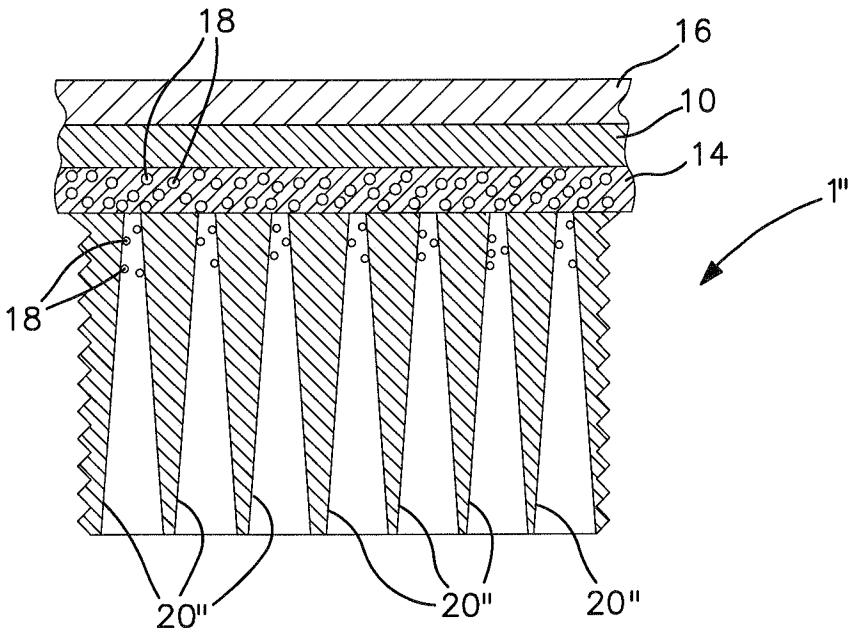

FIG. 3

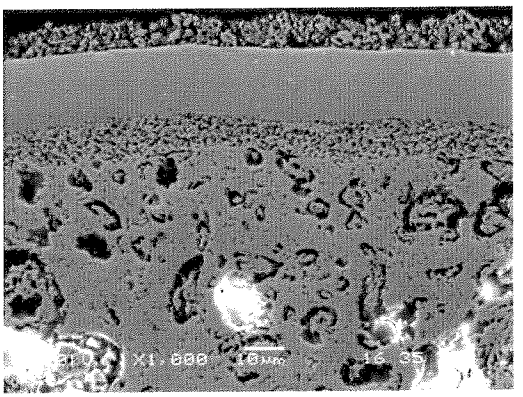

Fig. 4

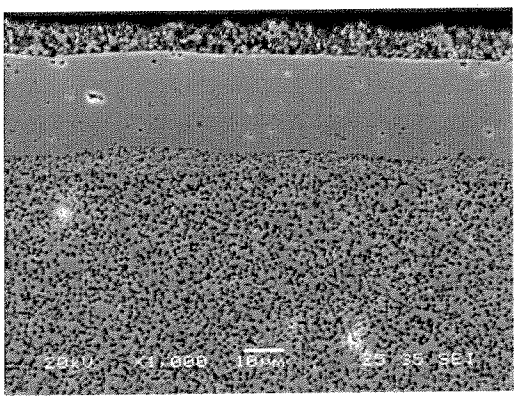

Fig. 5

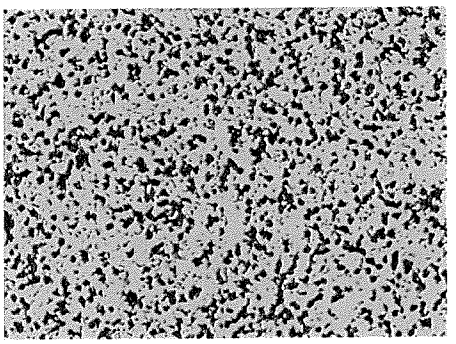

Fig. 6

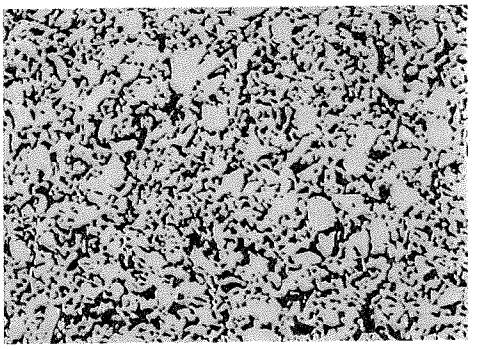

Fig. 7